Novel Halogenation and Pallado-Biology Strategies for Biological Probes

A Thesis Submitted to the Board of the Faculty of Physical Science
in Partial Fulfilment of the Requirements for
the Degree of Doctor of Philosophy at the University of Oxford

Anuchit Phanumartwiwath

St. Cross College, University of Oxford

August 2016

Supervisor : Professor Benjamin G. Davis, FRS

Author Declaration

The work presented in this thesis was conducted at the Department of Chemistry, University of Oxford under the supervision of Professor Benjamin Davis. All the work is my own, except where otherwise stated, and has not been submitted for any other degree at this or any other university.

Anuchit Phanumartwiwath

Abstract

Novel Halogenation and Pallado-Biology Strategies for Biological Probes

Anuchit Phanumartwiwath

St. Cross College, University of Oxford

Post-translational modifications (PTMs), which biochemically modify proteins to generate diversity and control functionality, are important in the field of chemical biology research. However, typical bioconjugation methods involving nucleophilic addition of cysteine and lysine residues are limited by their lack of site-specificity. In this thesis, we have demonstrated the site-selective chemical modification of a variety of proteins through protein halogenation and subsequent pallado-biology strategies.

The "Tag-and-Modify" approach, developed previously in our group and involving the creation of a protein tag for further manipulation, is a useful tool for site-selective chemical modification. Here, we envisioned extending its utility to a novel concept of [^{18}F]-radiolabelling of proteins involving direct electrophilic fluorination, thus forming a C-F bond at a specific modification site and leading to the generation of protein species applicable for *in vivo* [^{18}F]-PET imaging and diagnosis.

We also explored several alternative methods for the installation of C-Br/C-I bonds onto a protein of interest. Our first attempts involved the biosynthetic incorporation of a synthetic bromotryptophan into the protein, however these processes were unsuccessful. As a workaround, we found IPy_2BF_4, an iodinating agent, to be very effective as a direct method for the site-specific installation of C-I bonds on tyrosine/histidine residues of proteins. We subsequently demonstrated novel and efficient palladium-catalysed cross-couplings of the resultant iodinated tyrosine/histidine moieties, leading to the creation of new C-C bonds. This approach was compatible with a wide range of functionally diverse boronic acids, using a water-soluble and phosphine-ligand-free Pd-complex catalyst under fully aqueous conditions.

Our novel, successful method for C-C bond formation onto proteins is potentially applicable to the initial investigation of challenging *in vivo* Pd cross-coupling of thyroglobulin, based on our achievement of protein labelling under *ex vivo* conditions. In summary, we are able to create new chemical tools for the site-selective/site-specific chemical modification of proteins, enabling their use as biological probes.

Acknowledgements

First of all, I would like to thank my supervisor, Prof. Ben Davis for giving me this opportunity to work on these interesting and challenging projects in the field of chemical biology, and I appreciate his advice, continuing support and encouragement especially during difficult times. Also thanks to him for supporting my participation in international conferences and training courses, having faith in me from the beginning of this DPhil study until the end and sharing his knowledge and scientific skills; I really appreciate it.

Some parts of my DPhil thesis would not have been completed without help and advice kindly offered from many great collaborators; Prof. Daniel Anthony, Prof. Olof Solin, Prof. Merja Haaparanta-Solin, Dr. Matthew Schombs, Dr. Alex Dickens, Dr. Anna Kirjavainen, and Dr. Sarita Forsback for [^{18}F]-radiolabelling of proteins and preclinical animal studies using [^{18}F]-PET imaging technique. I am also especially grateful to Prof. Daniel Anthony and Dr. Nan Yang for experiments and discussions relevant to *ex vivo*/*in vivo* labelling of proteins. Furthermore, I give special thanks to Marie-Laëtitia Thézénas and Prof. Benedikt Kessler for MSMS analysis service. I owe gratitude to Prof. Tim Claridge, Dr. Barbara Odell, and Tina Jackson for the NMR service as well as Dr. James Wickens and Sébastien Galan for any help with Protein Mass Spectrometry. Also, plasmids including annexin V(pET12a PAPI) and ubiquitin(WT-UbcH5c) were kindly provided by the Addgene company.

Secondly, I am grateful to Dr. Chris Spicer and Dr. Anaëlle Dumus for taking care of me and supervising me in the first year of DPhil at Oxford. I greatly acknowledge all people including Dr. Charlie Fehl, Matthew Bilyard, Dr. Jitka Dadova, Dr. Brian Lyons, Dr. Nan Yang, and Dr. Sylvain Royer for proofreading, comments, and suggestions in this DPhil thesis. As the continuation support, I have been honourably granted a fellowship of the Development and Promotion of Science and Technology Talents Project (DPST), Bangkok, Thailand that provided me an opportunity to study from secondary school level until DPhil. Moreover, the Office of Educational Affairs, Royal Thai Embassy, London, United Kingdom, took care of whilst also providing an official documentation with useful guidance and suggestions whilst living in the UK.

Finally, I would like to express so many thanks to my parents and family members, St. Cross College and all my previous/current BGD lab mates, thanks for all their support, help and friendship. Also, I give sincere thanks to all people who were involved in these projects during my DPhil study, whether directly or not.

Table of Contents

Abbreviations

ADHP	2-Amino-4,6-dihydroxypyrimidine
IME	2-Imino-2-methoxyethyl
β-ME	2-Mercaptoethanol
DBHDA	2,5-Dibromohexanediamide
3-BrTyr	3-Bromotyrosine
3-ClTyr	3-Chlorotyrosine
IAA	3-Indoleacrylic acid
3-ITyr	3-Iodotyrosine
MIT	3-Iodotyrosine
DIT	3,5-Iodotyrosine
4-BPhe	4-Boronophenylalanine
4-BrPhe	4-Bromophenylalanine
4-ClPhe	4-Chlorophenylalanine
4-FPhe	4-Fluorophenylalanine
4-IPhe	4-Iodophenylalanine
4-OT	4-Oxolocrotonate tautomerase
BCIP/NBT	5-Bromo-4-chloro-3-indolyl phosphate/ Nitro blue tetrazolium
5-BrTrp	5-Bromotryptophan
5-FTrp	5-Fluorotryptophan
5-OHTrp	5-Hydroxytryptophan
5-MeTrp	5-Methyltryptophan
DTNB	5,5-Dithio-bis-(2-nitrobenzoic acid)
6-BrTrp	6-Bromotryptophan
6-ClTrp	6-Chlorotryptophan
7-AzaTrp	7-Azatryptophan
aaRS	Aminoacyl-tRNA synthetase
Amp	Ampicillin
ANV	Annexin V
ACDs	Antibody-drug conjugates
aq	Aqueous
AIM	Auto induction medium

SBL	*Bacillus lentus* subtilisin
BT	Benzothienylalanine
BSA	Bovine serum albumin
NBS	*N*-Bromosuccinimide
CalB	*Candida antarctica* lipase B
C	Celsius
CD	Circular dichroism
CID	Collision-induced dissociation
CuAAC	Copper catalysed azide-alkyne cycloaddition
J	Coupling constant
CXM	Cycloheximide
Dha	Dehydroalanine
Dfa	Dehydrofluoroalanine
DNA	Deoxyribonucleic acid
DIBO	Dibenzocyclooctyne
DCM	Dichloromethane
DIFO	Difluorinated cyclooctyne
DHFR	Dihydrofolate reductase
DMF	Dimethylformamide
DMSO	Dimethylsulfoxide
DTT	Dithiothreitol
DMEM	Dulbecco's modified eagle's medium
S_EAr	Electrophilic aromatic substitution
ESI	Electrospray ionisation
EPO	Eosinophil peroxidase
equiv.	Equivalents
EDTA	Ethylenediaminetetraacetic acid
E. coli	*Escherichia coli*
FBS	Fetal bovine serum
FITC	Fluorescein thiocyanate
FA	Formic acid
FGly	Formylglycine
GST	Glutathione *S*-transferase
g	Gram(s)

GFP	Green fluorescent protein
GYG	Glycogenin-1
h	Hour(s)
Hb	Hemoglobin
Hz	Hertz
HPLC	High-performance liquid chromatography
HRMS	High resolution mass spectrometry
GFPHS	Highly stable green fluorescent protein
H3	Histone
HGH	Human growth hormone
LH	Human luteinising hormone
HEK	Human embryonic kidney
Hfa	Hydroxyfluoroalanine
L-Hpg	L-Homoproparylglycine
NHS	*N*-Hydroxysuccinimide
IR	Infrared
IPTG	Isopropyl-β-D-1-thiogalactopyranoside
NCS	Isothiocyanate
p-IPhe	*para*-Iodophenylalanine
Kan	Kanamycin
KDa	Kilodalton
L. lactis	*Lactococcus lactis*
LC-MS	Liquid chromatography mass spectroscopy
lit	Literature
L	Litre
LRMS	Low resolution mass spectrometry
LB	Lysogenyl broth
MBP	Maltose binding protein
MHz	Megahertz
m.p.	Melting point
M. jann	*Methanococcus jannaschii*
µg	Microgram
µL	Microlitre
µmol	Micromole

MBq	Megabecquerel
mg	Milligram
mL	Millilitre
mM	Millimolar
mmol	Millimole
min	Minute
M	Molar
mol	Mole
MW	Molecular weight
MCP-1	Monocyte chemoattractant protein-1
MPO	Myeloperoxidase
MIDA	*N*-Methyliminodiacetic acid
MSH	*O*-Mesitylenesulfonylhydroxylamine
nmol	Nanomole
NCL	Native chemical ligation
NMM	New minimal medium
NDM-1	New Delhi metallo-β-lactamase
NGMs	Next-genearation maleimides
Np	*Nostoc punctiforme*
NMR	Nuclear magnetic resonance
OD	Optical density
OmpC	Outer membrane protein C
OspF	Outer surface protein F
ppm	part per million
PpiB	Peptidyl-Pro *cis-trans* isomerase
PheRS	Phenylalanyl-tRNA synthetase
PBS	Phosphate-buffered saline
PS	Phosphatidylserine
PEG	Polyethylene glycol
PCR	Polymerase chain reaction
PET	Positron Emission Tomography
PTMs	Post-translational modifications
PI	Propidium iodide
RP-HPLC	Reversed phase high-performance liquid chromatography

rpm	Revolutions per minute
RNA	Ribonucleic acid
rt	Room temperature
SPI	Selective pressure incorporation
SDS-PAGE	Sodium dodecyl sulfate polyacrylamide gel electrophoresis
SM	Starting material
SPAAC	Strain-promoted azide-alkyne cycloaddition
SPIEDAC	Strain-promoted inverse electron-demand Diels-Alder cycloaddition
SsβG	*Sulfolobus solfataricus* β-galactosidase
SMC	Suzuki-Miyaura cross-coupling
[^{18}F]SFB	*N*-Succinimidyl-4-[^{18}F]-fluorobenzoate
TBAB	Tetra-n-butylammonium bromide
TLC	Thin layer chromatography
Tg	Thyroglobulin
TPO	Thyroid peroxidase
TSH	Thyroid-stimulating hormone
T4	Thyroxine
tRNA	Transfer-ribonucleic acid
TFA	Trifluoroacetatic acid
FBA	Trifluorobromo acetone
T3	Triiodothyronine
TAE	Tris-acetate EDTA
TBS	Tris-buffered saline
TPPTS	Trisphenylphosphine-3,3′,3″-trisulfonic acid trisodium salt
TPPMS	Trisphenylphosphine-3-monosulfonic acid monosodium salt
TXPTS	Tris(2,4-dimethyl-5-sulfophenyl)phosphine trisodium salt
TrpRS	Tryptophanyl-tRNA synthetase
TyrRS	Tyrosyl-tRNA synthetase
Boc	*N*-Tert-butoxycarbonyl
UBQ	Ubiquitin
UV	Ultraviolet
UAA	Unnatural amino acid
WT	Wild-type

Publications

1. T. H. Wright, B. J. Bower, J. M. Chalker, G. J. L. Bernardes, R. Wiewiora, W.-L. Ng, R. Raj, S. Faulkner, M. R. J. Vallée, **A. Phanumartwiwath**, O. D. Coleman, M.-L. Thézénas, M. Khan, S. R. G. Galan, L. Lercher, M. W. Schombs, S. Gerstberger, M. E. Palm-Espling, A. J. Baldwin, B. M. Kessler, T. D. W. Claridge, S. Mohammed and B. G. Davis, ***Science, 2016, 354, 597***. "Post-Translational Mutagenesis: a Chemical Synthetic Strategy for Exploration of Protein Side-Chain Diversity"

2. O. Boutureira, M. Schombs, **A. Phanumartwiwath**, R. L. C. Leung, G. J. L. Bernardes, M. Sánchez-Navarro, A. Kirjavainen, S. Forsback, I. S. R. Stenhagen, A. M. Dickens, A. L. Thompson, M. Haaparanta-Solin, O. Solin, V. Gouverneur, D. C. Anthony, and B. G. Davis, ***Manuscript in revision***, "A Protein-based Umpolung Allows Direct Electrophilic C–F Bond Formation at Dehydroalanine"

Presentations

UK Chemical Biology Symposium (RSC), the United Kingdom, *2016* (Poster Presentation: Selected Abstract for RSC Symposium Bursary)

251st American Chemical Society (ACS) National Meeting, the United States, *2016* (Oral Presentation: Division of Biological Chemistry, Young Investigators in Biological Chemistry Session)

2016 International Symposium on Chemical Biology (NCCR), Switzerland, *2016* (Poster Presentation: Selected Abstract for Travel Grant Award)

IKCOC-13: International Kyoto Conference on New Aspect of Organic Chemistry, Japan, *2015* (Poster Presentation)

ECBS & ICBS Joint Meeting, Germany, *2015* (Poster Presentation: Poster Prize Award)

ISACS-16: Challenges in Chemical Biology (RSC), Switzerland, *2015* (Poster Presentation)

Chapter 1

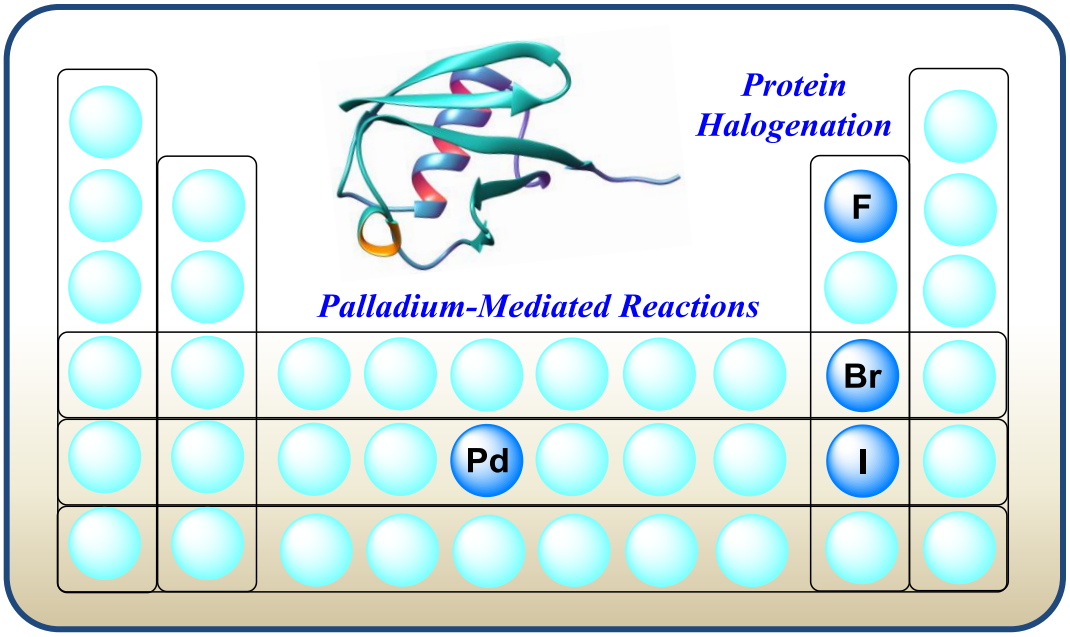

Introduction

1.1 Chemical Protein Modification

1.1.1 Chemical Protein Modifications of Natural Amino Acids

1.1.2 Chemical Protein Modifications of Unnatural Amino Acids

1.2 Protein Halogenation

1.2.1 Fluorination

1.2.2 Chlorination

1.2.3 Bromination

1.2.4 Iodination

1.3 Palladium-Mediated Reactions of Proteins

1.3.1 Suzuki-Miyaura Cross-Coupling Reactions

1.3.2 Sonogashira Cross-Coupling Reactions

1.3.3 Heck Cross-Coupling Reactions

1.4 The Aims of this Thesis

1.5 Bibliography

1.1 Chemical Protein Modification

Many useful chemical tools for site-selective chemical protein modification have been developed for widespread use over the past few decades[1-4]. These chemical tools can greatly expand the diversity of protein constructs, resulting in extensions to protein function and structural diversity[1-6]. The most common strategy for bioconjugation is the nucleophilic attack of lysine side-chains on electrophiles, which has been widely used in the field of biochemistry[4,7]. However, the maintenance of protein structure and function may be significantly impaired by such non-specific protein labelling methods. To maintain natural protein functions, a variety of chemical approaches for site-selective modification of both natural and synthetic amino acid residues of proteins is required[2-4,6]. Many chemical tools have been designed for specific protein reaction types through the introduction of either a genetic or chemical tag on the target proteins[2-4,6]. For example, Caddick and Baker developed protein labelling through maleimide-cysteine modification by a reaction between a thiol protein residue and maleimide derivatives[8,9]. A concept of the "Tag-and-Modify" approach, developed in the Davis group, can utilise site-selective protein modification by introduction of a designed chemical protein tag and subsequent (specific) derivatisation[10,11]. Other approaches based on the copper-catalysed azide-alkyne cycloaddition (CuAAC) and strain-promoted azide-alkyne cycloaddition (SPAAC), known as click chemistry, are also widely used for protein labelling in the complex aqueous conditions required to probe biological systems[4,12-16]. Details of each chemical approach for protein modification are described in the following sections.

1.1.1 Chemical Protein Modifications of Natural Amino Acids

Both natural lysine and cysteine residues of the protein are generally chosen as reactive nucleophiles for protein labelling. Either nucleophilic amines or thiols can potentially react with an electrophile, resulting in a simple bioconjugation of the protein of interest.

Chemical Modifications at Cysteine Thiols

The low natural abundance of the cysteine residue found in proteins can enable site-specific protein modification. The thiol of the cysteine residue acts as a nucleophile which can be alkylated by either alkyl halides or maleimides, leading to the formation of a thioether (C-S) bond on proteins (Figure **1.1**)[8,9,17-19]. Originally, cysteine alkylation with alkyl halides was used as a simple and straightforward method which to modify the protein of interest containing a solvent-exposed and sterically-accessible cysteine. Chalker and Davis reported the site-specific chemical conjugation of a cysteine variant of *Bacillus lentus* subtilisin (SBL-S156C) with 4-iodobenzyl bromide, resulting in the installation of *para*-iodophenyl group, linked by the resulting thioether, as a coupling partner for Pd-mediated Suzuki-Miyaura cross-coupling reactions[20]. The cysteine alkylation approach also facilitated a site-specific methylation of histone H3(K9C) through a reaction between its single cysteine and an aminoethylating agent (Scheme **1.1**)[21]. The methylated amino thioether could be used as a mimic of an enzymatically methylated-lysine H3. A simple and convenient method for protein labelling through maleimide-thiol coupling has been demonstrated on many protein substrates including enzymes and antibodies. For example, bovine hemoglobin (Hb) was site-selectively glycosylated by treatment of a cysteine residue of Hb with a lactose-linked maleimide, and this glycosylated Hb served as a high affinity oxygen carrier[22].

Also, Caddick and Baker developed a bifunctional label specific for cysteines using what they term next-generation maleimides (NGMs), able to further extend protein functionalities[8,9,23]. For example, selective chemical labelling of the Grb2 SH2 Domain was demonstrated via dibromomaleimide-cysteine modification, leading to bioconjugation with dual functionality[9]. The resultant maleimide-linked thioether protein could be reversibly cleaved by a thiol (2-mercaptoethanol or glutathione), thereby regenerating the non-modified protein. Also, the formation of a succinimide bridge of an antibody fragment was achieved by treatment of a cysteine of an anti-CEA ds-scFv with PEG-substituted phenoxymaleimide[8]. Recently, a 'plug-and-play' approach for selective protein labelling has been introduced by the Caddick group[24]. This method can facilitate a construction of next generation of antibody-drugs conjugates (ACDs) through dibromopyridazinedione-cysteine conjugation and subsequent dual click chemistry[24]. Cysteine-mediated protein modification is still attractive to biochemists due to its high

reliability as a site-specific chemical conjugation that is also straightforward as a scalable protein reaction.

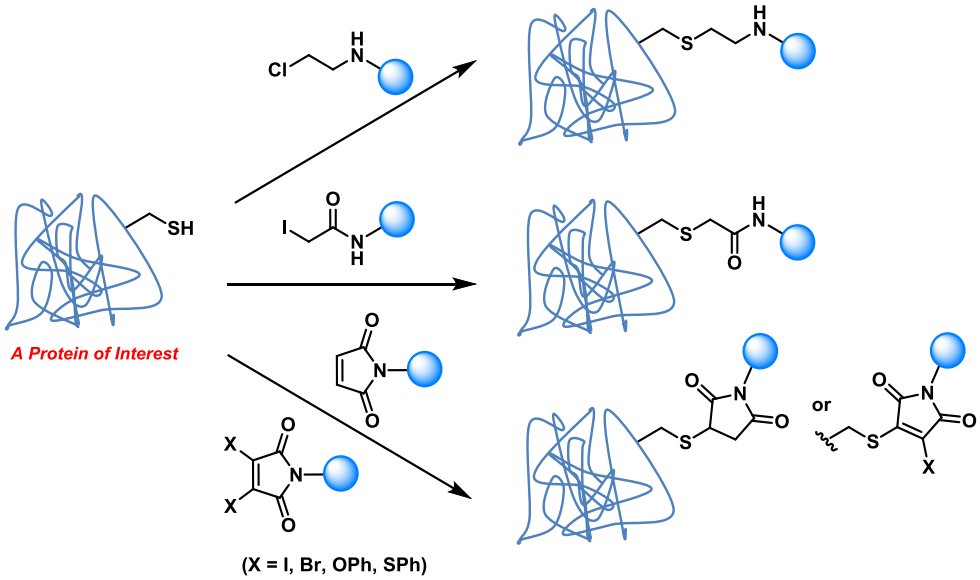

Figure 1.1 Chemical protein modifications through reactions of a nucleophilic cysteine with alkyl halides or maleimides[8,9,17-19].

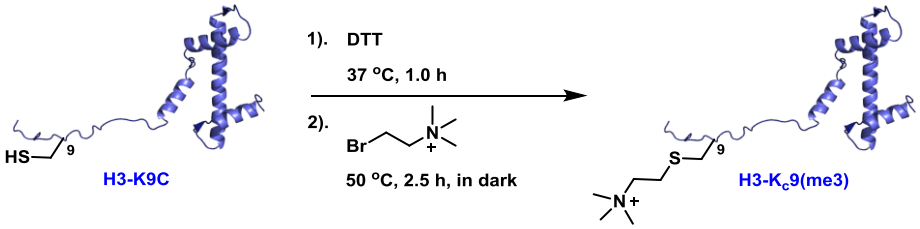

Scheme 1.1 Site-specific installation of a mimic methylated lysine of H3(K9C) through cysteine alkylation[21].

Chemical Modifications at Lysine and *N*-Terminal Amines

The lysine residue is the most abundant nucleophilic amine of the natural amino acids found in nature. This makes it attractive for simple nucleophilic methods of protein modification. Meanwhile, a modification of the *N*-terminus can be achieved via native chemical ligation (NCL), resulting in the formation of a new peptide bond between two polypeptides (Figure **1.2**)[25]. This method has been utilised in the construction of synthetic polypeptides as well as in the production of either small or medium-sized synthetic proteins. Within the sequence of amino acids, lysine residues on the protein surface may be accessible for selective lysine modification by the reaction of the NH_2 group with electrophiles such as *N*-hydroxysuccinimide (NHS), isothiocyanate (NCS), 2-imino-2-

methoxyethyl (IME), (Figure **1.3**)[4,7,26]. Generally, the lysine modification is commonly used for an installation of fluorescent tags by the reaction between fluorophore NHS or NCS derivatives and lysine side-chains of the protein. This results in the formation of covalent bonds between fluorescent dye and protein. However, uncontrolled multiple-site protein labelling through lysine modification is still an issue, due to the difficulty to achieve site-selective labelling on such an abundant amino acid residue.

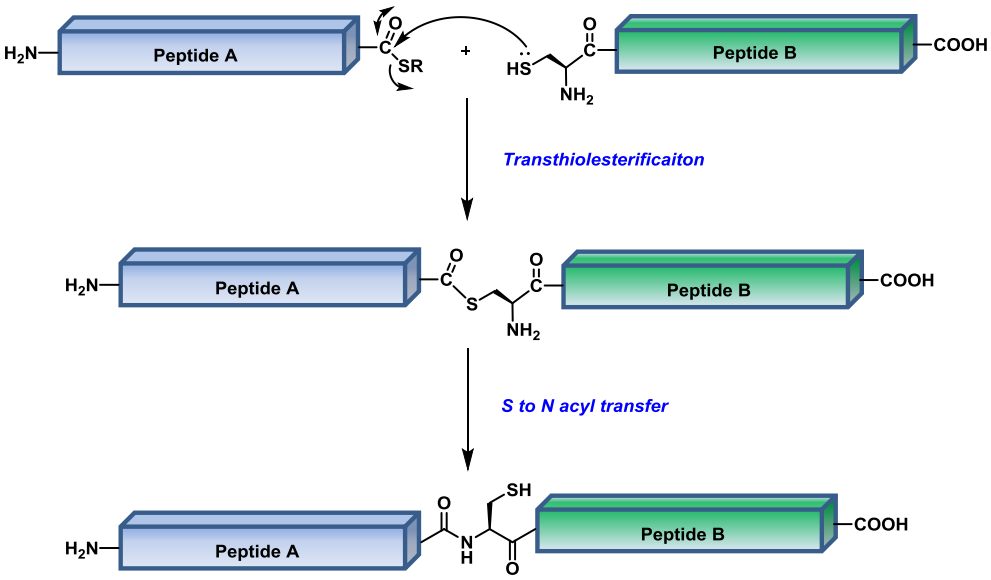

Figure 1.2 An efficient ligation method for the construction of synthetic polypeptides through native chemical ligation (NCL)[25].

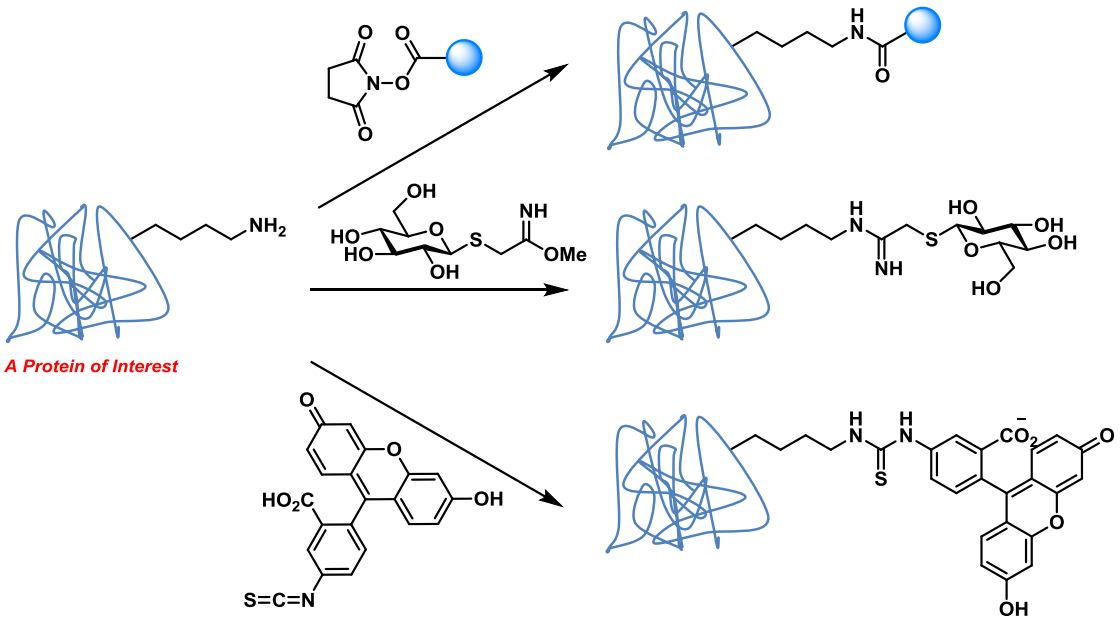

Figure 1.3 Chemical protein modifications through selective lysine modification with some designed electrophiles (NHS, NCS or IME)[2,4,26].

1.1.2 Chemical Protein Modifications of Unnatural Amino Acids

Whilst a protein labelling method involving lysine side-chains modification is simple and practical, it is limited by reaction selectivity. Owing to uncontrollable multiple-site labelling, these methods are difficult to apply to site-selective protein modification in biological conditions. To achieve site-selective protein conjugation, the concept of "Tag-and-Modify" approach can be employed to modify the protein of interest at pre-defined sites[10,11,19]. There are several genetic methods for incorporation of unnatural amino acids as protein tags by use of auxotrophic strains[27-31] or amber codon suppression technology[32-36]. Also, a chemical tag installed at pre-defined sites of proteins allows subsequent site-selective chemical protein modification. Within the field of chemical biology, there are various approaches which have been developed using novel concepts in chemistry and genetic engineering.

Chemical Modifications at Dehydroalanine

Dehydroalanine (Dha) is a synthetic precursor useful for the installation of a range of post-translational protein modifications (PTMs) including phosphorylation, glycosylation or methylation[10,11,37-40]. Dha is formed by treatment of a cysteine residue with an alkylating agent that can undergo elimination, including *O*-mesitylenesulfonyl hydroxylamine (MSH), 2,5-dibromohexanediamide (DBHDA) or 2,5-dibromovalerate. A "Tag-and-Modify" approach through the formation of Dha as a protein tag and its subsequent modification by nucleophilic attack has been developed and reported by Davis and co-workers (Figure **1.4**)[10,37,41]. For example, treatment of Np276-C61 expressed from *Nostoc punctiforme* with DBHDA gave a Dha-tagged protein which was subsequently glycosylated to afford Np276-GlcNAc61 (Scheme **1.2**)[11,41]. In a further study, this method enabled site-selective chemical phosphorylation of proteins, in particular of cAbLys and p38α, with both phosphorylated proteins retaining their protein function after modification[39,40]. Caddick and co-workers have used our alkylating agent (DBHDA) to intentionally form Dha onto green fluorescent protein (GFP), and surprisingly a cyclic sulfonium intermediate was detected by LC-MS analysis[42,43]. To confirm the existence of this intermediate, the stable cyclic sulfonium-formed GFP was treated with a nucleophilic thiol, and it clearly showed a corresponding thiolated product

as expected. Alternatively, Morrison and Webb have presented a method for the chemical formation of Dha onto peptides by use of 2,5-dibromovalerate as an alternative alkylating agent[23]. This reagent is able to form multiple Dha-sites on the peptide, and is also compatible with protein reactions.

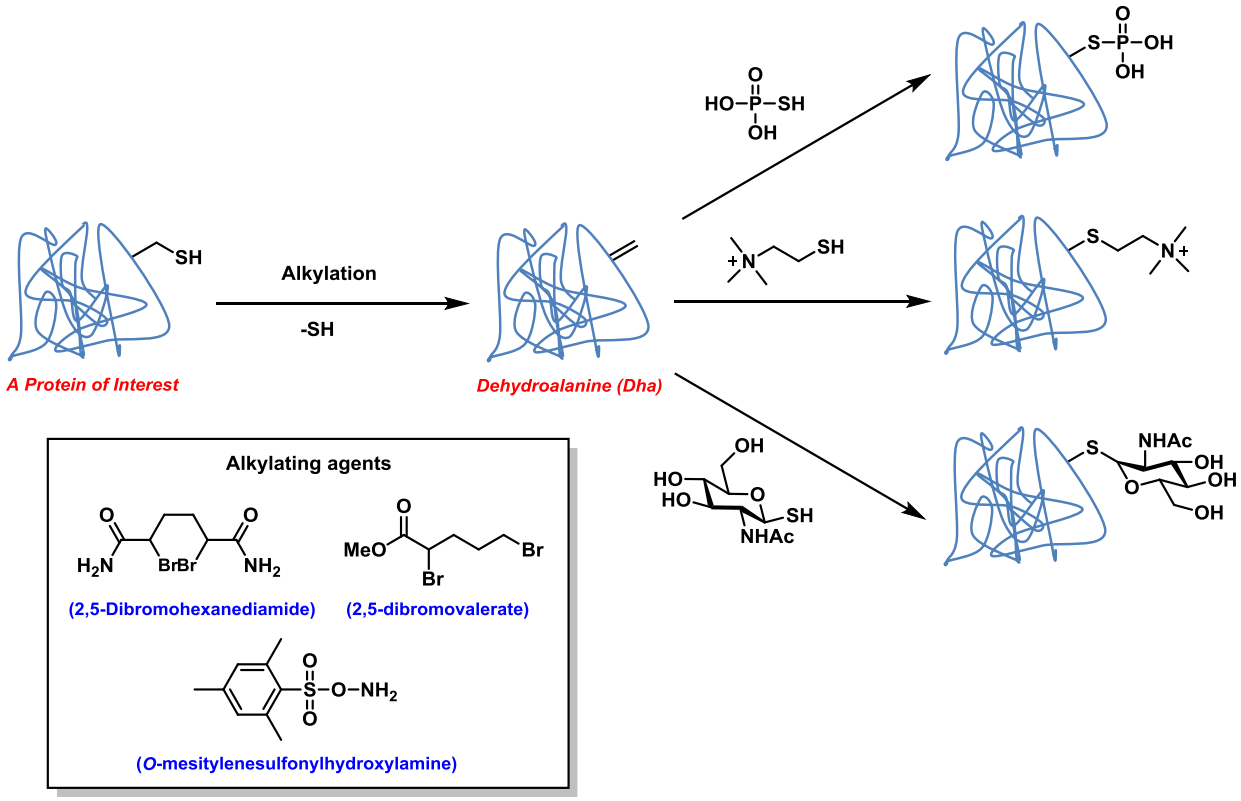

Figure 1.4 Chemical protein modifications through "Tag-and-Modify" approach using Dha as a protein tag[10,11,23,37].

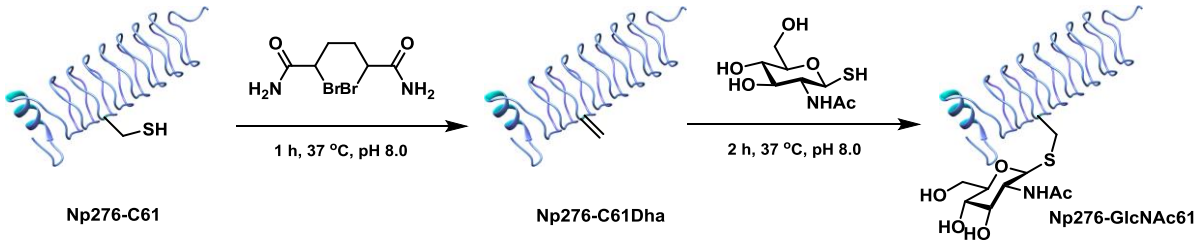

Scheme 1.2 Formation of Np276-GlcNAc61 through bis-alkylation elimination and subsequent glycosylation[11,41].

Chemical Modifications at Azido and Alkynyl Motifs

The Staudinger reaction, discovered by Hermann Staudinger, is a phosphine-mediated reduction in which an azide is converted into an amine via an iminophosphorane intermediate[44]. This method has been extensively applied for the chemical conjugation of

proteins in the field of chemical biology, especially as developed by the Bertozzi group[45-47]. The Staudinger ligation is widely used for a conjugation of an azide tag with a phosphine group, leading to the formation of an amide bond (Figure **1.5**)[47]. Alternatively, the original Staudinger ligation may be slightly modified by the use of a thioester electrophile instead of the ester group. This method, called the "traceless" Staudinger ligation, facilitates removal of the phosphine group and additionally prevents oxidation of the phosphine group during a protein reaction[46,48]. In recent years, the copper-catalysed azide-alkyne cycloaddition (CuAAC) reaction has become widespread in protein bioconjugation reactions due to the fact that the reaction proceeds efficiently and is compatible with aqueous systems[12,13,15,16]. A reaction of an azide-tagged protein with a terminal alkyne probe in the presence of Cu(I) catalyst/ligands affords 1,2,3-triazole products (Figure **1.6**). Applications of the CuAAC reactions are illustrated by many examples of site-specific protein labelling. However, such reactions exhibit a limitation with regards to labelling under biological conditions, possibly due to the toxicity of the Cu catalyst towards living cells[49]. This problem can be solved by use of strain-promoted azide-alkyne cycloaddition (SPAAC) reaction in which neither Cu catalyst or associated ligand are required[50]. The SPAAC reactions also lead to the formation of a 1,2,3-triazole product through a reaction between a highly strained cyclooctyne and an azide-incorporated protein. This SPAAC chemical conjugation method is compatible with protein labelling in biological environments including *in vitro, in cellulo* and *in vivo* conditions[15,50-52]. The reaction rate of SPAAC reactions can be significantly improved by use of modified cyclooctyne rings such as difluorinated cyclooctynes (DIFO) and dibenzocyclooctynes (DIBO)[53].

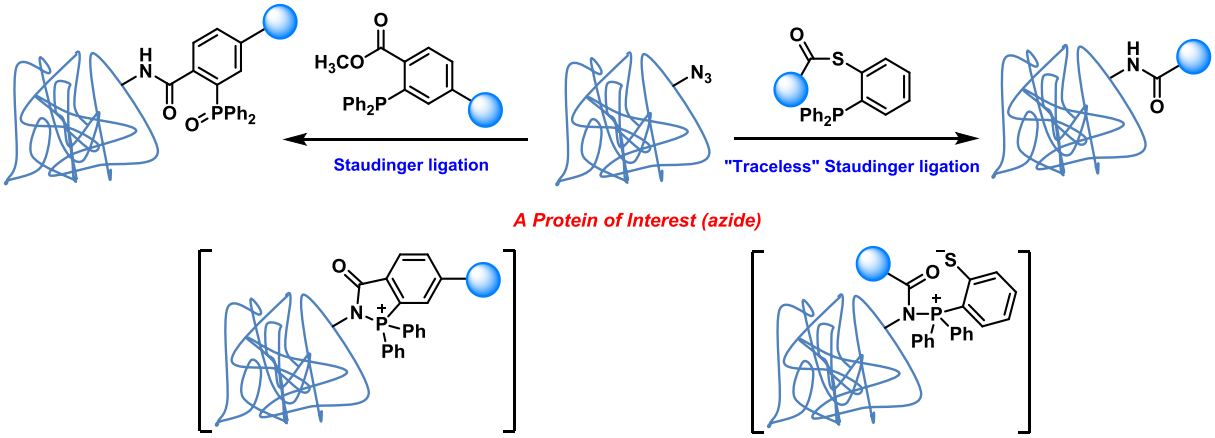

Figure 1.5 Chemical protein modification through either Staudinger ligation or "Traceless" Staudinger ligation[45-48].

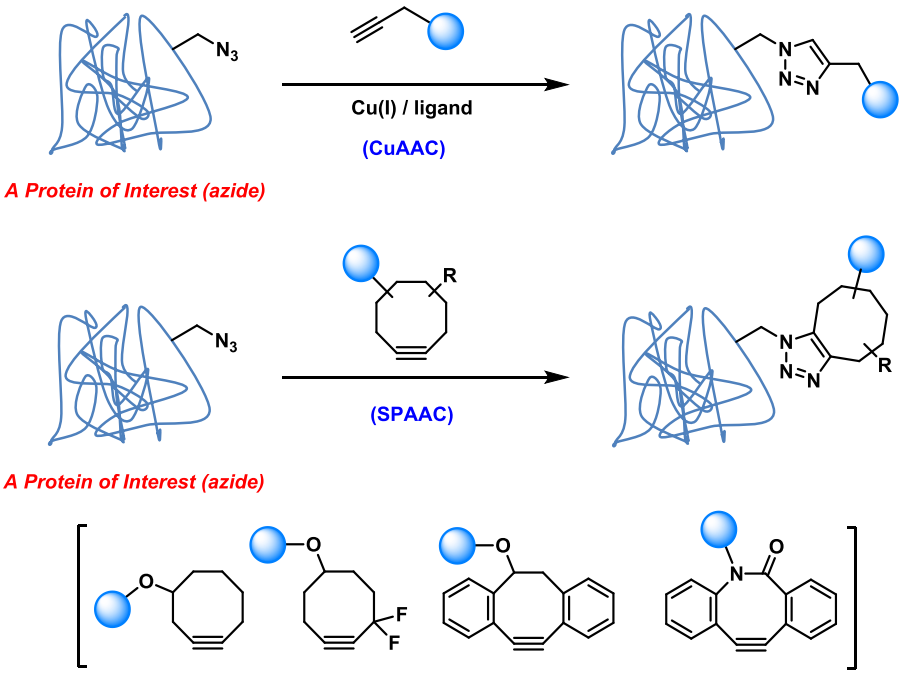

Figure 1.6 Chemical protein modification through either copper-catalysed azide-alkyne cycloaddition (CuAAC)[12,13,15,16] or strain-promoted azide-alkyne cycloaddition (SPAAC) reactions[15,50-53].

On the other hand, alkyne handles such as homoproparylglycine, alkynyl-pyrrolysine and cyclooctyne can also be biosynthetically incorporated into proteins using genetic approaches[33,54-56]. Alkynyl-tagged proteins can also react efficiently with azide moieties under either CuAAC or SPAAC reaction conditions (Figure **1.7**)[54,55].

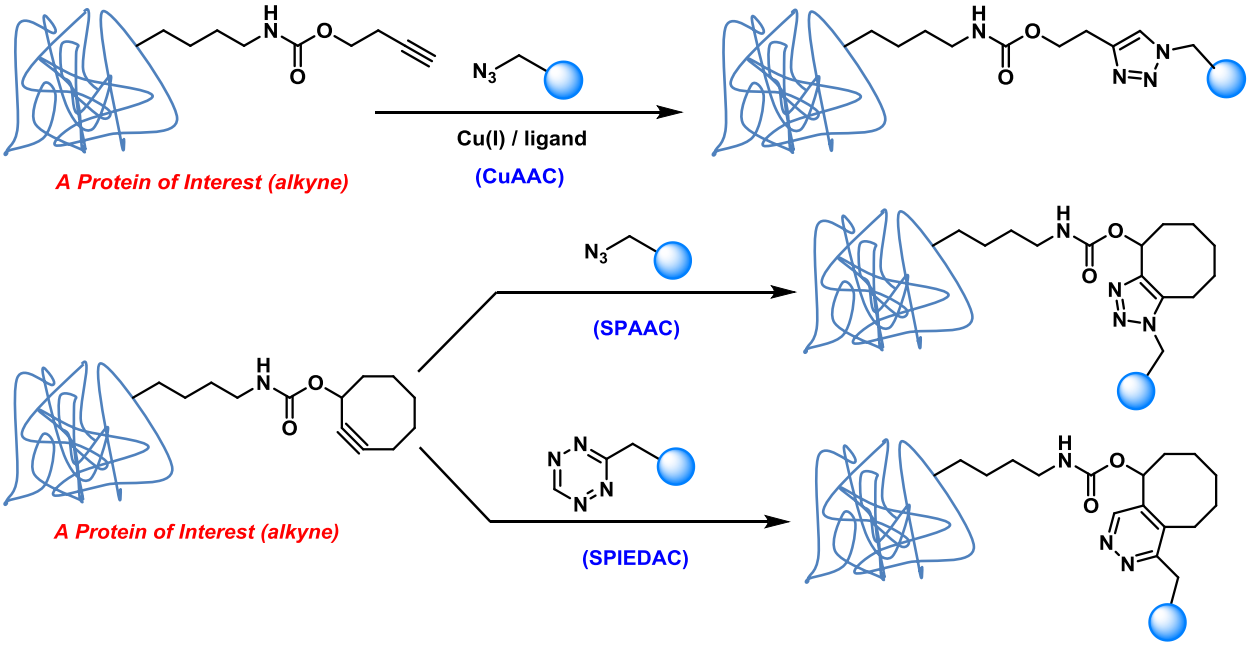

Figure 1.7 Chemical protein modification through either CuAAC or SPAAC/SPIEDAC reaction[54,55,57].

Chemical Modifications at Aldehydes and Ketones

A carbonyl handle, such as an aldehyde or ketone group, represents an alternative choice as a tag for subsequent site-specific chemical protein labelling. These resultant modified proteins can be site-selectively labelled via nucleophilic attack of specific amino functional groups of synthetic probes (Figure **1.8**)[58-60]. For example, Bertozzi reported the introduction of a short peptide bearing a formylglycine (FGly) moiety into recombinant proteins expressed in mammalian cells[60]. The FGly served as a unique aldehyde handle that could be chemically modified through reaction with an aminooxy fluorescent probe, leading to the formation of an oxime analogue (Figure **1.9**)[60].

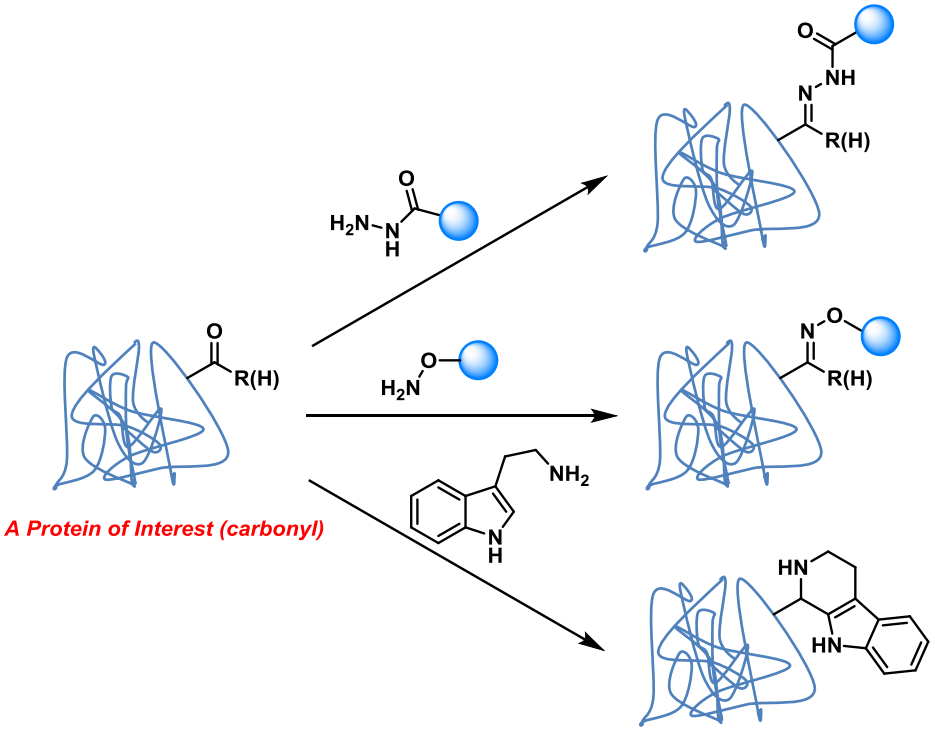

Figure 1.8 Chemical protein modification through reactions of nucleophilic amines with genetically carbonyl-encoded proteins[58-60].

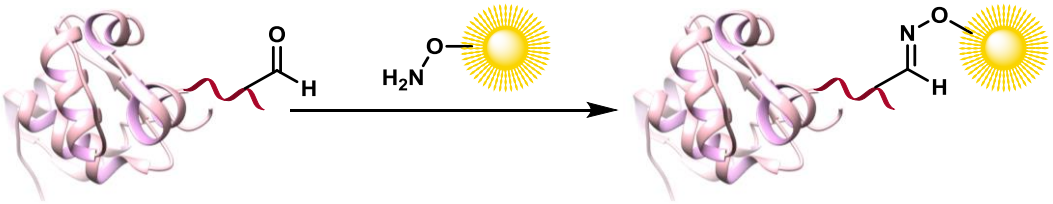

Figure 1.9 Site-selective protein labelling of the aldehyde-tagged recombinant protein with aminooxy fluorescent probe[60].

1.2 Protein Halogenation

1.2.1 Fluorination

Several strategies for an introduction of a fluorine atom into proteins have been developed and reported using either genetic incorporation or chemical protein fluorination methods[27,29,61]. Fluorinated proteins are incredibly useful for [^{19}F]-NMR studies of protein structure and conformational changes, as well as in the [^{18}F]-radiolabelling of proteins for preclinical animal studies using [^{18}F]-PET imaging[29,62-65].

Genetic Incorporation Methods for the Introduction of Fluorine

A simple method for the incorporation of fluorine into proteins has been reported using a specific auxotrophic strain which can recognise relevant fluorinated amino acids. Biosynthetic incorporation, known as selective pressure incorporation (SPI), usually involves the use of auxotrophic strain for the introduction of fluorine into proteins mostly expressed in *E. coli* via supplementation with synthetic fluorinated amino acids. Several fluorinated amino acids including aliphatic and aromatic residues have been successfully incorporated into proteins of interest (Figure **1.10**)[27,29,61]. For example, 4-fluorophenylalanine (4-FPhe) was globally incorporated into annexin V and azurin using selective pressure incorporation[66]. Budisa and co-workers also reported a set of monofluorinated phenylalanine, tyrosine and tryptophan analogues that was biosynthetically incorporated into *Candida antarctica* lipase B through the use of auxotrophic strains[28]. The disadvantages of this method include low incorporation efficiency and uncontrolled, global incorporation, possibly due to competitive incorporation between synthetic amino acids and natural amino acids for all compatible codons in the genome. As an alternative, residue-specific incorporation of non-canonical amino acids into proteins has been achieved by amber codon suppression technology as developed by the Schultz group[32,33,35,36]. This method involves the design of an orthogonal aminoacyl-tRNA synthetase/suppressor aminoacyl tRNA (aaRS/tRNA) pair; it is now widely used and can also enable higher levels of incorporation.

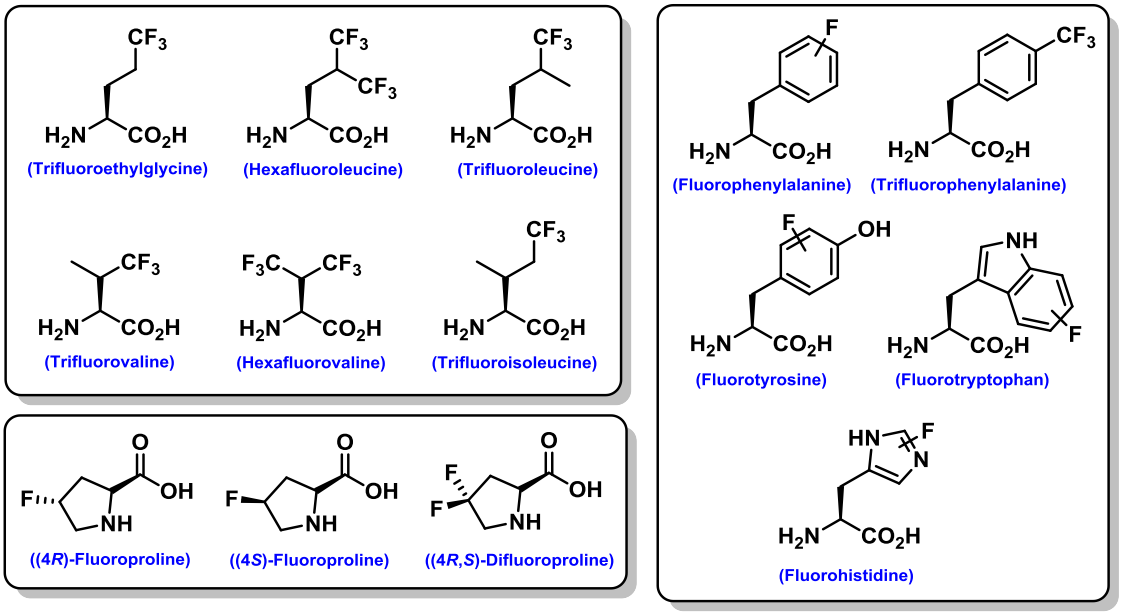

Figure 1.10 Genetic incorporation of fluorinated amino acid analogues into proteins[27-29,61,66,67].

Chemical Methods for Protein Fluorination

Several incorporation methods of fluorinated amino acids into proteins are based on SPI and amber codon suppression methods. Alternatively, chemical methods can also furnish proteins with synthetic fluorinated molecules through either nucleophilic attack or CuAAC reaction. For example, nucleophilic attack of a cysteine of the New Delhi metallo-β-lactamase (NDM-1) on an electrophilic fluorinating agent (trifluorobromo acetone, FBA) resulted in site-selective protein labelling[64]. This fluorinated NDM-1 was used in a study of ligand-metal binding using ^{19}F-NMR spectroscopy (Scheme **1.3**).

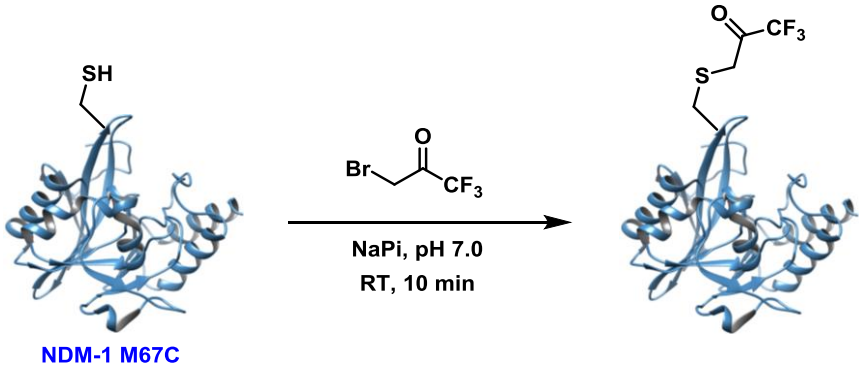

Scheme 1.3 Site-selective fluorine labelling of the NDM-1 through a reaction of the cysteine with FBA[64].

Furthermore, the common protein labelling technique of lysine side-chains can be applied to protein fluorination. For example, [^{18}F]-Radiolabelling of Avastin (Bevacizumab) as a human IgG antibody was performed by multiple labelling of lysine residues with *N*-succinimidyl 4-[^{18}F]fluorobenzoate ([^{18}F]SFB), shown in Scheme **1.4**[62,65]. This resulted in the formation of [^{18}F]-radiolabelled Avastin which was analysed by radio-HPLC to confirm its high radiochemical purity of 95%.

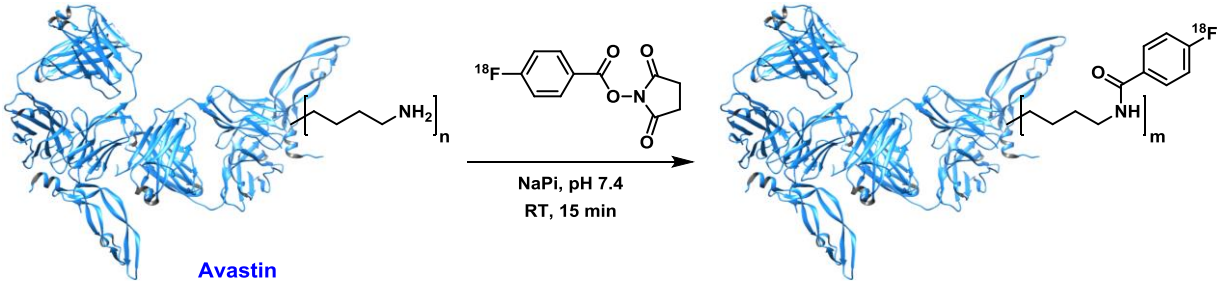

Scheme 1.4 [^{18}F]-radiolabelling of Avastin with [^{18}F]-SFB as an [^{18}F]-radiolabelled agent[65].

Many site-selective protein labelling strategies have become popular for protein fluorination reactions. Davis and co-workers reported a chemical method of site-specific chemical protein fluorination by reactions of an alkynyl-tagged protein with fluoroglucosyl azides through Cu(I)-catalysed 1,3-cycloaddition reaction (Scheme **1.5**)[68]. Also, our "Tag-and-Modify" approach enabled chemical incorporation of a fluoroglycosyl thiol as well as [^{18}F]-radiolabelling of proteins. SBL-S156C as a model protein was treated with MSH to form Dha as a protein tag, and subsequently attacked by a thiofluoroglycoside at a pre-defined Dha site (Scheme **1.6**)[69]. The advantage of the chemical methods lies with the ease of their application to the [^{18}F]-radiolabelling of proteins; biosynthetic incorporation methods, on the other hand, are limited in this regard, in part due to the half-life of the [^{18}F]-radiotracer (~110 min).

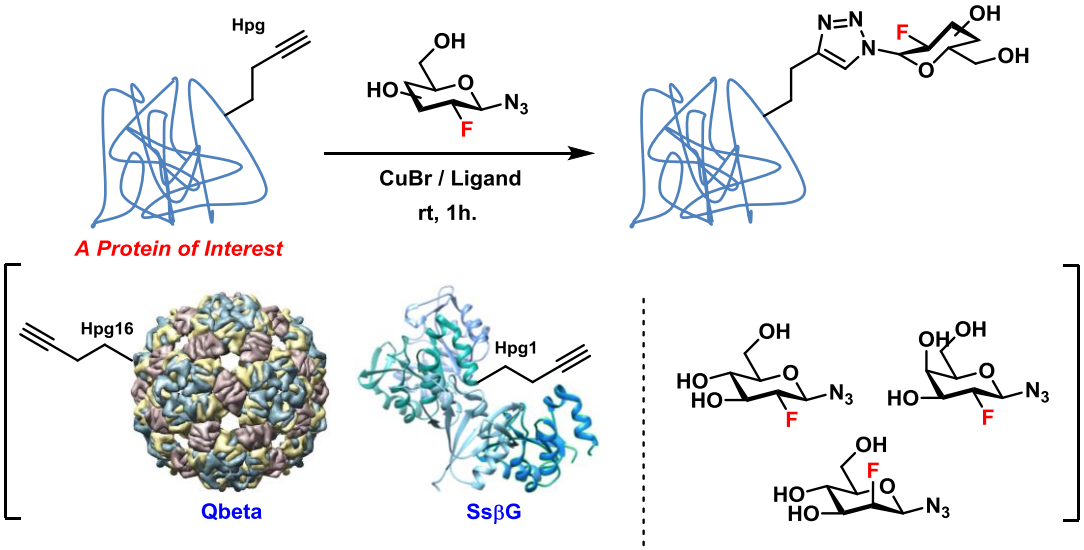

Scheme 1.5 Site-specific chemical installation of fluorosugars into proteins (Qbeta and SsβG) through CuAAC reactions[68].

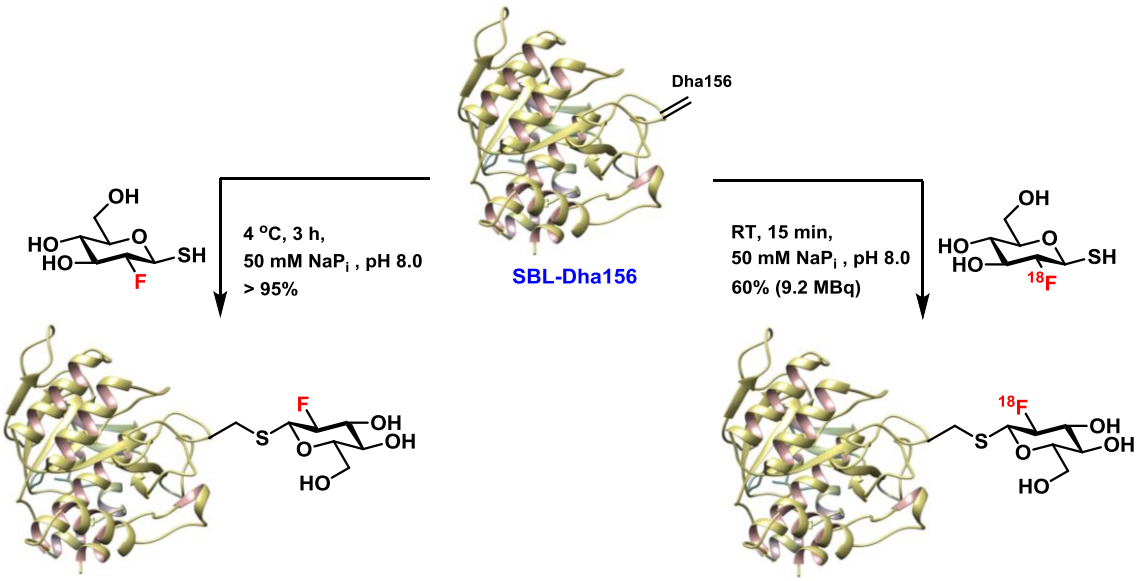

Scheme 1.6 Either [^{19}F]-substitution or [^{18}F]-radiolabelling of the SBL-156Dha through "Tag-and-Modify" approach[10,69].

1.2.2 Chlorination

Genetic Incorporation Methods for the Introduction of Chlorine

There are few reports of biosynthetic incorporation of chlorinated amino acids into proteins; however, chlorine substitution onto proteins is still attractive to extend the functionality of proteins. Some chlorinated aliphatic amino acid analogues including

chlorinated valine and leucine residues were successfully incorporated into *E. coli* peptidyl-Pro *cis-trans* isomerase B (PpiB) by cell-free protein synthesis methods[70]. On the other hand, no incorporation of chlorinated isoleucine analogues into PpiB was observed by protein mass spectrometry analysis. Some non-canonical aromatic amino acid derivatives containing chlorine atoms can be also incorporated into proteins by use of either SPI or UAG stop-codon suppression. Residue-specific incorporation of 4-chlorophenylalanine (4-ClPhe) into luciferase showed a replacement of the natural phenylalanine with its chlorinated analogue through association with a phenylalanyl-tRNA synthetase mutant (A294G PheRS)[71]. Similarly, 3-chlorotyrosine (3-ClTyr) was biosynthetically incorporated into either green fluorescent protein (GFP) or highly stable green fluorescent protein (GFPHS) by use of *E. coli* tyrosine-auxotrophic cells (JW2581)[72]. Also, an efficient incorporation of 6-chlorotryptophan (6-ClTrp) into recombinant proteins was demonstrated using *Lactococcus lactis* Trp auxotrophic cells via co-expression of a tryptophanyl-tRNA synthetase (TrpRS) of *L. lactis*[30].

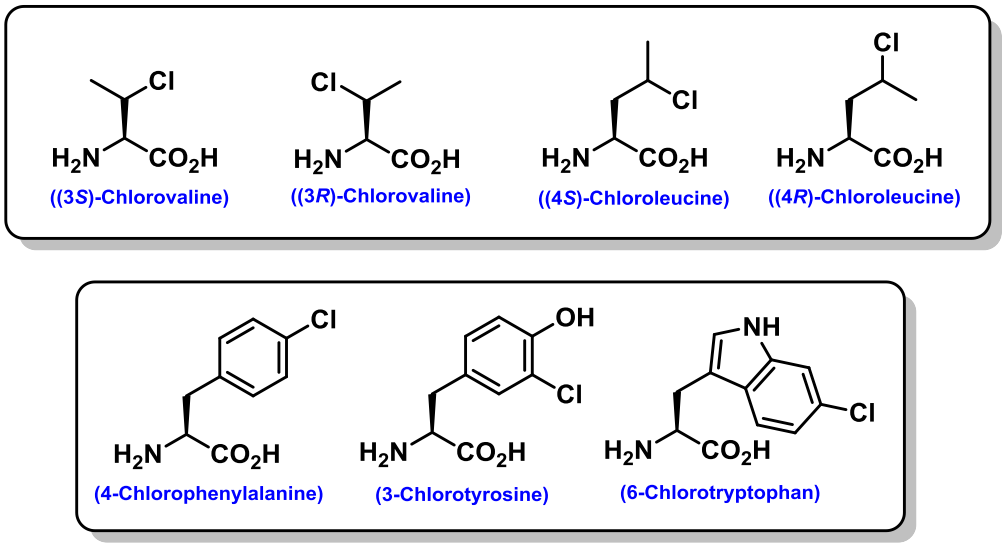

Figure 1.11 Genetic incorporation of chlorinated amino acid analogues into proteins[30,70-72].

Chemical Methods for Protein Chlorination

There are also few studies of either enzymatic or direct chemical methods for protein chlorination. One such report, by Kettle and co-workers, used a system of myeloperoxidase / human neutrophils with a combination of both hydrogen peroxide

(H_2O_2) and chloride (Cl^-), generating a hypochlorous acid (HOCl)[73]. This chlorinating agent directly reacted with tyrosine residues of a short model peptide, Gly-Gly-Tyr-Arg. This reaction proceeded via the formation of a chloramine (generated through reaction of an amino group with HOCl) and subsequent tyrosine chlorination. Also, Dean and co-workers used HOCl to investigate a chlorination reaction of tyrosine residues in the presence of a mixture of tyrosine amino acids (free) and proteins (bovine serum albumin, BSA and low density lipoprotein)[74]. 3,5-dichlorotyrosine residues were detected, derived from both BSA and lipoproteins. However, the HOCl reagent as a strong oxidising agent, would be difficult to apply to protein chlorination under mild conditions.

1.2.3 Bromination

Genetic Incorporation Methods for the Introduction of Bromine

Several strategies have been developed for the biosynthetic incorporation of non-canonical aromatic amino acid analogues with bromo substituents into proteins. These brominated proteins can be useful as coupling partners for palladium-mediated cross-coupling reactions. Via a similar strategy to that adopted for the aforementioned 4-ClPhe, site-specific incorporation of the *p*-bromophenylalanine residue (4-BrPhe) into luciferase was achieved by using a nonsense suppressor of the phenylalanyl-tRNA synthetase (A294G PheRS)[71]. Alternatively, incorporation of 4-BrPhe into dihydrofolate reductase (DHFR) was demonstrated through an expression system involving a phenylalanyl-tRNA synthetase (PheRS) and *E. coli* phenylalanine auxotroph[75]. Also, 3-bromotyrosine (3-BrTyr) residues were site-specifically introduced into glutathione *S*-transferase (GST) using an engineered codon translation machinery (a tyrosine aaRS/tRNA pair from *Methanocaldococus jannaschii*)[76]. In a study of the structural stability of GST, a significant stability enhancement was found upon multiple-site incorporation of bulky halogenated groups, due to their occupancy of an internal space and induction of stabilising interaction between non-canonical and neighbouring amino acid residues. Bromotryptophan analogues (5-BrTrp/6-BrTrp) could be site-specifically incorporated into bacterial proteins with fidelity through the use of either *L. lactis* Trp auxotrophic cells or amber codon suppression (yeast phenylalanyl-tRNA synthetase (yPheRS (T415G))/amber suppressor tRNA ($ytRNA^{Phe}_{CUA\_UG}$))[30,77].

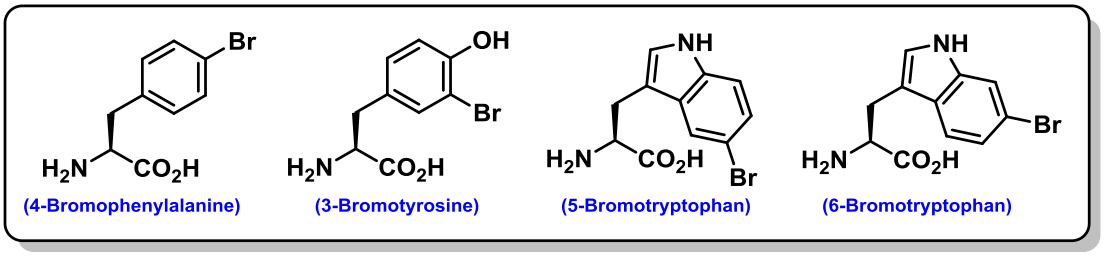

Figure 1.12 Genetic incorporation of brominated aromatic amino acid analogues into proteins[30,75-78].

Chemical Methods for Protein Bromination

There are not many reports of direct chemical methods for protein bromination. Wu and Hazen investigated an enzymatic system for a study of oxidative tissue damage *in vivo* through aromatic bromination of protein tyrosine residues using either eosinophil peroxidase (EPO) or myeloperoxidase (MPO) and a reactive brominating species ($HOBr/OBr^-$)[79]. It was found that EPO-catalysed bromination system was effective under physiological conditions of halides and H_2O_2. A mixture of brominated products (3-bromotyrosine and 3,5-dibromotyrosine) derived from EPO-induced protein oxidation served as biomarkers for indication of tissue injury *in vivo*. Furthermore, Kato and Osawa reported a chemical method for the installation of bromotyrosine residues on bovine serum albumin (BSA) and other immunogens using *N*-bromosuccinimide (NBS) as a brominating agent[80].

1.2.4 Iodination

Genetic Incorporation Methods for the Introduction of Iodine

Protein iodination is a useful method for the installation of "tags" for further chemical protein modification as well as to facilitate protein structure determination using X-ray crystallography. Iodinated proteins can be a good candidate for subsequent C-C bond formation through palladium-mediated cross-coupling reactions. Schultz reported the site-specific introduction of *p*-iodo-L-phenylalanine (4-IPhe) into bacteriophage T4 lysozyme using a tyrosine aaRS/tRNA pair from *M. jannaschii*[81]. This method is able to selectively introduce heavy iodine atoms into proteins without a perturbation of the original protein structure, sometimes needed to solve the phasing problem in protein

crystallography. By a similar procedure, 3-iodo-L-tyrosine (3-ITyr) was also site-specifically incorporated into proteins in mammalian cells using an amber suppressor *Bacillus stearothermophilus* TyrRS and $tRNA^{Tyr}$ pair[82]. A combination of engineering a designed *E.coli* tyrosyl-tRNA synthetase (V37C195) and an amber suppressor $tRNA^{Tyr}$ could allow site-specific incorporation of the 3-ITyr into proteins in eukaryotic translation systems[83].

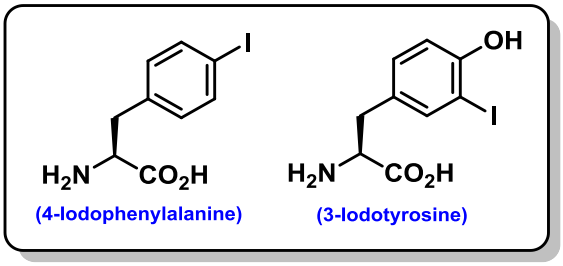

Figure 1.13 Genetic incorporation of iodinated aromatic amino acid analogues into proteins[81-83].

Chemical Methods for Protein Iodination

Biosynthetic incorporation methods of iodinated aromatic amino acids into proteins by use of bioengineering technology have been previously described. A few reports show chemical methods for protein iodination through either direct electrophilic aromatic substitution (S_EAr) or indirect protein iodination. For example, *bis*(pyridine)iodinium (I) tetrafluoroborate (IPy_2BF_4) as a mild iodinating agent can react with tyrosine residues existing in peptides or proteins[84]. Direct iodination of proteins through S_EAr was demonstrated by treatment of model proteins (insulin, lysozyme, and 1,3-1,4-*β*-D-4-gluconohydrolase) with IPy_2BF_4 in an aqueous media[84]. Multiple-site labelling of tyrosine residues was confirmed by both MALDI-TOF and MSMS analysis. The advantages of this method are its fast, direct, site-selective protein iodination and its biocompatibility. Alternatively, a method for indirect protein iodination through CuAAC reaction has been described, in which a reaction between Hpg-tagged protein and 2-azido-5-iodobenzoic acid in the presence of Cu(II) catalyst (Scheme **1.7**) affords a 1,2,3-triazole ring with iodinated substituents[85].

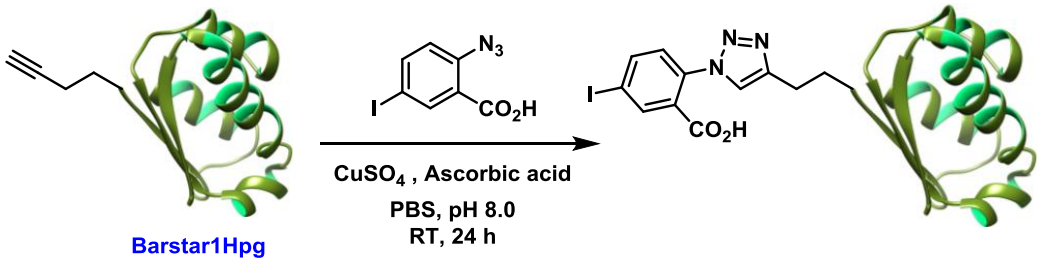

Scheme 1.7 Indirect chemical method for protein iodination through CuAAC reaction[85].

Furthermore, [^{125}I] or [^{131}I] radioisotopes are often used in protein radiolabelling, and the resultant [^{125}I] / [^{131}I]-labelled protein can be used for an investigation of biodistribution in preclinical animal studies. For example, [^{125}I]-radiolabelling of three protein hormones (including human growth hormone (HGH), thyroid-stimulating hormone (TSH), and human luteinising hormone (LH)) was achieved by treatment with a combination of *N*-hydroxysuccinimidyl-3-(4-hydroxyphenyl)propionate (known as the Bolton-Hunter reagent), Na^{125}I, and chloramine-T as an oxidising agent[86]. This reaction occurred via nucleophilic attack of lysine residues, leading to the formation of covalent amide bonds. Aside from the Bolton-Hunter reagent, Iodogen® (1,3,4,6-tetrachloro-3α,6α-diphenylglycoluril) acts as an oxidising agent and is widely used for radioiodination of proteins[87]. This reagent can potentially generate a reactive iodine species from oxidation of Na^{125}I source. The application of the Iodogen® for protein [^{125}I]-radiolabelling was first reported by Fraker and Speck[88]. For example, tyrosine residues of fibrinogen and urokinase were labelled by use of a combination of Iodogen® and ^{125}I, leading to high labelling efficiency and minimal disruption of the protein function[89].

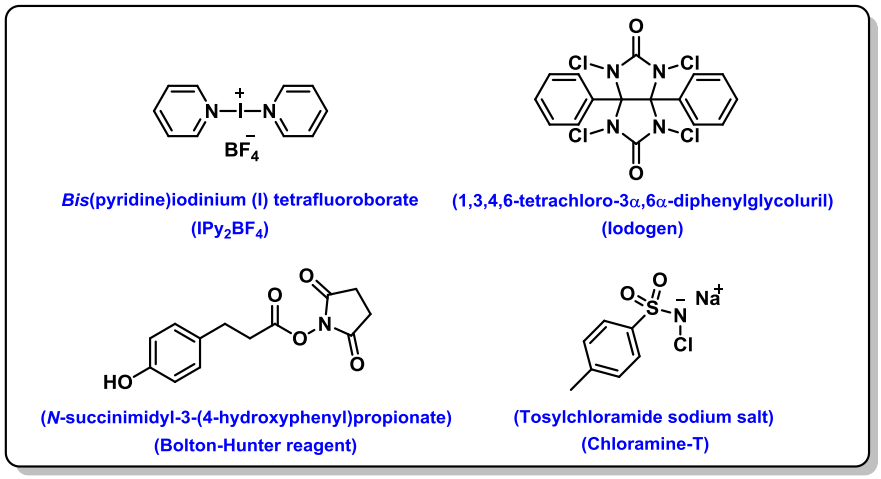

Figure 1.14 Structures of IPy_2BF_4, Iodogen®, Bolton-Hunter reagent, and chloramine-T, respectively[84,86-89].

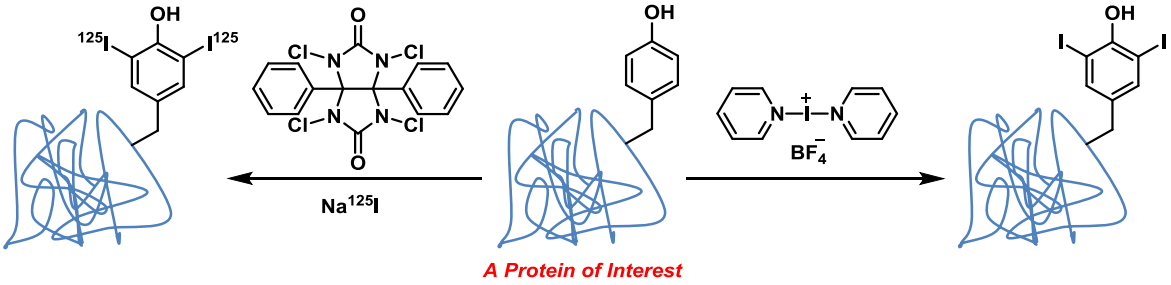

Figure 1.15 Direct iodination of proteins by use of IPy_2BF_4 or a combination of Iodogen® and $Na^{125}I$[84,87-89].

1.3 Palladium-Mediated Reactions of Proteins

Recent advances in transition metal-catalysed reactions in the field of chemical biology have been demonstrated and are widely used for chemical protein modification[90,91] such as Cu-catalysed reaction (CuAAC)[12,13,15,16,57], Pd-mediated reactions (Suzuki-Miyaura[20,92-94], Sonogashira[95-98] or Heck[99,100]), Rh-mediated reactions[101,102], and Ru-catalysed reactions (Olefin cross metathesis)[103,104]. In this chapter, we mainly focus on Pd-catalysed cross-coupling reactions, which are suitable to site-specifically modify proteins in aqueous systems. For example, a protein containing a genetically encoded 4-IPhe can undergo site-specific cross-coupling to a variety of boronic acid substrates, leading to extended protein functionality via C-C bond formation[92-94].

1.3.1 Suzuki-Miyaura Cross-Coupling Reaction

The Suzuki-Miyaura cross-coupling reaction, discovered by Akira Suzuki, is widely used in organic synthesis, particularly in C-C bond formation[105,106]. The reaction proceeds through a coupling of an organoboron compound to either a vinyl or an aryl halide in the presence of palladium catalyst and base[105-107]. The mechanism of the Suzuki-Miyaura reaction proceeds via sequential oxidative addition, transmetallation and reductive elimination stages (Figure **1.16**)[107]. The oxidative addition of R'X to Pd (0) forms an organopalladium intermediate, which is followed by transmetallation of a boron-ate complex (R = aryl, vinyl or alkyl) with palladium, giving a second organopalladium species. Subsequent reductive elimination generates Pd(0) from Pd(II), forming a new C-C bond (R-R') and turning over the catalytic cycle.

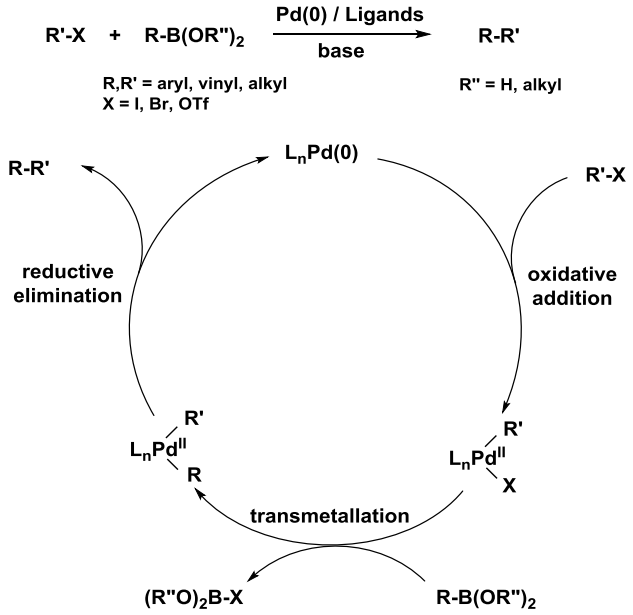

Figure 1.16 Mechanism of Suzuki-Miyaura Cross-Coupling Reaction[105-107].

An initial study of Suzuki-Miyaura cross-couplings of proteins proceeded from the investigation of the coupling of a 4-IPhe-incorporated WW domain peptide of the Pin1 protein to a series of phenylboronic acids, in the presence of disodium tetrachloropalladate (Na_2PdCl_4)[108]. This method was able to catalyse the formation of C-C coupling products with excellent yields, quantified by HPLC and MALDI-TOF analysis. A further study of the Pd-mediated Suzuki reaction on proteins was demonstrated by residue specific incorporation of *p*-boronophenylalanine (4-BPhe) into T4 lysozyme, and subsequent treatment of the modified T4 lysozyme with a fluorescent aryl iodide and $Pd_2(dba)_3$[109]. Unfortunately, this method gave a low coupling protein yield and was unsuitable for most protein substrates, due to the harsh and denaturing conditions required (high temperature (70 °C) and long reaction times (15 h). Various water-soluble phosphine ligands such as TPPMS, TPPTS, and TXPTS have been suitable for aqueous Pd cross-couplings of small molecules, but these ligands are highly expensive and require an inert atmosphere[110]. We have previously reported a new Pd catalyst system containing a simple ligand (2-amino-4,6-dihydroxypyrimidine, ADHP = **L1**), which has since been widely used in aqueous Pd-mediated reactions of proteins[20]. This Pd catalyst is highly soluble in aqueous systems, is air-stable, and does not require phosphine ligands. Chalker and Davis demonstrated aqueous Suzuki-Miyaura cross-couplings using a *Bacillus lentus* subtilisin (SBL) variant as a model protein[20]. To start

with, the SBL variant (SBL-C156) was treated with *p*-iodobenzyl bromide, leading to the formation of a 4-iodobenzyl residues as a chemical protein tag. The iodobenzyl SBL was subsequently tested for Pd cross-coupling reactions with a series of boronic acids in the presence of the water-soluble Pd catalyst (Scheme **1.8**). These reactions proceeded under mild conditions (37 °C, pH 8.0) that could also be applied to other protein substrates[92-94,111].

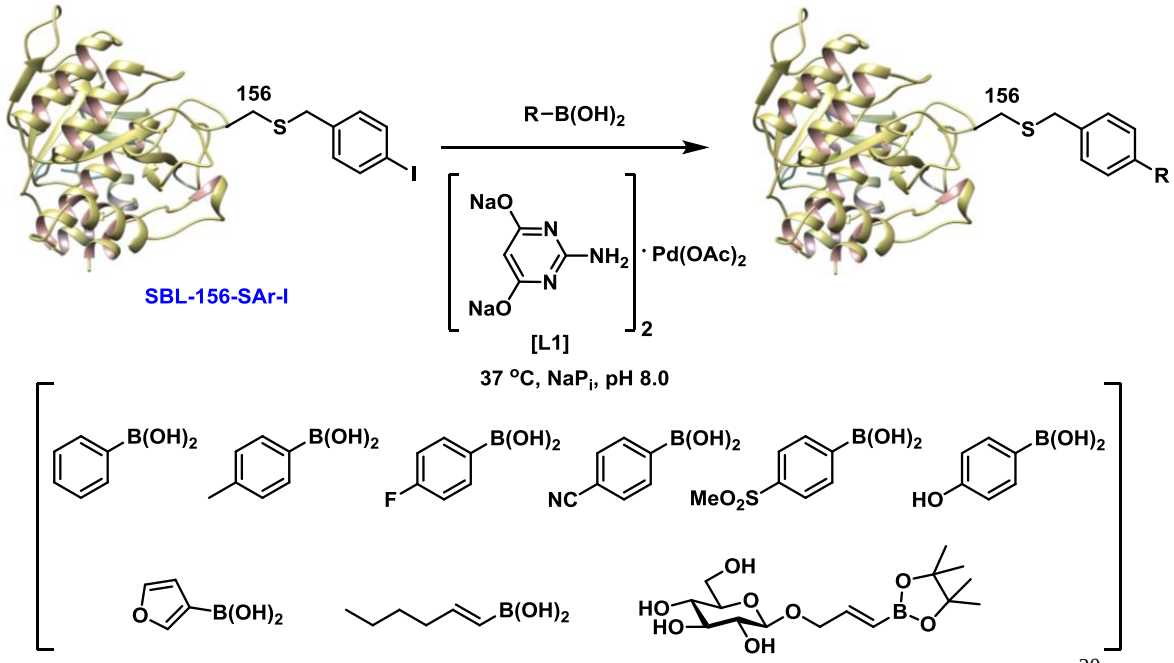

Scheme 1.8 Suzuki-Miyaura cross-coupling of the iodoaryl SBL with R-$B(OH)_2$[20].

To extend the capabilities of this aqueous Pd-catalysed system, Spicer and Davis reported an efficient system for site-selective Suzuki-Miyaura cross-couplings of furan-3-boronic acid to a moltaose binding protein (MBP) mutant containing a genetically encoded 4-IPhe residue, in the presence of $[\mathbf{L1}]_2Pd(OAc)_2$[93]. After 2 h reaction time, full conversion to the C-C coupled protein product was observed by LC-MS analysis. Also, 3-mercaptopropionic acid was discovered to be an efficient Pd scavenger, causing a significant improvement in LC-MS signal as compared to untreated protein samples, and thus facilitating analysis. Furthermore, this Pd catalyst with ADHP ligands was used to facilitate C-C bond formation between the 4-IPhe-encoded Z-domain protein and a fluorescent dye, 3-(dansylamino)phenylboronic acid[112]. The formation of the fluorescent cross-coupled protein was confirmed by LC-MS, and a protein band on SDS-PAGE was clearly visualised under UV light (365 nm) to give a bright yellow fluorescent signal.

Davis and co-workers have also reported site-selective protein PEGylation through Pd-catalysed reactions[92]. A study of the Pd-catalysed C-C bond formation onto a model iodinated amino acid (*N*HBoc-4-iodophenylalaine, Boc-*p*-IPhe) with monomethoxy PEG phenylboronic acids (including 2kDa and 20kDa) was initially investigated by use of Pd catalysts bearing various pyrimidine or guanidine ligands (**L1-L4**)[92]. Formation of C-C coupling products (with good to excellent yields, 68-93%) containing either a shorter or longer PEG linkage was monitored by ^{1}H-NMR and MS spectrometry, indicating high efficiency of either pyrimidine or guanidine-based Pd catalysts. Optimised reaction conditions were further applied to an investigation of Pd-catalysed Suzuki-Miyaura PEGylation reactions of proteins[92]. Both chemically/genetically iodinated Np276 and SBL proteins were partially coupled to the mPEG2k phenylboronic acid, as observed by SDS-PAGE, MALDI-TOF and MSMS analysis, giving PEGlyated proteins with a good level of product conversion (up to 70%) (Scheme **1.9**).

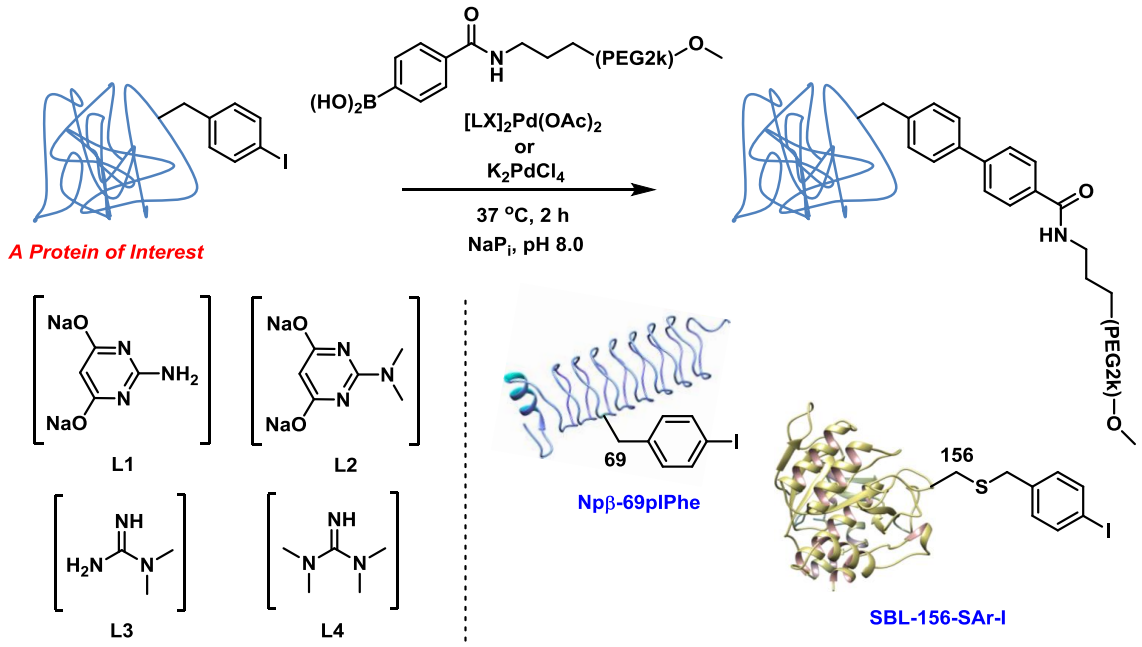

Scheme 1.9 Site-specific Pd-mediated Suzuki-Miyaura PEGylation of model proteins using Pd catalysts with various pyrimidine and guanidine ligands[92].

Spicer and Davis further investigated the application of our Pd catalyst to biological systems through Pd-mediated cell-surface labelling of *E.coli* outer membrane protein C (OmpC)[94]. Fluorescent signals of fluorescein-coupled OmpC could be clearly detected on the outer membrane of *E.coli* bacterial surface via confocal laser scanning microscopy. Also, a flow cytometry-based study of cell viability to palladium toxicity was performed

after treatment of cells with trypan blue. It was found that Pd catalyst used at high concentrations (2000 µM) showed no significant level of Pd toxicity towards cells.

1.3.2 Sonogashira Cross-Coupling Reaction

The Sonogashira cross-coupling reaction, discovered by Kenkichi Sonogashira, is important and is widely used in organic synthesis[113-115]. The Pd-mediated reaction through Sonogashira cross-coupling also facilitates the formation of C-C bonds through a coupling between a terminal alkyne and an aryl/vinyl halide under mild conditions[113-115]. In terms of its mechanism, the Sonogashira reaction is similar to the Pd-catalysed Suzuki-Miyaura cycle but incorporates an additional catalytic cycle of the copper catalyst , required for substrate activation (Figure **1.17**)[113,114].

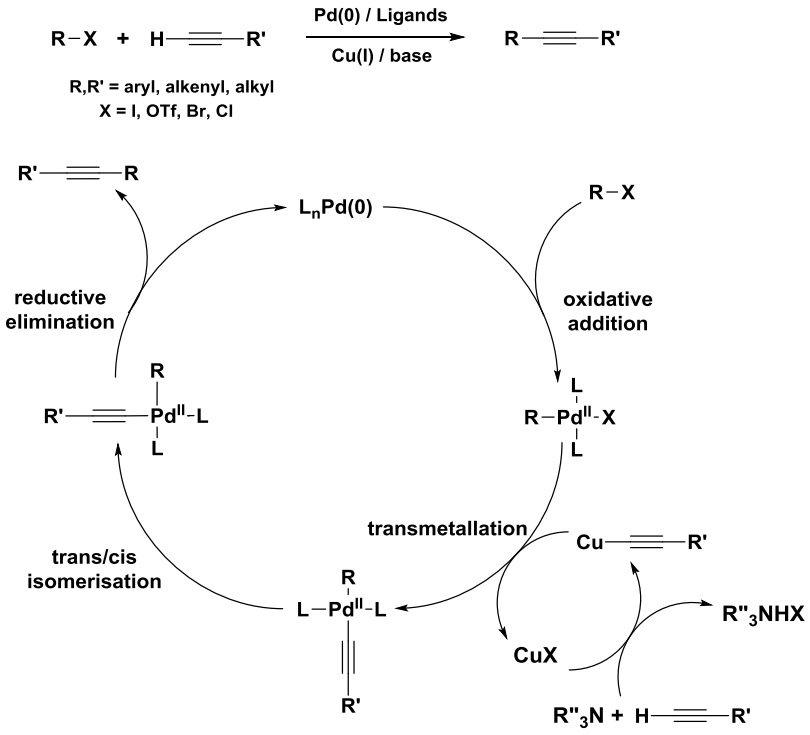

Figure 1.17 Mechanism of Sonogashira Cross-Coupling Reaction[113,114].

Pd-catalysed protein modification based on Sonogashira reactions was first reported by Kodama et.al[116]. This method proceeded via site-specific incorporation of a 4-IPhe residue into Ras protein through amber codon suppression. The iodinated Ras protein was subsequently coupled to a biotinylated alkyne in the presence of a combination of

$Pd(OAc)_2$, TPPTS, and CuOTf, leading to site-specific biotinylation of the Ras protein[116]. The presence of biotinylated protein was confirmed by western blot and MS spectrometry analysis including LC-MS and MSMS. In a similar vein, the Davis water-soluble Pd catalyst has been widely used not only in Suzuki cross-couplings, but also in Sonogashira reactions. Lin and co-workers reported copper-free Sonogashira reactions for protein functionalisation by treatment of ubiquitin containing a genetically incorporated alkyne with a broad range of functionalised aromatic iodide substrates in the presence of a water-soluble Pd catalyst[97]. A further example of Sonogashira cross-coupling between *para*-iodophenyl dihydrofolate reductase (eDHFR) and 5-ethylnyl fluorescein, by use of the $Pd(OAc)_2(ADHP)_2$ catalyst, was reported by Wombacher et.al[95]. This work presented a two-step protein labelling approach involving enzyme-mediated peptide labelling and palladium-mediated Sonogashira cross-coupling, leading to site-specific C-C bond installation of the fluorescent probe. Chen and co-workers reported a method of Pd-catalysed Sonogashira cross-coupling for site-specific protein labelling inside *E.coli* bacterial cells by treatment of either an alkyne-incorporated GFP or OspF with an iodophenyl fluorescent probe (Iphe-FL525) in the presence of $Pd(NO_3)_2$ catalyst (Figure **1.18**)[96].

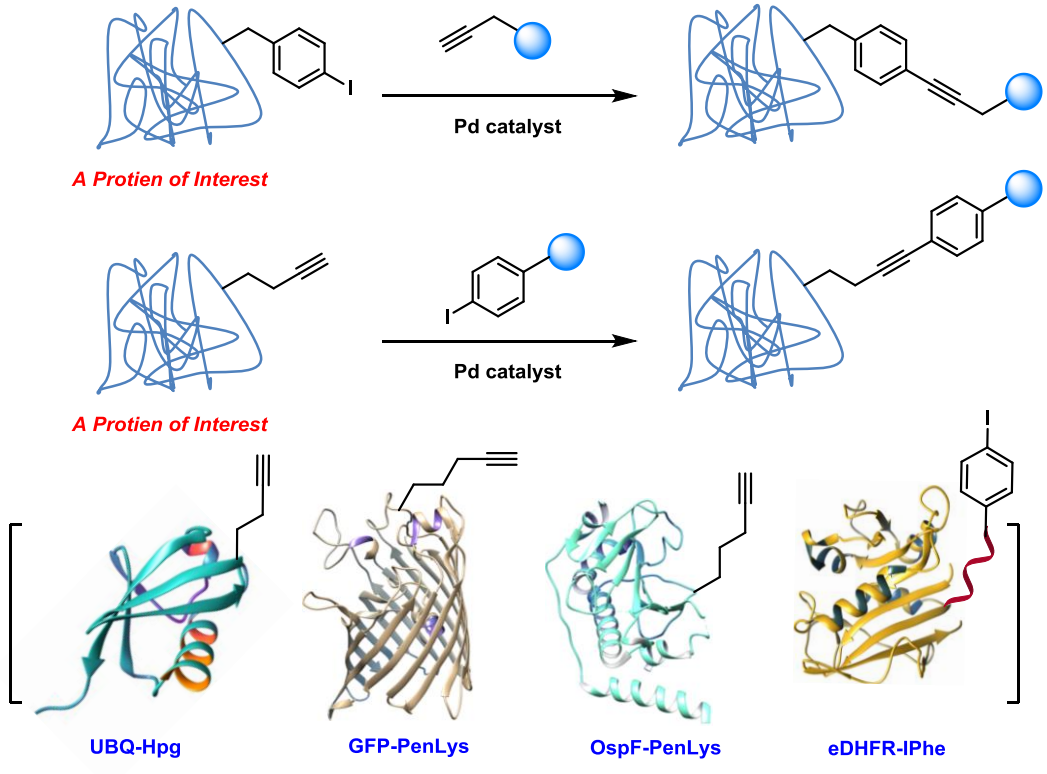

Figure 1.18 Chemical protein modification through Sonogashira cross-coupling reactions[95-97].

1.3.3 Heck Cross-Coupling Reaction

The Heck cross-coupling reaction is also crucial for the formation of C-C bonds from the reaction of an aryl/vinyl halide and an olefin in the presence of Pd catalyst and base[117-119]. The palladium catalytic cycle of the Heck cross-coupling reaction proceeds via sequential oxidative addition, syn-addition, β-hydride elimination and reductive elimination stages (Figure **1.19**)[107,117]. The oxidative addition of R'X to Pd (0) forms an organopalladium intermediate followed by insertion of an activated alkene with palladium, giving an organopalladium species. Subsequent β-hydride elimination then generates a new C-C bond. The Pd(0) catalyst is finally regenerated by reaction of the resultant palladium complex with a base.

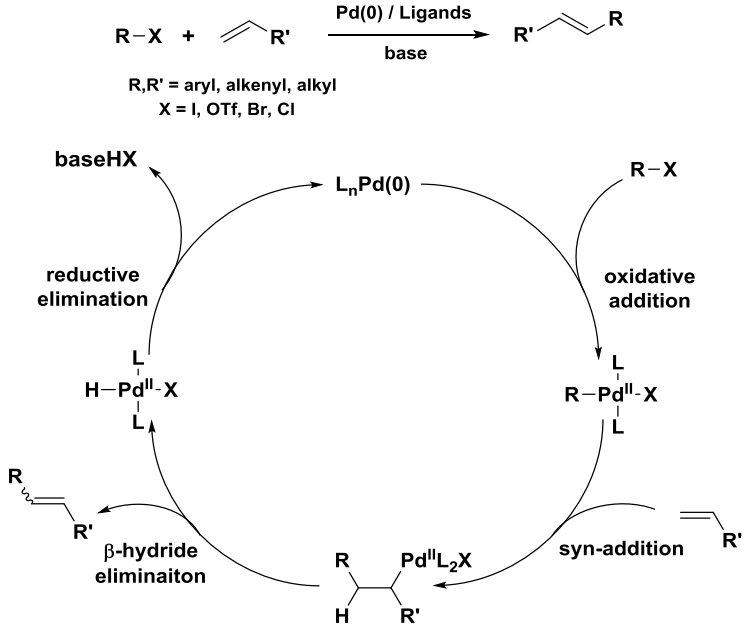

Figure 1.19 Mechanism of Heck Cross-Coupling Reaction[107,117].

The Pd-catalysed Heck reaction is also applicable to chemical protein modification in aqueous systems. An initial study of this Heck reaction of proteins was carried out by treatment of the 4-IPhe-incoporated Ras protein with a biotinylated alkene substrate in the presence of $Pd(OAc)_2$ and TPPTS[120]. Disappointingly, this reaction condition gave the cross-coupled protein with very low conversion (2%). Recently, Dekker and co-workers reported a new method for protein labelling through aqueous Pd-catalysed oxidative Heck reaction which was successfully demonstrated on a model study of an enzyme 4-oxolocrotonate tautomerase variant (4-OT R61C)[100]. A cysteine residue of the

4-OT (R61C) was first converted into a maleimide linker with a terminal olefin, and subsequently treated with a series of substituted phenylboronic acids in the presence of $Pd(OAc)_2$/BIAN (Scheme **1.10**). The resulting C-C coupled products were detected by LC-MS analysis in excellent to quantitative yields. This oxidative Heck cross-coupling system showed an efficient fluorescent labelling of the terminal alkene-tagged 4-OT in cell lysates. In a previous study, Dekker and co-workers applied this method to fluorescently label terminal alkene-tagged histones *in vitro* through aqueous oxidative Heck cross-coupling reaction[99]. Cross-coupling of the alkene-bound 4-OT with a biotinylated phenylboronic acid was performed by use of $Pd(OAc)_2$ with EDTA as a ligand, instead of the original Pd/BIAN catalyst[99]. Full conversion of the biotinylated protein was observed by LC-MS, comparable to results obtained with two other Pd complex catalysts (BIAN or ADHP).

This current approach would be applicable to *in vitro* monitor labelling of histone lysine acylation by using terminal alkenyl carboxylates and biotinylated phenylboronic acid, leading to the detection of luminescent signals of the modified histones.

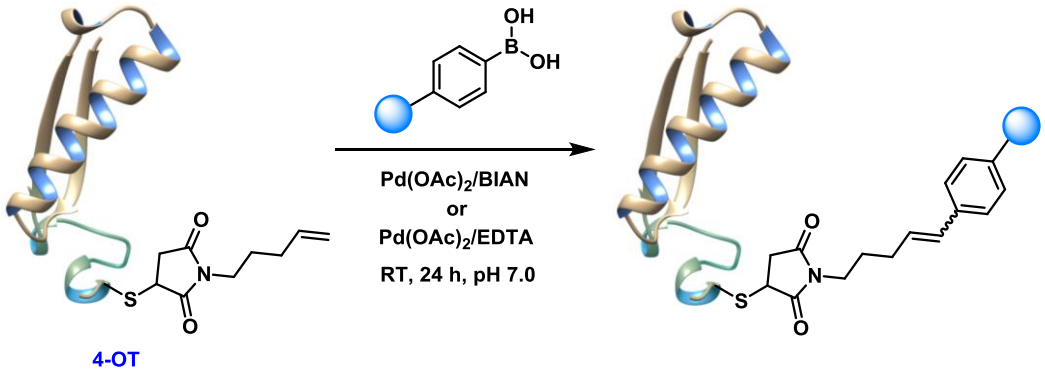

Scheme 1.10 Aqueous Pd-catalysed oxidative Heck cross-coupling of alkene-bound 4-OT with a series of substituted phenylboronic acids[99,100].

1.4 The Aims of this Thesis

Advances in chemical protein modification methods have in turn led to an ever-expanding range of applications, such as the generation of antibody drug conjugates (ADCs), extension of protein functionality, and monitoring of protein reactions in biological systems. It is therefore apparent that the further development of new tools for selective chemical protein modification is crucial in the field of chemical biology and bioengineering.

In this thesis, we mainly focus on two topics of chemical protein modification: protein halogenation and subsequent palladium-mediated cross-coupling reactions. First, we develop a direct chemical method for electrophilic protein fluorination through an extension of our "Tag-and-Modify" concept as a proof of principle, and also apply this method to direct [^{18}F]-radiolabelling of proteins. Next, we explore either genetic incorporation or direct chemical methods for site-specific installation of C-X bonds (X = Br, I) onto proteins as coupling partners for subsequent Pd-catalysed cross-coupling reactions. To start with, biosynthetic incorporation of unnatural aromatic amino acids into proteins of interest is investigated using auxotrophic bacterial strains with unnatural tRNA synthetases. In an alternative approach, we investigate protein iodination through direct chemical installation of C-I bonds onto proteins, utilising a mild iodinating agent. To further investigate site-specific Pd-mediated bioconjugation, a model study of small molecules/proteins based on our aqueous Pd-mediated Suzuki-Miyaura cross-coupling system is discussed. Finally, we extend the application of our pallado-biology strategy to protein labelling under challenging biological conditions. It is expected that our research can extend the scope of chemical protein modification as well as enable new applications of our chemical toolkit in the context of biological probes.

1.5 Bibliography

(1) Walsh, C. T.; Garneau-Tsodikova, S.; Gatto, G. J., Jr. Protein posttranslational modifications: the chemistry of proteome diversifications. *Angew. Chem. Int. Ed. Engl.* **2005**, *44*, 7342-7372.

(2) Boutureira, O.; Bernardes, G. J. Advances in chemical protein modification. *Chem. Rev.* **2015**, *115*, 2174-2195.

(3) Spicer, C. D.; Davis, B. G. Selective chemical protein modification. *Nat Commun* **2014**, *5*, 4740.

(4) Sletten, E. M.; Bertozzi, C. R. Bioorthogonal chemistry: fishing for selectivity in a sea of functionality. *Angew. Chem. Int. Ed. Engl.* **2009**, *48*, 6974-6998.

(5) Krall, N.; da Cruz, F. P.; Boutureira, O.; Bernardes, G. J. Site-selective protein-modification chemistry for basic biology and drug development. *Nat. Chem.* **2016**, *8*, 103-113.

(6) Gong, Y.; Pan, L. Recent advances in bioorthogonal reactions for site-specific protein labeling and engineering. *Tetrahedron Lett.* **2015**, *56*, 2123-2132.

(7) Basle, E.; Joubert, N.; Pucheault, M. Protein chemical modification on endogenous amino acids. *Chemistry & biology* **2010**, *17*, 213-227.

(8) Marculescu, C.; Kossen, H.; Morgan, R. E.; Mayer, P.; Fletcher, S. A.; Tolner, B.; Chester, K. A.; Jones, L. H.; Baker, J. R. Aryloxymaleimides for cysteine modification, disulfide bridging and the dual functionalization of disulfide bonds. *Chem. Commun.* **2014**, *50*, 7139-7142.

(9) Smith, M. E. B.; Schumacher, F. F.; Ryan, C. P.; Tedaldi, L. M.; Papaioannou, D.; Waksman, G.; Caddick, S.; Baker, J. R. Protein Modification, Bioconjugation, and Disulfide Bridging Using Bromomaleimides. *J. Am. Chem. Soc.* **2010**, *132*, 1960-1965.

(10) Chalker, J. M.; Bernardes, G. J.; Davis, B. G. A 'Tag and Modify' Approach to Site-Selective Protein Modification. *Acc. Chem. Res.* **2011**, *44*, 730-741.

(11) Chalker, J. M.; Gunnoo, S. B.; Boutureira, O.; Gerstberger, S. C.; Fernández-González, M.; Bernardes, G. J. L.; Griffin, L.; Hailu, H.; Schofield, C. J.; Davis, B. G. Methods for converting cysteine to dehydroalanine on peptides and proteins. *Chem. Sci.* **2011**, *2*, 1666.

(12) Link, A. J.; Tirrell, D. A. Cell Surface Labeling of Escherichia coli via Copper(I)-Catalyzed [3+2] Cycloaddition. *J. Am. Chem. Soc.* **2003**, *125*, 11164-11165.

(13) Link, A. J.; Vink, M. K. S.; Tirrell, D. A. Presentation and Detection of Azide Functionality in Bacterial Cell Surface Proteins. *J. Am. Chem. Soc.* **2004**, *126*, 10598-10602.

(14) Rostovtsev, V. V.; Green, L. G.; Fokin, V. V.; Sharpless, K. B. A Stepwise Huisgen Cycloaddition Process: Copper(I)-Catalyzed Regioselective "Ligation" of Azides and Terminal Alkynes. *Angew. Chem. Int. Ed.* **2002**, *41*, 2596-2599.

(15) Sletten, E. M.; Bertozzi, C. R. From Mechanism to Mouse: A Tale of Two Bioorthogonal Reactions. *Acc. Chem. Res.* **2011**, *44*, 666-676.

(16) Wang, Q.; Chan, T. R.; Hilgraf, R.; Fokin, V. V.; Sharpless, K. B.; Finn, M. G. Bioconjugation by Copper(I)-Catalyzed Azide-Alkyne [3 + 2] Cycloaddition. *J. Am. Chem. Soc.* **2003**, *125*, 3192-3193.

(17) Gunnoo, S. B.; Madder, A. Chemical Protein Modification through Cysteine. *Chembiochem.* **2016**, *17*, 529-553.

(18) Tedaldi, L. M.; Smith, M. E. B.; Nathani, R. I.; Baker, J. R. Bromomaleimides: new reagents for the selective and reversible modification of cysteine. *Chem. Commun.* **2009**, 6583.

(19) Chalker, J. M.; Bernardes, G. J.; Lin, Y. A.; Davis, B. G. Chemical modification of proteins at cysteine: opportunities in chemistry and biology. *Chem Asian J* **2009**, *4*, 630-640.

(20) Chalker, J. M.; Wood, C. S. C.; Davis, B. G. A Convenient Catalyst for Aqueous and Protein Suzuki−Miyaura Cross-Coupling. *J. Am. Chem. Soc.* **2009**, *131*, 16346-16347.

(21) Simon, M. D.; Chu, F.; Racki, L. R.; de la Cruz, C. C.; Burlingame, A. L.; Panning, B.; Narlikar, G. J.; Shokat, K. M. The site-specific installation of methyl-lysine analogs into recombinant histones. *Cell* **2007**, *128*, 1003-1012.

(22) Zhang, Y.; Bhatt, V. S.; Sun, G.; Wang, P. G.; Palmer, A. F. Site-Selective Glycosylation of Hemoglobin on Cys β93. *Bioconjug. Chem.* **2008**, *19*, 2221-2230.

(23) Morrison, P. M.; Foley, P. J.; Warriner, S. L.; Webb, M. E. Chemical generation and modification of peptides containing multiple dehydroalanines. *Chem. Commun.* **2015**, *51*, 13470-13473.

(24) Maruani, A.; Smith, M. E.; Miranda, E.; Chester, K. A.; Chudasama, V.; Caddick, S. A plug-and-play approach to antibody-based therapeutics via a chemoselective dual click strategy. *Nat Commun* **2015**, *6*, 6645.

(25) Dawson, P. E.; Muir, T. W.; Clark-Lewis, I.; Kent, S. B. H. Synthesis of proteins by native chemical ligation. *Science* **1994**, *266*, 776-778.

(26) Robinson, M. A.; Charlton, S. T.; Garnier, P.; Wang, X. T.; Davis, S. S.; Perkins, A. C.; Frier, M.; Duncan, R.; Savage, T. J.; Wyatt, D. A.; Watson, S. A.; Davis, B. G. LEAPT: lectin-directed enzyme-activated prodrug therapy. *Proc. Natl. Acad. Sci. U.S.A.* **2004**, *101*, 14527-14532.

(27) Biava, H.; Budisa, N. Evolution of fluorinated enzymes: An emerging trend for biocatalyst stabilization. *Engineering in Life Sciences* **2014**, *14*, 340-351.

(28) Budisa, N.; Wenger, W.; Wiltschi, B. Residue-specific global fluorination of Candida antarctica lipase B in Pichia pastoris. *Mol Biosyst* **2010**, *6*, 1630-1639.

(29) Salwiczek, M.; Nyakatura, E. K.; Gerling, U. I.; Ye, S.; Koksch, B. Fluorinated amino acids: compatibility with native protein structures and effects on protein-protein interactions. *Chem. Soc. Rev.* **2012**, *41*, 2135-2171.

(30) Petrovic, D. M.; Leenhouts, K.; van Roosmalen, M. L.; Broos, J. An expression system for the efficient incorporation of an expanded set of tryptophan analogues. *Amino acids* **2013**, *44*, 1329-1336.

(31) El Khattabi, M.; van Roosmalen, M. L.; Jager, D.; Metselaar, H.; Permentier, H.; Leenhouts, K.; Broos, J. Lactococcus lactis as expression host for the biosynthetic incorporation of tryptophan analogues into recombinant proteins. *Biochem. J* **2008**, *409*, 193-198.

(32) Chin, J. W.; Cropp, T. A.; Anderson, J. C.; Mukherji, M.; Zhang, Z.; Schultz, P. G. An Expanded Eukaryotic Genetic Code. *Science* **2003**, *301*, 964-967.

(33) Liu, C. C.; Schultz, P. G. Adding new chemistries to the genetic code. *Annu. Rev. Biochem* **2010**, *79*, 413-444.

(34) Wang, F.; Robbins, S.; Guo, J.; Shen, W.; Schultz, P. G. Genetic incorporation of unnatural amino acids into proteins in Mycobacterium tuberculosis. *PLoS One* **2010**, *5*, e9354.

(35) Wang, L.; Brock, A.; Herberich, B.; Schultz, P. G. Expanding the Genetic Code of Escherichia coli. *Science* **2001**, *292*, 498-500.

(36) Wang, L.; Schultz, P. G. Expanding the genetic code. *Angew. Chem. Int. Ed. Engl.* **2004**, *44*, 34-66.

(37) Bernardes, G. J. L.; Chalker, J. M.; Errey, J. C.; Davis, B. G. Facile Conversion of Cysteine and Alkyl Cysteines to Dehydroalanine on Protein Surfaces: Versatile and Switchable Access to Functionalized Proteins. *J. Am. Chem. Soc.* **2008**, *130*, 5052-5053.

(38) Chalker, J. M.; Lercher, L.; Rose, N. R.; Schofield, C. J.; Davis, B. G. Conversion of cysteine into dehydroalanine enables access to synthetic histones bearing diverse post-translational modifications. *Angew. Chem. Int. Ed. Engl.* **2012**, *51*, 1835-1839.

(39) Chooi, K. P.; Galan, S. R.; Raj, R.; McCullagh, J.; Mohammed, S.; Jones, L. H.; Davis, B. G. Synthetic phosphorylation of p38alpha recapitulates protein kinase activity. *J. Am. Chem. Soc.* **2014**, *136*, 1698-1701.

(40) Gunnoo, S. B.; Finney, H. M.; Baker, T. S.; Lawson, A. D.; Anthony, D. C.; Davis, B. G. Creation of a gated antibody as a conditionally functional synthetic protein. *Nat Commun* **2014**, *5*, 4388.

(41) Fernández-González, M.; Boutureira, O.; Bernardes, G. J. L.; Chalker, J. M.; Young, M. A.; Errey, J. C.; Davis, B. G. Site-selective chemoenzymatic construction of synthetic glycoproteins using endoglycosidases. *Chem. Sci.* **2010**, *1*, 709.

(42) Nathani, R.; Moody, P.; Smith, M. E.; Fitzmaurice, R. J.; Caddick, S. Bioconjugation of green fluorescent protein via an unexpectedly stable cyclic sulfonium intermediate. *Chembiochem.* **2012**, *13*, 1283-1285.

(43) Nathani, R. I.; Moody, P.; Chudasama, V.; Smith, M. E.; Fitzmaurice, R. J.; Caddick, S. A novel approach to the site-selective dual labelling of a protein via chemoselective cysteine modification. *Chem. Sci.* **2013**, *4*, 3455-3458.

(44) Staudinger, H.; Meyer, J. Über neue organische Phosphorverbindungen III. Phosphinmethylenderivate und Phosphinimine. *Helv. Chim. Acta* **1919**, *2*, 635-646.

(45) Kiick, K. L.; Saxon, E.; Tirrell, D. A.; Bertozzi, C. R. Incorporation of azides into recombinant proteins for chemoselective modification by the Staudinger ligation. *Proc. Natl. Acad. Sci. U.S.A.* **2002**, *99*, 19-24.

(46) Saxon, E.; Bertozzi, C. R. Cell Surface Engineering by a Modified Staudinger Reaction. *Science* **2000**, *287*, 2007-2010.

(47) van Berkel, S. S.; van Eldijk, M. B.; van Hest, J. C. Staudinger ligation as a method for bioconjugation. *Angew. Chem. Int. Ed. Engl.* **2011**, *50*, 8806-8827.

(48) Bernardes, G. J. L.; Linderoth, L.; Doores, K. J.; Boutureira, O.; Davis, B. G. Site-Selective Traceless Staudinger Ligation for Glycoprotein Synthesis Reveals Scope and Limitations. *Chembiochem.* **2011**, *12*, 1383-1386.

(49) Hong, V.; Steinmetz, N. F.; Manchester, M.; Finn, M. G. Labelling Live Cells by Copper-Catalysed Alkyne-Azide Click Chemistry. *Bioconjug. Chem.* **2010**, *21*, 1912-1916.

(50) Agard, N. J.; Prescher, J. A.; Bertozzi, C. R. A Strain-Promoted [3 + 2] Azide−Alkyne Cycloaddition for Covalent Modification of Biomolecules in Living Systems. *J. Am. Chem. Soc.* **2004**, *126*, 15046-15047.

(51) Laughlin, S. T.; Baskin, J. M.; Amacher, S. L.; Bertozzi, C. R. In Vivo Imaging of Membrane-Associated Glycans in Developing Zebrafish. *Science* **2008**, *320*, 664-667.

(52) Chang, P. V.; Prescher, J. A.; Sletten, E. M.; Baskin, J. M.; Miller, I. A.; Agard, N. J.; Lo, A.; Bertozzi, C. R. Copper-free click chemistry in living animals. *Proc. Natl. Acad. Sci. U.S.A.* **2010**, *107*, 1821-1826.

(53) Jewett, J. C.; Sletten, E. M.; Bertozzi, C. R. Rapid Cu-Free Click Chemistry with Readily Synthesized Biarylazacyclooctynones. *J. Am. Chem. Soc.* **2010**, *132*, 3688-3690.

(54) Plass, T.; Milles, S.; Koehler, C.; Schultz, C.; Lemke, E. A. Genetically encoded copper-free click chemistry. *Angew. Chem. Int. Ed. Engl.* **2011**, *50*, 3878-3881.

(55) Plass, T.; Milles, S.; Koehler, C.; Szymanski, J.; Mueller, R.; Wiessler, M.; Schultz, C.; Lemke, E. A. Amino acids for Diels-Alder reactions in living cells. *Angew. Chem. Int. Ed. Engl.* **2012**, *51*, 4166-4170.

(56) Li, Y.; Pan, M.; Li, Y.; Huang, Y.; Guo, Q. Thiol-yne radical reaction mediated site-specific protein labeling via genetic incorporation of an alkynyl-L-lysine analogue. *Org Biomol Chem* **2013**, *11*, 2624-2629.

(57) McKay, C. S.; Finn, M. G. Click chemistry in complex mixtures: bioorthogonal bioconjugation. *Chemistry & biology* **2014**, *21*, 1075-1101.

(58) Agarwal, P.; van der Weijden, J.; Sletten, E. M.; Rabuka, D.; Bertozzi, C. R. A Pictet-Spengler ligation for protein chemical modification. *Proc. Natl. Acad. Sci. U.S.A.* **2013**, *110*, 46-51.

(59) King, M.; Wagner, A. Developments in the field of bioorthogonal bond forming reactions-past and present trends. *Bioconjug. Chem.* **2014**, *25*, 825-839.

(60) Wu, P.; Shui, W.; Carlson, B. L.; Hu, N.; Rabuka, D.; Lee, J.; Bertozzi, C. R. Site-specific chemical modification of recombinant proteins produced in mammalian cells by using the genetically encoded aldehyde tag. *Proc. Natl. Acad. Sci. U.S.A.* **2009**, *106*, 3000-3005.

(61) Buer, B. C.; Marsh, E. N. Fluorine: a new element in protein design. *Protein Sci.* **2012**, *21*, 453-462.

(62) Kuchar, M.; Pretze, M.; Kniess, T.; Steinbach, J.; Pietzsch, J.; Loser, R. Site-selective radiolabeling of peptides by (18)F-fluorobenzoylation with [(18F)]SFB in solution and on solid phase: a comparative study. *Amino acids* **2012**, *43*, 1431-1443.

(63) Marsh, E. N. Fluorinated proteins: from design and synthesis to structure and stability. *Acc. Chem. Res.* **2014**, *47*, 2878-2886.

(64) Rydzik, A. M.; Brem, J.; van Berkel, S. S.; Pfeffer, I.; Makena, A.; Claridge, T. D.; Schofield, C. J. Monitoring conformational changes in the NDM-1 metallo-beta-lactamase by 19F NMR spectroscopy. *Angew. Chem. Int. Ed. Engl.* **2014**, *53*, 3129-3133.

(65) Tang, G.; Zeng, W.; Yu, M.; Kabalka, G. Facile synthesis ofN-succinimidyl 4-[18F]fluorobenzoate ([18F]SFB) for protein labeling. *J. Labelled Compd. Radiopharm.* **2008**, *51*, 68-71.

(66) Budisa, N.; Pipitone, O.; Siwanowicz, I.; Rubini, M.; Pal, P. P.; Holak, T. A.; Gelmi, M. L. Efforts towards the Design of 'Teflon' Proteins: In vivo Translation with Trifluorinated Leucine and Methionine Analogues. *Chemistry & Biodiversity* **2004**, *1*, 1465-1475.

(67) Eichler, J. F.; Cramer, J. C.; Kirk, K. L.; Bann, J. G. Biosynthetic incorporation of fluorohistidine into proteins in E. coli: a new probe of macromolecular structure. *Chembiochem.* **2005**, *6*, 2170-2173.

(68) Boutureira, O.; D'Hooge, F.; Fernandez-Gonzalez, M.; Bernardes, G. J.; Sanchez-Navarro, M.; Koeppe, J. R.; Davis, B. G. Fluoroglycoproteins: ready chemical

site-selective incorporation of fluorosugars into proteins. *Chem. Commun.* **2010**, *46*, 8142-8144.

(69) Boutureira, O.; Bernardes, G. J.; D'Hooge, F.; Davis, B. G. Direct radiolabelling of proteins at cysteine using [18F]-fluorosugars. *Chem. Commun.* **2011**, *47*, 10010-10012.

(70) Stigers, D. J.; Watts, Z. I.; Hennessy, J. E.; Kim, H. K.; Martini, R.; Taylor, M. C.; Ozawa, K.; Keillor, J. W.; Dixon, N. E.; Easton, C. J. Incorporation of chlorinated analogues of aliphatic amino acids during cell-free protein synthesis. *Chem. Commun.* **2011**, *47*, 1839-1841.

(71) Ibba, M.; Hennecke, H. Relaxing the substrate specificity of an aminoacyl-tRNA synthetase allows in vitro and in vivo synthesis of proteins containing unnatural amino acids. *FEBS Lett.* **1995**, *364*, 272-275.

(72) Ayyadurai, N.; Deepankumar, K.; Prabhu, N. S.; Budisa, N.; Yun, H. Evaluation and biosynthetic incorporation of chlorotyrosine into recombinant proteins. *Biotechnology and Bioprocess Engineering* **2012**, *17*, 679-686.

(73) Domigan, N. M.; Charlton, T. S.; Duncan, M. W.; Winterbourn, C. C.; Kettle, A. J. Chlorination of Tyrosyl Residues in Peptides by Myeloperoxidase and Human Neutrophils. *J. Biol. Chem.* **1995**, *270*, 16542-16548.

(74) Fu, S.; Wang, H.; Davies, M.; Dean, R. Reactions of Hypochlorous Acid with Tyrosine and Peptidyl-tyrosyl Residues Give Dichlorinated and Aldehydic Products in Addition to 3-Chlorotyrosine. *J. Biol. Chem.* **2000**, *275*, 10851-10858.

(75) Sharma, N.; Furter, R.; Kast, P.; Tirrell, D. A. Efficient introduction of aryl bromide functionality into proteins in vivo. *FEBS Lett.* **2000**, *467*, 37-40.

(76) Ohtake, K.; Yamaguchi, A.; Mukai, T.; Kashimura, H.; Hirano, N.; Haruki, M.; Kohashi, S.; Yamagishi, K.; Murayama, K.; Tomabechi, Y.; Itagaki, T.; Akasaka, R.; Kawazoe, M.; Takemoto, C.; Shirouzu, M.; Yokoyama, S.; Sakamoto, K. Protein stabilization utilizing a redefined codon. *Sci Rep* **2015**, *5*, 9762.

(77) Kwon, I.; Tirrell, D. A. Site-Specific Incorporation of Tryptophan Analogues into Recombinant Proteins in Bacterial Cells. *J. Am. Chem. Soc.* **2007**, *129*, 10431-10437.

(78) Kwon, I.; Wang, P.; Tirrell, D. A. Design of a Bacterial Host for Site-Specific Incorporation of p-Bromophenylalanine into Recombinant Proteins. *J. Am. Chem. Soc.* **2006**, *128*, 11778-11783.

(79) Wu, W.; Chen, Y.; Avignon, A. d.; Hazen, S. L. 3-Bromotyrosine and 3,5-Dibromotyrosine Are Major Products of Protein Oxidation by Eosinophil Peroxidase: Potential Markers for Eosinophil-Dependent Tissue Injury in Vivo *Biochemistry* **1999**, *38*, 3538-3548.

(80) Kato, Y.; Kawai, Y.; Morinaga, H.; Kondo, H.; Dozaki, N.; Kitamoto, N.; Osawa, T. Immunogenicity of a brominated protein and successive establishment of a monoclonal antibody to dihalogenated tyrosine. *Free Radic Biol Med* **2005**, *38*, 24-31.

(81) Xie, J.; Wang, L.; Wu, N.; Brock, A.; Spraggon, G.; Schultz, P. G. The site-specific incorporation of p-iodo-L-phenylalanine into proteins for structure determination. *Nat. Biotechnol.* **2004**, *22*, 1297-1301.

(82) Hino, N.; Hayashi, A.; Sakamoto, K.; Yokoyama, S. Site-specific incorporation of non-natural amino acids into proteins in mammalian cells with an expanded genetic code. *Nat Protoc* **2006**, *1*, 2957-2962.

(83) Kiga, D.; Sakamoto, K.; Kodama, K.; Kigawa, T.; Matsuda, T.; Yabuki, T.; Shirouzu, M.; Harada, Y.; Nakayama, H.; Takio, K.; Hasegawa, Y.; Endo, Y.; Hirao, I.; Yokoyama, S. An engineered Escherichia coli tyrosyl-tRNA synthetase for site-

specific incorporation of an unnatural amino acid into proteins in eukaryotic translation and its application in a wheat germ cell-free system. *Proc. Natl. Acad. Sci. U.S.A.* **2002**, *99*, 9715-9720.

(84) Espuña, G.; Andreu, D.; Barluenga, J.; Pérez, X.; Planas, A.; Arsequell, G.; Valencia, G. Iodination of Proteins by IPy2BF4, a New Tool in Protein Chemistry. *Biochemistry* **2006**, *45*, 5957-5963.

(85) Dong, S.; Moroder, L.; Budisa, N. Protein Iodination by Click Chemistry. *Chembiochem.* **2009**, *10*, 1149-1151.

(86) Bolton, A. E.; Hunter, W. M. The Labelling of Proteins to High Specific Radioactivities by Conjugation to a ^{125}I-Containing Acylating Agent. *Biochem. J* **1973**, *133*, 529-539.

(87) Ynak, T.; Akgυn, Z.; Yildirim, Y.; Duman, Y.; Erenel, G. Self-radioiodination of iodogen. *Appl. Radiat. Isot.* **2001**, *54*, 749-752.

(88) Fraker, R. J.; Speck, J. C. Protein and cell membrane iodination with a sparingly soluble chloramide 1,3,4,6-tetrachloro 5,6-diphenylglycouril. *Biochem. Biophys. Res. Commun.* **1978**, *80*, 849-857.

(89) Millar, W. T.; Smith, J. F. B. Protein Iodination Using Iodogen(R). *Int. J. Appl. Radiat. Isot.* **1983**, *34*, 639-641.

(90) Antos, J. M.; Francis, M. B. Transition metal catalyzed methods for site-selective protein modification. *Curr. Opin. Chem. Biol.* **2006**, *10*, 253-262.

(91) Yang, M.; Li, J.; Chen, P. R. Transition metal-mediated bioorthogonal protein chemistry in living cells. *Chem. Soc. Rev.* **2014**, *43*, 6511-6526.

(92) Dumas, A.; Spicer, C. D.; Gao, Z.; Takehana, T.; Lin, Y. A.; Yasukohchi, T.; Davis, B. G. Self-liganded Suzuki-Miyaura coupling for site-selective protein PEGylation. *Angew. Chem. Int. Ed. Engl.* **2013**, *52*, 3916-3921.

(93) Spicer, C. D.; Davis, B. G. Palladium-Mediated Site-Selective Suzuki-Miyaura Protein Modification at Genetically Encoded Aryl Halides. *Chem. Commun.* **2011**, *47*, 1698-1700.

(94) Spicer, C. D.; Triemer, T.; Davis, B. G. Palladium-Mediated Cell-Surface Labeling. *J. Am. Chem. Soc.* **2012**, *134*, 800-803.

(95) Hauke, S.; Best, M.; Schmidt, T. T.; Baalmann, M.; Krause, A.; Wombacher, R. Two-step protein labeling utilizing lipoic acid ligase and Sonogashira cross-coupling. *Bioconjug. Chem.* **2014**, *25*, 1632-1637.

(96) Li, J.; Lin, S.; Wang, J.; Jia, S.; Yang, M.; Hao, Z.; Zhang, X.; Chen, P. R. Ligand-free palladium-mediated site-specific protein labeling inside gram-negative bacterial pathogens. *J. Am. Chem. Soc.* **2013**, *135*, 7330-7338.

(97) Li, N.; Lim, R. K. V.; Edwardraja, S.; Lin, Q. Copper-Free Sonogashira Cross-Coupling for Functionalization of Alkyne-Encoded Proteins in Aqueous Medium and in Bacterial Cells. *J. Am. Chem. Soc.* **2011**, *133*, 15316-15319.

(98) Li, N.; Ramil, C. P.; Lim, R. K.; Lin, Q. A genetically encoded alkyne directs palladium-mediated protein labeling on live mammalian cell surface. *ACS Chem Biol* **2015**, *10*, 379-384.

(99) Ourailidou, M. E.; Dockerty, P.; Witte, M.; Poelarends, G. J.; Dekker, F. J. Metabolic alkene labeling and in vitro detection of histone acylation via the aqueous oxidative Heck reaction. *Org Biomol Chem* **2015**, *13*, 3648-3653.

(100) Ourailidou, M. E.; van der Meer, J. Y.; Baas, B. J.; Jeronimus-Stratingh, M.; Gottumukkala, A. L.; Poelarends, G. J.; Minnaard, A. J.; Dekker, F. J. Aqueous oxidative Heck reaction as a protein-labeling strategy. *Chembiochem.* **2014**, *15*, 209-212.

(101) Antos, J. M.; Francis, M. B. Selective Tryptophan Modification with Rhodium Carbenoids in Aqueous Solution. *J. Am. Chem. Soc.* **2004**, *126*, 10256-10257.

(102) Antos, J. M.; McFarland, J. M.; Iavarone, A. T.; Francis, M. B. Chemoselective Tryptophan Labeling with Rhodium Carbenoids at Mild pH. *J. Am. Chem. Soc.* **2009**, *131*, 6301-6308.

(103) Lin, Y. A.; Chalker, J. M.; Davis, B. G. Olefin metathesis for site-selective protein modification. *Chembiochem.* **2009**, *10*, 959-969.

(104) Lin, Y. A.; Chalker, J. M.; Floyd, N.; Bernardes, G. J. L.; Davis, B. G. Allyl Sulfides Are Privileged Substrates in Aqueous Cross-Metathesis: Application to Site-Selective Protein Modification. *J. Am. Chem. Soc.* **2008**, *130*, 9642-9643.

(105) Miyaura, N.; Suzuki, A. Palladium-Catalyzed Cross-Coupling Reactions of Organoboron Compounds. *Chem. Rev.* **1995**, *95*, 2457-2483.

(106) Suzuki, A. Recent advances in the cross-coupling reactions of organoboron derivatives with organic electrophiles, 1995-1998. *J. Organomet. Chem.* **1999**, *576*, 147-168.

(107) Johansson Seechurn, C. C.; Kitching, M. O.; Colacot, T. J.; Snieckus, V. Palladium-catalyzed cross-coupling: a historical contextual perspective to the 2010 Nobel Prize. *Angew. Chem. Int. Ed. Engl.* **2012**, *51*, 5062-5085.

(108) Ojida, A.; Tsutsumi, H.; Kasagi, N.; Hamachi, I. Suzuki coupling for protein modification. *Tetrahedron Lett.* **2005**, *46*, 3301-3305.

(109) Brustad, E.; Bushey, M. L.; Lee, J. W.; Groff, D.; Liu, W.; Schultz, P. G. A genetically encoded boronate-containing amino acid. *Angew. Chem. Int. Ed. Engl.* **2008**, *47*, 8220-8223.

(110) Polshettiwar, V.; Decottignies, A.; Len, C.; Fihri, A. Suzuki-Miyaura cross-coupling reactions in aqueous media: green and sustainable syntheses of biaryls. *ChemSusChem* **2010**, *3*, 502-522.

(111) Gao, Z.; Gouverneur, V.; Davis, B. G. Enhanced Aqueous Suzuki–Miyaura Coupling Allows Site-Specific Polypeptide 18F-Labeling. *J. Am. Chem. Soc.* **2013**, *135*, 13612-13615.

(112) Wang, Y. S.; Russell, W. K.; Wang, Z.; Wan, W.; Dodd, L. E.; Pai, P. J.; Russell, D. H.; Liu, W. R. The de novo engineering of pyrrolysyl-tRNA synthetase for genetic incorporation of L-phenylalanine and its derivatives. *Mol Biosyst* **2011**, *7*, 714-717.

(113) Sonogashira, K.; Tohda, Y.; Hagihara, N. A Convenient Synthesis of Acetylenes: Catalytic Substitutions of Acetylenic Hydrogen with Bromoalkenes, Iodoarenes, and Bromopyridines. *Tetrahedron Lett.* **1975**, *16*, 4467-4470.

(114) Chinchilla, R.; Najera, C. Recent advances in Sonogashira reactions. *Chem. Soc. Rev.* **2011**, *40*, 5084-5121.

(115) Doucet, H.; Hierso, J. C. Palladium-based catalytic systems for the synthesis of conjugated enynes by sonogashira reactions and related alkynylations. *Angew. Chem. Int. Ed. Engl.* **2007**, *46*, 834-871.

(116) Kodama, K.; Fukuzawa, S.; Nakayama, H.; Sakamoto, K.; Kigawa, T.; Yabuki, T.; Matsuda, N.; Shirouzu, M.; Takio, K.; Yokoyama, S.; Tachibana, K. Site-specific functionalization of proteins by organopalladium reactions. *Chembiochem.* **2007**, *8*, 232-238.

(117) Whitcombe, N. J.; Hii, K. K.; Gibson, S. E. Advances in the Heck chemistry of aryl bromides and chlorides. *Tetrahedron* **2001**, *57*, 7449-7476.

(118) Heck, R. F. The palladium-catalyzed arylation of enol esters, ethers, and halides. A new synthesis of 2-aryl aldehydes and ketones. *J. Am. Chem. Soc.* **1968**, *90*, 5535-5538.

(119) Heck, R. F. Acylation, methylation, and carboxyalkylation of olefins by Group VIII metal derivatives. *J. Am. Chem. Soc.* **1968**, *90*, 5518-5526.

(120) Kodama, K.; Fukuzawa, S.; Nakayama, H.; Kigawa, T.; Sakamoto, K.; Yabuki, T.; Matsuda, N.; Shirouzu, M.; Takio, K.; Tachibana, K.; Yokoyama, S. Regioselective carbon-carbon bond formation in proteins with palladium catalysis; new protein chemistry by organometallic chemistry. *Chembiochem.* **2006**, *7*, 134-139.

Chapter 2

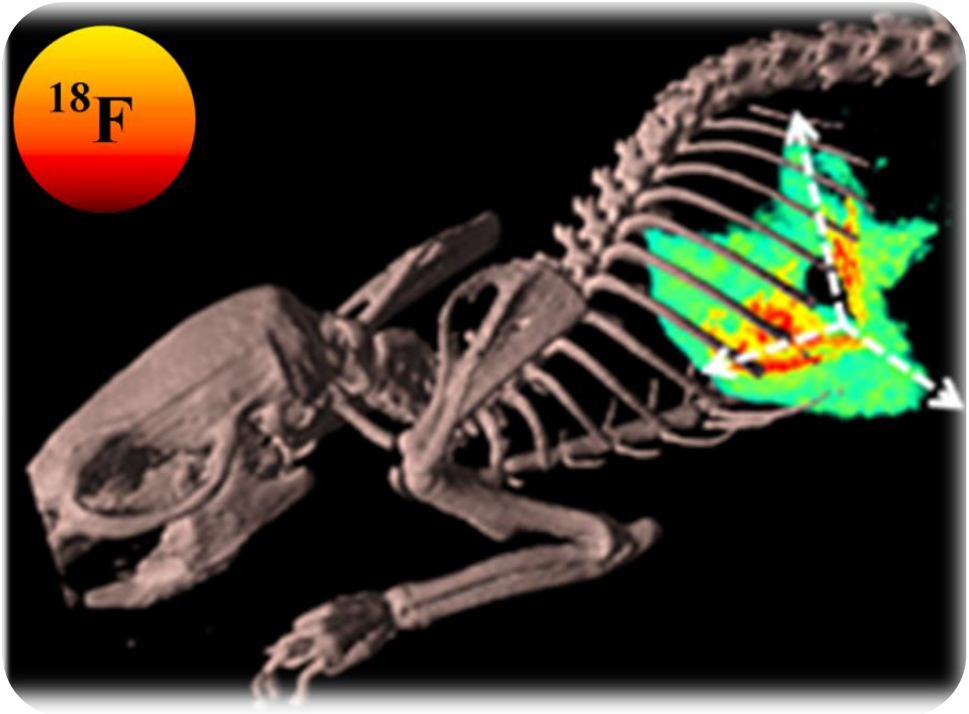

Site-Selective and Direct Electrophilic C-F Bond Formation on Proteins

2.1 Introduction

2.1.1 Methods for C-F Bond Formation

2.1.2 Fluorination Tools in Biology

2.2 A Novel "Tag-and-Modify" Approach for Direct Electrophilic Protein Fluorination

2.3 Site-Selective [^{18}F]-Radiolabelling of Proteins for Preclinical Animal Studies

2.4 Direct Electrophilic Aromatic Fluorination of Proteins

2.5 Conclusion

2.6 Experimental

2.7 Bibliography

2.1 Introduction

The aim of this chapter is to investigate a novel concept of direct electrophilic protein fluorination through "Tag-and-Modify" approach and is applicable to direct [^{18}F]-radiolabelling of proteins for a preclinical animal study.

2.1.1 Methods for C-F Bond Formation

Several chemical methods for fluorination have been developed and are useful in application in a number of organic syntheses involving the formation of fluorinated natural products or pharmaceutical molecules[1-6]. The fluorination reaction can be essentially classified into two reaction classes depending on the polarity of the X-F bond; nucleophilic fluorination and electrophilic fluorination. Currently, a variety of powerful fluorinating agents are commercially available for use in each fluorination reaction type (Figure **2.1**)[1,2,4,5,7].

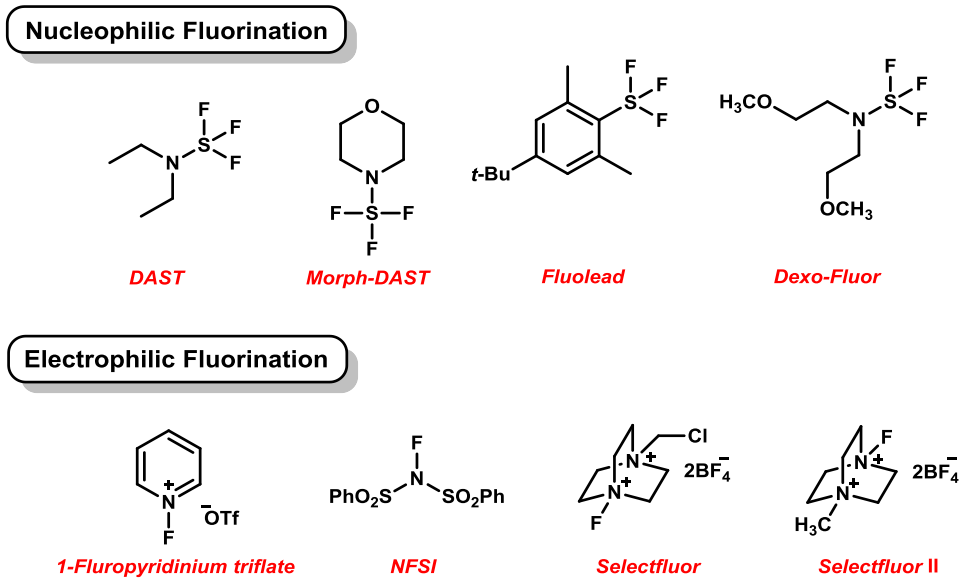

Figure 2.1 Useful fluorinating agents suitable for nucleophilic or electrophilic fluorination reactions[1,2,4,5,7].

1-Chloromethyl-4-fluoro-1,4-diazoniabicyclo[2.2.2]octane *bis* (tetrafluoroborate) (F-TEDA-BF_4), known as Selecfluor *bis*(tetrafluorborate), is used as an strongly electrophilic fluorine source, and this commercially available reagent is stable, non-toxic

and also suitable for some reactions performed in aqueous systems[4,7-9]. For example, treatment of estrone with Selectfluor *bis*(tetrafluoroborate) in an aqueous medium gave a 10*β*-fluorinated-1,4-estradiene-3,17-dione (Scheme **2.1**)[10]. The reaction of this fluorinating reagent with a cinchona alkaloid has also been demonstrated, affording a cinchona alkaloid *N*-fluoroammonium salts that was useful for subsequent catalytic enantioselective fluorination[11,12].

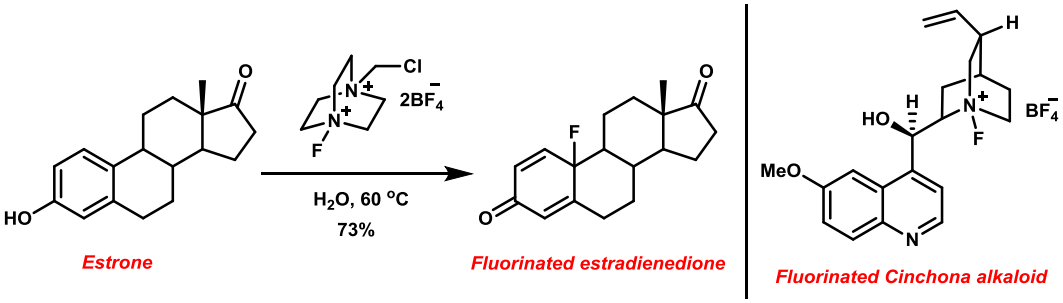

Scheme 2.1 Use of Selectfluor *bis*(tetrafluoroborate) for electrophilic fluorination reactions of small molecules[10-12].

2.1.2 Fluorination Tools in Biology

There are several different ways to introduce fluorine atoms to a protein of interest, which use either direct or indirect fluorination methods[13-18]. Budisa and co-workers reported the biosynthetic incorporation of monofluorinated variants of phenylalanine, tyrosine and tryptophan into a non-glycosylated mutant of *Candida antarctica* lipase B (CalB N74D) using *P. pastoris* auxotrophic strains for each respective amino acid analogue (Figure **2.2**)[16]. Incorporation of each fluorinated analogue was achieved and confirmed by LC-MS analysis.

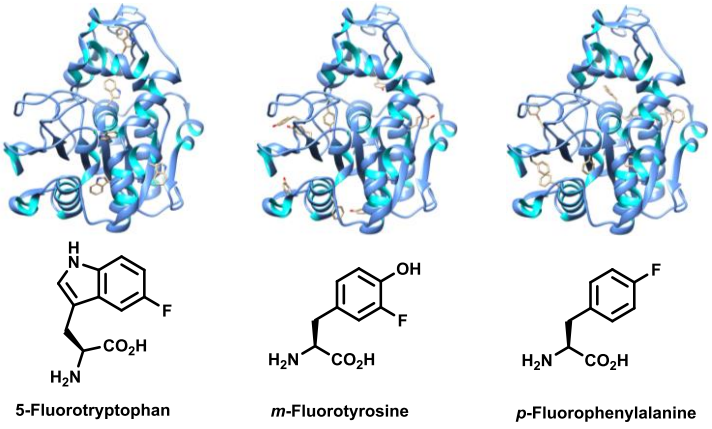

Figure 2.2 Biosynthetic incorporation of monofluorinated analogues into CalB N74D[16].

Furthermore, we have previously demonstrated site-specific ^{19}F or [^{18}F]-labelling of a model protein SBL-156ArI with *para*-^{19}F or [^{18}F]-radioactive phenylboronic acid through aqueous Suzuki-Miyaura reaction in the presence of the efficient Pd catalyst (Scheme **2.2**)[19]. The radiolabelled SBL was confirmed by both UV and radioactive HPLC profiles, leading to the first Pd-catalysed incorporation of an [^{18}F]-radiosynthetic compound into the protein.

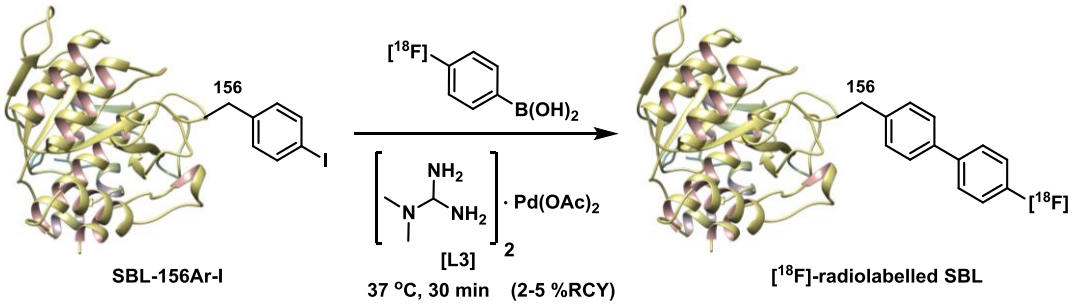

Scheme 2.2 [^{18}F]-labelling of SBL-156ArI via Suzuki-Miyaura cross-coupling[19].

A useful strategy for [^{18}F] atom incorporation into either peptides or proteins is now widely used for radiopharmaceutical and *in vivo* [^{18}F]-PET imaging purposes[20-25]. An [^{18}F]-labelled annexin V was prepared from the reaction of *N*-succinimidyl 4-[^{18}F]fluorobenzoic acid with the multiple lysine side-chains of wild-type annexin V (Scheme **2.3**)[23,25]. Annexin V is well-known as an apoptosis biomarker, which can detect cell-death phenomena[26-29]. For example, *in vivo* imaging of an animal model induced by intravenous injection of cycloheximide (CXM) showed a higher uptake of [^{18}F]-radiolabelled annexin V as compared to an untreated animal[30]. Whilst such a simple [^{18}F]-labelling of proteins through nucleophilic attack of lysine residues can be achieved, the method still requires a prosthetic group for the [^{18}F]-labelled molecules, and the non-specificity of the labelling method may lead to interference with protein function.

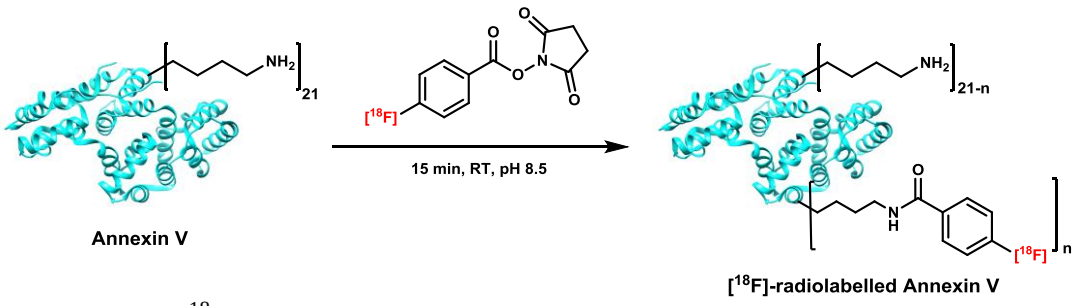

Scheme 2.3 [^{18}F]-radiolabelling of wild-type annexin V using *N*-succinimidyl 4-[^{18}F]fluorobenzoic acid[23,25].

2.2 A Novel "Tag-and-Modify" Approach for Direct Electrophilic Protein Fluorination

Prior work in our group showed successful direct fluorination of small molecules using our "Tag-and-Modify" approach. We then moved forward to a set of model proteins including Np276, Qbeta, and Histone (H3) to study novel method for direct C-F bond formation on proteins. A particular focus of this thesis was the study of a biologically functional protein, Annexin V (ANV), and its application as a biomarker for apoptosis. The wild-type ANV contains a single cysteine residue (C316), which can be chemically modified to Dehydroalanine (Dha). The use of Dha as a protein tag has been developed by our group, and this tag facilitates site-selective protein modification by nucleophilic attacks (from various nucleophiles e.g. thiosugar, thiophosphate) at pre-defined Dha sites from cysteines[31-35]. There are several methods for the introduction of fluorine atoms into proteins using either direct or indirect labelling. However, some methods suffer from a lack of selectivity and show a loss of protein function after non-specific protein labelling. In proof-of-concept work, we have demonstrated the novel concept of direct, fast, and site-selective C-F bond formation on proteins, resulting in the creation of new C-F bonds at Dha-sites with minimal perturbation of protein function and structure (Scheme **2.4**).

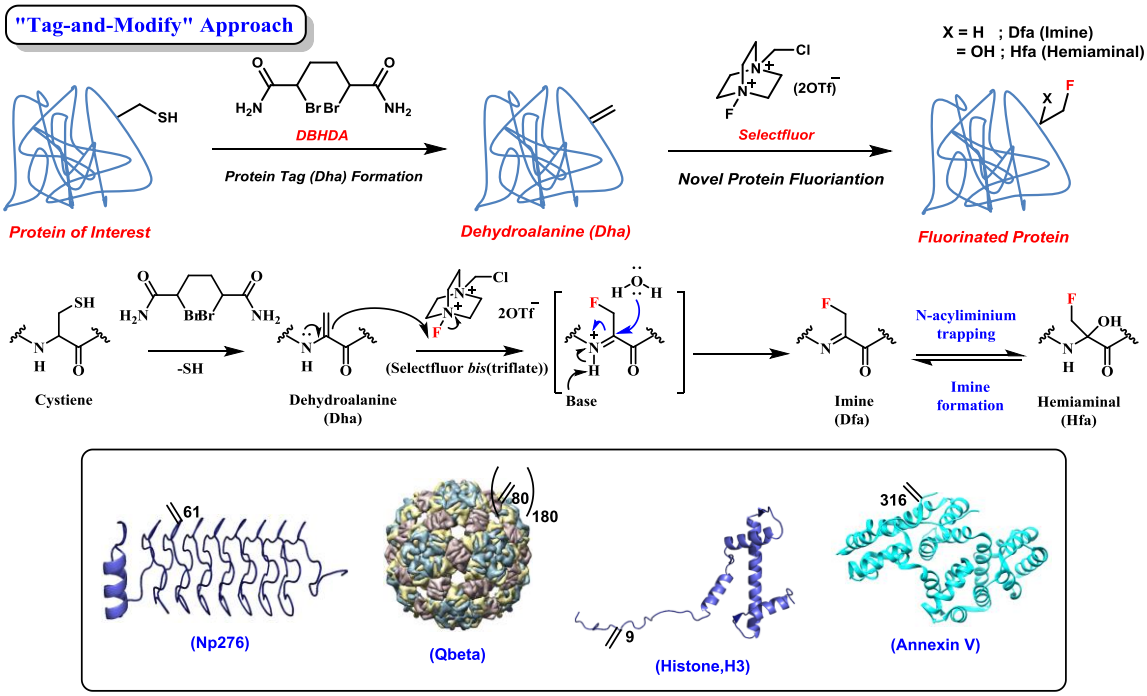

Scheme 2.4 A novel concept of direct electrophilic C-F bond formation of proteins through "Tag-and-Modify" approach.

Initially, treatment of wild-type ANV(C316) with dithiothreitol (DTT) as a reducing agent cleaved a disulfide bond to give a monomer prior to the bis-alkylation elimination of a free cysteine. After DTT treatment, we attempted to prepare the Dha-containing protein for investigation of the fluorination reaction by treatment of the reduced cysteine with 2,5-dibromohexanediamide (DBHDA) as an alkylating agent. However, LC-MS analysis showed no Dha formation onto ANV (Figure **2.3**), possibly due to the inaccessibility of the cysteine residue which is buried in a helix portion of the protein (Figure **2.4**).

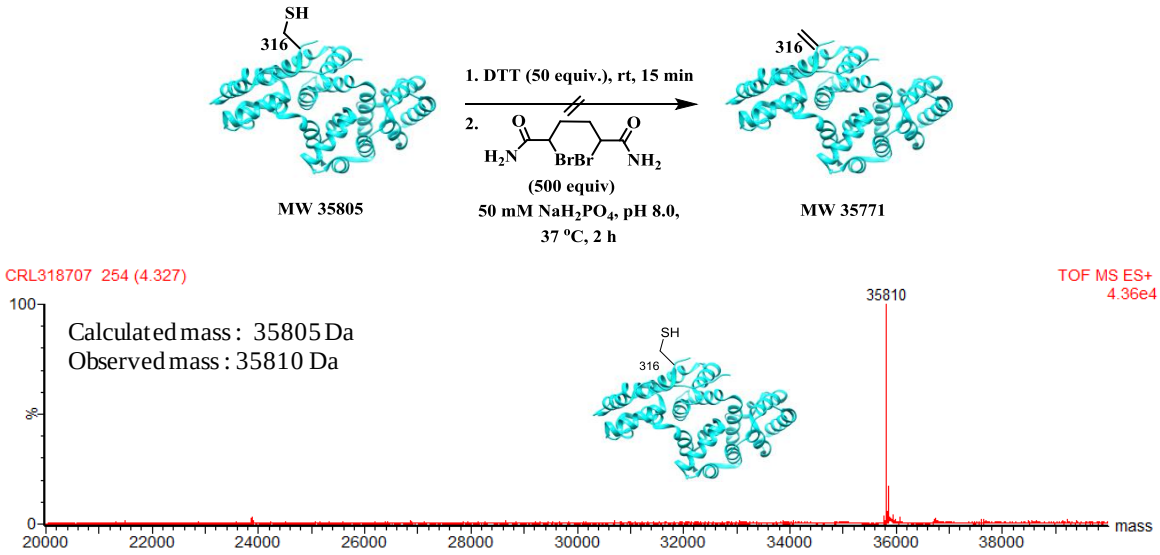

Figure 2.3 ESI-MS spectrum of wild-type ANV(C316) after attempted Dha formation by use of DBHDA as an alkylating agent.

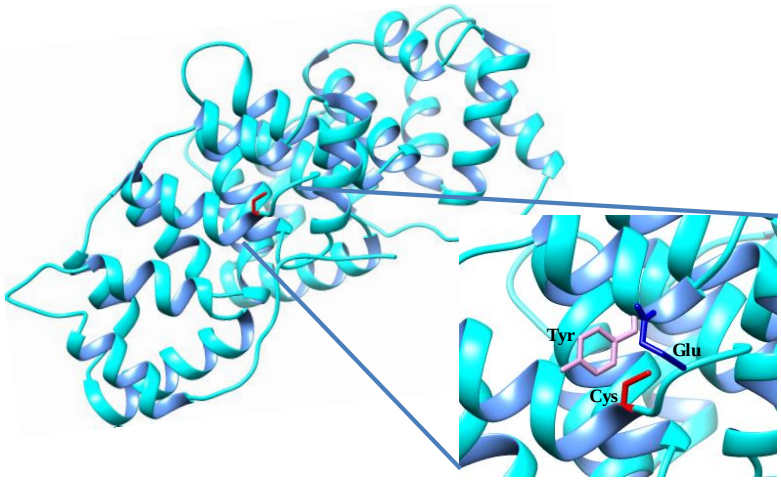

Figure 2.4 X-ray crystal structure (RCSB PDB-1ANW) shows a cysteine residue of wild-type ANV buried in helices (red highlighted).

Unfortunately, several attempts of Dha formation onto ANV in mild conditions failed. Reactions performed in denaturing conditions were envisioned as one possible way to solve this problem in order to increase the accessibility of the Dha reaction site. Thus, wild-type ANV(C316) was treated with DBHDA under denaturing conditions (3M GdmCl, pH 8.0). It was found that ANV(Dha316) completely formed, and was detected by LC-MS with the observed peak of Dha (MW: 35773 Da) corresponding to its calculated mass (MW: 35771 Da) (Figure **2.5**).

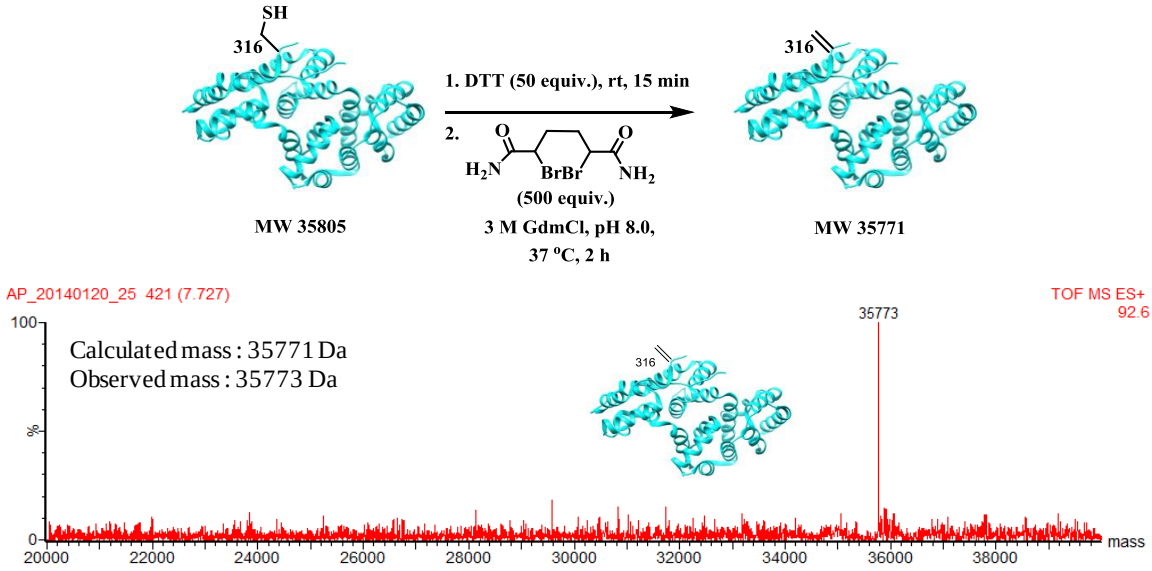

Figure 2.5 ESI-MS spectrum of wild-type ANV(C316) treated with DBHDA in denaturing conditions.

Unfortunately, despite the improved reaction conversion, subsequent refolding of ANV(Dha316) failed completely. Thus, we considered increasing the temperature as an alternative, mildly unfolding condition. A slight increase of temperature from 37 to 45 °C showed that ANV(Dha316) was successfully formed, and confirmed by LC-MS (Figure **2.6**).

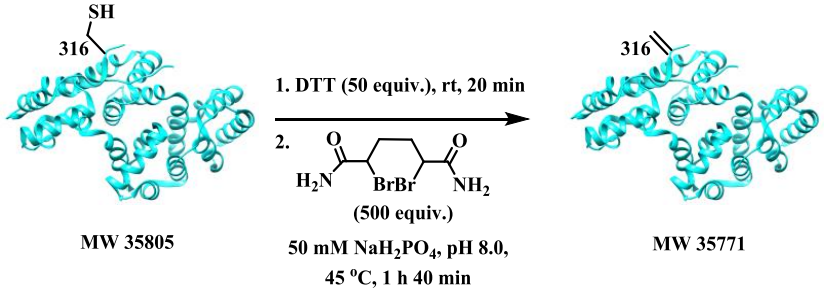

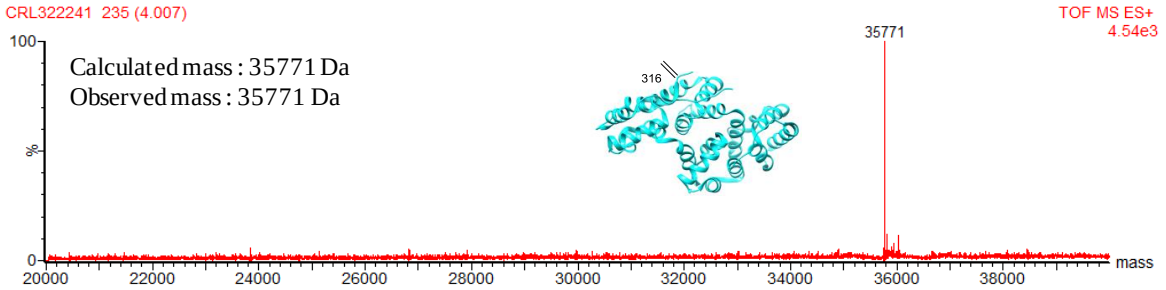

Figure 2.6 ESI-MS spectrum of wild-type ANV(C316) treated with DBHDA at 45°C.

To confirm installation of the Dha tag, we carried out two chemical control experiments. Treatment of ANV(Dha316) with 2-mercaptoethanol (*β*-ME) indeed showed a *β*-ME adduct formed by nucleophilic attack of thiol (*β*-ME) on Dha. On the other hand, no disulfide bridge formation of ANV(Dha316) after DTNB treatment was detected by LC-MS, confirming the absence of any remaining cysteine (Figure **2.7**).

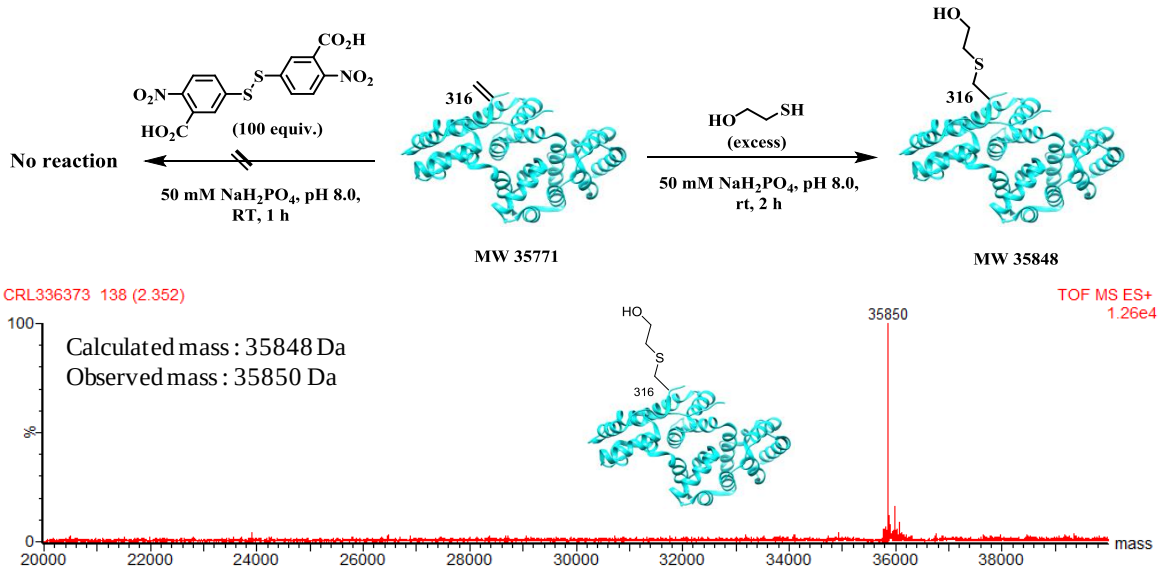

Figure 2.7 ESI-MS spectrum of *β*-ME adduct confirmed by treatment of ANV(Dha316) with *β*-ME and DTNB as chemical controls.

After bis-alkylation/elimination of the wild-type annexin V, ANV(Dha316) was used as a starting material for an initial study of protein fluorination reactions. A chemical method for direct C-F bond formation onto protein was initially investigated by treatment of ANV(Dha316) with Selectfluor *bis*(triflate) (0.5-2.0 equiv.), resulting in the formation of a mixture of fluorinated products (Dfa/Hfa) detected by LC-MS (Table **2.1**).

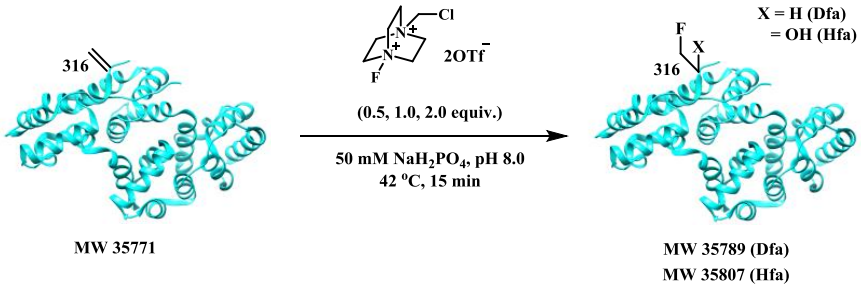

Entry	ANV(Dha316) (equiv.)	Selectfluor *bis*(triflate) (equiv.)	Reaction conditions[a]	Product conversion (%)[b]
1	1.0	0.5	42 °C, 15 min	Dha (63), Dfa (27), Hfa (13)
2	1.0	1.0	42 °C, 15 min	Dha (42), Dfa (39), Hfa (19)
3	1.0	2.0	42 °C, 15 min	Dha (14), Dfa (34), Hfa (34)

General conditions: a). ANV(Dha316) in NaH_2PO_4 (50 mM, pH 8) and Selectfluor *bis*(triflate) in acetone at 42 °C for 15 min unless otherwise indicated. b). Calculated by LC-MS.

Table 2.1 Optimisation of fluorination reactions of ANV(Dha316) using Selectfluor *bis*(triflate) as a fluorinating agent.

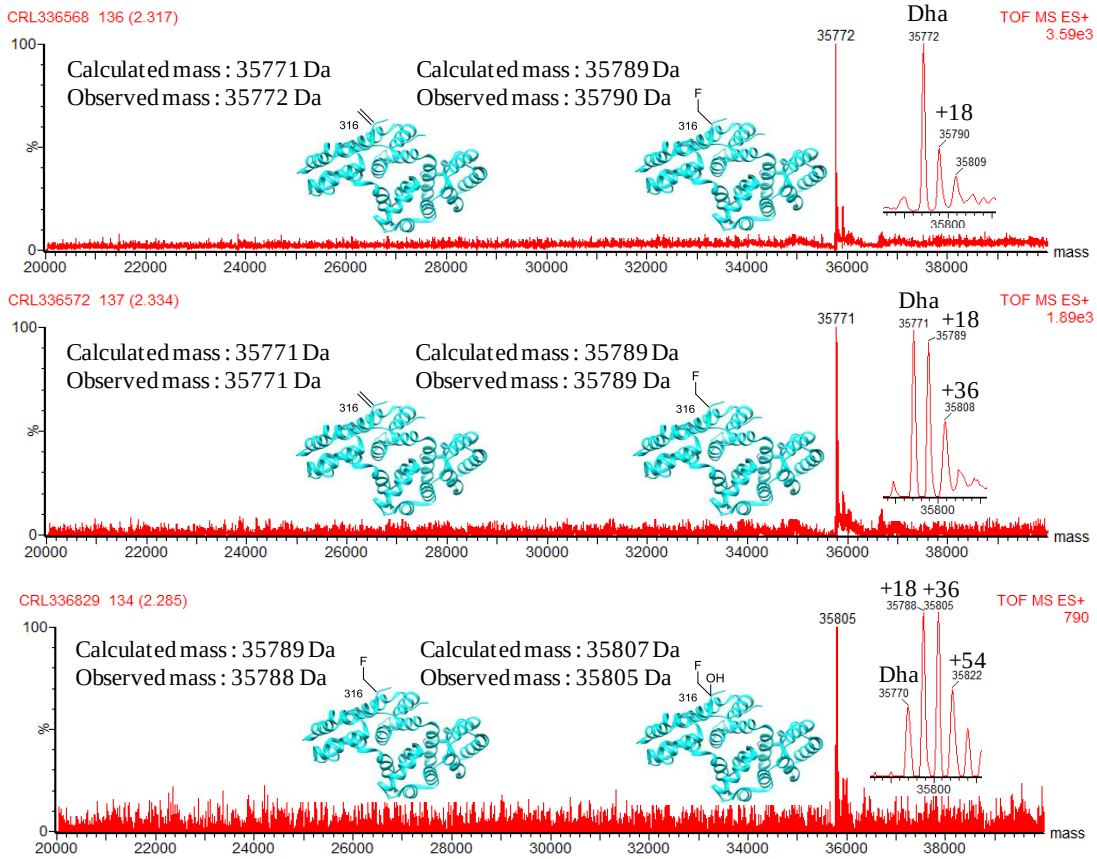

Figure 2.8 ESI-MS spectra of fluorinated ANV from reactions of ANV(Dha316) treated with 0.5-2.0 equiv. Selectfluor *bis*(triflate) as a fluorinating agent.

We further investigated chemoselectivity between the Dha-tagged ANV and the wild-type ANV by reactions of either ANV(Dha316) or ANV(C316) with 20 equiv. Selectfluor *bis*(triflate) (Scheme **2.5**). Unfortunately, the fluorinated protein was not clearly detected by LC-MS analysis which generated a complex ESI-MS spectrum. The fluorinated annexin V was alternatively characterised by SDS-PAGE, western blot, CD and MSMS, which clearly showed the protein was not degraded. When analysed by MSMS, it was found that ANV(Dha316) showed a preferential chemoselectivity over wild-type ANV by the detection of the corresponding fluorinated ANV (Dfa/Hfa). In the case of wild-type annexin V, a methionine-oxidised product was the major product observed by MSMS, and the fluorinated tyrosine was also shown at a low level of detection based on comparative expectation values. (See experimental details, Table **2.5**).

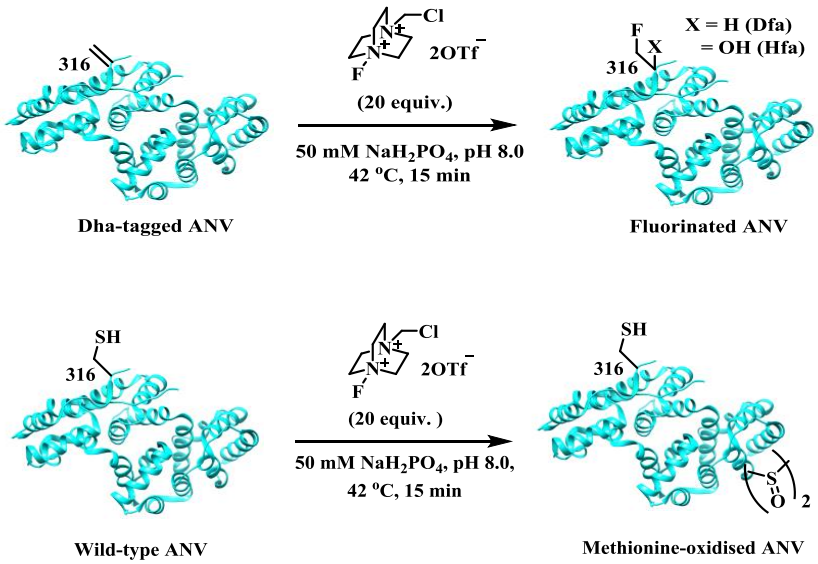

Scheme 2.5 A chemoselectivity comparison of Dha-tagged ANV and wild-type ANV.

A mixture of the fluorinated products was further examined by MSMS analysis, indicating that formation of dehydrofluoroalanine (Dfa) on the protein backbone was found on the desired peptide (ALLLLCGEDD) (Figure **2.9**). Furthermore, hydroxyfluoroalanine (Hfa) existing in an equilibrium based on our proposed mechanism (Scheme **2.4**) was also detected, which showed the desired modification at Dha316 (Figure **2.9**). As a side reaction, some methionine residues were oxidised by Selectfluor

bis(triflate), but these oxidised products had no major effect on the protein function (See a following session).

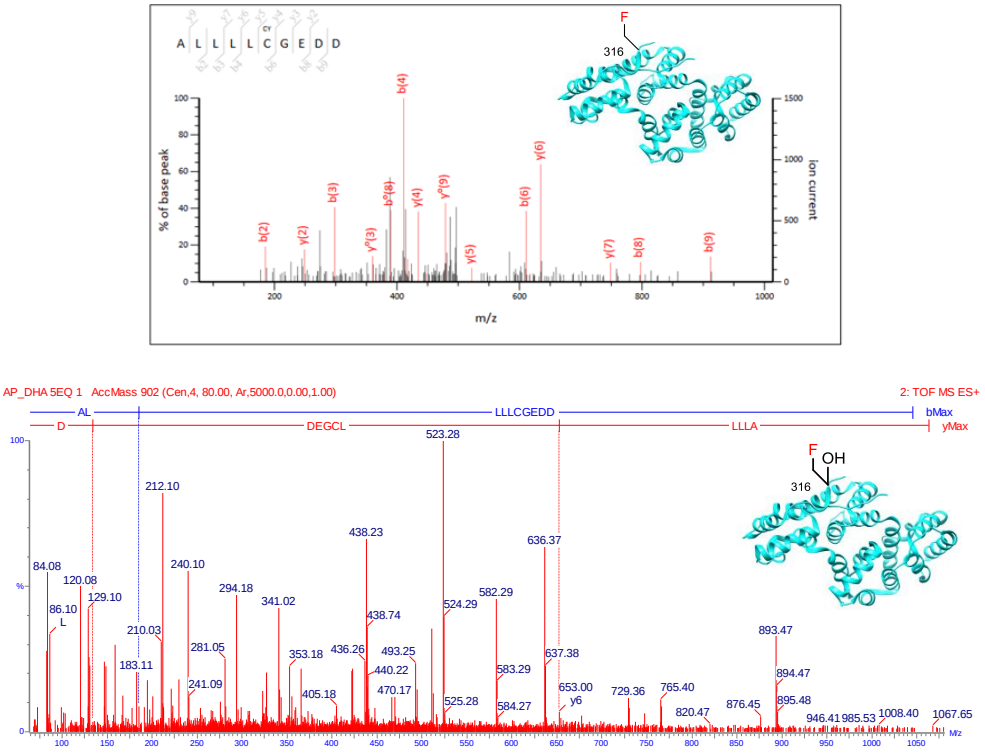

Figure 2.9 Peptide fragmentation (ALLLLCGEDD) shows modification sites of either Dfa or Hfa using Mascot and Biolynx software, respectively.

Biologically, ANV acts as a biomarker for cell-death detection, and shows specific binding to phosphatidylserine (PS), which allows movement from the inner to the outer cellular membranes caused by apoptosis[26-29]. For apoptosis experiments, we used Alexa Fluoro^{TM}488 NHS ester as a fluorescent dye, propidium iodide (PI) as a nuclei staining dye (a marker for dead cells), and actinomycin D as an apoptosis inducer. In order to test its activity, fluorescent labelling of a mixture of the fluorinated annexin V was successfully conducted by lysine modification of ANV(Dfa/Hfa316) with Alexa Fluoro^{TM}488 NHS ester (See experimental details, Figure **2.41**). The fluorescently-labelled ANV(Dfa/Hfa316) was used to investigate its binding activity to PS in the outer membrane, resulting in observation of green fluorescent signals on HEK293 cells' outer cellular membranes (Figure **2.10**). This ANV(Dfa/Hfa316) (**II**) showed a similar trend of the binding activity as compared to wild-type ANV (**I**) with a fluorescent tag. Two control experiments were used to investigate selectivity. The first control (**III**) showed no

binding of the labelled ANV(Dfa/Hfa316) on cellular membrane when apoptosis was not induced by actinomycin D in HEK293. The latter control (**IV**) also showed no binding affinity of the labelled fluorinated ANV, after all apoptotic HEK293 cells were blocked by pre-treatment with non-fluorescently-labelled wild-type ANV prior to addition of the labelled ANV(Dfa/Hfa316). According to the apoptosis experimental results, it was found that the chemically modified annexin V still remained its protein function post chemical fluorination reactions.

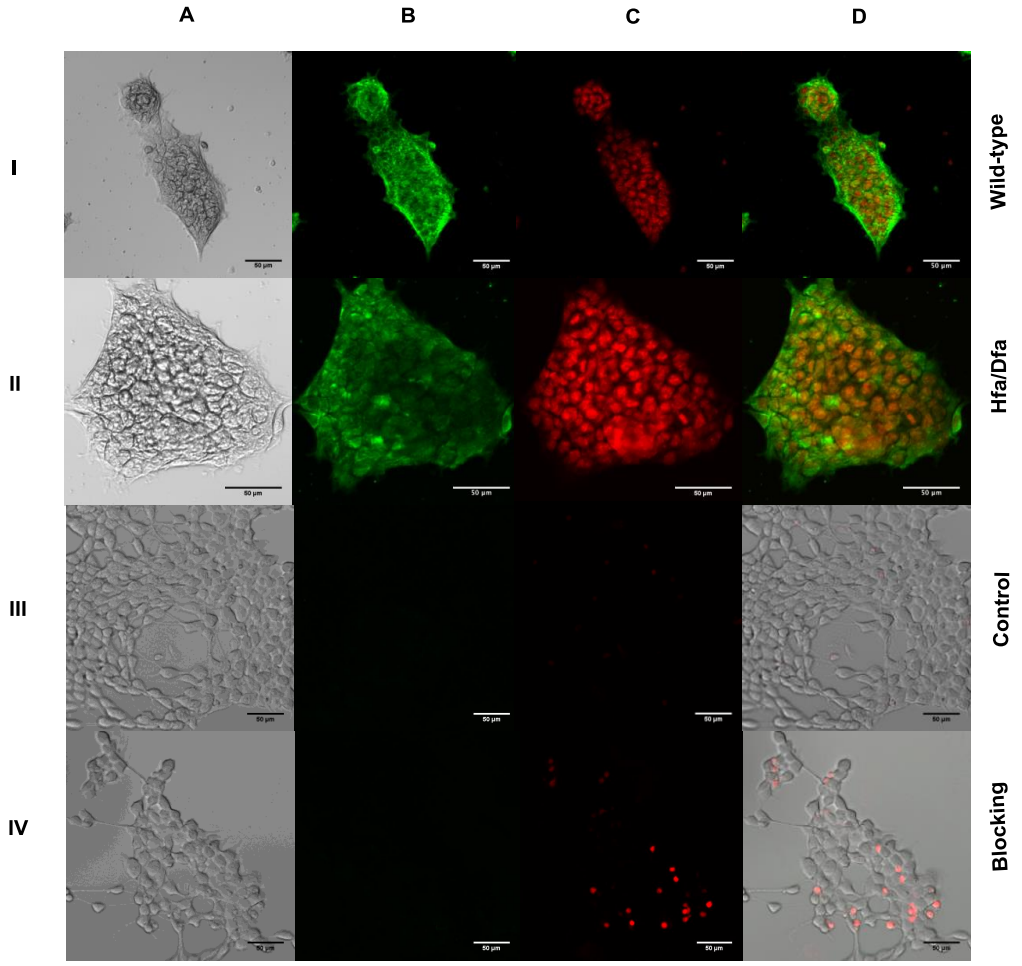

Figure 2.10 Fluorescent images of apoptosis detection in HEK293 cells treated with fluorescently-labelled ANV(wild-type and Dfa/Hfa316). Channel A = bright field; Channel B = AlexaFluor^{TM}488-labelled ANV (WT or Hfa/Dfa); Channel C = propidium iodide (PI); Channel D = merged Channels (A+B+C or B+C); Scale bar = 50 μm. (I) AlexaFluor^{TM}488-labelled WT-ANV (6 μg), Actinomycin D, and PI. (II) AlexaFluor^{TM} 488-labelled Dfa/Hfa (6 μg), Actinomycin D and PI. (III) AlexaFluor^{TM}488-labelled Dfa/Hfa (6 μg) and PI (negative control of (II) with no Actinomycin-D). (IV) Pre-incubation with unlabelled WT-ANV (27 μg), Actinomycin-D and PI followed by addition of AlexaFluor^{TM}488-labelled Dfa/Hfa (4.5 μg).

2.3 Site-Selective [^{18}F]-Radiolabelling of Protein for Preclinical Animal Studies

We were able to extend our new protein fluorination concept to [^{18}F]-radiolabelling of proteins as late-stage fluorination. As previously described, ANV(Dha316) used as a substrate was treated with [^{18}F]-Selectfluor *bis*(triflate) directly generated from a reaction of Selectfluor precursor with [^{18}F]F_2[36]. A reaction was then performed at 42 °C for 15 min prior to purification by simple desalting columns. After desalting, the [^{18}F]-labelled ANV was analysed by a radio-HPLC showing a protein peak labelled by [^{18}F]-radioactive Selectfluor *bis*(triflate). The wild-type ANV was also treated with radio-Selectfluor *bis*(triflate) as a control, resulting in no formation of [^{18}F]-labelled ANV detected by the radio-HPLC (Figure **2.11**). This result supports chemoselectivity for Dha residues over any naturally occurring residues of the wild-type protein.

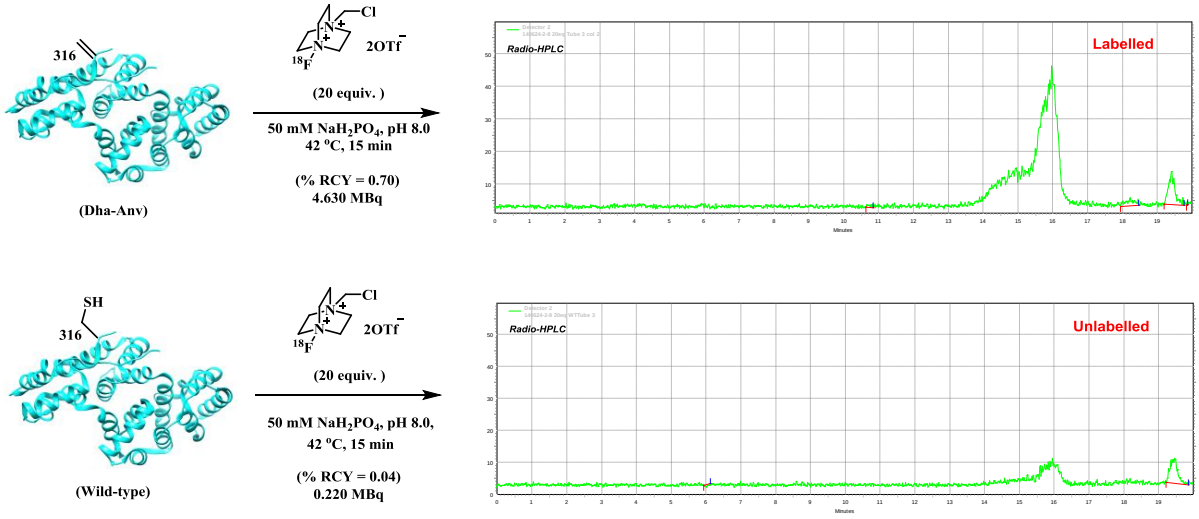

Figure 2.11 A comparison between [^{18}F]-radiolabelling of ANV(Dha316) and ANV(C316) shows a preferential labelling of the Dha-tag over the wild-type evidenced by each radio-HPLC profile.

The application of this methodology in a preclinical animal study was demonstrated by *in vivo* imaging of cell-death detection through positron emission tomography (PET) imaging. The radioactivity of the purified radiotracer was measured and subsequently injected intravenously, leading to imaging of cell-death in liver treated with cycloheximide as a potent inducer of apoptosis (Figure **2.12**). For blocking experiments as a control, excess non-radiolabelled annexin V was directly injected to mature rats pre-

treated by cycloheximide. After 1 h incubation, the [^{18}F]-radiolabelled annexin V was next injected to visualise cell-death in liver tissue (Figure **2.12**). In this control, lower binding of the radiolabelled annexin V was observed at cellular surfaces of the injured liver comparable to direct injection of the radiolabelled tracers, due to pre-treatment with non-radiolabelled protein. According to the plot, it clearly showed an increase binding caused by apoptosis, which could be blocked by pre-treatment of excess wild-type annexin V. This demonstrated that this novel method is both straightforward and useful in the [^{18}F]-radiolabelling of proteins without structural disruption.

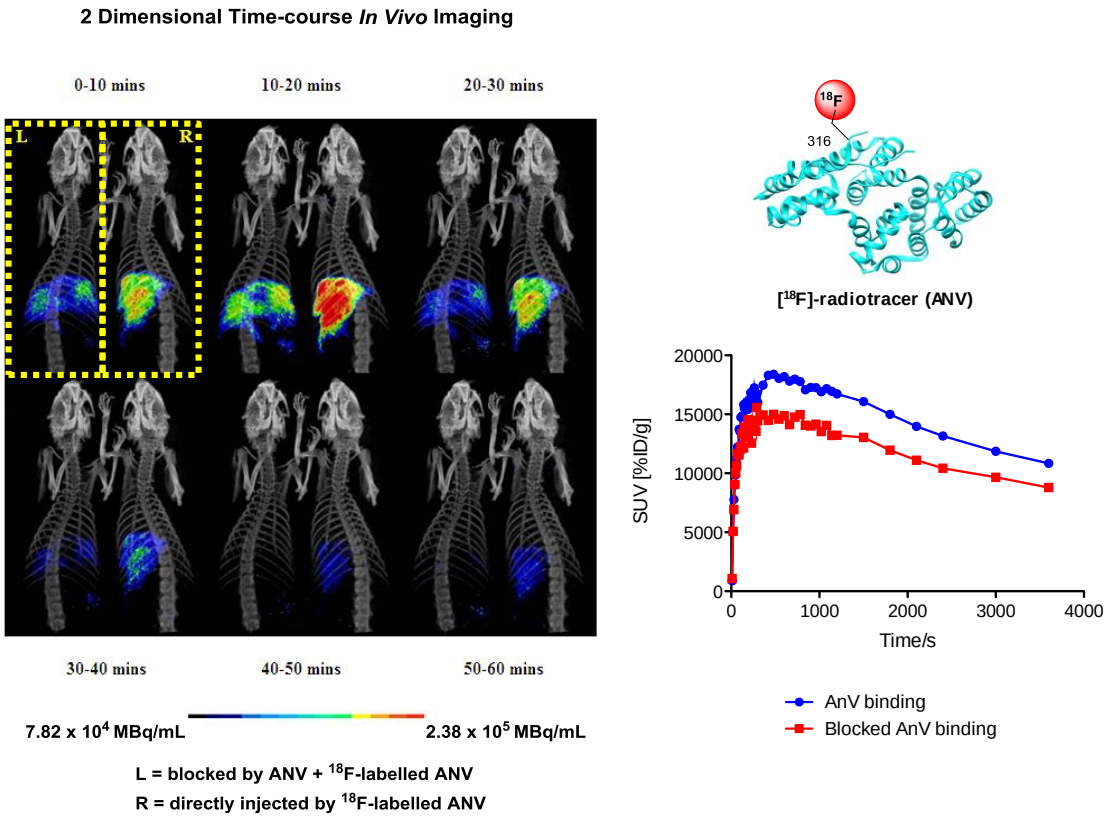

Figure 2.12 2D time-course [^{18}F]-PET imaging of the apoptosis detection of cell-death in liver injured by pre-treatment of cycloheximide as a potent apoptotic inducer. This plot shows an increased binding with direct injection of the [^{18}F]-radiotracer (ANV)(blue curve), which was reduced by cycloheximide-treated animals with excess amount of non-radiolabelled tracers (red curve).

2.4 Direct Electrophilic Aromatic Fluorination of Protein

As previously mentioned, we observed a low level of tyrosine fluorination upon treatment of wild-type annexin V with Selectfluor (as a control), although the predominant reaction in this case was methionine oxidation, possibly due to the elevated temperature. We reasoned that we could optimise this process towards direct electrophilic aromatic fluorination reactions on non-Dha-containing proteins, thus providing an alternative fluorination manifold to the previously discussed Dha-fluorination. The wild-type ANV contains 12 tyrosine residues, allowing the use of this protein as a model study of tyrosine fluorination. New C-F bonds formation at tyrosine residues was successfully observed upon treatment of wild-type ANV with Selectfluor *bis*(tetrafluoroborate) (Table **2.2**). A mixture of fluorinated products consisting of difluorotyrosine and oxidised methionine was observed by LC-MS and MSMS analysis.

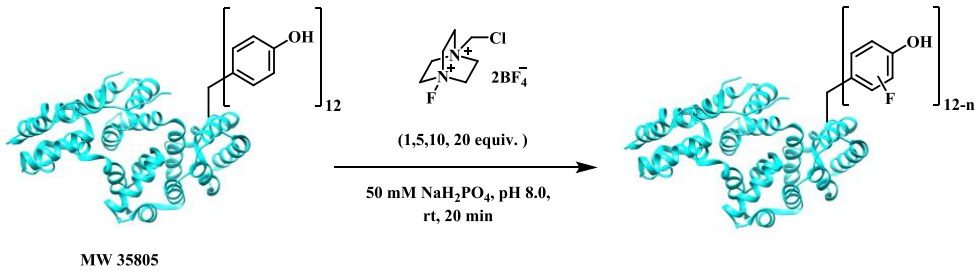

Entry	ANV (wild-type) (equiv.)	Selectfluor *bis*(tetrafluoroborate) (equiv.)	Reaction conditions[a]	Product conversion (%)[b]
1	1	1	25 °C, 20 min	SM (82) diF-Tyr (18)
2	1	5	25 °C, 20 min	diF-Tyr (91) diF-Tyr + Met(O) (9)
3	1	10	25 °C, 20 min	diF-Tyr (90) diF-Tyr + Met(O) (10)
3	1	20	25 °C, 20 min	diF-Tyr (72) diF-Tyr + Met(O) (18)

General conditions: a). ANV (wild-type) in NaH_2PO_4 (50 mM, pH 8) and Selectfluor *bis*(tetrafluoroborate) in H_2O at 25 °C for 20 min unless otherwise indicated; SM: starting material. b). Calculated by LC-MS. Met(O) = Methionine-oxidised products

Table 2.2 Optimisation of tyrosine fluorination of wild-type ANV using 1-20 equiv. Selectfluor *bis*(tetrafluoroborate) as a fluorinating agent.

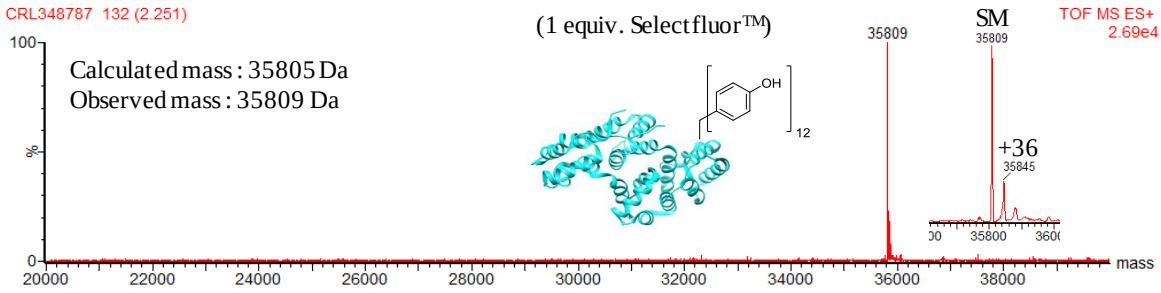

Figure 2.13 ESI-MS spectrum of wild-type ANV treated with 1 equiv. Selectfluor *bis*(tetrafluoroborate).

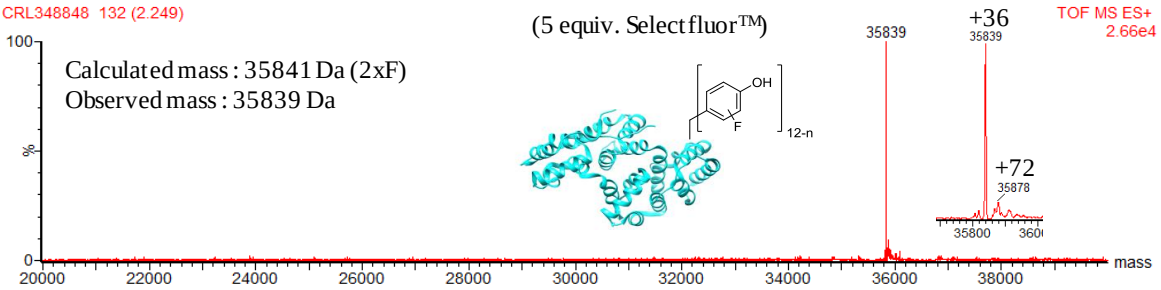

Figure 2.14 ESI-MS spectrum of wild-type ANV treated with 5 equiv. Selectfluor *bis*(tetrafluoroborate).

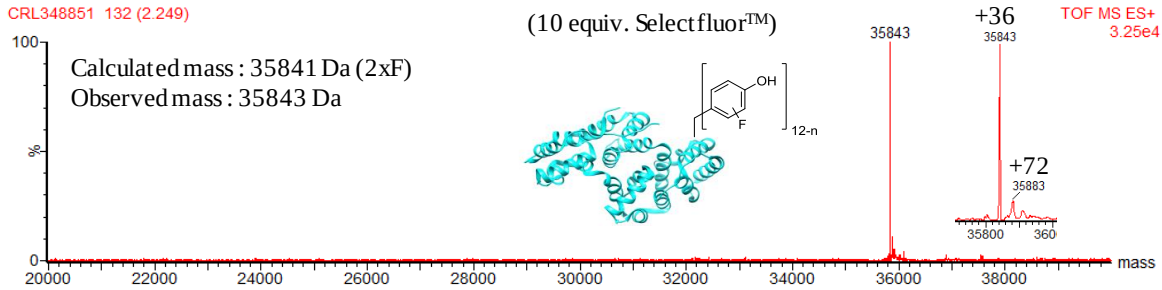

Figure 2.15 ESI-MS spectrum of wild-type ANV treated with 10 equiv. Selectfluor *bis*(tetrafluoroborate).

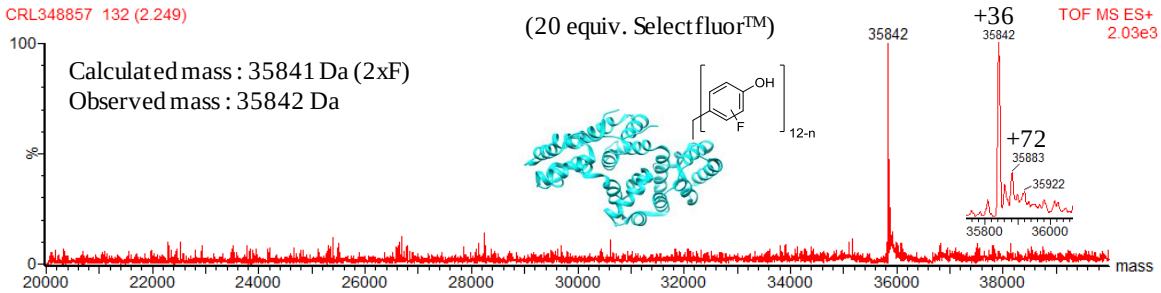

Figure 2.16 ESI-MS spectrum of wild-type ANV treated with 20 equiv. Selectfluor *bis*(tetrafluoroborate).

After protein modification, the function of the fluorinated annexin V was examined for apoptosis detection. Fluorescent labelling of both wild-type and fluorinated annexin V(diF-Tyr) was accomplished by treatment of wild-type and fluorinated proteins with 30 equiv. FITC (Figure **2.17**). The FITC-labelled proteins were then purified by fluorescent dye removal columns, prior to cell-death detection experiments.

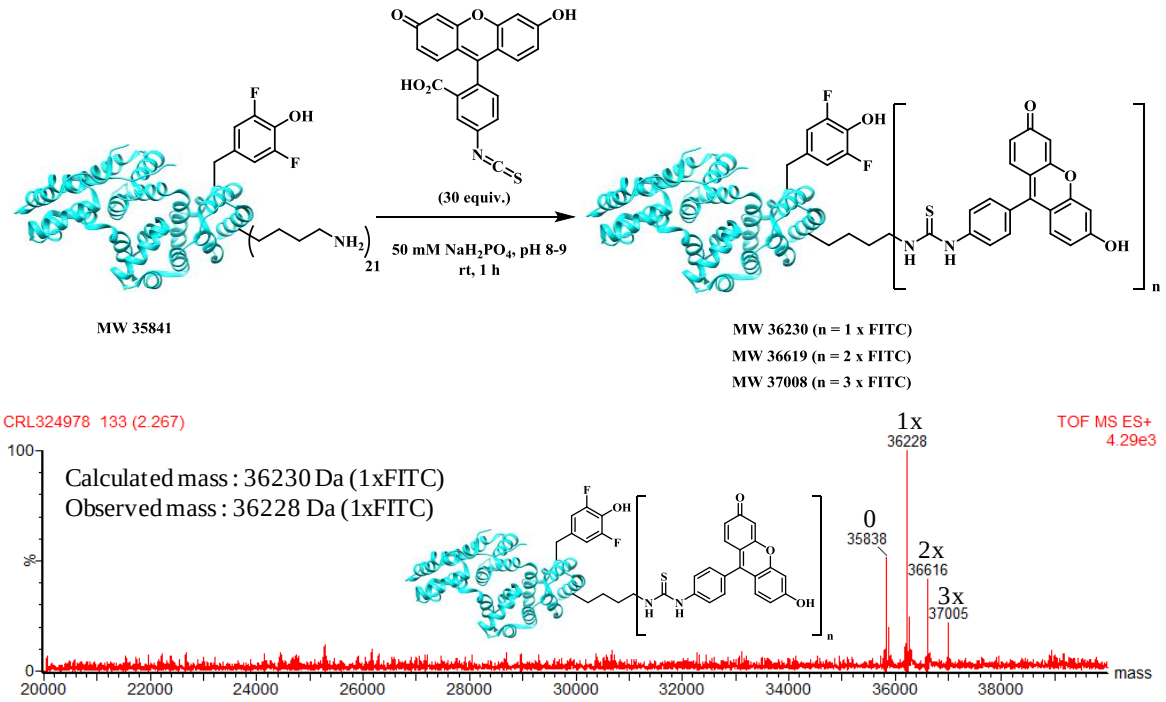

Figure 2.17 ESI-MS spectrum of fluorinated ANV (diF-Tyr) labelled with 30 equiv. FITC dye.

To confirm whether modified proteins are still active after fluorination reactions, we have demonstrated apoptosis detection. All fluorescent images of apoptotic-induced HEK293 cells were acquired by treatment of cells with fluorescent proteins/dyes prior to imaging using a confocal laser scanning microscope (Figure **2.18**). All active modified proteins showed fluorescent signals from apoptotic-induced HEK 293 cells (inducer: actinomycin D). Entries (**I-III**), the wild-type and fluorinated ANV (treated by 5 and 20 equiv. Selectfluor *bis*(tetrafluorborate)) showed both green (proteins) and red (nuclei) fluorescent signals, but the entry (**IV**) as a control showed no signals due the absence of actinomycin D. According to the blocking experiment, entry (**V**) revealed only red fluorescent signals from pre-treated cells by actinomycin D and subsequent non-fluorescent labelled wild-type ANV. Similarly to a previous study, this method also had

no influence on protein function. The modified annexin V after fluorination reaction was still active.

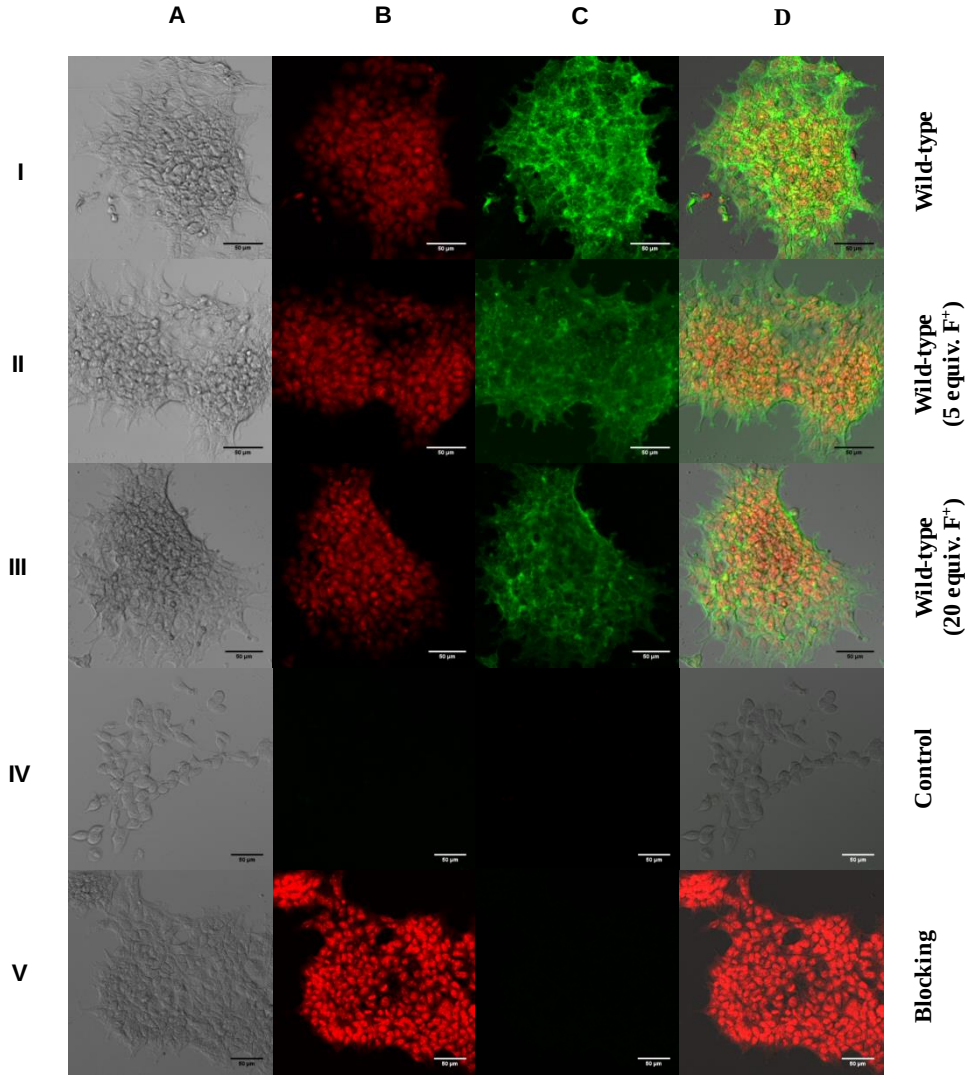

Figure 2.18 Fluorescent images of apoptosis detection in HEK293 cells treated with fluorescently-labelled ANV(wild-type and diF-Tyr): Channel A = bright field; Channel B = propidium iodide (PI); Channel C = FITC-labelled ANV (WT or diF-Tyr); Channel D = merged channels (A+B+C); Scale bar = 50 μm. (I) FITC-labelled WT-ANV (4.4 μg), Actinomycin D, and PI. (II) FITC-labelled ANV (treated by 5 equiv. Selectfluor *bis*(BF_4), diF-Tyr) (4.4 μg), Actinomycin D and PI. (III) FITC-labelled ANV(treated by 20 equiv. Selectfluor *bis*(BF_4), diF-Tyr) (4.4 μg) Actinomycin D and PI. (IV) FITC-labelled ANV(treated by 5 equiv. Selectfluor *bis*(BF_4), diF-Tyr) (4.4 μg) and PI (negative control of (II) with no Actinomycin D). (V) Pre-incubation with unlabelled WT-ANV (27 μg), Actinomycin D and PI; followed by addition of the FITC-labelled ANV (treated by 5 equiv. Selectfluor *bis*(BF_4), diF-Tyr) (4.4 μg).

2.5 Conclusion

In conclusion, our "Tag-and-Modify" approach enables direct C-F bond formation at pre-chemically installed sites (Dha) onto proteins of interest. A modified annexin V (Dha316) was used as a model protein to show fluorination on a protein backbone with minimal perturbation of wild-type structure. Based on this strategy, we were able to develop an efficient method for the [^{18}F]-radiolabelling of annexin V, thus enabling *in vivo* apoptosis detection of cell-death in liver by [^{18}F]-PET imaging. This novel approach shows the first report of direct, rapid and chemoselective incorporation of C-F bonds on protein, with applications for late-stage fluorination as well as application of real-time imaging of biologically-relevant processes. Furthermore, we are able to extend this methodology to create new C(sp^2)-F bonds on accessible tyrosine residues of the wild-type annexin V through direct chemoselective electrophilic aromatic fluorination.

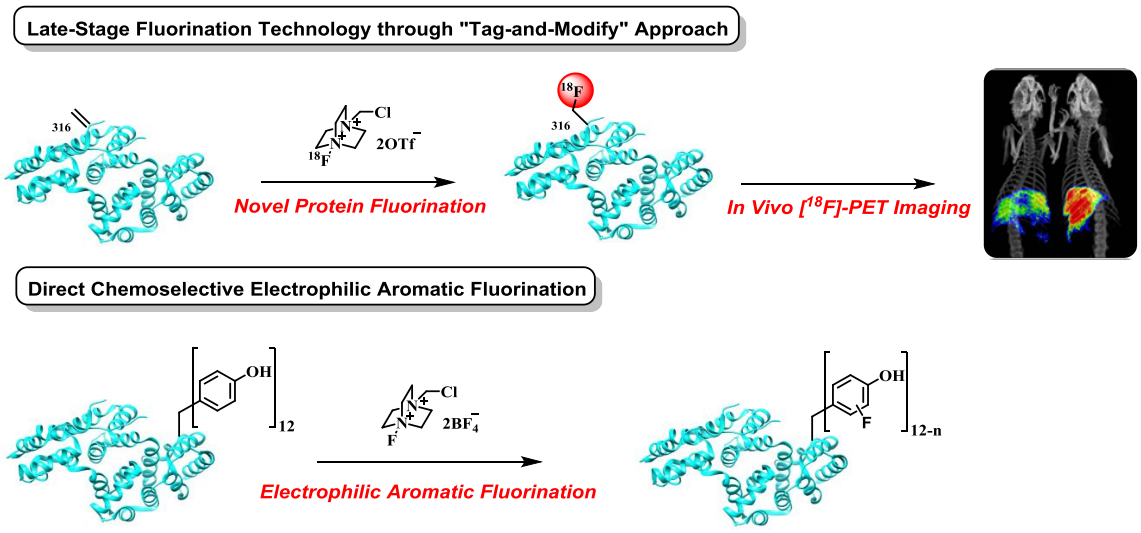

Scheme 2.5 Two novel strategies for protein fluorination through a "Tag-and-Modify" approach as well as direct electrophilic aromatic fluorination for C-F bond formation of proteins.

2.6 Experimental

Direct Electrophilic C-F Bond Formation of Annexin V at Dha-Site

2.6.1 Expression of Wild-type Annexin V[37]

The protein expression of wild-type annexin V was initially started from the transformation of the plasmid DNA, pET12a PAPI, (1 µL, conc. 150 ng/µL) into Novagen *E.coli* BL21/(DE3) singles competent cells. A single colony of annexin V bacterial cells was picked up and grown in 10 mL of LB media as a small starting culture containing ampicillin (100 µg/mL). This starting culture was incubated at 37 °C overnight, and was then used to inoculate 1 L of LB media containing ampicillin (100 µg/mL). Cell cultures were incubated at 37 °C until an optical density value (OD_{600} ~0.6-0.7) was observed. The protein expression was induced by addition of 1 mM IPTG, and was further incubated at 37 °C for 4 h. After the incubation periods complete, the cell cultures were harvested by centrifugation (7,000 rpm, 10 min, 4 °C). The cell pellet was re-suspended in 40 mL of TBS buffer (50 mM Tris.HCl, 150 mM NaCl, pH 8.0), and was then centrifuged (7,000 rpm, 10 min, 4 °C). The cell pellet was re-suspended in 40 mL of $CaCl_2$ buffer (50 mM Tris.HCl, 10 mM $CaCl_2$, pH 7.2), and was then lysed with a combination of DNase (5 mg) and EDTA-free protease inhibitor cocktail (0.5 tablet). The cell suspension was gently shaken at 4 °C for 10 min on the rocking shaker, then sonicated (3 x 2 min), and the cell debris was harvested by centrifugation (20,000 rpm, 20 min, 4 °C). The supernatant was gently decanted and further discarded. The cell pellet was re-suspended in 20 mL of EDTA buffer (50 mM Tris.HCl, 20 mM EDTA, pH 7.2), and was then centrifuged (20,000 rpm, 20 min, 4 °C). The supernatant was collected and filtered through a 0.45 µm membrane filter, and was then dialysed with 3 x 2 L of Tris buffer (20 mM Tris.HCl, pH 8.0) at 4 °C overnight. The dialysed solution was purified by anion exchange column chromatography by running a gradient between buffer A (20 mM Tris.HCl, pH 7.8) and buffer B (20 mM Tris.HCl, 500 mM NaCl, pH 7.8) to afford the purified protein. This protein was then concentrated and ultrafiltered using a vivaspin column concentrator with a 10,000 Da MW cut-off membrane (3,750 rpm, 15 min, 4 °C). The protein was then filtered through a 0.20 µm membrane filter, and dialysed with 4 x 1 L of HEPES-Na buffer (20 mM HEPES-Na, 100 mM NaCl, pH 7.4) at 4 °C. The final

concentration of the purified protein was calculated as 33.6 mg/L using a NanoDrop 1000 A_{280} spectrophotometry. Annexin V was further filtered through a 0.20 µm membrane filter, then aliquoted into 20 x 200 µL of aliquots which were flash frozen with liquid nitrogen and stored at -80 °C for further manipulation. The desired protein was analysed by LC-MS spectrometry (Calc: 35805 Da (Met-truncation) and Obs: 35805 Da), and further structural analysis was done using circular dichroism (CD) spectrometry. The secondary structure of this protein was found to contain a pattern of α-helices, and its melting temperature (T_m) was approximately 50 °C.

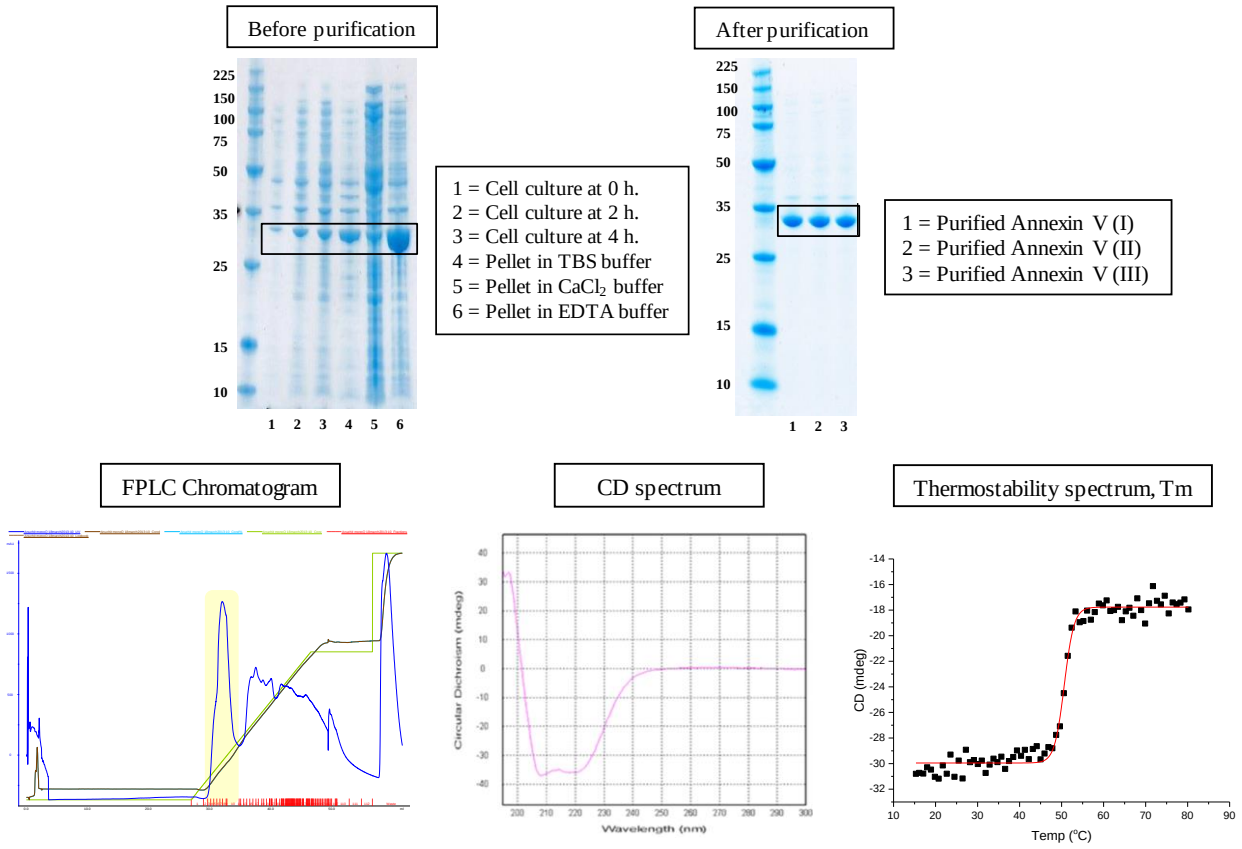

Figure 2.19 SDS-PAGEs and FPLC chromatogram show purification of wild-type annexin V expressed in *E.coli* BL21 (DE3), CD spectrum of the wild-type annexin V (conc. 0.5 mg/mL in 50 mM NaH_2PO_4 pH 8.0) and its melting temperature, T_m = 50 °C.

Sequence of Wild-type Annexin V

MAQVLRGTVT DFPGFDERAD AETLRKAMKG LGTDEESILT LLTSRSNAQR QEISAAFKTL
FGRDLLDDLK SELTGKFEKL IVALMKPSRL YDAYELKHAL KGAGTNEKVL TEIIASRTPE
ELRAIKQVYE EEYGSSLEDD VVGDTSGYYQ RMLVVLLQAN RDPDAGIDEA QVEQDAQALF
QAGELKWGTD EEKFITIFGT RSVSHLRKVF DKYMTISGFQ IEETIDRETS GNLEQLLLAV
VKSIRSIPAY LAETLYYAMK GAGTDDHTLI RVMVSRSEID LFNIRKEFRK NFATSLYSMI
KGDTSGDYKK ALLLLCGEDD

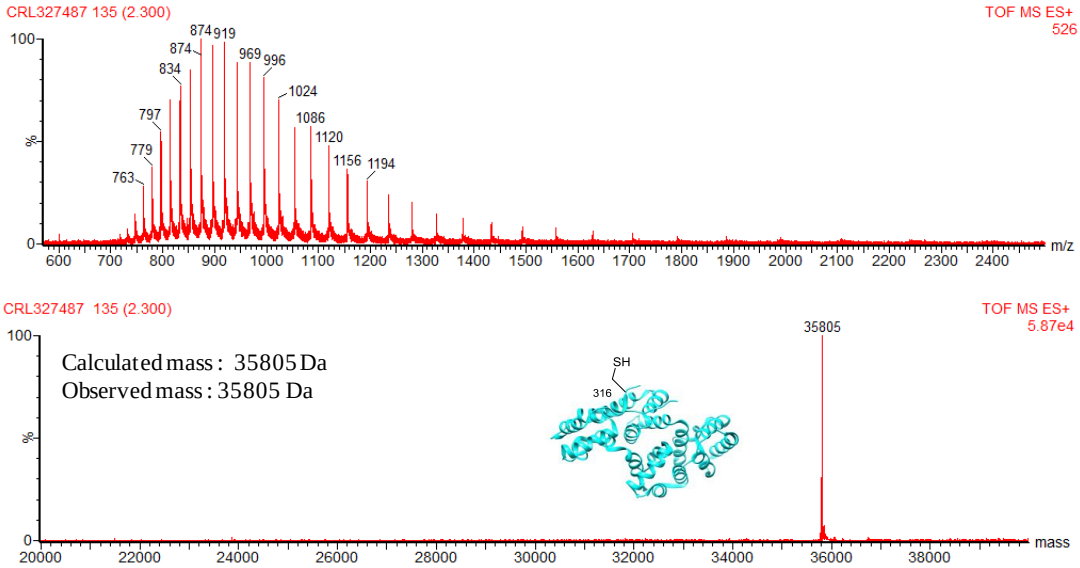

Figure 2.20 ESI-MS spectrum of wild-type annexin V expressed from *E.coli* BL21(DE3).

Control : Ellman's Reagent (DTNB) Addition

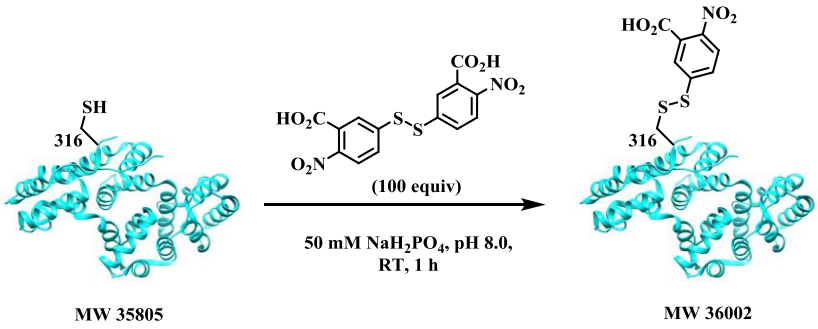

An aliquot of wild-type annexin V (C316) (4.19 nmol, 1.50 mg/mL, 100 µL) in 50 mM NaH_2PO_4, pH 8.0 was treated with a solution of DTNB in DMSO (0.419 µmol, 8.3 µL from a stock solution, conc. 20 mg/mL), and the reaction mixture was shaken at room temperature for 1 h. The protein was purified using a vivaspin column concentrator with a 10,000 Da MW cut-off membrane (9x times) loading fresh 50 mM NaH_2PO_4, pH 8.0 each time. The purified protein was analysed by LC–MS spectrometry (Calc: 36002 Da and Obs: 36005 Da).

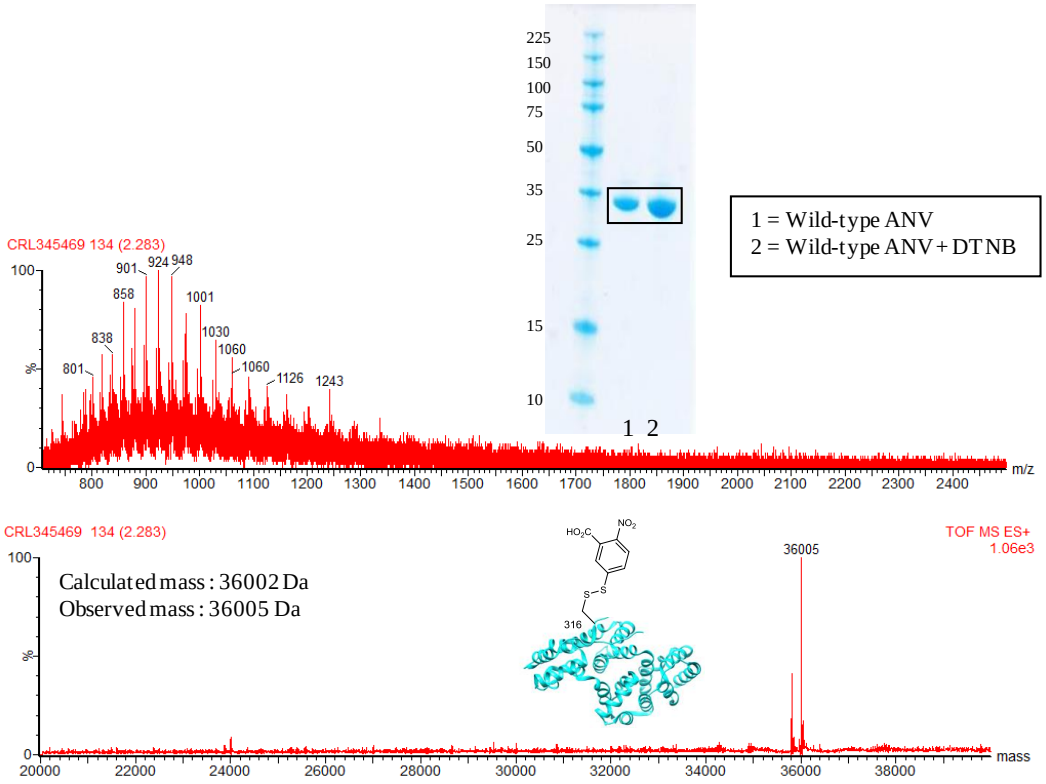

Figure 2.21 SDS-PAGE and ESI-MS spectrum of wild-type annexin V(C316) treated with 100 equiv. DTNB.

2.6.2 Dehydroalanine (Dha) Formation of the Annexin V(C316)

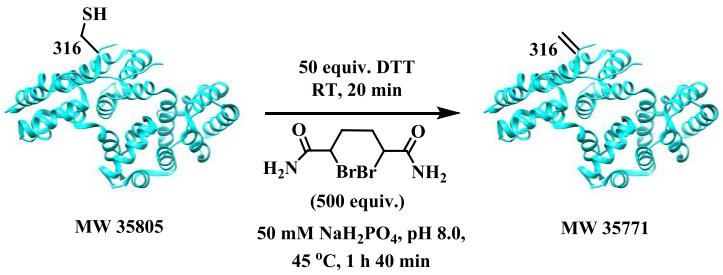

An aliquot of wild-type annexin V(C316) (48.3 nmol, 1.92 mg/mL, 0.9 mL) in 50 mM NaH_2PO_4, pH 8.0 was treated with a solution of DTT in H_2O (2.42 µmol, 43 µL from a stock solution, (8.6 mg/mL), and the reaction mixture was shaken at room temperature for 20 min. A solution of DBHDA in DMF (24.2 µmol, 9 x 5.4 µL from a stock solution, conc. 150 mg/mL) was added to each aliquot of the protein mixture (9 x 100 µL), then was vortexed briefly. Each reaction mixture was allowed to shake at 45 °C for 1 h 40 min. After the reactions complete, each sample was combined and collected as an aliquot

(10 µL) which was analysed by LC-MS spectrometry (Calc: 35771 Da and Obs: 35773 Da). The protein was purified using a vivaspin column concentrator with a 10,000 Da MW cut-off membrane (9x times) loading fresh 50 mM NaH_2PO_4, pH 8.0 each time.

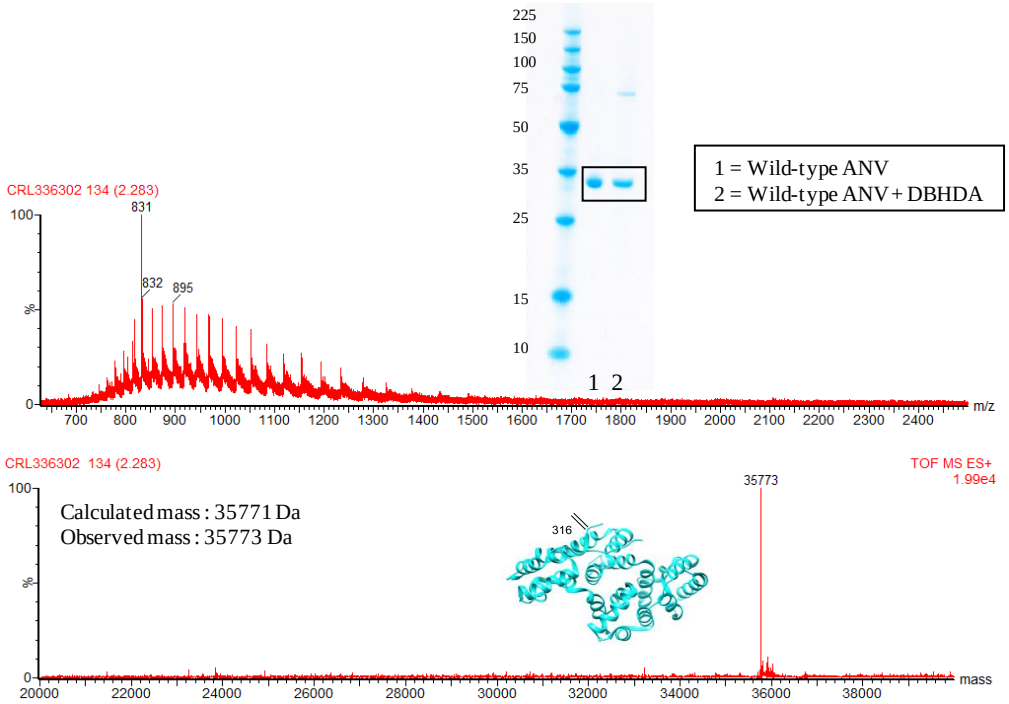

Figure 2.22 SDS-PAGE and ESI-MS spectrum of wild-type annexin V(C316) treated with 500 equiv. DBHDA.

Control: Ellman's Reagent (DTNB) Addition

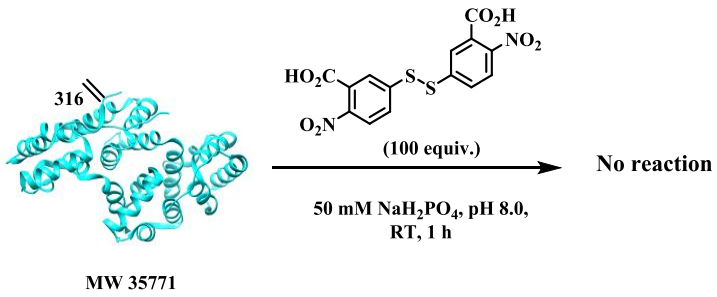

An aliquot of annexin V (Dha316) (4.33 nmol, 1.55 mg/mL, 100 µL) in 50 mM NaH_2PO_4, pH 8.0 was treated with a solution of DTNB in DMSO (0.433 µmol, 8.6 µL from a stock solution, conc. 20 mg/mL), and was shaken at room temperature for 1 h. The protein was purified using a vivaspin column concentrator with a 10,000 Da MW cut-off membrane (9x times) loading fresh 50 mM NaH_2PO_4, pH 8.0 each time. The

purified protein was analysed by LC–MS spectrometry (Calc: 35771 Da and Obs: 35771 Da).

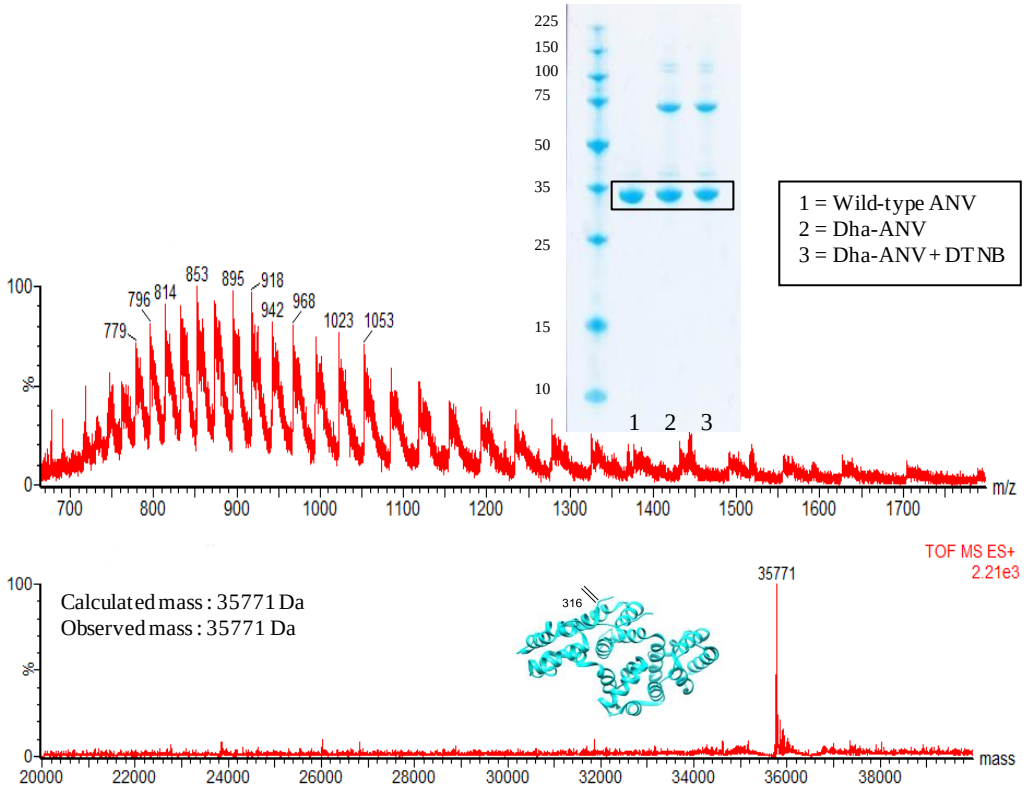

Figure 2.23 SDS-PAGE and ESI-MS spectrum of annexin V (Dha316) treated with 100 equiv. DTNB.

Control: 2-Mercaptoethanol (*β*-ME) Addition

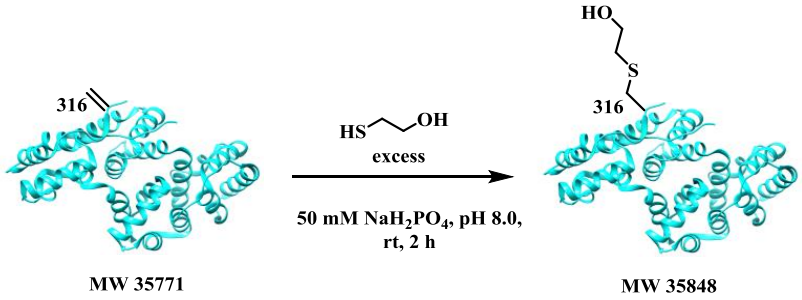

An aliquot of annexin V(Dha316) (0.81 nmol, 1.45 mg/mL, 20 µL) in 50 mM NaH_2PO_4, pH 8.0 was mixed with a solution of 2-mercaptoethanol (*β*-ME) (1.0 µL) by vortexing briefly. The reaction mixture was allowed to shake at room temperature for 2 h. An aliquot (5 µL) was directly analysed by LC–MS spectrometry (Calc: 35848 Da and Obs: 35850 Da).

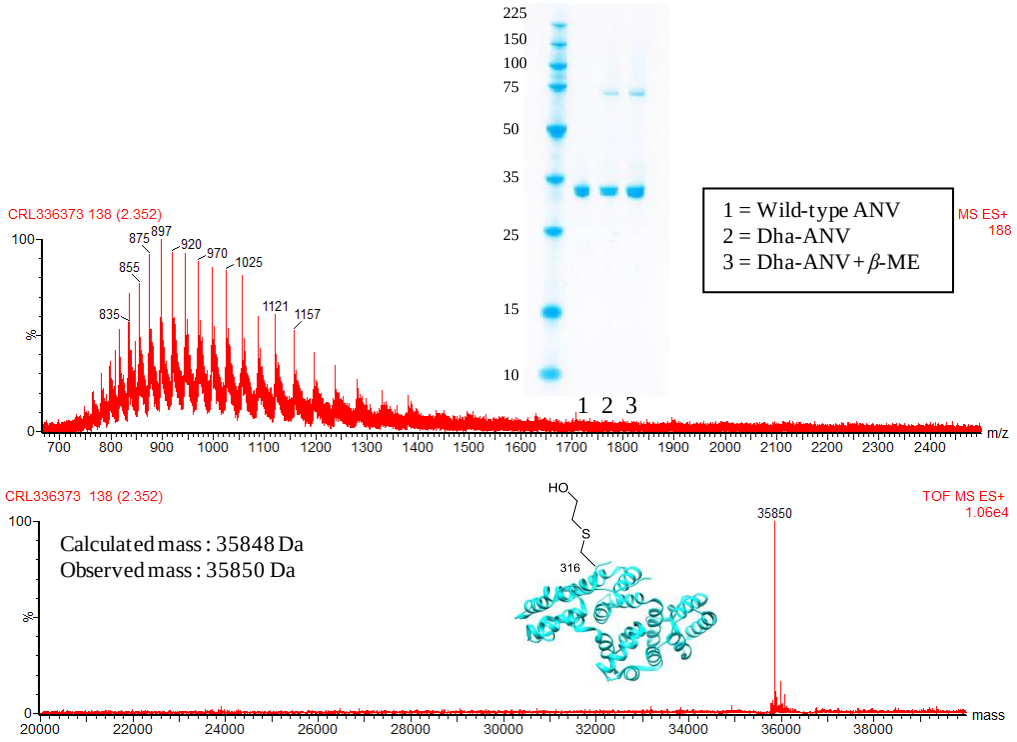

Figure 2.24 SDS-PAGE and ESI-MS spectrum of annexin V (Dha316) treated with excess *β*-ME.

2.6.3 Direct Electrophilic Fluorination Reactions of Annexin V

Fluorination of the Annexin V(Dha316)

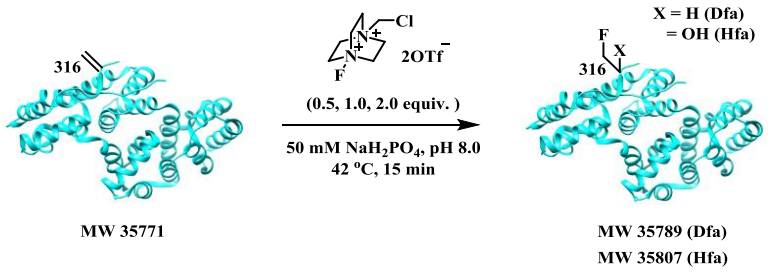

Each aliquot of annexin V(Dha316) (8.67 nmol, 1.55 mg/mL, 200 µL) in 50 mM NaH_2PO_4, pH 8.0 was mixed with a solution of Selectfluor *bis*(triflate) in acetone (4.34, 8.67, 17.3 nmol, 1.0, 2.0, 4.1 µL from a stock solution, conc. 2.0 mg/mL) by vortexing briefly. After 15 min of shaking at 42 °C, each aliquot was analysed by LC–MS spectrometry (Dfa; Calc: 35789 Da and Obs: 35789 Da, Hfa; Calc: 35807 Da and Obs: 35808 Da) after desalting by vivaspin column concentrators with a 10,000 Da MW cut-

off membrane (6x times) loading fresh 50 mM NaH_2PO_4, pH 8.0 each time. Protein samples were flash frozen with liquid nitrogen and stored at –80 ºC.

Entry	ANV(Dha316) (equiv.)	Selectfluor *bis*(triflate) (equiv.)	Reaction conditions[a]	Results (Da)	Product conversion (%)[b]
1	1.0	0.5	42 °C, 15 min	35772 (Dha) 35790 (Dfa) 35809 (Hfa)	63 27 13
2	1.0	1.0	42 °C, 15 min	35771 (Dha) 35789 (Dfa) 35808 (Hfa)	42 39 19
3	1.0	2.0	42 °C, 15 min	35770 (Dha) 35788 (Dfa) 35805 (Hfa)	14 34 34

General conditions: a). ANV(Dha316) in NaH_2PO_4 (50 mM, pH 8) and Selectfluor *bis*(triflate) in acetone at 42 °C for 15 min unless otherwise indicated. b). Calculated by LC-MS.

Table 2.3 Optimisation of fluorination reactions of ANV(Dha316) using Selectfluor *bis*(triflate) as a fluorinating agent.

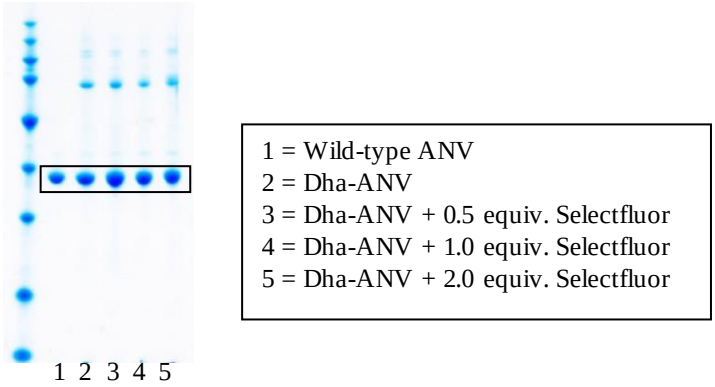

Figure 2.25 SDS-PAGE of wild-type annexin V (C316), annexin V(Dha316), and annexin V(Dha316) treated with 0.5, 1.0, and 2.0 equiv. Selectfluor *bis*(triflate), respectively.

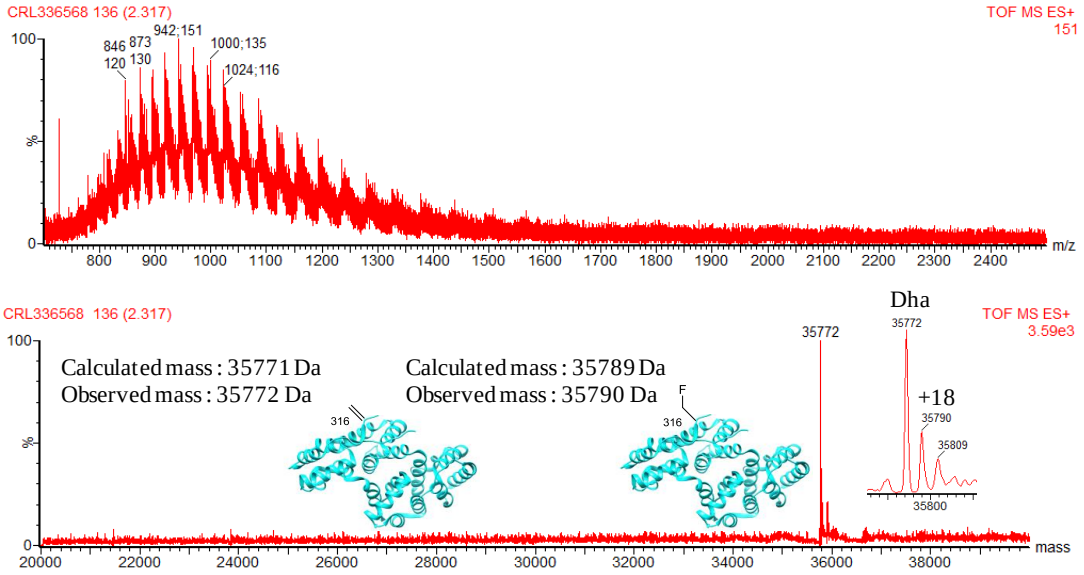

Figure 2.26 ESI-MS spectrum of annexin V (Dha316) treated with 0.5 equiv. Selectfluor *bis*(triflate).

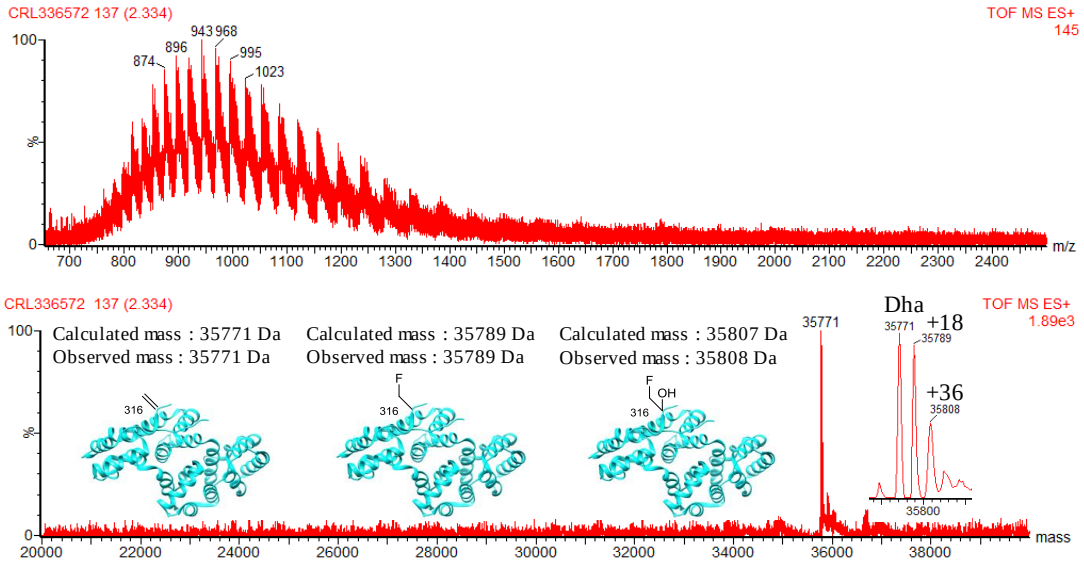

Figure 2.27 ESI-MS spectrum of annexin V (Dha316) treated with 1.0 equiv. Selectfluor *bis*(triflate).

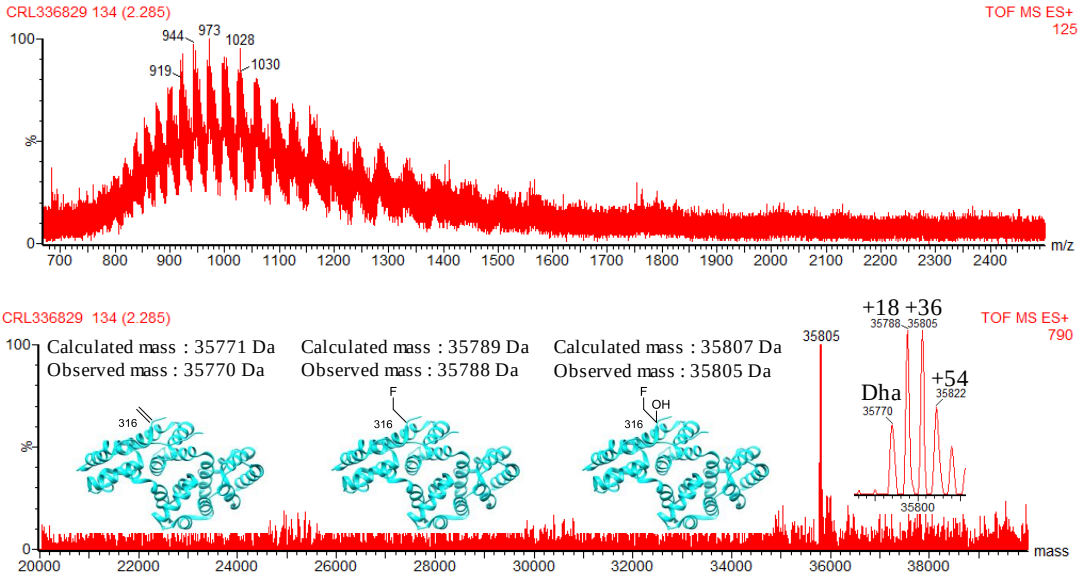

Figure 2.28 ESI-MS spectrum of annexin V (Dha316) treated with 2.0 equiv. Selectfluor *bis*(triflate).

Fluorination of the Annexin V(Dha316)

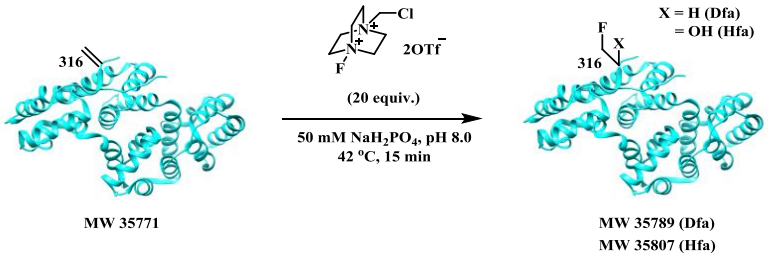

An aliquot of annexin V(Dha316) (8.67 nmol, 1.55 mg/mL, 200 µL) in 50 mM NaH_2PO_4, pH 8.0 was mixed with a solution of Selectfluor *bis*(triflate) in acetone (173 nmol, 7.5 µL from a stock solution, 11.0 mg/mL) by vortexing briefly. After 15 min of shaking at 42 °C, an aliquot was analysed by LC–MS spectrometry after desalting by a vivaspin column concentrator with a 10,000 Da MW cut-off membrane (6 x times) loading fresh 50 mM NaH_2PO_4, pH 8.0 each time. The LC-MS showed a complex ESI-MS spectrum, which was then further investigated by MS/MS analysis. Dfa and Hfa were observed on the desired peptide (ALLLLCGED), and some methionine-oxidised products were also found. A protein sample was flash frozen with liquid nitrogen and stored at –80 ºC.

Figure 2.29 SDS-PAGE of wild-type annexin V(C316), annexin V(Dha316), and annexin V(Dha316) treated with 20 equiv. Selectfluor *bis*(triflate).

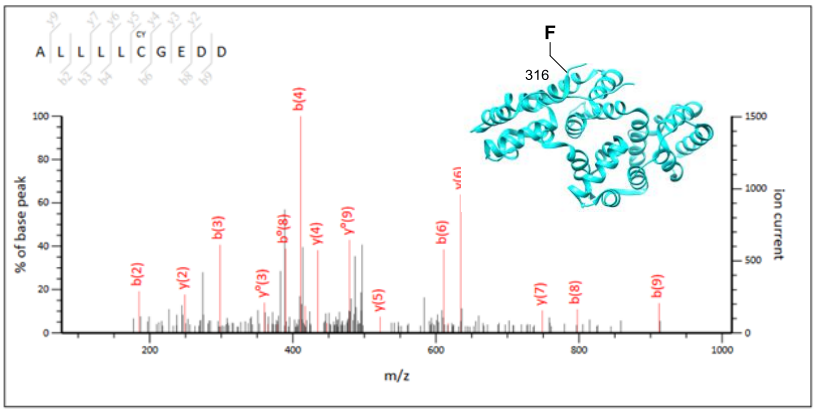

Figure 2.30 Peptide fragmentation of Dfa (C-316) ALLLLCGEDD analysed by Mascot database.

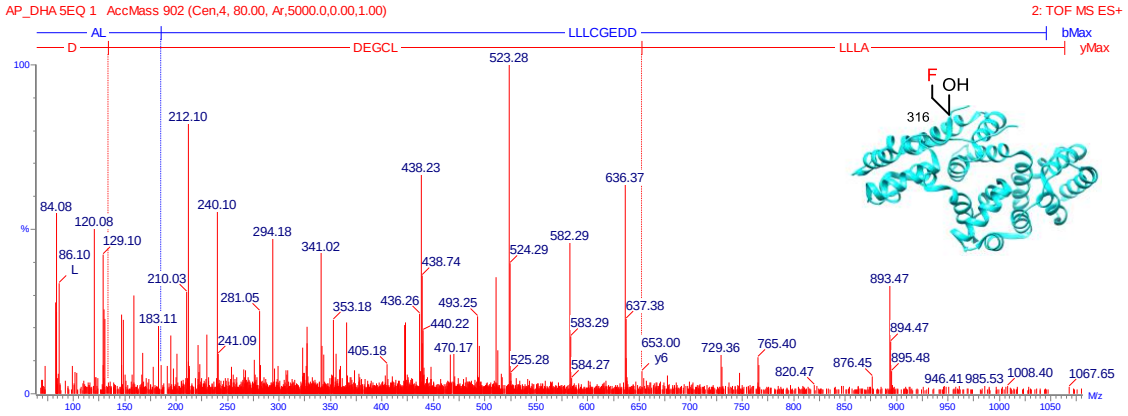

Figure 2.31 Peptide fragmentation of Hfa (C-316) ALLLLCGEDD analysed by Biolynx.

Control: Fluorination of Wild-type Annexin V(C316)

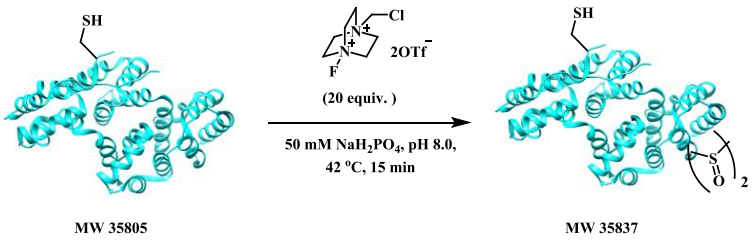

An aliquot of wild-type annexin V(C316) (6.79 nmol, 1.62 mg/mL, 150 µL) in 50 mM NaH_2PO_4, pH 8.0 was mixed with a solution of Selectfluor *bis*(triflate) in acetone (136 nmol, 5.9 µL from a stock solution, conc. 11.0 mg/mL) by vortexing briefly. After 15 min of shaking at 42 °C, each aliquot was analysed by LC–MS spectrometry (Calc: 35837 Da and Obs: 35840 Da) after desalting by a vivaspin column concentrator with a 10,000 Da MW cut-off membrane (6 x times) loading fresh 50 mM NaH_2PO_4, pH 8.0 each time. Also, MSMS analysis showed a majority of methionine-oxidised products, and also detected a monofluorinated tyrosine product. The purified protein sample was flash frozen with liquid nitrogen and stored at –80 ºC.

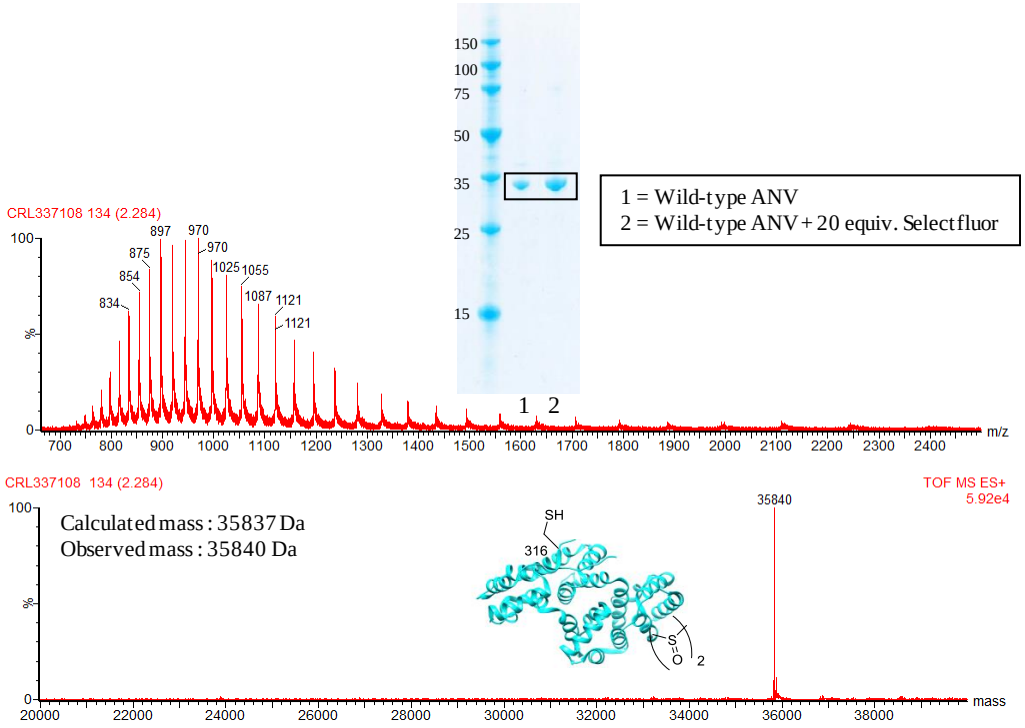

Figure 2.32 SDS-PAGE and ESI-MS spectrum of wild-type annexin V(C316) treated with 20 equiv. Selectfluor *bis*(triflate).

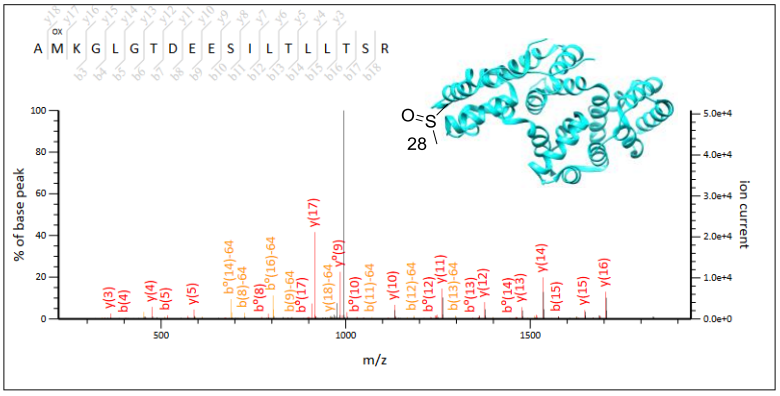

Figure 2.33 Peptide fragmentation of oxidised methionine (M-28) AMKGLGTDEESIL TLLTSR analysed by Mascot database.

2.6.4 Proteins Characterisation

Circular Dichroism (CD) Spectroscopy

Each protein sample (200 µL) was prepared at a concentration of 0.5 mg/mL in 50 mM NaH_2PO_4, pH 8.0, transferred into a quartz cuvette (1.0 mm path length, Starna scientific) and analysed by CD spectroscopy. Parameters on the Chirascan CD spectrometer were as follows;

1. Millidegrees
   - Absorbance
   - Auto PM
2. Temperature (°C) 25.0
3. Wavelength
   - Low 195.0 nm
   - High 300.0 nm
   - Step 1.0
4. Sampling
   - Time per point (s) 1.000
   - Current Time per point (s) 1.000
5. Baseline
   - 50 mM NaH_2PO_4, pH 8.0

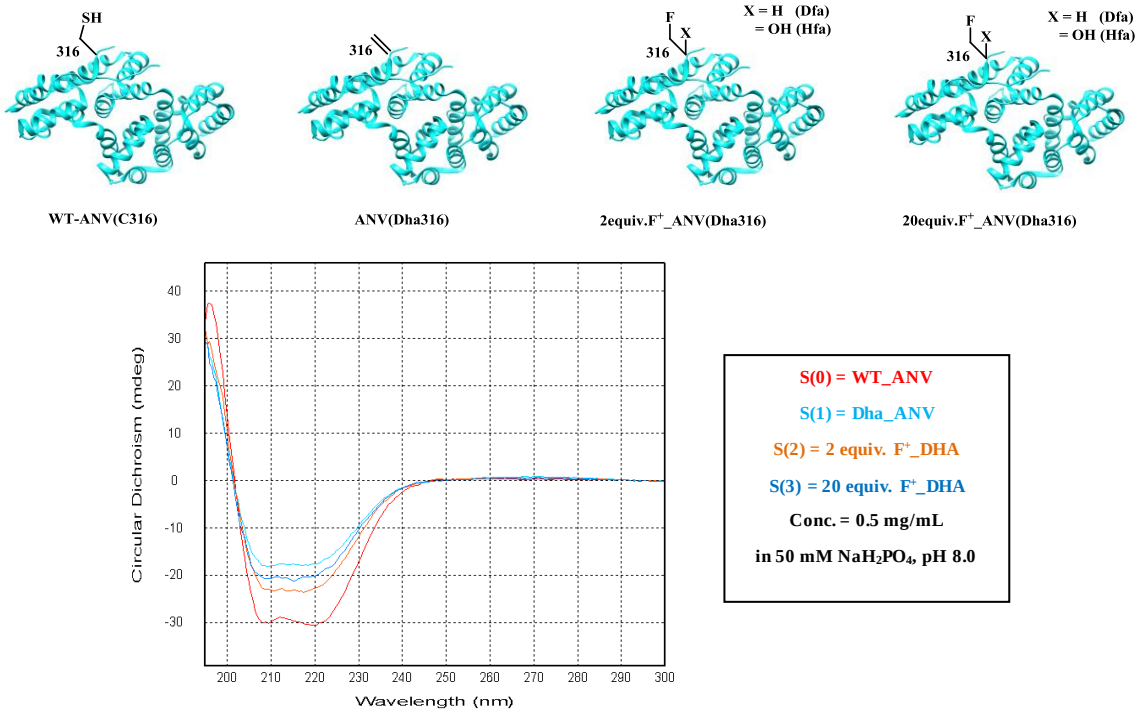

Figure 2.34 A comparison of circular dichroism (CD) spectra of wild-type annexin V(C316), annexin V(Dha316), and annexin V(Dha316) treated with 2 and 20 equiv. Selectfluor *bis*(triflate), respectively.

Western Blotting Analysis

(See general experimental considerations in appendix)

Entry	Antibodies	Blocking agent	Dilution	Conditions
1	Anti-Human Annexin V monoclonal antibody produced in mouse ***(Primary) IgG2a***	BSA in TBST	1 : 20,000	1 h, RT
	Anti-Mouse IgG (whole molecule) alkaline phosphatase antibody produced in goat ***(Secondary)***	BSA in TBST	1 : 20,000	1h, RT
2	Anti-Human Annexin V monoclonal antibody produced in mouse ***(Primary)IgG1***	BSA in TBST	1 : 20,000	1 h, RT
	Anti-Mouse IgG (whole molecule) alkaline phosphatase antibody produced in goat ***(Secondary)***	BSA in TBST	1 : 20,000	1h, RT

BCIP/NBT used as an alkaline phosphatase substrate.

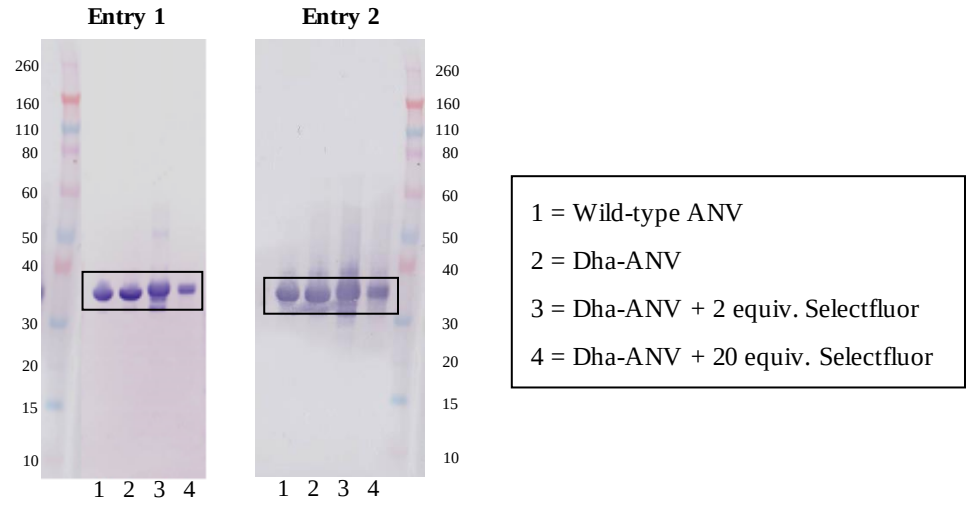

Figure 2.35 Western blot of wild-type and modified annexin V (Dha, 2equiv.F^+_Dha, and 20equiv.F^+_Dha) stained by both anti-human annexin V monoclonal antibody produced in mouse (primary antibody) and anti-mouse IgG alkaline phosphatase antibody produced in goat (secondary antibody).

Peptide Mapping of Fluorinated Annexin V (Dfa/Hfa316)

(See general experimental considerations in appendix)

Fluorinated Annexin V (Dfa/Hfa316):

Annexin V (Dha316) treated with 20 equiv. Selectfluor *bis*(triflate).

Entry	Score	Mr(found)	Mr(Calc)	Expect	Modification	Sequence
1	41.2	1044.5332	1044.5139	9.8×10^{-4}	Cys → Dfa (C-316)	ALLLLCGEDD
2	68.9	2050.0616	2050.0647	6.4×10^{-6}	Oxidation (M-28)	AMKGLGTDEESI LTLLTSR
3	54.1	1142.6845	1142.6893	3.5×10^{-5}	Oxidation (M-85)	LIVALMKPSR
4	105.8	1817.8506	1817.8508	2.1×10^{-10}	Oxidation (M-214)	YMTISGFQIEETI DR
5	77.8	1748.8695	1748.8670	5.1×10^{-8}	Oxidation (M-259)	SIPAYLAETLYY AMK
6	71.9	1289.6326	1289.6330	2.1×10^{-7}	Oxidation (M-299)	NFATSLYSMIK

Table 2.4 Peptide fragmentation of Dfa (C-316) ALLLLCGEDD and methionine-oxidised products (M-28, M-85, M-214, M-259, M-299) analysed by Mascot database.

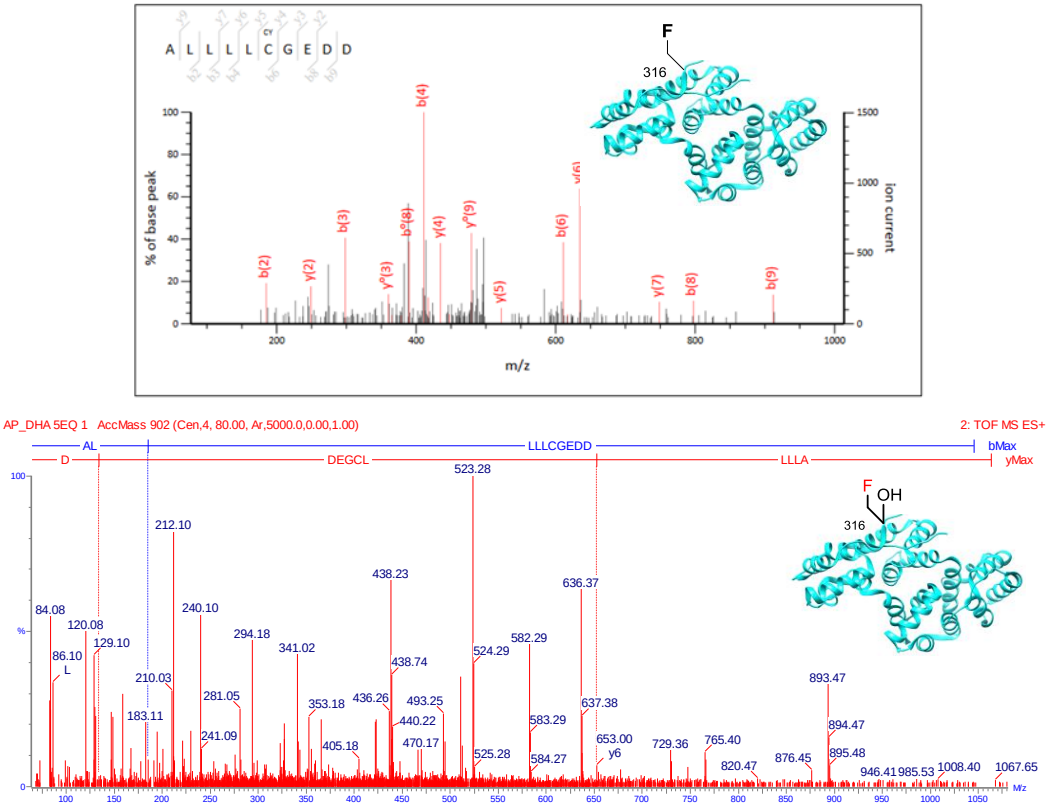

Figure 2.36 Peptide fragmentation of Dfa and Hfa (C-316) ALLLLCGEDD analysed by Mascot and Biolynx, respectively.

Methionine-Oxidised Annexin V:

Wild-type annexin V (C316) treated with 20 equiv. Selectfluor *bis*(triflate).

Entry	Score	Mr(found)	Mr(Calc)	Expect	Modification	Sequence
1	116.6	2050.0616	2050.0616	2.2×10^{-11}	Oxidation (M-28)	AMKGLGTDEESI LTLLTSR
2	105.0	1817.8507	1817.8506	1.7×10^{-10}	Oxidation (M-214)	YMTISGFQIEETI DR
3	90.6	1748.8654	1748.8695	5.9×10^{-9}	Oxidation (M-259)	SIPAYLAETLYY AMK
4	100.0	2112.9684	2112.9674	4.2×10^{-10}	Oxidation (M-299)	NFATSLYSMIKG DTSGDYK
5	42.2	2437.2167	2437.1999	0.00021	Fluoro (Y-213)	KVFDKYMTISGF QIEETIDR

Table 2.5 Peptide fragmentation of methionine-oxidised products (M-28, M-214, M-259, M-299) and monofluorotyrosine (Y-213) analysed by Mascot database.

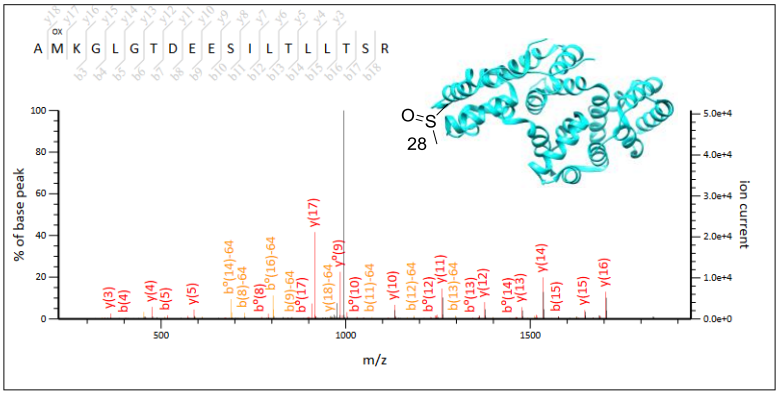

Figure 2.37 Peptide fragmentation of oxidised methionine (M-28) AMKGLGTDEESIL TLLTSR analysed by Mascot database.

Protein Stability

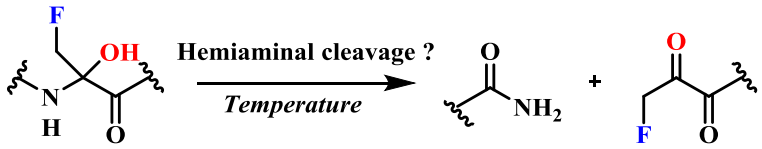

After fluorination (ANV (Dha316) treated with 2 and 20 equiv. Selectfluor *bis*(triflate)), each set of fluorinated proteins (Dfa/Hfa316) was incubated at different temperature (-80, 4, 25, and 37 °C). After a completion of incubation period, each protein aliquot was further run on SDS-PAGE, it showed no hemiaminal cleavage onto protein backbone.

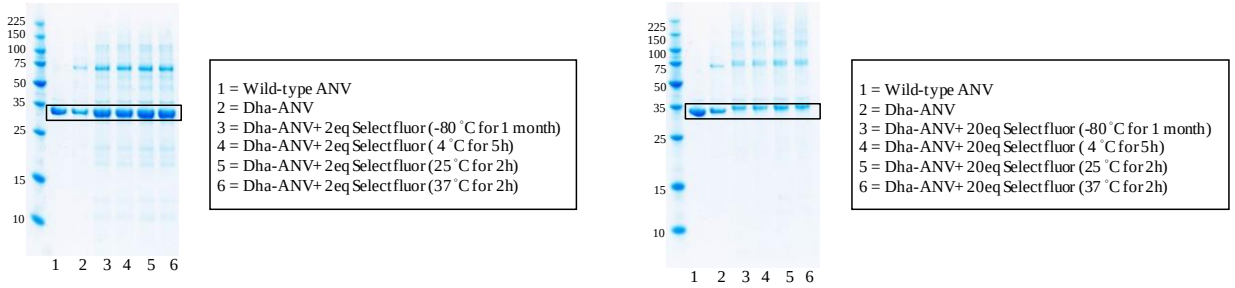

Figure 2.38 SDS-PAGEs show protein stability of the fluorinated ANV (2equiv.F^+ and 20 equiv. F^+_Dha) comparable to wild-type ANV performed at different temperature.

2.6.5 Fluorescent Labelling of the Annexin V

Labelling of Wild-type Annexin V(C316) with Alexa Fluor™ 488 NHS Ester Dye

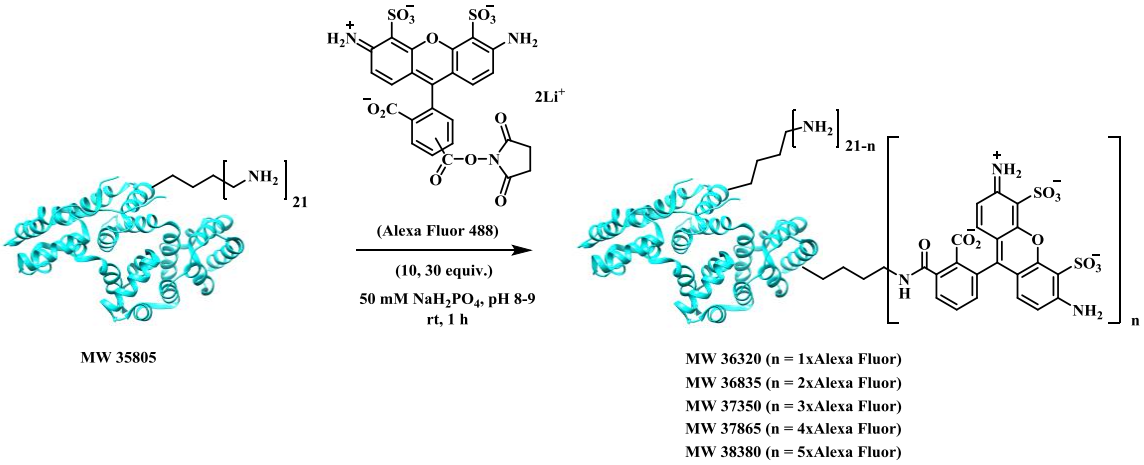

Each aliquot of wild-type annexin V in 50 mM NaH_2PO_4 (7.21 nmol, 1.29 mg/mL, 200 µL) was added 10 µL freshly prepared 1 M $NaHCO_3$ solution, then followed by addition of a solution of Alexa Fluor™ 488 NHS ester dye in DMSO (72.1, 216 nmol, 4.6, 13.9 µL from a stock solution, conc. 10.0 mg/mL). Each reaction mixture was incubated at room temperature for 1 h, then unconjugated dyes were removed by dye removal columns (according to the Thermo Scientific's instruction). The fluorescent-conjugated annexin V was observed by either LC-MS analysis (10 equiv. Alexa Fluor™ 488 NHS ester dye) or SDS-PAGEs visualised by both visible and UV light (365 nm). Protein samples were flash frozen with liquid nitrogen and stored at –80 ºC.

Entry	ANV(C316) (equiv.)	Alexa Fluor™ 488 NHS ester dye (equiv.)	Reaction conditions[a]	Results (Da)
1	1	10	RT, 1 h	36324 (1x) 36840 (2x) 37356 (3x) 37873 (4x) 38389 (5x)
2	1	30	RT, 1 h	ND.

General conditions: a). ANV(C316) in NaH_2PO_4 (50 mM, pH 8) and Alexa Fluor™ 488 dye in DMSO at 25 °C for 1 h unless otherwise indicated. ND. = Not Detectable

Table 2.6 Fluorescent labelling of wild-type ANV(C316) with 10 or 30 equiv. Alexa Fluor™ 488 NHS ester dye.

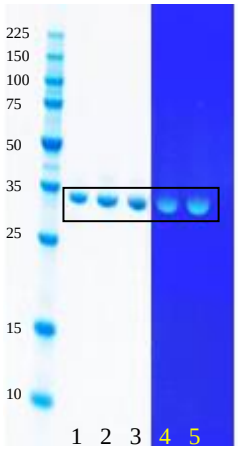

1 = Wild-type ANV

2 = Wild-type ANV + 10 equiv. Alexa Fluor 488 dye

3 = Wild-type ANV + 30 equiv. Alexa Fluor 488 dye

4 = Wild-type ANV + 10 equiv. Alexa Fluor 488 dye (UV)

5 = Wild-type ANV + 30 equiv. Alexa Fluor 488 dye (UV)

Figure 2.39 SDS-PAGE of wild-type annexin V treated with 10 and 30 equiv. Alexa Fluor™ 488 NHS ester dye detected by visible and UV light (365 nm).

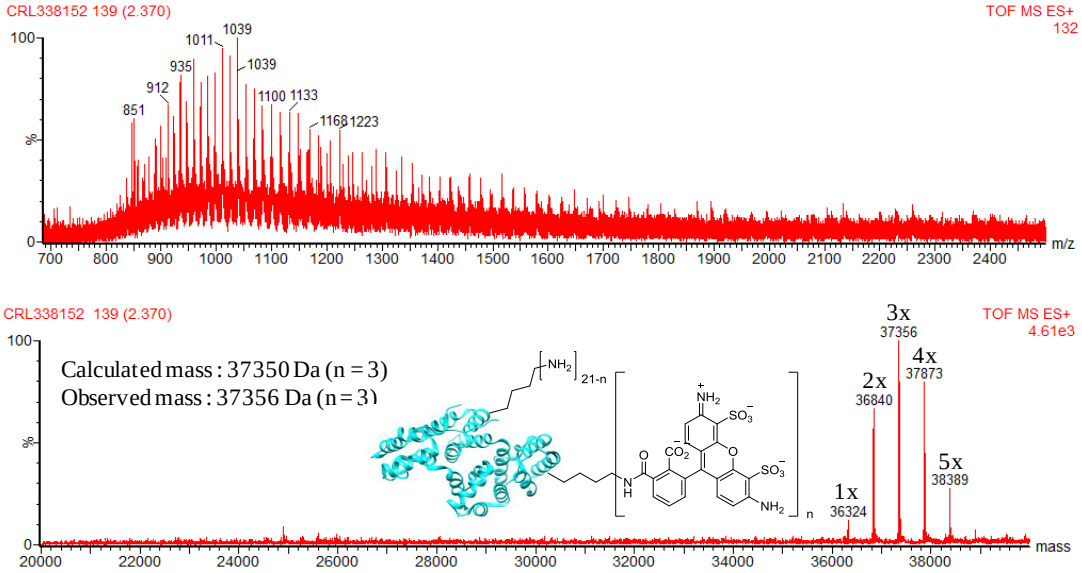

Figure 2.40 ESI-MS spectrum of wild-type annexin V treated with 10 equiv. Alexa Fluor™ 488 NHS ester dye.

Labelling of Fluorinated Annexin V(Dfa/Hfa) with Alexa Fluor™ 488 NHS Ester Dye

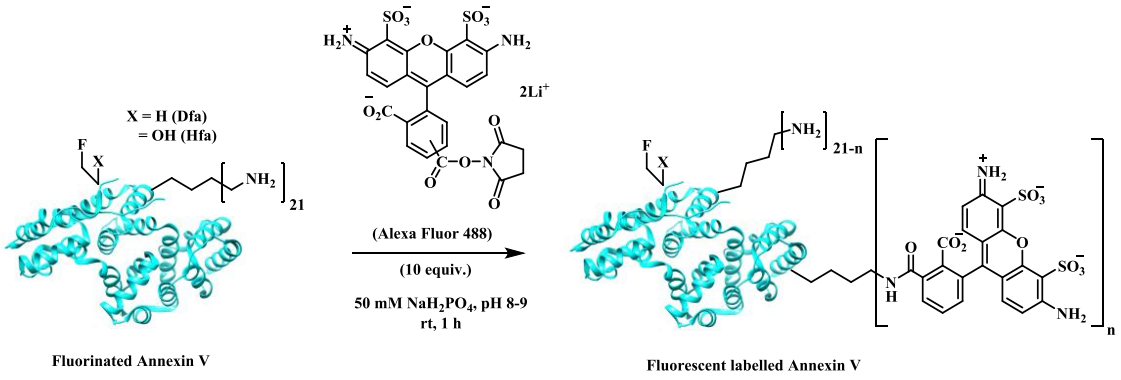

Each aliquot of fluorinated annexin V (2 equiv. F^+ and 20 equiv. F^+_Dha) in 50 mM NaH_2PO_4 (6.87, 6.26 nmol, 1.23, 1.12 mg/mL, 200 µL) was added 10 µL freshly prepared 1 M $NaHCO_3$ solution, then followed by addition of a solution of Alexa Fluor™ 488 NHS ester dye in DMSO (68.7, 62.6 nmol, 4.4, 4.0 µL from a stock solution, conc. 10.0 mg/mL). Each reaction mixture was stirred at room temperature for 1 h, then unconjugated dyes were removed by dye removal columns (according to the Thermo Scientific's instruction). The LC-MS showed complex ESI-MS spectra, which were then further investigated by SDS-PAGE and Western blot. The fluorescent-conjugated annexin V run on SDS-PAGEs was visualised by visible and UV light. Protein samples were flash frozen with liquid nitrogen and stored at –80 ºC.

Entry	ANV(Dfa/Hfa316) (equiv.)	Alexa Fluor™ 488 NHS ester dye (equiv.)	Reaction conditions[a]	Results (Da)
1	1 (2 equiv. F^+_Dha)	10	RT, 1 h	ND.
2	1 (20 equiv. F^+_Dha)	10	RT, 1 h	ND.

General conditions: a). ANV(Dfa/Hfa316) in NaH_2PO_4 (50 mM, pH 8) and Alexa Fluor™ 488 dye in DMSO at 25 °C for 1 h unless otherwise indicated. ND. = Not Detectable

Table 2.7 Fluorescent labelling of wild-type ANV(Dfa/Hfa316) with 10 equiv. Alexa Fluor™ 488 NHS ester dye.

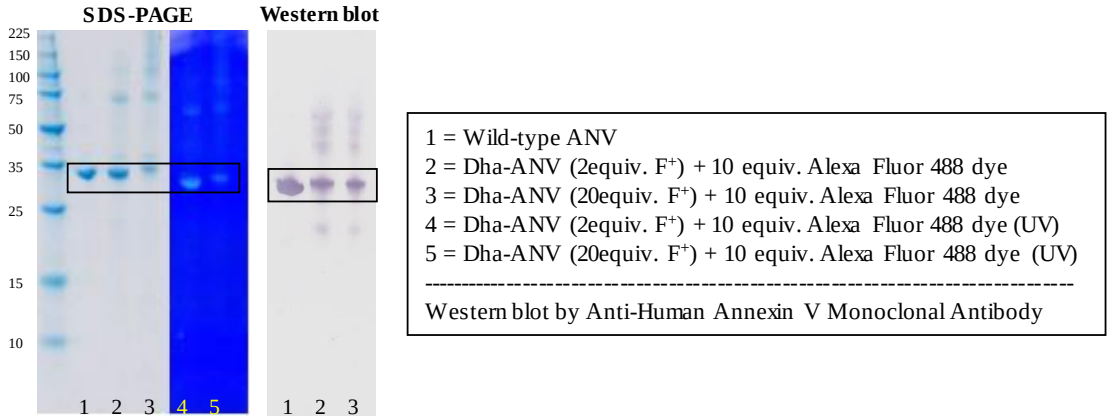

Figure 2.41 SDS-PAGEs of fluorinated ANV (2 equiv. F^+ and 20 equiv. F^+_Dha) treated with 10 equiv. Alexa Fluor™ 488 NHS ester dye and detected under visible and UV light (365 nm), and Western blot of the fluorescently-labelled fluorinated ANV (2 equiv. F^+ and 20 equiv. F^+_Dha) using anti-human annexin V monoclonal antibody.

2.6.6 Biological Activity of Wild-type and Modified Annexin V

Investigation of the *In Vitro* Apoptosis Assay

HEK 293 cells were grown in 20 mL of dulbecco's modified eagle's medium (DMEM) containing 10% fetal bovine serum (FBS) and a 1% mixture of streptomycin and penicillin. A HEK 293 cells suspension (1 mL) was diluted in 10 mL media, then incubated at 37 °C for 3 days. After the incubation period complete, a suspension of HEK 293 cells (100 µL) was diluted with 200 µL fresh DMEM media for each well of slide chamber (8 x wells), then continuously incubated at 37 °C overnight. HEK 293 cells were apoptotic-induced by a solution of actinomycin D in DMSO (10 µL, conc. 1.0 µg/mL) and incubated at 37 °C for 30 min. Cells were washed with cold-PBS buffer (200 µL), then re-suspended in 200 µL of annexin-binding buffer (10 mM HEPES-Na, 140 mM NaCl, and 2.5 mM $CaCl_2$, pH 7.4). Each cell suspension was stained by Alexa Fluor™488-labelled annexin V (WT_ANV, 2equiv. F^+_Dha, and 20equiv. F^+_Dha) (6 µg, conc. 1.5-2.0 mg/mL) and a solution of propidium iodide (PI) in PBS buffer (10 µL, conc. 100 µg/mL). For a blocking experiment, apoptotic-induced HEK 293 cells were pre-treated by an excess amount of the non-fluorescent labelled wild-type ANV (27 µg, conc. 9.0 mg/mL) for 5-10 min at room temperature, and subsequently treated with both PI and Alexa Fluor™488-labelled wild-type ANV or fluorinated ANV. The cell suspension was allowed to incubate at room temperature for 15 min in the dark, washed

twice with annexin-binding buffer (200 µL), then cell samples were observed by a confocal laser scanning microscopy (LEICA).

Entry	Proteins/Dyes (C = 1.5-2.0 mg/mL)	Act-D (1.0 µg/mL)	PI (100 µg/mL)	Remarks
1	Alexa Fluor™ 488_WT_ANV (6 µg)	10 µL	10 µL	Late apoptosis
2	Alexa Fluor™ 488_2eqF_Dha (6 µg)	10 µL	10 µL	Late apoptosis
3	Alexa Fluor™ 488_20eqF_Dha (6 µg)	10 µL	10 µL	Late apoptosis
4	Alexa Fluor™ 488_WT_ANV (6 µg)	-	10 µL	Control: Apoptosis not induced
5	Alexa Fluor™ 488_2eqF_Dha (6 µg)	-	10 µL	Control: Apoptosis not induced
6	Alexa Fluor™ 488_20eqF_Dha (6 µg)	-	10 µL	Control: Apoptosis not induced
7	-	-	-	Control: Live cells
8	-	10 µL	10 µL	Control: Necrotic cells
9	Alexa Fluor™ 488 dye (6 µg)	-	-	Control: Non-specific binding
10	Alexa Fluor™ 488 dye (6 µg)	10 µL	10 µL	Control: Non-specific binding
11	Fluorescein diacetate dye (6 µg)	-	10 µL	Control: Live/dead cells staining
12	WT_ANV (27 µg) + Alexa Fluor™ 488_WT_ANV (4.5 µg)	10 µL	10 µL	Blocking experiment
13	WT_ANV (27 µg) + Alexa Fluor™ 488_2eqF_Dha (4.5 µg)	10 µL	10 µL	Blocking experiment
14	WT_ANV (27 µg) + Alexa Fluor™ 488_20eqF_Dha (4.5 µg)	10 µL	10 µL	Blocking experiment

The incubation period for apoptotic induction was at 37 °C for 0.5h. ANV = Annexin V, WT = Wild-type, 2eqF_Dha / 20 eqF_Dha = Fluorinated Annexin V, Act-D = Actinomycin D, PI = Propidium iodide,

Table 2.8 Apoptotic detection experiments of HEK 293 cells induced by actinomycin D and subsequtnely stainned by fluorescent-labelled ANV and PI.

1. Wild-type ANV labelled with Alexa Fluor™ 488 dye (Entry **1**)

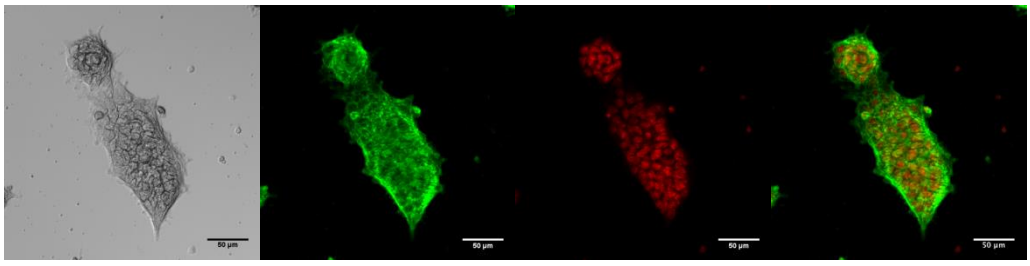

2. Fluorinated ANV (2equiv.F^+_Dha) labelled with Alexa Fluor^{TM} 488 dye (Entry **2**)

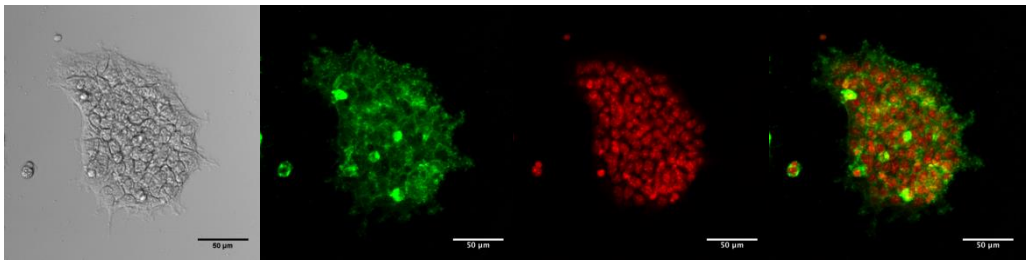

3. Fluorinated ANV (20equiv.F^+_Dha) labelled with Alexa Fluor^{TM} 488 dye (Entry **3**)

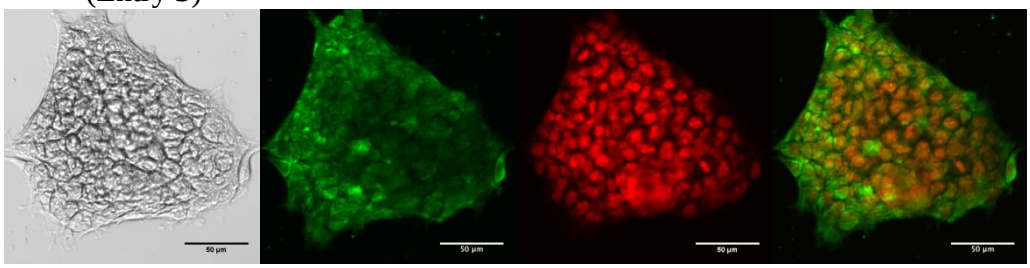

4. Wild-type ANV labelled with Alexa Fluor^{TM} 488 dye, control (Entry **4**)

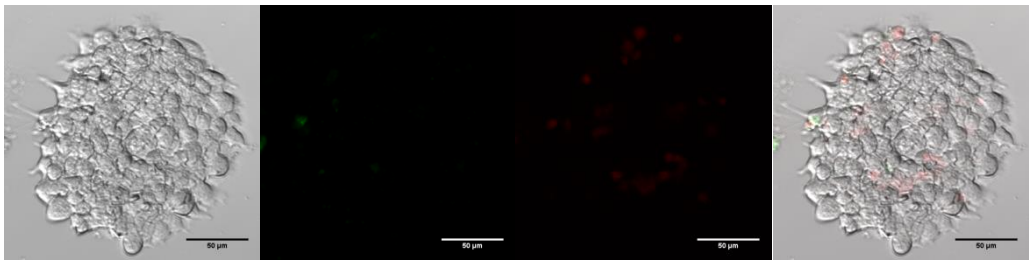

5. Fluorinated ANV (2equiv.F^+_Dha) labelled with Alexa Fluor^{TM} 488 dye, control (Entry **5**)

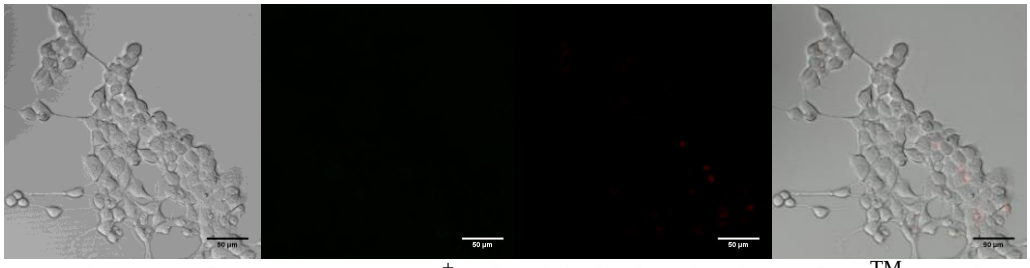

6. Fluorinated ANV (20equiv.F^+_Dha) labelled with Alexa Fluor^{TM} 488 dye, control (Entry **6**)

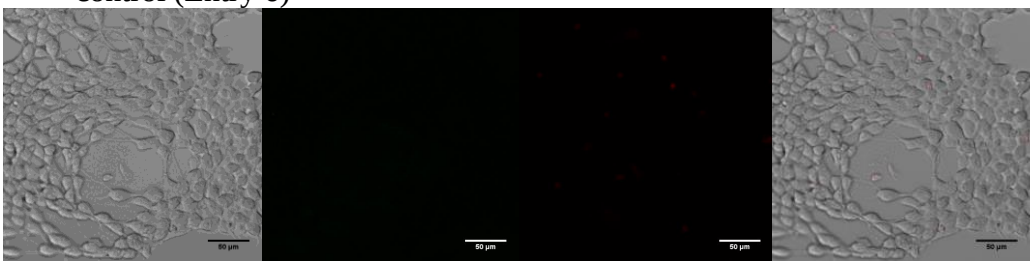

7. Live cells (Entry **7**)

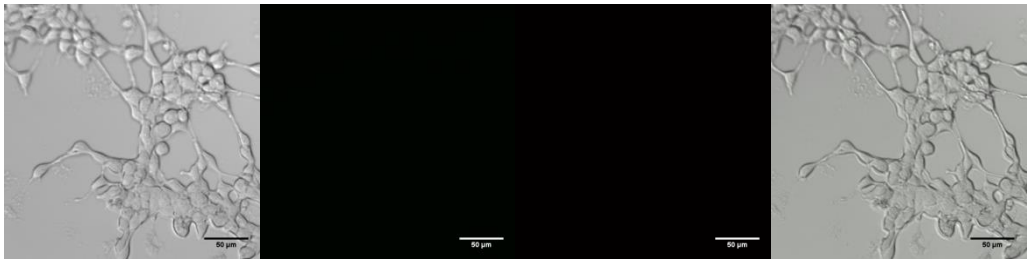

8. Necrotic cells (Entry **8**)

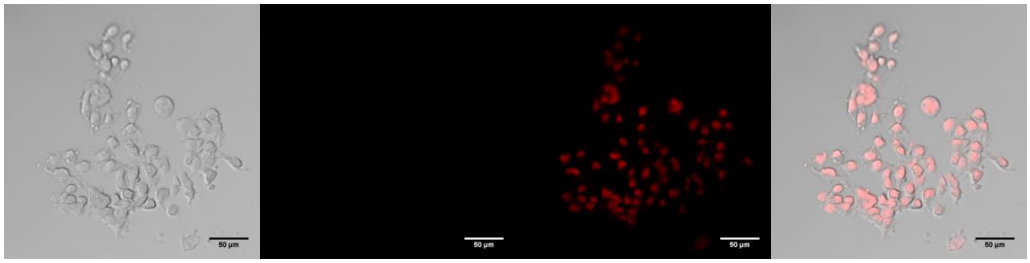

9. Non-specific binding – Live cells (Entry **9**)

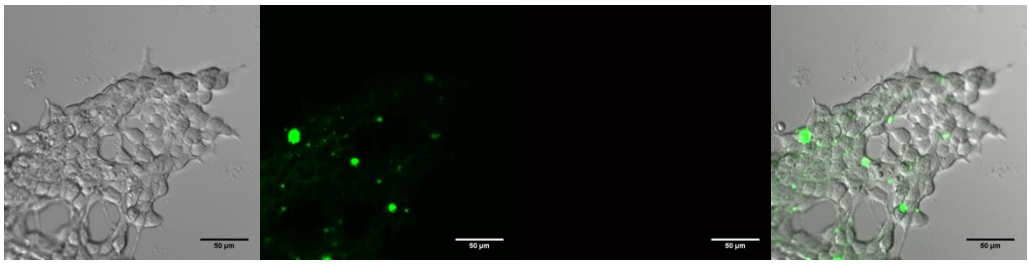

10. Non-specific binding – Dead cells (Entry **10**)

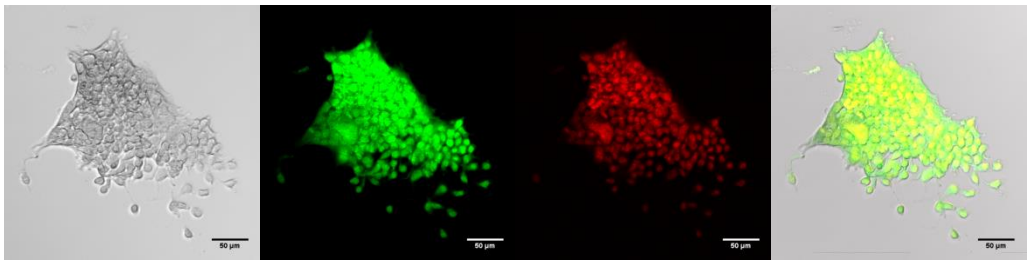

11. Live and dead cells staining (Entry **11**)

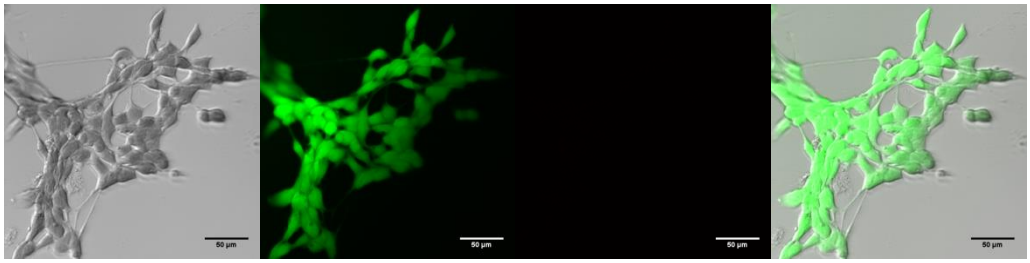

12. Non-labelled wild-type ANV, and wild-type ANV labelled with Alexa Fluor^{TM} 488 dye, blocking experiment (Entry **12**)

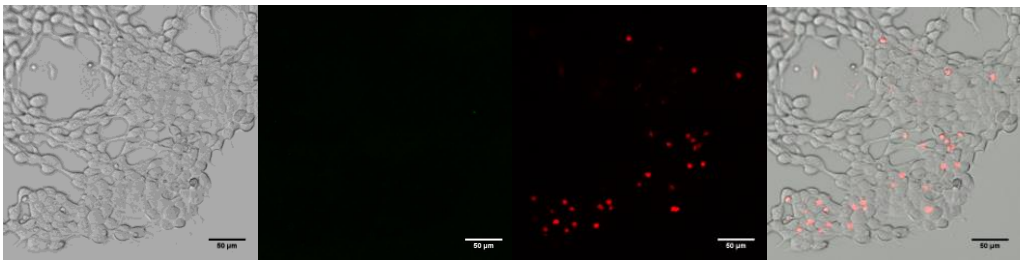

13. Non-labelled wild-type ANV, and fluorinated ANV (2 equiv. F^{+}_Dha) labelled with Alexa Fluor^{TM} 488 dye, blocking experiment (Entry **13**)

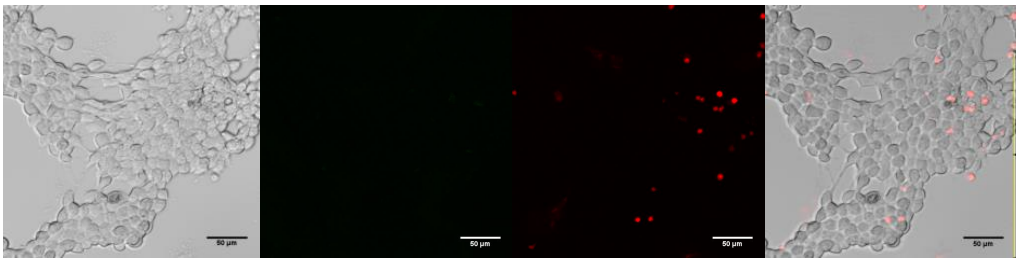

14. Non-labelled wild-type ANV, and fluorinated ANV (20 equiv. F^{+}_Dha) labelled with Alexa Fluor^{TM} 488 dye, blocking experiment (Entry **14**)

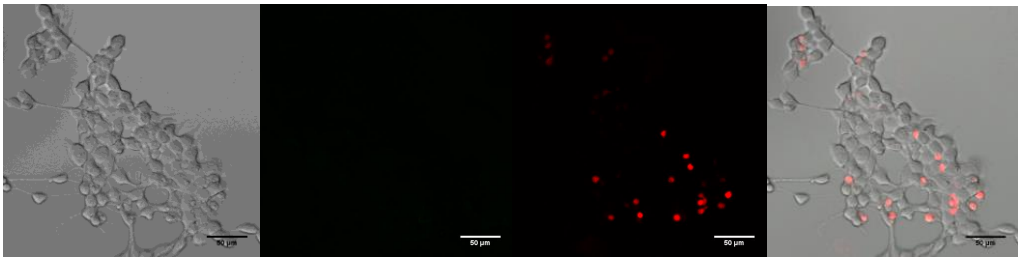

Figure 2.42 Fluorescent images of apoptotic-induced HEK 293 cells using a confocal laser scanning microscopy (LEICA) and scale bar 50 µm : channel I = bright field, channel II = fluorescent-labelled annexin V or dye, channel III = propidium iodide (PI), and channel IV = merged channels I+II+III/II+III.

2.6.7 [^{18}F]-Radiolabelling of the Annexin V using [^{18}F]-Selectfluor *bis*(Triflate)

(Performed by Dr. Anna Kirjavainen, Dr. Sarita Forsback, Prof. Olof Solin: Turku PET Centre, and Dr. Matthew Schombs: Department of Chemistry, University of Oxford.)

Radiosynthesis of [^{18}F]-Selectfluor *bis*(Triflate) followed a procedure which was reported by Gouverneur and co-workers[36].

[^{18}F]-Radiolabelling of the Annexin V (Dha316)

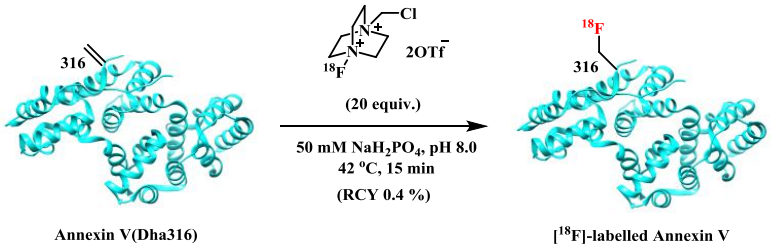

An aliquot of annexin V (Dha316) (20.27 nmol, 1.45 mg/mL, 500 µL) in 50 mM NaH_2PO_4, pH 8.0 was mixed with a solution of [^{18}F]-Selectfluor *bis*(triflate) in acetone (405.4 nmol, 16.2 µL from a stock solution, conc. 2.0 µmol, 80 µL) by vortexing briefly. After 15 min of shaking at 42 °C, the reaction mixture was desalted by a PD 10 minitrap G-25 column pre-equilibrated with PBS buffer, pH 7.3. Each protein fraction (200 µL) was collected in eppendorf tubes, then analysed by RP-HPLC with both UV and radioactivity detectors.

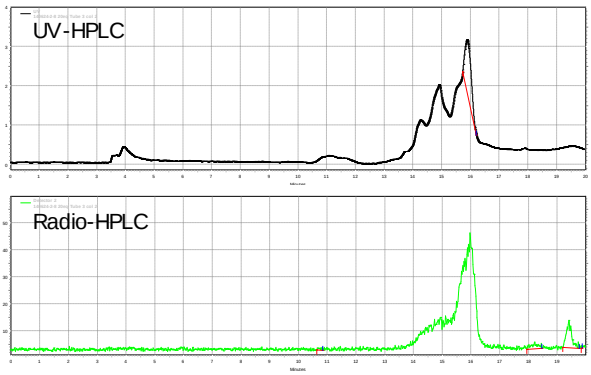

Figure 2.43 UV and radio-HPLC profiles of annexin V(Dha316) treated with 20 equiv. [^{18}F]-Selectfluor *bis*(triflate).

Control: [^{18}F]-Radiolabelling of Wild-type Annexin V(C316)

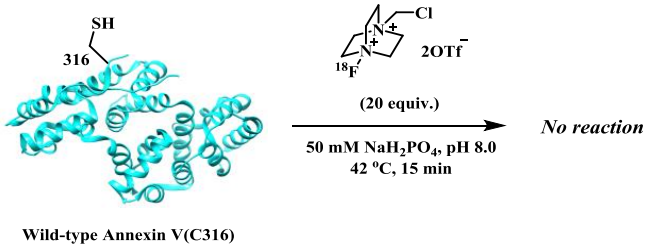

An aliquot of wild-type annexin V(C316) (22.34 nmol, 1.60 mg/mL, 500 µL) in 50 mM NaH_2PO_4, pH 8.0 was mixed with a solution of [^{18}F]-Selectfluor *bis*(triflate) in acetone (446.8 nmol, 17.8 µL from a stock solution, conc. 2.0 µmol, 80 µL) by vortexing briefly. After 15 min of shaking at 42 °C, the reaction mixture was desalted using a PD 10 minitrap G-25 column pre-equilibrated with PBS buffer, pH 7.3. Each protein fraction (200 µL) was collected in eppendorf tubes, then analysed by RP-HPLC with both UV and radioactivity detectors.

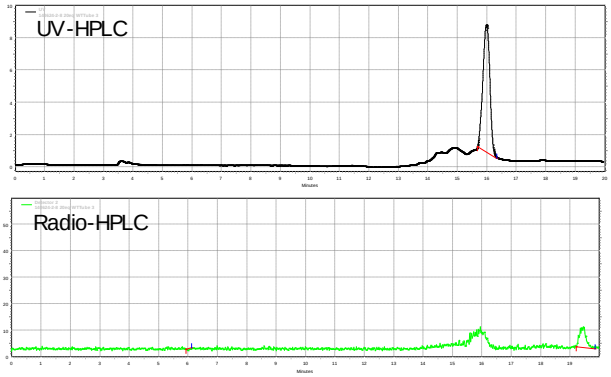

Figure 2.44 UV and radio-HPLC profiles of wild-type annexin V(C316) treated with 20 equiv. [^{18}F]-Selectfluor *bis*(triflate).

Preparation of [^{18}F]-radiolabelled Annexin V

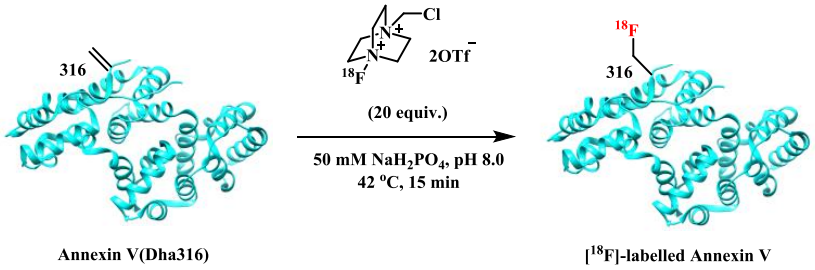

Annexin V(Dha316) [^{18}F]-labelled Annexin V

(Same procedure mentioned in section 2.6.7)

Entry	ANV(Dha316) (equiv.)	Selectfluor *bis*(triflate) (equiv.)	Reaction Conditions	Radioactivity (MBq)	RCY (%)
1	1 (1.45 mg/mL)	20	42 °C, 15 min	3.38	0.4
2	1 (1.79 mg/mL)	20	42 °C, 15 min	2.38	0.5
3	1 (1.79 mg/mL)	20	42 °C, 15 min	7.00	0.8
4	1 (1.42 mg/mL)	20	42 °C, 15 min	5.80	0.5
5	1 (1.42 mg/mL)	20	42 °C, 15 min	4.00	0.3
6	1 (1.25 mg/mL)	20	42 °C, 15 min	3.92	0.5
7	1 (1.25 mg/mL)	20	42 °C, 15 min	4.63	0.7
8	1 (1.25 mg/mL)	20	42 °C, 15 min	3.23	0.5
9	1 (1.42 mg/mL)	20	42 °C, 15 min	1.31	0.1

General conditions: ANV(Dha316) in NaH_2PO_4 (50 mM, pH 8) and [^{18}F]-Selectfluor *bis*(triflate) in acetone (c = 2.0 µmol) at 42 °C for 15 min, unless otherwise indicated.

Table 2.9 Preparation of [^{18}F]-radiolabelled annexin V by treatment of ANV(Dha316) with 20 equiv. [^{18}F]-Selectfluor *bis*(triflate).

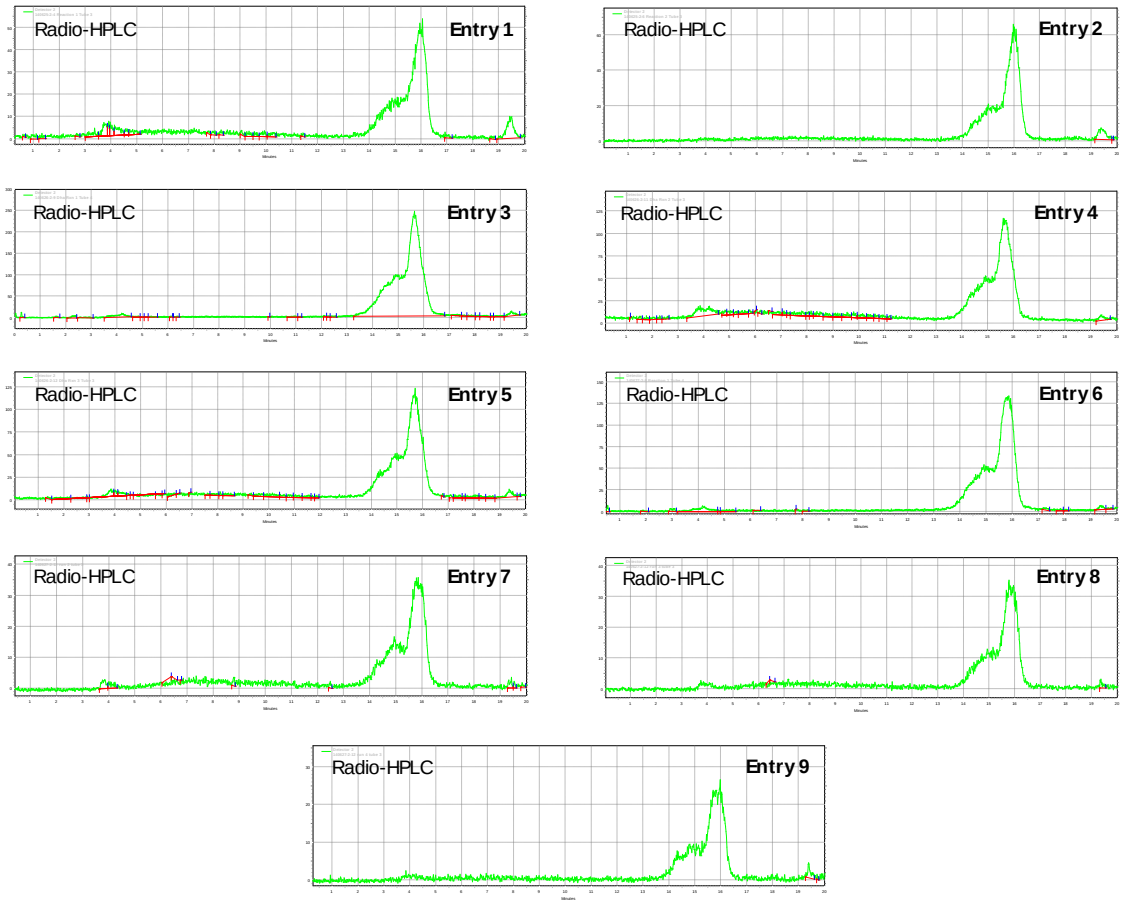

Figure 2.45 Radio-HPLC profiles of [^{18}F]-radiolabelled annexin V by treatment of ANV(Dha316) with 20 equiv. [^{18}F]-Selectfluor *bis*(triflate).

2.6.8 Preclinical Animal Studies by [^{18}F]-PET Imaging Technique

(Performed by Dr. Alex M. Dickens, Prof. Daniel C. Anthony: Department of Phramacology, University of Oxford and Prof. Merja Haaparanta-Solin: Turku PET Centre.)

Adult male SD rats (200-250 g) were anesthetised using 2.5% isoflurane in air. All animal experiments followed by current EU guidelines were ethically approved by the Southern board of Finland for animal ethics (ESAVI-2010-04454/Ym-23). An intravenous injection of cycloheximide (CXM) (10 mg) into animals (n = 4) was performed to induce the liver injury 4 h prior to imaging. For control model, animals (n = 4) was intravenously injected by saline and left for 4 h prior to *in vivo* imaging. For the control studies, an injection of non-radiolabelled annexin V into animals was first carried out before subsequent injection of the [^{18}F]-labelled ANV(Dfa/Hfa). The two animals

treated by CXM were subjected to a monitor of time-course PET/CT 2D images by PET/CT scanner during a time period of 60 min. One animal was pre-treated with wild-type annexin V (on the left) for 30 min, where as, the animal (on the right) received a vehicle control injection 30 min before straight injection of the [^{18}F]-labelled annexin V. According to experiments between control and apoptosis induction, a mixture of [^{18}F]-labelled ANV(Dfa/Hfa) (1.73 ± 0.8 MBq) was injected into the lesioned (n=4) or control animals (n=4). During imaging, one lesioned animal (treated by CXM) died was therefore excluded from experimental analysis. These PET/CT 3D images were captured by PET/CT scanner after addition of entire radioactivity in the liver for 45 min. The uptake of the [^{18}F]-radiotracer in the liver spherical ROI's of the same volumes was quantified, and the average SUV value was also calculated.

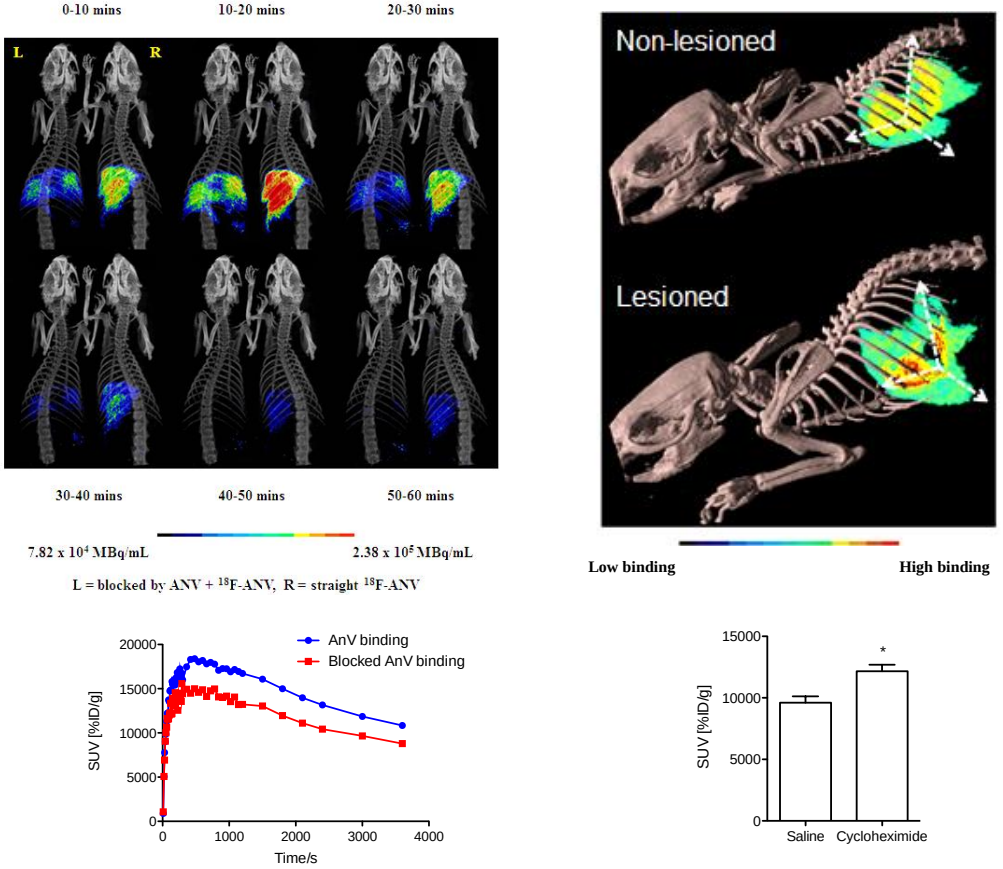

Figure 2.46 Time-course PET/CT 2D images of a comparative study of the apoptosis detection of cell-death liver injured by injection of CXM (L = blocking, R = straight injection) and PET/CT 3D images between CXM-treated and untreated animals. The plot shows an increased binding with direct injection of the [^{18}F]-radiotracer (ANV) (blue curve), which was reduced by CXM-treated animals with excess amount of cold tracer (red curve). Comparison binding of [^{18}F]-radiotracer in CXM-treated and untreated animals

Direct Electrophilic Aromatic Fluorination of Wild-type Annexin V

2.6.9 Fluorination of Wild-type Annexin V using Selectfluor *bis*(tetrafluoro borate)

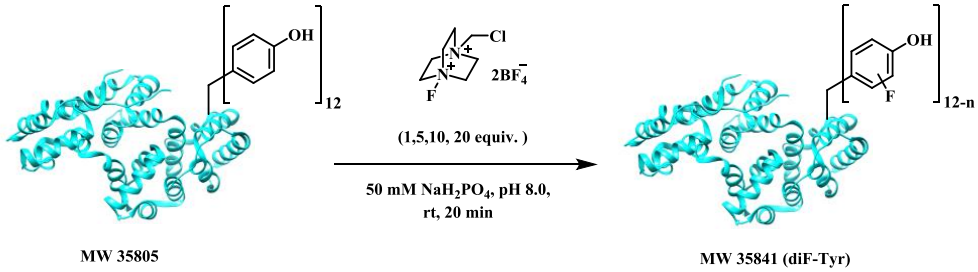

Each aliquot of wild-type annexin V (4.2 nmol, 1.52 mg/mL, 100 µL) in 50 mM NaH_2PO_4, pH 8.0 was mixed with a solution of Selectfluor *bis*(tetrafluoroborate) in H_2O (4.2, 21, 42, 84 nmol, 0.3, 1.5, 3.0, 6.0 µL from stock solution, conc. 5.0 mg/mL) by vortexing briefly. After 20 min of shaking at room temperature, each aliquot was analysed by LC–MS spectrometry (diF-Tyr; Calc: 35841 Da and Obs: 35839 Da) after desalting by vivaspin column concentrators with a 10,000 Da MW cut-off membrane (8-9 x times) loading fresh 50 mM NaH_2PO_4, pH 8.0 each time. Protein samples were flash frozen with liquid nitrogen and stored at –80 ºC.

Entry	ANV (wild-type) (equiv.)	Selectfluor *bis*(tetrafluoroborate) (equiv.)	Reaction conditions[a]	Product conversion (%)[b]
1	1	1	25 °C, 20 min	SM (82) diF-Tyr (18)
2	1	5	25 °C, 20 min	diF-Tyr (91) diF-Tyr + Met(O) (9)
3	1	10	25 °C, 20 min	diF-Tyr (90) diF-Tyr + Met(O) (10)
3	1	20	25 °C, 20 min	diF-Tyr (72) diF-Tyr + Met(O) (18)

General conditions: a). ANV (wild-type) in NaH_2PO_4 (50 mM, pH 8) and Selectfluor *bis*(tetrafluoroborate) in H_2O at 25 °C for 20 min unless otherwise indicated; SM: starting material. b). Calculated by LC-MS. Met(O) = Methionine-oxidised products

Table 2.10 Optimisation of tyrosine fluorination of wild-type ANV using 1-20 equiv. Selectfluor *bis*(tetrafluoroborate) as a fluorinating agent.

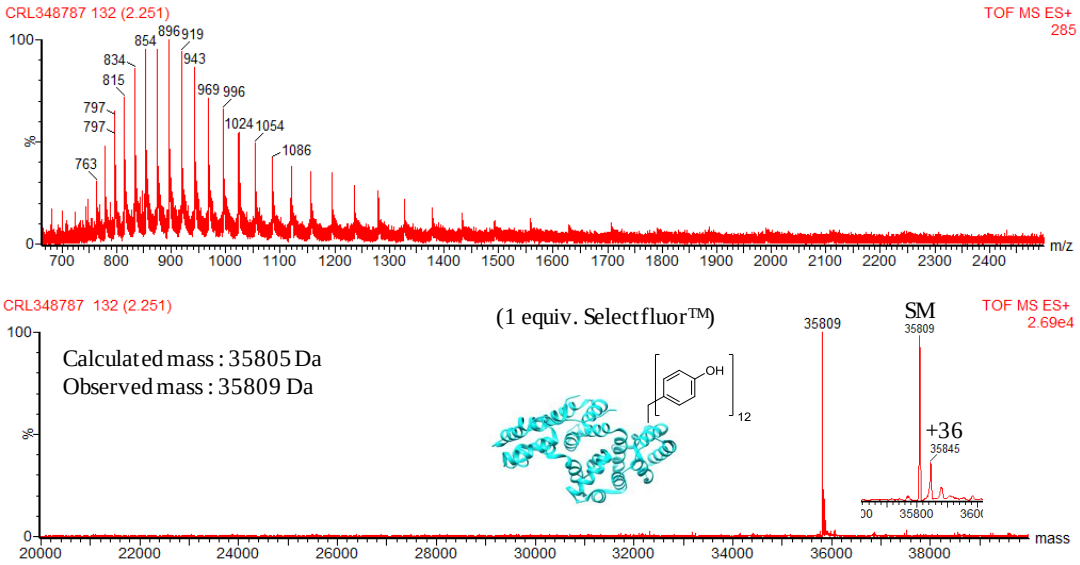

Figure 2.47 ESI-MS spectrum of wild-type annexin V treated with 1 equiv. Selectfluor *bis*(tetrafluoroborate).

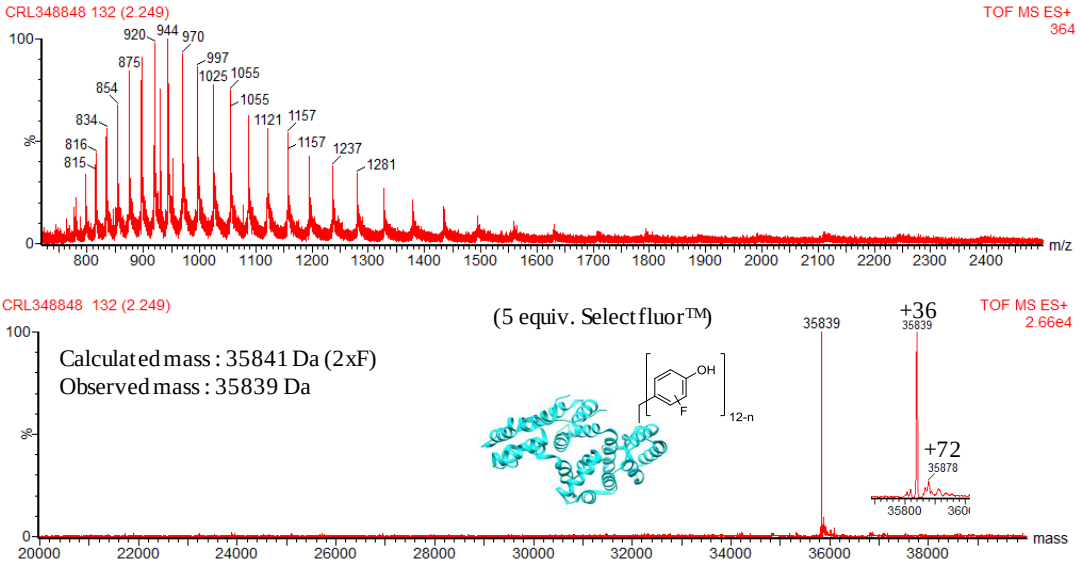

Figure 2.48 ESI-MS spectrum of wild-type annexin V treated with 5 equiv. Selectfluor *bis*(tetrafluoroborate).

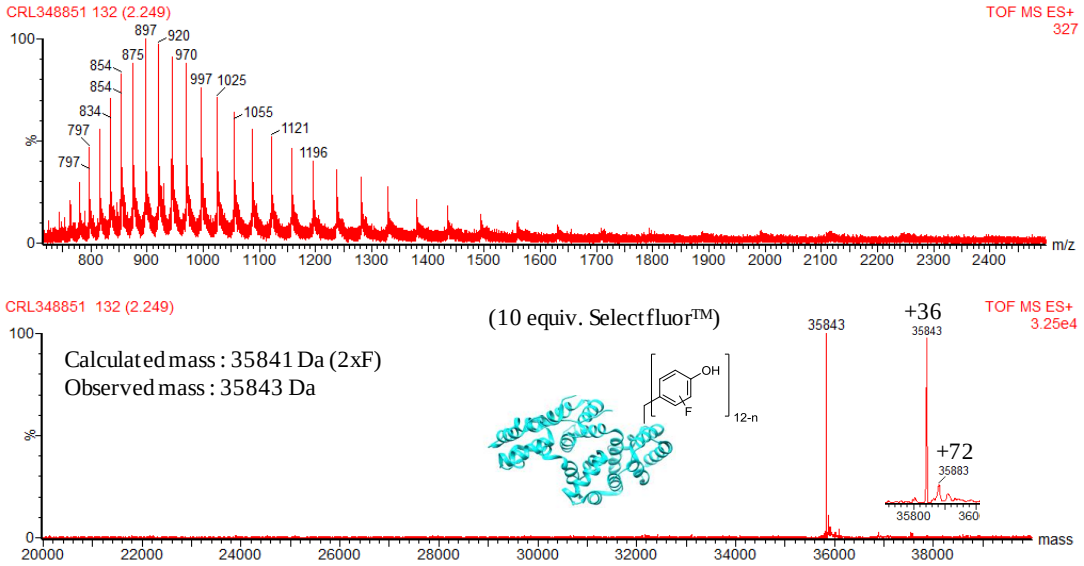

Figure 2.49 ESI-MS spectrum of wild-type annexin V treated with 10 equiv. Selectfluor *bis*(tetrafluoroborate).

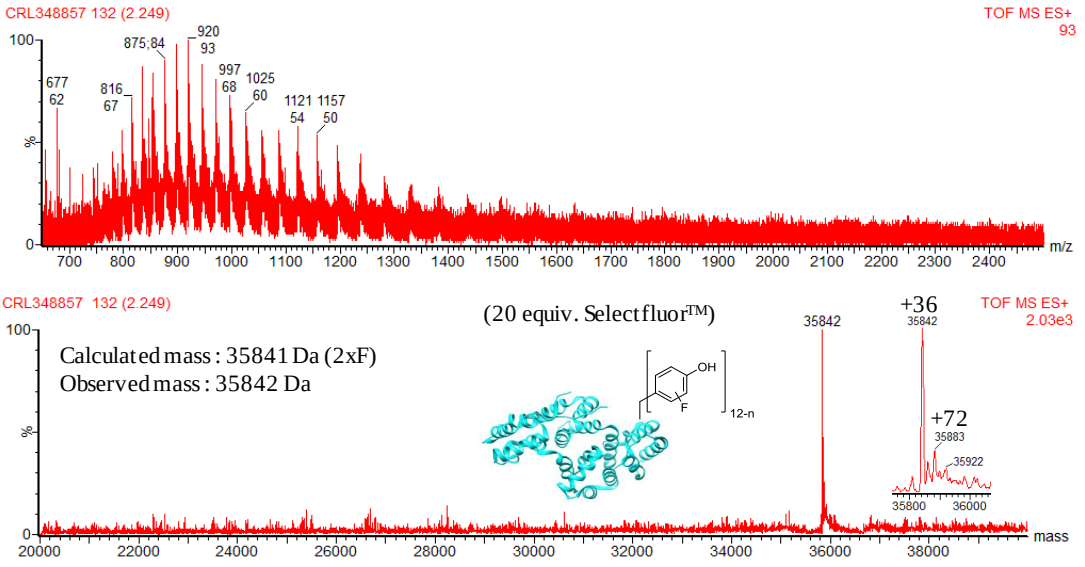

Figure 2.50 ESI-MS spectrum of wild-type annexin V treated with 20 equiv. Selectfluor *bis*(tetrafluoroborate).

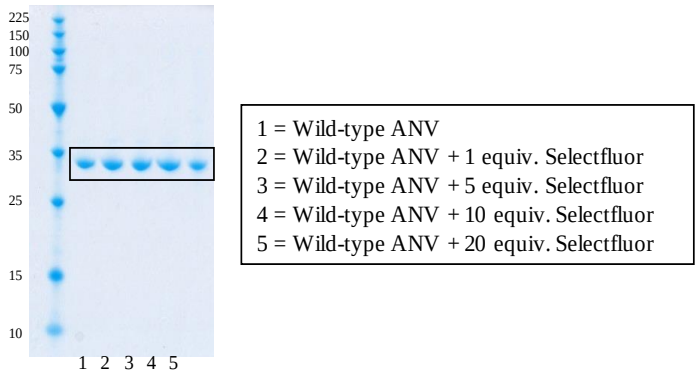

Figure 2.51 SDS-PAGE of wild-type annexin V treated with 1, 5, 10, and 20 equiv. Selectfluor *bis*(tetrafluoroborate), respectively.

Control: Ellman Addition to Fluorinated Annexin V (diF-Tyr)

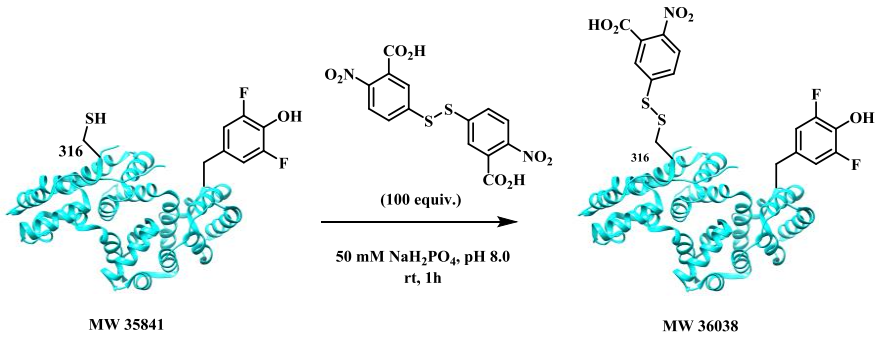

An aliquot of fluorinated annexin V (5 equiv.F^+_ANV) (3.07 nmol, 2.20 mg/mL, 50 µL) in 50 mM NaH_2PO_4, pH 8.0 was mixed with a solution of DTNB in DMSO (307 nmol, 6.1 µL from stock solution, conc. 20 mg/mL) by vortexing briefly. After 1h of shaking at room temperature, an aliquot was analysed by LC–MS spectrometry (Calc: 36038 Da and Obs: 36036 Da) after desalting by a vivaspin column concentrator with 10,000 Da MW cut-off membrane (8-9 x times) loading fresh 50 mM NaH_2PO_4, pH 8.0 each time. A protein sample was flash frozen with liquid nitrogen and stored at –80 ºC.

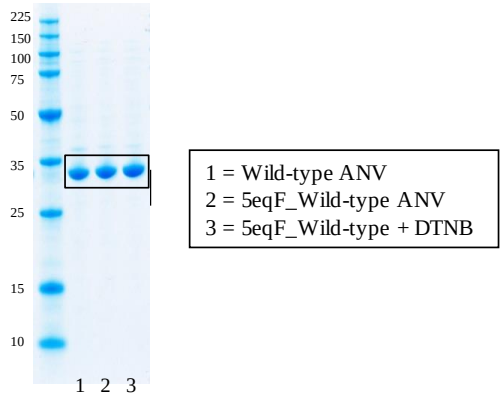

Figure 2.52 SDS-PAGE of fluorinated annexin V (5 equiv.F^+_ANV) treated with 100 equiv. DTNB.

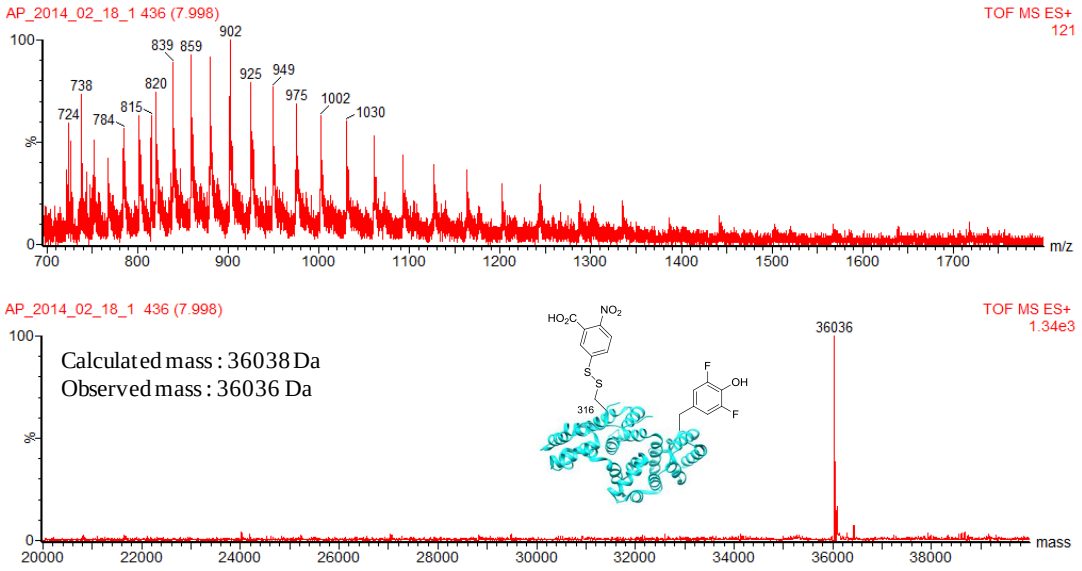

Figure 2.53 ESI-MS spectrum of fluorinated annexin V(diF-Tyr) treated with 100 equiv. Ellman's reagent.

2.6.10 Proteins Characterisation

Circular Dichroism (CD) Spectroscopy

(Same procedure mentioned in section 2.6.4)

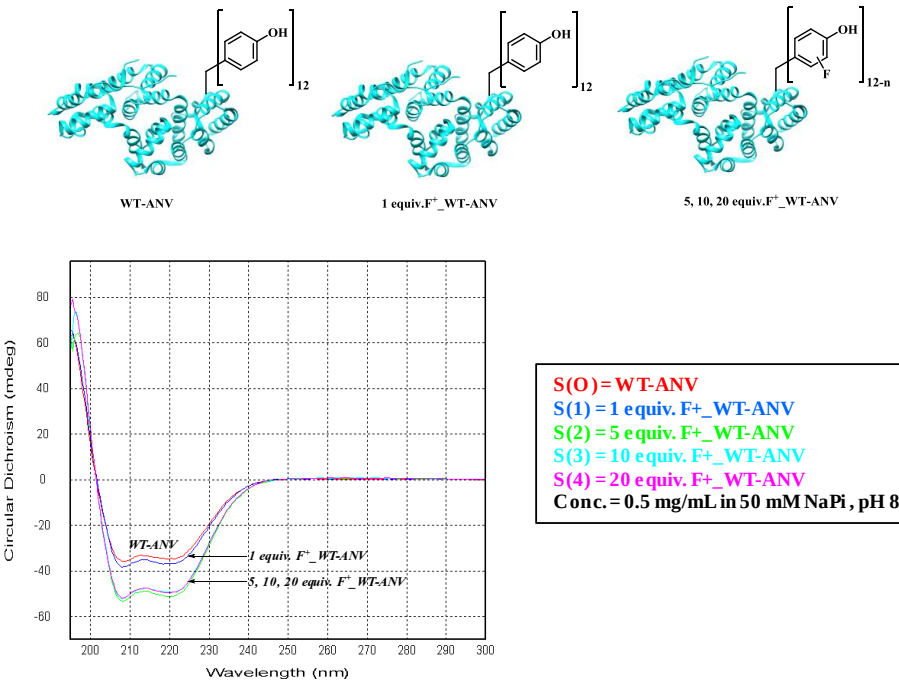

Figure 2.54 A comparison of circular dichroism (CD) spectra of wild-type annexin V, and wild-type annexin V treated with 1, 5, 10 and 20 equiv. Selectfluor *bis* (tetrafluoroborate), respectively.

Western Blotting Analysis

(See general experimental considerations in appendix)

Entry	Antibodies	Blocking agent	Dilution	Conditions
1	Anti-Human Annexin V monoclonal antibody produced in mouse ***(Primary)IgG1***	BSA in TBST	1 : 20,000	1 h, RT
	Anti-Mouse IgG (whole molecule) alkaline-phosphatase antibody produced in goat ***(Secondary)***	BSA in TBST	1 : 20,000	1h, RT

BCIP/NBT used as an alkaline phosphatase substrate.

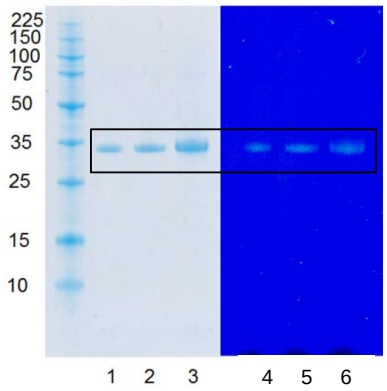

1 = Wild-type ANV + FITC
2 = Wild-type ANV (5 equiv. F^+) + FITC
3 = Wild-type ANV (20 equiv. F^+) + FITC
4 = Wild-type ANV + FITC (UV)
5 = Wild-type ANV (5 equiv. F^+) + FITC (UV)
6 = Wild-type ANV (20 equiv. F^+) + FITC (UV)

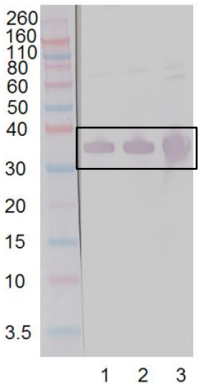

1 = Wild-type ANV + FITC
2 = Wild-type ANV (5 equiv. F^+) + FITC
3 = Wild-type ANV (20 equiv. F^+) + FITC

Figure 2.55 SDS-PAGEs and Western blot of wild-type ANV labelled with FITC dye and fluorinated ANV (diF-Tyr) labelled with FITC.

Peptide Mapping of the Fluorinated Annexin V(diF-Tyr)

(See general experimental considerations in appendix)

Entry	Score	Mr(found)	Mr(Calc)	Expect	Modification	Sequence
1	61.1	2924.1560	2923.2120	1.9×10^{-6}	Difluoro (Y-129)	QVYEEEYGSSL EDDVVGDTSGY YQR
2	92.8	2242.0640	2241.0623	1.2×10^{-8}	Oxidation (M-299)	NFATSLYSMIKG DTSGDYKK

Table 2.11 Peptide fragmentation of difluoro-Tyr (Y-129) QVYEEEYGSSLEDDVV GDTSGYYQR and methionine-oxidised product (M-299) NFATSLYSMIKGDTSG DYKK analysed by Mascot database.

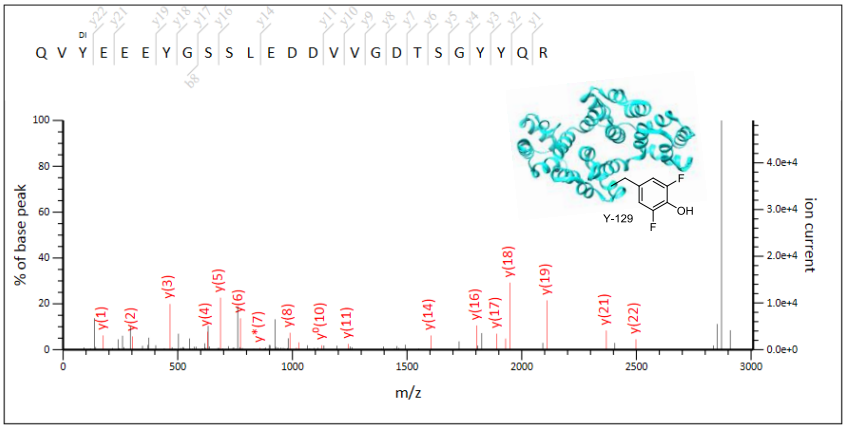

Figure 2.56 Peptide fragmentation of difluorotyrosine (Y-129) QVYEEEYGSSLEDDV VGDTSGYYQR analysed by Mascot database.

Protein Stability

(Same procedure mentioned in section 2.6.4)

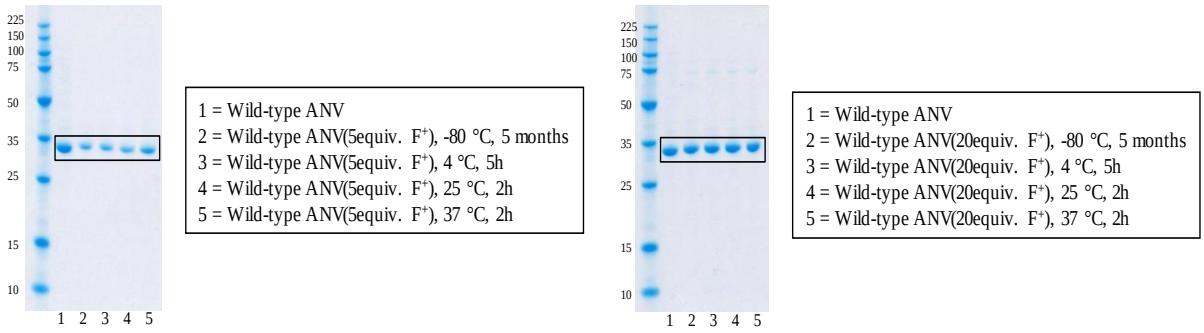

Figure 2.57 SDS-PAGEs show protein stability of fluorinated ANV (5 equiv.F^+ and 20 equiv. F^+_ANV) comparable to wild-type ANV performed at different temperature.

2.6.11 Fluorescent Labelling of the Annexin V

Labelling of Wild-type Annexin V with Fluorescein Isothiocyanate (FITC) Dye

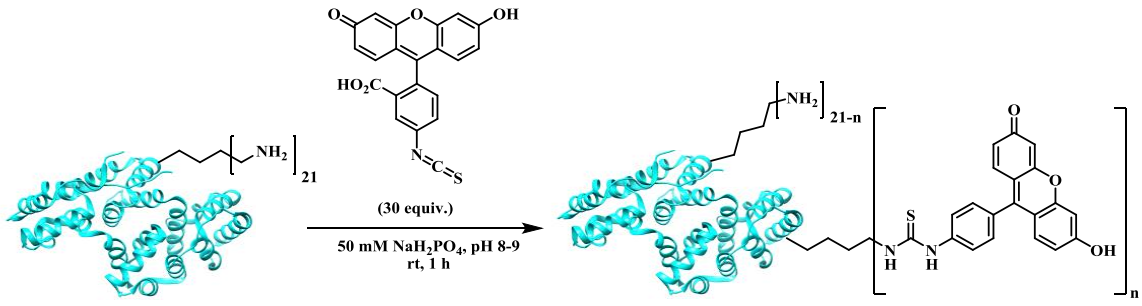

An aliquot of wild-type annexin V (9.22 nmol, 1.65 mg/mL, 200 µL) in 50 mM NaH_2PO_4, pH 8.0 was mixed with a freshly prepared solution of 1 M $NaHCO_3$ (40 µL) and a solution of FITC dye in DMSO (276 nmol, 3.56 µL from stock solution, conc. 30 mg/mL) by vortexing briefly. After 1h of shaking at room temperature, an aliquot was analysed by LC-MS after removal of excess FITC dye using a dye removal column (according to the Thermo Scientific's instruction). The purified protein sample was flash frozen with liquid nitrogen and stored at –80 ºC.

Entry	ANV (wild-type) (equiv.)	FITC (equiv.)	Reaction conditions[a]	Product (Da)
1	1	30	25 °C, 60 min	35804 (SM) 36194 (1xFITC) 36583 (2xFITC) 36973 (3xFITC) 37362 (4xFITC)

General conditions: a). ANV (wild-type) in NaH_2PO_4 (50 mM, pH 8) and FITC in DMSO at 25 ºC for 60 min unless otherwise indicated; SM: starting material.

Table 2.12 Fluorescent labelling of wild-type ANV with 30 equiv. FITC.

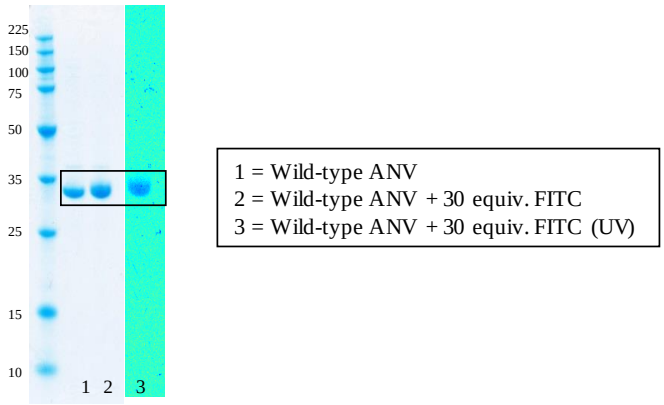

Figure 2.58 SDS-PAGE of wild-type annexin V labelled with 30 equiv. FITC dye under visible and UV (365 nm) light.

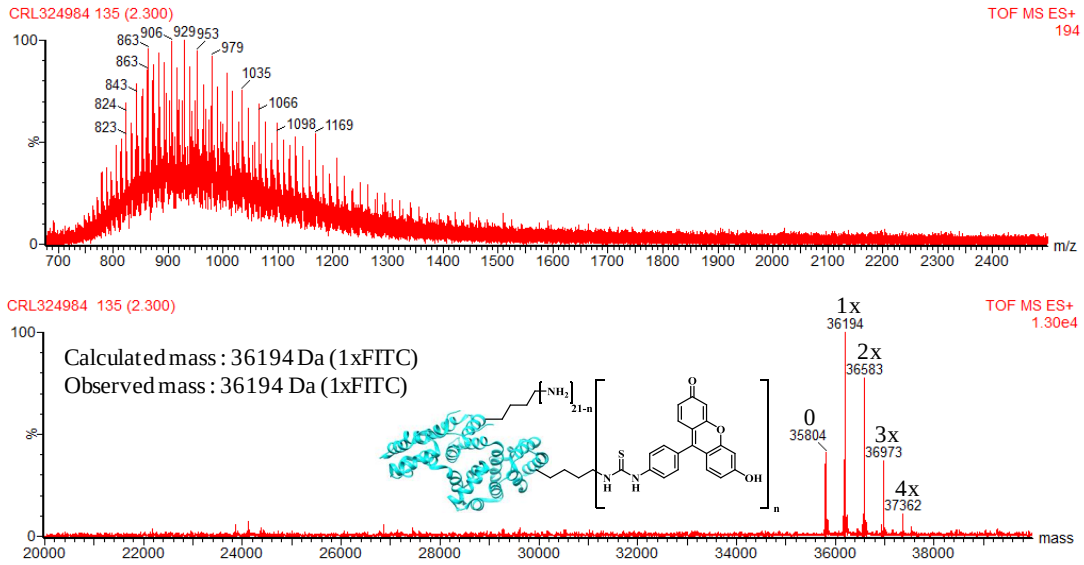

Figure 2.59 ESI-MS spectrum of wild-type annexin V labelled with 30 equiv. FITC.

Labelling of Fluorinated Annexin V with Fluorescein Isothiocyanate (FITC) Dye

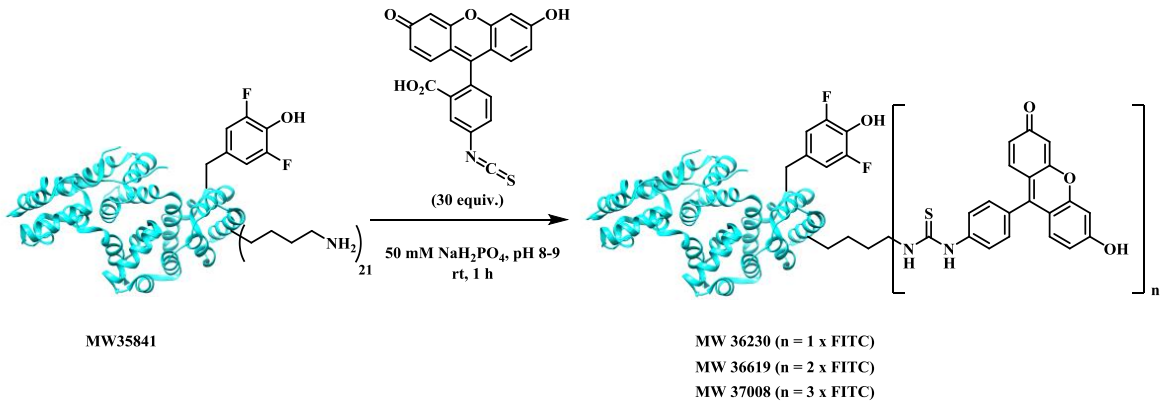

Each aliquot of fluorinated annexin V (5 equiv. F^+_ANV: 9.04 nmol, 1.69 mg/mL, 200 µL and 20 equiv. F^+_ANV: 8.93 nmol, 1.60 mg/mL, 200 µL) in 50 mM NaH_2PO_4, pH 8.0 was mixed with a freshly prepared solution of 1 M $NaHCO_3$ (40 µL) and a solution of FITC dye in DMSO (271 nmol (5 equiv. F^+_ANV), 3.50 µL and 268 nmol (20 equiv. F^+_ANV), 3.50 µL from stock solution, conc. 30 mg/mL) by vortexing briefly. After 1h of shaking at room temperature, an aliquot was analysed by LC-MS after removal of excess FITC dye using a dye removal column (according to the Thermo Scientific's

instruction). The purified protein samples were flash frozen with liquid nitrogen and stored at –80 ºC.

Entry	ANV (equiv.)	FITC (equiv.)	Reaction conditions[a]	Product (Da)
1	1 (5equiv. F^+_ANV)	30	25 °C, 60 min	35838 (SM) 36228 (1xFITC) 36616 (2xFITC) 37005 (3xFITC)
2	1 (20equiv. F^+_ANV)	30	25 °C, 60 min	35898 (SM) 36289 (1xFITC) 36678 (2xFITC)

General conditions: a). ANV (diF-Tyr) in NaH_2PO_4 (50 mM, pH 8) and FITC in DMSO at 25 °C for 60 min unless otherwise indicated; SM: starting material.

Table 2.13 Fluorescent labelling of the fluorinated ANV with 30 equiv. FITC.

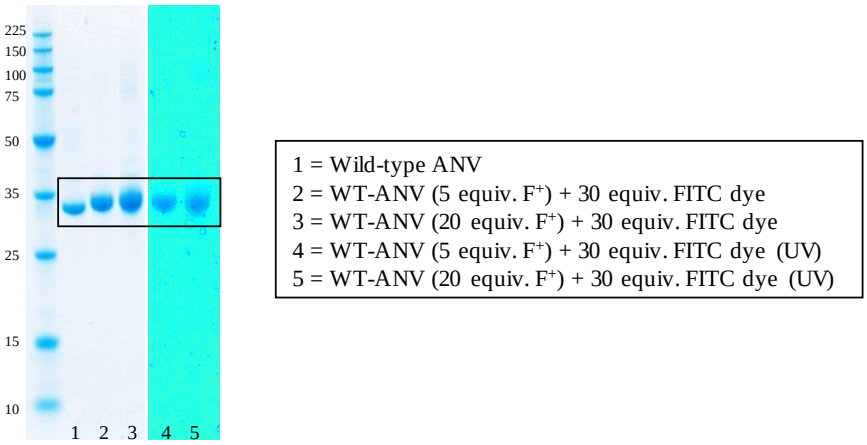

Figure 2.60 SDS-PAGE of fluorinated annexin V (5 equiv. F^+ and 20 equiv. F^+_ANV, respectively) labelled with 30 equiv. FITC fluorescent dye.

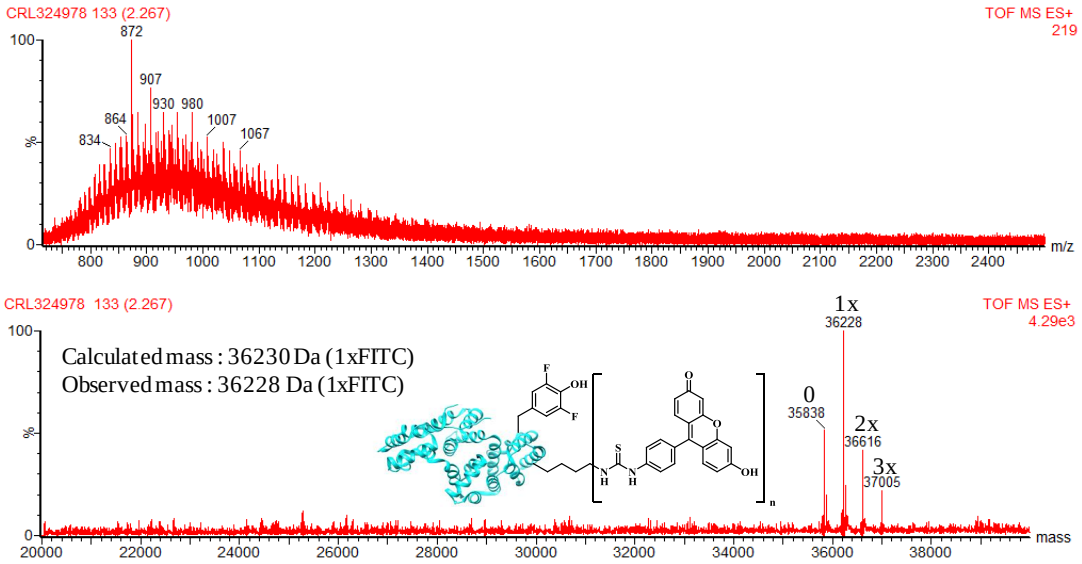

Figure 2.61 ESI-MS spectrum of fluorinated annexin V (5 equiv. F^+_ANV) labelled with 30 equiv. FITC.

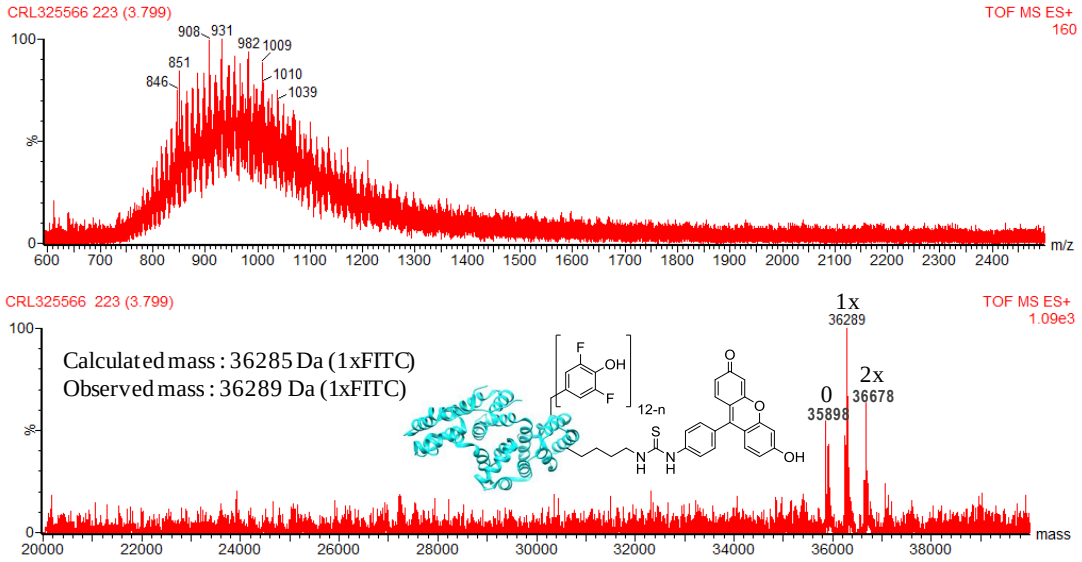

Figure 2.62 ESI-MS spectrum of fluorinated annexin V (20 equiv. F^+_ANV) labelled with 30 equiv. FITC.

2.6.12 Apoptotic Detection of the FITC-labelled Annexin V

(Same procedure mentioned in section 2.6.6)

Entry	Proteins/ Dyes (2.2 mg/mL)	Actinomycin D (1.0 µg/mL)	PI (100 µg/mL)	Comments
1	FITC_WT_ANV (4.4 µg)	10 µL	10 µL	Late apoptosis
2	FITC_5eqF _ANV (4.4 µg)	10 µL	10 µL	Late apoptosis
3	FITC_20eqF _ANV (4.4 µg)	10 µL	10 µL	Late apoptosis
4	FITC_WT_ANV (4.4 µg)	-	10 µL	Control : apoptosis not induced
5	FITC_5eqF _ANV (4.4 µg)	-	10 µL	Control : apoptosis not induced
6	FITC_20eqF _ANV (4.4 µg)	-	10 µL	Control : apoptosis not induced
7	-	10 µL	10 µL	Control : necrotic cells
8	FITC (4.4 µg)	-	-	Control : non-specific binding
9	FITC (4.4 µg)	10 µL	10 µL	Control : non-specific binding
10	Fluorescein diacetate (4.4 µg)	-	10 µL	Control : live/dead cells staining
11	WT_ANV (unlabelled, 27 µg) FITC_WT_ANV (4.4 µg)	10 µL	10 µL	Blocking experiment
12	WT_ANV (unlabelled, 27 µg) FITC_5eqF_ANV (4.4 µg)	10 µL	10 µL	Blocking experiment
13	WT_ANV (unlabelled, 27 µg) FITC_20eqF_ANV (4.4 µg)	10 µL	10 µL	Blocking experiment

The incubation period for apoptotic induction was at 37 °C for 1h.
ANV = Annexin V, WT = Wild-type, FITC = Fluorescein isothiocyanate, PI = Propidium iodide
5eqF_ANV / 20 eqF_ANV = Fluorinated Annexin V

Table 2.14 Apoptotic detection of HEK 293 cells induced by actinomycin D and subsequently stainned by fluorescent-labelled annexin V and PI.

1. Wild-type ANV labelled with FITC dye (Entry **1**)

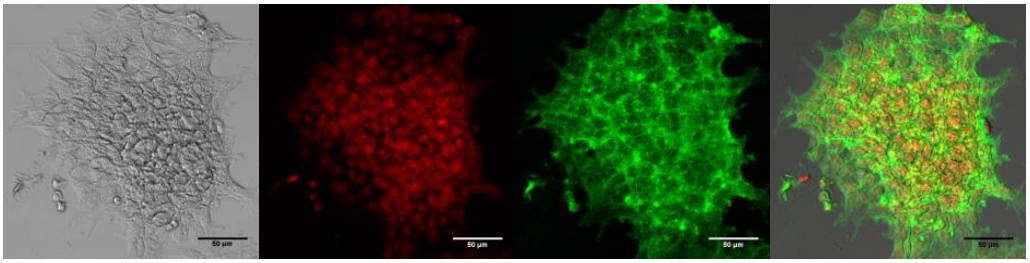

2. Fluorinated ANV (5 equiv.F^+_ANV) labelled with FITC dye (Entry **2**)

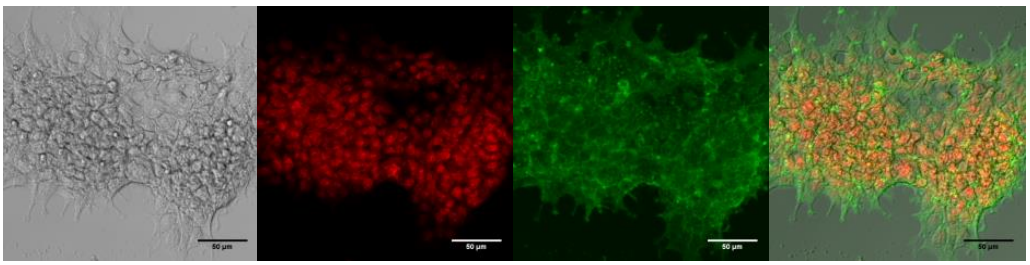

3. Fluorinated ANV (20 equiv.F^+_ANV) labelled with FITC dye (Entry **3**)

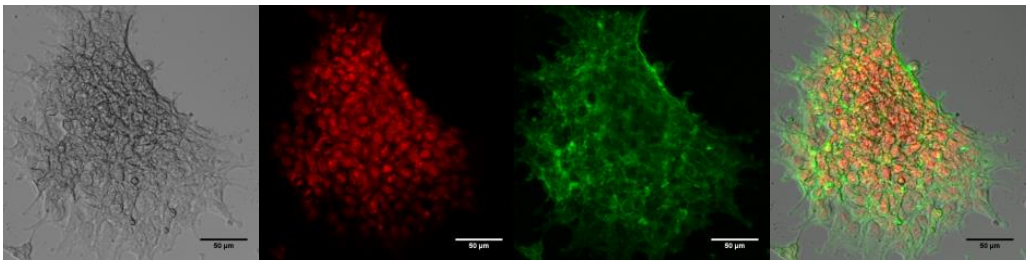

4. Wild-type ANV labelled with FITC dye, control (Entry **4**)

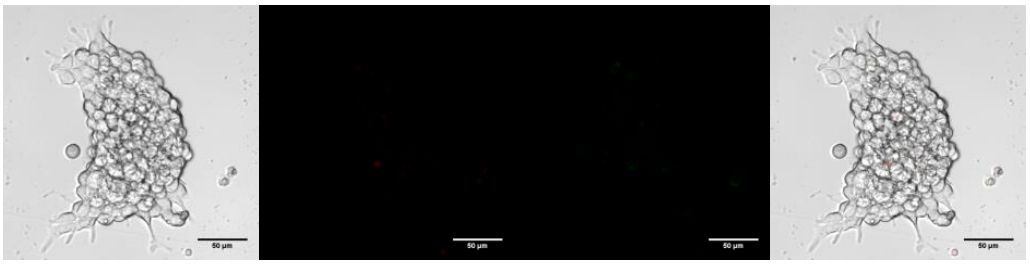

5. Fluorinated ANV (5 equiv.F^+_ANV) labelled with FITC dye, control (Entry **5**)

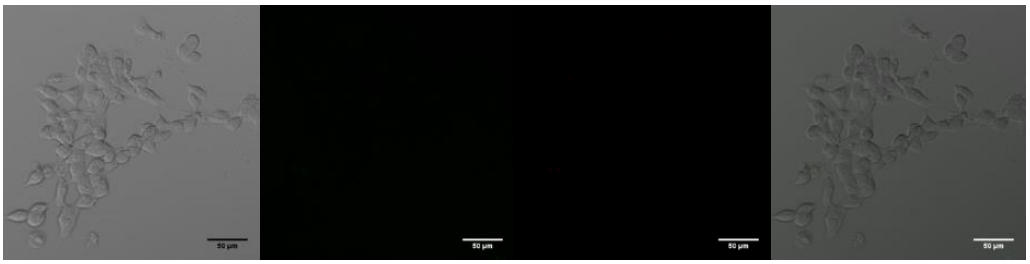

6. Fluorinated ANV (20 equiv.F^+_ANV) labelled with FITC dye, control (Entry **6**)

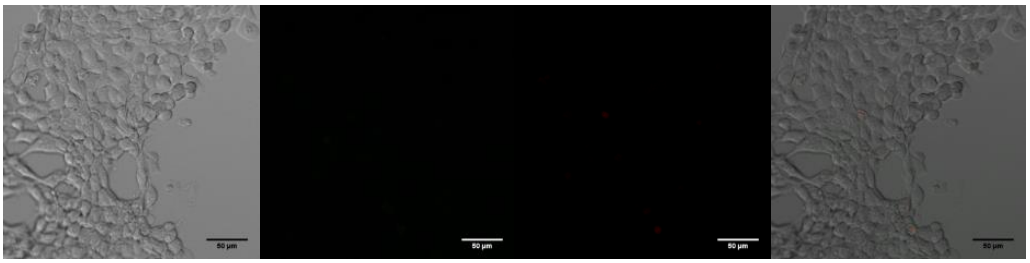

7. Necrotic cells (Entry **7**)

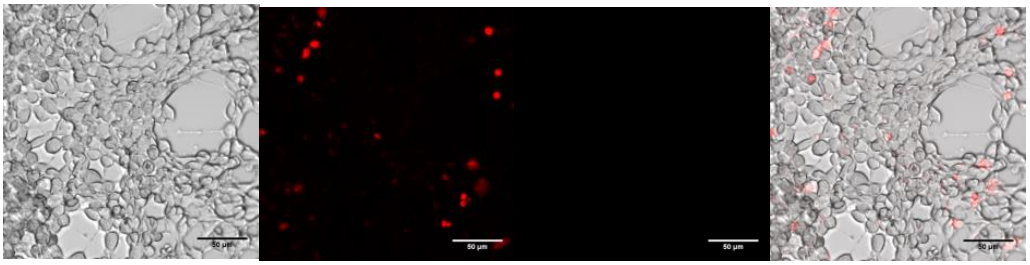

8. Non-specific binding – Live cells (Entry **8**)

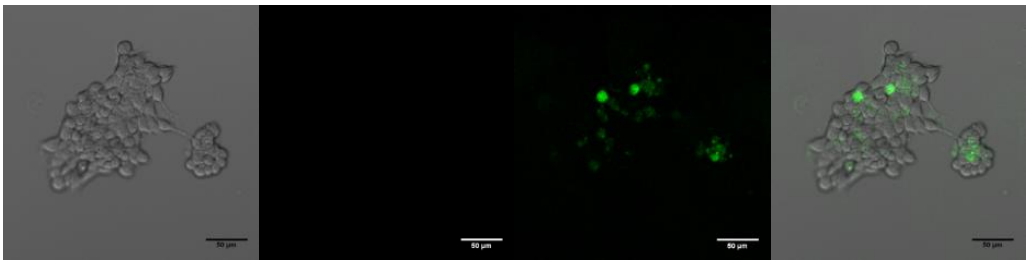

9. Non-specific binding – Dead cells (Entry **9**)

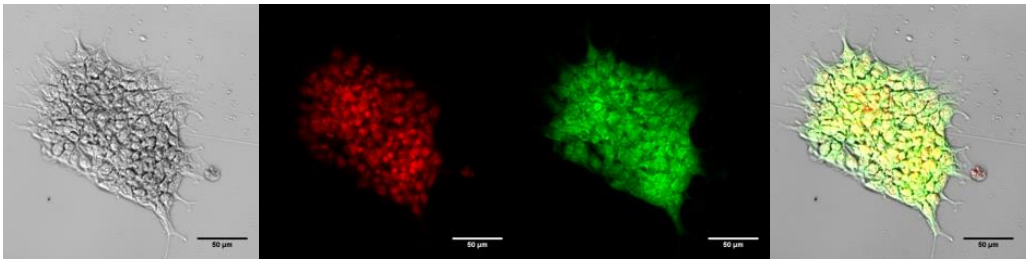

10. Live and dead cells staining (Entry **10**)

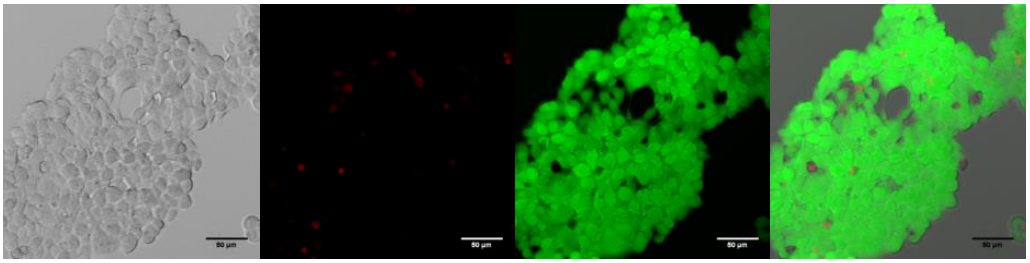

11. Non-labelled wild-type ANV, and wild-type ANV labelled with FITC dye, blocking experiment (Entry **11**)

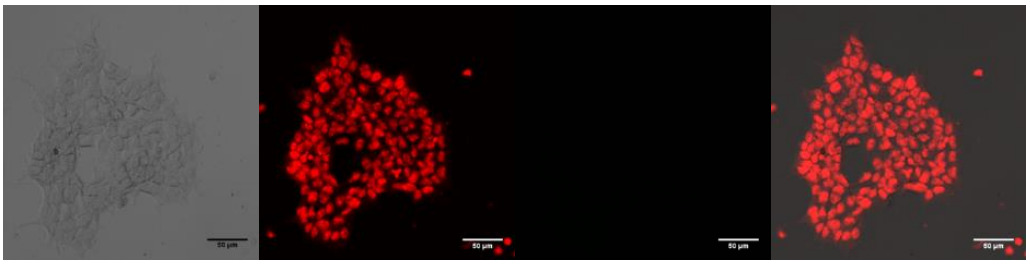

12. Non-labelled wild-type ANV, and fluorinated ANV (5 equiv.F^+_ANV) labelled with FITC dye, blocking experiment (Entry **12**)

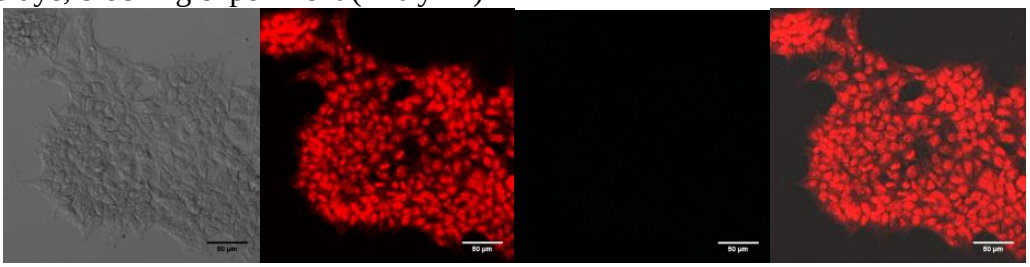

13. Non-labelled wild-type ANV, and fluorinated ANV (20 equiv.F^+_ANV) labelled with FITC dye, blocking experiment (Entry **13**)

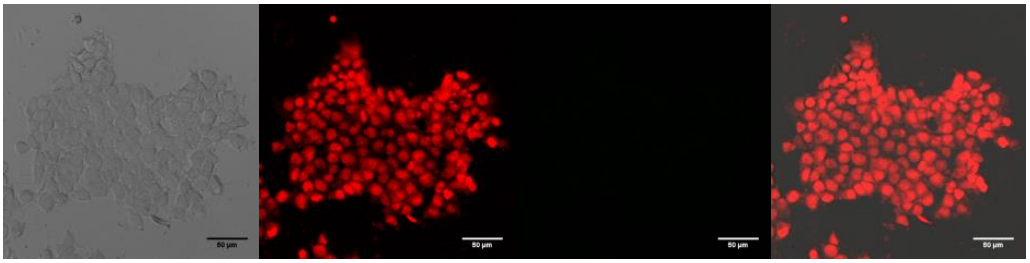

Figure 2.63 Fluorescent images of the apoptotic-induced HEK 293 cells using a confocal laser scanning microscopy (LEICA) and scale bar 50 µm : channel I = bright field, channel II = PI, channel III = fluorescent-labelled annexin V or dye, and channel IV = merged channels I+II+III.

2.7 Bibliography

(1) Campbell, M. G.; Ritter, T. Late-Stage Fluorination: From Fundamentals to Application. *Org. Process Res. Dev.* **2014**, *18*, 474-480.

(2) Champagne, P. A.; Desroches, J.; Hamel, J. D.; Vandamme, M.; Paquin, J. F. Monofluorination of Organic Compounds: 10 Years of Innovation. *Chem. Rev.* **2015**, *115*, 9073-9174.

(3) Gerstenberger, M. R. C.; Hass, A. Methods of Fluorination in Organic Chemistry. *Angew. Chem. Int. Ed.* **1981**, *20*, 647-667.

(4) Liang, T.; Neumann, C. N.; Ritter, T. Introduction of fluorine and fluorine-containing functional groups. *Angew. Chem. Int. Ed. Engl.* **2013**, *52*, 8214-8264.

(5) Shimizu, M.; Hiyama, T. Modern synthetic methods for fluorine-substituted target molecules. *Angew. Chem. Int. Ed. Engl.* **2004**, *44*, 214-231.

(6) Zhou, Y.; Wang, J.; Gu, Z.; Wang, S.; Zhu, W.; Acena, J. L.; Soloshonok, V. A.; Izawa, K.; Liu, H. Next Generation of Fluorine-Containing Pharmaceuticals, Compounds Currently in Phase II-III Clinical Trials of Major Pharmaceutical Companies: New Structural Trends and Therapeutic Areas. *Chem. Rev.* **2016**, *116*, 422-518.

(7) Nyffeler, P. T.; Duron, S. G.; Burkart, M. D.; Vincent, S. P.; Wong, C. H. Selectfluor: mechanistic insight and applications. *Angew. Chem. Int. Ed. Engl.* **2004**, *44*, 192-212.

(8) Banks, R. E. Selectfluor™ reagent F-TEDA-BF4 in action: tamed fluorine at your service. *J. Fluorine Chem.* **1998**, *87*, 1-17.

(9) Borodkin, G. I.; Zaikin, P. A.; Shakirov, M. M.; Shubin, V. G. Mechanism of electrophilic fluorination of aromatic compounds with NF-reagents. *Russ. J. Org. Chem.* **2007**, *43*, 1451-1459.

(10) Stavber, G.; Zupan, M.; Jereb, M.; Stavber, S. Selective and Effective Fluorination of Organic Compounds in Water Using Selectfluor F-TEDA-BF_4. *Org. Lett.* **2004**, *6*, 4973-4976.

(11) J.-A., M.; Cahard, D. Asymmetric Fluorination, Trifluoromethylation, and Perfluoroalkylation Reactions. *Chem. Rev.* **2004**, *104*, 6119-6146.

(12) Shibata, N.; Suzuki, E.; Asahi, T.; Shiro, M. Enantioselective Fluorination Mediated by Cinchona Alkaloid Derivatives/Selectfluor Combinations: Reaction Scope and Structural Information for N-Fluorocinchona Alkaloids. *J. Am. Chem. Soc.* **2001**, *123*, 7001-7009.

(13) Biava, H.; Budisa, N. Evolution of fluorinated enzymes: An emerging trend for biocatalyst stabilization. *Engineering in Life Sciences* **2014**, *14*, 340-351.

(14) Boutureira, O.; Bernardes, G. J.; D'Hooge, F.; Davis, B. G. Direct radiolabelling of proteins at cysteine using [18F]-fluorosugars. *Chem. Commun.* **2011**, *47*, 10010-10012.

(15) Boutureira, O.; D'Hooge, F.; Fernandez-Gonzalez, M.; Bernardes, G. J.; Sanchez-Navarro, M.; Koeppe, J. R.; Davis, B. G. Fluoroglycoproteins: ready chemical site-selective incorporation of fluorosugars into proteins. *Chem. Commun.* **2010**, *46*, 8142-8144.

(16) Budisa, N.; Wenger, W.; Wiltschi, B. Residue-specific global fluorination of Candida antarctica lipase B in Pichia pastoris. *Mol Biosyst* **2010**, *6*, 1630-1639.

(17) Buer, B. C.; Marsh, E. N. Fluorine: a new element in protein design. *Protein Sci.* **2012**, *21*, 453-462.

(18) Salwiczek, M.; Nyakatura, E. K.; Gerling, U. I.; Ye, S.; Koksch, B. Fluorinated amino acids: compatibility with native protein structures and effects on protein-protein interactions. *Chem. Soc. Rev.* **2012**, *41*, 2135-2171.

(19) Gao, Z.; Gouverneur, V.; Davis, B. G. Enhanced Aqueous Suzuki–Miyaura Coupling Allows Site-Specific Polypeptide 18F-Labeling. *J. Am. Chem. Soc.* **2013**, *135*, 13612-13615.

(20) Kuchar, M.; Pretze, M.; Kniess, T.; Steinbach, J.; Pietzsch, J.; Loser, R. Site-selective radiolabeling of peptides by (18)F-fluorobenzoylation with [(18F)]SFB in solution and on solid phase: a comparative study. *Amino acids* **2012**, *43*, 1431-1443.

(21) Tang, G.; Zeng, W.; Yu, M.; Kabalka, G. Facile synthesis ofN-succinimidyl 4-[18F]fluorobenzoate ([18F]SFB) for protein labeling. *J. Labelled Compd. Radiopharm.* **2008**, *51*, 68-71.

(22) Li, X.; Link, J. M.; Stekhova, S.; Yagle, K. J.; Smith, C.; Krohn, K. A.; Tait, J. F. Site-Specific Labeling of Annexin V with F-18 for Apoptosis Imaging. *Bioconjug. Chem.* **2008**, *19*.

(23) Murakami, Y.; Takamatsu, H.; Taki, J.; Tatsumi, M.; Noda, A.; Ichise, R.; Tait, J. F.; Nishimura, S. 18F-labelled annexin V: a PET tracer for apoptosis imaging. *Eur. J. Nucl. Med. Mol. Imaging* **2004**, *31*, 469-474.

(24) Perreault, A.; Knight, J. C.; Wang, M.; Way, J.; Wuest, F. 18F-Labeled wild-type annexin V: comparison of random and site-selective radiolabeling methods. *Amino acids* **2016**, *48*, 65-74.

(25) Yagke, K. J.; Eary, J. F.; Grierson, J. R.; Link, J. M.; Lewellen, B.; Gibson, D. F.; Krohn, K. A. Evaluation of 18F-annexin V as a PET imaging agent in an animal model of apoptosis. *J. Nucl. Med.* **2005**, *46*, 658-666.

(26) Blankenberg, F. G.; Katsikis, P. D.; Tait, J. F.; Davis, R. E.; Naumovski, L.; Ohtsuki, K.; Kopiwoda, S.; Abrams, M. J.; Darkes, M.; Robbins, R. C.; Maecker, H. T.; Strauss , H. W. In vivo detection and imaging of phosphatidylserine expression during programmed cell death *Proc. Natl. Acad. Sci. U.S.A.* **1998**, *95*, 6349-6354.

(27) Koopman, G.; Reutelingsperger, C. P.; Kuijten, G. A.; Keehnen, R. M.; Pals, S. T.; van Oers, M. H. Annexin V for flow cytometric detection of phosphatidylserine expression on B cells undergoing apoptosis. *Blood* **1994**, *84*, 1415-1420.

(28) Raynal, P.; Pollard, H. B. Annexins: the problem of assessing the biological role for a gene family of multifunctional calcium- and phospholipid-binding proteins. *Biochem. Biophys. Acta* **1994**, *1197*, 63-93.

(29) Thiagarajan, P.; Tait, J. F. Binding of annexin V/placental anticoagulant protein I to platelets. Evidence for phosphatidylserine exposure in the procoagulant response of activated platelets. *J. Biol. Chem.* **1990**, *265*, 17420-17423.

(30) Hu, S.; Kiesewetter, D. O.; Zhu, L.; Guo, N.; Gao, H.; Liu, G.; Hida, N.; Lang, L.; Niu, G.; Chen, X. Longitudinal PET imaging of doxorubicin-induced cell death with 18F-Annexin V. *Mol. Imaging Biol.* **2012**, *14*, 762-770.

(31) Bernardes, G. J. L.; Chalker, J. M.; Errey, J. C.; Davis, B. G. Facile Conversion of Cysteine and Alkyl Cysteines to Dehydroalanine on Protein Surfaces: Versatile and Switchable Access to Functionalized Proteins. *J. Am. Chem. Soc.* **2008**, *130*, 5052-5053.

(32) Chalker, J. M.; Bernardes, G. J.; Davis, B. G. A 'Tag and Modify' Approach to Site-Selective Protein Modification. *Acc. Chem. Res.* **2011**, *44*, 730-741.

(33) Chalker, J. M.; Gunnoo, S. B.; Boutureira, O.; Gerstberger, S. C.; Fernández-González, M.; Bernardes, G. J. L.; Griffin, L.; Hailu, H.; Schofield, C. J.; Davis, B. G. Methods for converting cysteine to dehydroalanine on peptides and proteins. *Chem. Sci.* **2011**, *2*, 1666.

(34) Fernández-González, M.; Boutureira, O.; Bernardes, G. J. L.; Chalker, J. M.; Young, M. A.; Errey, J. C.; Davis, B. G. Site-selective chemoenzymatic construction of synthetic glycoproteins using endoglycosidases. *Chem. Sci.* **2010**, *1*, 709.

(35) Gunnoo, S. B.; Finney, H. M.; Baker, T. S.; Lawson, A. D.; Anthony, D. C.; Davis, B. G. Creation of a gated antibody as a conditionally functional synthetic protein. *Nat Commun* **2014**, *5*, 4388.

(36) Teare, H.; Robins, E. G.; Kirjavainen, A.; Forsback, S.; Sandford, G.; Solin, O.; Luthra, S. K.; Gouverneur, V. Radiosynthesis and evaluation of [18F]Selectfluor bis(triflate). *Angew. Chem. Int. Ed. Engl.* **2010**, *49*, 6821-6824.

(37) Wood, B. L.; Gibson, D. F.; Tait, J. F. Increased Erythrocyte Phosphatidylserine Exposure in Sickle Cell Disease: Flow-Cytometric Measurement and Clinical Associations. *Blood* **1996**, *88*, 1873-1880.

Chapter 3

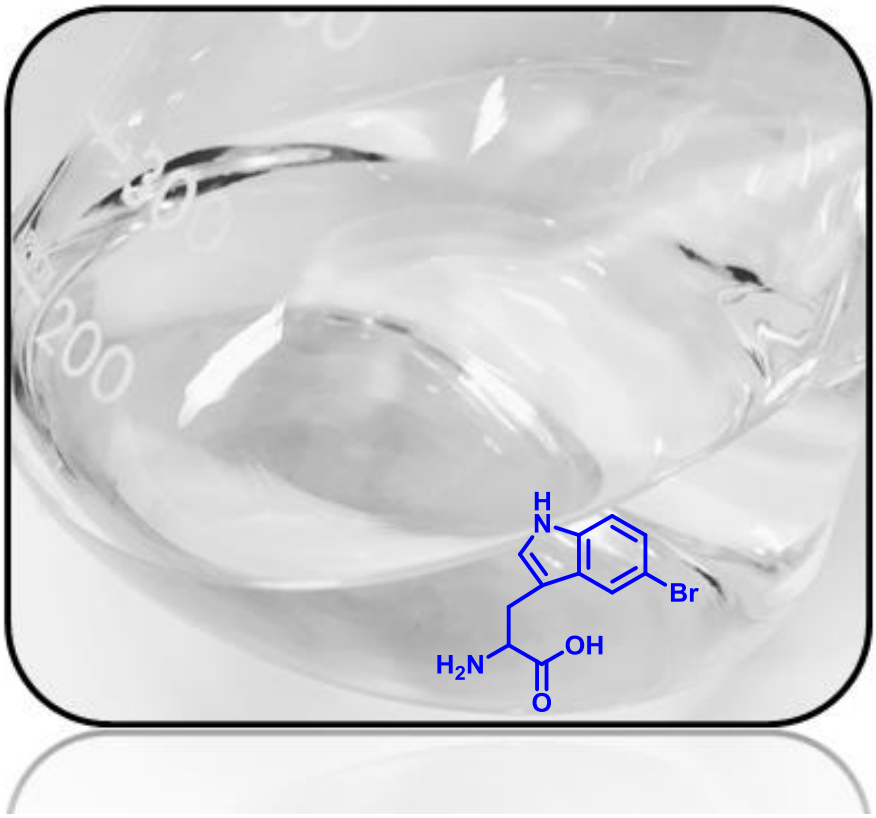

Biosynthetic Incorporation of Synthetic Tryptophan Analogue into Proteins

3.1 Introduction

3.1.1 Synthesis of Bromotryptophan

3.1.2 Biosynthetic Incorporation of Tryptophan Analogues into Proteins

3.1.3 Suzuki-Miyaura Cross-Coupling Reaction of Proteins

3.2 Synthetic Strategy of 5-Bromotryptophan

3.3 Model Studies of Suzuki-Miyaura Cross-Coupling Reactions

3.4 Investigation of Biosynthetic Incorporation Systems

3.5 Conclusion

3.6 Experimental

3.7 Bibliography

3.1 Introduction

The aim of this chapter is to investigate new biosynthetic incorporation systems for introduction of bromotryptophan into the protein and subsequent site-specific protein modification using aqueous Pd-mediated Suzuki-Miyaura reactions.

3.1.1 Synthesis of Bromotryptophan

The photophysical characteristics of tryptophan (Trp) and its analogues can be used to investigate many vital protein functions including protein-protein interactions, protein folding or unfolding mechanisms or ligand binding[1-3]. Nagarathnam and Johnson described a synthesis of 5-bromo-DL-tryptophan (5-Br-Trp) **1** using indole chemistry (Scheme **3.1**)[4]. The synthesis of 5-Br-Trp **1** proceeded from treatment of 4-bromophenylhydrazine **2** with 2-ketobutyric acid **3** under acid conditions, affording 5-bromoindole ethyl ester **4**. Subsequent base-promoted decarboxylation, followed by *N*-protection and bromination of the resultant species **5**, gave corresponding *N*-protected 3-bromoethylindole **6**. Treatment of **6** with diethyl acetamidomalonate in the presence of NaH in THF gave the intermediate **7** followed by deprotection and hydrolysis to afford 5-bromotryptophan **1**.

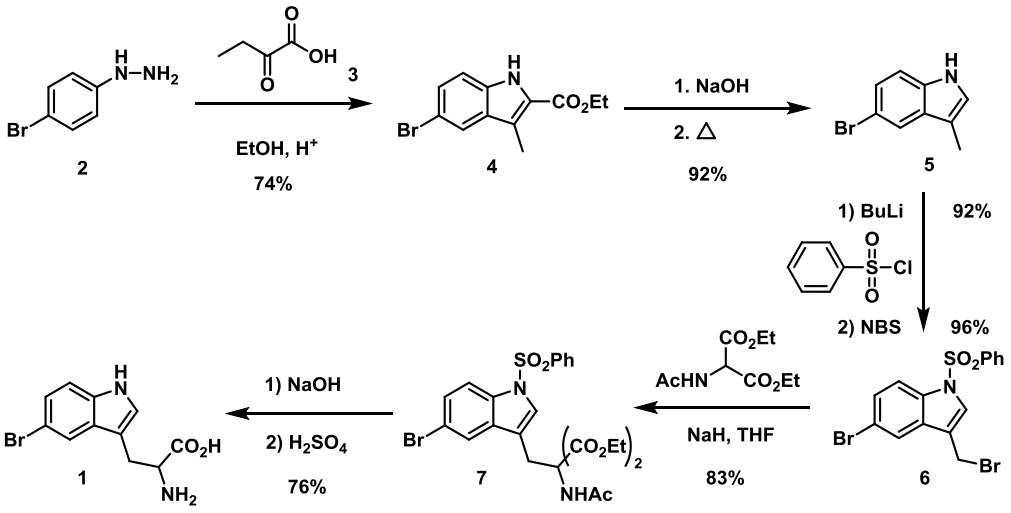

Scheme 3.1 Synthesis of 5-bromotryptophan **1**[4].

An alternative synthesis of 5-bromo-DL-tryptophan **1,** and *N*-protected 5-bromo-DL-tryptophan **13,** using 5-bromoindole **8** as a precursor was reported by Prasitpan and co-

workers in excellent yield (Scheme **3.2**)[5]. An alkylation of 5-bromoindole **8** with hydroxyiminopropanoate **9** gave bromoindolyl ester **10**. Reduction of **10** was achieved using zinc powder under acidic conditions affording tryptophanyl ethyl ester **11**. This amine **11** was used as an intermediate in the formation of 5-bromotryptophan **1** and its *N*-protected analogue **13**. Formation of target tryptophan **1** was successful after hydrolysis of amine **11** under basic conditions. Alternatively, Boc protection of the amine followed by ester saponification gave *N*-Boc-5-bromo-Trp **13**.

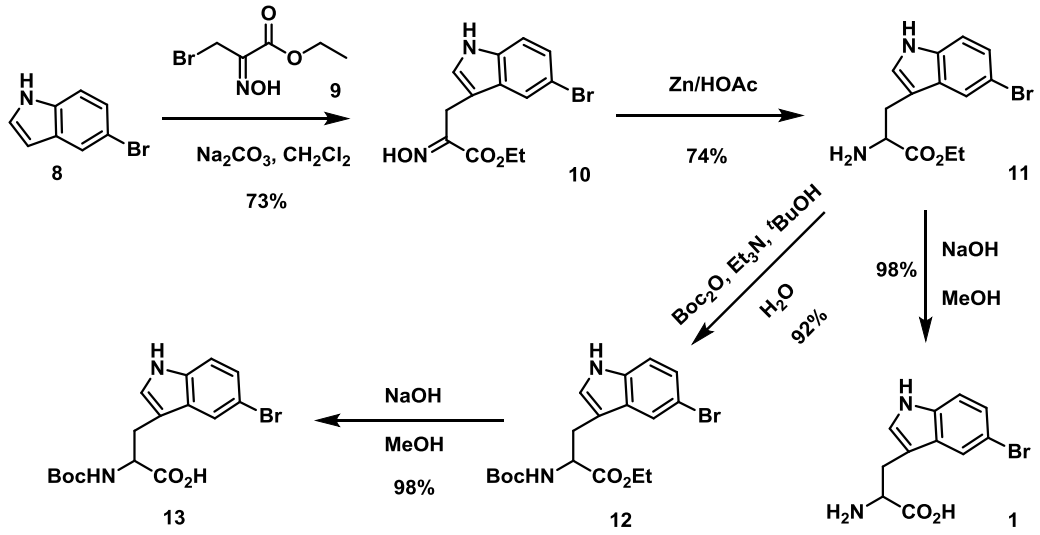

Scheme 3.2 Formation of 5-bromotryptophan **1** and its *N*-protected analogue **13**[5].

3.1.2 Biosynthetic Incorporation of Tryptophan Analogues into Proteins

Recent advances have described different methods for genetic incorporation of unnatural amino acids into recombinant proteins using auxotrophic strains, stop codon suppression or genetic engineering [1-3,6-10]. 5-Hydroxytryptophan (5-OH-Trp) **14** and 7-azatryptophan (7-Aza-Trp) **15** are Trp analogues which have been previously introduced into bacterial proteins due to their structural similarity to natural tryptophan located in proteins[1-3]. Hogue and co-workers studied the biosynthetic incorporation of 5-OH-Trp **14** and 7-Aza-Trp **15** into bacterial proteins, with the tryptophanyl-tRNA synthetase (TrpRS) playing a key role in the incorporation of these analogues[1,2]. These could be applied to investigating protein-protein interactions as characteristic fluorescent probes.

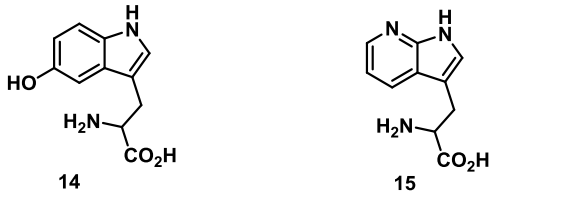

Figure 3.1 Structures of 5-hydroxytryptophan **14** and 7-azatryptophan **15**.

5-Fluorotryptophan (5-F-Trp) **16** was biosynthetically incorporated into protein J, which was originally from *Salmonella typhimurium*, by use of a tryptophan auxotroph with 70% incorporation efficiency[11]. Broos and co-workers described the use of *Lactococcus lactis* as an expression host for incorporation of Trp analogues into recombinant proteins[6]. Tryptophan auxotrophs of *L. lactis* were modified by deletion of Trp synthase genes. This approach allowed the high efficiency of 7-Aza-Trp **15**, 5-F-Trp **16** and 5-OH-Trp **14** incorporations (97%, 97% and 89% respectively). 5-Methyltryptophan (5-Me-Trp) **17** was also successfully biosynthetically incorporated into recombinant proteins, with evidence of incorporation from MALDI-TOF mass spectra, shown in Figure **3.2**.

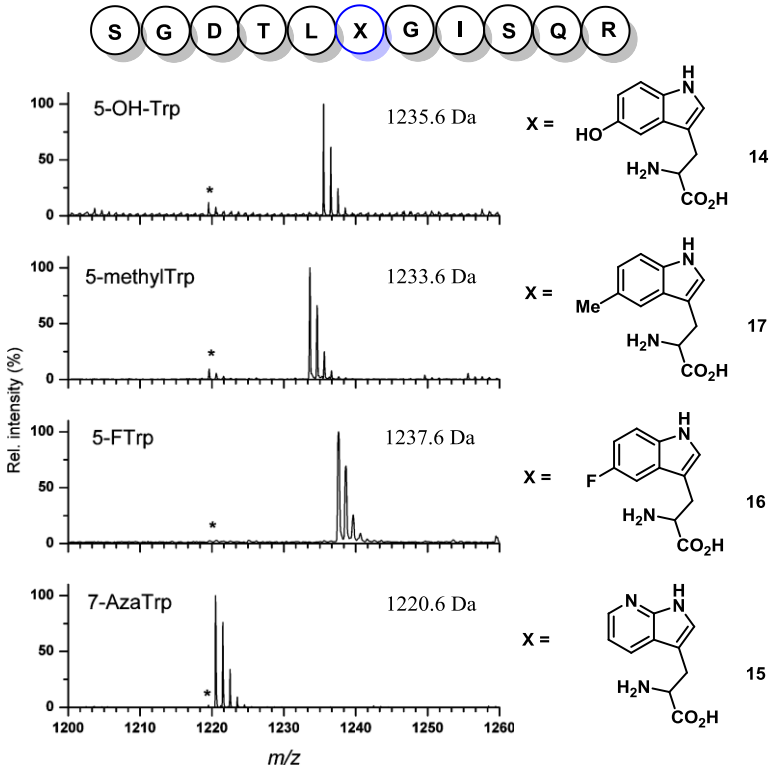

Figure 3.2 Tryptic fragment of PA6* (natural tryptophan, m/z = 1219.6 Da) with the incorporation of different Trp analogues and subsequent analysis by MALDI-TOF[6]. The figure is adapted with permission by *Biochem. J*. **2008**, 409, 193-198. Copyright 2008 Portland Press.

Halogenated tryptophan derivatives including 6-bromotryptophan (6-Br-Trp) **18**, 6-chlorotryptophan (6-Cl-Trp) **19** and benzothienylalanine (BT) **20** have all been incorporated into murine dihydrofolate reductase (mDHFR) with ≥98% fidelity using a designed phenylalanyl-tRNA synthetase, yPheRS (T415G)[12]. SDS-PAGE analysis of mDHFR incorporated with different halogenated tryptophan derivatives is shown in Figure **3.3**.

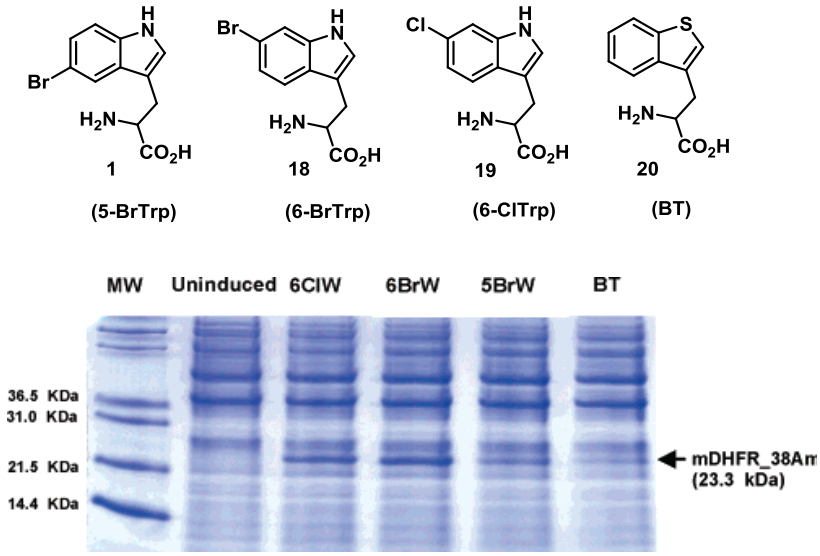

Figure 3.3 SDS-PAGE analysis of mDHFR incorporated with different Trp analogues[12]. The figure is adapted with permission by *J. Am. Chem. Soc.* **2007**, 129, 10431-10437. Copyright 2007 American Chemical Society.

3.1.3 Suzuki-Miyaura Cross-Coupling Reaction of Proteins

Previous work in our group has led to the development of an efficient Pd-pyrimidine catalyst, [**L1**]$_2$Pd(OAc)$_2$, which is generated from treatment of 2-amino-4,6-dihydroxypyrimidine with sodium hydroxide and addition of palladium acetate (Scheme **3.3**)[13-16]. This catalyst is useful in the Suzuki-Miyaura cross-coupling of amino acids and proteins in fully aqueous media.

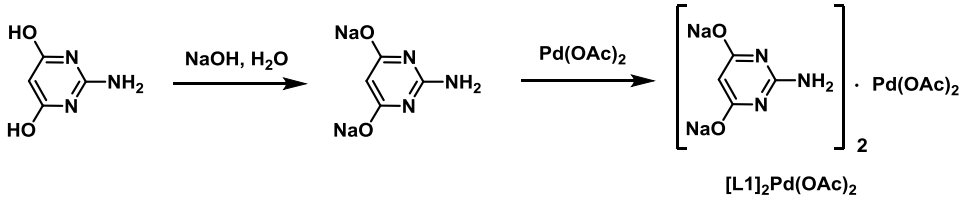

Scheme 3.3 Preparation of Pd-pyrimidine catalyst [**L1**]$_2$Pd(OAc)$_2$[13-16].

Chalker and Davis described the cross-coupling of halo-phenylalanine and tyrosine derivatives with phenyl boronic acid using the aforementioned soluble Pd catalyst, [**L1**]$_2$Pd(OAc)$_2$ in excellent yields, except the chloro- variant (Table **3.1**)[13].

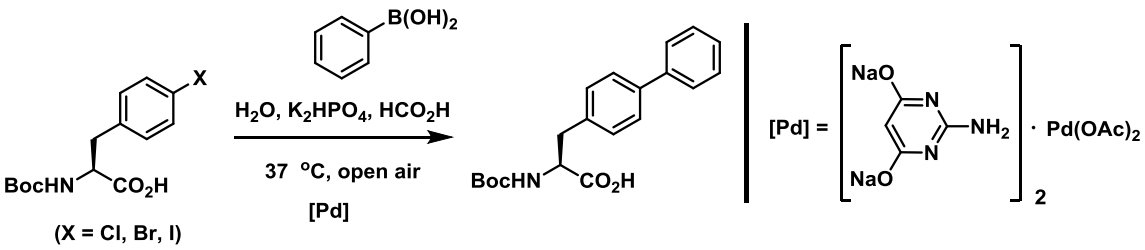

Entry	SM	Pd Loading	Conditions	Coupling product	Yield (%)
1	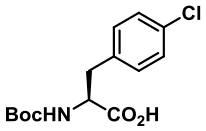	1%	37 °C, 4h	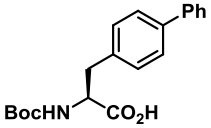	0
2	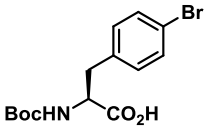	1%	37 °C, 4h	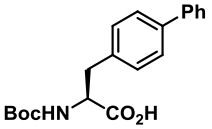	98
3	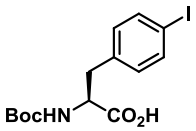	1%	37 °C, 4h	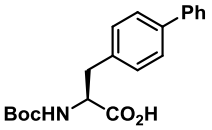	95
4	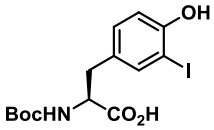	1%	37 °C, 4h	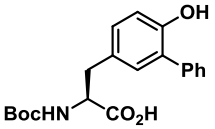	94

Table 3.1 A model study of Suzuki reactions using aqueous pyrimidine-based Pd catalyst[13].

Interestingly, Wang and co-workers have reported a synthesis of aromatic-substituted bulky and hydrophobic tryptophan derivatives through Suzuki-Miyaura cross-coupling reactions in the presence of Pd(OAc)$_2$, P(*o*-tolyl)$_3$ and K_2CO_3 (Scheme **3.4**)[17].

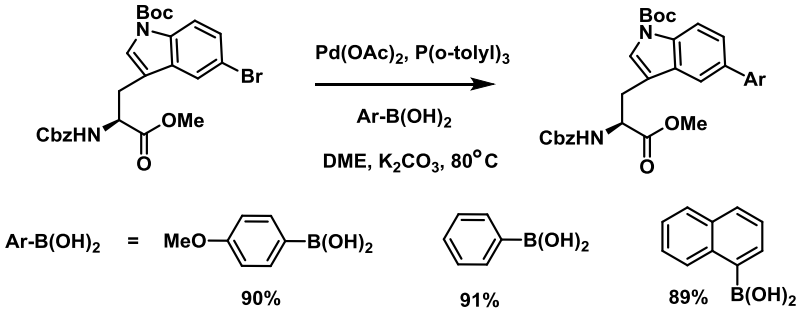

Scheme 3.4 Palladium-catalysed cross-coupling reactions of tryptophan derivatives with aryl boronic acids[17].

3.2 Synthetic Strategy of 5-Bromotryptophan

Our synthesis of the target 5-bromo-DL-tryptophan **1** followed the synthetic approach originally described by Prasitpan et. al[5]. The synthesis of 5-Br-Trp **1** proceeded from a preparation of hydroxyiminopropanoate **9** obtained by the reaction of ethyl bromopyruvate **21** with NH_2OH•HCl in a solvent mixture of 1:1 $CHCl_3/H_2O$ (Scheme **3.5**). Formation of oxime **10** was achieved by a C3-alkylation of 5-bromoindole **8** with hydroxyimino propanoate **9** in dichloromethane in the presence of Na_2CO_3.

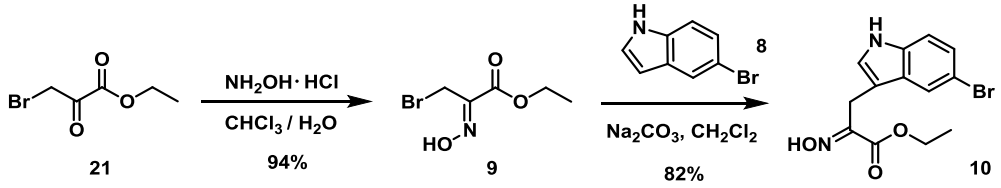

Scheme 3.5 Synthesis of oxime **10**.

Reduction of oxime **10** using zinc powder under acidic conditions resulted in the formation of amino acid ethyl ester **11** in 76% yield (Scheme **3.6**). The resulting tryptophanyl ethyl ester **11** was hydrolysed using NaOH in methanol, affording the desired 5-bromo-DL-tryptophan **1** in 73% yield.

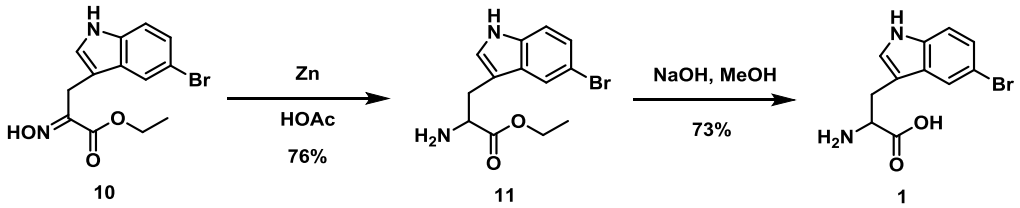

Scheme 3.6 Preparation of target tryptophan **1**.

The amino group of **11** was protected using Boc_2O in the presence of Et_3N and ^tBuOH to afford *N*-Boc-5-bromotryptophan ester **12** and subsequent hydrolysis of **12** using NaOH/MeOH gave the corresponding *N*-Boc-5-bromotryptophan **13** in 65% yield over 2 steps (Scheme **3.7**).

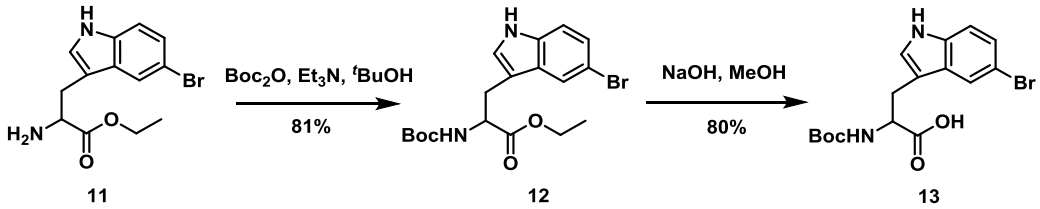

Scheme 3.7 Formation of *N*-Boc-5-bromotryptophan **13**.

3.3 Model Studies of Suzuki-Miyaura Cross-Coupling Reactions

To extend our aqueous Pd cross-coupling system to challenging halogenated tryptophan residues, we investigated cross-coupling of the model substrate *N*-protected-5-bromotryptophan **13** to phenylboronic acid in the presence of Pd catalyst solution at 37 °C. Pleasingly, we observed the formation of a new C-C bond at C-5 of the indole ring, providing 5-phenyl-*N*-Boc-tryptophan **22** in 98% yield (Scheme **3.8**).

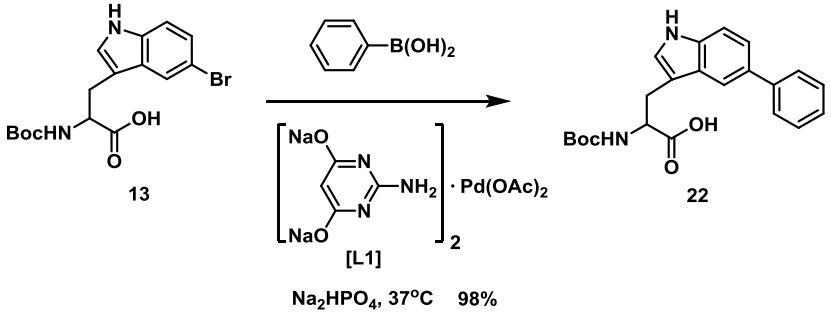

Scheme 3.8 Formation of 5-phenyl-*N*-Boc-tryptophan **22** through aqueous Suzuki-Miyaura cross-coupling.

The pyrimidine-based Pd catalyst $[\mathbf{L1}]_2Pd(OAc)_2$ was assembled by the reaction of 2-amino-4,6-hydroxypyrimidine as a ligand with NaOH to generate an intermediate able to co-ordinate to palladium acetate, as previously shown in Scheme **3.3**[13-16]. The advantages of this catalyst are its solubility in aqueous media and stability at ambient temperature for months, which are useful for protein modification through aqueous Suzuki-Miyaura cross-coupling. Additional halogenated tryptophan derivatives were also tested under

similar conditions (Table **3.2**). It was found that *N*-Boc-5-bromotryptophan was accessible to the Suzuki reaction with $PhB(OH)_2$ to give *N*-Boc-5-phenyltryptophan as a product in excellent yield (Entry **1**). Surprisingly, *N*-Boc-6-bromotrptophan was unreactive, possibly due to electronic effects of the indole ring system (Entry **2**). *N*-Boc-5-chlorotryptophan gave no desired product, despite the reaction the forcing conditions of reflux and tetra-n-butylammonium bromide (TBAB) used as bromide additive (Entry **3**,**4**). Alternatively, a coupling of *N*HAc-5-bromotryptophan with $PhB(OH)_2$ afforded 5-phenyl-acetamidotryptophan in 80% yield, but *N*HAc-5-chlorotryptophan showed no reaction (Entry **5**,**6**).

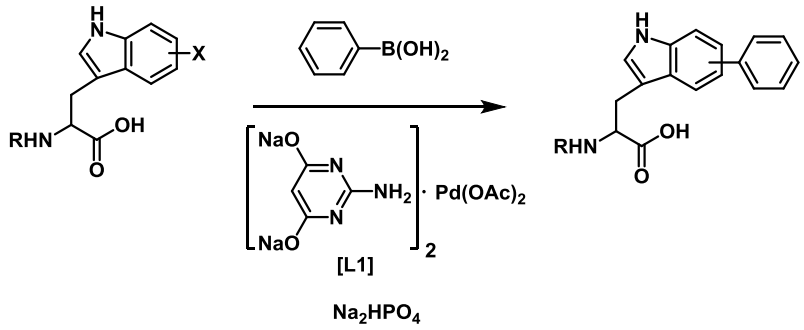

Entry	R	X	Temperature (°C)	Reaction time (h)	Yield (%)
1	*N*-Boc	5-Bromo	37	6	98
2	*N*-Boc	6-Bromo	37	6	SM
3	*N*-Boc	5-Chloro	37	6	SM
4 [a]	*N*-Boc	5-Chloro	105	6	SM
5	*N*HAc	5-Bromo	37	6	80
6	*N*HAc	5-Chloro	37	6	SM

a). The reaction was performed with TBAB (2.0 equiv). All reactions were carried out in aqueous media. SM = starting material.

Table 3.2 Suzuki-Miyaura cross-coupling of halogenated Trp analogues with $PhB(OH)_2$ in the presence of $[\mathbf{L1}]_2Pd(OAc)_2$ catalyst.

Next, we investigated the efficiency of different Pd catalysts by loading different ligands for the cross-coupling of 5-bromo-*N*-Boc tryptophan **13** with $PhB(OH)_2$ (Scheme **3.9**).

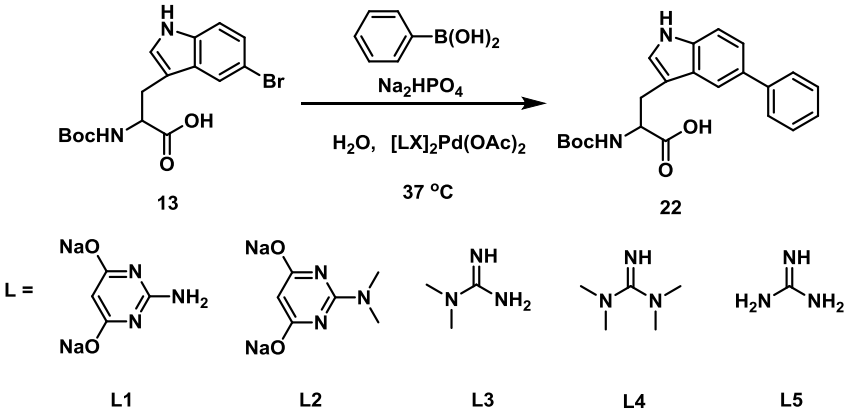

Scheme 3.9 Investigation of Pd catalyst efficiency on a model study of Suzuki reaction.

A set of pyrimidine-based Pd catalysts, involving 2-amino-4,6-dihydroxypyrimidine **L1** and (*N*,*N*-dimethyl)-2-amino-4,6-dihydroxypyrimidine **L2** ligands, was tested on Suzuki reactions, resulting in the formation of phenyl-coupled products in quantitative yield (Table **3.3**). Based on guanidine-based Pd catalysts, 1,1,3,3-tetramethylguanidine **L4** gave the desired product, but unfortunately 1,1-dimethylguanidine **L3** was unreactive under these conditions. Surprisingly, guanidine hydrochloride **L5** used as a ligand did not form a complex with $Pd(OAc)_2$.

Entry	Ligands	Crude Product Yield (%)	$[M+Na]^+$
1	L1	100	403.2
2	L2	100	403.2
3	L3	0	405.1 (Br^{79})
4	L4	100	403.2
5	L5	-	-

Table 3.3 A comparative study of efficiency of $[\mathbf{LX}]_2Pd(OAc)_2$ catalyst through Suzuki reactions.

To investigate a rate of product formation, a ratio of starting material and C-C coupled products was monitored using 500 MHz NMR spectrometry on each different reaction time point (0.5, 1.5, and 2.5h). It was found that all ligands showed excellent coupling ability between 5-bromo-*N*-Boc tryptophan **13** and $PhB(OH)_2$ after 1.5 h reaction time (Table **3.4**). Furthermore, Pd-catalysts with **L2** and **L4** ligands showed a completion of Pd cross-coupling reactions within 30 minutes.

Entry	Ligands	Reaction Time (h)			Crude Product Yields (%)	$[M+Na]^+$
		0.5	1.5	2.5		
		Ratio (starting material : product)				
1	L1	3:4	0:1	0:1	100	403.2
2	L2	0:1	0:1	0:1	100	403.2
3	L4	0:1	0:1	0:1	100	403.2

Table 3.4 Rate of phenyl-coupled product formation monitored by ^{1}H-NMR spectrometry and confirmed by MS.

The coupling product **22** was detected by observation of ^{1}H-NMR spectra from each different reaction time point using the well-resolved proton peak of the NHBoc group. It was found that conversion was complete from starting material **13** to product **22**. For example, [**L2**]$_2$Pd(OAc)$_2$ palladium complex gave the coupling product **22** in quantitative yield within 30 minutes (Figure **3.4**).

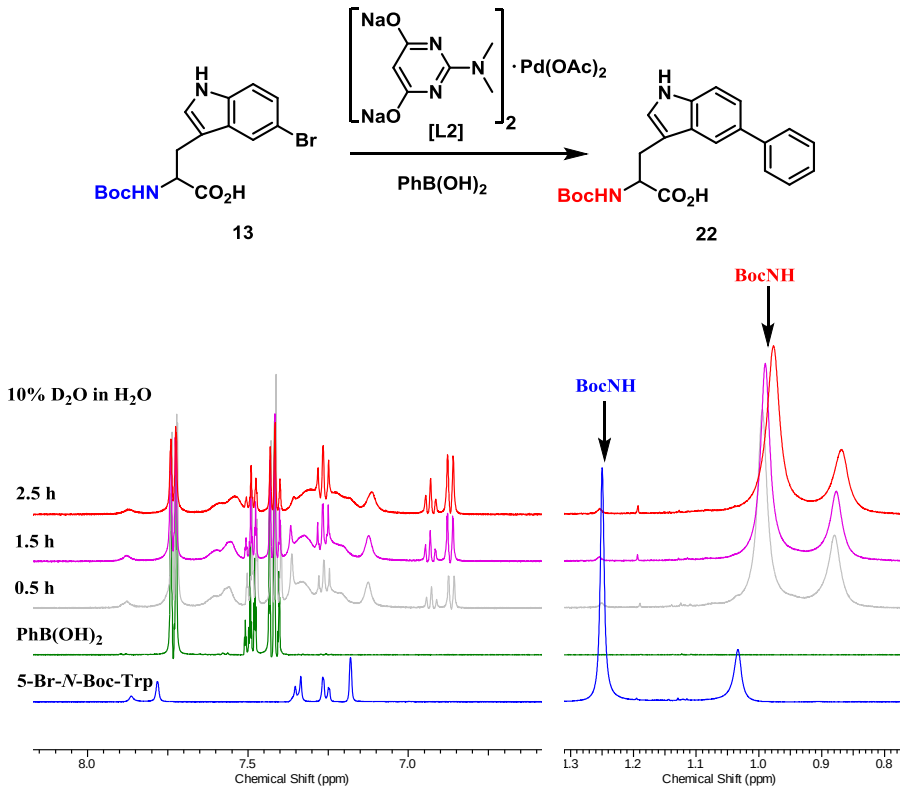

Figure 3.4 ^{1}H-NMR spectra of 5-phenyl-N-Boc-tryptophan **22** from each different reaction time point using [**L2**]$_2$Pd(OAc)$_2$.

3.4 Investigation of Biosynthetic Incorporation Systems

To investigate and optimise biosynthetic incorporation systems of the synthetic tryptophan analogue **1** into proteins, we initially tested this system with annexin V due to its presence of a single tryptophan (W-187) (Scheme **3.10**). As mentioned previously (chapter 2), this protein has utility as a potential biomarker for the detection of apoptosis.

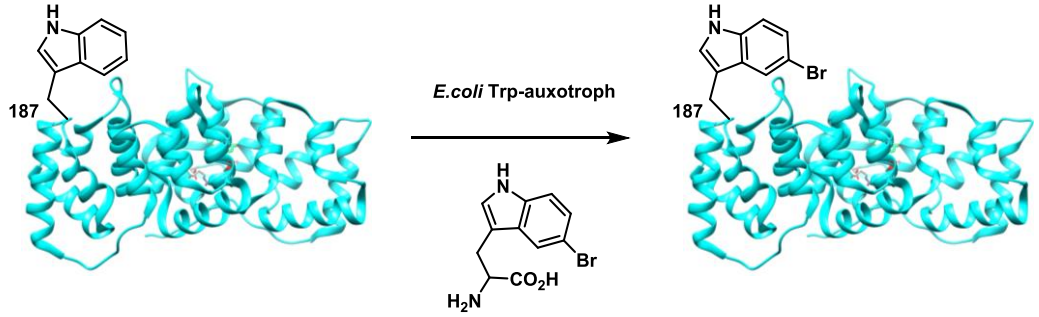

Scheme 3.10 A model study for biosynthetic incorporation of 5-Br-Trp into wild-type annexin V (W187) using *E. coli* Trp-auxotroph.

We first attempted to incorporate 5-bromotryptophan (5-Br-Trp) into annexin V using the Trp-auxotroph *E.coli* ATCC49980. After replacing L-Trp with 5-Br-Trp in new minimal medium (NMM), protein expression was induced by addition of IPTG and then incubated at 30 °C overnight. Samples were further prepared for SDS-PAGE analysis, however no bands corresponding to the mutant protein could be observed, compared to wild-type annexin V as a marker (Figure **3.5**).

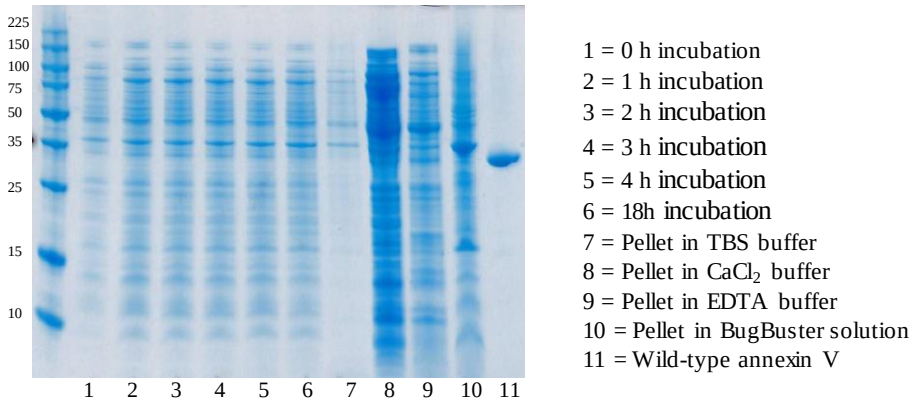

Figure 3.5 SDS-PAGE shows unsuccessful incorporation system of the annexin V supplemented with 5-Br-Trp using ATCC 49980 as a Trp-auxotroph.

Since no labelled protein was observed, the tryptophan auxotroph (ATCC 49980) may not be compatible for biosynthetic incorporation of 5-Br-Trp into annexin V. As such, two alternative Trp-auxotrophic strains, JW 1254-2 and CAG 18455, were selected to investigate the expression of the 5-Br-Trp incorporated annexin V under similar growth conditions. Disappointingly, no mutant annexin V was detected on the SDS-PAGE from expression conditions shown in Table **3.5**, possibly due to unsuitable conditions or toxicity of the synthetic tryptophan.

Entry	Trp-auxotrophs	Supplements	Media	Expression Conditions
1	ATCC 49980	5-Br-Trp	NMM	1 mM IPTG, 30 °C, 16 h
2	JW 1254-2	5-Br-Trp	NMM	1 mM IPTG, 30 °C, 16 h
3	CAG 18455	5-Br-Trp	NMM	1 mM IPTG, 30 °C, 16 h

Table 3.5 Attempted incorporations of 5-Br-Trp into annexin V using various tryptophan auxothrophs (ATCC 49980, JW 1254-2, and CAG 18455, respectively).

Given the successful expression of wild-type annexin V in *E.coli* BL21(DE3), we envisioned that this strain could be used to express the mutant annexin V (5-Br-ANV) in the presence of glyphosate as an enzyme inhibitor of the synthesis of aromatic amino acids[18,19]. However, after protein purification, LC-MS analysis showed no evidence of bromotryptophan incorporation, with only wild-type annexin V detected, indicating that the glyphosate inhibition was not sufficient (Figure **3.7**).

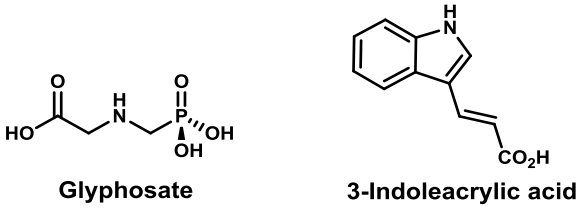

Figure 3.6 Structures of glyphosate and 3-indoleacrylic acid as enzyme inhibitors.

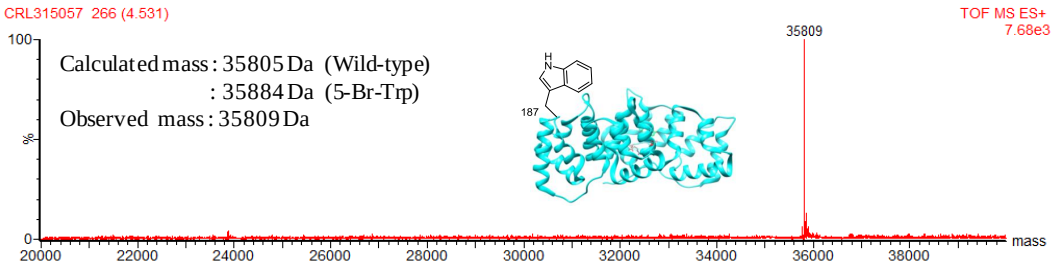

Figure 3.7 ESI-MS spectrum of wild-type annexin V expressed in *E.coli* BL21(DE3) using NMM supplemented with 5-Br-Trp and glyphosate.

As an alternative, a similar protocol was attempted but using 3-indoleacrylic acid (IAA) as a tryptophan synthase inhibitor[20]. However, no protein variant could be detected by LC-MS analysis (Figure **3.8**).

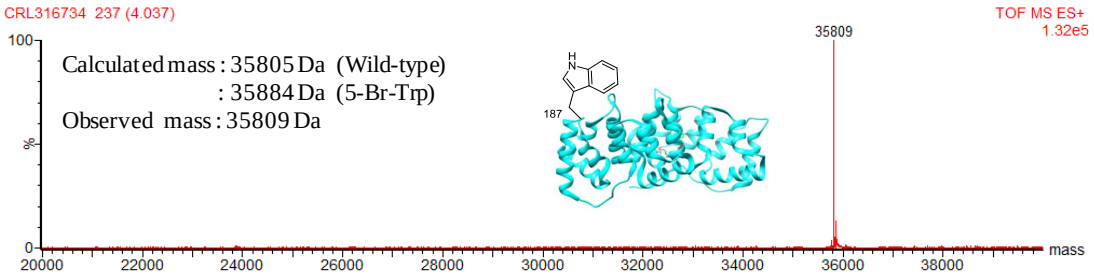

Figure 3.8 ESI-MS spectrum of wild-type annexin V expressed in *E.coli* BL21(DE3) using NMM supplemented with 5-Br-Trp, IAA and glyphosate.

After several unsuccessful attempts involving the use of Trp-auxotrophs, we focused instead on ability of the *V. cholerae* tryptophanyl-tRNA synthetase (TrpRS) to carry synthetic tryptophan residues and incorporate them into the protein. To start with, incorporation of 5-Br-Trp into annexin V was tested by co-transformation of the annexin V and TrpRS plasmids in *E. coli* BL21(DE3). Unfortunately, incorporation systems failed and showed only wild-type annexin V detected by LC-MS analysis (Figure **3.9**). Several expression conditions were tested on this TrpRS-associated incorporation system, but no incorporation of the synthetic tryptophan into annexin V was seen in any case (Table **3.6**).

Entry	Bacterial cells	Supplements	Media	Expression Conditions	Results (Da)
1	*E.coli* BL21(DE3)	-	NMM	1 mM IPTG, 30 °C, 16 h	35805
2	*E.coli* BL21(DE3)	5-Br-Trp	NMM	1 mM IPTG, 30 °C, 16 h	35805
3	*E.coli* BL21(DE3)	5-OH-Trp + IAA	NMM	1 mM IPTG, 30 °C, 16 h	35806
4	*E.coli* BL21(DE3)	5-Br-Trp + IAA	NMM	1 mM IPTG, 30 °C, 16 h	35805
5	*E.coli* BL21(DE3)	5-Br-Trp + glyphosate	NMM	1 mM IPTG, 30 °C, 16 h	35805

Table 3.6 Investigation of biosynthetic incorporation systems using tryptophanyl t-RNA synthetase (TrpRS).

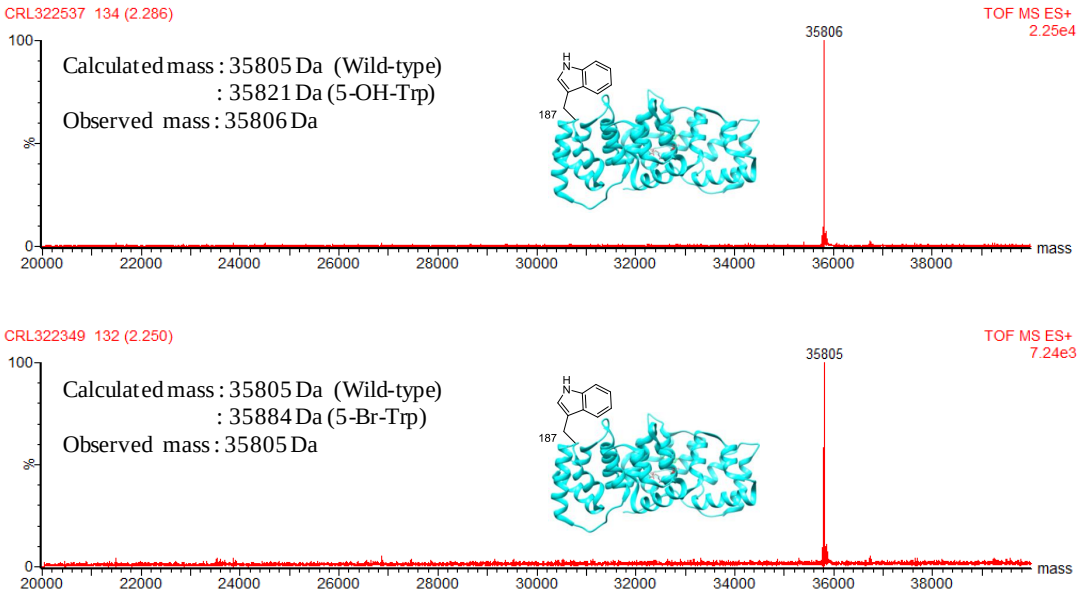

Figure 3.9 ESI-MS spectra of wild-type annexin V expressed with TrpRS in *E.coli* BL21(DE3) using NMM supplemented with either 5-OH-Trp or 5-Br-Trp, respectively.

Further examination of the molecular biology revealed that the original plasmid of annexin V (pET12a PAPI) possessed a T7-promoter which may be incompatible with these tryptophan auxotrophs, so the modification of this plasmid has been further investigated. The pQE80L-Kan vector (6xHis-tag) containing a T5-promoter may be suitable for the protein expression by use of a newly constructed plasmid. First, the annexin V gene was amplified by polymerase chain reaction (PCR) using designed DNA primers and was analysed by agarose gel electrophoresis, with subsequent purification. Next, either PCR fragments or the pQE80L-Kan vector was doubly digested by both HindIII-HF and BamHI-HF as restriction enzymes. After digestion, the annexin V gene was inserted into the digested vector. The ligation mixture was finally transformed into *E.coli* tryptophan auxotroph ATCC 49980, and also incubated at 37 °C overnight. Unfortunately, no presence of single bacterial colonies was observed (Figure **3.10**).

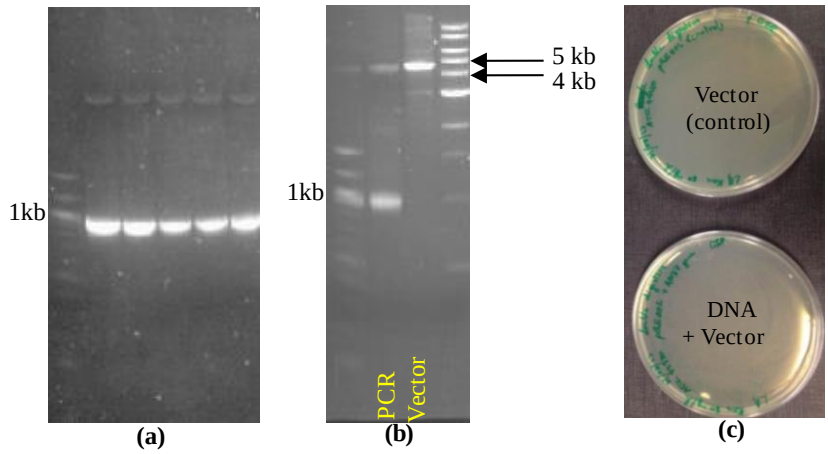

Figure 3.10 a). PCR fragments, b). Double digestion of PCR and pQE80L-Kan vector, and c). Transformation of the ligation mixture into *E.coli* tryptophan auxotroph ATCC 49980.

The plasmid construction was repeated with the same procedure mentioned above, but the ligation mixture was transformed into different types of bacterial cells (Table **3.7**). Trp-auxotroph, ATCC 49980 was initially attempted to use as bacterial cells, there was no single colony on LB agar plate observed. Alternatively, *E.coli* BL21 (DE3) was also investigated, but there was no detection of the presence of any single colonies. Furthermore, some ultracompetent cells (XL10-Gold and XL1-Blue) offering the highest transformation efficiencies were used for this transformation of the ligation mixture. It was found that only XL10-Gold cells showed the presence of many single colonies on the LB agar plate.

Entry	Bacterial cells	Restriction enzymes	Vector	Results
1	ATCC 49980			-
2	*E.coli* BL21 (DE3)	BamHI-HF & HindIII-HF	pQE80L-Kan	-
3	XL10-Gold	(Double digestion)	(T5-promoter)	+
4	XL1-Blue			-

Table 3.7 Transformation of the newly constructed plasmid (annexin V gene and pQE80L-Kan vector) into different bacterial cells.

This plasmid construct was confirmed by DNA sequencing and showed an insertion of annexin's gene with a correct amino acid sequence corresponding to the original plasmid (pET12a PAPI). Initial investigation of the new plasmid construct transformed into *E.coli*

tryptophan auxotroph ATCC4 9980 showed many single colonies on a NMM agar plate containing L-tryptophan. Incorporation systems of 5-Br-Trp into annexin V using Trp-auxotrophic strains were investigated by optimisation of several expression conditions. However, no detection of bromotryptophan incorporation into annexin V was observed using different Trp-auxotrophic strains, possibly due to unsuitable conditions or non-efficient Trp-auxotrophs (Table **3.8**). The purified protein was further analysed by LC-MS, and the ESI-MS spectrum showed a molecular weight of 37219 Da, which correlated to a wild-type annexin V (6xHis-tag) (Figure **3.11**).

Entry	Plasmids	Bacterial strains	Conditions	Results
1	pQE80L-Kan (T5-promoter and 6xHis-tag)	ATCC 49980	LB, 1 mM IPTG, 30 °C, 16 h	Wild-type (37221 Da)
2		CAG 18455		
3		ATCC 49980	NMM, 5-Br-Trp, 1 mM IPTG, 30 °C, 16 h	Not incorporated (37219 Da)

Table 3.8 Attempted incorporation of 5-Br-Trp into annexin using new plasmid construct and Trp-auxotrophs.

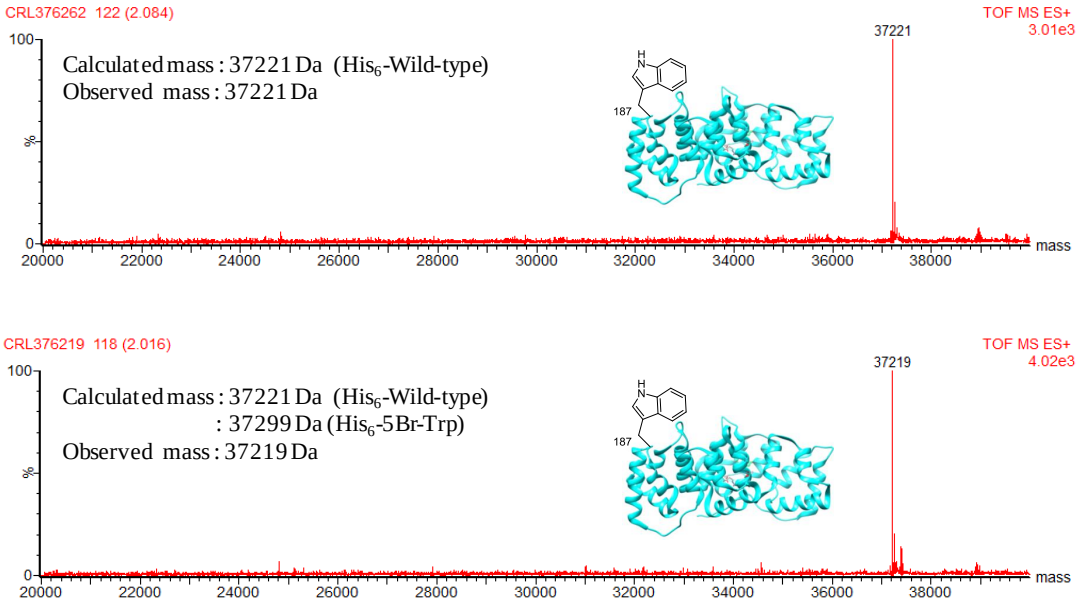

Figure 3.11 ESI-MS spectra of the His_6-wild-type annexin V expressed in Trp-auxotrophic strain (ATCC 49980) using LB or NMM supplemented with 5-Br-Trp, respectively.

3.5 Conclusion

Synthesis of 5-bromotryptophan **1** and its protected analogue **13** was achieved in excellent yield by the synthetic route reported by Prasitpan and co-workers[5]. *N*-Boc-5-bromotryptophan **13** was used as a substrate for the optimisation of Suzuki reaction conditions. All pyrimidine analogues (**L1** and **L2**) and the guanidine (**L4)** were excellent ligands for a model study of 5-Br-Trp with $PhB(OH)_2$. We initially investigated biosynthetic incorporation systems for annexin V which would be used to perform biological Suzuki reactions. However, our attempts toward the incorporation of 5-Br-Trp **1** into annexin V were unsuccessful by use of either *E. coli* BL21(DE3) or *E. coli* Trp-auxotrophic strains (ATCC 49980, JW1254-2, and CAG 18455) under different growth conditions. No modified annexin V was produced in any bacterial strains (Table **3.9**), possibly due to unsuitable growth conditions or the toxicity of the tryptophan analogues. Also, the new plasmid construct (T5 promoter) was not compatible for biosynthetic incorporation systems and was unable to introduce bromotryptophan into this protein by association of tryptophan auxotrophic strain (ATCC 49980). Hence, the incorporation of 5-Br-Trp into annexin V may need to be further investigated in order to afford the desired protein to allow chemical modification through Suzuki-Miyaura cross-coupling reactions.

Entry	Plasmids	Bacterial Strains	Supplements	Media	Expression Conditions	Results
1	pET12a PAPI (T7 promoter)	ATCC 49980	5-Br-Trp	NMM	1 mM IPTG, 30 °C, 16 h	No protein expression
2		JW 1254-2	5-Br-Trp	NMM	1 mM IPTG, 30 °C, 16 h	
3		CAG 18455	5-Br-Trp	NMM	1 mM IPTG, 30 °C, 16 h	
4		BL21(DE3)	5-Br-Trp glyphosate	NMM or AIM	1 mM IPTG, 30 °C, 16 h	Wild-type annexin V
5		BL21(DE3)	5-Br-Trp IAA	NMM	1 mM IPTG, 30 °C, 16 h	
6		BL21(DE3) + TrpRS	5-Br-Trp	NMM	1 mM IPTG, 30 °C, 16 h	
7	pQE80L-Kan (T5 promoter)	ATCC 49980	-	LB	1 mM IPTG, 30 °C, 16 h	
8		CAG 18455	-	LB	1 mM IPTG, 30 °C, 16 h	
9		ATCC 49980	5-Br-Trp	NMM	1 mM IPTG, 30 °C, 16 h	

Table 3.9 Attempted expression of the 5-Br-Trp incorporated annexin V by either Trp-auxotrophic strains or *E.coli* BL21(DE3).

3.6 Experimental

The numbering of the core structure used in this study is initially counted from nitrogen atom used as the first position in the indole ring;

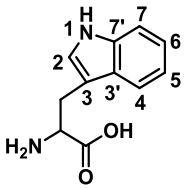

3.6.1 Chemical Synthesis

Ethyl-3-bromo-2-hydroxyiminopropanoate (9)

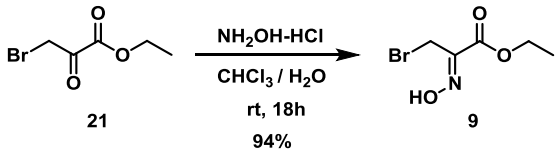

Hydroxylamine hydrochloride (10.4 g, 150 mmol) was dissolved in a 1:1 mixture of distilled water (60 mL) and chloroform (60 mL). Ethyl bromopyruvate **21** (19.5 g, 12.6 mL, 100 mmol) was added dropwise to the rapidly stirred biphasic mixture which was left overnight at room temperature. The reaction mixture was diluted with a 1:1 mixture of distilled water (50 mL) and DCM (50 mL) and the layers were separated. The aqueous layer was extracted with DCM (2 x 50 mL) and the organic layers were combined and dried over $MgSO_4$. Removal of the solvent *in vacuo* afforded ethyl-3-bromo-2-hydroxyiminopropanoate **9** as a white solid (19.8 g, 94%); mp: 75-76 °C, *lit.*[21] 75-77 °C; IR (ν_{max}, KBr): 3316, 1725, 1445, 1374, 1326, 1272, 1227, 1199, 1115, 1028 cm^{-1}; δ_H (400 MHz, $CDCl_3$) 10.09 (1H, br. s, NOH), 4.39 (2H, q, *J* 7.2, OCH_2), 4.27 (1H, s, CH_2Br), 1.39 (3H, t, *J* 7.2, CH_3); δ_C (100 MHz, $CDCl_3$) 161.6 (C=O), 147.9 (C=N), 62.5 (OCH_2), 15.1 (CH_2Br), 14.0 (CH_3); LRMS m/z (ESI): Found 210.0 $[M+H]^+$, calc $C_5H_9Br^{79}NO_3$ (210.0), found 212.0 $[M+H]^+$, calc $C_5H_9Br^{81}NO_3$ (212.0). Spectroscopic data in accordance with the literature[21,22].

Ethyl-2-hydroxyimino-3-(5-bromoindol-3-yl)-propanoate (10)

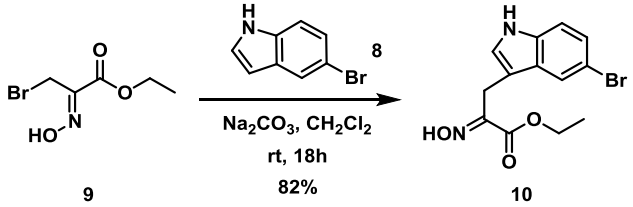

A solution of ethyl-3-bromo-2-hydroxyiminopropanoate **9** (3.00 g, 14.0 mmol) in dry CH_2Cl_2 (20 mL) was added dropwise to a stirred solution of 5-bromoindole **8** (5.49 g, 28.0 mmol) and Na_2CO_3 (2.97 g, 28.0 mmol) in dry CH_2Cl_2 (30 mL) under a nitrogen atmosphere. The reaction mixture was stirred overnight at room temperature. The precipitate was collected by filtration and washed with CH_2Cl_2 (20 mL) and water (2 x 20 mL). The solid collected was suspended in hot CH_2Cl_2 and filtered to afford the desired product, ethyl-2-hydroxyimino-3-(5-bromoindol-3-yl)-propanoate **10** as a white solid (3.79 g, 82%); mp: 179-180 °C, *lit.*[5]180-181 °C; IR (ν_{max}, KBr): 3384, 3260, 2988, 1707, 1423, 1380, 1300, 1206, 1132, 1102, 1041, 1023 cm^{-1}; δ_H (400 MHz, DMSO-d_6) 12.47 (1H, s, NH-indole), 11.11 (1H, br. s, NOH), 7.75 (1H, d, *J* 1.7, H-4), 7.30 (1H, d, *J* 8.6, H-7), 7.17 (2H, m, H-2 and H-6), 4.14 (2H, q, *J* 7.1, OCH_2), 3.87 (2 H, s, CH_2), 1.19 (3H, t, *J* 7.1, CH_3); δ_C (100 MHz, DMSO-d_6) 163.9 (C=O), 149.7 (C=N), 134.6 (C-7'), 128.8 (C-3'), 125.7 (C-3), 123.4 (C-6), 121.0 (C-4), 113.5 (C-7), 111.1 (C-2), 108.6 (C-5), 60.8 (OCH_2), 19.9 (CH_2), 14.0 (CH_3); LRMS m/z (ESI): Found 325.0 $[M+H]^+$, calc $C_{13}H_{14}Br^{79}N_2O_3$ (325.0), found 327.0 $[M+H]^+$, calc $C_{13}H_{14}Br^{81}N_2O_3$ (327.0). Spectroscopic data in accordance with the literature[5].

5-Bromo-DL-tryptophan ethyl ester (11)

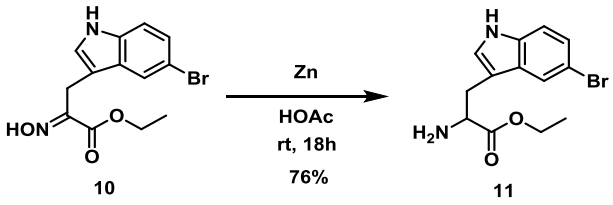

Zinc dust (2.00 g, 30.4 mmol) was added portionwise to a stirred solution of ethyl-2-hydroxyimino-3-(5-bromoindol-3-yl)-propanoate **10** (3.30 g, 10.1 mmol) in HOAc (75 mL). The reaction mixture was stirred overnight under a nitrogen atmosphere at room

temperature. The zinc was removed by filtration and washed with HOAc (20 mL). The filtrate was concentrated *in vacuo* to afford yellow oil which was triturated with 1 M HCl (15 mL). The formed precipitate was collected by filtration and washed with chilled distilled water (2 x 15 mL) and dried to give 5-bromo-DL-tryptophan ethyl ester hydrochloride **11** as a white solid (2.40 g, 76%); mp: 125-126 °C; IR (ν_{max}, KBr): 3271, 2889, 1737, 1591, 1517, 1463, 1435, 1319, 1282, 1252, 1206, 1106, 1053, 1017, 1085 cm^{-1}; δ_H (400 MHz, DMSO-d_6) 11.4 (1H, s, NH-indole), 8.62 (2H, br. s, NH_2), 7.71 (1H, d, *J* 2.0, H-4), 7.35 (1H, d, *J* 8.6, H-7), 7.32 (1H, d, *J* 2.4, H-2), 7.19 (1H, dd, *J* 8.6, 2.0, H-6), 4.19 (1H, app t, CH), 4.06 (2H, m, OCH_2), 3.42 (1H, dd, *J* 12.0, 4.0, CH_2), 3.23 (1H, dd, *J* 12.0, 8.0, CH_2), 1.10 (3H, t, *J* 7.1, CH_3); δ_C (100 MHz, DMSO-d_6) 169.3 (C=O), 135.0 (C-7'), 128.9 (C-3'), 126.9 (C-3), 123.7 (C-6), 120.5 (C-4), 113.7 (C-7), 111.4 (C-2), 106.4 (C-5), 61.8 (OCH_2), 52.7 (CH), 25.9 (CH_2), 13.8 (CH_3); LRMS m/z (ESI): Found 311.0 $[M+H]^+$, calc $C_{13}H_{15}Br^{79}N_2O_2$ (311.0), found 313.0 $[M+H]^+$, calc $C_{13}H_{15}Br^{81}N_2O_2$ (313.1). Spectroscopic data in accordance with the literature[5].

5-Bromo-DL-tryptophan (1)

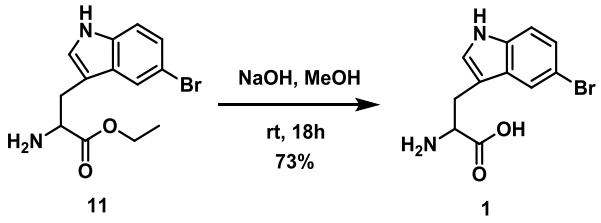

A solution of 1M NaOH (12.9 mL, 12.9 mmol) was added dropwise to a stirred solution of 5-bromo-DL-tryptophan ethyl ester **11** (2.00 g, 6.43 mmol) in MeOH (40 mL). The reaction mixture was left to stir overnight under a nitrogen atmosphere at room temperature. The solution was filtered and concentrated *in vacuo* and then neutralised with 1 M HCl. The white precipitate formed was collected by filtration and dried thoroughly to afford 5-bromo-DL-tryptophan **1** as a white solid (1.33 g, 73%); mp: 253-255 °C, *lit*.[5] 261-262 °C; IR (ν_{max}, KBr): 3448, 3408, 3023, 1665, 1584, 1460, 1407, 1355, 1144, 1100 cm^{-1}; δ_H (400 MHz, DMSO-d_6) 11.13 (1H, br. s, NH-indole), 7.75 (1H, d, *J* 1.7, H-7), 7.31 (1H, d, *J* 8.6, H-4), 7.25 (1H, d, *J* 2.2, H-2), 7.16 (1H, dd, *J* 8.6, 1.7, H-6), 3.41 (1H, dd, *J* 12.7, 5.6, CH), 3.22 (1H, dd, *J* 12.7, 5.6, CH_2), 2.99 (1H, dd, *J* 12.7,

5.6, CH_2); δ_C (100 MHz, DMSO-d_6) 169.8 (C=O), 135.0 (C-7'), 129.3 (C-3'), 125.9 (C-3), 123.3 (C-6), 120.9 (C-4), 113.3 (C-7), 111.0 (C-2), 109.5 (C-5), 54.8 (CH), 26.8 (CH_2); LRMS m/z (ESI): Found 283.0 $[M+H]^+$, calc $C_{11}H_{12}Br^{79}N_2O_2$ (283.0), found 285.0 $[M+H]^+$, calc $C_{11}H_{12}Br^{81}N_2O_2$ (285.0). Spectroscopic data in accordance with the literature[5].

_N_-Boc-5-bromo-DL-tryptophan ethyl ester (12)

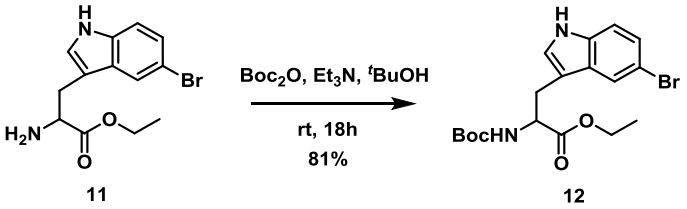

Di-*tert*-butyl-dicarbonate (2.55 mL, 11.1 mmol) was added to a stirred solution of 5-bromo-DL-tryptophan ethyl ester **11** (1.50 g, 4.82 mmol) in ^{t}BuOH (45 mL) under a nitrogen atmosphere at room temperature. Triethylamine (1.55 mL, 11.1 mmol) was added dropwise to the reaction mixture and allowed to stir overnight. The solution was concentrated *in vacuo* and the solid obtained was purified using flash chromatography (100% DCM) to afford *N*-Boc-5-bromo-DL-tryptophan ethyl ester **12** as a white solid (1.60 g, 81%); mp: 149-150 °C, *lit.*[5] 149-150 °C; IR (ν_{max}, KBr): 3396, 2985, 1736, 1673, 1518, 1454, 1368, 1351, 1293, 1267, 1220, 1170, 1100, 1058, 1025 cm^{-1}; δ_H (400 MHz, DMSO-d_6) 11.09 (1H, s, NH-indole), 7.67 (1H, s, H-4), 7.31 (1H, d, *J* 8.6, H-7), 7.24 (2H, m, H-2 and Boc-NH), 7.16 (1H, dd, *J* 8.6, 1.7, H-6), 4.13 (1H, td, *J* 8.3, 5.6, CH), 4.03 (2H, m, OCH_2), 3.07 (1H, dd, *J* 16.0, 8.0, CH_2), 2.99 (1H, dd, *J* 12.0, 8.0, CH_2), 1.32 (8H, s, Boc-H), 1.23 (1H, br. s, Boc-H), 1.10 (3H, t, *J* 7.1, CH_3); δ_C (100 MHz, DMSO-d_6) 172.2 (C=O), 155.3 (NHC=O), 134.8 (C-7'), 129.1 (C-3'), 125.6 (C-3), 123.4 (C-6), 120.6 (C-4), 113.4 (C-7), 111.1 (C-2), 109.9 (C-5), 78.2 ($(CH_3)_3\underline{C}$-Boc), 60.4 (OCH_2), 54.9 (CH), 28.1 (Boc-CH_3), 26.6 (CH_2), 14.0 (CH_3); LRMS m/z (ESI): Found 433.1 $[M+Na]^+$, calc $C_{18}H_{23}Br^{79}N_2O_4Na$ (433.1), found 435.1 $[M+Na]^+$, calc $C_{18}H_{23}Br^{81}N_2O_4Na$ (435.1). Spectroscopic data in accordance with the literature[5].

N-Boc-5-bromo-DL-tryptophan (13)

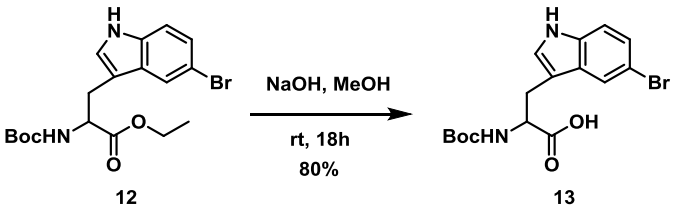

N-Boc-5-bromo-DL-tryptophan ethyl ester **12** (500 mg, 1.22 mmol) was dissolved in MeOH (10 mL) under N_2 and 1 M NaOH (2.44 mL, 2.44 mmol) added dropwise. The reaction was left to stir overnight. The solution was concentrated to half volume *in vacuo* and then neutralised with 1 M HCl. The white precipitate was collected by filtration and dried thoroughly to afford *N*-Boc-5-bromo-DL-tryptophan **13** (320 mg, 80%) as a white solid; mp: 161-163 °C, *lit*.[5] 162-163 °C; IR (ν_{max}, KBr): 3359, 2978, 1714, 1649, 1403, 1368, 1247, 1204, 1163, 1106, 1053, 1027 cm^{-1}; δ_H (400 MHz, DMSO-d_6) 11.08 (1H, s, NH-indole), 7.72 (1H, s, H-4), 7.31 (1H, d, *J* 8.6, H-7), 7.22 (1H, d, *J* 2.0, H-2), 7.17 (1H, dd, *J* 8.6, 1.7, H-6), 7.02 (1H, d, *J* 8.2, Boc-NH), 4.11 (1H, td, *J* 8.7, 4.7, CH), 3.11 (1H, dd, *J* 14.5, 6.9, CH_2), 2.95 (1H, dd, *J* 14.5, 6.9, CH_2), 1.32 (8H, s, Boc-H), 1.21 (1H, s, Boc-H); δ_C (100 MHz, DMSO-d_6) 174.2 (C=O), 155.3 (NHC=O), 134.8 (C-7'), 129.2 (C-3'), 125.5 (C-3), 123.3 (C-6), 120.7 (C-4), 113.4 (C-7), 111.1 (C-2), 110.3 (C-5), 78.0 (Boc-$\underline{C}(CH_3)_3$), 54.8 (CH), 28.2 (Boc-CH_3), 26.7 (CH_2); LRMS m/z (ESI): Found 405.0 $[M+Na]^+$, calc $C_{16}H_{19}Br^{79}N_2O_4Na$ (405.0), found 407.0 $[M+Na]^+$, calc $C_{16}H_{19}Br^{81}N_2O_4Na$ (407.0). Spectroscopic data in accordance with the literature[5].

Preparation of palladium catalyst solution $[L1]_2Pd(OAc)_2$

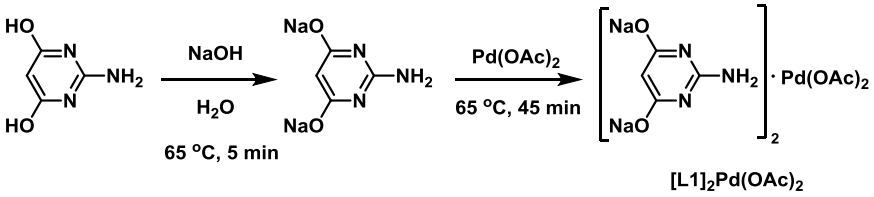

0.1 M NaOH (2.00 mL) was added to 2-amino-4,6-dihydroxypyrimidine (13.0 mg, 0.10 mmol) and the pyrimidine was fully dissolved by stirring rapidly at 65°C for 5 minutes. $Pd(OAc)_2$ (11.0 mg, 0.05 mmol) was added to the resulting solution which was stirred at

the same temperature for further 45 minutes. [**L1**]$_2$Pd(OAc)$_2$ catalyst was obtained as a homogenous golden-orange solution which was diluted to 5 mL with distilled water to yield a 0.01 M catalyst stock solution[13-16,23].

2-Dimethylamino-4,6-dihydroxypyrimidine (L2)

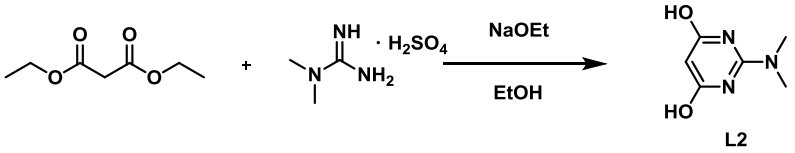

Dimethylmalonate (0.28 mL, 1.84 mmol) and dimethylguanidine sulfate (0.50 g, 1.84 mmol) were dissolved in ethanol. NaOEt (21% w/v in EtOH, 2.38 mL, 7.36 mmol) was added dropwise in the reaction mixture, then allowed to stir overnight at room temperature. The white precipitate formed in solution was diluted with 5 mL H_2O, then neutralised with 1M HCl. The resulting white solid was filtered, washed with H_2O and dried, then crude product was used for the next step without purification. δ_H (400 MHz, DMSO-d_6) 10.55 (2H, br. s, OH), 4.67 (1H, s, H-3), 3.00 (6H, s, 2xCH_3); δ_C (100 MHz, DMSO-d_6) 168.0 (C-3), 155.0 (C-2, C-4), 78.3 (C-6), 37.1 (2xCH_3); LRMS m/z (ESI): Found 178.0 $[M+Na]^+$, calc $C_6H_9N_3O_2Na$ (178.1), Spectroscopic data in accordance with the literature[14,24].

Preparation of palladium catalyst solution [L2]$_2$Pd(OAc)$_2$

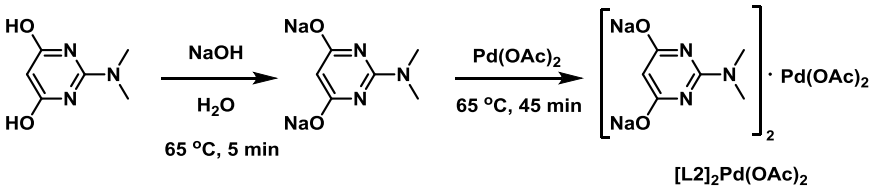

0.1 M NaOH (1.00 mL) was added to a solution of 2-dimethylamino-4,6-dihydroxy pyrimidine (7.75 mg, 0.05 mmol) in H_2O, the pyrimidine was fully dissolved by stirring rapidly at 65°C for 5 min. Pd(OAc)$_2$ (5.5 mg, 0.025 mmol) was added to the resulting solution which was stirred at the same temperature for further 45 min. [**L2**]$_2$Pd(OAc)$_2$ catalyst was obtained as a homogenous golden-orange solution which was diluted with distilled water (2.5 mL) to yield a 0.01 M catalyst stock solution[14,23,24].

Preparation of palladium catalyst solution $[L3]_2Pd(OAc)_2$

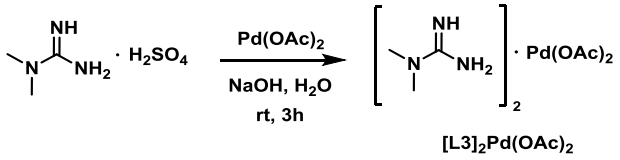

0.1 M NaOH (1.50 mL) was added to a solution of 1,1-dimethylguanidine sulfate (40.9 mg, 0.15 mmol) in H_2O, then allowed to stir for 5 min at room temperature. $Pd(OAc)_2$ (16.8 mg, 0.075 mmol) was added to the reaction mixture stirred at the same temperature for further 3 h. [**L3**]$_2$Pd(OAc)$_2$ catalyst was obtained as a homogenous dark brown solution which was diluted with distilled water (3 mL) to yield a 0.01 M catalyst stock solution[14,23].

Preparation of palladium catalyst solution $[L4]_2Pd(OAc)_2$

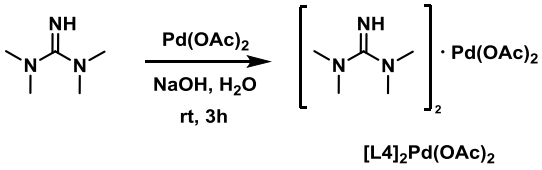

0.1 M NaOH (1.50 mL) was added to a solution of 1,1,3,3-tetramethylguanidine (17.3 mg, 0.15 mmol) in H_2O, then allowed to stir for 5 min at room temperature. $Pd(OAc)_2$ (16.8 mg, 0.075 mmol) was added to the reaction mixture stirred at the same temperature for further 3 h. [**L4**]$_2$Pd(OAc)$_2$ catalyst was obtained as a homogenous dark brown solution which was diluted with distilled water (3 mL) to yield a 0.01 M catalyst stock solution[14,23].

***N*-Boc-5-phenyl-DL-tryptophan (22)**

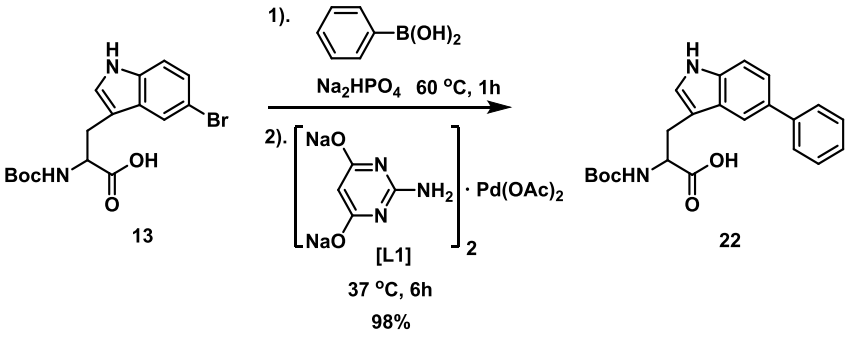

N-Boc-5-bromo-DL-tryptophan **13** (50 mg, 0.13 mmol), phenyl boronic acid (48 mg, 0.39 mmol) and Na_2HPO_4 (992 mg, 6.50 mmol) were dissolved in distilled water (5 mL), the reaction mixture was stirred at 60°C for 1h. The reaction was then cooled to 37 °C, [**L1**]$_2$Pd(OAc)$_2$ catalyst solution (0.65 mL, 6.5 μmol) was added and allowed to stir rapidly for 6 h. The reaction mixture was diluted with ethyl acetate (15 mL) and 1 M HCl (15 mL). The aqueous layer was extracted with EtOAc (2 x 15 mL) and the combined organic layers were washed with brine (20 mL), dried over $MgSO_4$. The solution was filtered and concentrated *in vacuo* to yield a colourless oil which was purified by flash chromatography (10-20% MeOH/DCM) to give *N*-Boc-5-phenyl-DL-tryptophan **22** as a light golden solid (49 mg, 98%); mp: 320 °C (decomposed); IR (ν_{max}, KBr): 3324, 2923, 2853, 1649, 1578, 1407, 1368, 1250, 1162, 1051 cm^{-1}; δ_H (400 MHz, MeOD) 7.83 (1H, s, H-2), 7.65 (2H, d, *J* 7.1, 2 x Ar-H), 7.40 (4H, m, 2 x Ar-H, H-6 and H-7), 7.25 (1H, app t, Ar-H), 7.11 (1H, s, H-4), 4.38 (1H, app t, CH), 3.42 (1H, app dd, CH_2), 3.17 (1H, dd *J* 13.9, 6.7, CH_2), 1.31 (7H, s, Boc-H), 1.13 (2H, br. s, Boc-H); δ_C (126 MHz, MeOD) 157.7 (C=O), 144.4 (NHC=O), 137.6 (C-7'), 133.5 (C-5), 129.7 (Ar-C_{ipso}), 129.6 (2 x Ar-C and C-3'), 128.3 (2 x Ar-C), 127.1 (Ar-C), 125.4 (C-4), 122.0 (C-6), 118.2 (C-2), 112.5 (C-7), 112.2 (C-3), 80.4 (Boc-$\underline{C}(CH_3)_3$), 57.6 (CH), 28.7 (Boc-CH_3), 29.2 (CH_2); HRMS m/z (ESI): Found 403.1626 $[M+Na]^+$, calc $C_{22}H_{24}N_2O_4Na$ (403.1628).

5-Phenyl-*N*HAc-DL-tryptophan (24)

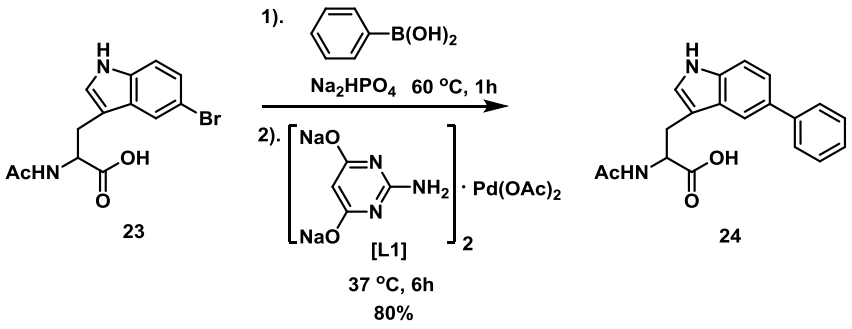

5-Bromo-*N*HAc-DL-tryptophan **23** (50 mg, 0.15 mmol), phenyl boronic acid (56 mg, 0.46 mmol) and Na_2HPO_4 (1.09 g, 7.70 mmol) were dissolved in distilled water (5 mL), the reaction mixture was stirred at 60°C for 1h. The reaction had cooled to 37 °C, Pd-pyrimidine catalyst solution [**L1**]$_2$Pd(OAc)$_2$ (0.77 mL, 7.7 μmol) was added and allowed

to stir rapidly for 6 h. The reaction mixture was diluted with ethyl acetate (15 mL) and 1 M HCl (15 mL). The aqueous layer was extracted with EtOAc (2 x 15 mL) and the combined organics were washed with brine (20 mL), dried over $MgSO_4$. The solution was filtered and concentrated *in vacuo* to yield a colourless oil which was purified by flash chromatography (15-20% MeOH/DCM) to afford 5-Phenyl-*N*HAc-DL-tryptophan **24** as a light yellow solid (40 mg, 80%); mp: 300 °C (decomposed); IR (ν_{max}, KBr): 2923, 2853, 1579, 1460, 1096 cm^{-1}; δ_H (400 MHz, MeOD) 7.84 (1H, s, H-2), 7.64 (2H, d, *J* 7.3, 2 x Ar-H), 7.38 (4H, m, 2 x Ar-H, H-6 and H-7), 7.23 (1H, m, Ar-H), 7.12 (1H, s, H-4), 4.62 (1H, app t, CH), 3.43 (1H, dd *J* 14.6, 6.1, CH_2), 3.17 (1H, dd *J* 14.6, 6.1, CH_2), 1.83 (3H, s, CH_3); δ_H (126 MHz, MeOD) 172.8 (C=O), 144.2 (NHC=O), 137.5 (C-7'), 133.3 (C-5), 129.9 (Ar-C_{ipso}), 129.6 (2 x Ar-C), 128.1 (2 x Ar-C and C-3'), 127.0 (Ar-C), 125.2 (C-4), 121.9 (C-6), 117.9 (C-2), 112.6 (C-3), 112.5 (C-7), 57.1 (CH), 28.8 (CH_2), 22.8 (CH_3); HRMS m/z (ESI): Found 345.1196 $[M+Na]^+$, calc $C_{19}H_{18}N_2O_3Na$ (345.1210).

Efficiency of Pd catalysts with different ligands (L1-L4)

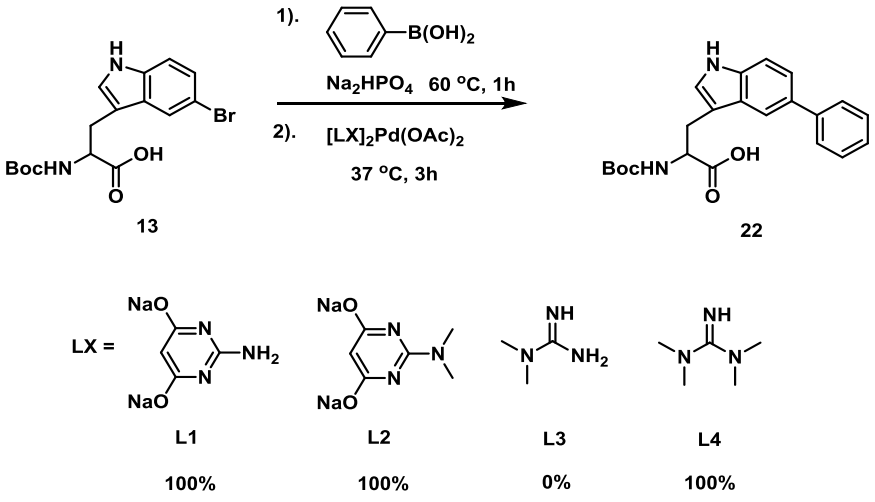

N-Boc-5-bromo-DL-tryptophan **13** (25 mg, 0.065 mmol), phenyl boronic acid (23.8 mg, 0.195 mmol) and Na_2HPO_4 (227 mg, 1.95 mmol) were dissolved into distilled water (3 mL), the reaction mixture was stirred at 60°C for 1 h. The reaction had cooled to 37 °C. Each Pd-catalyst solution [**LX**]$_2$Pd(OAc)$_2$ (0.32 mL, 3.25 μmol) was added to the reaction mixture, then allowed to stir rapidly for 3 h. The reaction mixture was diluted

with ethyl acetate (5 mL) and 1 M HCl (5 mL). The aqueous layer was extracted with EtOAc (2 x 10 mL), then the combined organics were washed with brine (10 mL) and dried over $MgSO_4$. The solution was filtered and concentrated *in vacuo* to yield a yellow solid as a crude product of *N*-Boc-5-phenyl-DL-tryptophan **22** ; LRMS m/z (ESI): Found 403.2 $[M+Na]^+$, calc $C_{22}H_{24}N_2O_4Na$ (403.2).

Entry	Ligands	Reaction Time (h)	Crude Product Yield (%)	$[M+Na]^+$
1	L1	3	100	403.2
2	L2	3	100	403.2
3	L3	3	0	405.1 (Br^{79})
4	L4	3	100	403.2

Table 3.10 Comparative study of the efficiency of Pd catalysts with different ligands (L1-L4) for Suzuki-Miyaura cross-coupling reactions of **13** with $PhB(OH)_2$.

^{1}H-NMR study of a ratio of product formation using Pd-catalyst (L1-L4)

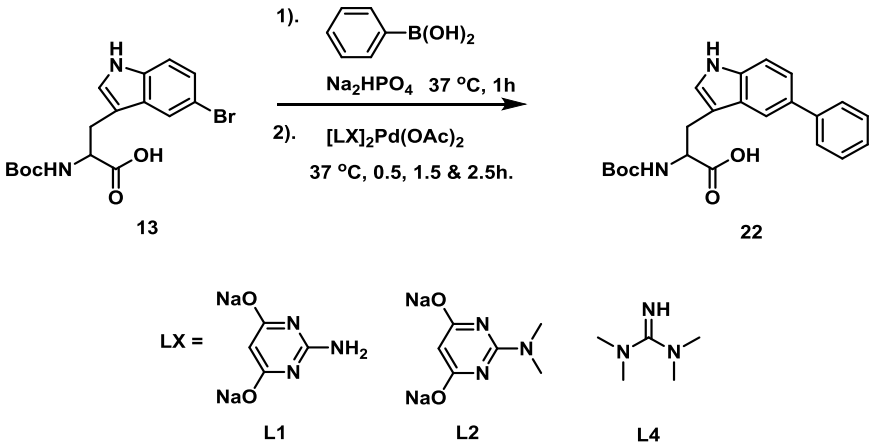

N-Boc-5-bromo-DL-tryptophan **13** (9 mg, 0.024 mmol), phenyl boronic acid (8.78 mg, 0.072 mmol) and Na_2HPO_4 (102 mg, 0.72 mmol) were dissolved into distilled water (2.5 mL), the reaction mixture was stirred using thermoshaker at 37 °C for 1 h. Each $[\mathbf{LX}]_2Pd(OAc)_2$ catalyst solution (0.12 mL, 1.20 μmol) was added, then allowed to stir at 37 °C for 3 h. The solution (0.60 mL) was collected at each different time (0.5, 1.5 and 2.5 h.), then solution was added 1 M HCl (0.10 mL). Each solution was transferred into

the NMR tubes, then 10 % volume of D_2O was also added and mixed together. All samples were monitored by observation of ^{1}H-NMR spectra compared with starting material and phenylboronic acid using 500 MHz NMR spectrometry.

Entry	Ligands	Reaction Time (h)			Crude Product Yields (%)	$[M+Na]^+$
		0.5	1.5	2.5		
		Ratio (starting material : product)				
1	L1	3:4	0:1	0:1	100	403.2
2	L2	0:1	0:1	0:1	100	403.2
3	L4	0:1	0:1	0:1	100	403.2

Table 3.11 Efficiency of Pd-catalysts monitored by ^{1}H-NMR spectrometry.

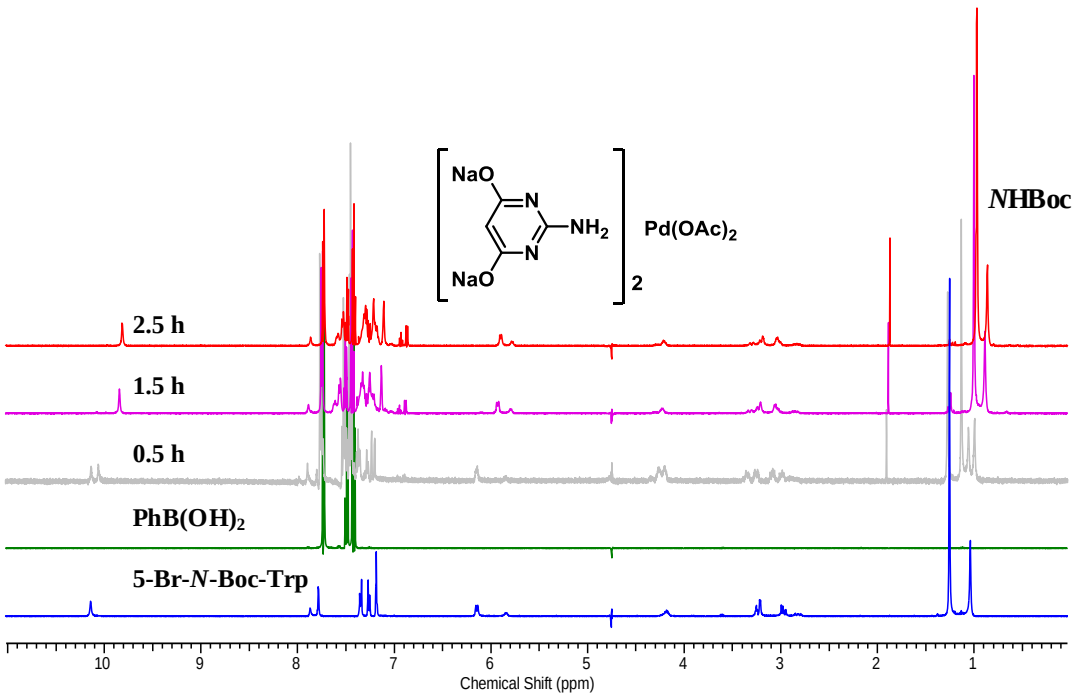

Figure 3.12 ^{1}H-NMR spectra of Suzuki reactions using $[\mathbf{L1}]_2Pd(OAc)_2$.

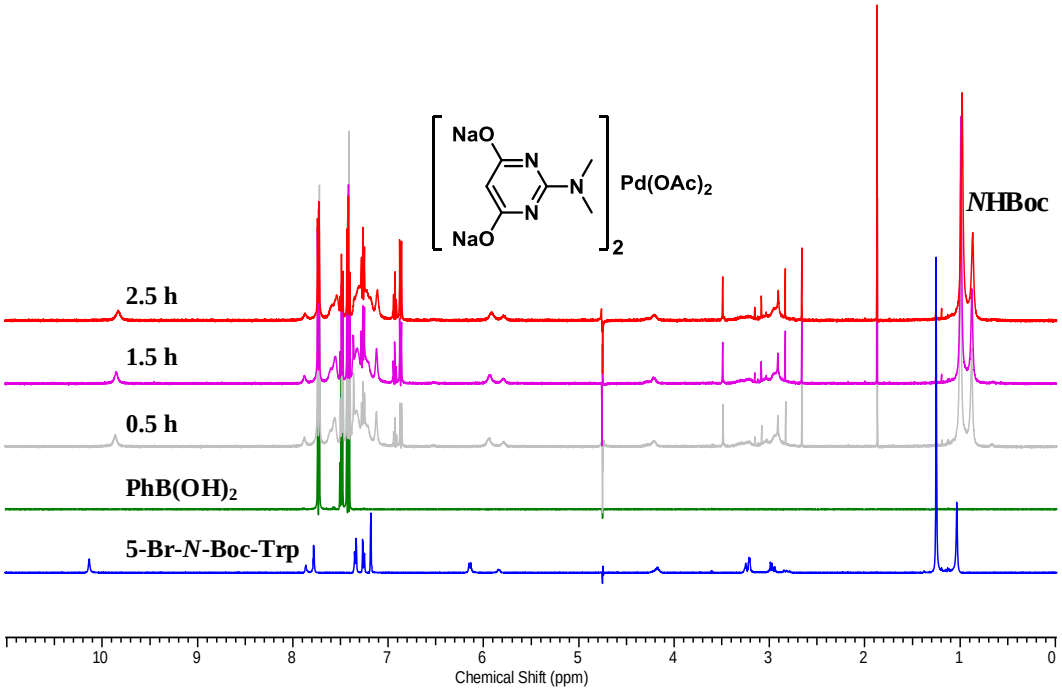

Figure 3.13 ^{1}H-NMR spectra of Suzuki reactions using [**L2**]$_2$Pd(OAc)$_2$.

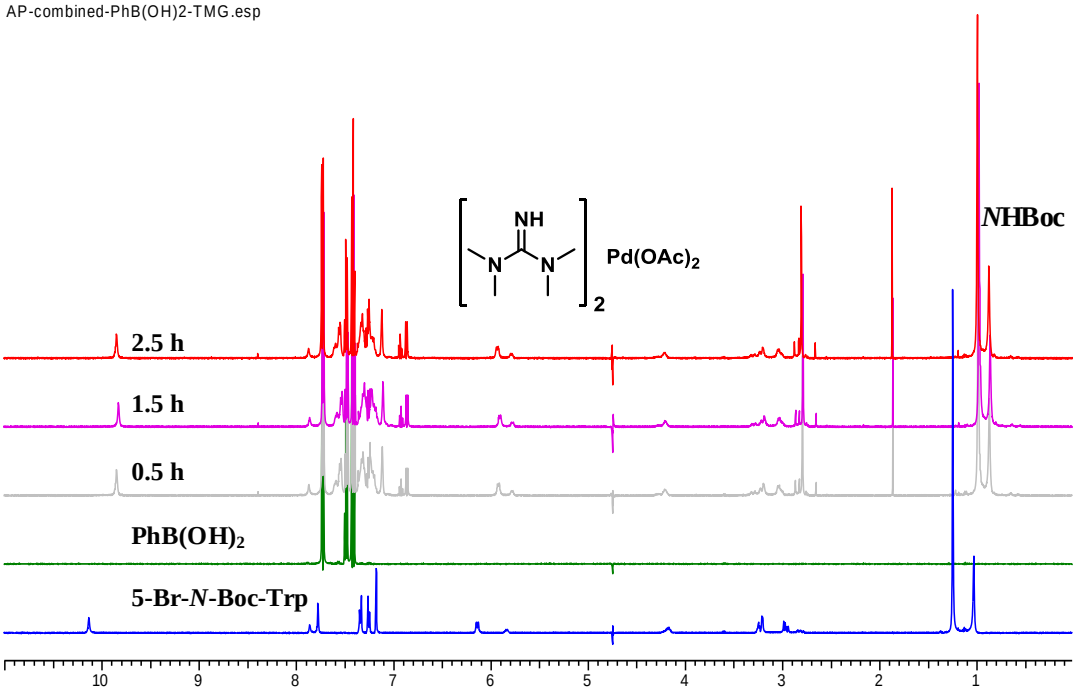

Figure 3.14 ^{1}H-NMR spectra of Suzuki reactions using [**L4**]$_2$Pd(OAc)$_2$.

3.6.3 Biosynthetic Incorporation of Unnatural Aromatic Amino Acids into Annexin V

General Procedure for Biosynthetic Incorporation Systems and Protein purification

Attempted protein expression proceeded from transformation of the plasmid pET12a-PAPI (T7 promoter) or pQE80L-Kan (T5 promoter and 6xHis-tag) in Trp-auxotrophs (ATCC49980, JW1254-2 or CAG 18455) or Novagen *E.coli* BL21(DE3) singles competent cells. A single colony of annexin V bacterial cells was picked and grown in 5 mL of LB medium at 37 °C overnight, then the pellet was transferred into 200 mL of NMM containing an appropriate antibiotic. Cell cultures were inoculated at 37 °C until OD_{600} ~0.6-0.7 observed and boosted with supplements (See each table). Protein expression was induced by addition of 1 mM IPTG. Cell cultures were incubated at 30 °C for 16 h, then centrifuged (7000 rpm, 10 min, 4 °C) and re-suspended in 40 mL of TBS buffer (50 mM Tris.HCl, 150 mM NaCl, pH 8.0), and followed by further centrifugation (7,000 rpm, 10 min, 4 °C). The cell pellet was re-suspended in 40 mL of $CaCl_2$ buffer (50 mM Tris.HCl, 10 mM $CaCl_2$, pH 7.2) and lysed with DNase (5 mg) and 0.5 tablet of free-EDTA protease inhibitor. The cell suspension was gently stirred at 4 °C for 10 min, then sonicated (3 x 2 min), and the cell debris was collected by centrifugation (17,000 rpm, 20 min, 4 °C). The supernatant was decanted and discarded, then the cell pellet was re-suspended in 20 mL of EDTA buffer (50 mM Tris.HCl, 20 mM EDTA, pH 7.2). The cell suspension was centrifuged (17,000 rpm, 20 min, 4 °C), then the supernatant was collected and filtered with 0.45 µm membrane filter. Each protein sample was analysed by either SDS-PAGE or LC-MS analysis.

Antibiotics used: Ampicillin (100 mg/L) for pET12a-PAPI (T7 promoter)
Kanamycin (50 mg/L) for pQE80L-Kan (T5 promoter)
Kanamycin (50 mg/L) for *V.* cholerae TrpRS plasmid

Expression scale used: 100, 200 and 1,000 mL

Supplements used: 5-OH or 5-Br-Trp for protein modification
glyphosate or 3-indoleacrylic as an enzyme inhibitor

Bacterial growth media recipes

1. Auto-induction medium 1 L (2 mL 1 M $MgSO_4$, 0.2 mL 1000 x trace elements, 20 mL 50 x 5052, 10 mL 25% aspartate, 20 mL 50 X M, 20 mg all amino acids, except tryptophan and cysteine, and 928 mL MilliQ water)[25].

   1000 x trace elements (100 mL)
   - 50 mL 0.1 M $FeCl_3.6H_2O$ (2.70 g)
   - 2 mL 1.0 M $CaCl_2.2H_2O$ (15.8 g)
   - 1 mL 1.0 M $MnCl_2.4H_2O$ (19.8 g)
   - 1 mL 1.0 M $ZnSO_4.7H_2O$ (28.8 g)
   - 1 mL 0.2 M $CoCl_2.6H_2O$ (4.76 g)
   - 2 mL 0.1 M $CuCl_2.2H_2O$ (1.70 g)
   - 1 mL 0.2 M $NiCl_2.6H_2O$ (4.76 g)
   - 2 mL 0.1 M $Na_2MoO_4.2H_2O$ (2.42 g)
   - 2 mL 0.1 M Na_2SeO_3 (1.73 g)
   - 2 mL 0.1 M H_3BO_3 (0.62 g)
   - 36 mL MilliQ water

   50 x 5052 (1 L)
   - 25 % glycerol (250 g)
   - 2.5 % D-glucose (25 g)
   - 10 % α-lactose (100 g)
   - MilliQ water (730 mL)

   50 x M (1 L)
   - 1.25 M Na_2HPO_4 (335 g)
   - 1.25 M $KHPO_4$ (170 g)
   - 2.5 M NH_4Cl (134 g)
   - 0.25 M Na_2SO_4 (35.5 g)
   - MilliQ water (700 mL)
   - 25 % aspartate (100 mL), pH 7
   - Aspartic acid (25 g)
   - MilliQ water (84 mL)

2. New minimal medium (NMM) 1 L (11.41 g 50 mM $K_2HPO_4.2H_2O$, 2.99 g 22 mM KH_2PO_4, 496 mg 8.5 mM NaCl, 991 mg 7.5 mM $MgSO_4$, 991 mg 7.5 mM $(NH4)_2SO_4$, 120 mg 1 mM $MgSO_4$, 3.60 g 20 mM D-glucose, 9.0 µL 1 M $CaCl_2$, 3.6 µL 1 M $FeSO_4.7H_2O$, 10 µL trace elements, 10 mg thiamine, 10 mg biothin, 50 mg each all amino acids, except tryptophan, and 1 L MilliQ water)[26,27].

   Trace elements (100 mL)
   - 250 mg $CuSO_4.5H_2O$
   - 5 g $ZnSO_4.7H_2O$
   - 50 mg $MnSO_4.H_2O$
   - 47 mg $(NH_4)_2.MoO_4$
   - 100 mL MilliQ water

Investigation of Biosynthetic Incorporation Systems using Trp-auxotroph

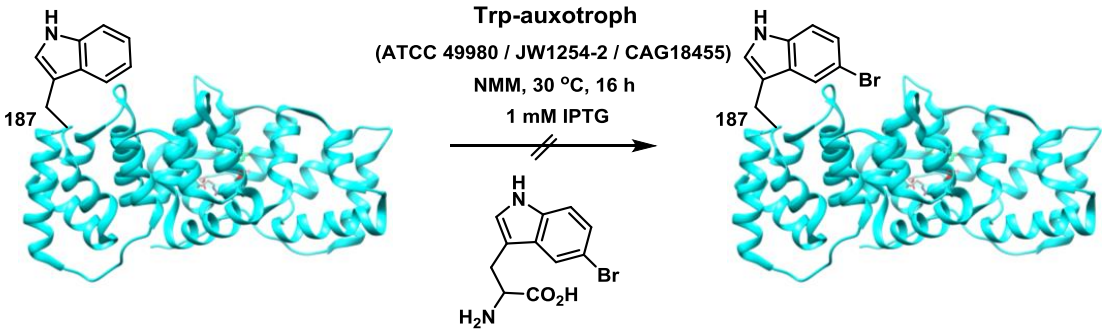

Entry	Trp-auxotrophs	Plasmids	Supplements	Media	Expression Conditions
1	ATCC 49980	pET12a-PAPI	5-Br-Trp	NMM	1 mM IPTG, 30 °C, 16 h
2	JW 1254-2	pET12a-PAPI	5-Br-Trp	NMM	1 mM IPTG, 30 °C, 16 h
3	CAG 18455	pET12a-PAPI	5-Br-Trp	NMM	1 mM IPTG, 30 °C, 16 h

Expression scale: entry 1, 1 L and entry 2-3, 200 mL
Supplement: entry 1, 5 mL and entry 2-3, 1 mL of the 5-Br-Trp stock solution (50 mM)
Protein extraction: entry 2-3, 300 µL BugBuster® protein extraction reagent

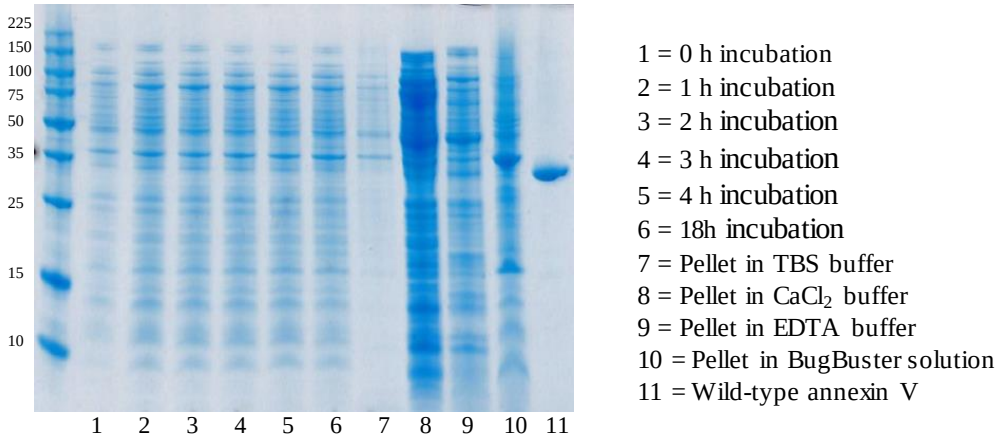

Figure 3.15 SDS-PAGE of the attempted incorporation of 5-Br-Trp into annexin V using *E.coli* tryptophan auxotroph ATCC 49980. No desired protein was detected by SDS-PAGE.

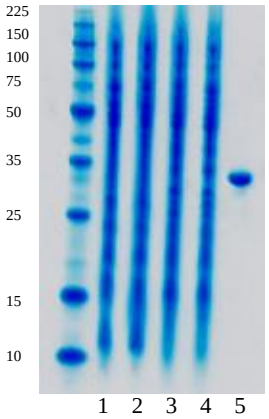

1 = JW 1254-2, LB, 30 °C, 16h
2 = CAG 18455, LB, 30 °C, 16h
3 = CAG 18455, NMM, 30 °C, 16h
4 = JW 1254-2, NMM, 30 °C, 16h
5 = Wild-type annexin V

Figure 3.16 SDS-PAGE of the attempted incorporation of 5-Br-Trp into annexin V using *E.coli* tryptophan auxotroph JW 1254-2 and CAG 18455, respectively. No desired protein was detected by SDS-PAGE.

Investigation of Biosynthetic Incorporation Systems using *E.coli* BL21(DE3) and Enzyme Inhibitor

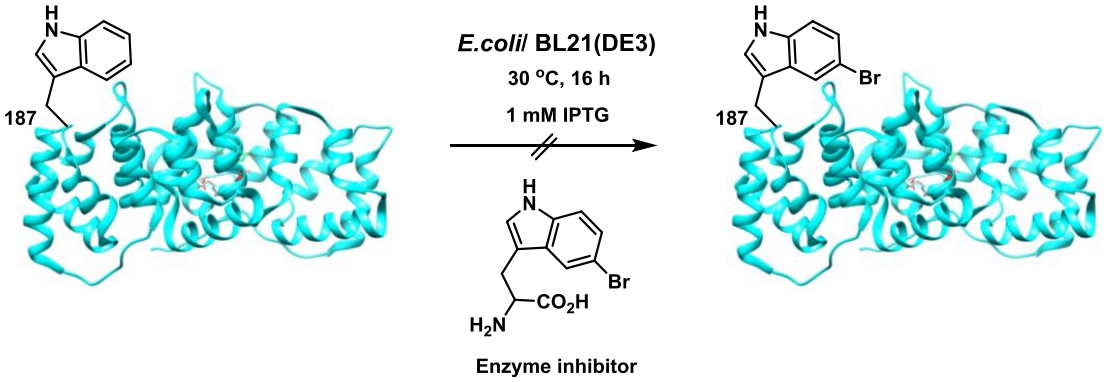

Entry	Bacterial cells	Plasmids	Supplements	Enzyme inhibitors	Media	Expression Conditions
1	*E.coli* BL21(DE3)	pET12a-PAPI	5-Br-Trp	glyphosate	NMM	1 mM IPTG, 30 °C, 16 h
2	*E.coli* BL21(DE3)	pET12a-PAPI	5-Br-Trp	glyphosate	AIM	1 mM IPTG, 30 °C, 16 h
3	*E.coli* BL21(DE3)	pET12a-PAPI	5-OH-Trp	glyphosate	AIM	1 mM IPTG, 30 °C, 16 h
4	*E.coli* BL21(DE3)	pET12a-PAPI	5-Br-Trp	IAA glyphosate	NMM	1 mM IPTG, 30 °C, 16 h

Expression scale: entry 1, 200 mL and entry 2-4, 100 mL
Supplements: entry 1, 150 mg and entry 2,4, 75 mg of 5-Br-Trp and entry 3, 75 mg of 5-OH-Trp
entry 1, 200 mg and entry 2-4,100 mg of glyphosate
entry 4, 100 µL of the IAA stock solution (10 mg/mL)

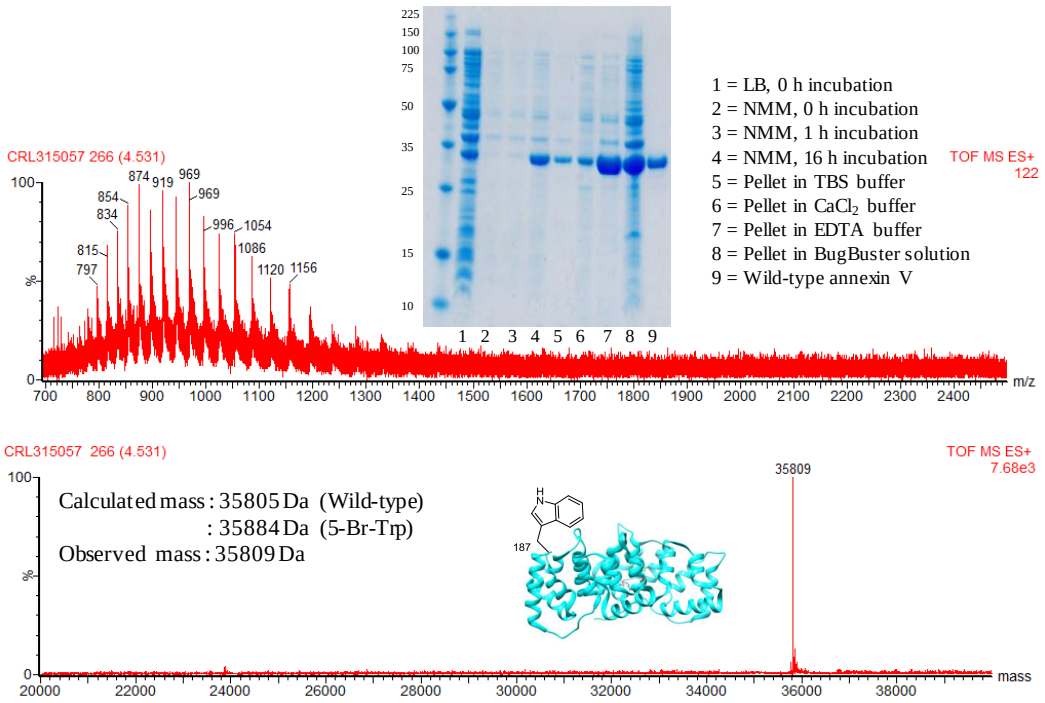

Figure 3.17 SDS-PAGE and ESI-MS spectrum of the attempted incorporation of 5-Br-Trp into annexin V expressed in *E. coli* BL21(DE3) using NMM supplemented with glyphosate

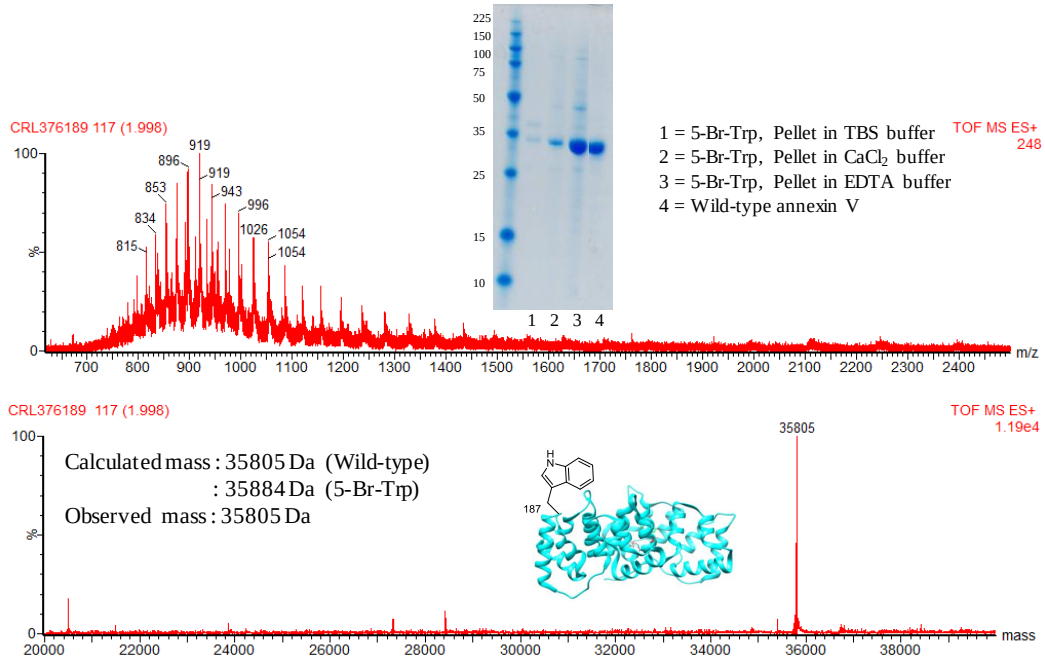

Figure 3.18 SDS-PAGE and ESI-MS spectrum of the attempted incorporation of 5-Br-Trp into annexin V expressed in *E. coli* BL21(DE3) using AIM supplemented with glyphosate.

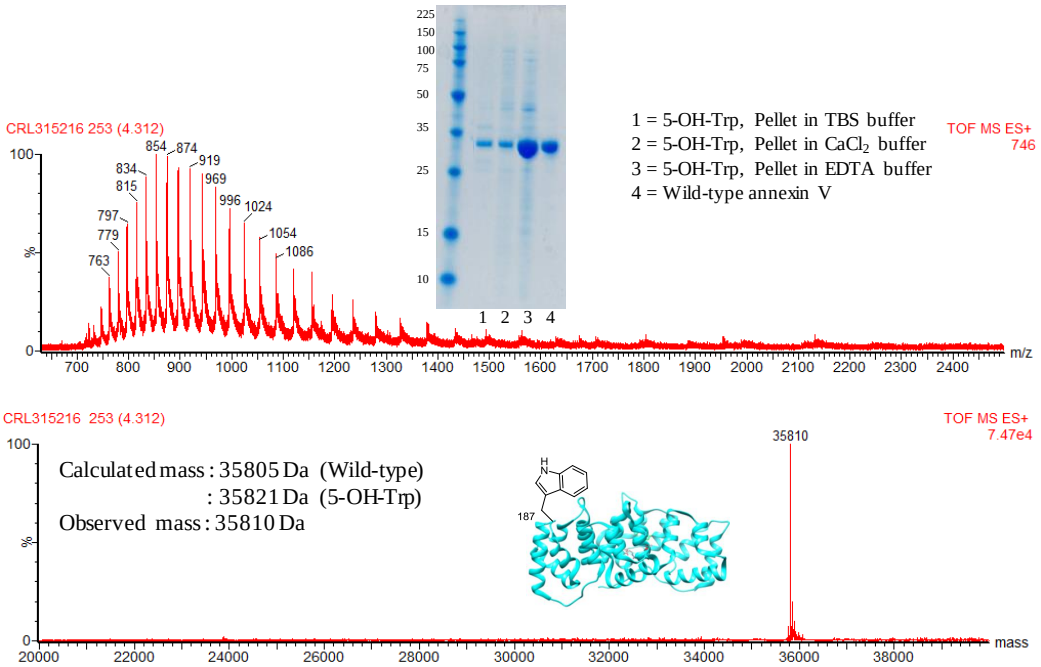

Figure 3.19 ESI-MS spectrum of the attempted incorporation of 5-OH-Trp into annexin V expressed in *E. coli* BL21(DE3) using AIM supplemented with glyphosate.

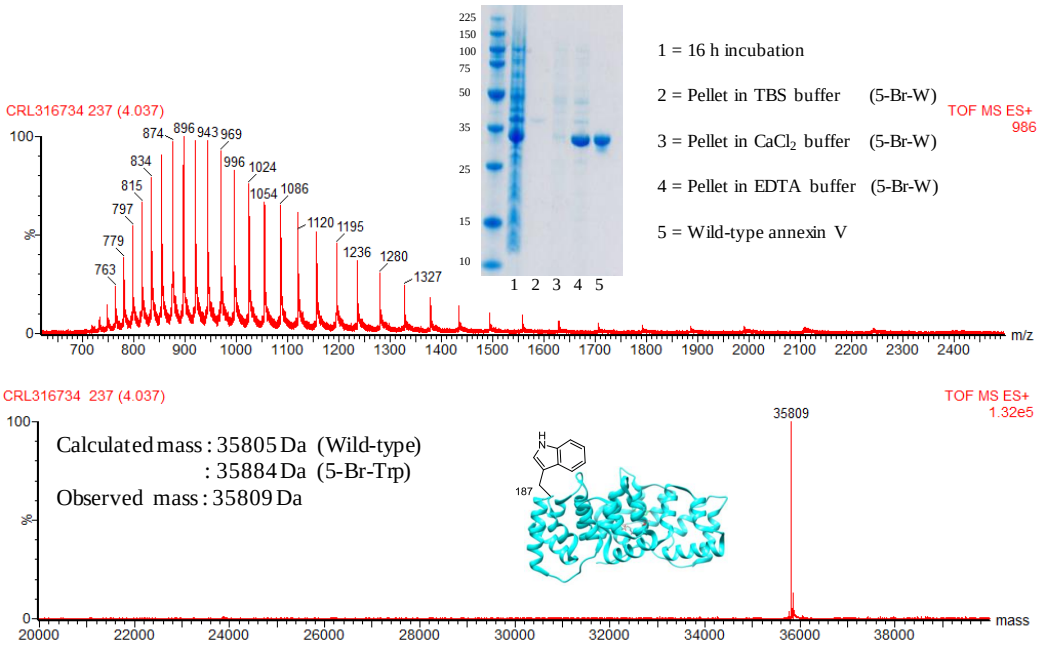

Figure 3.20 SDS-PAGE and ESI-MS spectrum of the attempted incorporation of 5-Br-Trp into annexin V expressed in *E. coli* BL21(DE3) using NMM supplemented with glyphosate and 3-indoleacrylic acid (IAA).

Investigation of Biosynthetic Incorporation Systems using *E.coli* BL21(DE3) and Tryptophanyl-tRNA Synthetase (TrpRS)

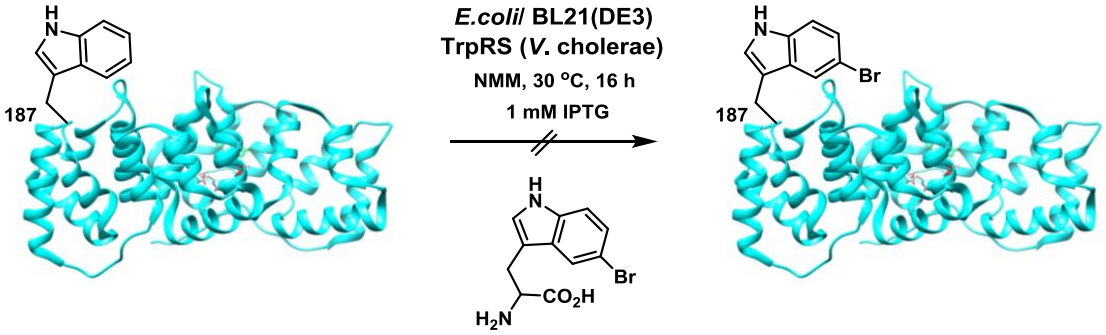

Entry	Bacterial cells	Plasmids	Supplements	Media	Expression Conditions
1	*E.coli* BL21(DE3)	pET12a-PAPI TrpRS (*V.* cholerae)	-	NMM	1 mM IPTG, 30 °C, 16 h
2	*E.coli* BL21(DE3)	pET12a-PAPI TrpRS (*V.* cholerae)	5-Br-Trp	NMM	1 mM IPTG, 30 °C, 16 h
3	*E.coli* BL21(DE3)	pET12a-PAPI TrpRS (*V.* cholerae)	5-OH-Trp+ IAA	NMM	1 mM IPTG, 30 °C, 16 h
4	*E.coli* BL21(DE3)	pET12a-PAPI TrpRS (*V.* cholerae)	5-Br-Trp+ IAA	NMM	1 mM IPTG, 30 °C, 16 h
5	*E.coli* BL21(DE3)	pET12a-PAPI TrpRS (*V.* cholerae)	5-Br-Trp + glyphosate	NMM	1 mM IPTG, 30 °C, 16 h

Expression scale: 200 mL
Supplements: entry 2,4-5, 100 µL of the 5-Br-Trp stock solution (20 mg/mL)
entry 3, 100 µL of the 5-OH-Trp stock solution (20 mg/mL)
entry 3-4, 25 µL of the IAA stock solution (10 mg/mL)
entry 5, 200 µL of the glyphosate stock solution (100 mg/mL)

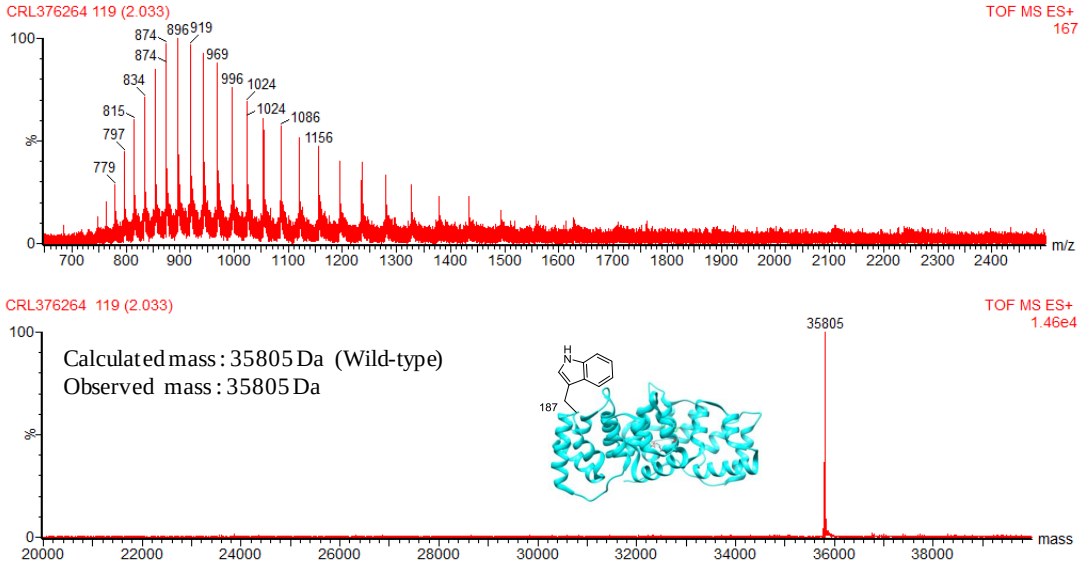

Figure 3.21 ESI-MS spectrum of wild-type annexin V expressed with *V.* chlolerae TrpRS in *E. coli* BL21(DE3) using NMM.

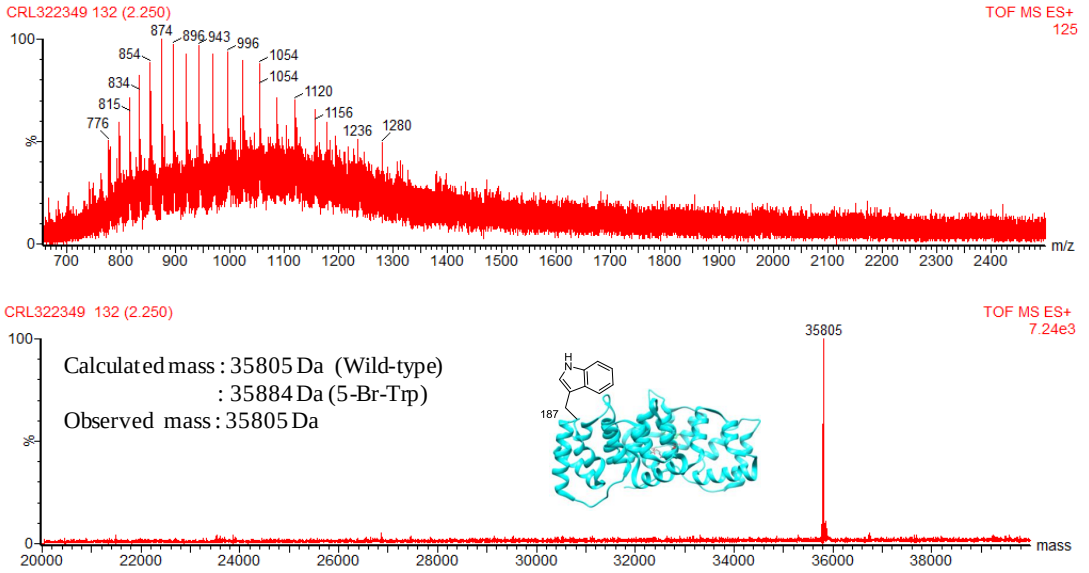

Figure 3.22 ESI-MS spectrum of wild-type annexin V expressed with *V.* chlolerae TrpRS in *E. coli* BL21(DE3) using NMM supplemented with 5-Br-Trp.

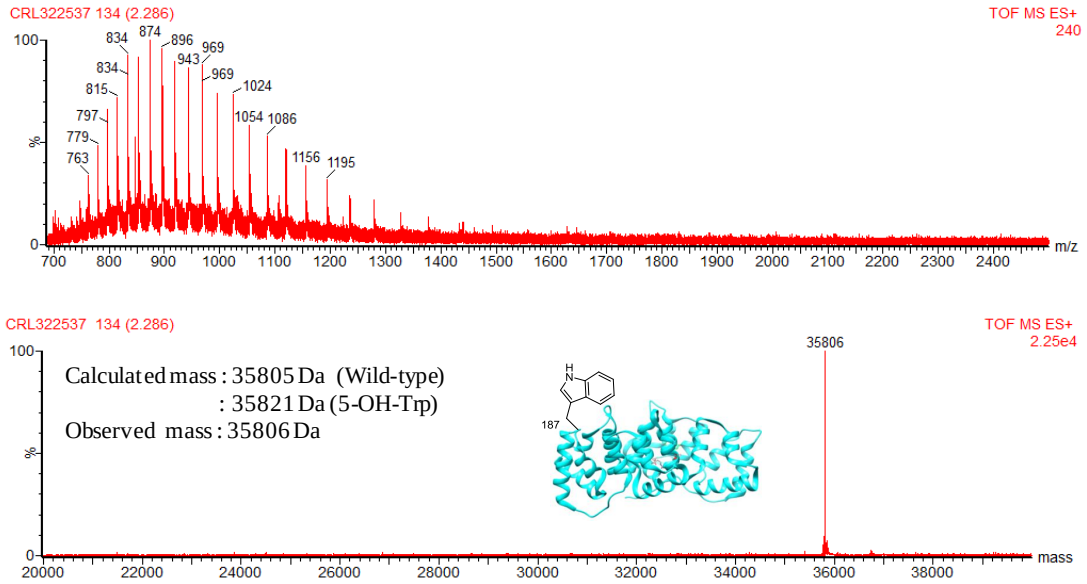

Figure 3.23 ESI-MS spectrum of wild-type annexin V expressed with *V.* chlolerae TrpRS in *E. coli* BL21(DE3) using NMM supplemented with 5-OH-Trp and IAA.

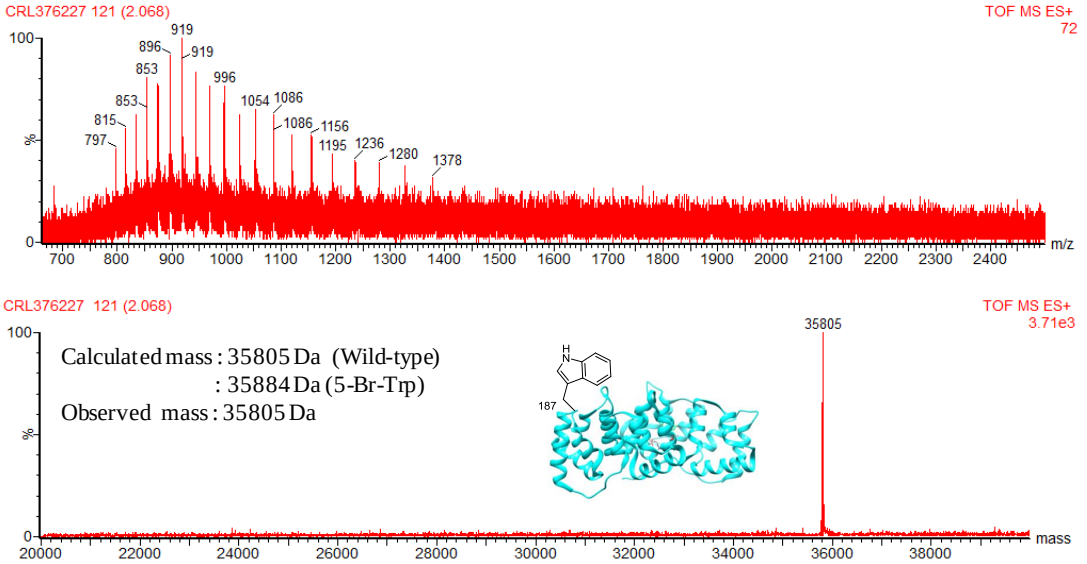

Figure 3.24 ESI-MS spectrum of wild-type annexin V expressed with *V.* chlolerae TrpRS in *E. coli* BL21(DE3) using NMM supplemented with 5-Br-Trp and IAA.

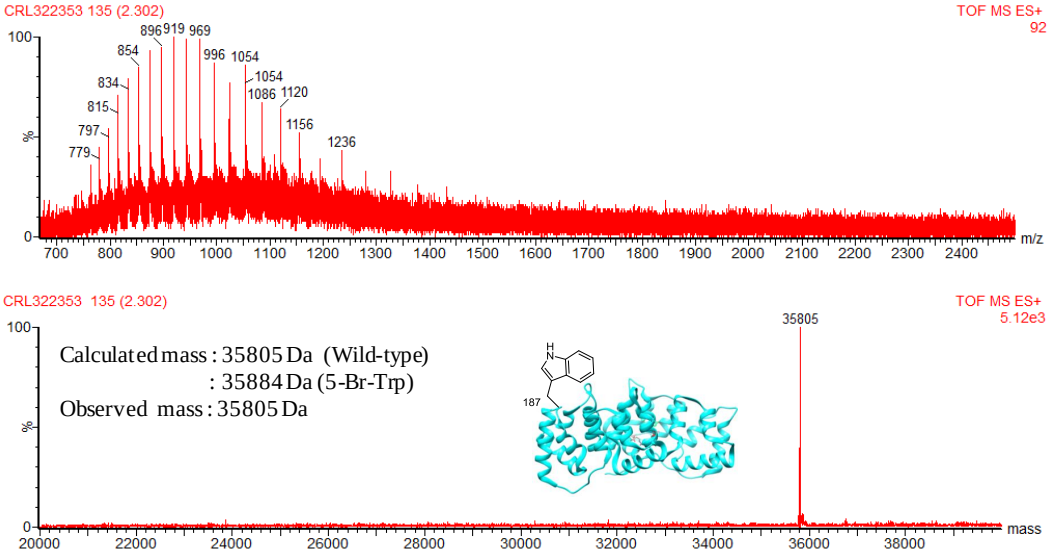

Figure 3.25 ESI-MS spectrum of wild-type annexin V expressed with *V.* chlolerae TrpRS in *E. coli* BL21(DE3) using NMM supplemented with 5-Br-Trp and glyphosate.

3.6.4 Plasmid Construction of the Annexin V Plasmid into pQE80L-Kan Vector

Forward primer: AGT CGT GGA TCC GCA CAG GTT CTC AGA GGC ACT GTG

Reverse primer: AGT CGT AAG CTT TTA GTC ATC TTC TCC ACA GAG CAG CAG

Each 10 µM forward and reserve primers (1 µL), DNA template of the annexin V plasmid (pET12a PAPI), and PfuUltra II Hotstart2 x Master Mix (25 µL) were added in a PCR eppendorf, then filled up with sterilised MilliQ water to a totally final volume of 50 µL. The reaction tube was placed in the PCR machine whose programme was set up as follows.

Segments	Number of cycles	Temperature	Duration
1	1	95 °C	2 min
2	30	95 °C	20 sec
		72 °C	20 sec
		72 °C	30 sec
3	1	72 °C	3 min

1% Agarose gel (0.5 g agarose, 50 mL 1 x TAE buffer, and 5 µL DNA visualising agent) was prepared to analyse the PCR product being extracted by QlAquick gel extraction kit

(Qiagen). DNA PCR fragment (14 µL) was re-suspended in the 10 x NEBuffer 4 (2 µL), then followed by addition of two restriction enzymes, BamHI-HF (2 µL) and HindIII-HF (2 µL). The pQE80L-Kan vector (10 µL) was also re-suspended in the 10 x NEBuffer 4 (2 µL), then followed by addition of the BamHI (2 µL) and HindIII (2 µL), and adjusted volume to 20 µL with sterilised MilliQ water (4 µL). Both DNA PCR fragment and pQE80L-Kan vector reaction tubes were incubated at 37 °C for 4 h, then further purified by PCR purification kit and eluted by sterilised MilliQ water (30 µL). A 3:1 ratio mixture of the digested PCR fragment and vector (9 µL) was dissolved in a 2 x quick ligation buffer (10 µL), then followed by addition of quick ligase (1 µL) and incubated at room temperature for 1 h. The ligation mixture was transformed into *E.coli* tryptophan auxotrophic strain ATCC 49980 and XL10-Gold ultracompetent cells, then plated on the LB agar plate containing kanamycin as an antibiotic.

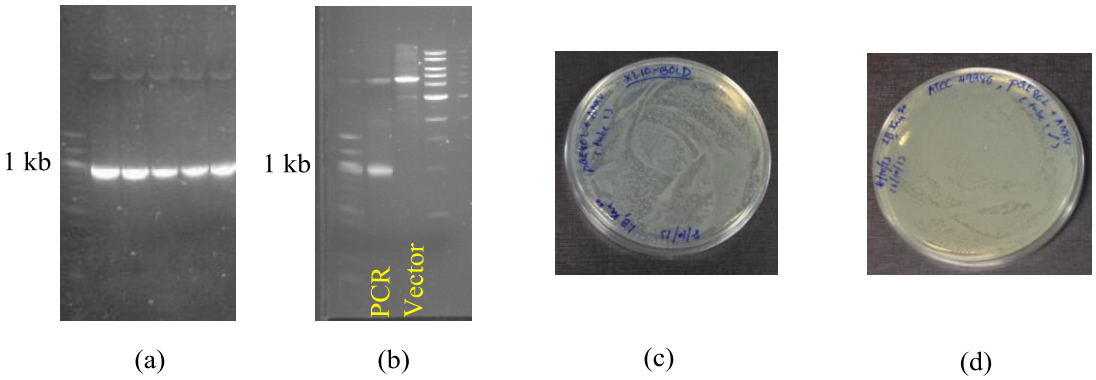

Figure 3.26 a). PCR band (~1 kb) on agarose gel, b). Digested PCR fragment (~1 kb) and pQE80L-Kan vector (4.7 kb), and c-d). Transformation of the ligation mixture into XL10-Gold ultracompetent cells and *E.coli* tryptophan auxotroph ATCC 49980, respectively.

Sequencing of the Colony PCR of pQE80L-Kan derived from XL10-Gold Ultracompetent Cells

Each 10 µM forward and reserve primers (1 µL), DNA template of the pQE80L-Kan derived from XL10-Gold ultracompetent cells, and PfuUltra II Hotstart2 x Master Mix (25 µL) were added in a PCR eppendorf, then filled up with sterilised MilliQ water to a totally final volume of 50 µL. The reaction tube was placed in the PCR machine whose programme was set up as follows.

Segments	Number of cycles	Temperature	Duration
1	1	95 °C	2 min
2	30	95 °C	20 sec
		72 °C	20 sec
		72 °C	30 sec
3	1	72 °C	3 min

1% Agarose gel (0.5 g agarose, 50 mL 1 x TAE buffer, and 5 µL DNA visualising agent) was prepared to analyse the PCR product being extracted by QlAquick gel extraction kit (Qiagen). The purified plasmid DNA (10 µL, 100 ng/µL) was prepared for DNA sequencing. The DNA sequence of the plasmid DNA (pQE80L-Kan) exactly matched with the original annexin V gene from the pET12a PAPI plasmid. This plasmid DNA was transformed into XL10-Gold and XL1-Blue cells on LB agar plate, then picked up in 5 mL LB culture. The overnight culture was prepared for 50% glycerol stock which was kept in the -80 °C freezer.

Met R G S H H H H H H G S A Q V L R G T V T D F P G F D E R A D A E T L R K A Met K G L G T D E E S I L T L L T S X S N A Q R Q E I S A A F K T L X G R D L L D D L K S E L T G K F E K L I V A L Met K P S R L Y D A Y E L K H A L K G A G T N E K V L T E I I A S R T P E E L R A I K Q V Y E E E Y G S S L E D D V V G D T S G Y Y Q R Met L V V L L Q A N R D P D A G I D E A Q V E Q D A Q A L F Q A G E L K W G T D E E K F I T I F G T R S V S H L R K V F D K Y Met T I S G F Q I E E T I D R E T S G N L E Q L L L A V V K S I R S I P A Y L A E T L Y Y A Met K G A G T D

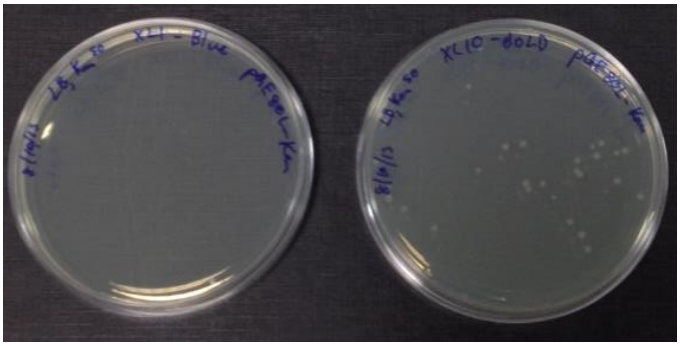

Figure 3.27 Amino acid sequence of the new plasmid construct (pQE80L-Kan), and transformation of the pQE80L-Kan into XL1-Blue and XL10-Gold cells.

Expression of Wild-type Annexin V (pQE80L-Kan) using Trp-auxotroph

Entry	Bacterial cells	Plasmids	Supplements	Media	Expression Conditions
1	ATCC 49980	pQE80L-Kan	-	LB	1 mM IPTG, 30 °C, 16 h
2	CAG 18455	pQE80L-Kan	-	LB	1 mM IPTG, 30 °C, 16 h
Expression scale: 200 mL					

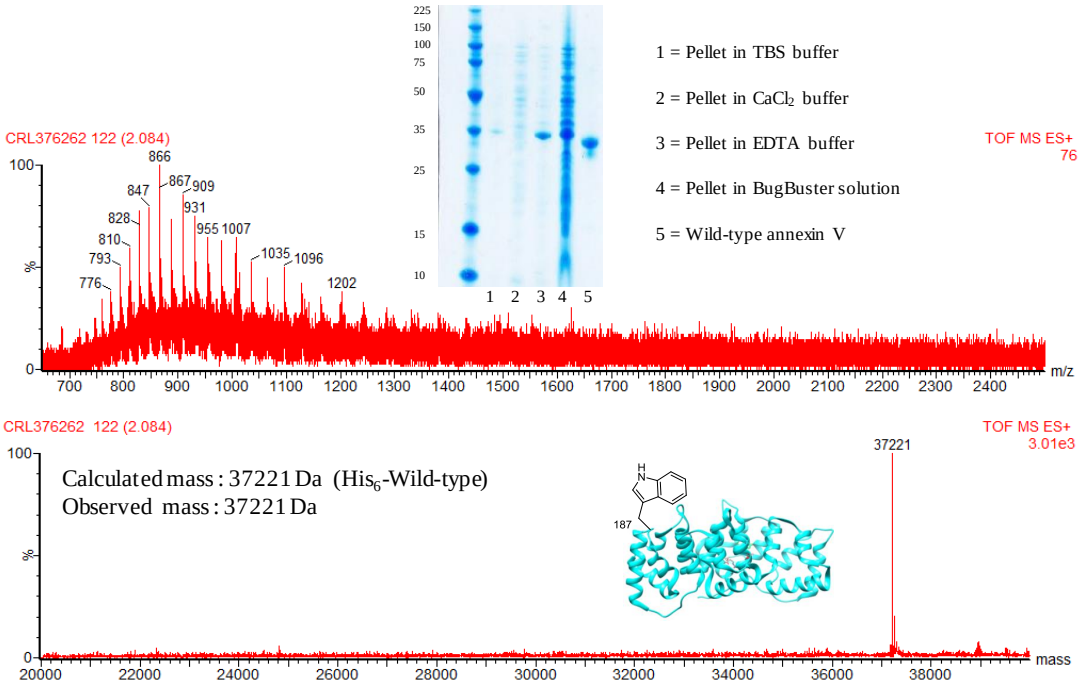

Figure 3.28 SDS-PAGE and ESI-MS spectrum of wild-type annexin V (6xHis-tag) expressed in *E.coli* tryptophan auxotroph ATCC 49980.

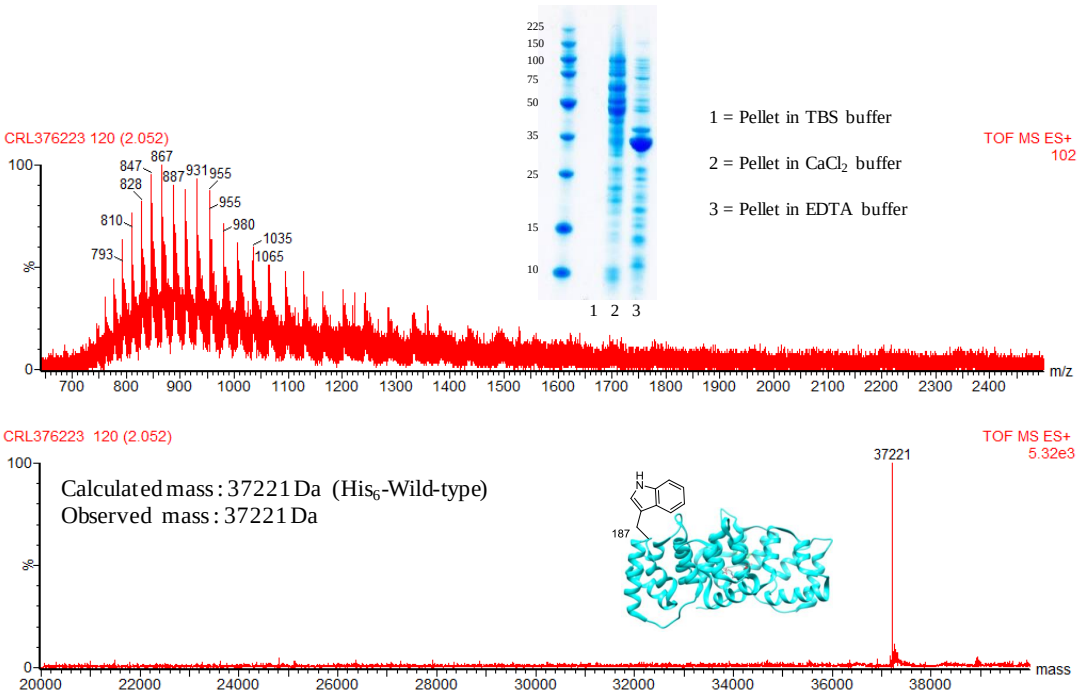

Figure 3.29 SDS-PAGE and ESI-MS spectrum of wild-type annexin V (6xHis-tag) expressed in *E.coli* tryptophan auxotroph CAG 18455.

Investigation of Biosynthetic Incorporation Systems using Trp-auxotroph (II)

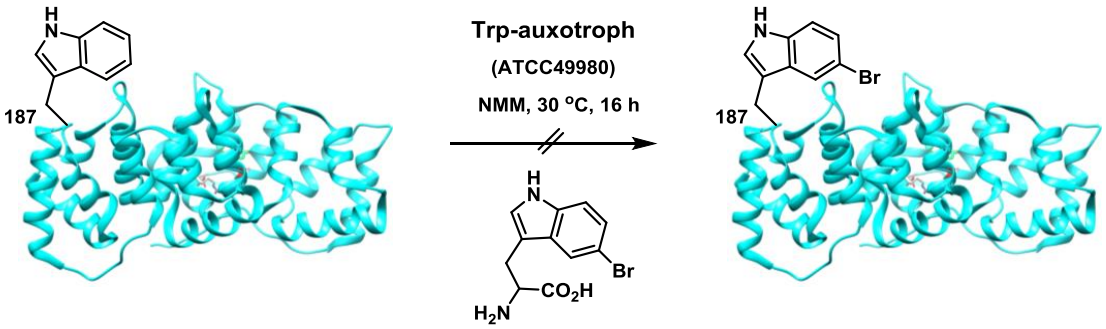

Entry	Bacterial cells	Plasmids	Supplements	Media	Expression Conditions
1	ATCC 49980	pQE80L-Kan	5-Br-Trp	NMM	1 mM IPTG, 30 °C, 16 h

Expression scale: 200 mL
Supplements: 3x20 mg of 5-Br-Trp

(For Western blot: See general experimental considerations in appendix)

Entry	Proteins	Antibodies		Dilution
		Primary	Secondary	
1	Annexin V (6xHis-tag)	Monoclonal anti-polyhistidine alkaline phosphatase antibody produced in mouse	-	1 : 5,000
BCIP/NBT used as an alkaline phosphatase substrate.				

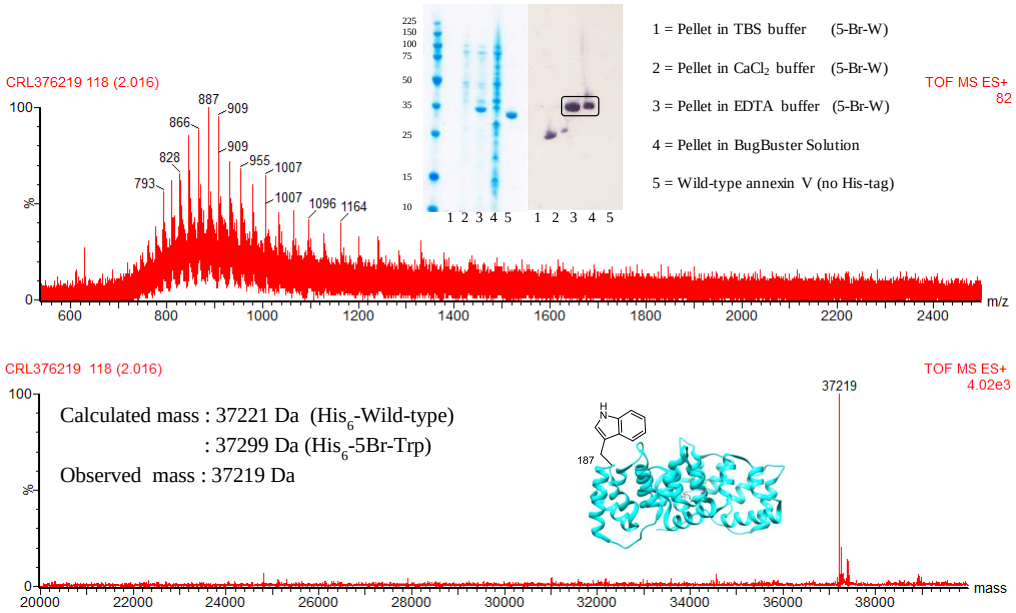

Figure 3.30 SDS-PAGE, corresponding Western blot (using monoclonal anti-polyhistidines alkaline phosphatase antibody) and ESI-MS spectrum of the attempted incorporation of 5-Br-Trp into annexin V expressed in *E.coli* tryptophan auxotroph ATCC 49980 using NMM supplemented with 5-Br-Trp.

3.7 Bibliography

(1) Hogue, C. W. V.; Rasquinha, I.; Szabo, A. G.; MacManus, J. P. A new intrinsic fluorescent probe for proteins Biosynthetic incorporation of 5-hydroxytryptophan into oncomodulin. *FEBS Lett.* **1992**, *310*, 269-272.

(2) Hogue, C. W. V.; Szabo, A. G. Characterization of aminoacyl-adenylates in B. tsubtilis tryptophanyl-tRNA synthetase, by the fluorescence of tryptophan analogs 5-hydroxytryptophan and 7-azatryptophan. *Biophys. Chem.* **1993**, *48*, 159-169.

(3) Ross, J. B. A.; Szabo, A. G.; Hogue, C. W. V. Enhancement of protein spectra with tryptophan analogs: fluorescence spectroscopy of protein-protein and protein-nucleic acid interactions. *Methods Enzymol.* **1997**, *278*, 151-190.

(4) Nagarathnam, D.; Johnson, M. E. A New Synthesis of 5-Bromo-DL-tryptophan. *Synth. Commun.* **1993**, *23*, 2011-2017.

(5) Prasitpan, N.; Johnson, M. E.; Currie, B. L. 5-Bromo-DL-tryptophan and Protected Intermediates for Peptide Synthesis. *Synth. Commun.* **1990**, *20*, 3459-3466.

(6) El Khattabi, M.; van Roosmalen, M. L.; Jager, D.; Metselaar, H.; Permentier, H.; Leenhouts, K.; Broos, J. Lactococcus lactis as expression host for the biosynthetic incorporation of tryptophan analogues into recombinant proteins. *Biochem. J* **2008**, *409*, 193-198.

(7) Chin, J. W.; Cropp, T. A.; Anderson, J. C.; Mukherji, M.; Zhang, Z.; Schultz, P. G. An Expanded Eukaryotic Genetic Code. *Science* **2003**, *301*, 964-967.

(8) Liu, C. C.; Schultz, P. G. Adding new chemistries to the genetic code. *Annu. Rev. Biochem* **2010**, *79*, 413-444.

(9) Wang, L.; Brock, A.; Herberich, B.; Schultz, P. G. Expanding the Genetic Code of Escherichia coli. *Science* **2001**, *292*, 498-500.

(10) Wang, L.; Schultz, P. G. Expanding the genetic code. *Angew. Chem. Int. Ed. Engl.* **2004**, *44*, 34-66.

(11) Post, J. F. M.; Cottam, P. F.; Simplaceanu, V.; Ho, C. Fluorine-19 Nuclear Magnetic Resonance Study of 5-Fluorotryptophan-labelled Histidine-binding Protein J of *Salmonella typhimurium*. *J. Mol. Biol.* **1984**, *179*, 729-743.

(12) Kwon, I.; Tirrell, D. A. Site-Specific Incorporation of Tryptophan Analogues into Recombinant Proteins in Bacterial Cells. *J. Am. Chem. Soc.* **2007**, *129*, 10431-10437.

(13) Chalker, J. M.; Wood, C. S. C.; Davis, B. G. A Convenient Catalyst for Aqueous and Protein Suzuki-Miyaura Cross-Coupling. *J. Am. Chem. Soc.* **2009**, *131*, 16346-16347.

(14) Dumas, A.; Spicer, C. D.; Gao, Z.; Takehana, T.; Lin, Y. A.; Yasukohchi, T.; Davis, B. G. Self-liganded Suzuki-Miyaura coupling for site-selective protein PEGylation. *Angew. Chem. Int. Ed. Engl.* **2013**, *52*, 3916-3921.

(15) Spicer, C. D.; Davis, B. G. Palladium-Mediated Site-Selective Suzuki-Miyaura Protein Modification at Genetically Encoded Aryl Halides. *Chem. Commun.* **2011**, *47*, 1698-1700.

(16) Spicer, C. D.; Triemer, T.; Davis, B. G. Palladium-Mediated Cell-Surface Labeling. *J. Am. Chem. Soc.* **2012**, *134*, 800-803.

(17) Wang, W.; Xiong, C.; Yang, J.; Hruby, V. J. Practical, asymmetric synthesis of aromatic-substituted bulky and hydrophobic tryptophan derivatives. *Tetrahedron Lett.* **2001**, *42*, 7717-7719.

(18) Hollαnder, H.; Amrhein, N. The Site of the Inhibition of the Shikimate Pathway by Glyphosate. *Plant Physiology* **1980**, *66*, 823-829.

(19) Roisch, U.; Lingens, F. Effect of the Herbicide N-Phosphonomethylglycine on the Biosynthesis of Aromatic Amino Acids. *Angew. Chem. Int. Ed.* **1974**, *13*, 400.

(20) Matchett, W. H. Inhibition of Tryptophan Synthetase by Indoleacrylic Acid. *J. Bacteriol.* **1972**, *110*, 146-154.

(21) Boger, D. L.; Corbett, W. L.; Curran, T. T.; Kasper, A. M. Inverse electron-demand Diels-Alder reactions of N-sulfonyl .alpha.,.beta.-unsaturated imines: a general approach to implementation of the 4.pi. participation of 1-aza-1,3-butadienes in Diels-Alder reactions. *J. Am. Chem. Soc.* **1991**, *113*, 1713-1729.

(22) Boger, D. L.; Corbett, W. L.; Wiggins, J. M. Room-temperature, endo-specific 1-aza-1,3-butadiene Diels-Alder reactions: acceleration of the LUMOdiene-controlled [4 + 2] cycloaddition reactions through noncomplementary aza diene substitution. *J. Org. Chem.* **1990**, *55*, 2999-3000.

(23) Gao, Z.; Gouverneur, V.; Davis, B. G. Enhanced Aqueous Suzuki–Miyaura Coupling Allows Site-Specific Polypeptide 18F-Labeling. *J. Am. Chem. Soc.* **2013**, *135*, 13612-13615.

(24) Li, N.; Lim, R. K. V.; Edwardraja, S.; Lin, Q. Copper-Free Sonogashira Cross-Coupling for Functionalization of Alkyne-Encoded Proteins in Aqueous Medium and in Bacterial Cells. *J. Am. Chem. Soc.* **2011**, *133*, 15316-15319.

(25) Studier, F. W. Protein production by auto-induction in high-density shaking cultures. *Protein Express. Purif.* **2005**, *41*, 207-234.

(26) Budisa, N.; Alefelder, S.; Bae, J. H.; Golbik, R.; Minks, C.; Huber, R.; Moroder, L. Proteins with beta-(thienopyrrolyl)alanines as alternative chromophores and pharmaceutically active amino acids. *Protein Sci.* **2001**, *10*, 1281-1292.

(27) Budisa, N.; Steipe, B.; Demange, P.; Eckerskorn, C.; Kellermann, J.; Huber, R. High-level biosynthetic substitution of methionine in proteins by its analogs 2-aminohexanoic acid, selenomethionine, telluromethionine and ethionine in Escherichia coli. *Eur. J. Biochem.* **1995**, *230*, 788-796.

Chapter 4

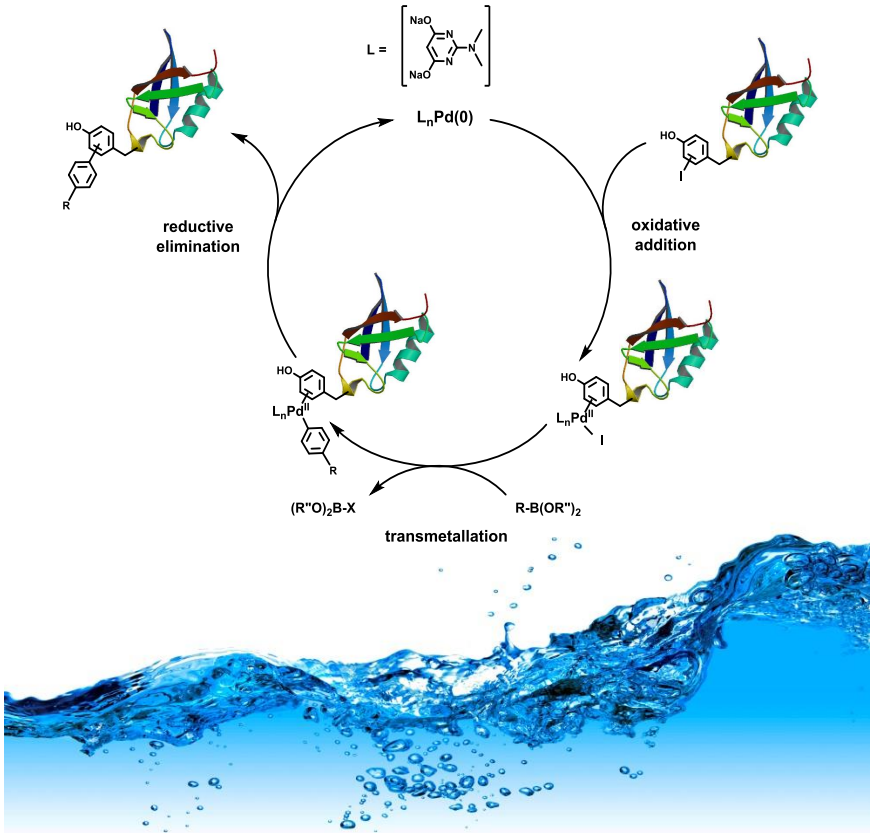

Site-Specific Bioconjugation through Pd(0)-Mediated Cross-Couplings

4.1 Introduction

4.1.1 Peptide and Protein Iodination Reactions

4.1.2 Palladium-Catalysed Cross-Coupling Reactions of Proteins

4.1.3 Ubiquitination

4.2 Site-Specific Protein Iodination Reactions

4.3 Palladium-Mediated Reactions of Proteins

4.3.1 Suzuki-Miyaura Cross-Coupling Reactions

4.3.2 Sonogashira Cross-Coupling Reactions

4.4 Palladium-Mediated Ubiquitination

4.5 Conclusion

4.6 Experimental

4.7 Bibliography

4.1 Introduction

The aim of this chapter is to optimise a chemical method for site-specific protein iodination reactions and also to investigate bioconjugation reactions of the iodinated protein using our aqueous palladium-catalysed systems through either Suzuki-Miyaura or Sonogashira cross-coupling. The application of this system to a novel chemical method for palladium-mediated ubiquitination is also investigated.

4.1.1 Peptide and Protein Iodination Reactions

A synthesis of *bis*(pyridine)iodinium(I) tetrafluoroborate (IPy_2BF_4), a potential iodinating agent, was first reported by Barluenga and co-workers[1,2]. Formation of the IPy_2BF_4 proceeded from treatment of $HgO{\bullet}2BF_4$-SiO_2 with both iodine and pyridine in DCM (Scheme **4.1**)[1,2]. Alternatively, this compound was also more safely synthesised by use of $AgBF_4$-SiO_2 instead of the original $HgO{\bullet}2BF_4$-SiO_2, as reported by Davis et. al (Scheme **4.1**)[3].

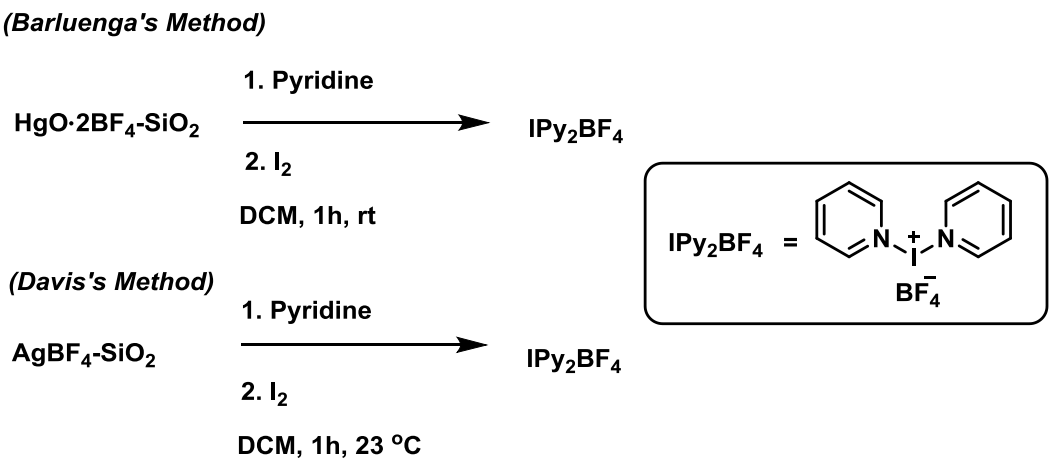

Scheme 4.1 Preparation of the IPy_2BF_4 as an iodinating agent by Barluenga and Davis' methods, respectively[1-3].

IPy_2BF_4 is also useful in iodination reactions of both peptides and proteins via electrophilic aromatic iodination (Scheme **4.2**)[1,4-6]. Furthermore, electrophilic aromatic iodination of proteins (bovine insulin, lysozyme, and 1,3-1,4-β-D-4-glucanohydrolase) has been demonstrated by use of IPy_2BF_4 as a mild and selective iodinating agent[4]. All

protein reactions showed multiple-site labelling of the most accessible tyrosine residues, as subsequently confirmed by MALDI-TOF and MSMS analysis. In the case of lysozyme, a histidine residue was also selectively iodinated by IPy_2BF_4 under acidic conditions (pH5.9).

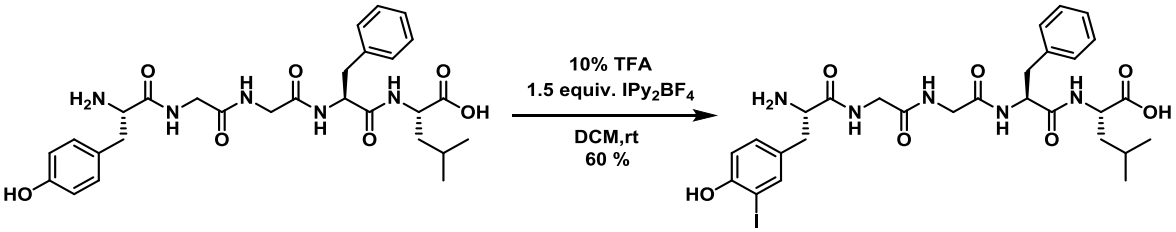

Scheme 4.2 Iodination reaction of activated aromatic residues in peptide[5].

4.1.2 Palladium-Catalysed Cross-Coupling Reactions of Proteins

Chemical modification of proteins is widely used in extension of the functionality of proteins and structural diversity. Many tools for this purpose now exist, such as native chemical ligation[7], C-C bond formation[8-11], glycosylation reactions[12,13] or cycloaddition[14-19]. Chalker and Davis reported a new pyrimidine-based Pd catalyst containing a simple ligand (2-amino-4,6-dihydroxypyrimidine, **L1**), which has since been widely used in aqueous Pd-mediated reactions of proteins[9,20,21]. This water-soluble Pd catalyst was used to facilitate new single C-C bond formation at *p*-iodobenzyl cysteine installed at position 156 of *Bacillus lentus* subtilisin (SBL) under aqueous conditions (Scheme **4.3**)[9].

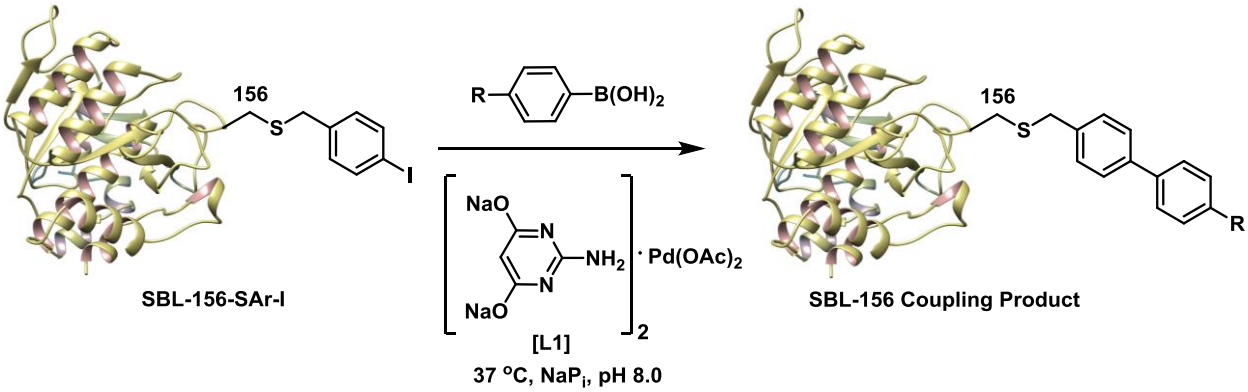

Scheme 4.3 Suzuki-Miyaura cross-coupling of iodoaryl SBL with R-$B(OH)_2$[9].

Spicer and Davis also reported genetic incorporation of *p*-iodophenylalanine into maltose binding protein (MBP) using UAG stop-codon suppression[20]. This protein could be chemically modified by use of a water-soluble and air-stable Pd catalyst to afford the cross-coupled product, as detected by LC-MS analysis (Scheme **4.4**).

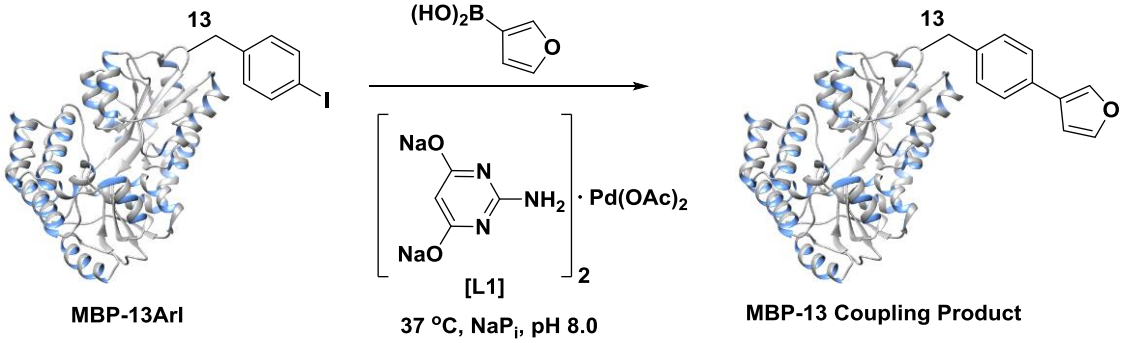

Scheme 4.4 Site-selective Suzuki-Miyaura cross-coupling of iodophenyl MBP[20].

Sonogashira cross-coupling is an alternative Pd-mediated reaction involving the formation of a new C-C bond between a terminal alkyne with an aryl or vinyl halide, in the presence of Pd catalyst. Copper-free Pd-mediated Sonogashira reactions of the ubiquitin (UBQ) bearing a genetically encoded alkyne with a set of functionalised aromatic iodide substrates were first reported by Lin and co-workers (Scheme **4.5**)[22]. These reactions were facilitated by a water-soluble Pd catalyst containing (*N,N'*-dimethyl)-2-amino-4,6-dihydroxy pyrimidine, **L2** as a ligand.

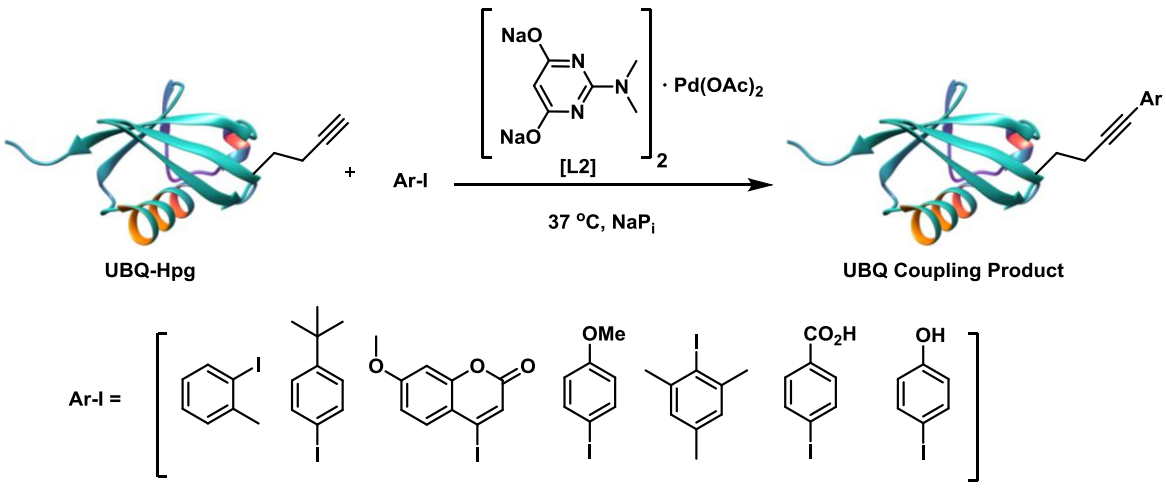

Scheme 4.5 A model study of aqueous copper-free Sonogashira reactions of the Hpg-tagged ubiquitin using our efficient Pd catalyst[22].

Furthermore, Sonogashira cross-coupling of *para*-iodophenyl dihydrofolate reductase (eDHFR) with 5-ethylnyl fluorescein as a fluorescent dye using a pyrimidine-based Pd catalyst was reported by Wombacher and co-workers[23]. Site-specific C-C bond formation between eDHFR and the fluorescent probe was achieved by a two-step protein modification process, via enzymatic peptide labelling and subsequent Sonogashira reaction.

4.1.3 Ubiquitination

Ubiquitin is a small protein containing 76 amino acids (8.5 kDa) that is found in almost all eukaryotic organisms[24,25]. Its conjugation to proteins, known as ubiquitination, targets the protein degradation. Ubiquitination occurs through three steps - activation, conjugation, and ligation - involving specific enzymes, which are ubiquitin-activating enzyme (E1), ubiquitin-conjugating enzyme (E2), and ubiquitin ligase (E3), respectively shown in Figure **4.1**[25,26]. A linkage between ubiquitin molecules and a lysine side-chain of the protein target is made via an isopeptide bond, leading to the attachment of either a single ubiquitin molecule (monoubiquitination) or several ubiquitin units (polyubiquitination) to the protein. This process is repeated to form a small ubiquitin tag, which associates with the proteasome, leading to protein degradation[25,26].

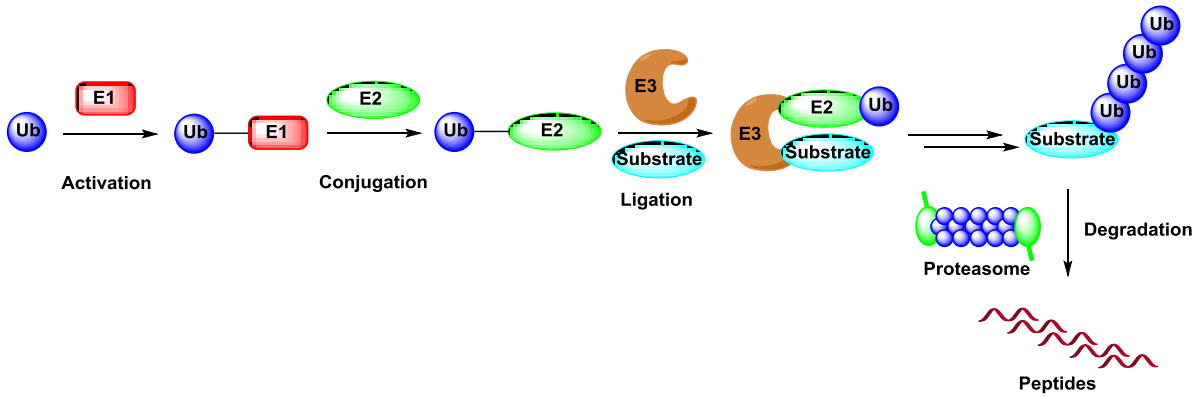

Figure 4.1 Ubiquitination mechanism involving activation, conjugation, ligation, and degradation[24-27].

Apart from enzymatic ubiquitination, a recent report shows chemical linkages generated by copper(I)-catalysed alkyne-azide cycloaddition (CuAAC) reaction between

genetically modified UBQ (based on amber codon suppression and use of Met-auxotroph) and a protein of interest containing a propargyl tag, leading to the formation of a polyubiquitin tag, as observed by SDS-PAGE (Scheme **4.6**)[28].

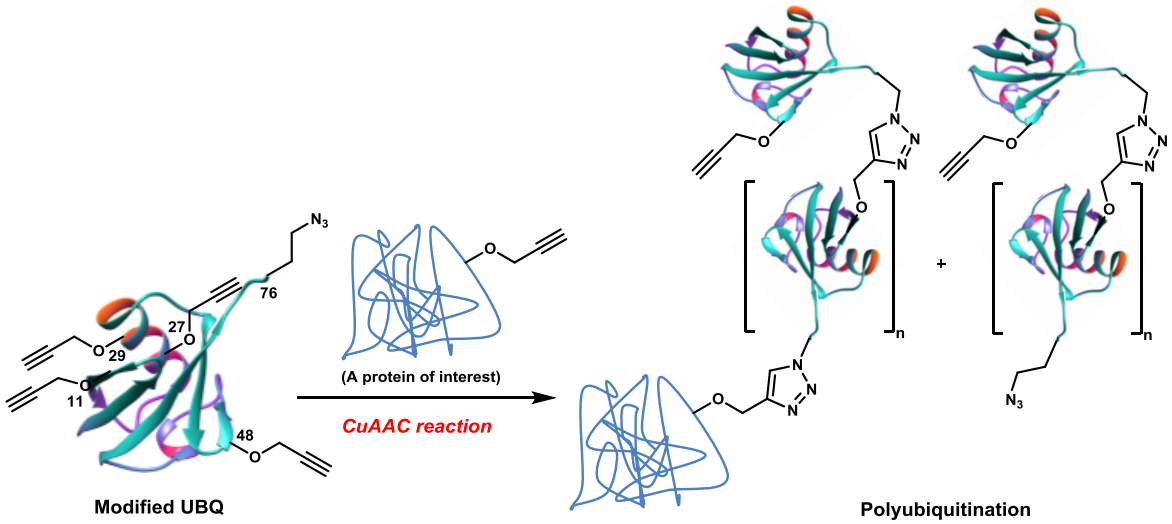

Scheme 4.6 A new method for chemical polyubiquitinaiton of the protein of interest through CuAAC reactions[28].

4.2 Site-specific Protein Iodination Reactions

As previously discussed in chapter 3, the biosynthetic incorporation of 5-Br-Trp into annexin V through either use of tryptophan auxotropic strain or Trp-tRNA synthetase (TrpRS) was unsuccessful, possibly due to incompatible incorporation systems during protein expression. In this chapter, we alternatively investigated a direct method to chemically install C-I bonds at tyrosine residues which could then be further modified by Pd-mediated reactions (Suzuki-Miyaura and Sonogashira cross-coupling reactions) for the creation of new C-C bonds. Initially, Barluenga's reagent (IPy_2BF_4) was investigated as a reactive iodinating agent for the installation of C-I bonds on tyrosine residues of a protein of interest. We tested a set of model proteins including insulin, monocyte chemoattractant protein-1 (MCP-1) or C-C motif chemokine (CCL2), and ubiquitin (UBQ) by treatment of these proteins with IPy_2BF_4 (Scheme **4.7**).

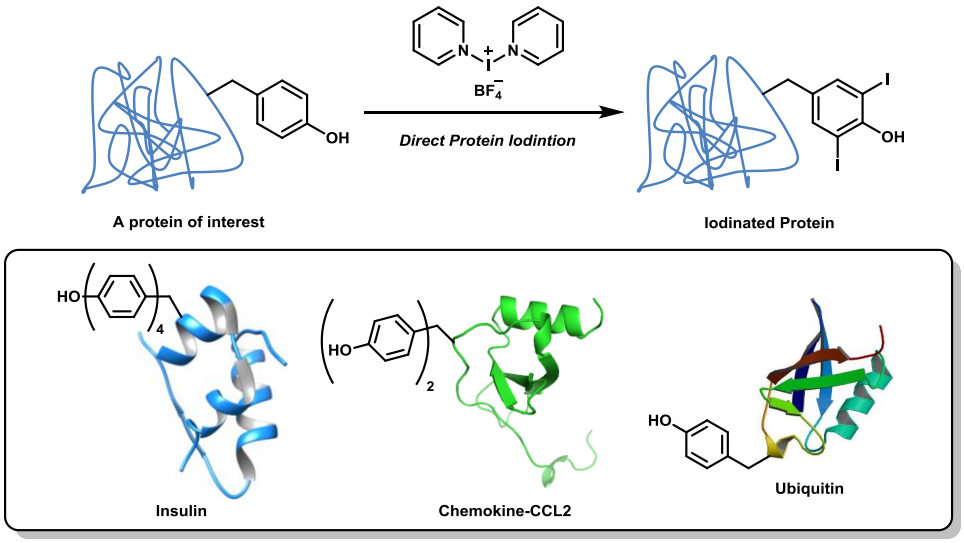

Scheme 4.7 A protein model study for direct protein iodination by use of Barluenga's reagent.

We chose insulin for our first model study based on a previous study[4]. Insulin as isolated from either human or bovine source has four natural tyrosine residues. Reactions of wild-type insulin were investigated by reacting with IPy_2BF_4, leading to the formation of multiply-iodinated products (Figure **4.2**). Surprisingly, we found that iodination occurred not only on tyrosine, but also on histidine (as previously observed only in lysozyme). The insulin iodinated by 20 equiv. IPy_2BF_4 was digested by trypsin, affording the peptides containing desired chemical modifications (C-I) at histidine (2x) and tyrosine (4x) moieties (See experimental details, Table **4.21**).

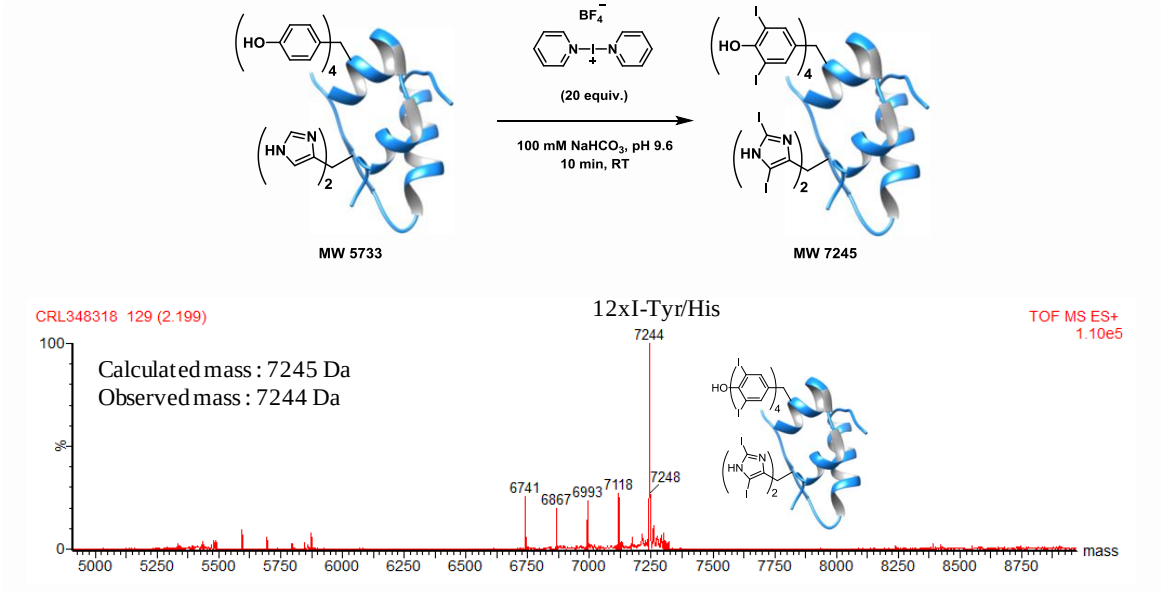

Figure 4.2 ESI-MS spectrum of wild-type insulin treated with 20 equiv. IPy_2BF_4.

Next, MCP-1, as a chemokine-CCL2, was also studied by treatment of wild-type MCP-1 with IPy_2BF_4 (10 equiv.), giving iodinated protein as observed by LC-MS (Figure **4.3**). Formation of new C-I bonds onto both tyrosine (2x) and histidine (1x) of the MCP-1 was also confirmed by MSMS analysis (See experimental details, Table **4.22**).

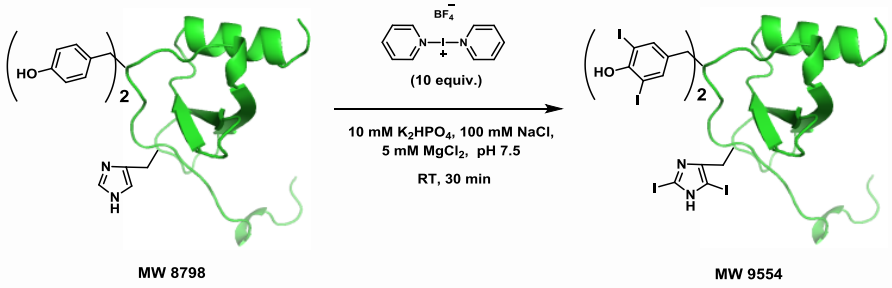

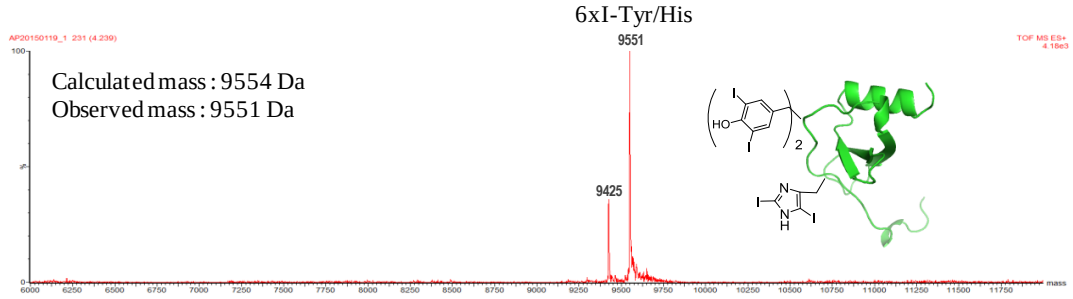

Figure 4.3 ESI-MS spectrum of wild-type MCP-1 treated with 10 equiv. IPy_2BF_4.

Alternatively, ubiquitin (UBQ), a small protein containing each single tyrosine (1x) and histidine (1x), is a good candidate for protein iodination. This protein was treated with IPy_2BF_4 (15 equiv.), giving iodinated products (including an oxidised methionine) observed by LC-MS (Figure **4.4**). Both iodinated tyrosine and histidine moieties of the UBQ and its oxidised methionine were also detected by MSMS analysis (See experimental details, Table **4.23**). Based on these results, we reasoned that this iodinated ubiquitin could be a useful model for investigation of Pd-mediated reactions to minimise undesired modification at undesired positions/sites.

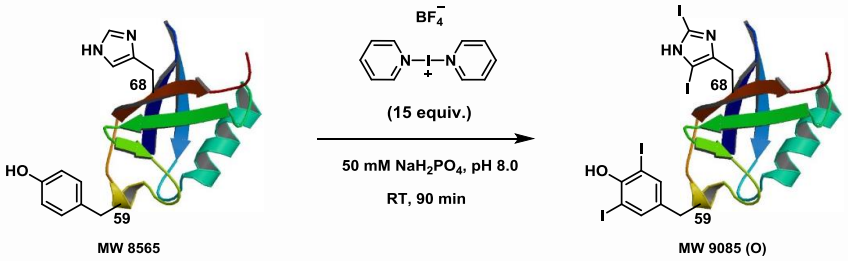

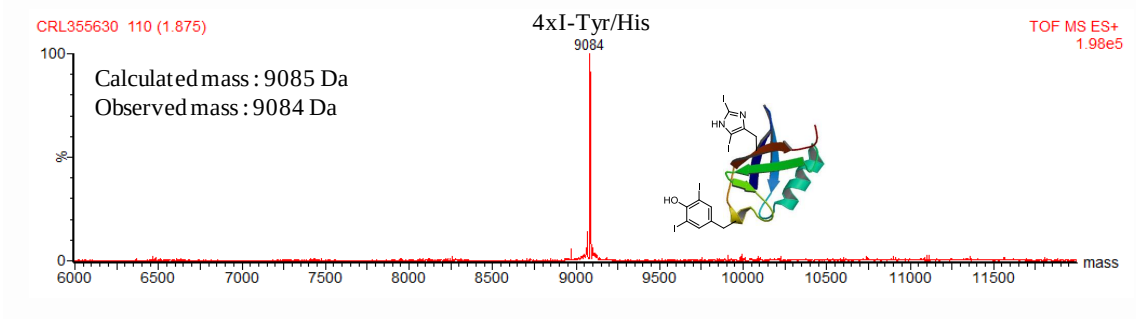

Figure 4.4 ESI-MS spectrum of wild-type ubiquitin treated with 15 equiv. IPy_2BF_4.

4.3 Palladium-Mediated Reactions of Proteins

4.3.1 Suzuki-Miyaura Cross-Coupling Reactions

A model study of aqueous Suzuki-Miyaura cross-coupling (SMC) reactions of the UBQ was investigated by use of our aqueous Pd catalysts containing various ligands, resulting in the formation of new C-C bonds at specific sites (Scheme **4.8**). Compared to our previous study of a genetically incorporated IPhe residue, tyrosine and histidine residues represent novel and challenging targets for Suzuki cross-coupling on proteins.

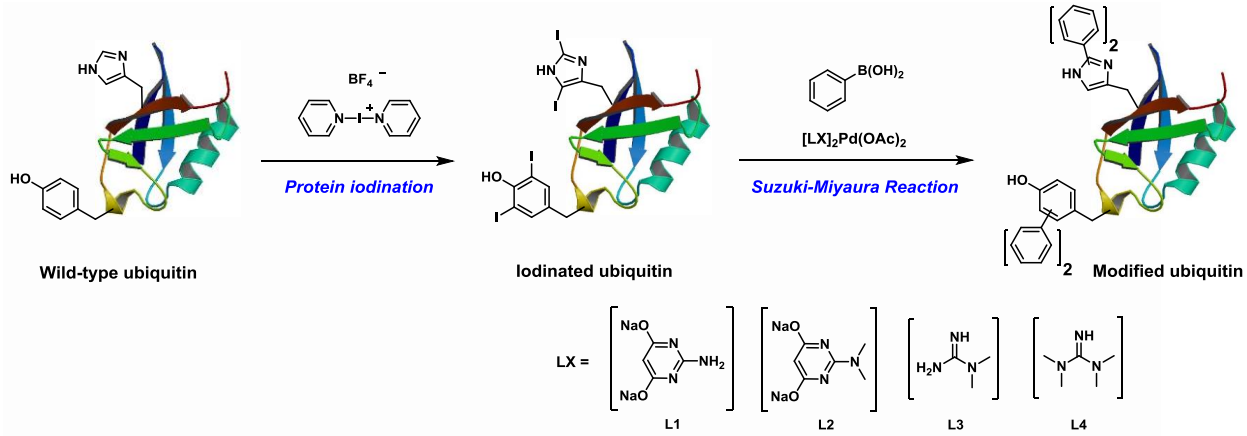

Scheme 4.8 A model study of Suzuki-Miyaura cross-coupling reactions of the iodinated ubiquitin with boronic acids in the presence of an aqueous Pd catalyst.

Initially, all ligands (**L1-L4**) of Pd catalysts were investigated by reactions of iodo-Tyr/His UBQ with $PhB(OH)_2$. It was found that two Pd catalysts containing **L2** or **L4** ligand showed a highly efficient conversion of a starting material to desired coupling products with full consumption of starting material. We decided to use $[\mathbf{L2}]_2Pd(OAc)_2$

catalyst for a further investigation of all Pd-mediated reactions. Optimisation of reaction conditions was studied by varying the amounts of $PhB(OH)_2$, ranging from 500 to 2000 equiv. in order to compare the conversion to C-C cross-coupled products. The reaction revealed that there was no significant change, even upon addition of excess amounts of $PhB(OH)_2$ to reactions (Figure **4.5**). The reaction would ideally use minimal and optimal amounts of boronic acid/Pd catalyst in order to avoid undesired side-reactions.

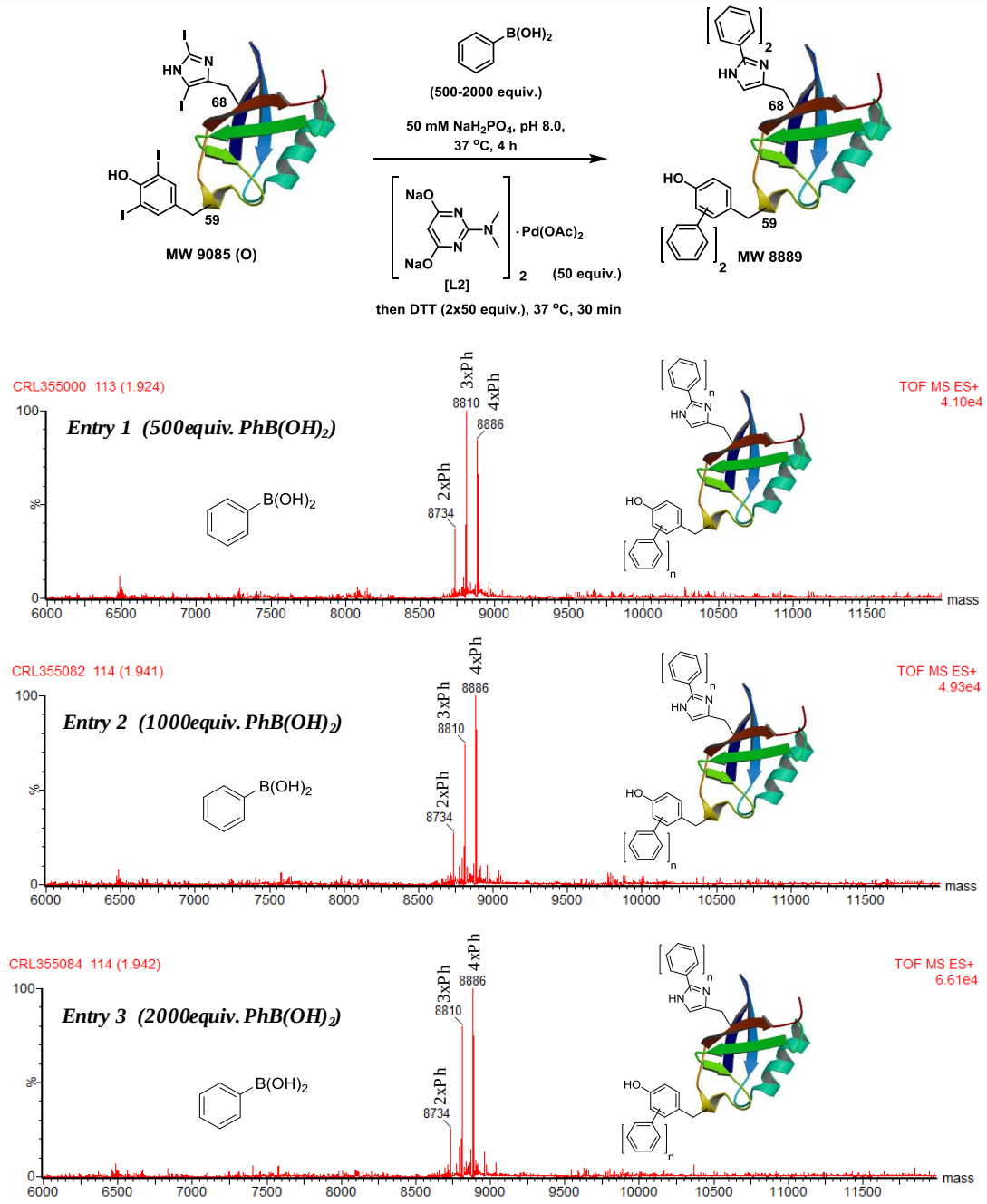

Figure 4.5 ESI-MS spectra of the iodo-Tyr/His ubiquitin treated with 500-2000 equiv. $PhB(OH)_2$ and 50 equiv. $[\mathbf{L2}]_2Pd(OAc)_2$.

To confirm an installation of new C-C bond at tyrosine and histidine residues, the phenyl-coupled product digested by trypsin was analysed by nanoLC-MSMS. Both post-translational modifications, diPh (Y-59) and diPh (H-68), on this peptide (TLSDYNIQKESTLHLVLR) were found by MSMS analysis (See experimental detail, Table **4.24**). To investigate the scope of our aqueous Pd cross-coupling reactions of iodinated ubiquitin to a wide range of boronic acids with diverse functionalities were carried out in the presence of the $[\mathbf{L2}]_2Pd(OAc)_2$ catalyst (Scheme **4.9**).

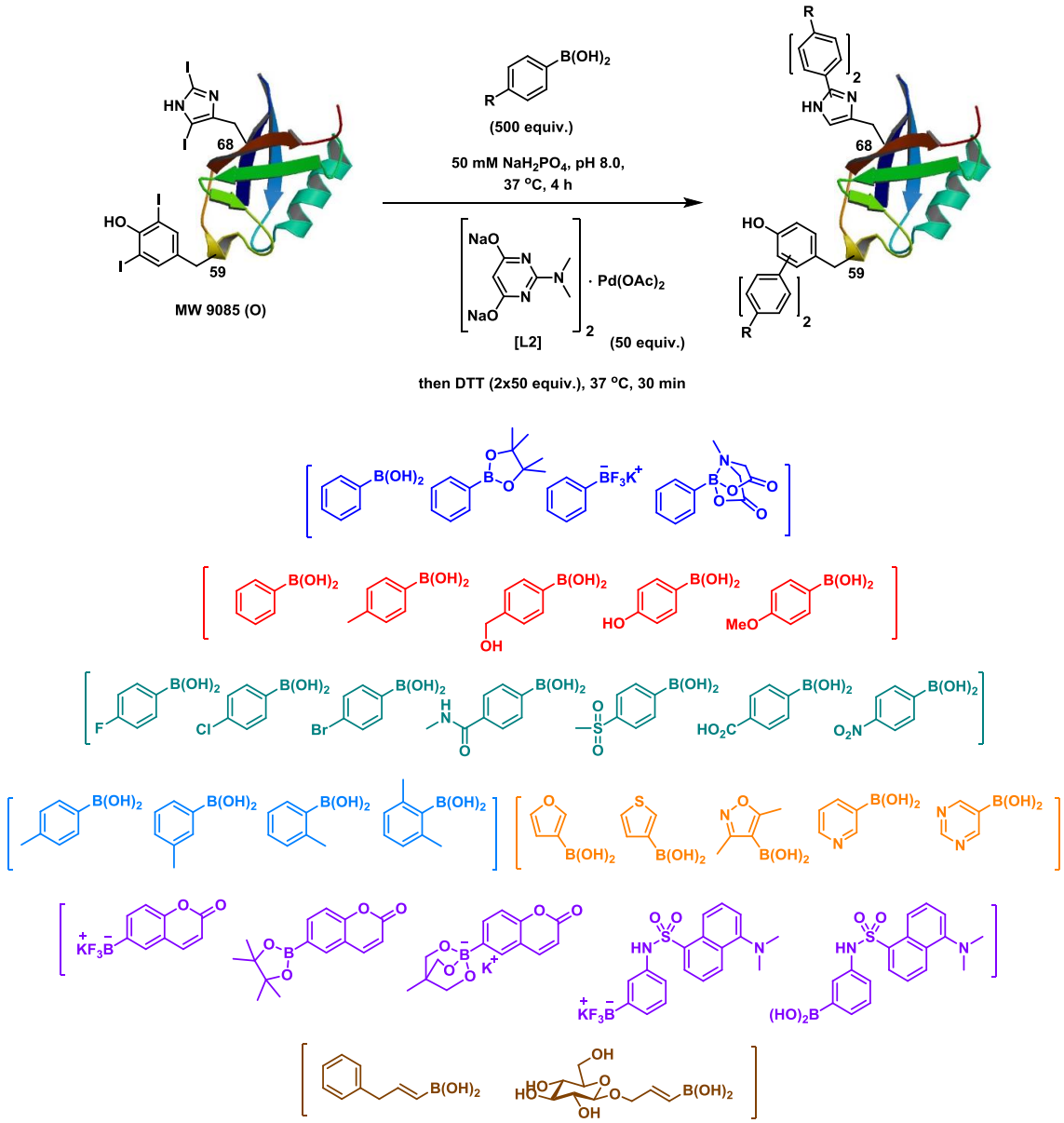

Scheme 4.9 Suzuki-Miyaura reactions of the iodo-Tyr/His ubiquitin with various boronic acids.

To compare the rate of conversion, we used some neutral phenylboronic acid derivatives. Both $B(OH)_2$ and $B(OR)_2$ (pinacol ester) showed a better conversion of C-I bonds to new C-C coupled bonds as compared to potassium trifluoroborate (BF_3K) and *N*-methyliminodiacetic acid (MIDA). For example, a reaction of the iodo-Tyr/His ubiquitin with phenylboronic acid pinacol ester gave multiple C-C bonds without remaining starting material as observed by LC-MS (Figure **4.6**).

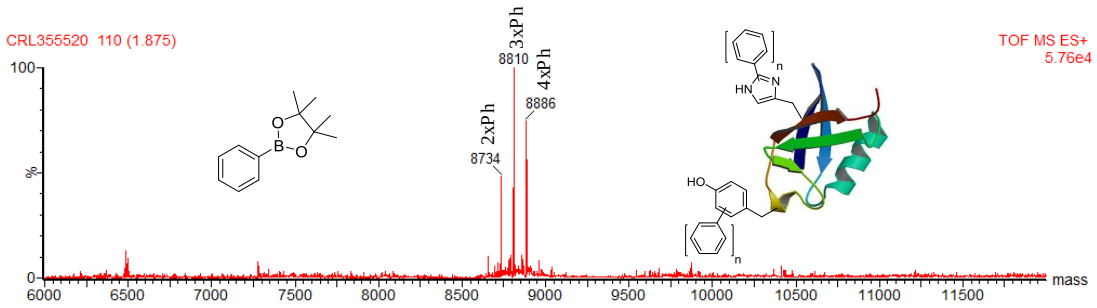

Figure 4.6 ESI-MS spectrum of the iodo-Tyr/His ubiquitin treated with 500 equiv. $PhB(OR)_2$ (R = pinacol ester) and 50 equiv. $[\mathbf{L2}]_2Pd(OAc)_2$.

For a further study of the SMC reactions, electron-rich substituents of the phenylboronic acids were tested on same conditions mentioned previously. All candidates worked very well in the presence of the $[\mathbf{L2}]_2Pd(OAc)_2$ catalyst, forming multiple C-C bonds with different ratio of the coupling products. For example, treatment of the iodo-Tyr/His ubiquitin with 4-methylphenylboronic acid showed predominantly three new C-C bonds on both residues as observed by LC-MS (Figure **4.7**).

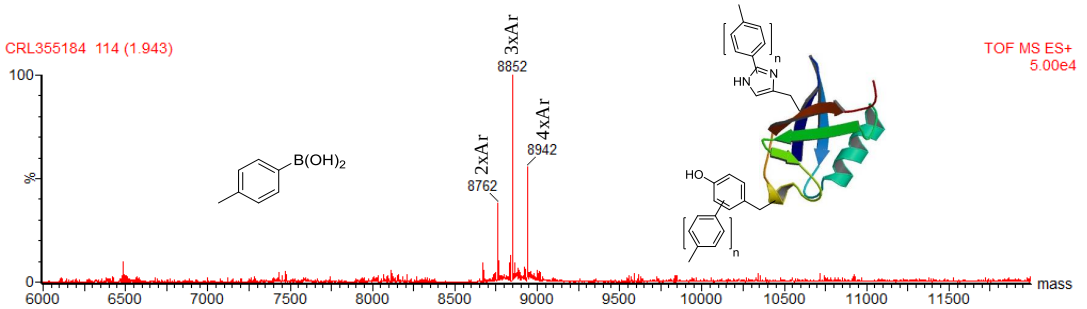

Figure 4.7 ESI-MS spectrum of the iodo-Tyr/His ubiquitin treated with 500 equiv. 4-Me-$PhB(OH)_2$ and 50 equiv. $[\mathbf{L2}]_2Pd(OAc)_2$.

In addition, phenylboronic acid derivatives bearing an electron withdrawing substituent were also investigated. Surprisingly, all possible coupling products were observed by LC-MS without remaining starting materials. For example, when the iodo-Tyr/His

ubiquitin was coupled to 4-nitrophenylboronic acid, the bi-, tri-, and tetra-arylated coupling products were detected by LC-MS (Figure **4.8**).

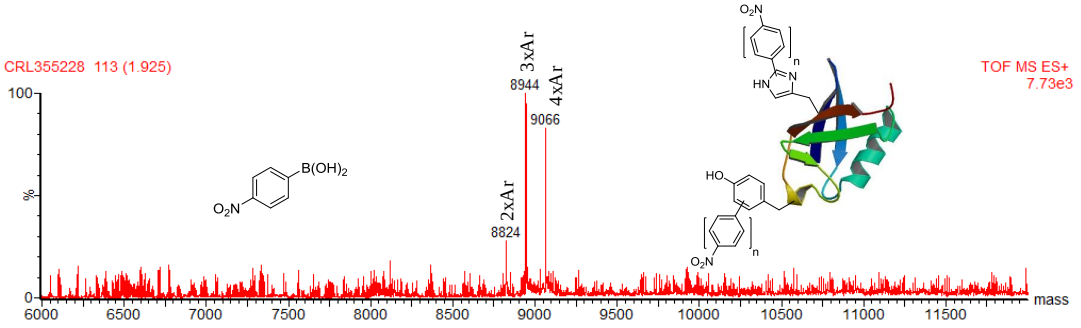

Figure 4.8 ESI-MS spectrum of the iodo-Tyr/His ubiquitin treated with 500 equiv. 4-NO_2-PhB$(OH)_2$ and 50 equiv. [**L2**]$_2$Pd$(OAc)_2$.

In terms of steric effects, we also investigated SMC reactions which were performed with some more hindered *ortho*-mono/dimethyl PhB$(OH)_2$. As expected, methyl groups at either *meta* or *para* position showed C-C forming bonds without a detection of remaining starting materials (Figure **4.9**), on the other hand, no desired product was detected by LC-MS when the iodo-Tyr/His ubiquitin reacted with 2,5-diMePhB$(OH)_2$ (Figure **4.10**). Only starting material (4xI) and deiodinated products (2-3xI) were observed by LC-MS.

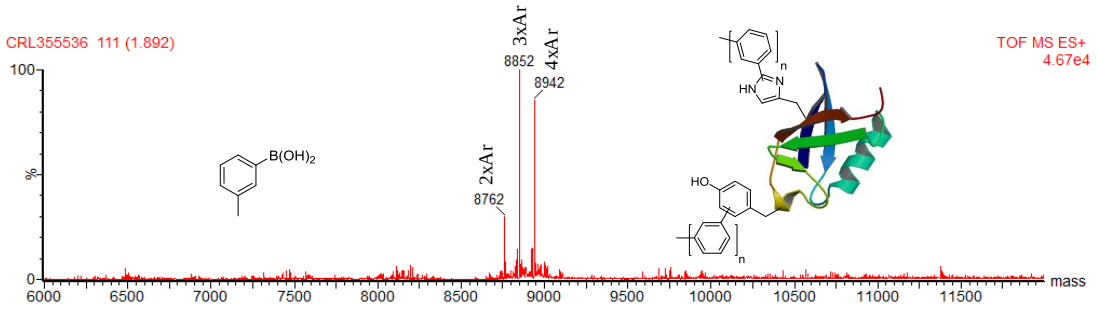

Figure 4.9 ESI-MS spectrum of the iodo-Tyr/His ubiquitin treated with 500 equiv. 3-Me-PhB$(OH)_2$ and 50 equiv. [**L2**]$_2$Pd$(OAc)_2$.

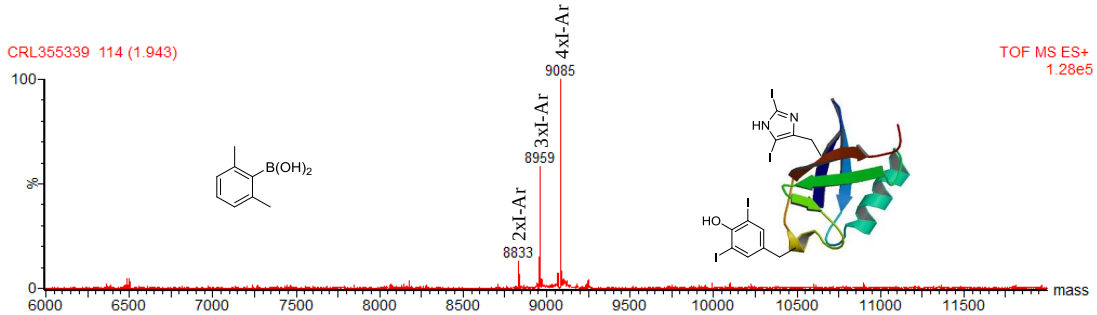

Figure 4.10 ESI-MS spectrum of the iodo-Tyr/His ubiquitin treated with 500 equiv. 2,5-diMe-PhB$(OH)_2$ and 50 equiv. [**L2**]$_2$Pd$(OAc)_2$.

We also investigated some electronically-challenging heterocyclic substrates on SMC reactions. Thienylboronic acids showed the best conversion of the coupling products shown in Figure **4.11**. A partial formation of C-C bond forming products was found by LC-MS upon treatment of the UBQ with furanylboronic acid. In case of *N*-heterocyclic boronic acids, there was no product formation observed by LC-MS, possibly due to their poor aqueous solubility or lowered reactivity.

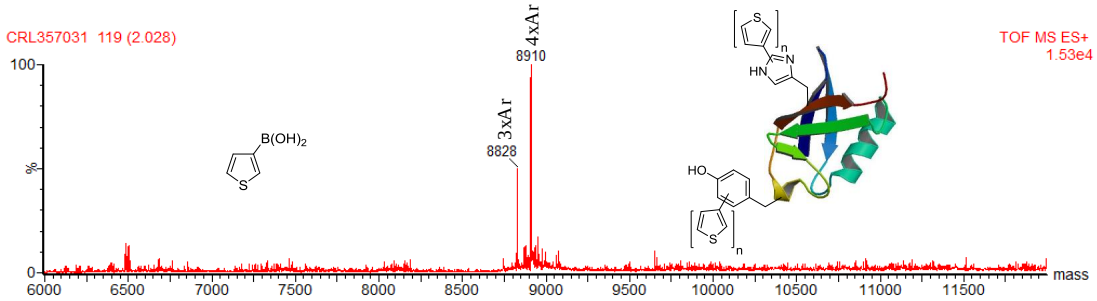

Figure 4.11 ESI-MS spectrum of the iodo-Tyr/His ubiquitin treated with 500 equiv. 3-thienylB(OH)$_2$ and 50 equiv. [**L2**]$_2$Pd(OAc)$_2$.

Apart from aromatic systems, Pd cross-coupling of the iodo-Tyr/His ubiquitin with alkenylboronic acids was demonstrated, but the reactivity was less good as compared to aromatic C(sp^2)-C(sp^2) systems. A mixture of 3-phenylpropene C-C coupling products was partially observed by LC-MS (Figure **4.12**), but the reaction failed when treating with a glucose-derived coupling partner.

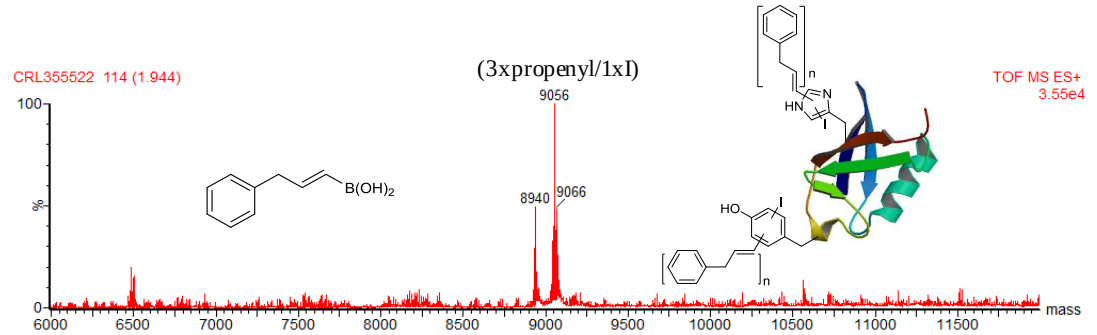

Figure 4.12 ESI-MS spectrum of the iodo-Tyr/His ubiquitin treated with 500 equiv. 3-phenylpropenylB(OH)$_2$ and 50 equiv. [**L2**]$_2$Pd(OAc)$_2$.

To extend this Pd-mediated system to the fluorescent labelling of proteins, the iodo-Tyr/His UBQ was coupled to various fluorescent boronic acids. Only two fluorophores, coumarinyl boronic acid pinacol ester and cyclictriolborate, were successful in SMC

coupling reactions of the UBQ (Figure **4.13**). Others, including coumarinyl trifluoroborate, and dansyl dye derivatives, caused protein degradation.

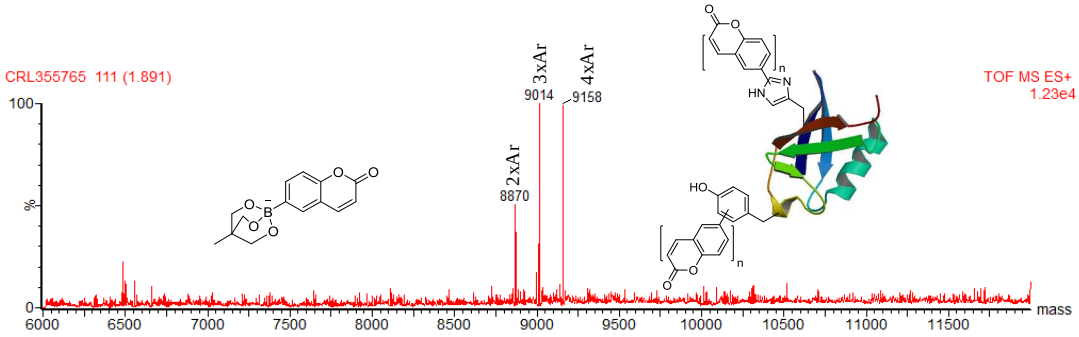

Figure 4.13 ESI-MS spectrum of the iodo-Tyr/His ubiquitin treated with 500 equiv. potassium coumarinyl cyclictriolborate and 50 equiv. [**L2**]$_2$Pd(OAc)$_2$.

4.3.2 Sonogashira Cross-Coupling Reactions

Our aqueous Pd-mediated system showed many successful examples of SMC reactions of the iodo-Tyr/His UBQ with various aromatic boronic acids. We then applied this system to another type of Pd-mediated reaction, the Sonogashira cross-coupling. To investigate Sonogashira cross-coupling reactions, the iodo-Tyr/His UBQ was treated with 1-propargyl-β-D-glucopyranose (propynyl-*O*-glucose) in the presence of the [**L2**]$_2$Pd(OAc)$_2$ catalyst. After 4 h at 37 °C, coupling products and unreactive iodinated ubiquitin were detected by LC-MS as shown in Table **4.1**. An increase in amounts of both propynyl-*O*-glucose (750-1000 equiv.) and [**L2**]$_2$Pd(OAc)$_2$ catalyst (75-100 equiv.) showed a better conversion to cross-coupled ubiquitin as compared to lesser amounts of alkyne and [**L2**]$_2$Pd(OAc)$_2$ catalyst, however, the ESI-MS signal resolution was poor. The iodo-Tyr/His ubiquitin was treated with 500 equiv. propynyl-*O*-glucose and 50 equiv. [**L2**]$_2$Pd(OAc)$_2$ catalyst, giving optimal conversion to C-C coupling product (Figure **4.14**).

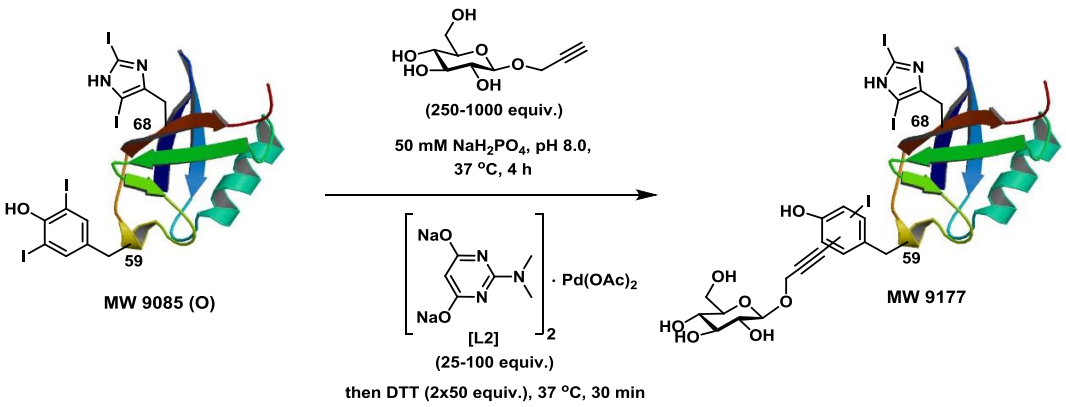

Entry	Iodo-UBQ (equiv.)	Propynyl-*O*-glucose (equiv.)	$[L2]_2Pd(OAc)_2$ (equiv.)	Products conversion (%)
1	1	250	25	9084 Da (4xI+O) (70) 9175 Da (3xI+O+glu-alkyne) (30)
2	1	500	50	9084 Da (4xI+O) (70) 9176 Da (3xI+O+glu-alkyne) (30)
3	1	750	75	9084 Da (4xI+O) (59) 9175 Da (3xI+O+glu-alkyne) (41)
4	1	1000	100	9084 Da (4xI+O) (62) 9176 Da (3xI+O+glu-alkyne) (38)

*The reaction mixture was treated with DTT (3 x Pd equiv.) for 30 min prior to mass analysis.
O = Met (oxidation) / ESI-MS baseline subtracted.

Table 4.1 Investigation of Sonogashira cross-couplings of the iodo-Tyr/His ubiquitin with various amounts of 1-propargyl-β-D-glucopyranose and $[\mathbf{L2}]_2Pd(OAc)_2$.

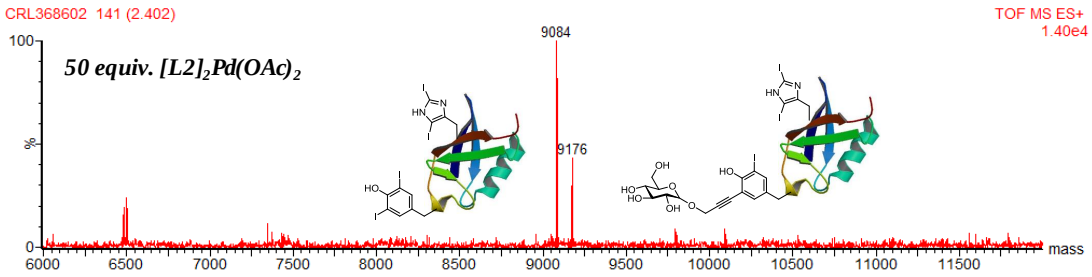

Figure 4.14 ESI-MS spectrum of the iodo-Tyr/His ubiquitin treated with 500 equiv. 1-propargyl-β-D-glucopyranose and 50 equiv. $[\mathbf{L2}]_2Pd(OAc)_2$.

Initially, DTT was used as a Pd scavenger, but we observed protein cleavage of ubiquitin (MW = 6.5 kDa) by LC-MS analysis. We thus sought a mild alternative Pd scavenger which would minimise undesired protein cleavage. QuadraSil™ MP (thiol) and AP

(amine) as a metal scavenger (functionalised silica gel) could potentially remove Pd metal from the protein without protein cleavage (Figure **4.15**). Both QuadraSil™ are useful in removal of Pd metal from the protein reaction prior to LC-MS analysis.

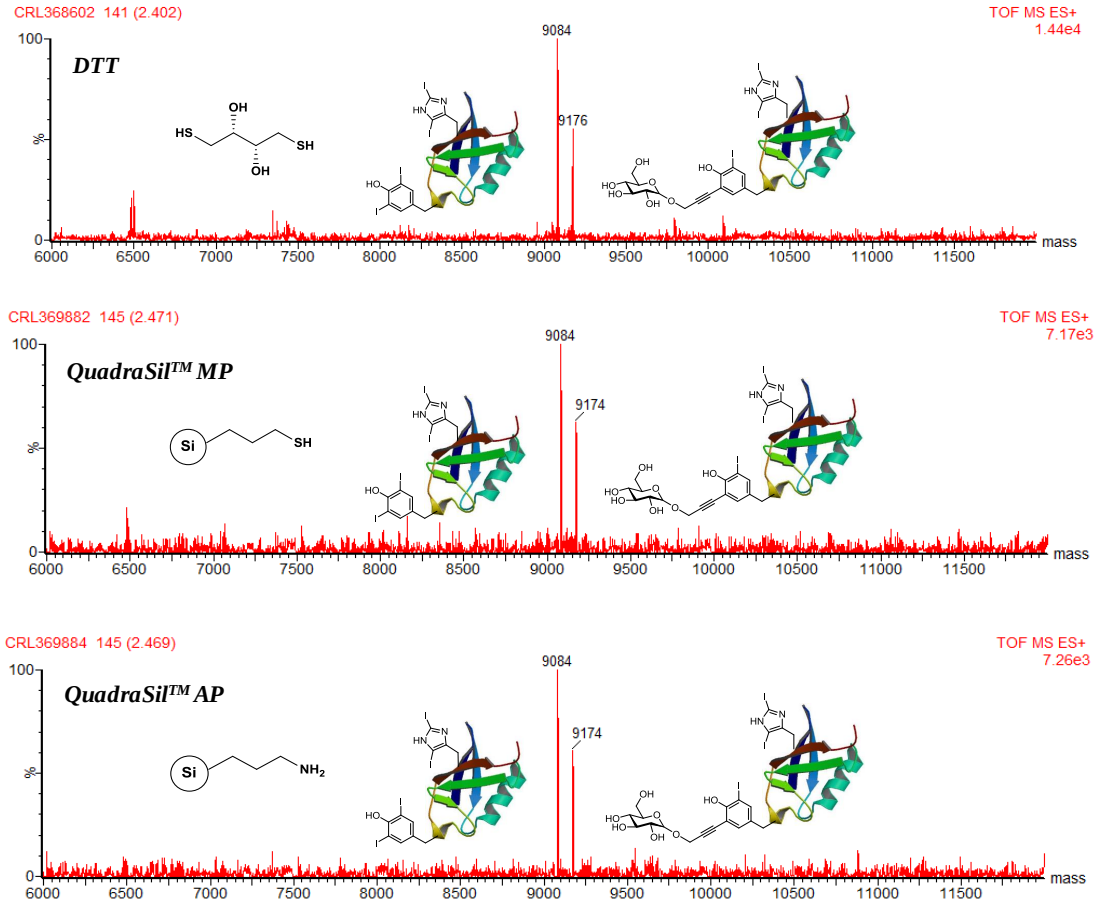

Figure 4.15 A comparative study of an efficiency of Pd scavengers for Sonogashira reactions.

4.4 Palladium-Mediated Ubiquitination

To extend the capabilities of this protein Pd-mediated cross-coupling reaction, a methionine of wild-type ubiquitin was biosynthetically transformed into a homopropargylglycine (L-Hpg) at the *N*-terminus by use of a Met-auxotroph. Subsequently, ubiquitination between Hpg-tagged ubiquitin and iodinated proteins of interest was initially investigated through Sonogashira reaction (Scheme **4.10**). This

system would be useful for *in vitro* protein degradation by Pd-mediated ubiquitination of the protein of interest.

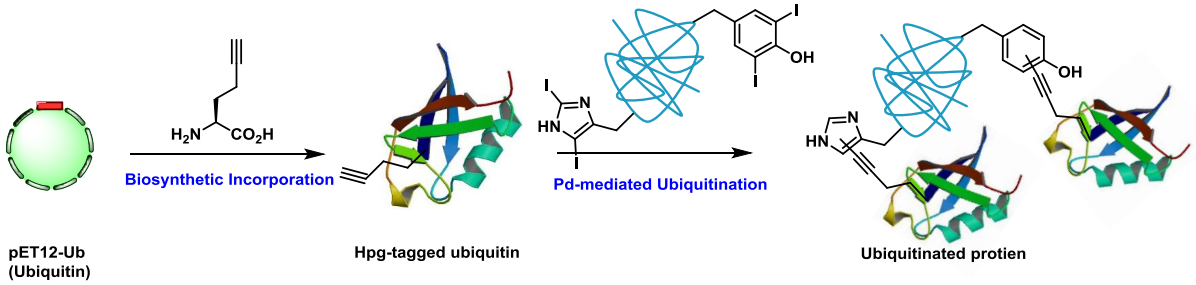

Scheme 4.10 Proposed pathway of chemical ubiquitnation through Pd-mediated reaction.

Biosynthetic incorporation of L-Hpg into the ubiquitin was achieved by use of Met-auxotroph (B834 (DE3)), resulting in an installation of an *N*-terminal alkyne tag of the UBQ. Unfortunately, there was not full incorporation of Hpg into ubiquitin, with 80% of the desired analogue observed by LC-MS analysis (Figure **4.16**). However, we deemed this enough to begin model studies since the Met-containing side-product should not be capable of cross-coupling.

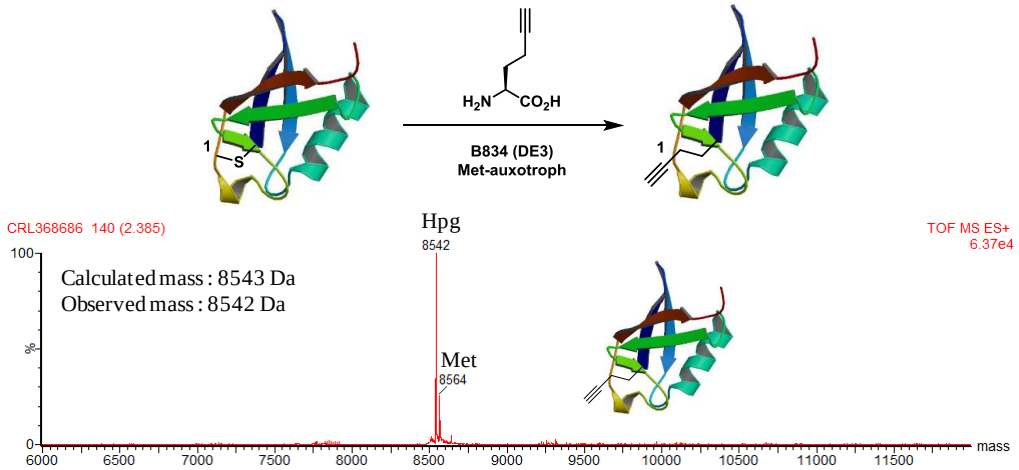

Figure 4.16 ESI-MS spectrum of the alkyne-incorporated ubiquitin using Met-auxotroph, B834 (DE3).

As a starting point for chemical ubiquitination, we reasoned that proteins containing a genetically encoded *p*-iodoPhe residue could represent good model systems for Pd cross-coupling reactions to this modified ubiquitin. IodoPhe-tagged glycogenin-1 (GYG) was initially tested with the ubiquitin containing the alkyne tag, unfortunately the cross-coupled proteins were not observed by either LC-MS or SDS-PAGE analysis. This may cause from an inaccessibility of the *p*-iodoPhe residue of the GYG protein (Figure **4.17**).

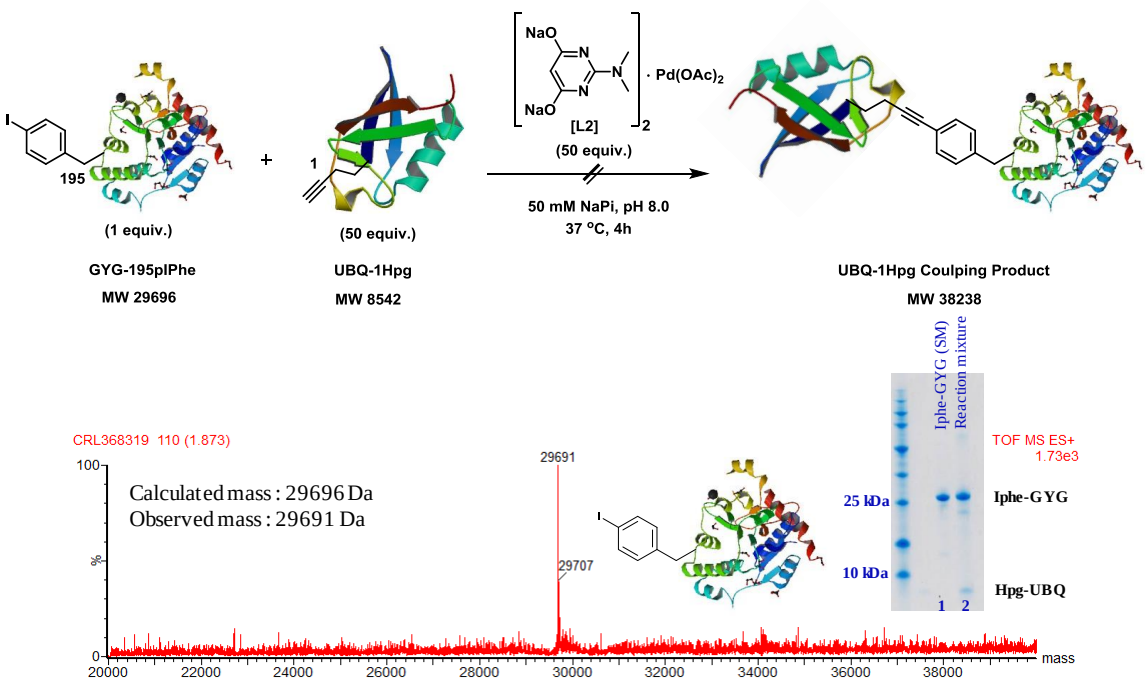

Figure 4.17 An attempted Sonogashira cross-coupling reaction of the *p*-iodoPhe GYG with Hpg-tagged ubiquitin.

Alternatively, genetically encoded *p*-iodoPhe maltose-binding protein (MBP) (6xHis-tag) was treated with an excess of the Hpg-tagged ubiquitin in the presence of the [**L2**]$_2$Pd(OAc)$_2$ catalyst, but no formation of cross-coupled proteins was observed by LC-MS, SDS-PAGE, and Western blot (using anti-polyhistidines antibody) (Figure **4.18**).

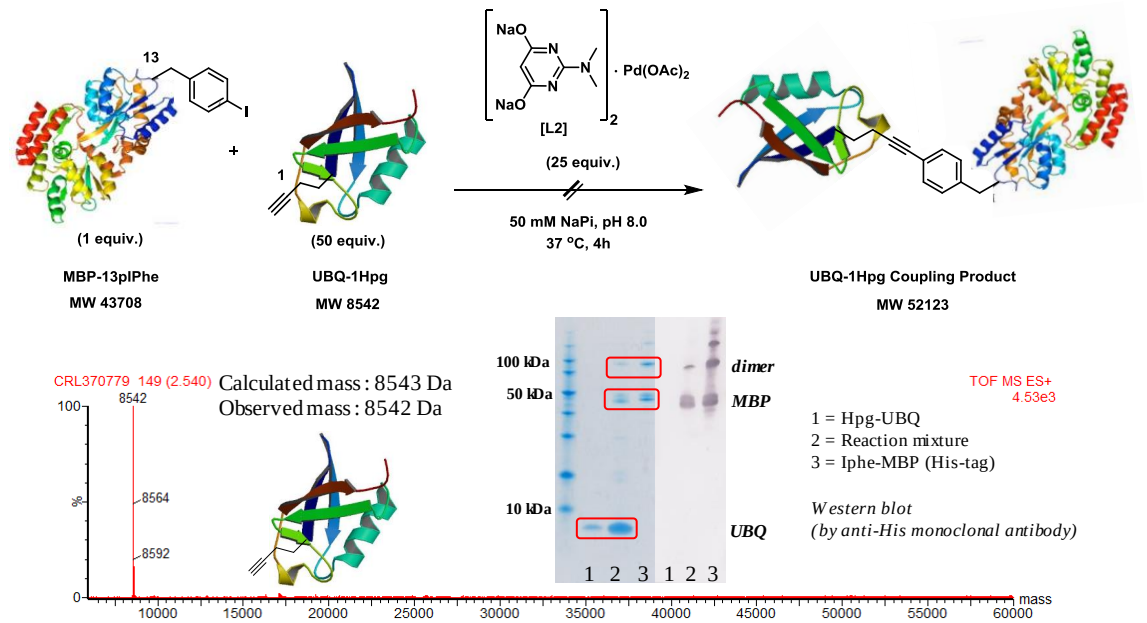

Figure 4.18 An attempted Sonogashira cross-coupling reaction of the *p*-iodoPhe MBP with Hpg-tagged ubiquitin.

Unfortunately, Pd-mediated ubiquitination was unsuccessful through Sonogashira cross-coupling reactions of the Hpg-UBQ with some model proteins bearing a *p*-iodoPhe residue. However, we further investigated the Pd cross-couplings between iodo-Tyr/His and Hpg-tagged UBQ. Treatment of the iodo-Tyr/His ubiquitin with the excess Hpg-tagged ubiquitin was performed at 37 °C for 4h in the presence of the $[\mathbf{L2}]_2Pd(OAc)_2$ catalyst (Table **4.2**). Unfortunately, no formation of cross-coupled ubiquitin species was observed by either LC-MS or SDS-PAGE (Figure **4.19** and **4.20**). On the other hand, the iodo-Tyr/His ubiquitin could undergo cross-coupling to propynyl-*O*-glucose under the same conditions used in the protein reactions shown in Figure **4.21**. The failure of these attempted Pd-mediated reactions may be due to an inaccessibility of the *N*-terminal alkyne tag of the ubiquitin. This may be further investigated by site-directed mutagenesis to install Met at a more accessible position on the protien surface, enabling its subsequent replacement with the Hpg alkyne tag at this position. The improved accessibility may improve the Pd-mediated reaction, leading to ubiquitination.

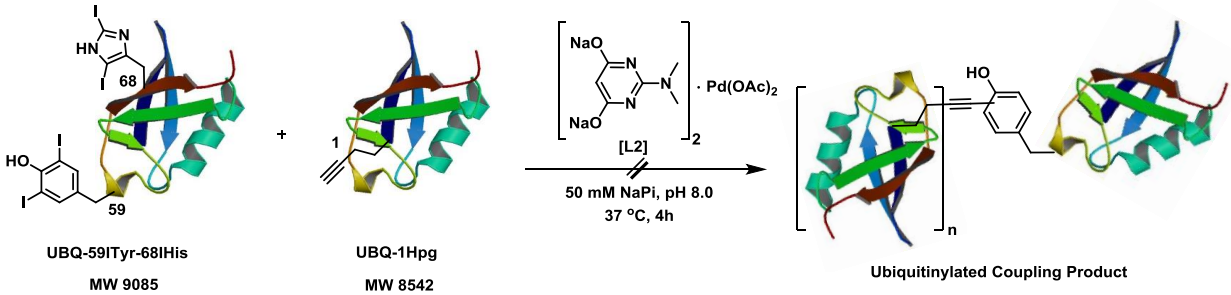

Entry	Iodo-UBQ (equiv.)	Hpg-UBQ (equiv.)	$[L2]_2Pd(OAc)_2$ (equiv.)	Reaction conditions	Results (LC-MS)
1	1	50	5	37 °C, 4 h	Unreactive Hpg-tagged Ubiquitin was only observed. (8543 Da)
2	1	50	10		
3	1	100	10		
4	1	100	20		
5	1	200	20		
6	50	1	5		

General conditions : Iodo-Tyr/His UBQ in NaH_2PO_4 (50 mM, pH 8), Hpg-UBQ in NaH_2PO_4 (50 mM, pH 8), $[\mathbf{L2}]_2Pd(OAc)_2$ in 0.1 M NaOH (c = 0.01 M) at 37 °C for 4h, unless otherwise indicated.

Table 4.2 Attempted Sonogashira cross-couplings of the iodo-Tyr/His ubiquitin and Hpg tagged ubiquitin.

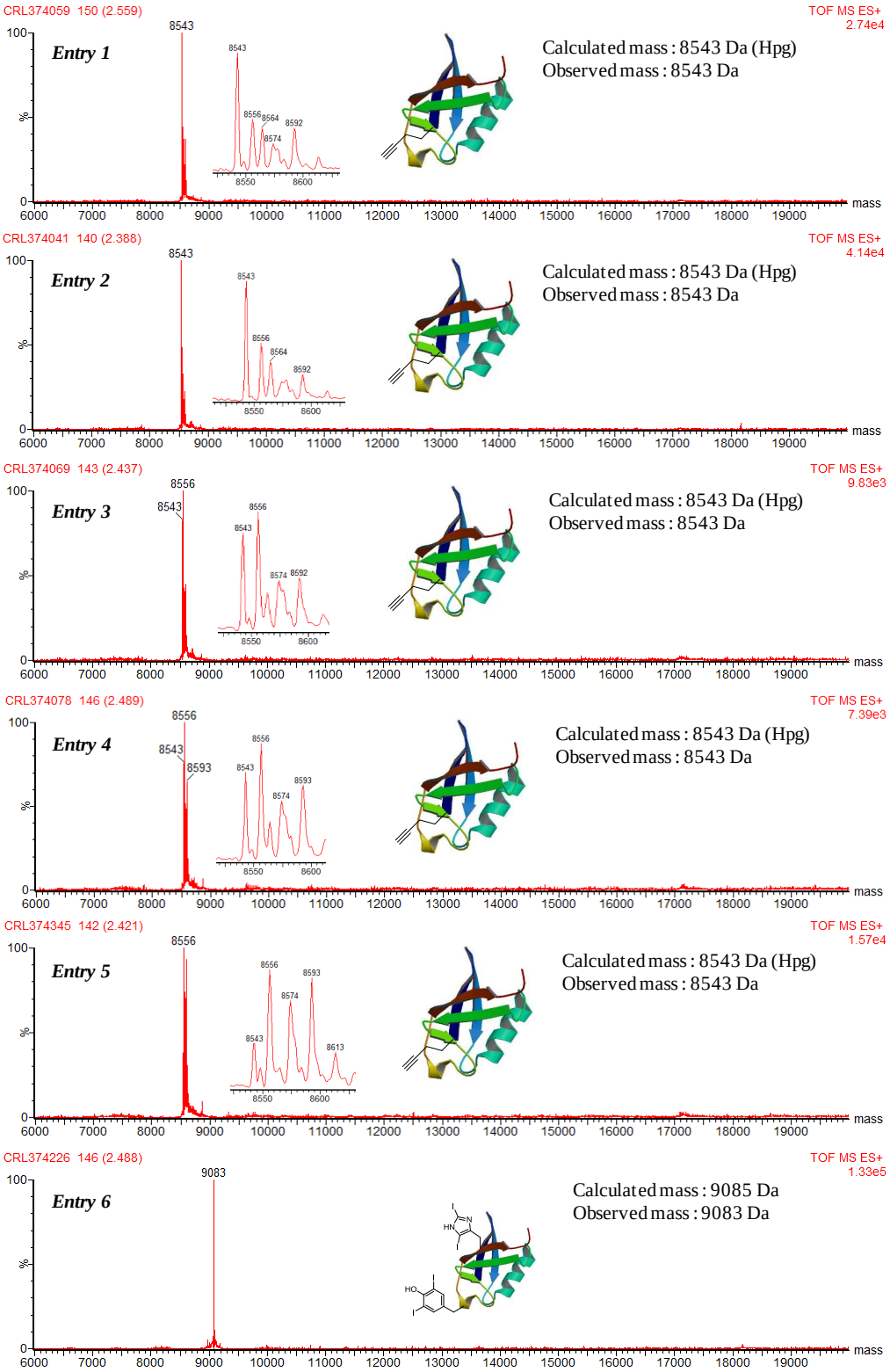

Figure 4.19 ESI-MS spectra of the iodo-Tyr/His ubiquitin (1 equiv.) with Hpg-tagged ubiquitin (50-200 equiv.) in the presence of $[\mathbf{L2}]_2Pd(OAc)_2$.catalyst (5-20 equiv.) [Entry 1-5], and the iodo-Tyr/His ubiquitin (50 equiv.) with Hpg-tagged ubiquitin (1 equiv.) in the presence of $[\mathbf{L2}]_2Pd(OAc)_2$.catalyst (5equiv.) [Entry 6].

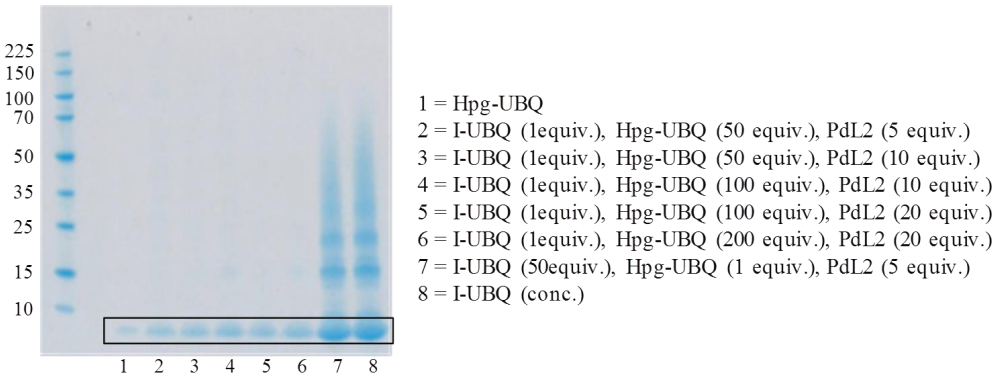

Figure 4.20 SDS-PAGE shows Hpg-tagged ubiquitin bands from each reaction mixture (Lane 2-6), on the other hand, the iodo-Tyr/His ubiquitin bands from the reaction mixture (Lane 7).

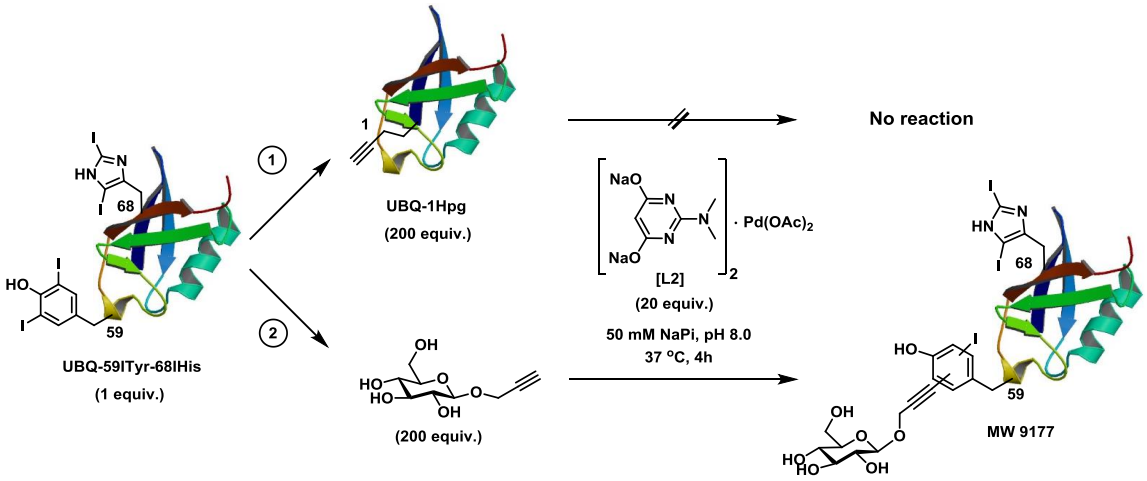

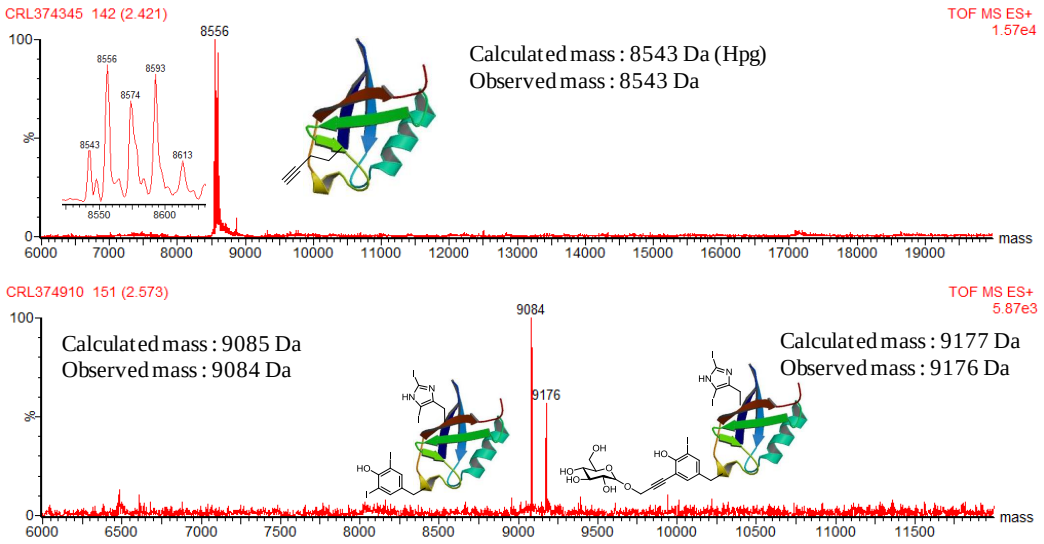

Figure 4.21 A comparative study of Pd-mediated Suzuki reactions between (1) iodo-Tyr/His UBQ + Hpg-tagged UBQ and (2) iodo-Tyr/His UBQ + propynyl-*O*-glucose.

4.5 Conclusion

Three model proteins including insulin, MCP-1, and UBQ were used for a study of protein iodination reactions by use of Barluenga's reagent (IPy_2BF_4) (Scheme **4.11**). Based on MSMS results, we found that naturally occurring tyrosine and histidine residues in model proteins reacted with this iodinating agent, resulting in the creation of new C-I bonds at specific modification sites. The IPy_2BF_4 is a good chemical tool for residue-specific iodination reactions of the protein of interest.

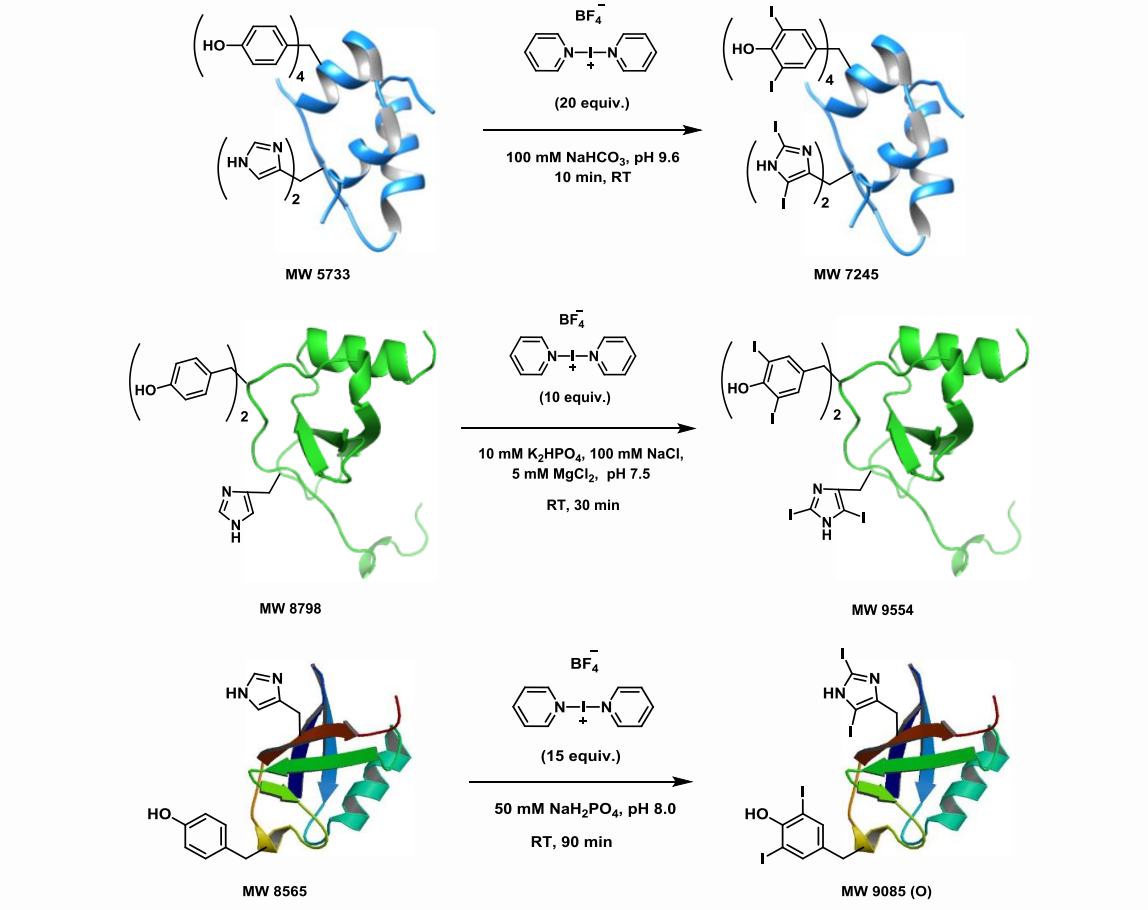

Scheme 4.11 Chemical approach for direct C-I bonds formation onto model proteins by use of IPy_2BF_4.

We decided to use the UBQ as a model study for aqueous Suzuki-Miyaura cross-coupling reactions, due to their presence of each single tyrosine and histidine residues. Treatment of the iodo-Tyr/His ubiquitin with various phenylboronic acid derivatives in the presence of the $[\mathbf{L2}]_2Pd(OAc)_2$ catalyst enabled C-C bond formation to an extensive

range of substrates (Scheme **4.12**). Our Pd cross-coupling system is useful for site-specific bioconjugation, including fluorescent labelling, at novel and challenging tyrosine/histidine residues of the UBQ. This soluble [**L2**]$_2$Pd(OAc)$_2$ catalyst is air-insensitive, soluble, and efficient for Suzuki reactions in aqueous systems.

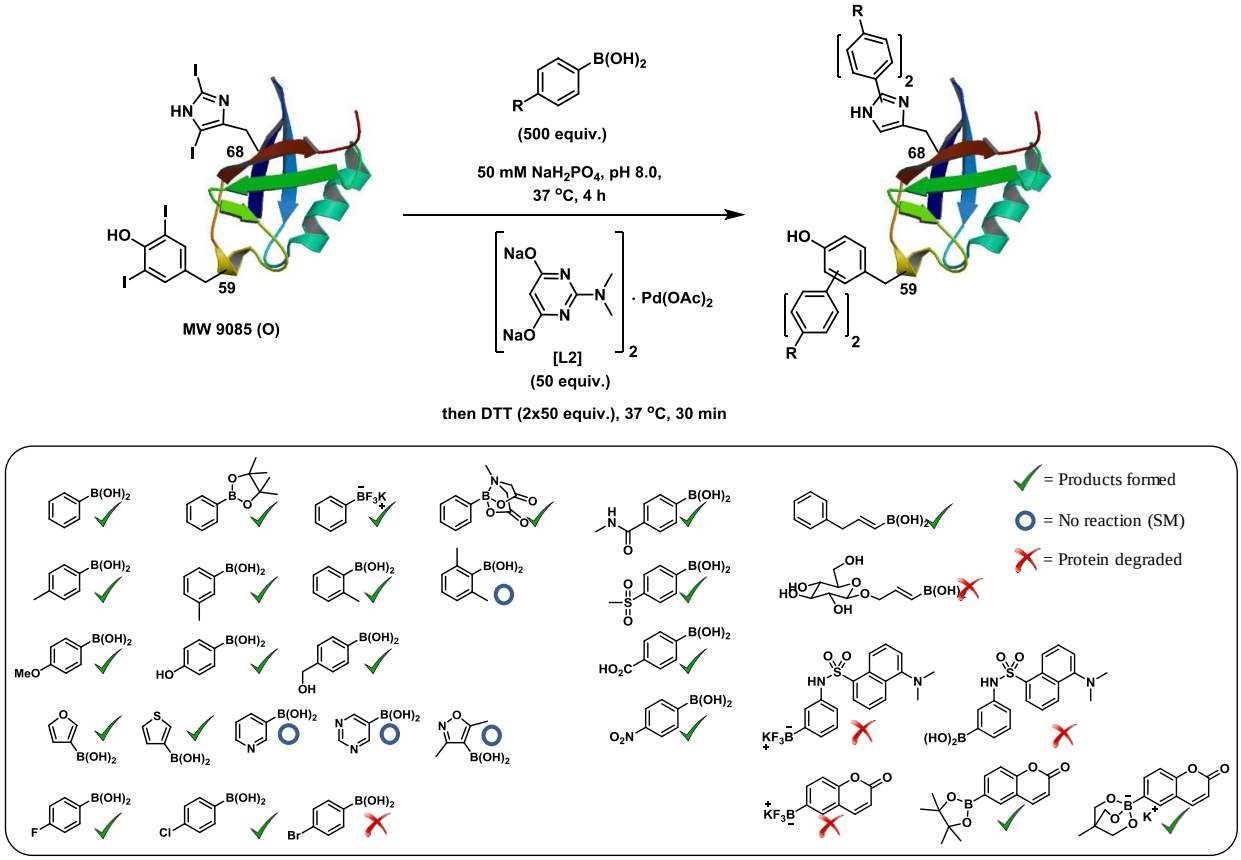

Scheme 4.12 Aqueous Suzuki-Miyaura cross-coupling reactions of the iodo-Tyr/His ubiquitin with a broad range of aromatic boronic acid derivatives.

We are now investigating chemical ubiquitination through Sonogashira/Suzuki cross-coupling reactions. A biosynthetic replacement of the Met of the ubiquitin with L-Hpg was achieved by use of Met-auxotroph (B834 (DE3)). Cross-coupling of this modified UBQ (with the terminal alkyne tag) to iodinated proteins was attempted. Unfortunately, cross-coupled proteins were not detected by either protein mass spectrometry or SDS-PAGE analysis; this may arise from many factors including steric effect or moderate efficiency of [**L2**]$_2$Pd(OAc)$_2$ catalyst through Sonogashira reactions.

4.6 Experimental Details

4.6.1 Protein Iodination

Iodination of Insulin

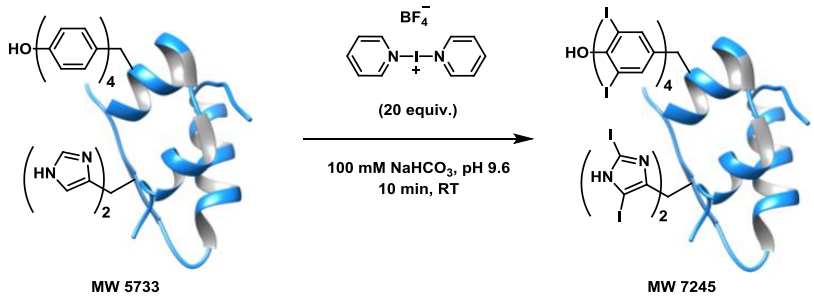

An aliquot of the bovine insulin (26.1 nmol, 1.0 mg/mL, 150 µL) in 100 mM $NaHCO_3$, pH 9.6 was mixed with a solution of IPy_2BF_4 in DMF (522 nmol, 3.9 µL from stock solution, conc. 50.0 mg/mL) by vortexing briefly. After 10 min of shaking at RT, an aliquot was analysed by LC–MS after desalting by PD SpinTrap G-25 column pre-equilibrated with 100 mM $NaHCO_3$, pH 9.6. A protein sample was flash frozen with liquid nitrogen and stored at –20 ºC.

Entry	Insulin (equiv.)	IPy_2BF_4 (equiv.)	Time (min)	Products (Da)
1	1	20	10	6741 (8xI), 6867 (9xI), 6993 (10xI), 7118 (11xI), 7244 (12xI)

General conditions : Insulin in $NaHCO_3$ (100 mM, pH 9.6), IPy_2BF_4 in DMF (c = 50 mg/mL), at 25 °C for 10 min.

Table 4.3 Tyrosine iodination of the insulin using IPy_2BF_4.

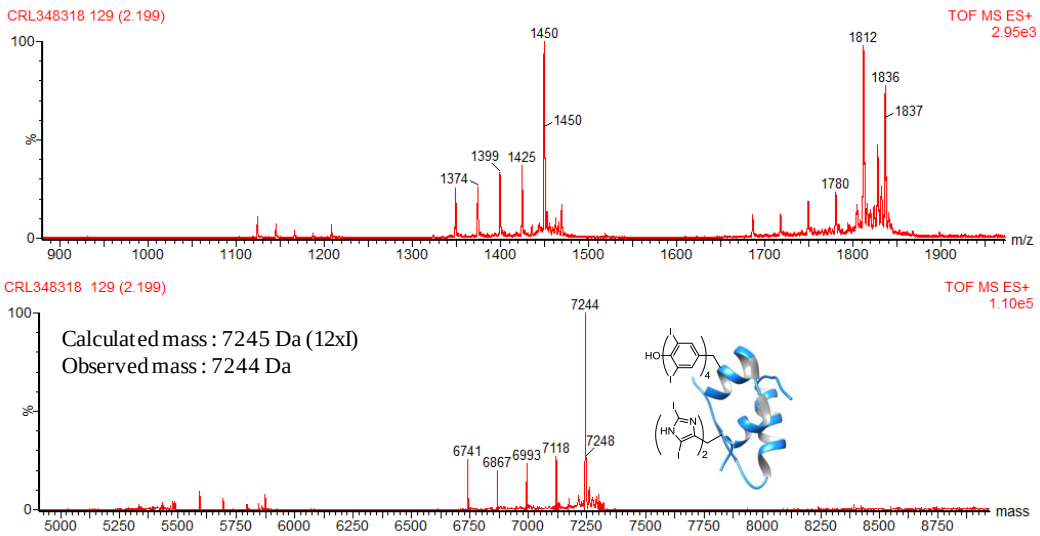

Figure 4.22 ESI-MS spectrum of the insulin treated with 20 equiv. IPy_2BF_4 (10 min).

Iodination of MCP-1

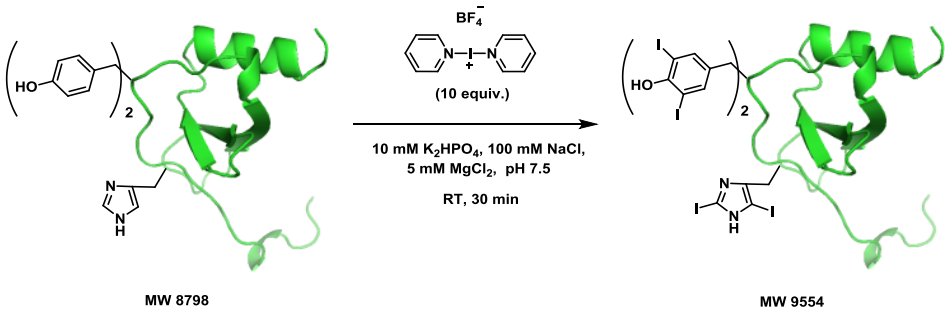

An aliquot of the MCP-1 (5.68 nmol, 1.0 mg/mL, 50 µL) in 10 mM K_2HPO_4, 100 mM NaCl, 5 mM $MgCl_2$, pH 7.5 was mixed with a solution of IPy_2BF_4 in DMF (56.8 nmol, 2.1 µL from stock solution, conc. 10.0 mg/mL) by vortexing briefly. After 30 min of shaking at RT, an aliquot was analysed by LC–MS after desalting by a vivaspin column concentrator with a 3,000 Da MW cut-off membrane (6x times) loading the sample and fresh 10 mM K_2HPO_4, 100 mM NaCl, 5 mM $MgCl_2$, pH 7.5 each time. A protein sample was flash frozen with liquid nitrogen and stored at –20 ºC.

Entry	MCP-1 (equiv.)	IPy_2BF_4 (equiv.)	Time (min)	Products (Da)
1	1	10	30	9425 (5xI), 9551 (6xI)

General conditions : MCP-1 in K_2HPO_4, NaCl, $MgCl_2$ (10 mM, 100 mM, 5 mM, pH 7.5), IPy_2BF_4 in DMF (c = 10 mg/mL), at 25 °C for 30 min.

Table 4.4 Tyrosine iodination of the MCP-1 using IPy_2BF_4.

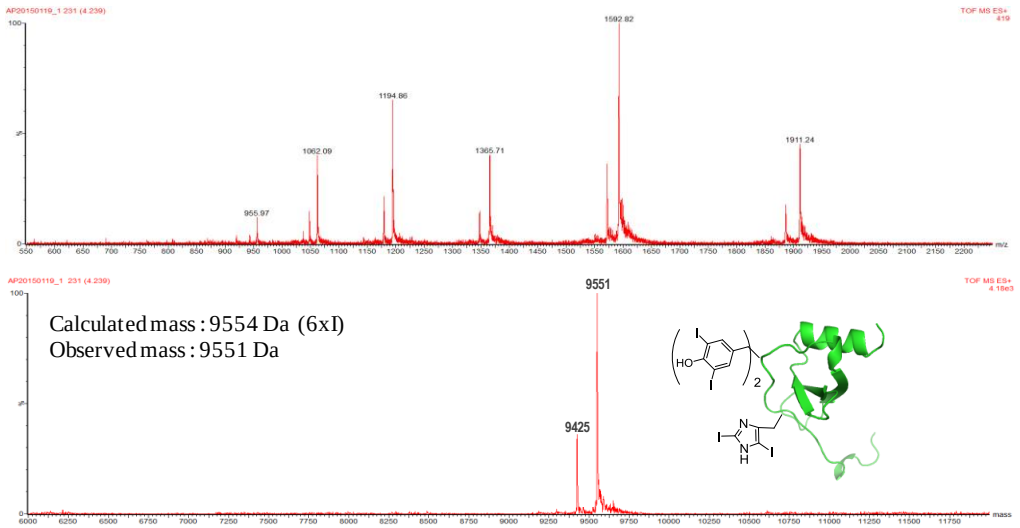

Figure 4.23 ESI-MS spectrum of the MCP-1 treated with 10 equiv. IPy_2BF_4 (30 min).

Iodination of UBQ

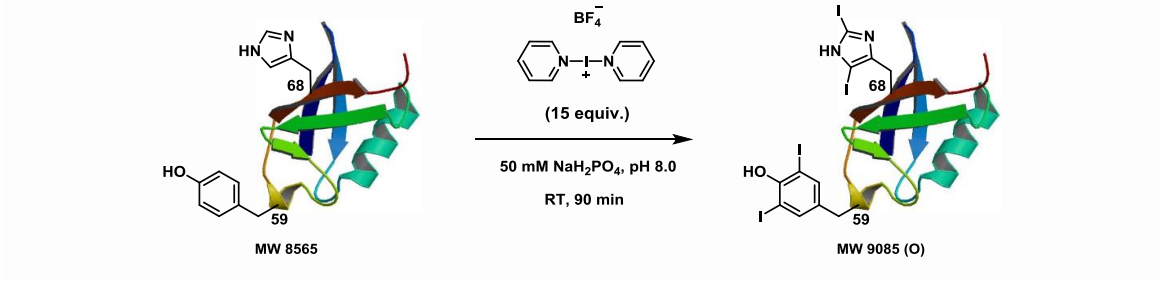

An aliquot of the UBQ (27.2 nmol, 2.33 mg/mL, 100 µL) in 50 mM NaH_2PO_4, pH 8.0 was mixed with a solution of IPy_2BF_4 in DMF (190 nmol, 7.1 µL from stock solution, conc. 10.0 mg/mL) by vortexing briefly. After 90 min of shaking at RT, an aliquot was analysed by LC–MS after desalting by PD SpinTrap G-25 column pre-equilibrated with 50 mM NaH_2PO_4, pH 8.0. A protein sample was flash frozen with liquid nitrogen and stored at –20 ºC.

Entry	UBQ (equiv.)	IPy_2BF_4 (equiv.)	Time (min)	Products (Da)
1	1	15	90	9084 (4xI+O)
General conditions : UBQ in NaH_2PO_4 (50 mM, pH 8.0), IPy_2BF_4 in DMF (c = 10 mg/mL), at 25 °C for 90 min. O = Oxidised methionine				

Table 4.5 Tyrosine iodination of the UBQ using IPy_2BF_4.

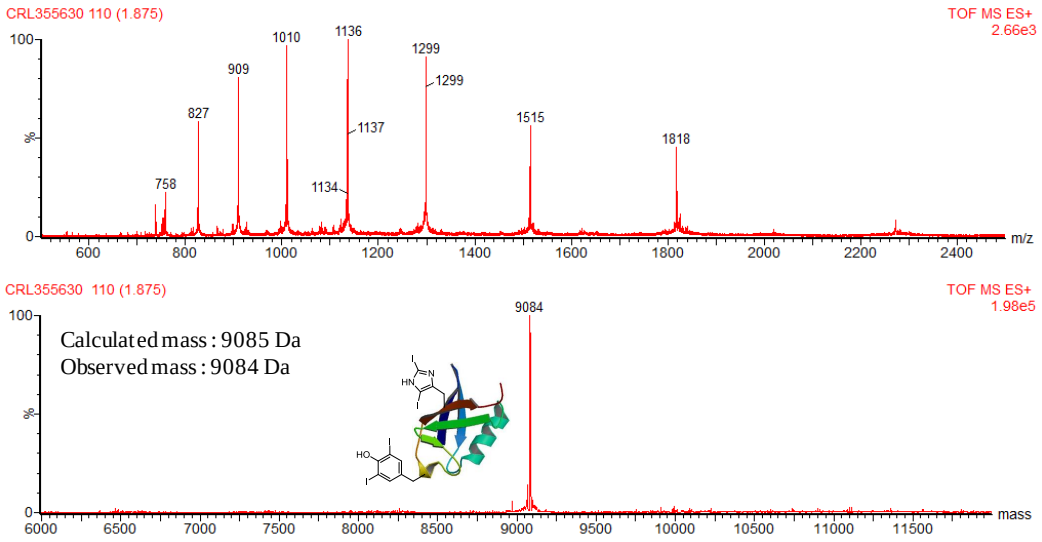

Figure 4.24 ESI-MS spectrum of the ubiquitin treated with 15 equiv. IPy_2BF_4 (90 min).

4.6.2 Aqueous Suzuki-Miyaura Cross-Coupling Reactions

Effects of ligands (L1-L4) of Pd catalysts

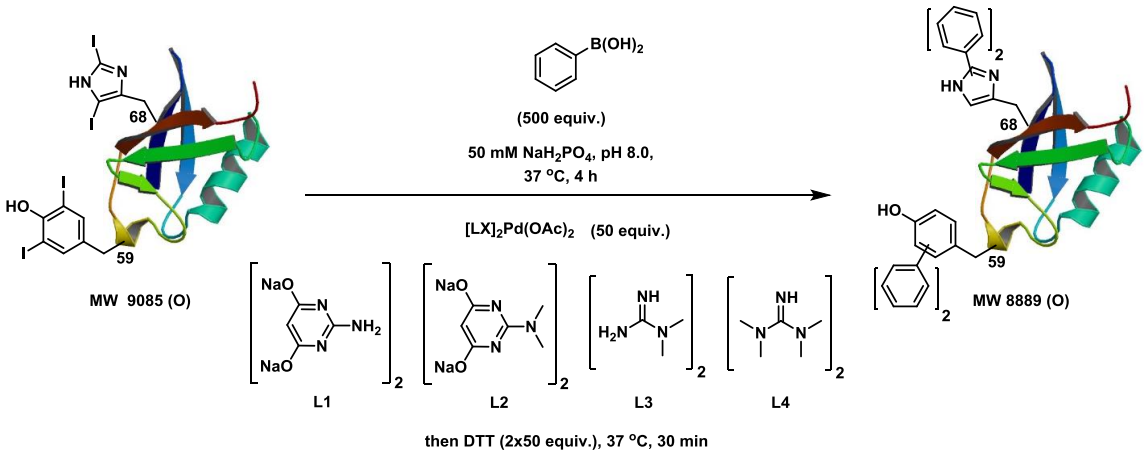

Each aliquot of the iodo-Try/His UBQ (3.3 nmol, 1.50 mg/mL, 20 µL) in 50 mM NaH_2PO_4, pH 8.0 was mixed with a solution of $PhB(OH)_2$ in a ratio of 1:3 DMF/50 mM NaH_2PO_4 mixture (1,650 nmol, 4 µL from stock solution, conc. 50.0 mg/mL) by vortexing briefly. Each [**LX**]$_2$Pd(OAc)$_2$ catalyst solution (165 nmol, 16.5 µL, conc. 0.01 M) was added to each reaction mixture which was vortexed briefly. After 4 h. of shaking at 37°C, each aliquot was analysed by LC–MS after addition of DTT solution in H_2O (2xtimes) (165 nmol, 1.25 µL, from stock solution, conc. 20.0 mg/mL) and stirring at 37 °C for 30 min. Protein samples were flash frozen with liquid nitrogen and stored at –20 °C.

Entry	Iodo-UBQ (equiv.)	$PhB(OH)_2$ (equiv.)	$[LX]_2Pd(OAc)_2$ (equiv.)	Time (h)	Products (Da)
1	1	500	-	1	9085 (4xI+O)
2	1	-	50 **[L1]**	1	9085 (4xI+O)
3	1	500	50 **[L1]**	4	8658 Da (1xPh+O), 8734 Da (2xPh+O), 8810 Da (3xPh+O), 8783 Da (1xI+1xPh+O), 8860 Da (1xI+2xPh+O), 8909 Da (2xI+1xPh+O), 8959 Da (3xI+O)
4	1	500	50 **[L2]**	4	8734 Da (2xPh+O), 8810 Da (3xPh+O), 8886 Da (4xPh+O)
5	1	500	50 **[L3]**	4	8658 Da (1xPh+O), 8734 Da (2xPh+O), 8810 Da (3xPh+O), 8886 Da (4xPh+O), 8784 Da (1xI+1xPh+O), 8860 Da (1xI+2xPh+O), 8908 Da (2xI+1xPh+O),
6	1	500	50 **[L4]**	4	8658 Da (1xPh+O), 8734 Da (2xPh+O), 8810 Da (3xPh+O), 8886 Da (4xPh+O)

General conditions: iodo-Tyr/His UBQ in NaH_2PO_4 (50 mM, pH 8), $PhB(OH)_2$ in 1:3 DMF/NaH_2PO_4 and 0.01 M $[\mathbf{LX}]_2Pd(OAc)_2$ in NaOH at 37 ^oC for 4 h, unless otherwise indicated. O = Oxidised methionine

Table 4.6 Investigation of Suzuki-Miyaura cross-couplings of the iodo-Tyr/His ubiquitin with $PhB(OH)_2$ using palladium $[\mathbf{LX}]_2Pd(OAc)_2$ catalysts.

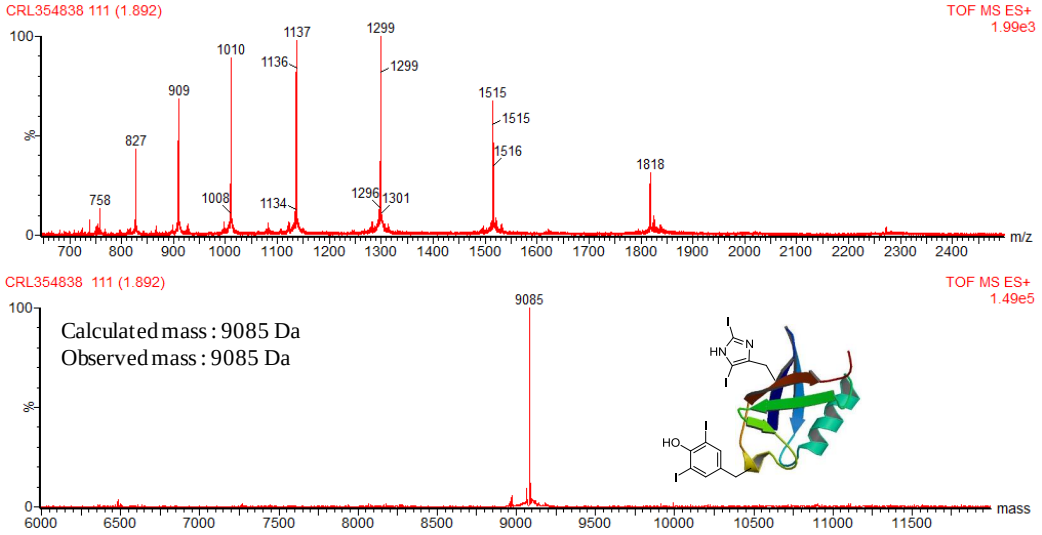

Figure 4.25 ESI-MS spectrum of the iodo-Tyr/His ubiquitin treated with 500 equiv. $PhB(OH)_2$ (control).

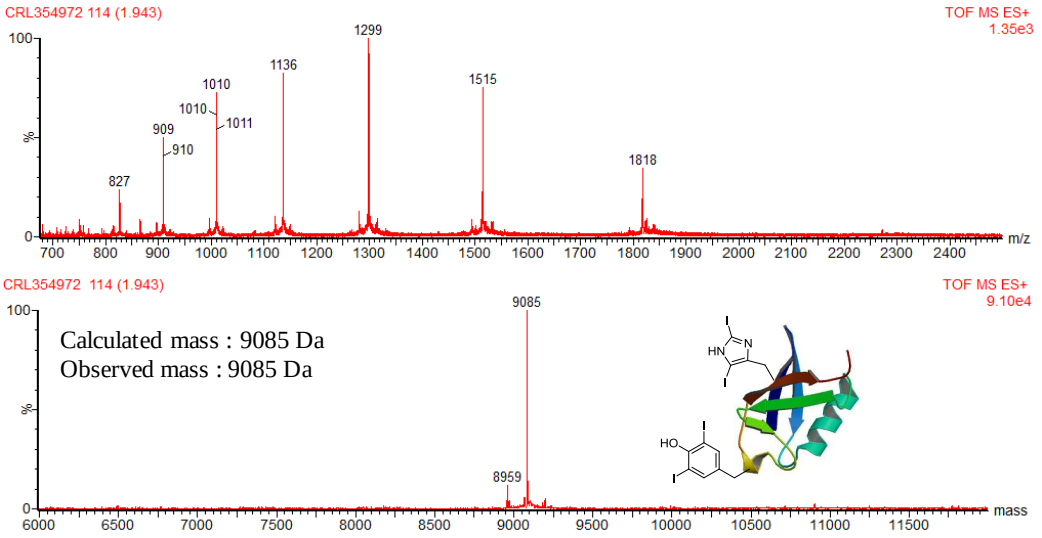

Figure 4.26 ESI-MS spectrum of the iodo-Tyr/His ubiquitin treated with 50 equiv. $[\mathbf{L1}]_2Pd(OAc)_2$ (control).

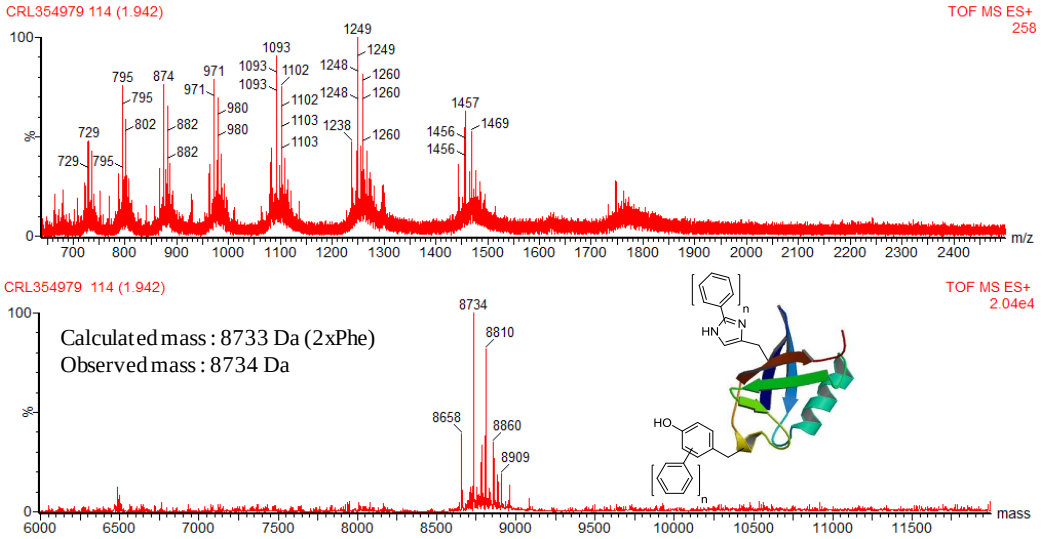

Figure 4.27 ESI-MS spectrum of the iodo-Tyr/His ubiquitin treated with 50 equiv. $[\mathbf{L1}]_2Pd(OAc)_2$ and 500 equiv. $PhB(OH)_2$.

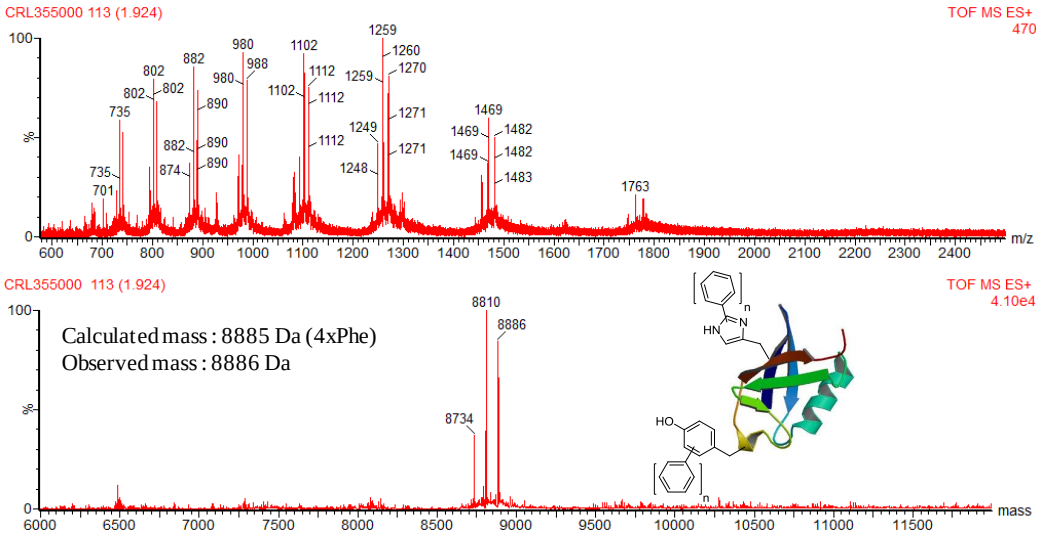

Figure 4.28 ESI-MS spectrum of the iodo-Tyr/His ubiquitin treated with 50 equiv. $[\mathbf{L2}]_2Pd(OAc)_2$ and 500 equiv. $PhB(OH)_2$.

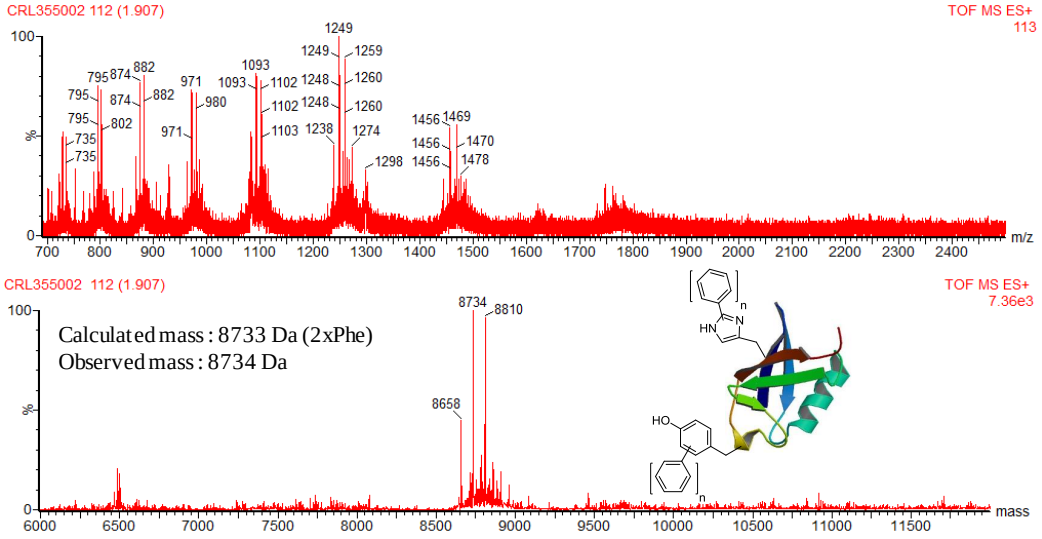

Figure 4.29 ESI-MS spectrum of the iodo-Tyr/His ubiquitin treated with 50 equiv. [**L3**]$_2$Pd(OAc)$_2$ and 500 equiv. PhB(OH)$_2$.

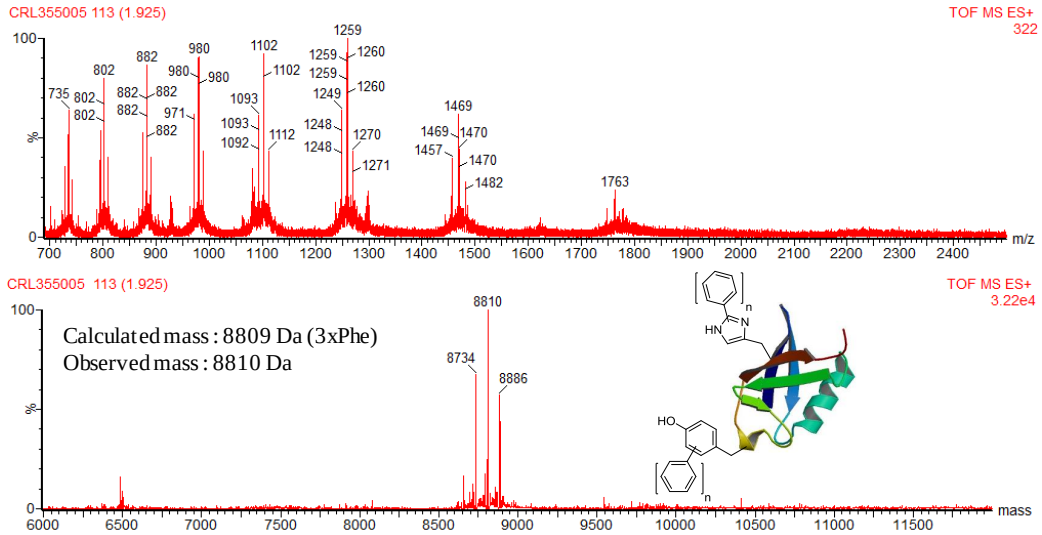

Figure 4.30 ESI-MS spectrum of the iodo-Tyr/His ubiquitin treated with 50 equiv. [**L4**]$_2$Pd(OAc)$_2$ and 500 equiv. PhB(OH)$_2$.

Effect of amounts of phenylboronic acid

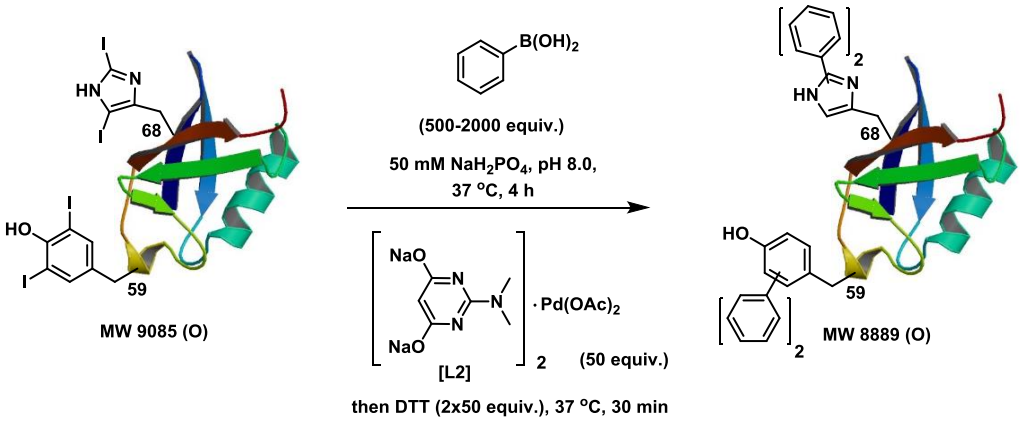

Each aliquot of the iodo-Try/His UBQ (3.3 nmol, 1.50 mg/mL, 20 µL) in 50 mM NaH_2PO_4, pH 8.0 was mixed with a solution of $PhB(OH)_2$ in a ratio of 1:3 DMF/50 mM NaH_2PO_4 mixture (1,650 nmol (500 equiv.), 4 µL from stock solution, conc. 50.0 mg/mL, 3,300 nmol (1,000 equiv.) 2 µL and 6,600 nmol (2,000 equiv.) 4 µL from stock solution, conc. 200.0 mg/mL) by vortexing briefly. A [**L2**]$_2$Pd(OAc)$_2$ catalyst solution (165 nmol, 16.5 µL, conc. 0.01 M) was added to each reaction mixture which was vortexed briefly. After 4 h. of shaking at 37°C, each aliquot was analysed by LC–MS after addition of DTT solution in H_2O (2xtimes) (165 nmol, 1.25 µL, from stock solution, conc. 20.0 mg/mL) and stirring at 37 °C for 30 min. Protein samples were flash frozen with liquid nitrogen and stored at –20 °C.

Entry	Iodo-UBQ (equiv.)	$PhB(OH)_2$ (equiv.)	$[L2]_2Pd(OAc)_2$ (equiv.)	Time (h)	Products (Da)
1	1	500	50	4	8734 (2xPh+O), 8810 (3xPh+O), 8886 (4xPh+O)
2	1	1000	50	4	8734 (2xPh+O), 8810 (3xPh+O), 8886 (4xPh+O)
3	1	2000	50	4	8734 (2xPh+O), 8810 (3xPh+O), 8886 (4xPh+O)

General conditions: iodo-Tyr/His UBQ in NaH_2PO_4 (50 mM, pH 8), $PhB(OH)_2$ in 1:3 DMF/ NaH_2PO_4 and 0.01 M [**L2**]$_2$Pd(OAc)$_2$ in NaOH at 37 °C for 4 h, unless otherwise indicated. O = Oxidised methionine

Table 4.7 Investigation of Suzuki-Miyaura cross-couplings of the iodo-Tyr/His ubiquitin with various amounts of $PhB(OH)_2$

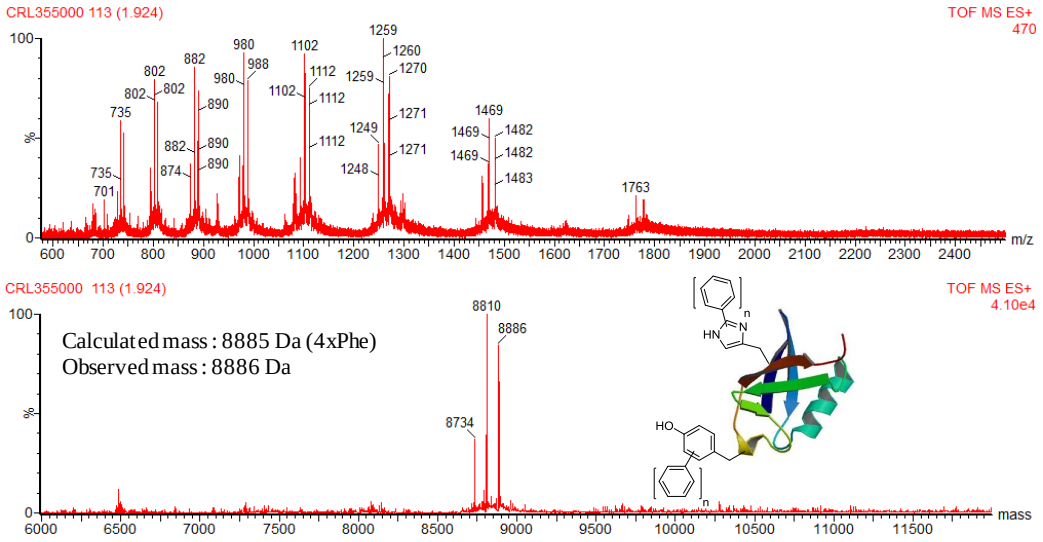

Figure 4.31 ESI-MS spectrum of the iodo-Tyr/His ubiquitin treated with 50 equiv. $[\mathbf{L2}]_2Pd(OAc)_2$ and 500 equiv. $PhB(OH)_2$.

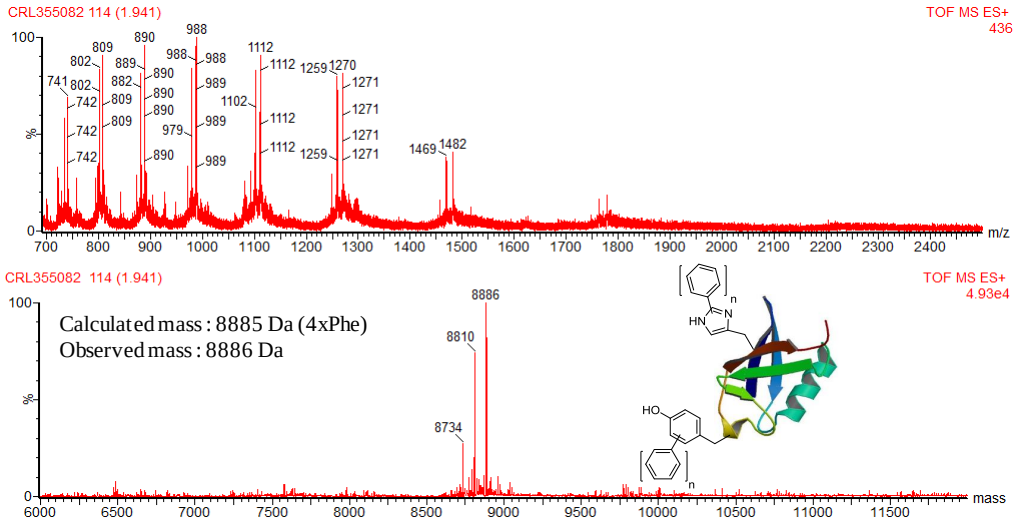

Figure 4.32 ESI-MS spectrum of the iodo-Tyr/His ubiquitin treated with 50 equiv. $[\mathbf{L2}]_2Pd(OAc)_2$ and 1000 equiv. $PhB(OH)_2$.

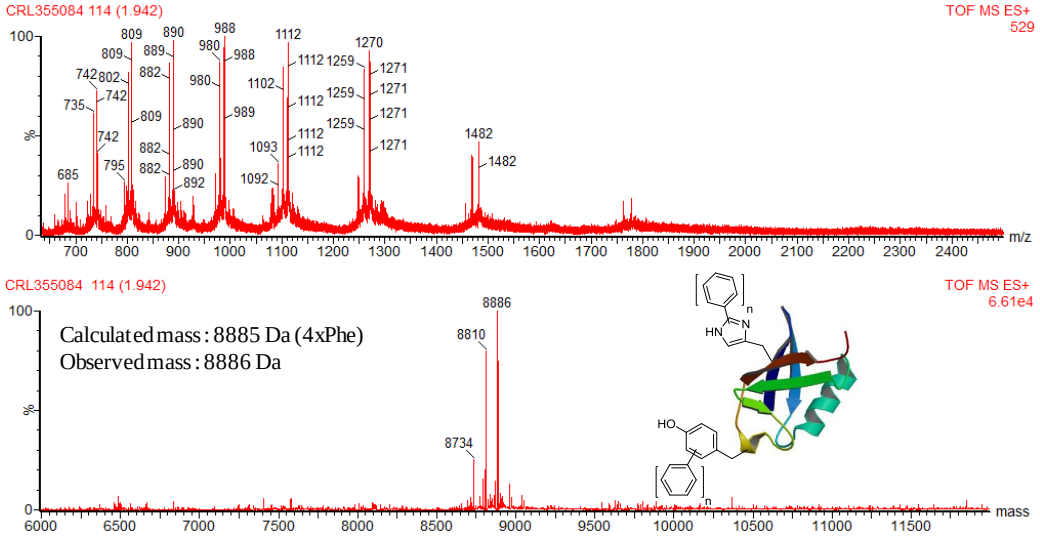

Figure 4.33 ESI-MS spectrum of the iodo-Tyr/His ubiquitin treated with 50 equiv. [**L2**]$_2$Pd(OAc)$_2$ and 2000 equiv. PhB(OH)$_2$.

Effect of electron donating groups as substituents of R-B(OH)$_2$

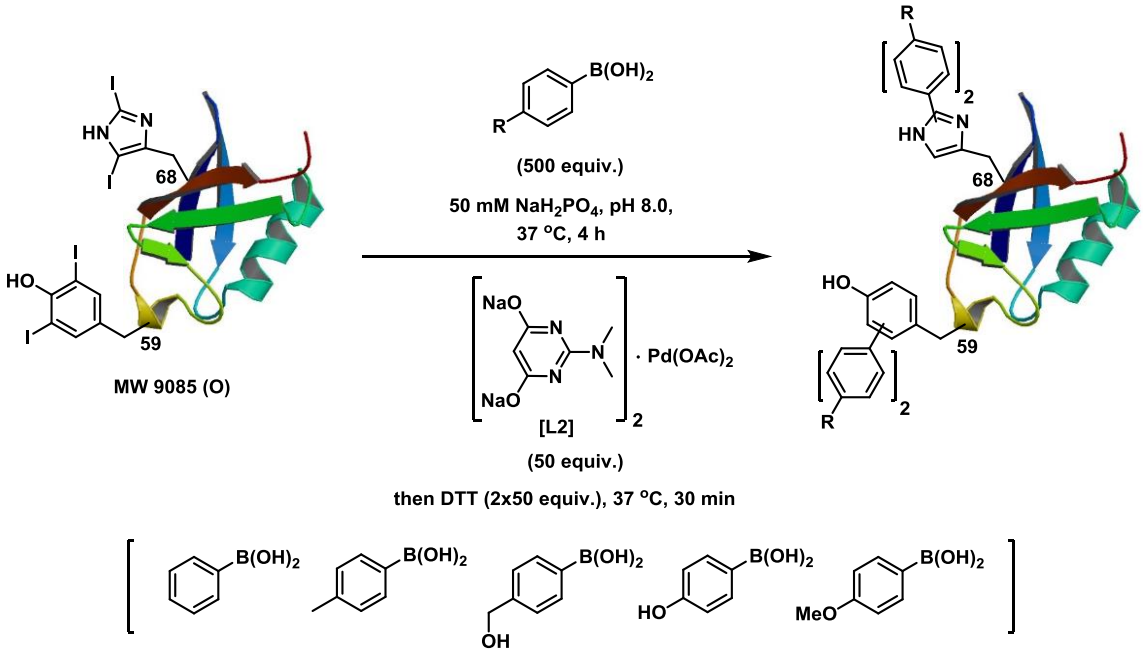

Each aliquot of the iodo-Tyr/His UBQ (3.3 nmol, 1.50 mg/mL, 20 µL) in 50 mM NaH_2PO_4, pH 8.0 was mixed with a solution of R-PhB(OH)$_2$ in a ratio of 1:3 DMF/50 mM NaH_2PO_4 mixture (1,650 nmol, 4-5 µL from stock solution, conc. 50.0 mg/mL) by vortexing briefly. A [**L2**]$_2$Pd(OAc)$_2$ catalyst solution (165 nmol, 16.5 µL, conc. 0.01 M) was added to each reaction mixture which was vortexed briefly. After 4 h. of shaking at 37°C, each aliquot was analysed by LC–MS after addition of DTT solution in H_2O

(2xtimes) (165 nmol, 1.25 µL, from stock solution, conc. 20.0 mg/mL) and stirring at 37 °C for 30 min. Protein samples were flash frozen with liquid nitrogen and stored at –20 °C.

Entry	**Iodo-UBQ (equiv.)**	**$PhB(OH)_2$ (equiv.)**	**$[L2]_2Pd(OAc)_2$ (equiv.)**	**Products (Da)**
1	1	500 (R = H)	50	8733 (2xPh+O) 8810 (3xPh+O) 8885 (4xPh+O)
2	1	500 (R = Me)	50	8671 (1xMe-Ph+O) 8762 (2xMe-Ph+O) 8852 (3xMe-Ph+O) 8942 (4xMe-Ph+O)
3	1	500 (R = CH_2OH)	50	8687 (1x$HOCH_2$-Ph+O) 8793 (2x$HOCH_2$-Ph+O) 8900 (3x$HOCH_2$-Ph+O) 9006 (4x$HOCH_2$-Ph+O)
4	1	500 (R = OH)	50	8673 (1xOH-Ph+O) 8765 (2xOH-Ph+O) 8799 (1xOH-Ph+O+1xI) 8858 (3xOH-Ph+O) 8892 (2xOH-Ph+O+1xI) 8950 (4xOH-Ph+O)
5	1	500 (R = OMe)	50	8687 (1xOMe-Ph+O) 8793 (2xOMe-Ph+O) 8900 (3xOMe-Ph+O) 9006 (4xOMe-Ph+O)

General conditions: iodo-Tyr/His UBQ in NaH_2PO_4 (50 mM, pH 8), R-$PhB(OH)_2$ in 1:3 DMF/ NaH_2PO_4 and 0.01 M [**L2**]$_2Pd(OAc)_2$ in NaOH at 37 °C for 4 h, unless otherwise indicated. O = Oxidised methionine

Table 4.8 Investigation of Suzuki-Miyaura cross-couplings of the iodo-Tyr/His ubiquitin with different electron donating groups of $PhB(OH)_2$.

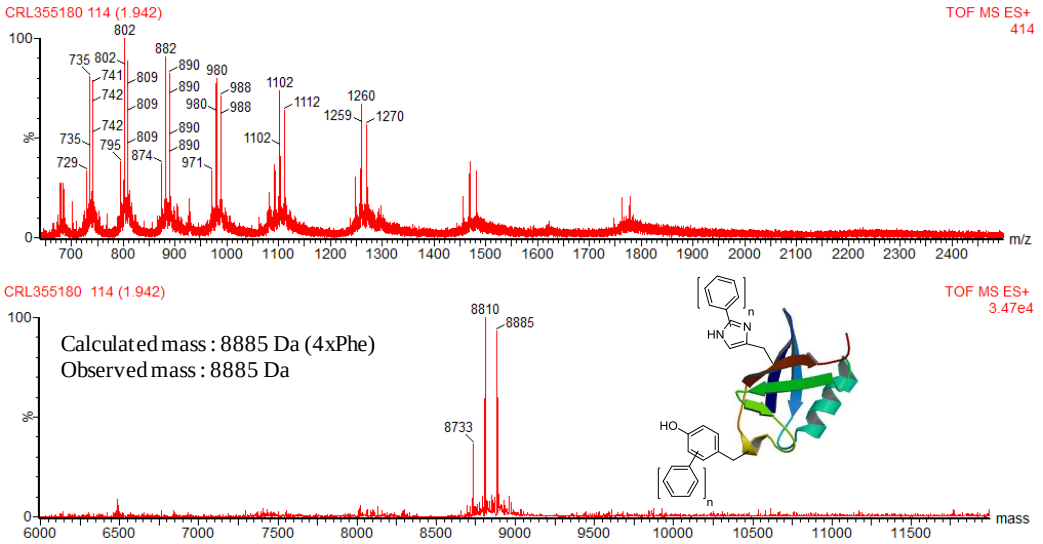

Figure 4.34 ESI-MS spectrum of the iodo-Tyr/His ubiquitin treated with 50 equiv. [**L2**]$_2$Pd(OAc)$_2$ and 500 equiv. PhB(OH)$_2$.

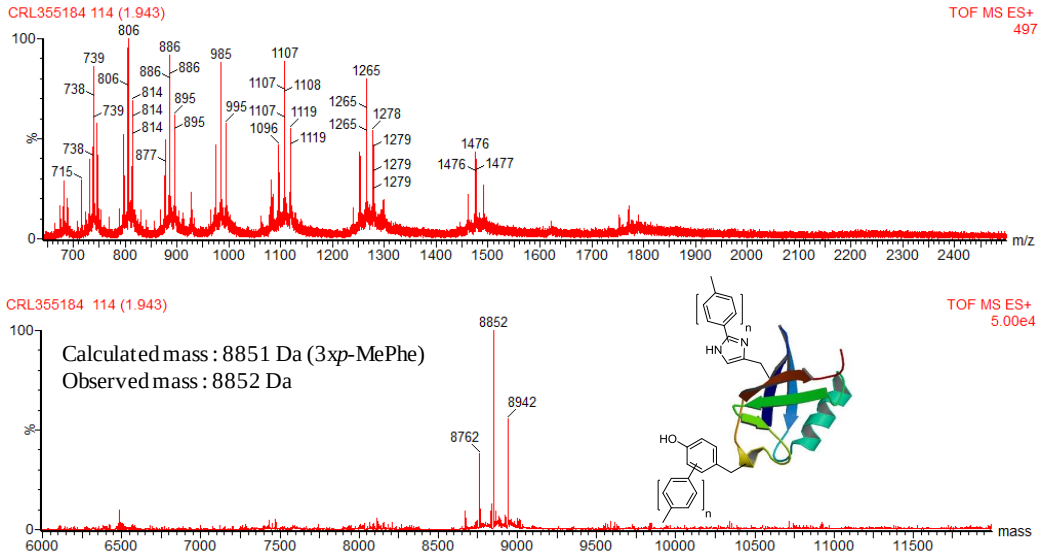

Figure 4.35 ESI-MS spectrum of the iodo-Tyr/His ubiquitin treated with 50 equiv. [**L2**]$_2$Pd(OAc)$_2$ and 500 equiv. *p*-Me-PhB(OH)$_2$.

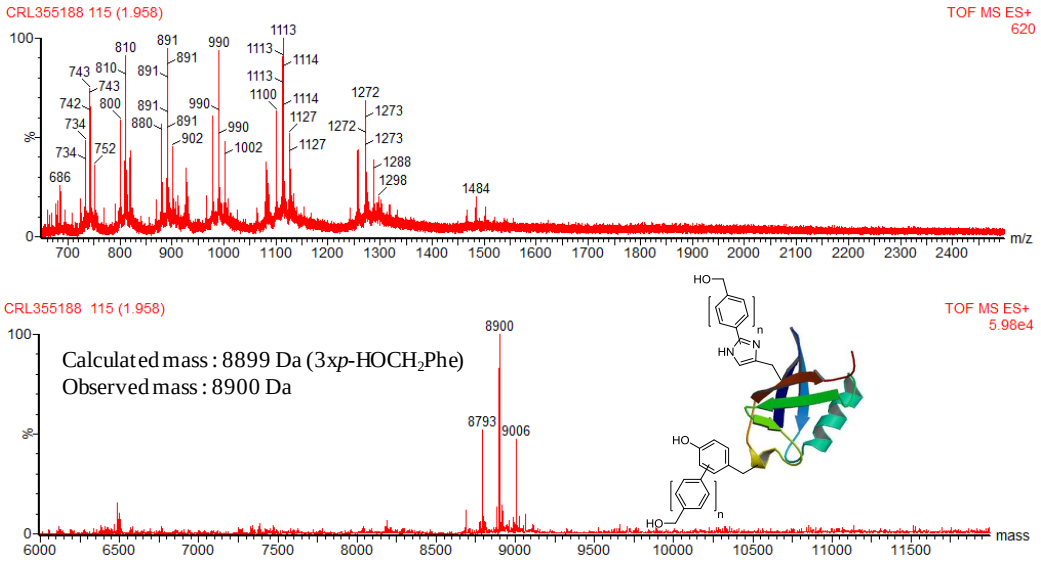

Figure 4.36 ESI-MS spectrum of the iodo-Tyr/His ubiquitin treated with 50 equiv. [**L2**]$_2$Pd(OAc)$_2$ and 500 equiv. *p*-HOCH$_2$-PhB(OH)$_2$.

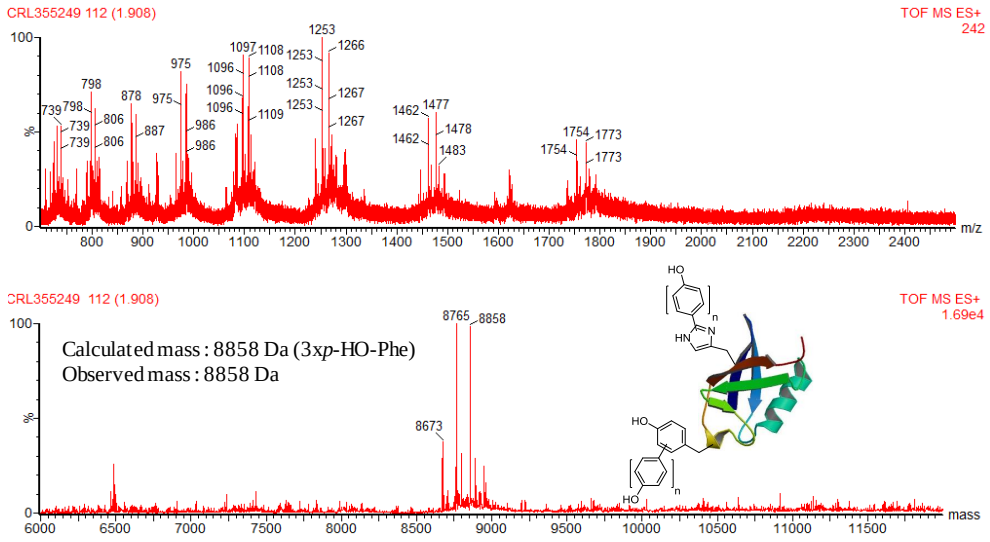

Figure 4.37 ESI-MS spectrum of the iodo-Tyr/His ubiquitin treated with 50 equiv. [**L2**]$_2$Pd(OAc)$_2$ and 500 equiv. *p*-HO-PhB(OH)$_2$.

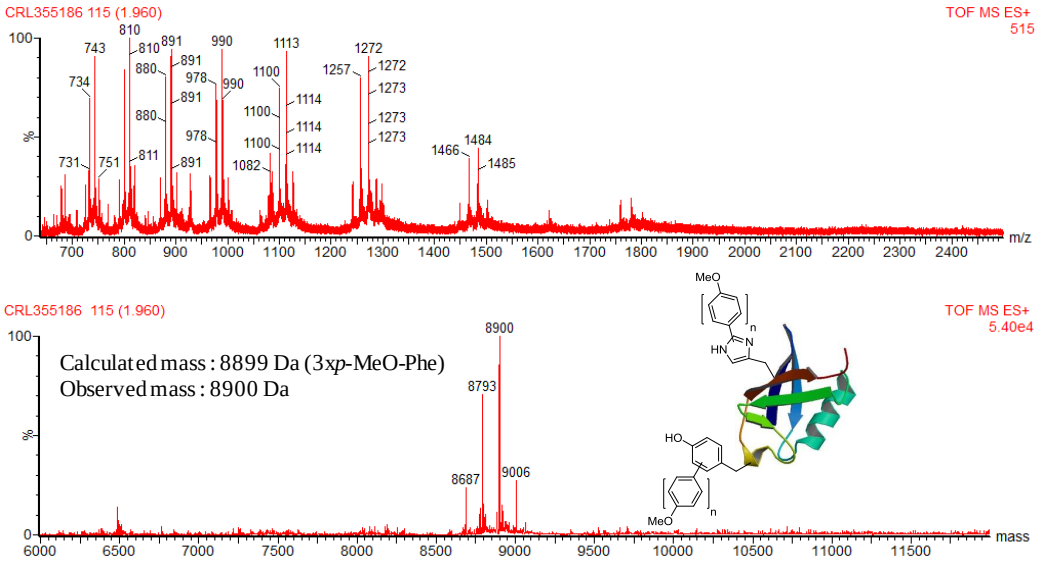

Figure 4.38 ESI-MS spectrum of the iodo-Tyr/His ubiquitin treated with 50 equiv. [**L2**]$_2$Pd(OAc)$_2$ and 500 equiv. *p*-OMe-PhB(OH)$_2$.

Effect of electron withdrawing groups as substituents of R-B(OH)$_2$

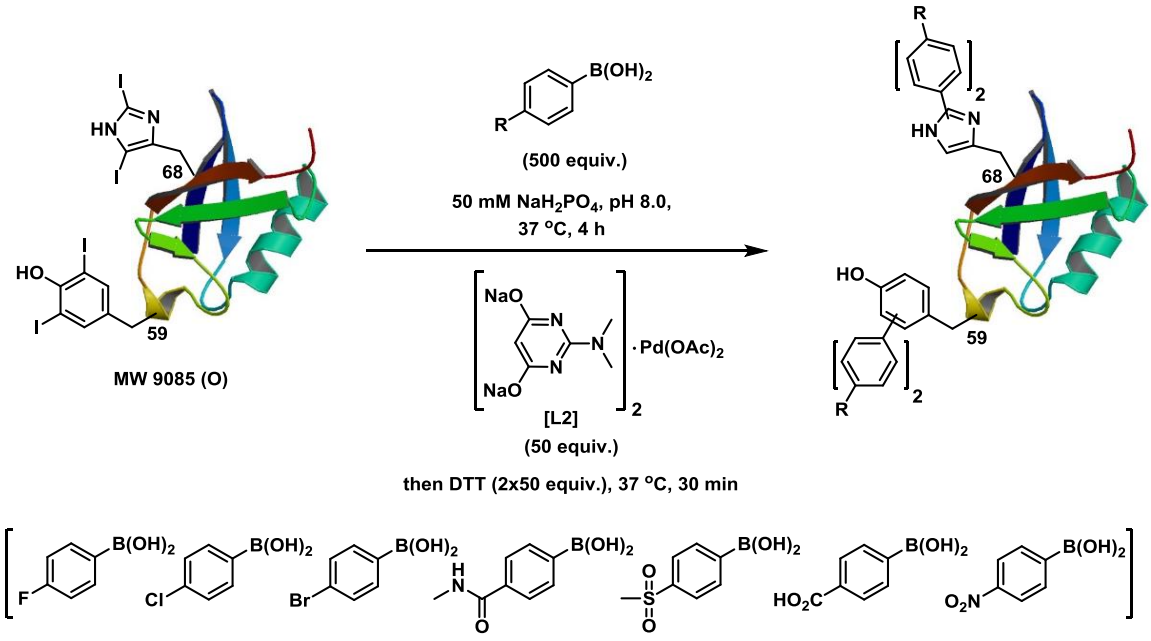

Each aliquot of the iodo-Tyr/His UBQ (3.3 nmol, 1.50 mg/mL, 20 µL) in 50 mM NaH_2PO_4, pH 8.0 was mixed with a solution of the R-PhB(OH)$_2$ in a ratio of 1:3 DMF/50 mM NaH_2PO_4 mixture (1,650 nmol, 4-6 µL from stock solution, conc. 50.0 mg/mL) by vortexing briefly. A [**L2**]$_2$Pd(OAc)$_2$ catalyst solution (165 nmol, 16.5 µL, conc. 0.01 M) was added to each reaction mixture which was vortexed briefly. After 4 h. of shaking at

37°C, each aliquot was analysed by LC–MS after addition of DTT solution in H_2O (2xtimes) (165 nmol, 1.25 µL, from stock solution, conc. 20.0 mg/mL) and stirring at 37 °C for 30 min. Protein samples were flash frozen with liquid nitrogen and stored at –20 °C.

Entry	**Iodo-UBQ (equiv.)**	**R-PhB(OH)$_2$ (equiv.)**	**[L2]$_2$Pd(OAc)$_2$ (equiv.)**	**Products (Da)**
1	1	500 (R = F)	50	8770 (2xF-Ph+O) 8864 (3xF-Ph+O) 8958 (4xF-Ph+O)
2	1	500 (R = Cl)	50	8803 (2xCl-Ph+O) 8913 (3xCl-Ph+O) 9023 (4xCl-Ph+O)
3	1	500 (R = Br)	50	Protein degraded
4	1	500 (R = NHCO)	50	8715 (1xMeNHCO-Ph+O) 8848 (2xMeNHCO-Ph+O) 8981 (3xMeNHCO-Ph+O) 9114 (4xMeNHCO-Ph+O)
5	1	500 (R = MeO_2S)	50	8736 (1xMeO_2S-Ph+O) 8890 (2xMeO_2S-Ph+O) 9044 (3xMeO_2S-Ph+O) 9198 (4xMeO_2S-Ph+O)
6	1	500 (R = CO_2H)	50	8701 (1xCOOH-Ph+O) 8822 (2xCOOH-Ph+O) 8942 (3xCOOH-Ph+O) 9062 (4xCOOH-Ph+O)
7	1	500 (R = NO_2)	50	8824 (2xNO_2-Ph+O) 8944 (3xNO_2-Ph+O) 9066 (4xNO_2-Ph+O)

General conditions: iodo-Tyr/His UBQ in NaH_2PO_4 (50 mM, pH 8), R-PhB(OH)$_2$ in 1:3 DMF/NaH_2PO_4 and 0.01 M [**L2**]$_2$Pd(OAc)$_2$ in NaOH at 37 °C for 4 h, unless otherwise indicated. O = Oxidised methionine

Table 4.9 Investigation of Suzuki-Miyaura cross-couplings of the iodo-Tyr/His ubiquitin with different electron withdrawing groups of PhB(OH)$_2$.

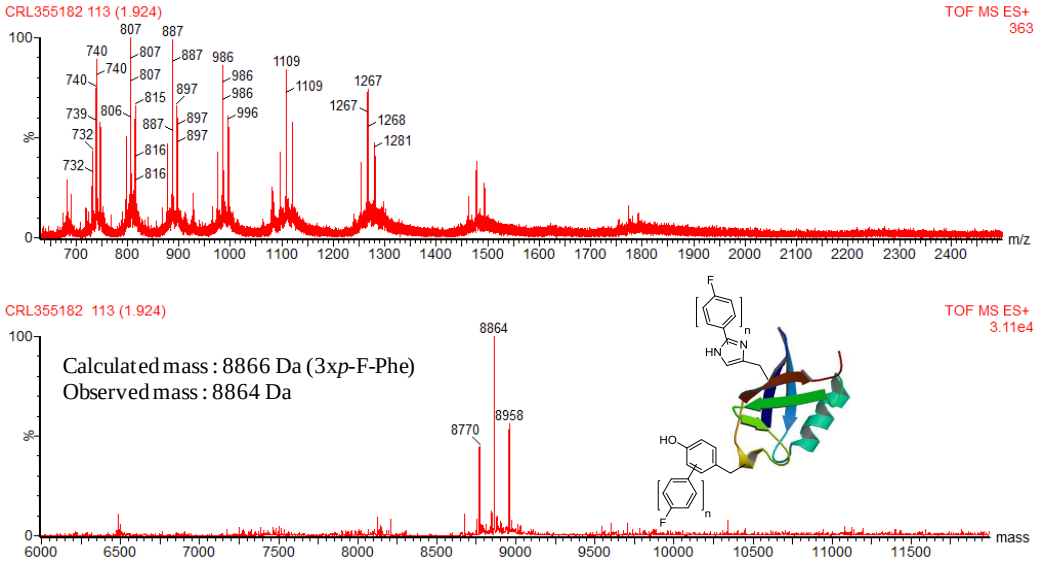

Figure 4.39 ESI-MS spectrum of the iodo-Tyr/His ubiquitin treated with 50 equiv. $[\mathbf{L2}]_2Pd(OAc)_2$ and 500 equiv. *p*-F-PhB$(OH)_2$.

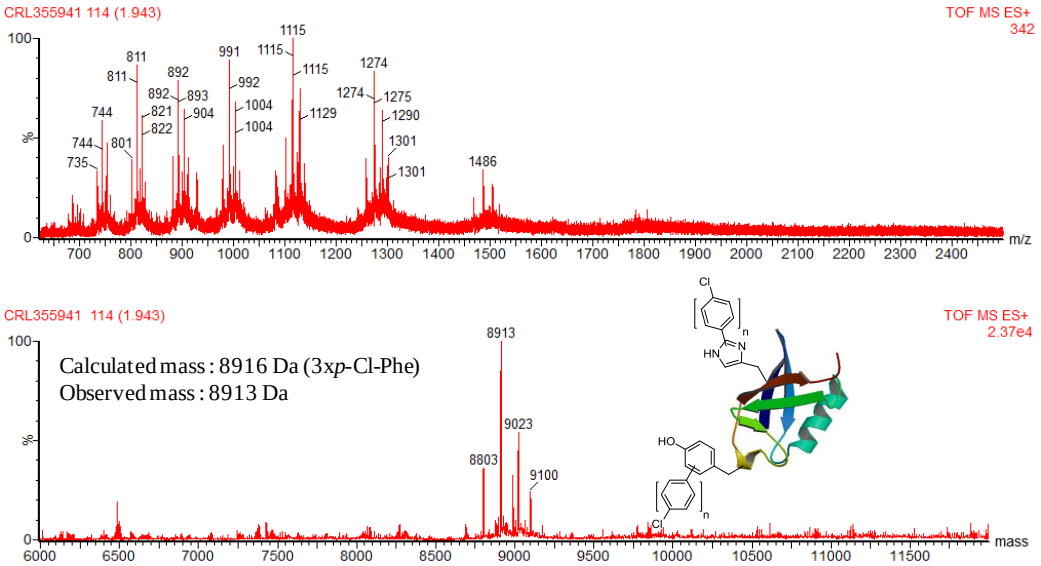

Figure 4.40 ESI-MS spectrum of the iodo-Tyr/His ubiquitin treated with 50 equiv. $[\mathbf{L2}]_2Pd(OAc)_2$ and 500 equiv. *p*-Cl-PhB$(OH)_2$.

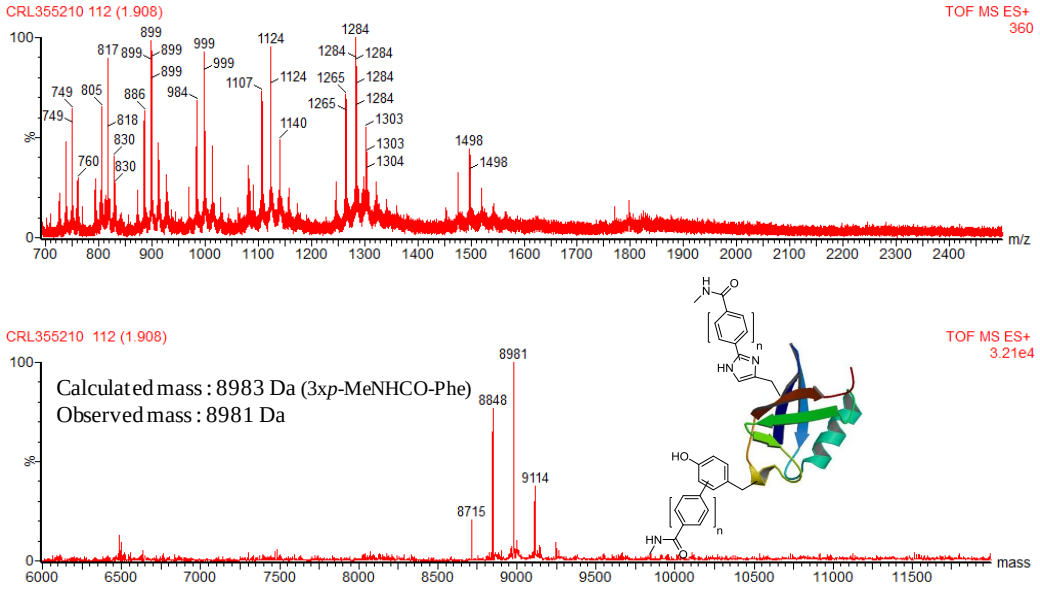

Figure 4.41 ESI-MS spectrum of the iodo-Tyr/His ubiquitin treated with 50 equiv. [**L2**]$_2$Pd(OAc)$_2$ and 500 equiv. *p*-MeNHCO-PhB(OH)$_2$.

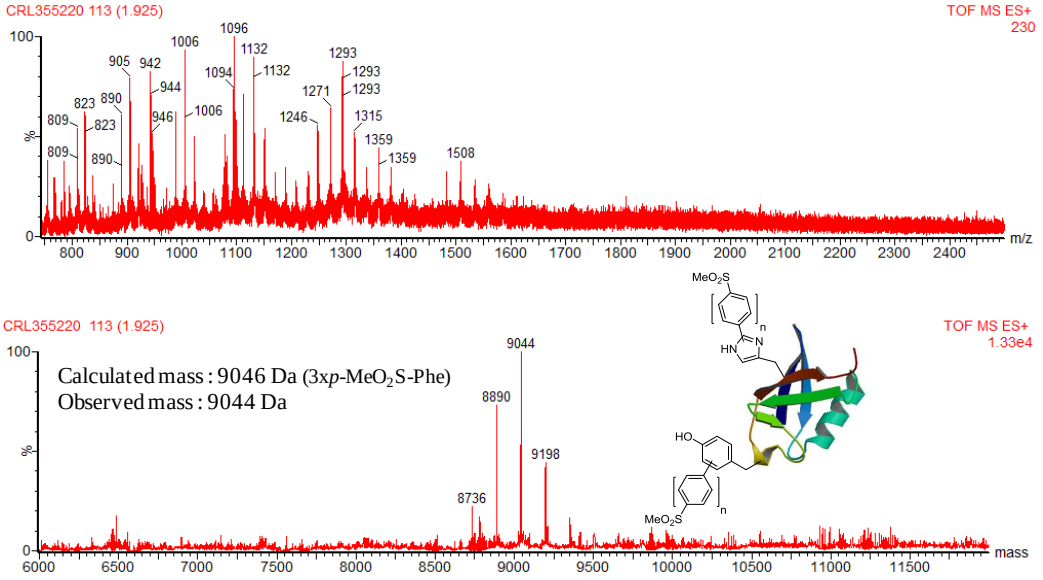

Figure 4.42 ESI-MS spectrum of the iodo-Tyr/His ubiquitin treated with 50 equiv. [**L2**]$_2$Pd(OAc)$_2$ and 500 equiv. *p*-MeO$_2$S-PhB(OH)$_2$.

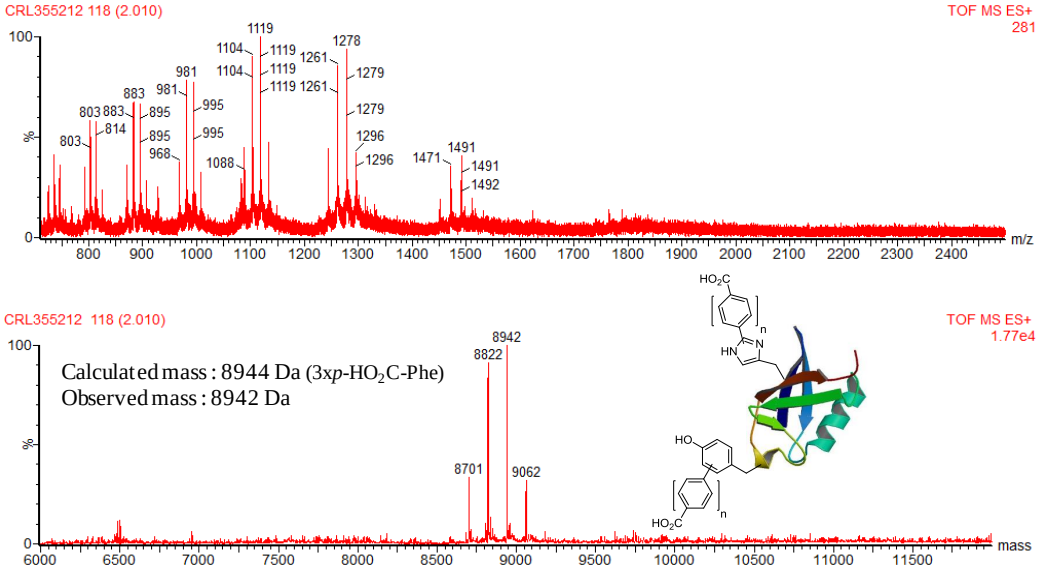

Figure 4.43 ESI-MS spectrum of the iodo-Tyr/His ubiquitin treated with 50 equiv. [**L2**]$_2$Pd(OAc)$_2$ and 500 equiv. *p*-HO$_2$C-PhB(OH)$_2$.

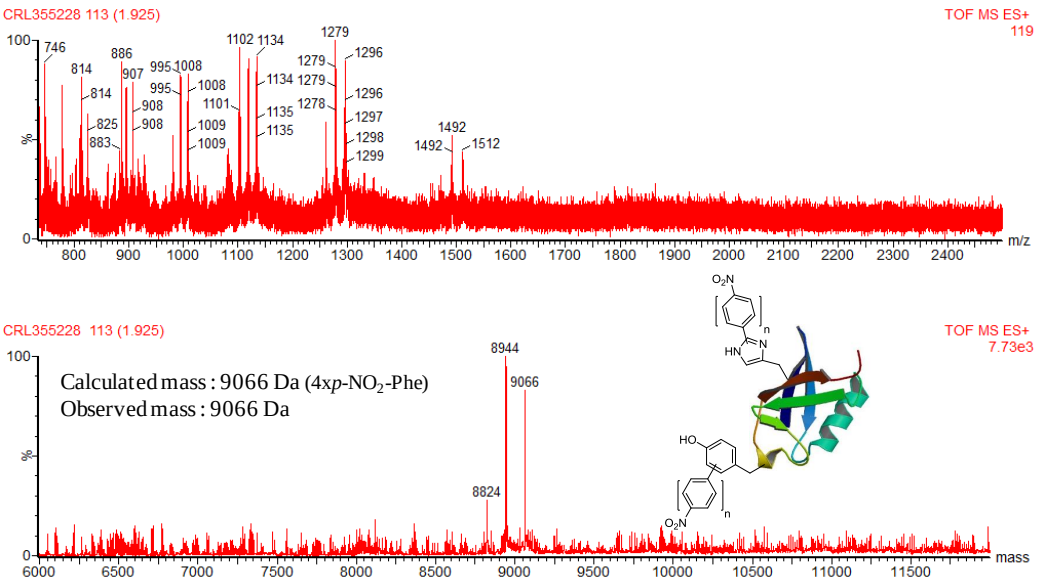

Figure 4.44 ESI-MS spectrum of the iodo-Tyr/His ubiquitin treated with 50 equiv. [**L2**]$_2$Pd(OAc)$_2$ and 500 equiv. *p*-NO$_2$-PhB(OH)$_2$.

Effect of boronic acid derivatives

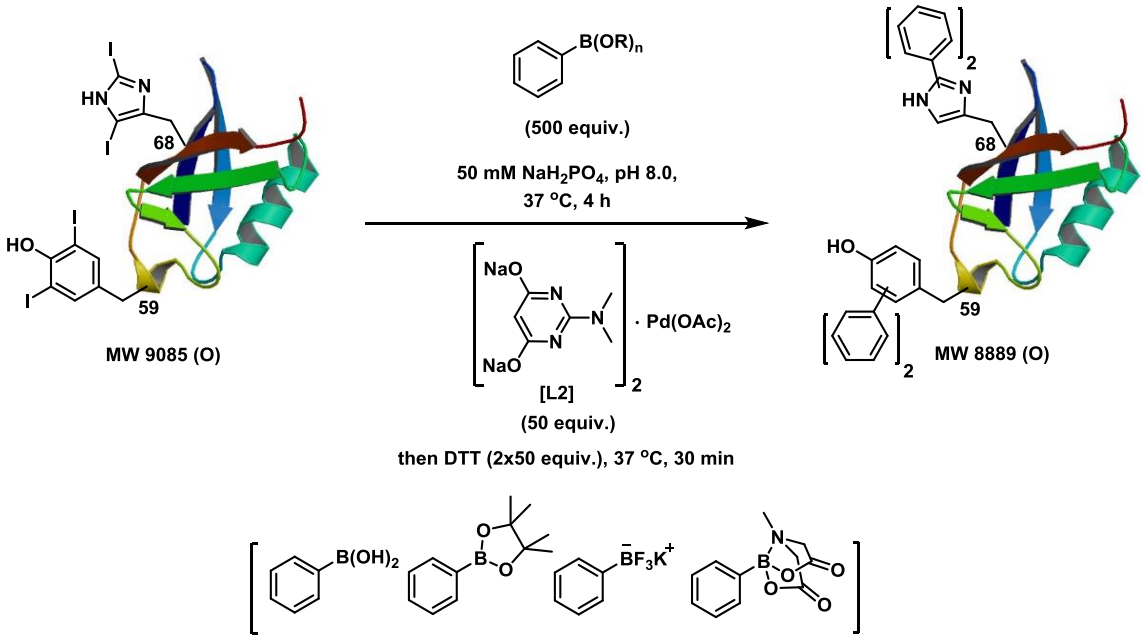

Each aliquot of the iodo-Try/His UBQ (3.3 nmol, 1.50 mg/mL, 20 µL) in 50 mM NaH_2PO_4, pH 8.0 was mixed with a solution of $PhB(OR)_n$ in a ratio of 1:3 DMF/50 mM NaH_2PO_4 mixture (1,650 nmol, 3-4 µL from stock solution, conc. 50.0 mg/mL for $PhB(OH)_2$ and conc. 100.0 mg/mL for pinacol ester, BF_3K, and MIDA) by vortexing briefly. A [**L2**]$_2$Pd(OAc)$_2$ catalyst solution (165 nmol, 16.5 µL, conc. 0.01 M) was added to each reaction mixture which was vortexed briefly. After 4 h. of shaking at 37°C, each aliquot was analysed by LC–MS after addition of DTT solution in H_2O (2xtimes) (165 nmol, 1.25 µL, from stock solution, conc. 20.0 mg/mL) and stirring at 37 °C for 30 min. Protein samples were flash frozen with liquid nitrogen and stored at –20 ºC.

Entry	Iodo-UBQ (equiv.)	$PhB(OR)_2$ (equiv.)	$[L2]_2Pd(OAc)_2$ (equiv.)	Products (Da)
1	1	500 (R = H)	50	8733 (2xPh+O) 8810 (3xPh+O) 8885 (4xPh+O)
2	1	500 (R = Pinacol ester)	50	8734 (2xPh+O) 8810 (3xPh+O) 8886 (4xPh+O)
3	1	500 (R = BF_3K)	50	8657 (1xPh+O) 8734 (2xPh+O) 8810 (3xPh+O)
4	1	500 (R = MIDA)	50	8658 (1xPh+O) 8734 (2xPh+O) 8810 (3xPh+O) 8886 (4xPh+O)

General conditions: iodo-Tyr/His UBQ in NaH_2PO_4 (50 mM, pH 8), R-$PhB(OH)_2$ in 1:3 DMF/NaH_2PO_4 and 0.01 M $[\mathbf{L2}]_2Pd(OAc)_2$ in NaOH at 37 °C for 4 h, unless otherwise indicated. O = Oxidised methionine

Table 4.10 Investigation of Suzuki-Miyaura cross-couplings of the iodo-Tyr/His ubiquitin with different bond acid derivatives of $PhB(OH)_2$.

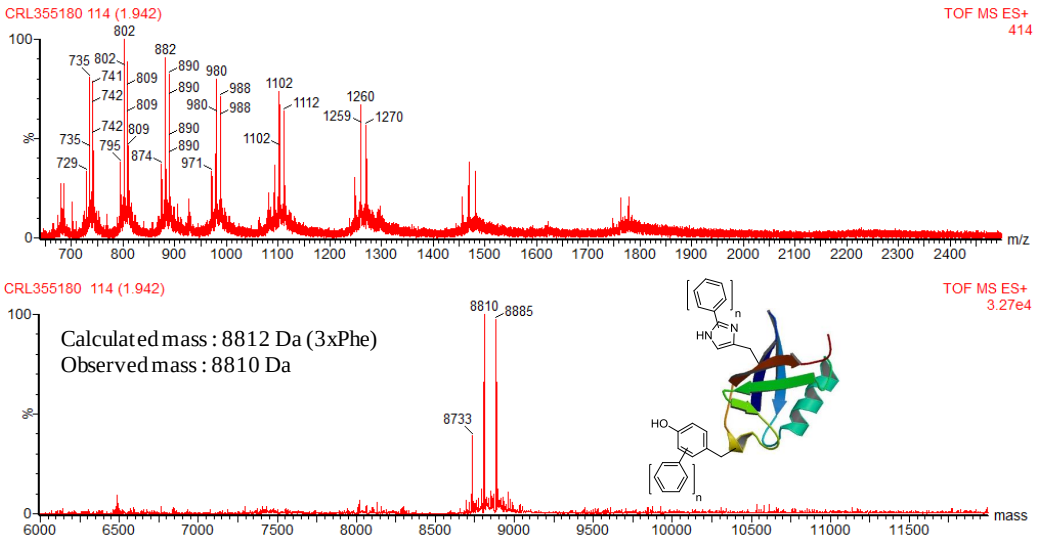

Figure 4.45 ESI-MS spectrum of the iodo-Tyr/His ubiquitin treated with 50 equiv. $[\mathbf{L2}]_2Pd(OAc)_2$ and 500 equiv. $PhB(OR)_2$, R = H.

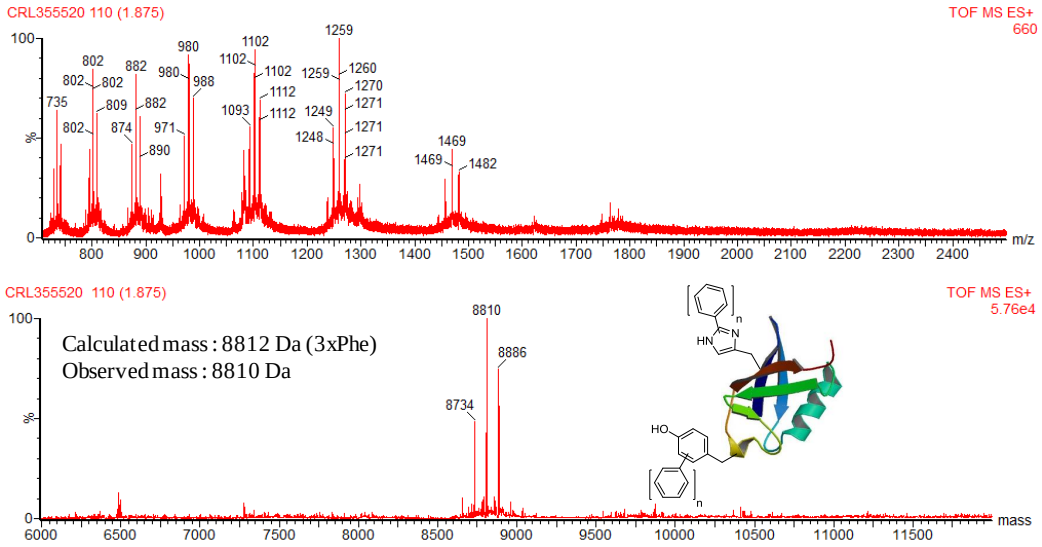

Figure 4.46 ESI-MS spectrum of the iodo-Tyr/His ubiquitin treated with 50 equiv. [**L2**]$_2$Pd(OAc)$_2$ and 500 equiv. PhB(OR)$_2$, R = pinacol ester.

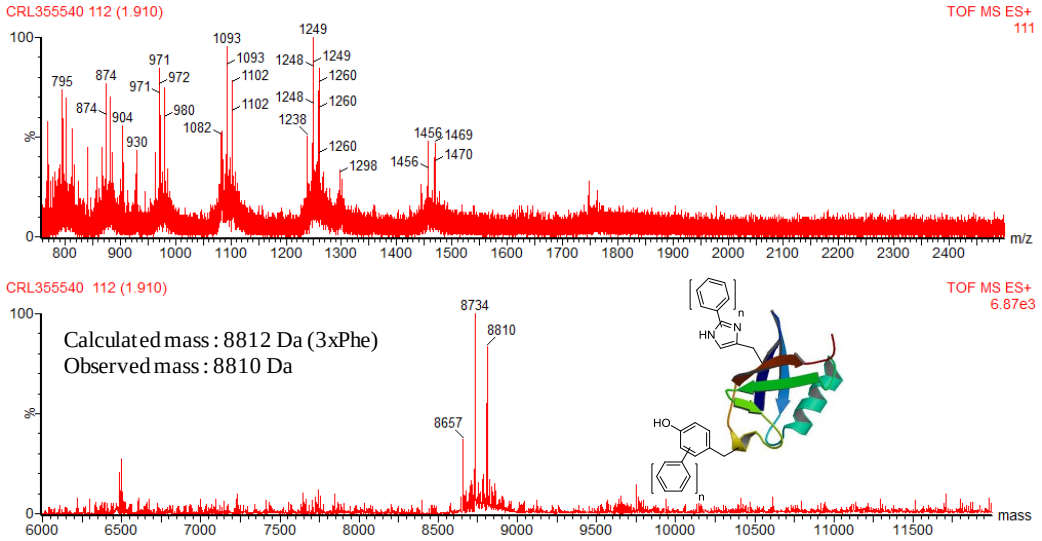

Figure 4.47 ESI-MS spectrum of the iodo-Tyr/His ubiquitin treated with 50 equiv. [**L2**]$_2$Pd(OAc)$_2$ and 500 equiv. PhB(OR)$_2$, R = BF_3K.

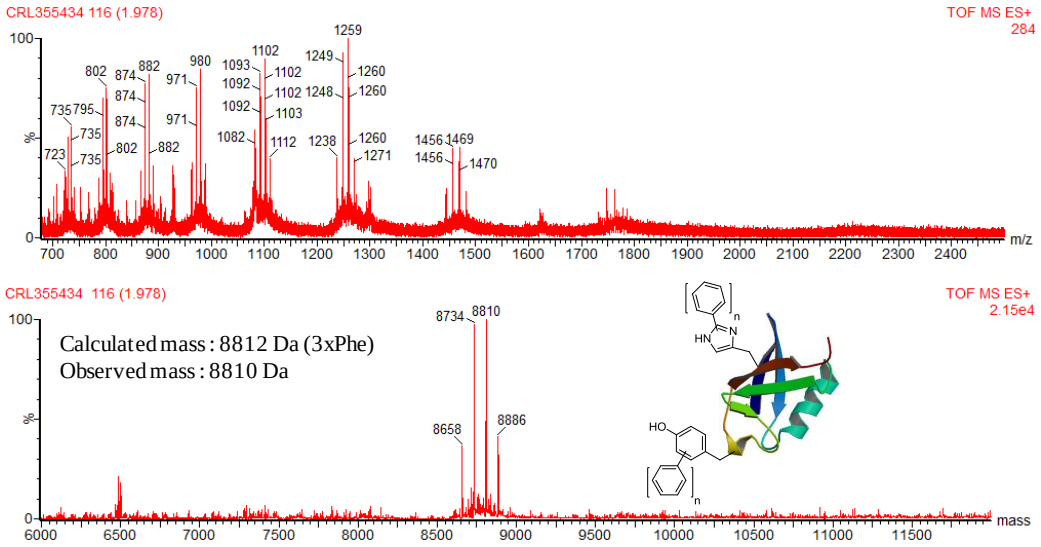

Figure 4.48 ESI-MS spectrum of the iodo-Tyr/His ubiquitin treated with 50 equiv. $[\mathbf{L2}]_2Pd(OAc)_2$ and 500 equiv. $PhB(OR)_2$, R = MIDA.

Effect of steric hindrance of boronic acids

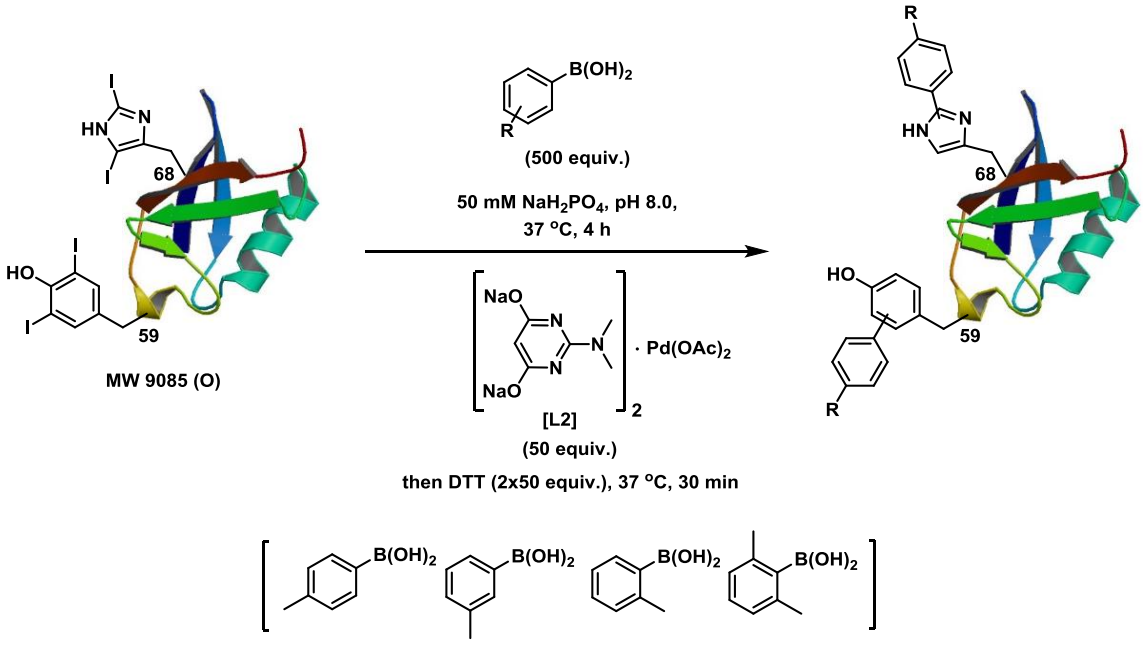

Each aliquot of the iodo-Tyr/His UBQ (3.3 nmol, 1.50 mg/mL, 20 µL) in 50 mM NaH_2PO_4, pH 8.0 was mixed with a solution of R-$PhB(OH)_2$ in a ratio of 1:3 DMF/50 mM NaH_2PO_4 mixture (1,650 nmol, 4.5-5 µL from stock solution, conc. 50.0 mg/mL) by vortexing briefly. A $[\mathbf{L2}]_2Pd(OAc)_2$ catalyst solution (165 nmol, 16.5 µL, conc. 0.01 M) was added to each reaction mixture which was vortexed briefly. After 4 h. of shaking at

37°C, each aliquot was analysed by LC–MS after addition of DTT solution in H_2O (2xtimes) (165 nmol, 1.25 µL, from stock solution, conc. 20.0 mg/mL) and stirring at 37 °C for 30 min. Protein samples were flash frozen with liquid nitrogen and stored at –20 °C.

Entry	**Iodo-UBQ (equiv.)**	**$PhB(OR)_2$ (equiv.)**	**$[L2]_2Pd(OAc)_2$ (equiv.)**	**Products (Da)**
1	1	500 (R = 4-Me)	50	8671 (1xMe-Ph+O) 8762 (2xMe-Ph+O) 8852 (3xMe-Ph+O) 8942 (4xMe-Ph+O)
2	1	500 (R = 3-Me)	50	8762 (2xMe-Ph+O) 8852 (3xMe-Ph+O) 8942 (4xMe-Ph+O)
3	1	500 (R = 2-Me)	50	8582 (WT+O) 8672 (1xMe-Ph+O) 8762 (2xMe-Ph+O) 8852 (3xMe-Ph+O) 8708 (1xI+O) 8834 (2xI+O) 8798 (1xI+1xMe-Ph+O) 8888 (1xI+2xMe-Ph+O) 8924 (2xI+1xMe-Ph+O)
4	1	500 (R = 2,5-DiMe)	50	8833 (2xI+O) 8959 (3xI+O) 9084 (4xI+O)

General conditions: iodo-Tyr/His UBQ in NaH_2PO_4 (50 mM, pH 8), R-$PhB(OH)_2$ in 1:3 DMF/NaH_2PO_4 and 0.01 M [**L2**]$_2$Pd$(OAc)_2$ in NaOH at 37 °C for 4 h, unless otherwise indicated. O = Oxidised methionine

Table 4.11 Investigation of Suzuki-Miyaura cross-couplings of the iodo-Tyr/His ubiquitin with different position of a methyl group of $PhB(OH)_2$.

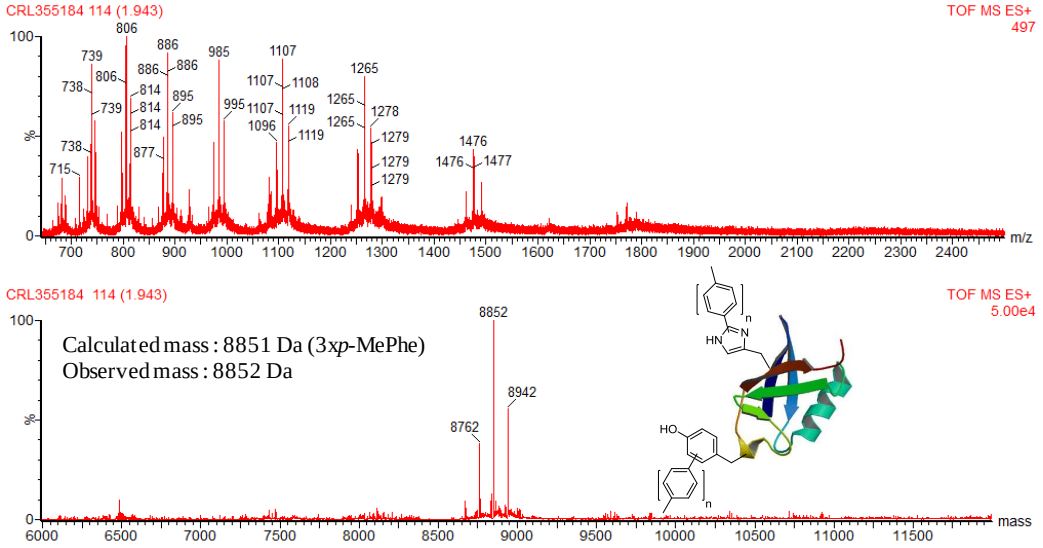

Figure 4.49 ESI-MS spectrum of the iodo-Tyr/His ubiquitin treated with 50 equiv. [**L2**]$_2$Pd(OAc)$_2$ and 500 equiv. *p*-Me-PhB(OH)$_2$.

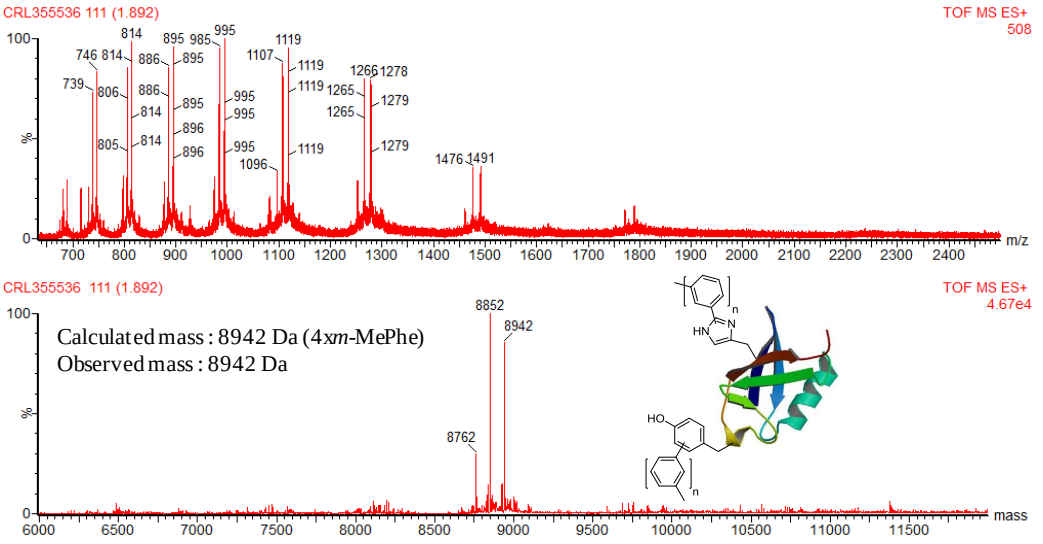

Figure 4.50 ESI-MS spectrum of the iodo-Tyr/His ubiquitin treated with 50 equiv. [**L2**]$_2$Pd(OAc)$_2$ and 500 equiv. *m*-Me-PhB(OH)$_2$.

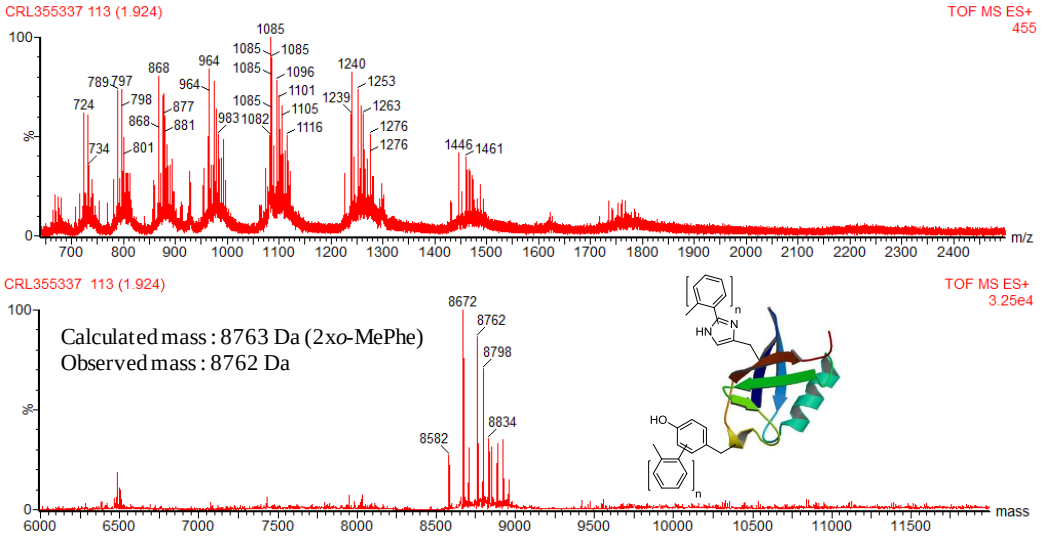

Figure 4.51 ESI-MS spectrum of the iodo-Tyr/His ubiquitin treated with 50 equiv. [**L2**]$_2$Pd(OAc)$_2$ and 500 equiv. *o*-Me-PhB(OH)$_2$.

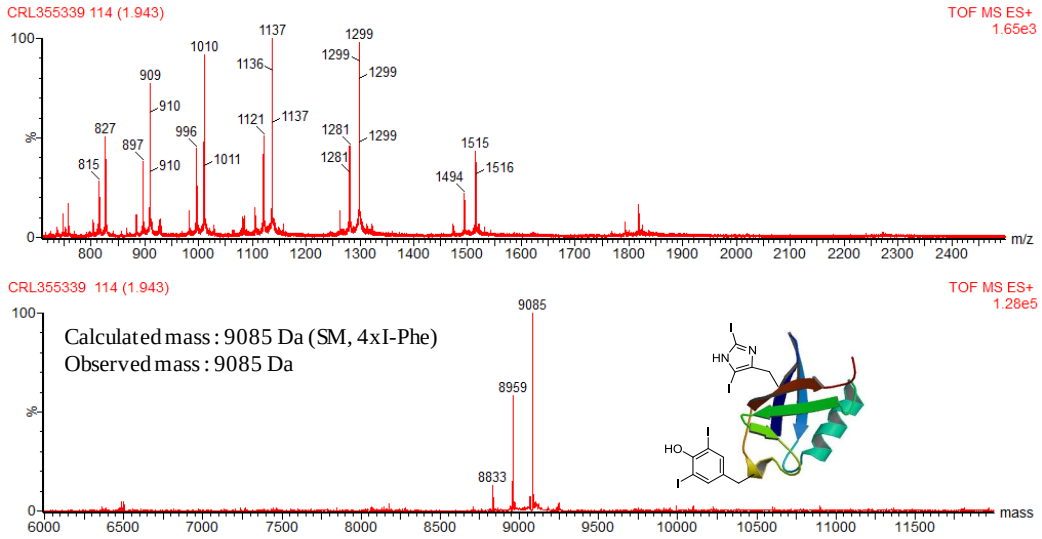

Figure 4.52 ESI-MS spectrum of the iodo-Tyr/His ubiquitin treated with 50 equiv. [**L2**]$_2$Pd(OAc)$_2$ and 500 equiv. 2,5-diMe-PhB(OH)$_2$.

Effect of heterocyclic boronic acids

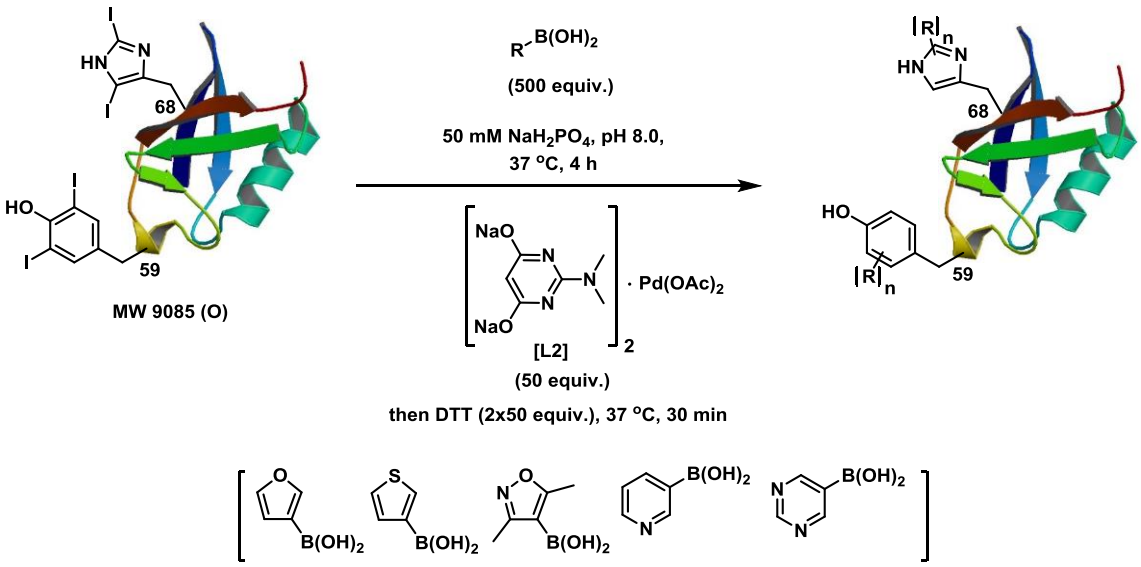

Each aliquot of the iodo-Tyr/His UBQ (3.3 nmol, 1.50 mg/mL, 20 µL) in 50 mM NaH_2PO_4, pH 8.0 was mixed with a solution of R-$B(OH)_2$ in a ratio of 1:1 DMF/50 mM NaH_2PO_4 mixture for R = furan, thienyl, isoxazole, in a ratio of 3:1 DMF/50 mM NaH_2PO_4 mixture for R = 3-pyridine, and in pure DMF for R = 5-pyrimidine (1,650 nmol, 2-5 µL from stock solution, conc. 50.0 mg/mL for furan, thienyl, isoxazole and conc. 100.0 mg/mL for 3-pyridine and 5-pyrimidine) by vortexing briefly. A [**L2**]$_2$Pd(OAc)$_2$ catalyst solution (165 nmol, 16.5 µL, conc. 0.01 M) was added to each reaction mixture which was vortexed briefly. After 4 h. of shaking at 37°C, each aliquot was analysed by LC–MS after addition of DTT solution in H_2O (2xtimes) (165 nmol, 1.25 µL, from stock solution, conc. 20.0 mg/mL) and stirring at 37 °C for 30 min. Protein samples were flash frozen with liquid nitrogen and stored at –20 ºC.

Entry	Iodo-UBQ (equiv.)	$PhB(OR)_2$ (equiv.)	$[L2]_2Pd(OAc)_2$ (equiv.)	Products (Da)
1	1	500 (R = Furan)	50	8714 (2xFuran+O) 8779 (3xFuran+O) 8840 (2xFuran+O+1xI) 8900 (1xFuran+Ox+2xI) 8959 Da (3xI+O)
2	1	500 (R = Thienyl)	50	8828 (3xThienyl+O) 8910 (4xThienyl+O)
3	1	500 (R = Isoxazole)	50	8959 (3xI+O) 9085 (4xI+O)
4	1	500 (R = 3-Pyridine)	50	8833 (2xI+O) 8959 (3xI+O) 9085 (4xI+O)
5	1	500 (R = 5-Pyrimidine)	50	8834 (2xI+O) 8958 (3xI+O) 9085 (4xI+O)

General conditions: iodo-Tyr/His UBQ in NaH_2PO_4 (50 mM, pH 8), R-$PhB(OH)_2$ in 1:1 or 3:1 DMF/NaH_2PO_4 and 0.01 M $[\mathbf{L2}]_2Pd(OAc)_2$ in NaOH at 37 °C for 4 h, unless otherwise indicated. O = Oxidised methionine

Table 4.12 Investigation of Suzuki-Miyaura cross-couplings of the iodo-Tyr/His ubiquitin with different heterocyclic boronic acids.

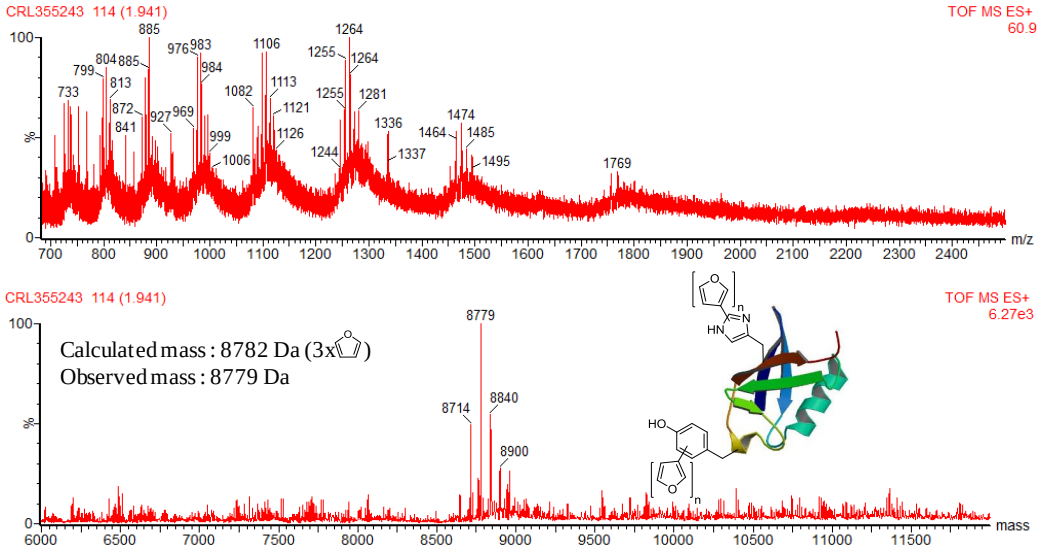

Figure 4.53 ESI-MS spectrum of the iodo-Tyr/His ubiquitin treated with 50 equiv. $[\mathbf{L2}]_2Pd(OAc)_2$ and 500 equiv. 3-furanylboronic acid.

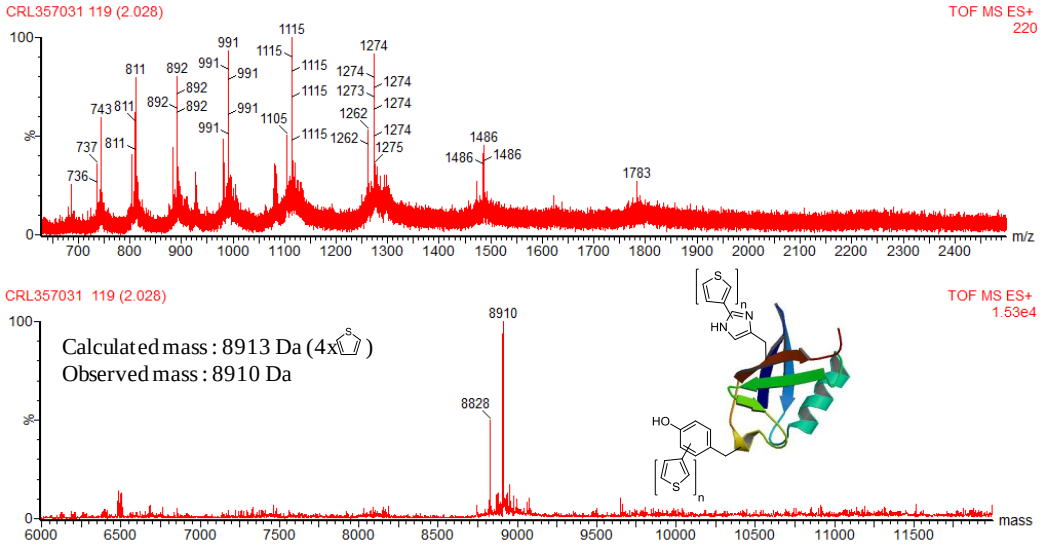

Figure 4.54 ESI-MS spectrum of the iodo-Tyr/His ubiquitin treated with 50 equiv. $[\mathbf{L2}]_2Pd(OAc)_2$ and 500 equiv. 3-thienylboronic acid.

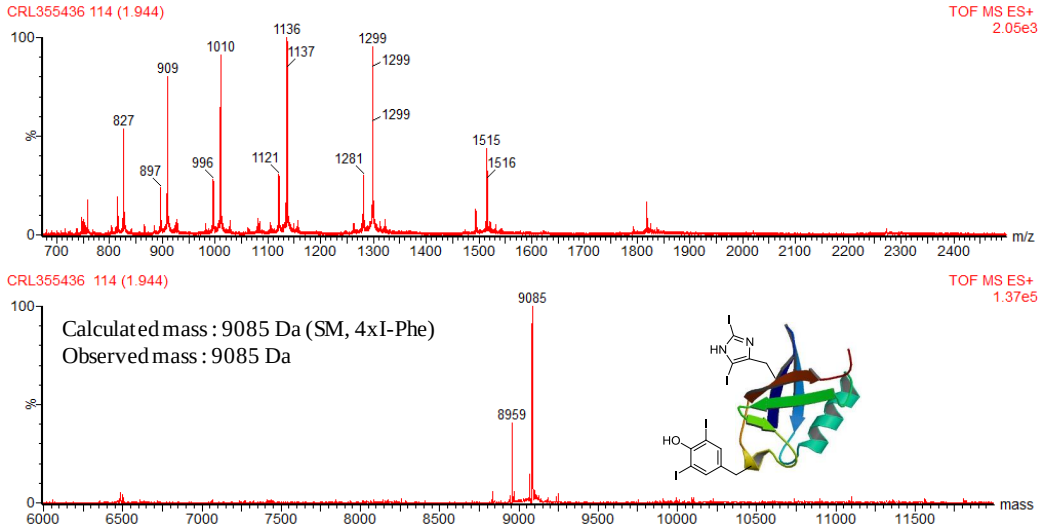

Figure 4.55 ESI-MS spectrum of the iodo-Tyr/His ubiquitin treated with 50 equiv. $[\mathbf{L2}]_2Pd(OAc)_2$ and 500 equiv. 3-isoxazolylboronic acid.

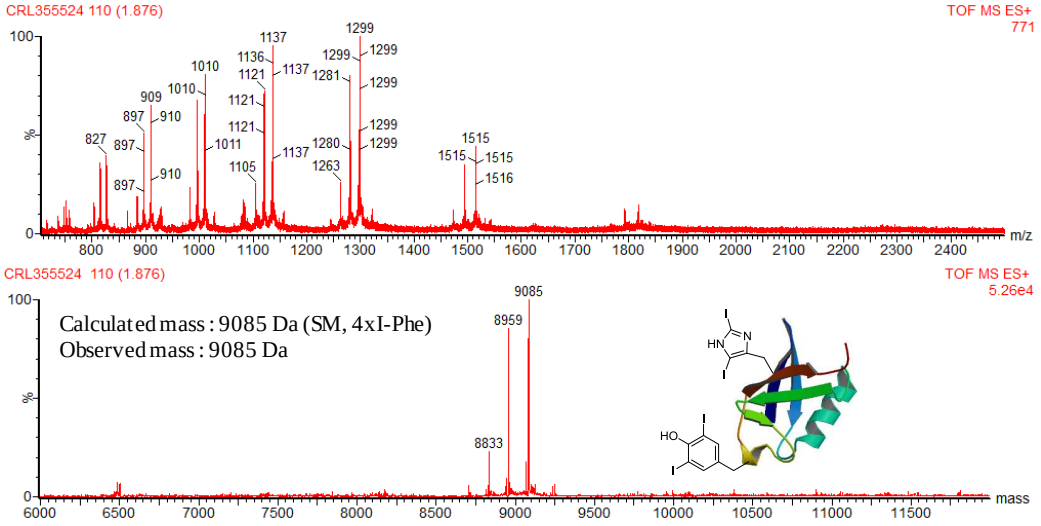

Figure 4.56 ESI-MS spectrum of the iodo-Tyr/His ubiquitin treated with 50 equiv. [**L2**]$_2$Pd(OAc)$_2$ and 500 equiv. 3-pyridinylboronic acid.

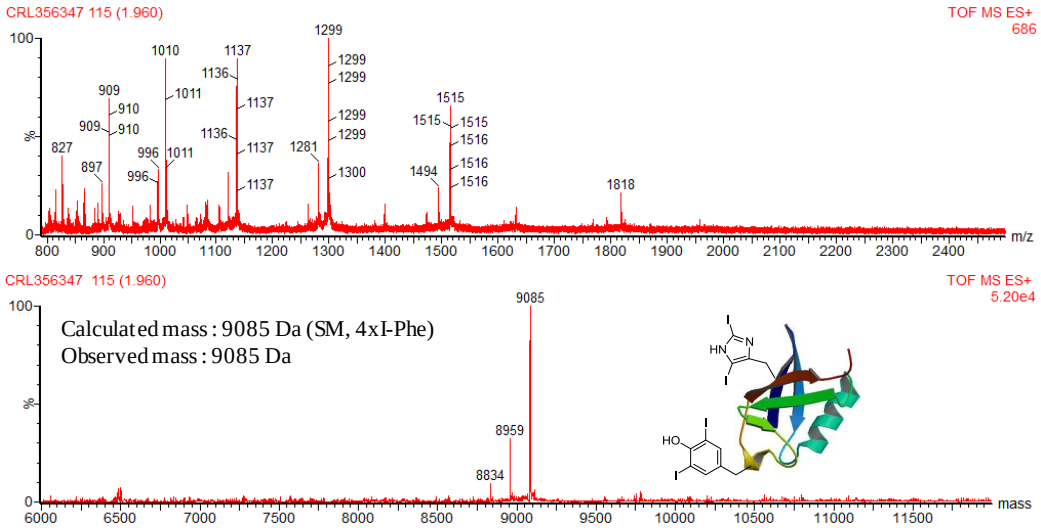

Figure 4.57 ESI-MS spectrum of the iodo-Tyr/His ubiquitin treated with 50 equiv. [**L2**]$_2$Pd(OAc)$_2$ and 500 equiv. 5-pyrimidinylboronic acid.

Effect of non-aromatic boronic acids

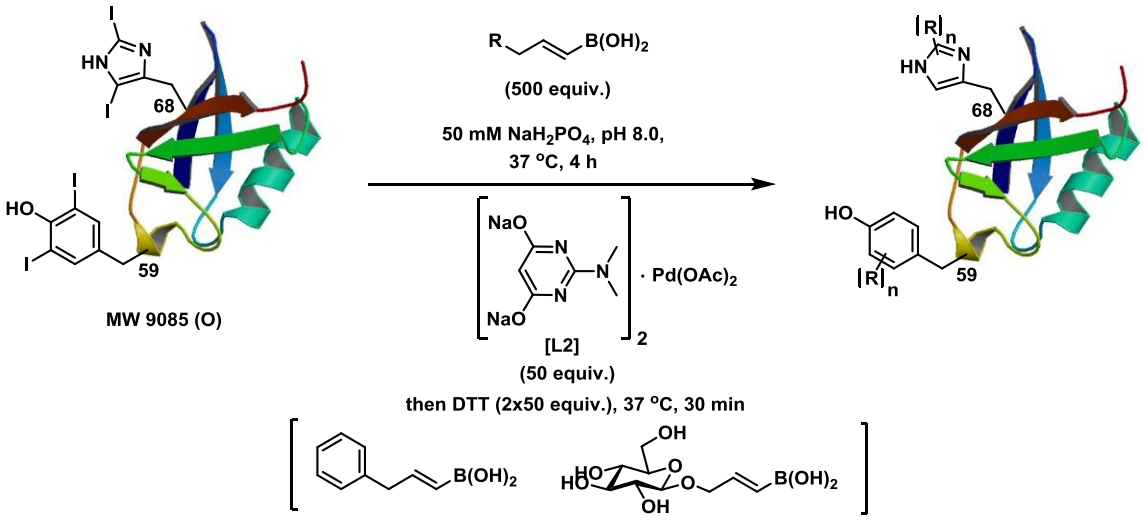

Each aliquot of the iodo-Tyr/His UBQ (3.3 nmol, 1.50 mg/mL, 20 µL) in 50 mM NaH_2PO_4, pH 8.0 was mixed with a solution of R-$B(OH)_2$ in a ratio of 1:3 DMF/50 mM NaH_2PO_4 mixture for R = phenyl, and in 50 mM NaH_2PO_4 mixture for R = glucosyl (1,650 nmol, 4-5 µL from stock solution, conc. 50.0 mg/mL for phenyl and conc. 100.0 mg/mL for glucosyl) by vortexing briefly. A [**L2**]$_2$Pd$(OAc)_2$ catalyst solution (165 nmol, 16.5 µL, conc. 0.01 M) was added to each reaction mixture which was vortexed briefly. After 4 h. of shaking at 37°C, each aliquot was analysed by LC–MS after addition of DTT solution in H_2O (2xtimes) (165 nmol, 1.25 µL, from stock solution, conc. 20.0 mg/mL) and stirring at 37 °C for 30 min. Protein samples were flash frozen with liquid nitrogen and stored at –20 °C.

Entry	Iodo-UBQ (equiv.)	PhB$(OR)_2$ (equiv.)	[L2]$_2$Pd$(OAc)_2$ (equiv.)	Products (Da)
1	1	500 (R = Phenyl)	50	8930 (2xpropenyl+O) 9046 (3xpropenyl+O) 8940 (1xI+2xpropenyl+O) 8949 (2xI+1xpropenyl+O) 9056 (1xI+3xpropenyl+O) 9066 (2xI+2xpropenyl+O) 9075 (3xI+1xpropenyl+O)
2	1.	500 (R = Glucosyl)	50	Protein degraded

General conditions: iodo-Tyr/His UBQ in NaH_2PO_4 (50 mM, pH 8), R-PhB$(OH)_2$ in 1:3 DMF/NaH_2PO_4 and 0.01 M [**L2**]$_2$Pd$(OAc)_2$ in NaOH at 37 °C for 4 h, unless otherwise indicated. O = Oxidised methionine

Table 4.13 Investigation of Suzuki-Miyaura cross-couplings of the iodo-Tyr/His ubiquitin with alkenyl boronic acids.

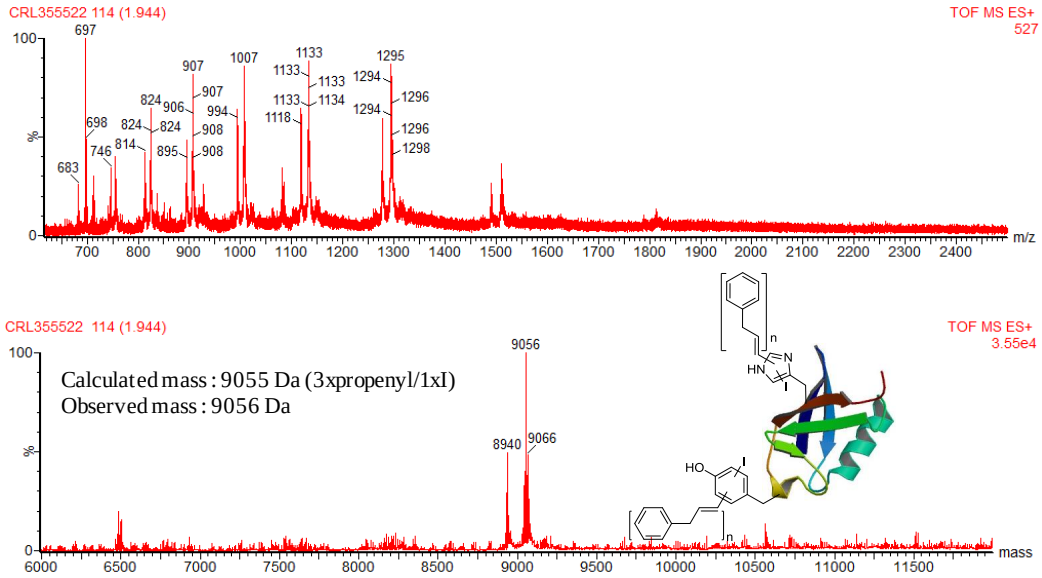

Figure 4.58 ESI-MS spectrum of the iodo-Tyr/His ubiquitin treated with 50 equiv. [**L2**]$_2$Pd(OAc)$_2$ and 500 equiv. trans-3-phenyl-1-propenylboronic acid.

Effect of fluorescent boronic acids

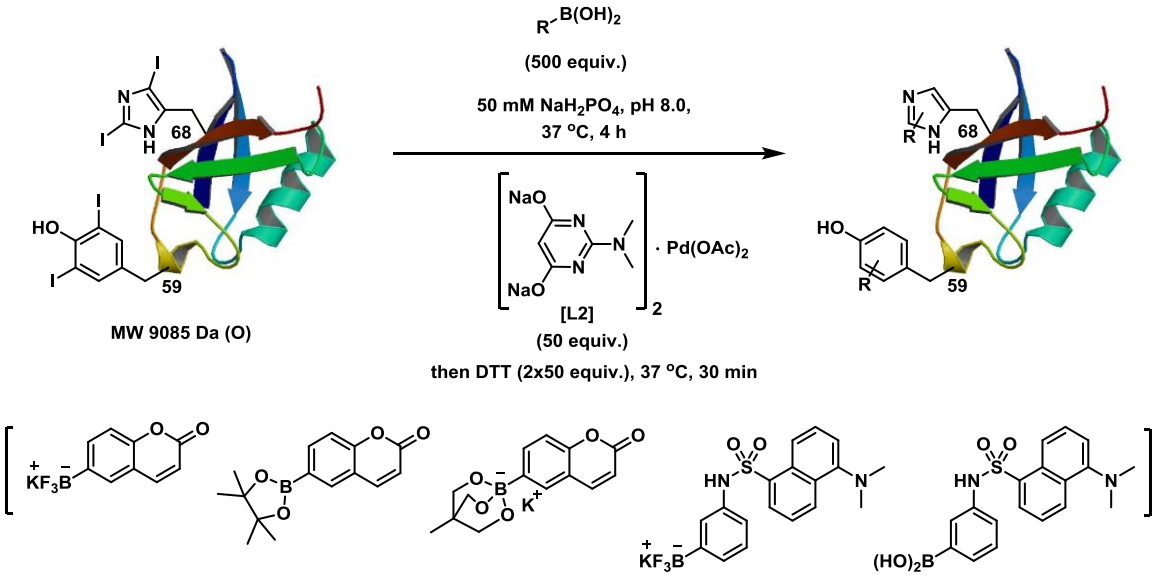

Each aliquot of the iodo-Tyr/His UBQ (3.3 nmol, 1.50 mg/mL, 20 µL) in 50 mM NaH_2PO_4, pH 8.0 was mixed with a solution of R-$B(OH)_2$ in pure DMF for R = coumarinyl dye, and in an 1:3 DMF/50 mM NaH_2PO_4 mixture for R = dansyl dye (1,650 nmol, 4-5 µL from stock solution, conc. 100.0 mg/mL for coumarinyl dye and conc. 150.0 mg/mL for dansyl dye) by vortexing briefly. A [**L2**]$_2$Pd(OAc)$_2$ catalyst solution (165 nmol, 16.5 µL, conc. 0.01 M) was added to each reaction mixture which was

vortexed briefly. After 4 h. of shaking at 37°C, each aliquot was analysed by LC–MS after addition of DTT solution in H_2O (2xtimes) (165 nmol, 1.25 µL, from stock solution, conc. 20.0 mg/mL) and stirring at 37 °C for 30 min. Protein samples were flash frozen with liquid nitrogen and stored at –20 ºC.

Entry	**Iodo-UBQ (equiv.)**	**$PhB(OR)_2$ (equiv.)**	**$[L2]_2Pd(OAc)_2$ (equiv.)**	**Products (Da)**
1	1	500 R = Coumarinyl (BF_3K)	50	Protein degraded
2	1	500 R = Coumarinyl (Pinacol ester)	50	8726 (1xCou+O) 8870 (2xCou+O) 9014 (3xCou+O) 9159 (4xCou+O)
3	1	500 R = Coumarinyl (Cyclictriolborate)	50	8870 (2xCou+O) 9014 (3xCou+O) 9158 (4xCou+O)
4	1	500 R = Dansyl (BF_3K)	50	Protein degraded
5	1	500 R = Dansyl ($B(OH)_2$)	50	Protein degraded

General conditions: iodo-Tyr/His UBQ in NaH_2PO_4 (50 mM, pH 8), R-$PhB(OH)_2$ in DMF or 1:3 DMF/NaH_2PO_4 and 0.01 M [**L2**]$_2Pd(OAc)_2$ in NaOH at 37 ^oC for 4 h, unless otherwise indicated. O = Oxidised methionine

Table 4.14 Investigation of Suzuki-Miyaura cross-couplings of the iodo-Tyr/His ubiquitin with fluorescent-coumarinyl/dansyl boronic acids.

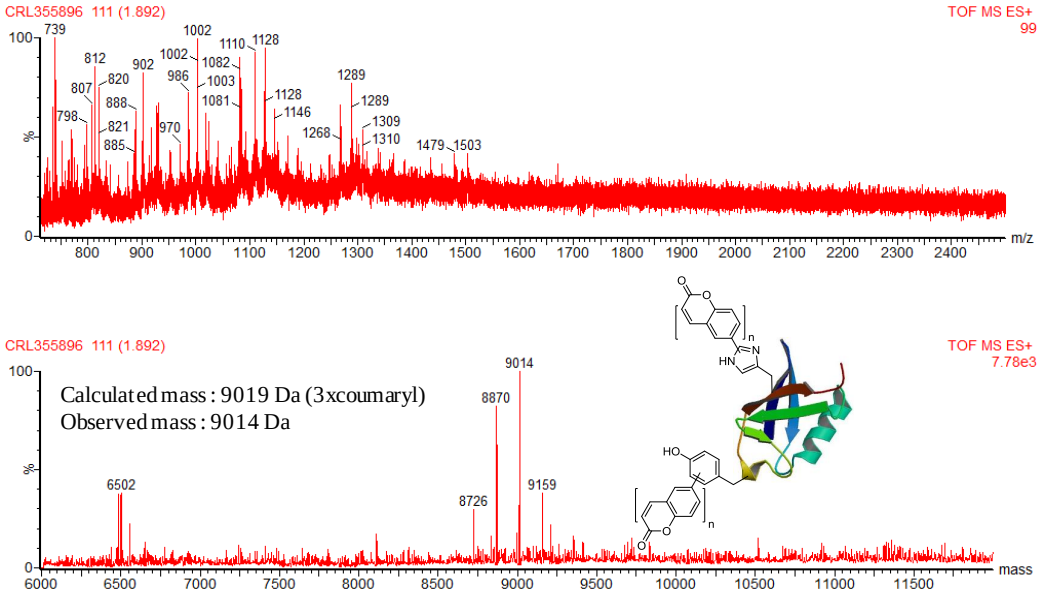

Figure 4.59 ESI-MS spectrum of the iodo-Tyr/His ubiquitin treated with 50 equiv. $[\mathbf{L2}]_2Pd(OAc)_2$ and 500 equiv. coumarinyl-6-boronic acid pinacol ester.

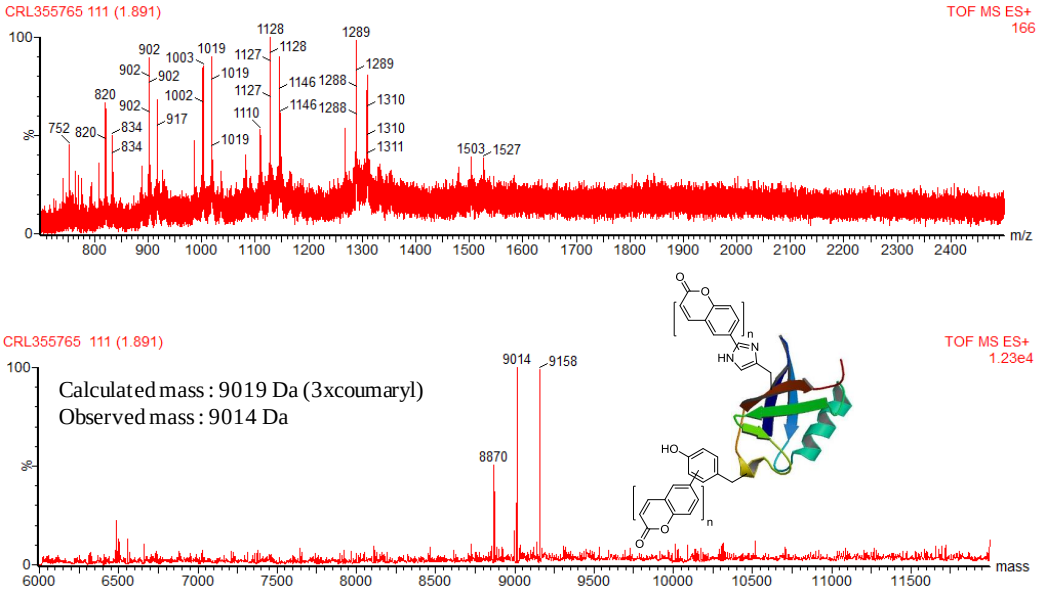

Figure 4.60 ESI-MS spectrum of the iodo-Tyr/His ubiquitin treated with 50 equiv. $[\mathbf{L2}]_2Pd(OAc)_2$ and 500 equiv. potassium coumarinyl-6-cyclic triolborate.

4.6.3 Aqueous Sonogashira Cross-Coupling Reactions

Effect of different ligands of palladium catalysts

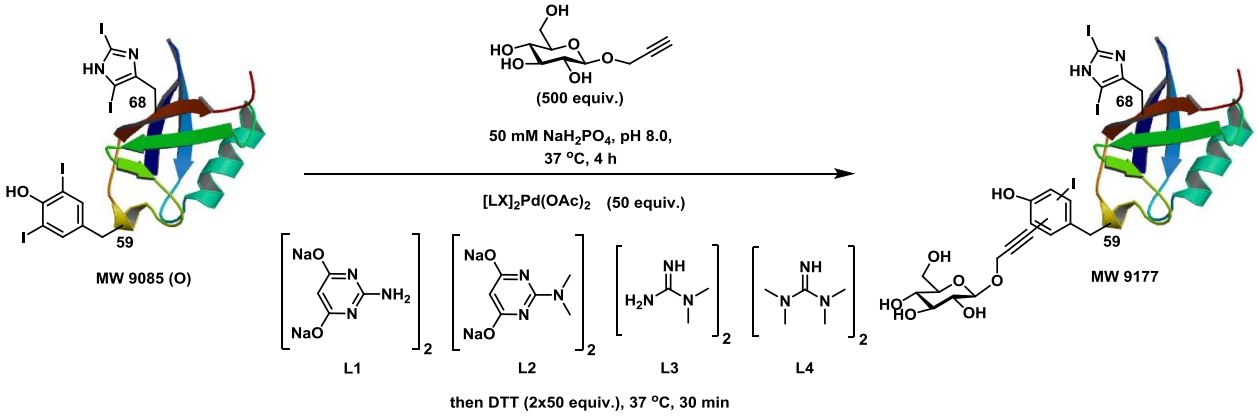

Each aliquot of the iodo-Tyr/His UBQ (3.3 nmol, 1.50 mg/mL, 20 µL) in 50 mM NaH_2PO_4 and 80 mM sodium ascorbate, pH 8.0 was mixed with a solution of 1-propargyl-β-D-glucopyranose in H_2O (1,650 nmol, 5.1 µL from stock solution, conc. 70.0 mg/mL) by vortexing briefly. Each $[\mathbf{LX}]_2Pd(OAc)_2$ catalyst solution (165 nmol, 16.5 µL, conc. 0.01 M) was added to each reaction mixture which was vortexed briefly. After 4 h. of shaking at 37°C, each aliquot was analysed by LC–MS after addition of DTT solution in H_2O (2xtimes) (165 nmol, 1.25 µL, from stock solution, conc. 20.0 mg/mL) and stirring at 37 °C for 30 min. Protein samples were flash frozen with liquid nitrogen and stored at –20 °C.

Entry	Iodo-UBQ (equiv.)	Glu-alkyne (equiv.)	$[LX]_2Pd(OAc)_2$ (equiv.)	Conversion products (%)
1	1	500	50	9085 Da (4xI+O) (72)
			L1	9177 Da (3xI+O+glu-alkyne) (28)
2	1	500	50	9085 Da (4xI+O) (56)
			L2	9177 Da (3xI+O+glu-alkyne) (44)
3	1	500	50	9085 Da (4xI+O) (74)
			L3	9177 Da (3xI+O+glu-alkyne) (26)
4	1	500	50	9085 Da (4xI+O) (68)
			L4	9177 Da (3xI+O+glu-alkyne) (32)
5	1	500	-	9086 Da (4xI+O)

General conditions: iodo-Tyr/His UBQ in NaH_2PO_4 (50 mM, pH 8), propargyl-*O*-glucose in H_2O and 0.01 M $[\mathbf{LX}]_2Pd(OAc)_2$ in NaOH at 37 °C for 4 h, unless otherwise indicated.
O = Oxidised methionine

Table 4.15 Investigation of Sonogashira cross-couplings of the iodo-Tyr/His ubiquitin with 1-propargyl-β-D-glucopyranose in the presence of $[\mathbf{LX}]_2Pd(OAc)_2$ catalysts.

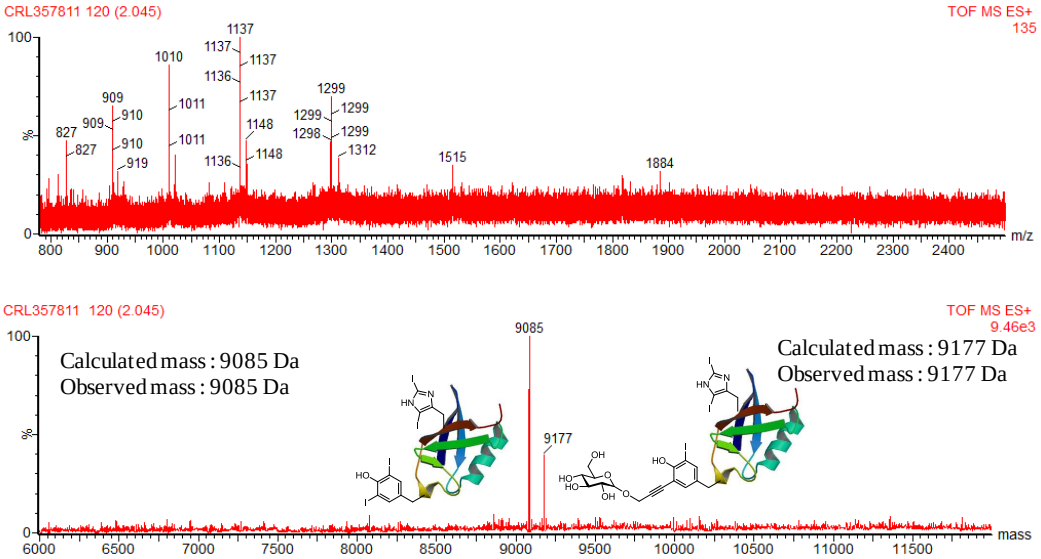

Figure 4.61 ESI-MS spectrum of the iodo-Tyr/His ubiquitin treated with 50 equiv. [**L1**]$_2$Pd(OAc)$_2$ and 500 equiv. 1-propargyl-β-D-glucopyranose.

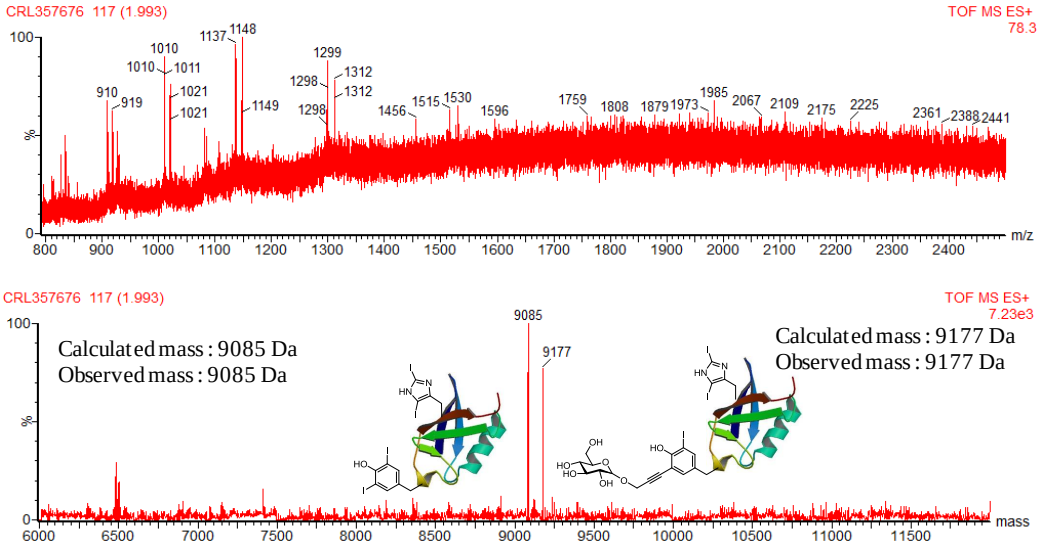

Figure 4.62 ESI-MS spectrum of the iodo-Tyr/His ubiquitin treated with 50 equiv. [**L2**]$_2$Pd(OAc)$_2$ and 500 equiv. 1-propargyl-β-D-glucopyranose.

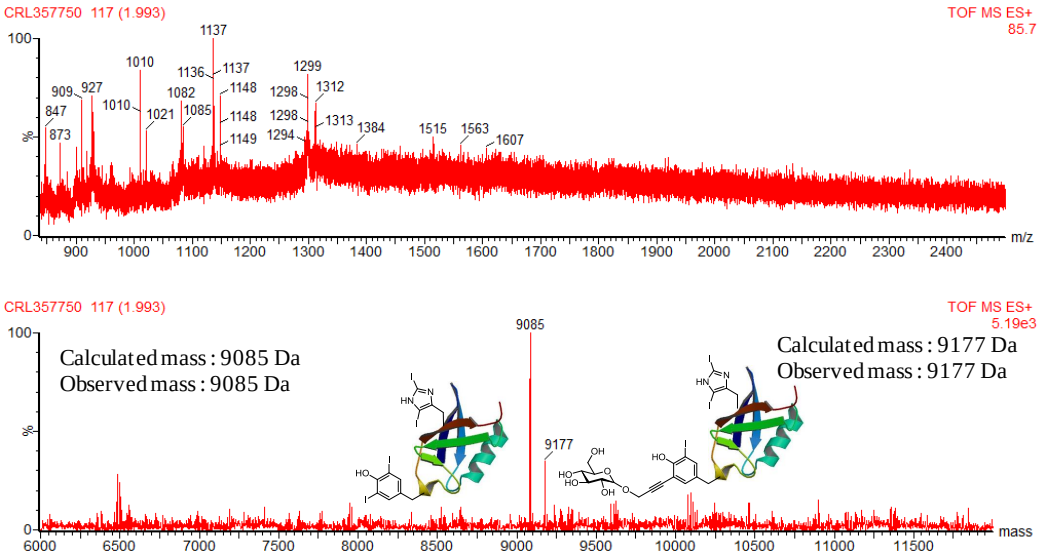

Figure 4.63 ESI-MS spectrum of the iodo-Tyr/His ubiquitin treated with 50 equiv. [**L3**]$_2$Pd(OAc)$_2$ and 500 equiv. 1-propargyl-β-D-glucopyranose.

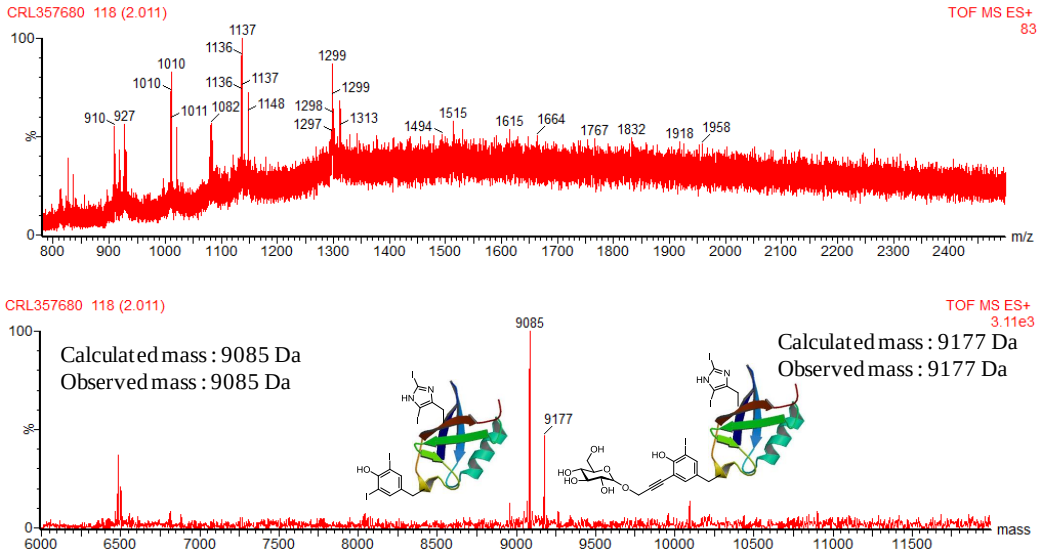

Figure 4.64 ESI-MS spectrum of the iodo-Tyr/His ubiquitin treated with 50 equiv. [**L4**]$_2$Pd(OAc)$_2$ and 500 equiv. 1-propargyl-β-D-glucopyranose.

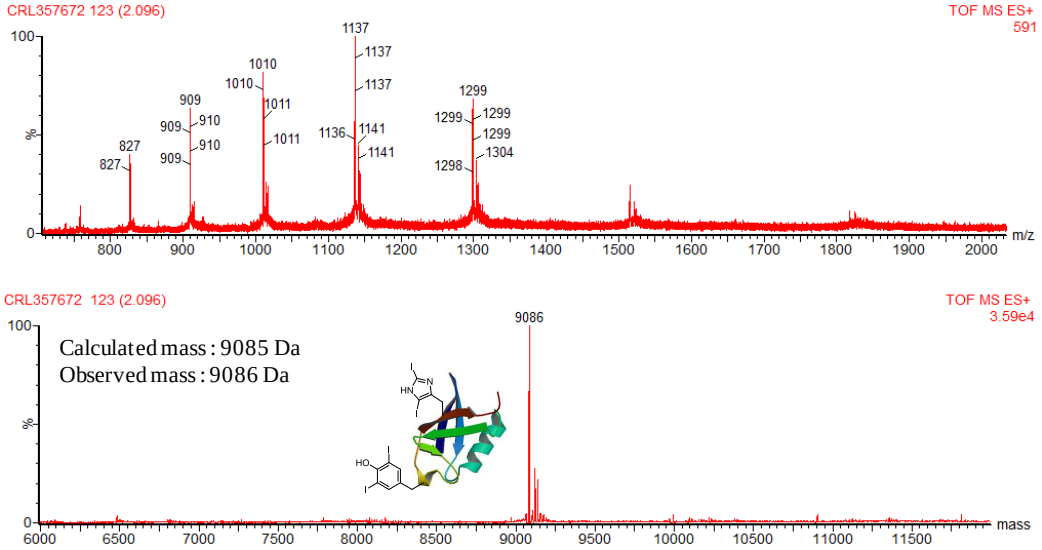

Figure 4.65 ESI-MS spectrum of the iodo-Tyr/His ubiquitin treated with 500 equiv. 1-propargyl-β-D-glucopyranose (control).

Effect of various amounts of alkyne and palladium catalyst

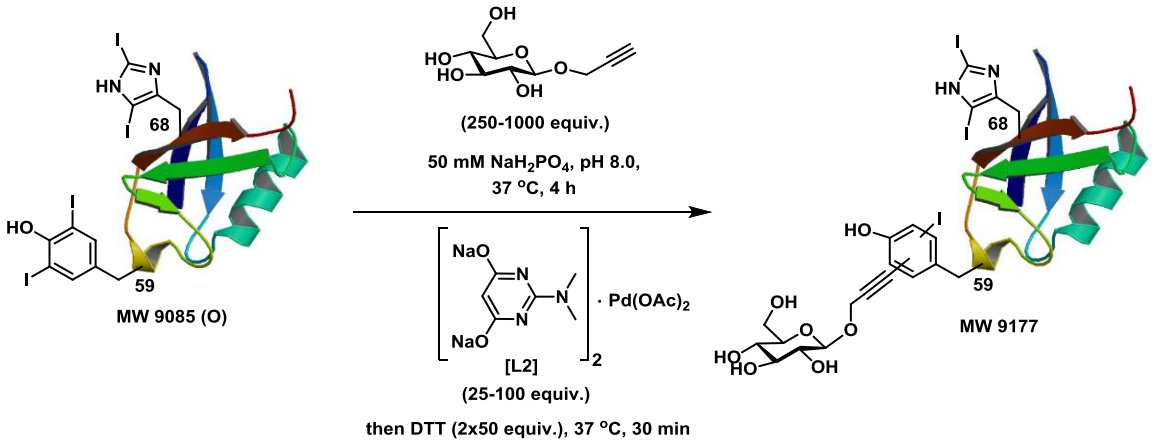

Each aliquot of the iodo-Tyr/His UBQ (3.3 nmol, 1.50 mg/mL, 20 µL) in 50 mM NaH_2PO_4 and 80 mM sodium ascorbate, pH 8.0 was mixed with a solution of 1-propargyl-β-D-glucopyranose in H_2O (0.82, 1.65, 2.47, 3.3 µmol, 1.8, 3.6, 5.4, 7.2 µL from stock solution, conc. 100.0 mg/mL) by vortexing briefly. A [**L2**]$_2$Pd(OAc)$_2$ catalyst solution (82, 165, 247, 330 nmol, 8.2, 16.5, 24.7, 33.0 µL, conc. 0.01 M) was added to each reaction mixture which was vortexed briefly. After 4 h. of shaking at 37°C, each aliquot was analysed by LC–MS after addition of DTT solution in H_2O (2xtimes) (82, 165, 247, 330 nmol, 0.65, 1.25, 1.87, 2.50 µL, from stock solution, conc. 20.0 mg/mL) and stirring at 37°C for 30 min. Protein samples were flash frozen with liquid nitrogen and stored at –20 °C.

Entry	Iodo-UBQ (equiv.)	Glu-alkyne (equiv.)	$[L2]_2Pd(OAc)_2$ (equiv.)	Products conversion (%)
1	1	250	25	9084 Da (4xI+O) (70) 9175 Da (3xI+O+glu-alkyne) (30)
2	1	500	50	9084 Da (4xI+O) (70) 9176 Da (3xI+O+glu-alkyne) (30)
3	1	750	75	9084 Da (4xI+O) (59) 9175 Da (3xI+O+glu-alkyne) (41)
4	1	1000	100	9084 Da (4xI+O) (62) 9176 Da (3xI+O+glu-alkyne) (38)

General conditions: iodo-Tyr/His UBQ in NaH_2PO_4 (50 mM, pH 8), propargyl-*O*-glucose in H_2O and 0.01 M $[\mathbf{L2}]_2Pd(OAc)_2$ in NaOH at 37 °C for 4 h, unless otherwise indicated.
O = Oxidised methionine / ESI-MS baseline subtracted

Table 4.16 Investigation of Sonogashira reactions of the iodo-Tyr/His ubiquitin with various amounts of 1-propargyl-β-D-glucopyranose in the presence of $[\mathbf{L2}]_2Pd(OAc)_2$.

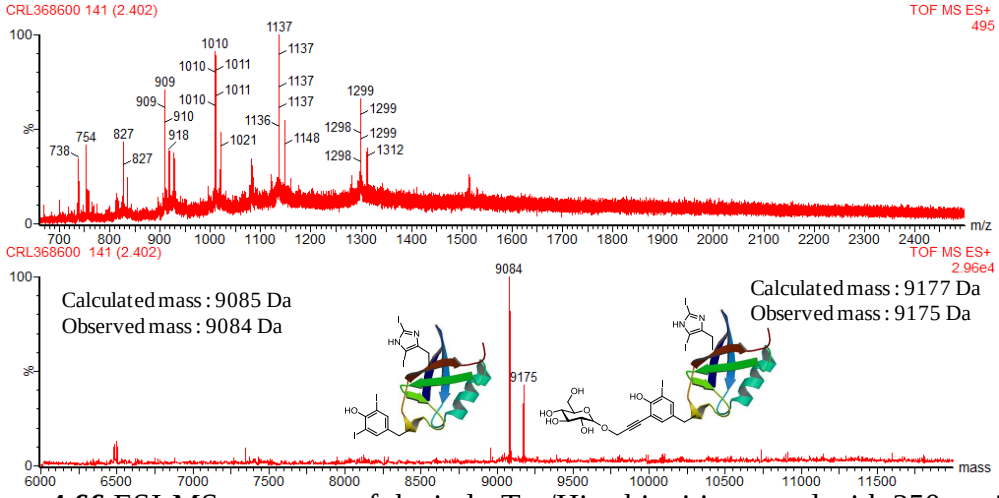

Figure 4.66 ESI-MS spectrum of the iodo-Tyr/His ubiquitin treated with 250 equiv. 1-propargyl-β-D-glucopyranose and 25 equiv. $[\mathbf{L2}]_2Pd(OAc)_2$.

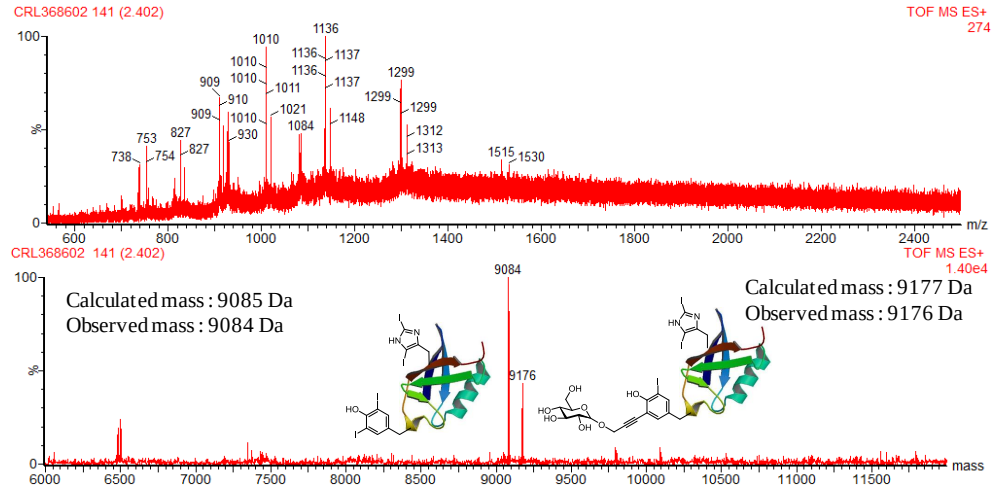

Figure 4.67 ESI-MS spectrum of the iodo-Tyr/His ubiquitin treated with 500 equiv. 1-propargyl-β-D-glucopyranose and 50 equiv. $[\mathbf{L2}]_2Pd(OAc)_2$.

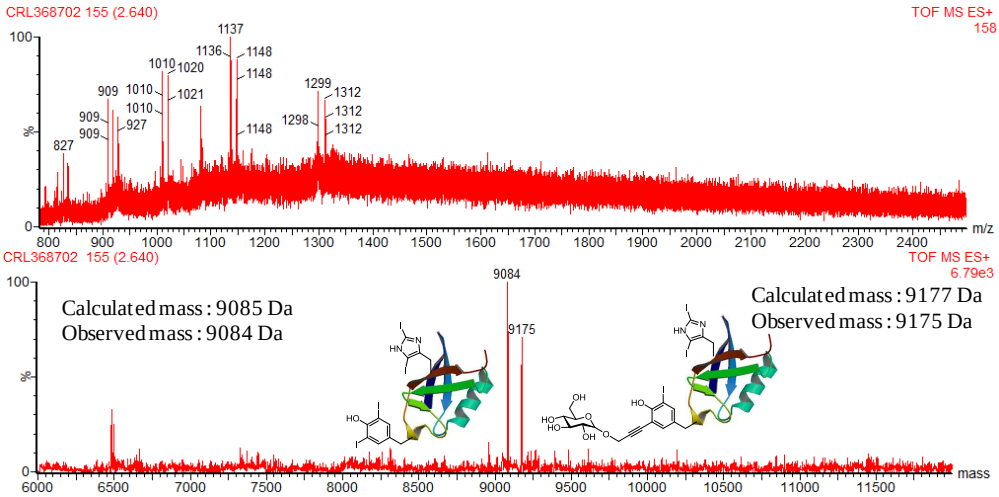

Figure 4.68 ESI-MS spectrum of the iodo-Tyr/His ubiquitin treated with 750 equiv. 1-propargyl-β-D-glucopyranose and 75 equiv. [**L2**]$_2$Pd(OAc)$_2$.

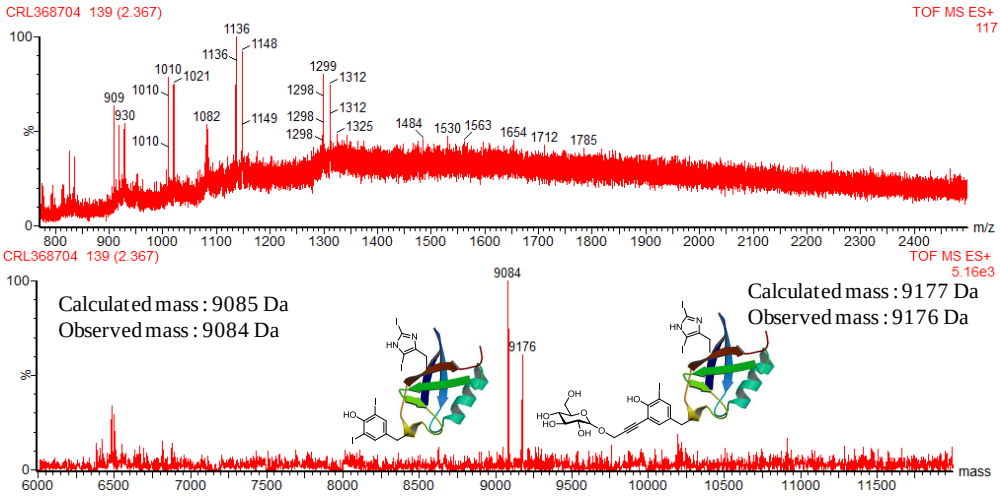

Figure 4.69 ESI-MS spectrum of the iodo-Tyr/His ubiquitin treated with 1000 equiv. 1-propargyl-β-D-glucopyranose and 100 equiv. [**L2**]$_2$Pd(OAc)$_2$.

Effect of Pd scavengers

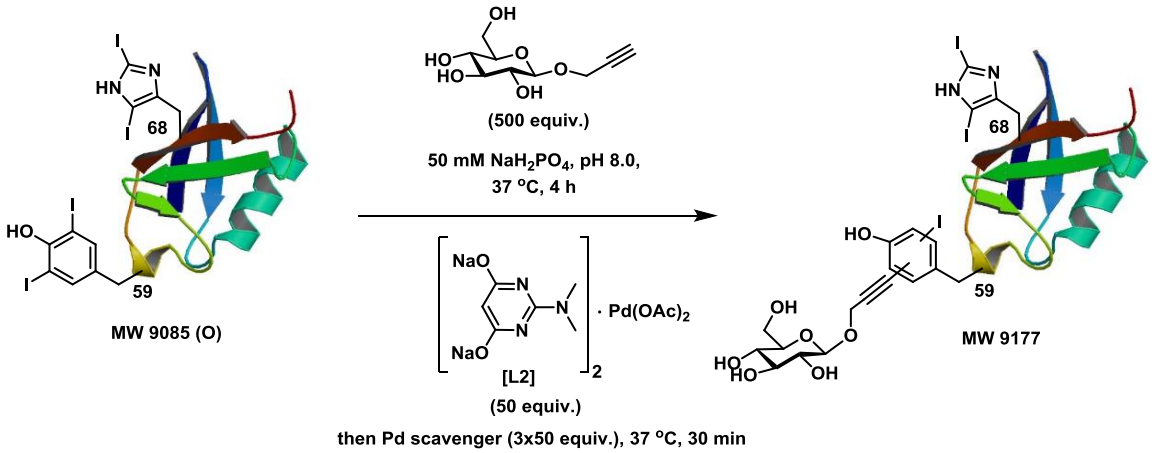

Each aliquot of the iodo-Tyr/His ubiquitin (3.3 nmol, 1.50 mg/mL, 20 µL) in 50 mM NaH_2PO_4 and 80 mM sodium ascorbate, pH 8.0 was mixed with a solution of 1-propargyl-β-D-glucopyranose in H_2O (1.65 µmol, 3.6 µL from stock solution, conc. 100.0 mg/mL) by vortexing briefly. A [**L2**]$_2$Pd(OAc)$_2$ catalyst solution (165 nmol, 16.5 µL, conc. 0.01 M) was added to each reaction mixture which was vortexed briefly. After 4 h. of shaking at 37°C, each aliquot was analysed by LC–MS after addition of different Pd scavengers (3xtimes) (1.25 µL, from DTT stock solution, conc. 20.0 mg/mL, 0.45 mg of QuadraSil MP, and 0.33 mg of QuadraSil AP) and stirring at 37°C for 30 min. Protein samples were flash frozen with liquid nitrogen and stored at –20 °C.

Entry	Iodo-UBQ (equiv.)	Alkyne (equiv.)	[L2]$_2$Pd(OAc)$_2$ (equiv.)	Scavenger (equiv.)	Remarks
1	1	500	50	150 (DTT)	Protein Cleavage
2	1	500	50	150 (QuadraSil MP) 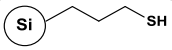	-
3	1	500	50	150 (QuadraSil AP) 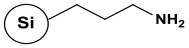	-

General conditions: iodo-Tyr/His UBQ in NaH_2PO_4 (50 mM, pH 8), propargyl-*O*-glucose in H_2O and 0.01 M [**L2**]$_2$Pd(OAc)$_2$ in NaOH at 37 °C for 4 h, unless otherwise indicated.
O = Oxidised methionine / ESI-MS baseline subtracted

Table 4.17 Investigation of Pd scavengers for Sonogashira reactions of iodo-Tyr/His ubiquitin with 1-propargyl-β-D-glucopyranose in the presence of [**L2**]$_2$Pd(OAc)$_2$.

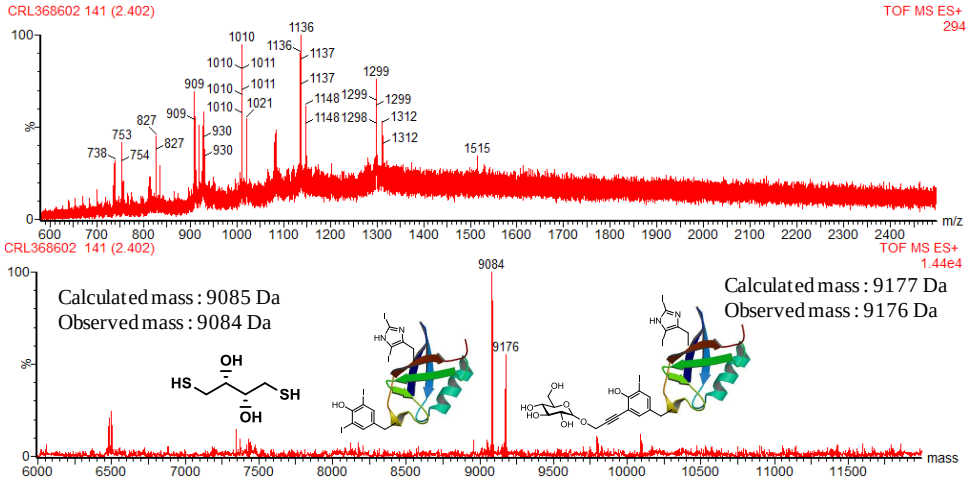

Figure 4.70 ESI-MS spectrum of the iodo-Tyr/His ubiquitin treated with 500 equiv. 1-propargyl-β-D-glucopyranose and 50 equiv. [**L2**]$_2$Pd(OAc)$_2$ (DTT as a Pd scavenger).

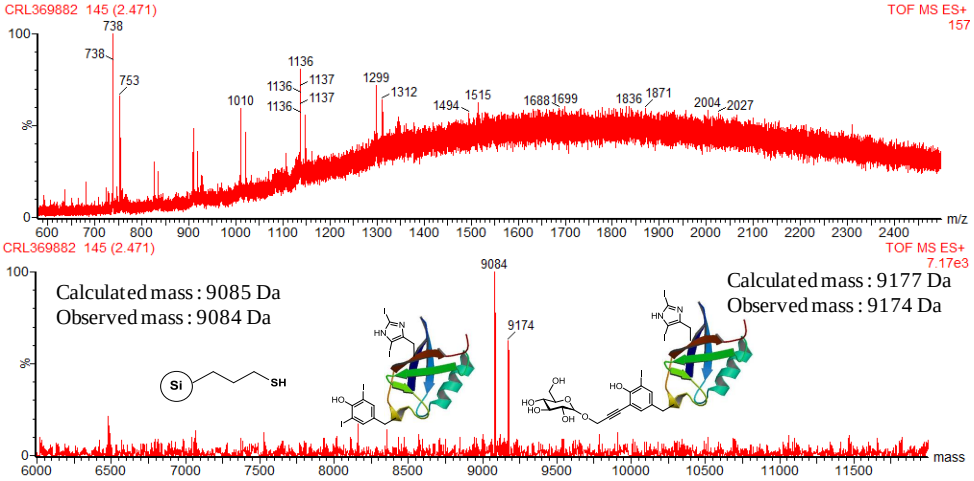

Figure 4.71 ESI-MS spectrum of the iodo-Tyr/His ubiquitin treated with 500 equiv. 1-propargyl-β-D-glucopyranose and 50 equiv. [**L2**]$_2$Pd(OAc)$_2$ (QuadraSil MP as a Pd scavenger).

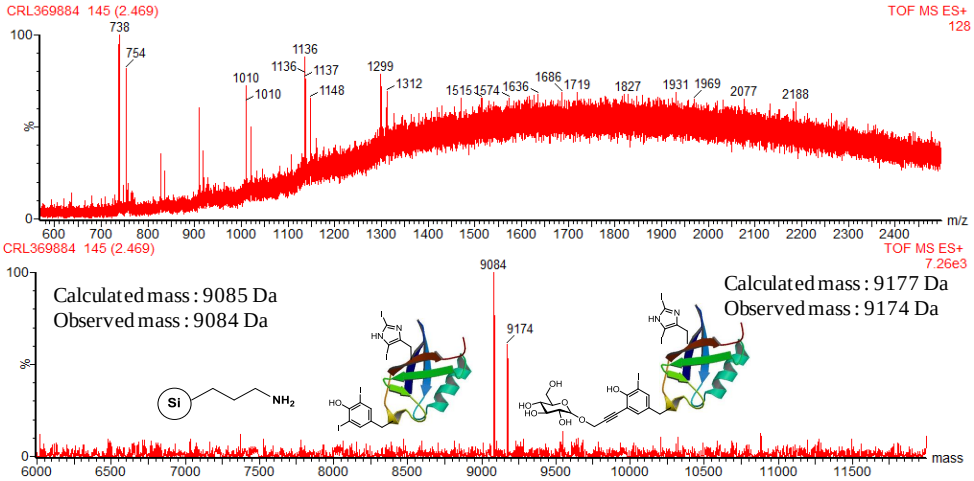

Figure 4.72 ESI-MS spectrum of the iodo-Tyr/His ubiquitin treated with 500 equiv. 1-propargyl-β-D-glucopyranose and 50 equiv. [**L2**]$_2$Pd(OAc)$_2$ (QuadraSil AP as a Pd scavenger).

4.6.4 Palladium-mediated Ubiquitination

L-Hpg incorporation into ubiquitin using Met-auxotroph, *E. coli* B834 (DE3)

1 µL of the plasmid DNA (WT-UbcH5)[29], conc. 100 ng/µL was transformed into Novagen *E.coli* B834 (DE3) single competent cells. The cells were next used to inoculate in LB media (5 mL) containing ampicillin (100 µg/mL), then were incubated overnight at 37 °C. These cells were plated on Agar/Amp plates and glycerol stocks being prepared were stored at -80 °C awaiting further manipulation. A single colony of ubiquitin bacterial cells was picked up and grown in a small starting culture of LB broth media (2.5 mL) containing ampicillin (100 µg/mL) at 37 °C overnight. For an expression of wild-type ubiquitin, the overnight starting culture (2.5 mL) was transferred into the 20 mL of LB media containing ampicillin (100 µg/mL). The cell cultures were incubated at 37 °C until an optical density value (OD_{600}) ~0.6-0.7 was observed. A protein expression was further induced by addition of 1 mM IPTG and further incubated at 37 °C for 4 h. In case L-Hpg incorporation, the starting culture was then used to inoculate 100 mL of SelenoMet base medium (21.6 g/L) containing 5 mL of nutrient mix (5.1 g/ 50mL), 0.4 mL of L-Met (10 mg/mL), and 0.1 mL of ampicillin (100 µg/mL). The cell cultures were incubated at 37 °C until an optical density value ($OD_{600)}$ ~0.6-0.7 was observed. Incubated cell cultures were briefly centrifuged (3,750 rpm, 10 min, 4 °C) and washed with SelenoMet base medium (3x15 mL) contain ampicillin only. The cell pellet was re-suspended in 50 mL of SelenoMet base medium containing 2.5 mL of nutrient mix, 1.0 mL of L-Hpg (50 mg/mL), and 0.05 mL of ampicillin, then was further incubated at 37 °C for 1h. The protein expression was induced by addition of 1 mM IPTG and further incubated at 37 °C for 4 h. Cell cultures were harvested by centrifugation (8,000 rpm, 15 min, 4 °C), and the cell pellet was re-suspended in 0.75 mL of Bugbuster Master mix solution, and 1/4 tablet of free-EDTA protease inhibitor. The cell suspension was shaken at rt for 1 h., and centrifuged (8,000 rpm, 15 min, 4 °C). Each protein supernatant was purified by a vivaspin column concentrator (10 kDa MW cut-off) first, then a flow-through was collected for a further purification using the vivaspin column concentrator (5 kDa MW cut-off) (5x times) loading a fresh 50 mM NaH_2PO_4, pH 8.0 each time. Final concentration of each purified protein was measured by NanoDrop 1000 A_{280}

spectrophotometry. Each modified protein was analysed by SDS-PAGE and LC-MS, then were flash frozen with liquid nitrogen and stored at -80 °C.

Sequence : Ubiquitin (UBQ)

XQIFVKTLTG KTITLEVEPS DTIENVKAKI QDKEGIPPDQ
QRLIFAGKQL EDGRTLSDYN IQKESTLHLV LRLRGG

X = Met (wild-type) or Hpq (alkyne)

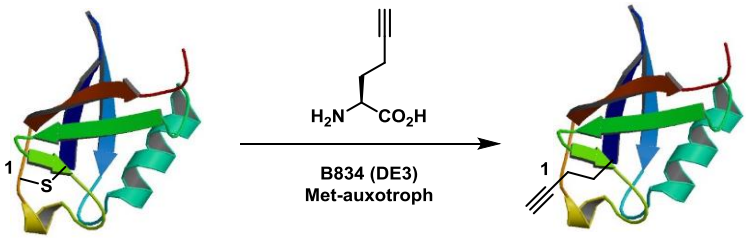

Entry	Met-auxotroph	Media	Additive	Incubation conditions	Results
1	B834 (DE3)	SelenoMet	L-Hpg	37 °C, 4 h	80% incorporation
2	B834 (DE3)	LB	-	37 °C, 4 h	-

Table 4.18 Protein expression systems for wild-type and modified ubiquitins (UBQ-1Hpg) expressed in *E.coli* B834 (DE3) as a Met-auxotroph.

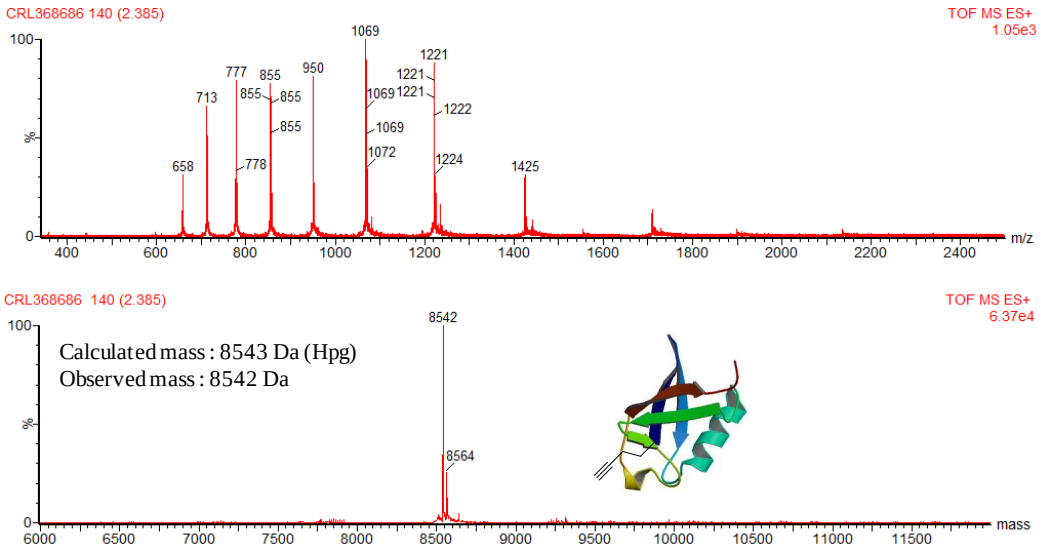

Figure 4.73 ESI-MS spectrum of the modified ubiquitin with *N*-terminal propargyl tag expressed in *E.coli* B834 (DE3) as a Met-auxotroph.

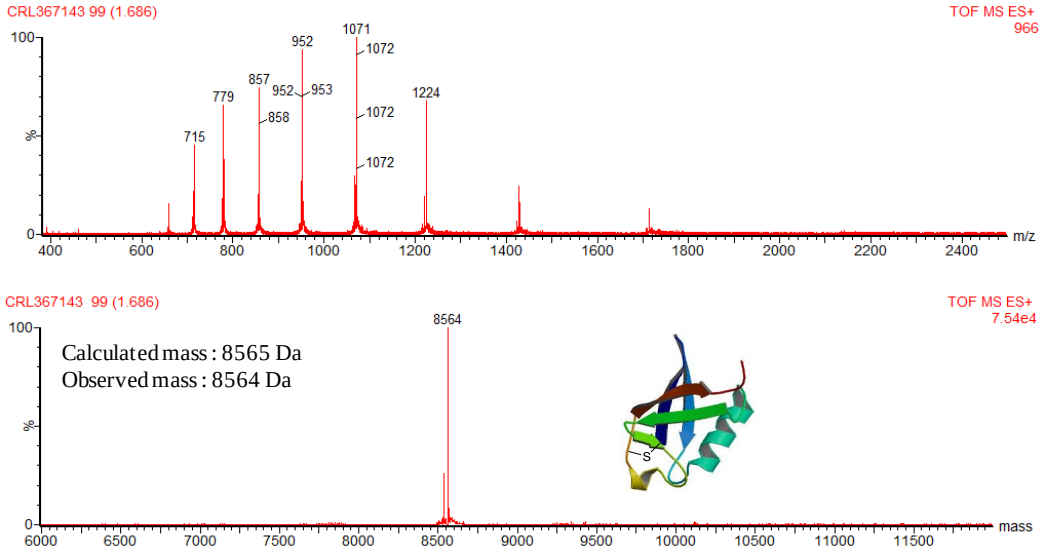

Figure 4.74 ESI-MS spectrum of wild-type ubiquitin expressed in *E.coli* B834 (DE3) as a Met-auxotroph.

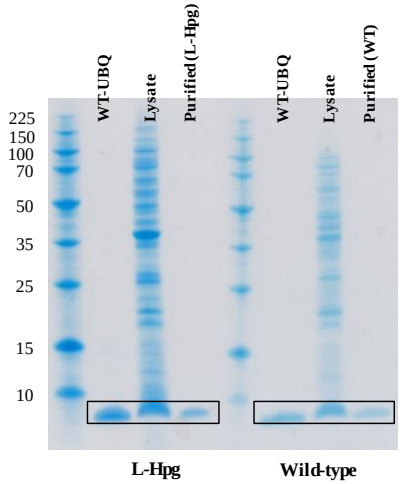

Figure 4.75 SDS-PAGEs show a purification of both wild-type/modified ubiquitin using 10kDa and 5 kDa MW cut-off vivaspin column concentrators, respectively.

Sonogashira cross-coupling of the GyG-Y195pIPhe with UBQ-M1Hpg

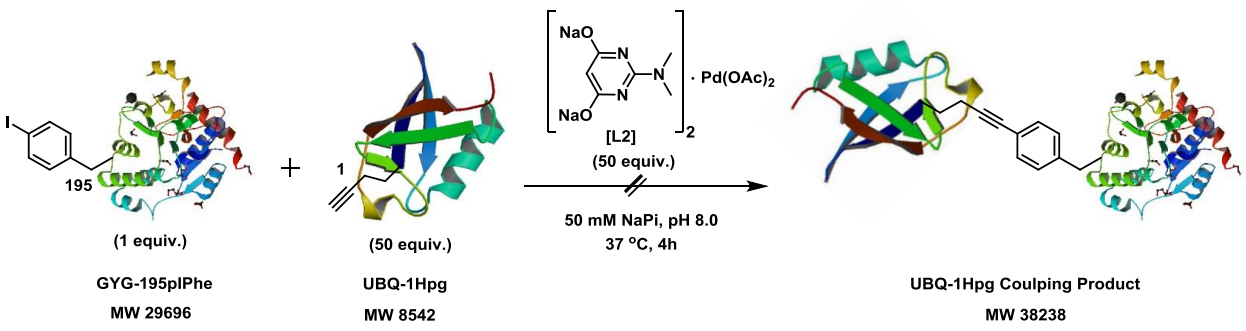

An aliquot of the GYG-Y195*p*IPhe (1.01 nmol, 1.50 mg/mL, 20 µL) in 50 mM NaH_2PO_4 and 80 mM sodium ascorbate, pH 8.0 was mixed with the UBQ-M1Hpg in 50 mM NaH_2PO_4 (50.5 nmol, 0.431 mg) by vortexing briefly. A $[\mathbf{L2}]_2Pd(OAc)_2$ catalyst solution (50.5 nmol, 5.0 µL, conc. 0.01 M) was added to the reaction mixture which was vortexed briefly. After 4 h. of shaking at 37 °C, an aliquot was analysed by LC–MS after addition of DTT solution (3xtimes) (0.39 µL, from stock solution, conc. 20.0 mg/mL) and stirred at 37 °C for 30 min. A protein sample was flash frozen with liquid nitrogen and stored at –20 ºC.

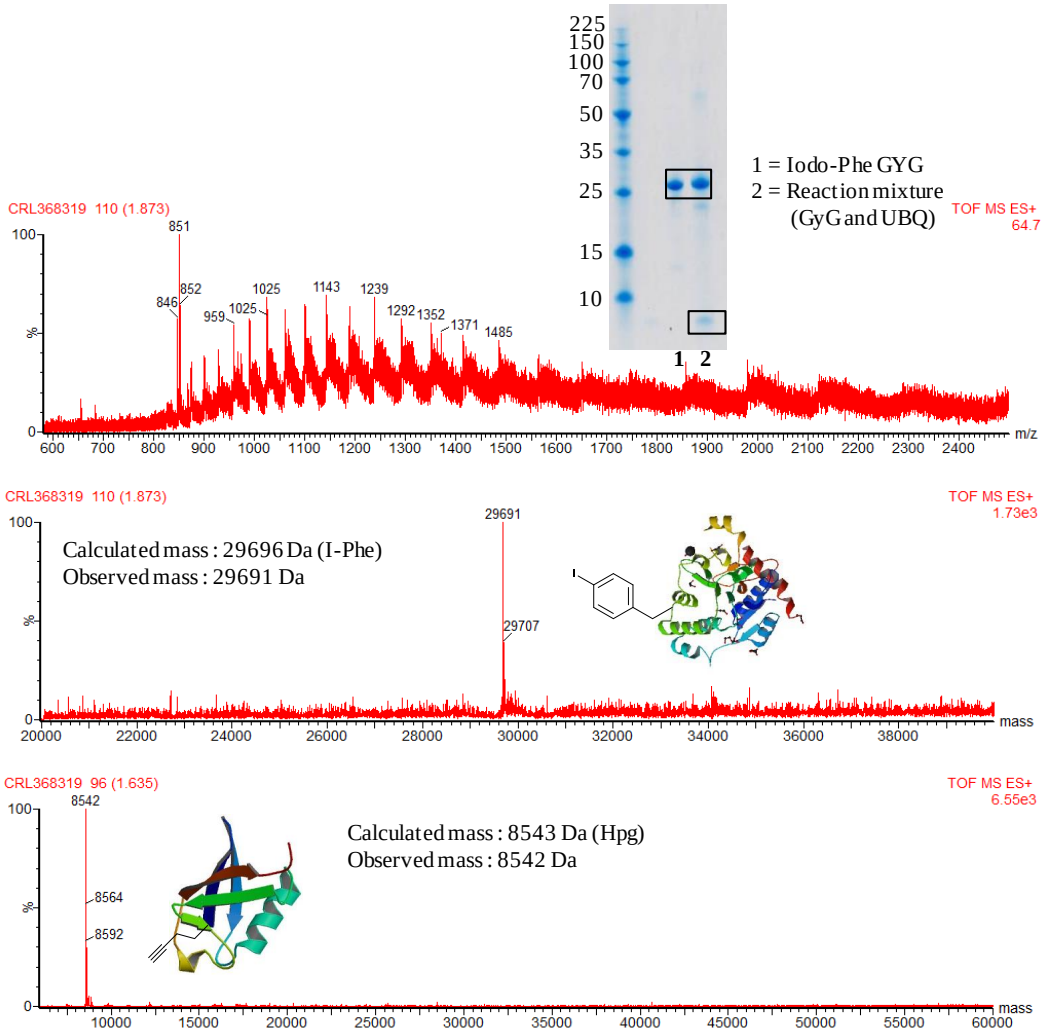

Figure 4.76 SDS-PAGE and ESI-MS spectrum of an attempted Pd-mediated cross-coupling of the GYG-195-pIPhe with UBQ-1Hpg.

Sonogashira cross-coupling of the MBP-E13pIPhe with UBQ-M1Hpg

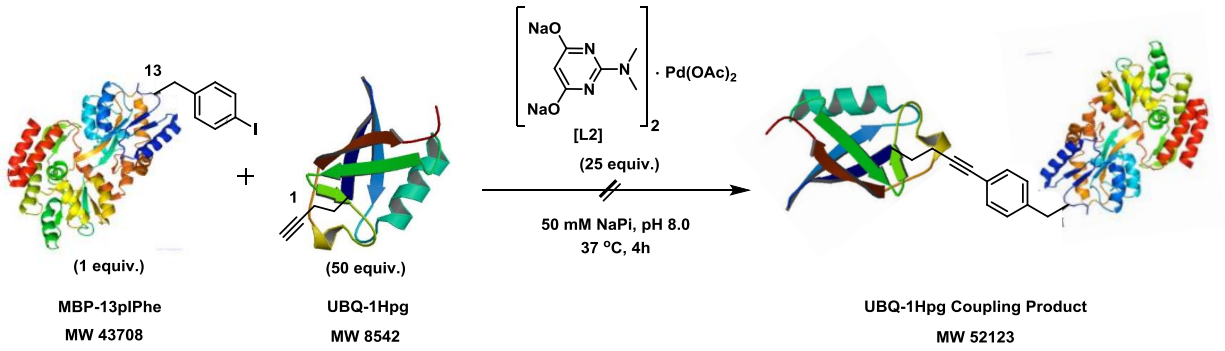

An aliquot of the MBP-E13pIPhe (1.14 nmol, 2.50 mg/mL, 20 µL) in 50 mM NaH_2PO_4 and 80 mM sodium ascorbate, pH 8.0 was mixed with the UBQ-M1Hpg in 50 mM NaH_2PO_4 (57.0 nmol, 14 µL from stock solution, conc. 35.0 mg/mL) by vortexing briefly. A $[\mathbf{L2}]_2Pd(OAc)_2$ catalyst solution (28.5 nmol, 2.9 µL, conc. 0.01 M) was added to the reaction mixture which was vortexed briefly. After 4 h. of shaking at 37 °C, an aliquot was analysed by LC–MS after addition of QuadraSil MP (1.50mg) and stirred at 37 °C for 30 min. A protein sample was flash frozen with liquid nitrogen and stored at –20 ºC.

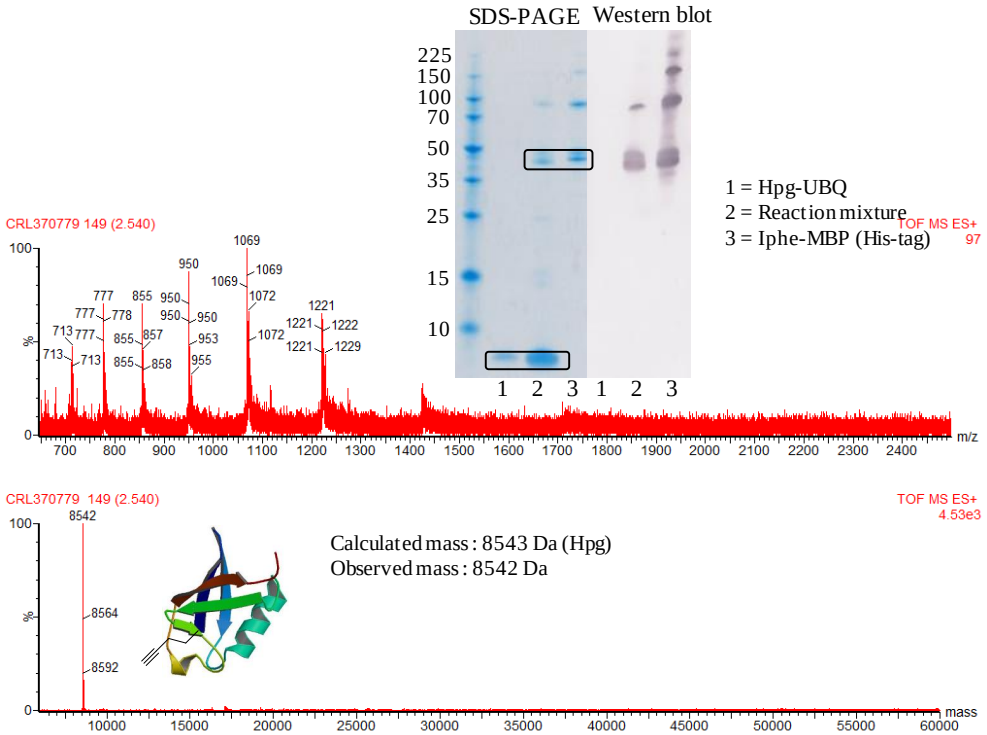

Figure 4.77 SDS-PAGE, Western blot (by monoclonal anti-polyhistidines alkaline phosphatase antibody) and ESI-MS spectrum of an attempted Pd-mediated cross-coupling of the MBP-E13pIPhe with UBQ-M1Hpg.

Sonogashira cross-coupling of the Iodo-Tyr/His UBQ with UBQ-M1Hpg

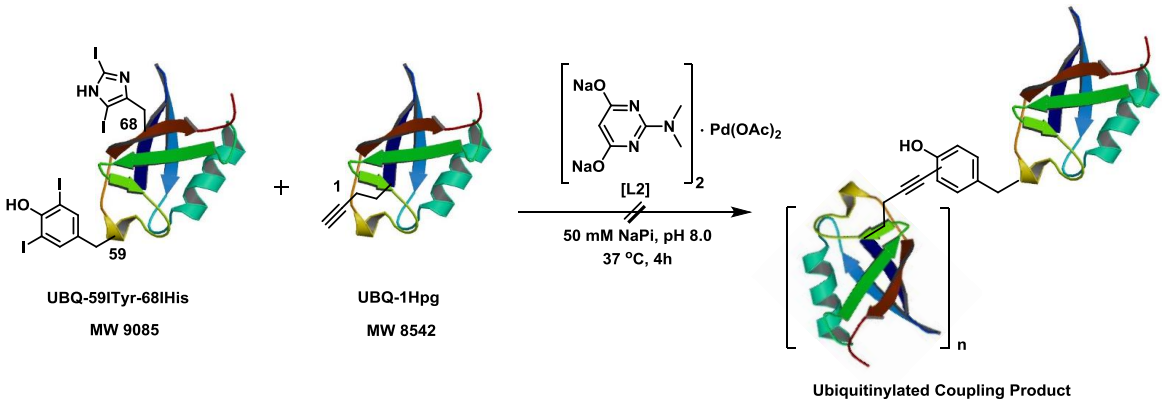

Each aliquot of the iodo-Tyr/His ubiquitin (3.30 nmol, 1.50 mg/mL, 20 µL) in 50 mM NaH_2PO_4 and 80 mM sodium ascorbate, pH 8.0 was mixed with the UBQ-M1Hpg in 50 mM NaH_2PO_4 (165.0, 330.0, 660.0 nmol, 17.6, 35.2, 70.5 µL from stock solution, conc. 80.0 mg/mL) by vortexing briefly. A [**L2**]$_2$Pd(OAc)$_2$ catalyst solution (16.5, 33.0, 66.0 nmol, 1.6, 3.3, 6.6 µL, conc. 0.01 M) was added to each reaction mixture which was vortexed briefly. After 4 h. of shaking at 37 °C, each aliquot was analysed by LC–MS after addition of DTT solution (3x 0.125, 0.25, 0.50 µL, from stock solution, conc. 20 mg/mL) and stirred at 37 °C for 30 min. Protein samples were flash frozen with liquid nitrogen and stored at –20 ºC.

Entry	Iodo-UBQ (equiv.)	Hpg-UBQ (equiv.)	PdL2 (equiv.)	Reaction conditions	Results
1	1	50	5	37 °C, 4 h	No detection of polyubiquitination
2	1	50	10		
3	1	100	10		
4	1	100	20		
5	1	200	20		
6	50	1	5		

General conditions : Iodo-Tyr/His UBQ in NaH_2PO_4 (50 mM, pH 8), UBQ-M1Hpg in NaH_2PO_4 (50 mM, pH 8), [**L2**]$_2$Pd(OAc)$_2$ in 0.1 M NaOH (c = 0.01 M) at 37 °C for 4h, unless otherwise indicated.

Table 4.19 Attempted Sonogashira cross-couplings of the iodo-Tyr/His ubiquitin and Hpg tagged ubiquitin.

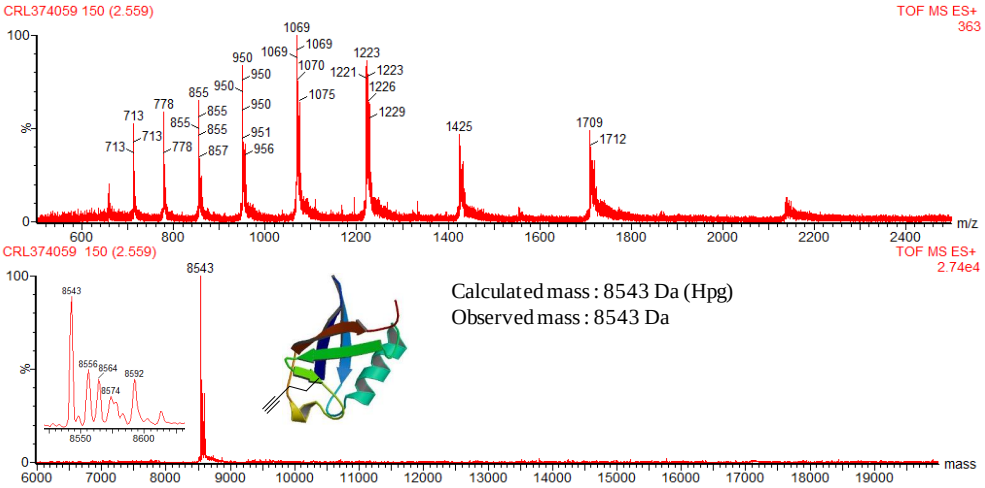

Figure 4.78 An attempted Sonogashira cross-coupling of the iodo-Tyr/His ubiquitin with Hpg-tagged ubiquitin (50 equiv.) and [**L2**]$_2$Pd(OAc)$_2$ catalyst (5 equiv.).

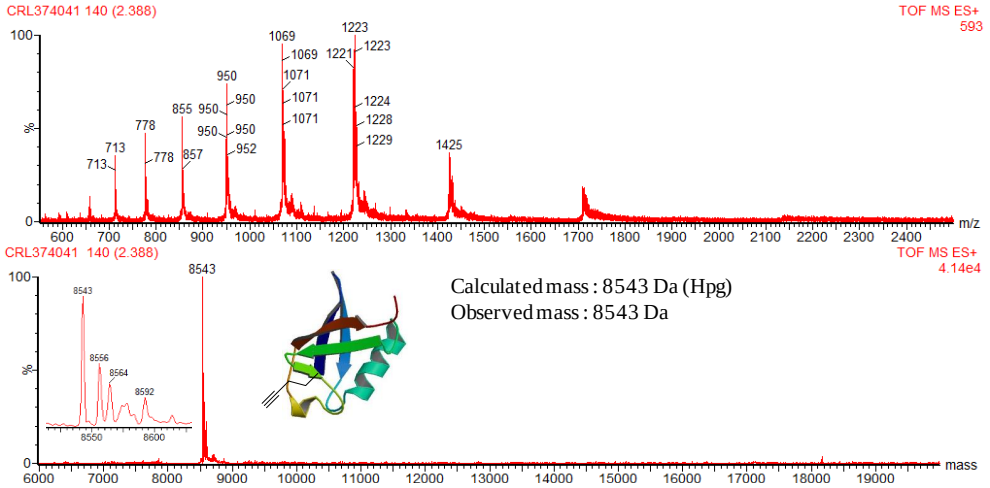

Figure 4.79 An attempted Sonogashira cross-coupling of the iodo-Tyr/His ubiquitin with Hpg-tagged ubiquitin (50 equiv.) and [**L2**]$_2$Pd(OAc)$_2$ catalyst (10 equiv.).

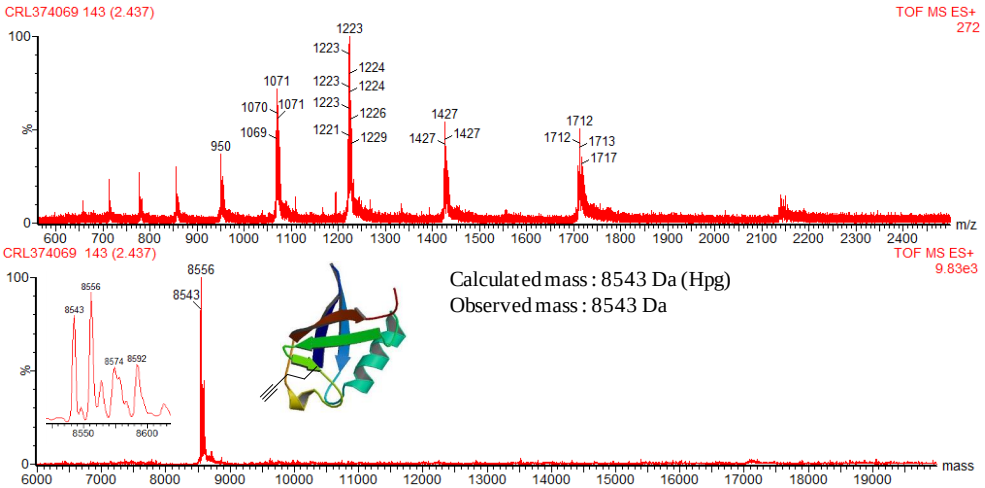

Figure 4.80 An attempted Sonogashira cross-coupling of the iodo-Tyr/His ubiquitin with Hpg-tagged ubiquitin (100 equiv.) and [**L2**]$_2$Pd(OAc)$_2$ catalyst (10 equiv.).

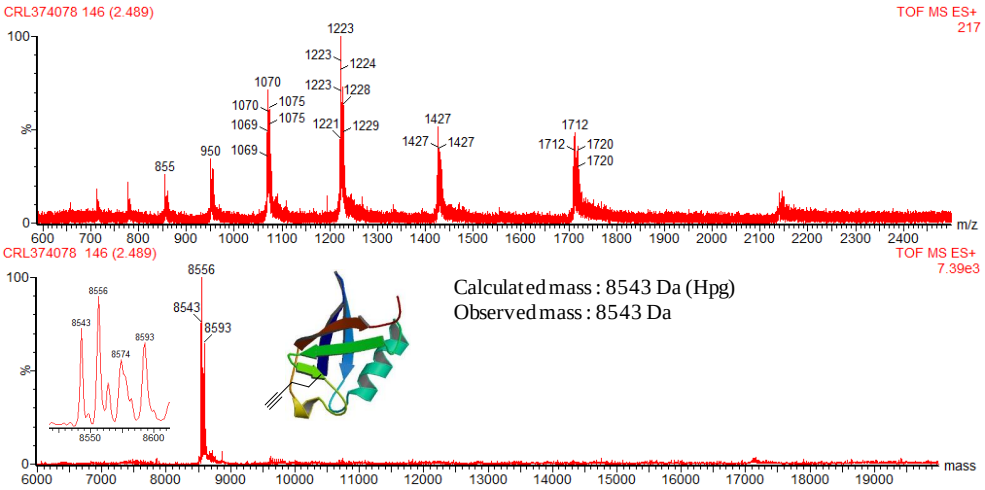

Figure 4.81 An attempted Sonogashira cross-coupling of the iodo-Tyr/His ubiquitin with Hpg-tagged ubiquitin (100 equiv.) and $[\mathbf{L2}]_2Pd(OAc)_2$ catalyst (20 equiv.).

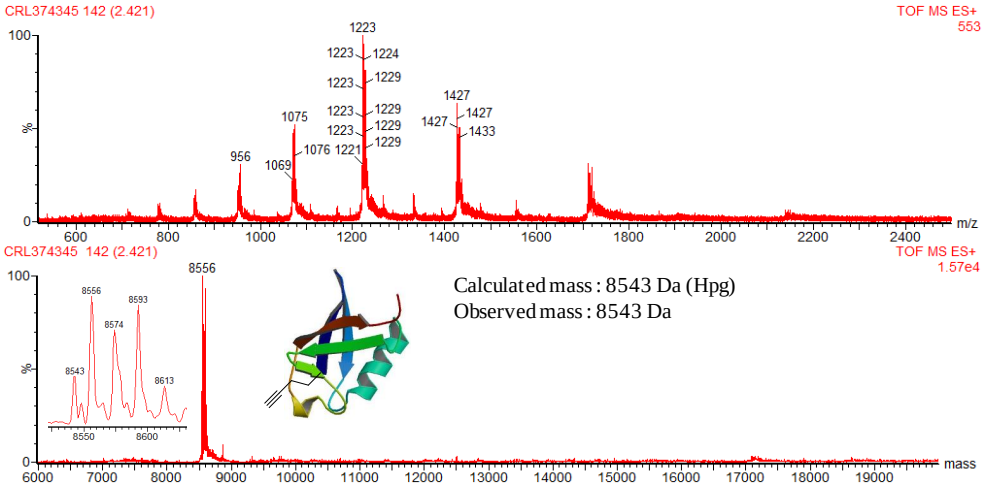

Figure 4.82 An attempted Sonogashira cross-coupling of the iodo-Tyr/His ubiquitin with Hpg-tagged ubiquitin (200 equiv.) and $[\mathbf{L2}]_2Pd(OAc)_2$ catalyst (20 equiv.).

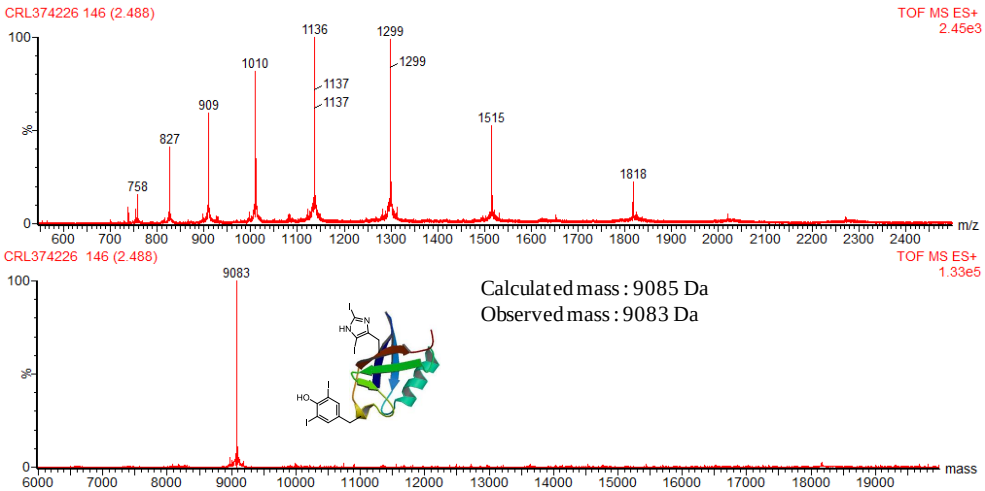

Figure 4.83 An attempted Sonogashira cross-coupling of the Hpg-tagged ubiquitin with iodo-Tyr/His ubiquitin (50 equiv.) and $[\mathbf{L2}]_2Pd(OAc)_2$ catalyst (5 equiv.).

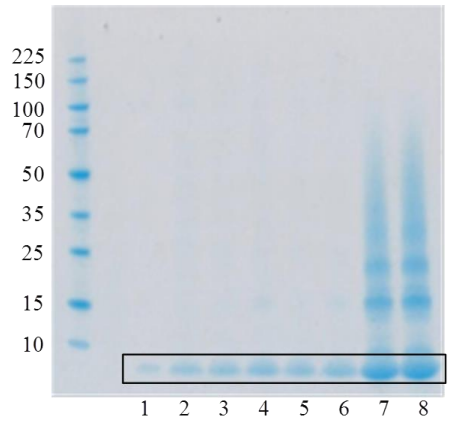

Figure 4.84 SDS-PAGE shows Hpg-tagged ubiquitin bands from each reaction mixture (Entry 2-6), on the other hand, the iodo-Tyr/His ubiquitin bands from the reaction mixture (Entry 7).

Control: Sonogashira cross-coupling of the Iodo-Tyr/His UBQ with propargyl-*o*-glucose

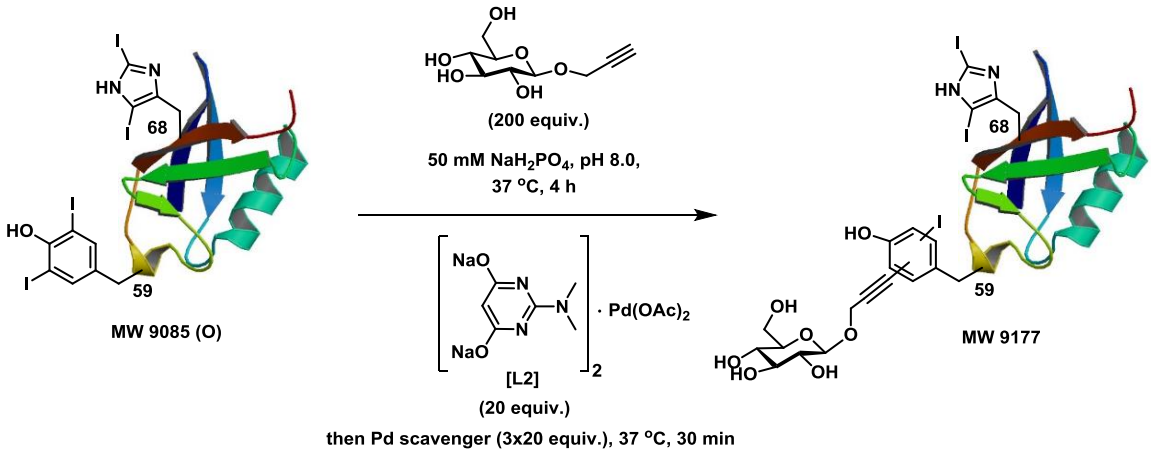

(Same procedure mentioned in section 4.6.3)

Entry	Iodo-UBQ (equiv.)	Glu-alkyne (equiv.)	$[L2]_2Pd(OAc)_2$ (equiv.)	Products conversion (%)
1	1	200	20	9084 Da (4xI+O) (64) 9176 Da (3xI+O+glu-alkyne) (36)
General conditions: iodo-Tyr/His UBQ in NaH_2PO_4 (50 mM, pH 8), propargyl-*O*-glucose in H_2O and 0.01 M $[\mathbf{L2}]_2Pd(OAc)_2$ in NaOH at 37 °C for 4 h, unless otherwise indicated. O = Oxidised methionine				

Table 4.20 Sonogashira reaction of the iodo-Tyr/His ubiquitin with 200 equiv. 1-propargyl-β-D-glucopyranose in the presence of $[\mathbf{L2}]_2Pd(OAc)_2$.

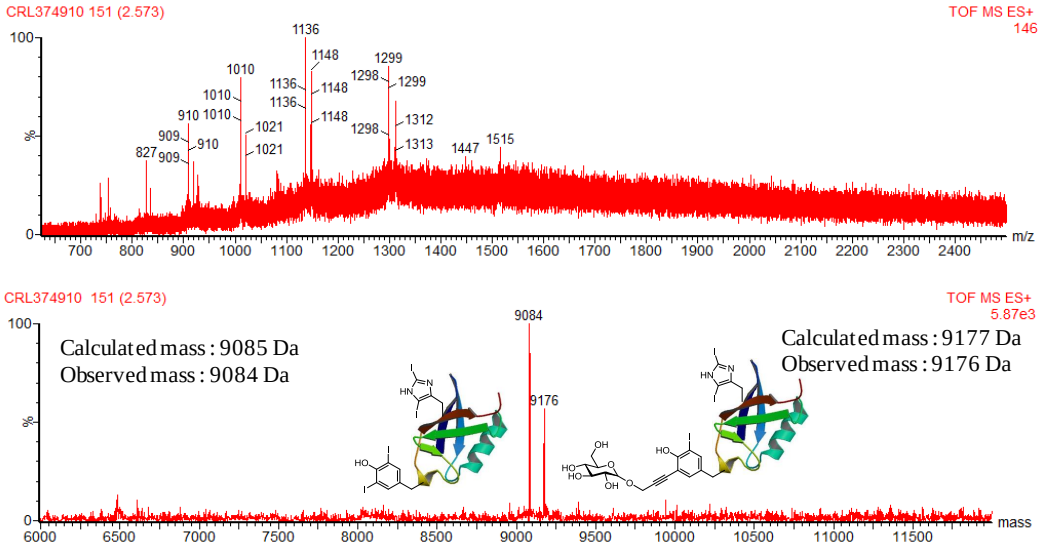

Figure 4.85 ESI-MS spectrum of the iodo-Tyr/His ubiquitin treated with 200 equiv. 1-propargyl-β-D-glucopyranose and 20 equiv. [**L2**]$_2$Pd(OAc)$_2$.

4.6.5 Peptide Mapping of Modified Proteins

(See general experimental consideration in appendix)

MSMS Investigation of Iodo-Tyr/His Insulin

Entry	Score	Mr(found)	Mr(Calc)	Expect	Modification	Sequence
1	25.5	1119.5543	3355.6427	0.032	H → Diiodo H (H-29, 34) Y → Diiodo Y (Y-40)	FVNQHLCGSHLVE ALYLVCGER
2	51.2	1035.6240	3103.8502	$7.8x10^{-5}$	H → Diiodo H (H-34) Y → Diiodo Y (Y-40)	FVNQHLCGSHLVE ALYLVCGER
3	33.9	591.6348	1181.2580	0.077	Y → Diiodo Y (Y-50)	GFFYTPKA
4	29.1	1191.3600	2380.7054	0.004	Y → Diiodo Y (Y-98)	GIVEQCCASVCSL YQLEN
5	6.7	1024.2233	3069.6480	0.95	Y → Diiodo Y (Y-98,103)	GIVEQCCASVCSL YQLENYCN

Table 4.21 Peptide fragmentation of iodinated Tyr and His (H-29, H-34, Y-40, Y-50, Y-98, Y103) analysed by Mascot database.

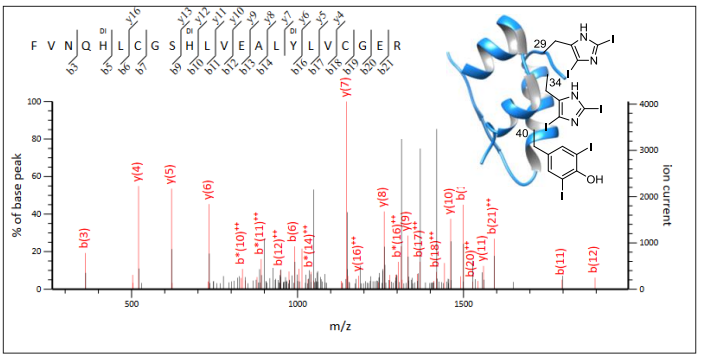

Figure 4.86 Peptide fragmentation of the diiodo-Tyr/His (H-29, H-34, Y-40) FVNQHLCGSHLVEALYLVCGER analysed by Mascot database.

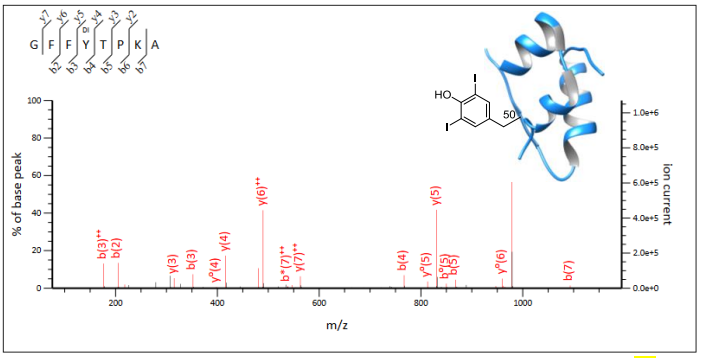

Figure 4.87 Peptide fragmentation of the diiodo-Tyr (Y-50) GFFYTPKA analysed by Mascot database.

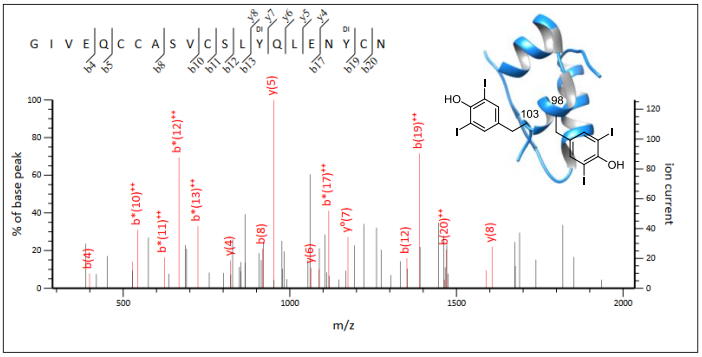

Figure 4.88 Peptide fragmentation of the diiodo-Tyr (Y-98, Y-103) GIVEQCCASVCSLYQLENYCN analysed by Mascot database.

MSMS Investigation of Iodo-Tyr/His MCP-1

Entry	Score	Mr(found)	Mr(Calc)	Expect	Modification	Sequence
1	67.3	1148.3696	2294.7235	$2.1x10^{-6}$	Y → Diiodo Y (Y-36)	DAINAPVTCCYNFTNRK
2	22.7	509.1164	1016.2114	0.25	Y → Diiodo Y (Y-51)	LASYRR
3	43.4	775.5924	2323.7566	0.0012	H → Diiodo H (H-89)	WVQDSMDHLDKQTQTPK

Table 4.22 Peptide fragmentation of the iodinated Tyr and His (Y-36, Y-51, H-89) analysed by Mascot database.

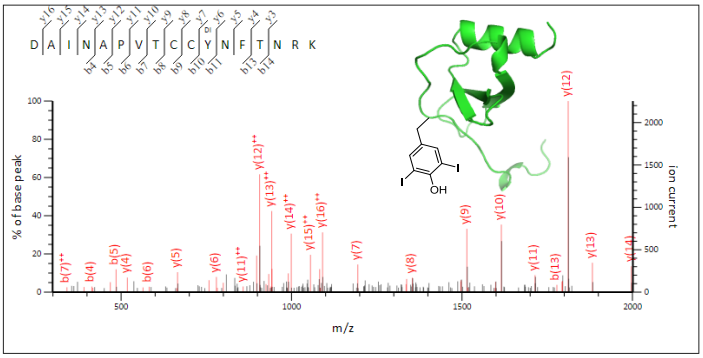

Figure 4.89 Peptide fragmentation of the diiodo-Tyr (Y-36) DAINAPVTCCYNFTNRK analysed by Mascot database.

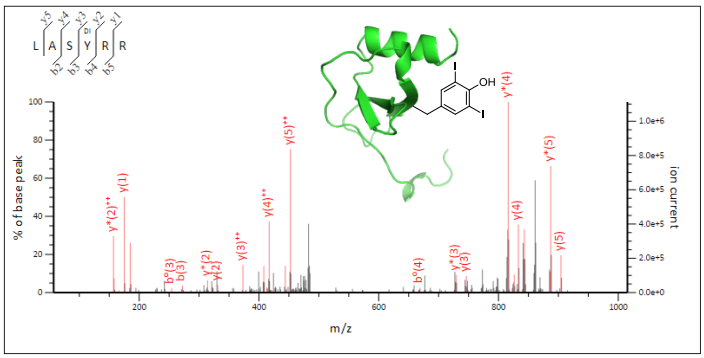

Figure 4.90 Peptide fragmentation of the diiodo-Tyr (Y-51) LASYRR analysed by Mascot database.

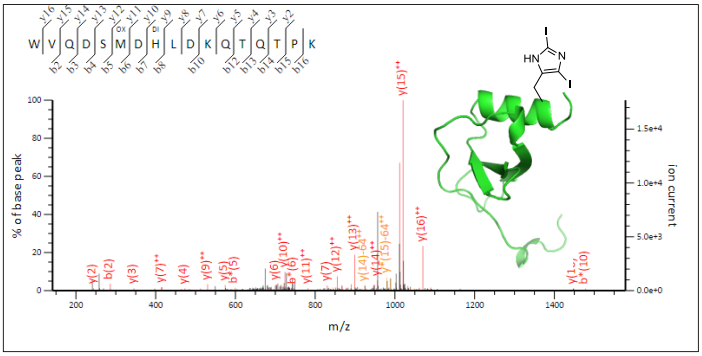

Figure 4.91 Peptide fragmentation of the diiodo-His (H-89) WVQDSMDHLDKQTQTPK analysed by Mascot database.

MSMS Investigation of Iodo-Tyr/His UBQ

Entry	Score	Mr(found)	Mr(Calc)	Expect	Modification	Sequence
1	45.2	660.2112	1318.4068	$5.8x10^{-5}$	H → Diiodo H (H-68)	ESTLHLVLR
2	44.5	667.1769	1332.3384	0.00013	Y → Diiodo Y (Y-59)	TLSDYNIQK
3	31.4	659.1908	2632.7346	0.0014	Y → Diiodo Y (Y-59) H → Diiodo H (H-68)	TLSDYNIQKEST LHLVLR

Table 4.23 Peptide fragmentation of the iodinated Tyr and His (Y-59, H-68) analysed by Mascot database.

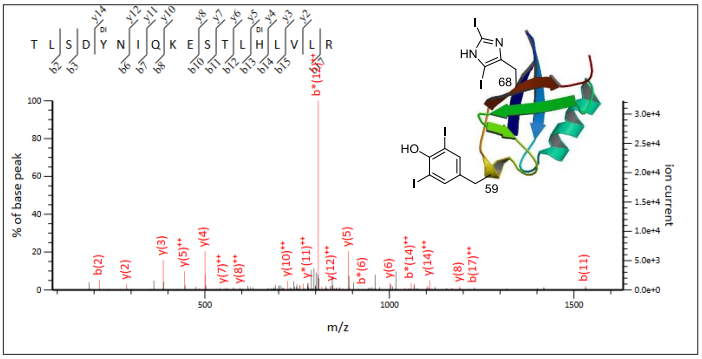

Figure 4.92 Peptide fragmentation of the diiodo-Tyr/His (Y-59, H-68) TLSDYNIQKESTLHLVLR analysed by Mascot database.

MSMS Investigation of Phenyl-Coupled UBQ

Entry	Score	Modification	Sequence
1	83.2	Y → Di-Ph Y (Y-59)	QLEDGRTLSDYNIQK
2	59.2	H → Di-Ph H (H-68)	ESTLHLVLR
3	59.0	Y → Di-Ph Y (Y-59) H → Di-Ph H (H-68)	TLSDYNIQKESTLHLVLR

Table 4.24 Peptide fragmentation of the phenyl-coupled Tyr and His (Y-59, H-68) analysed by Peaks.

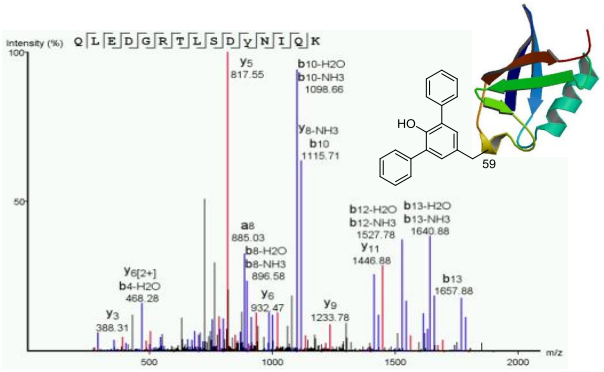

Figure 4.93 Peptide fragmentation of the DiPh-Tyr (Y-59) QLEDGRTLSDYNIQK analysed by Peaks.

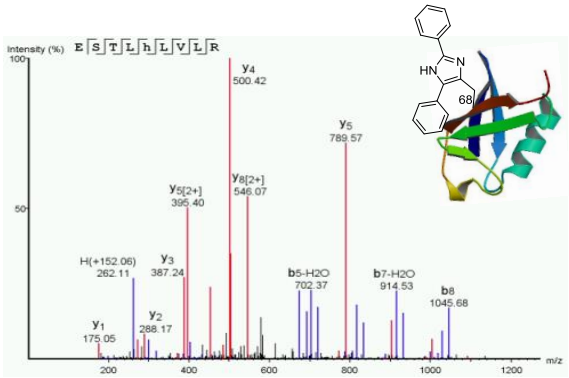

Figure 4.94 Peptide fragmentation of the DiPh-His (H-68) ESTLHLVLR analysed by Peaks.

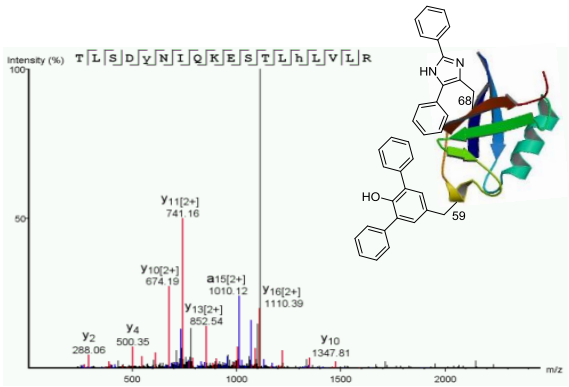

Figure 4.95 Peptide fragmentation of the DiPh-Tyr (Y-59) and DiPh-His (H-68) TLSDYNIQKESTLHLVLR analysed by Peaks.

MSMS Investigation of Propargyl-*O*-Glucose-Coupled UBQ

Entry	Score	Modification	Sequence
1	83.5	Y → MonoGlc Y (Y-59) H → MonoGlc H (H-68)	TLSDYNIQKESTLHLVLR

Table 4.24 Peptide fragmentation of the propargyl-*O*-glucose Tyr and His (Y-59, H-68) analysed by Peaks.

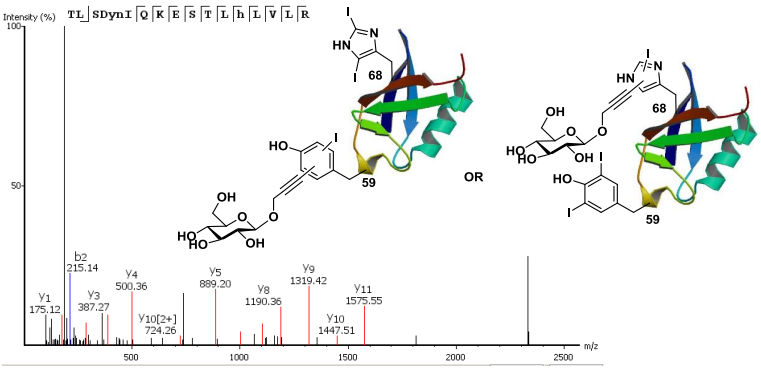

Figure 4.96 Peptide fragmentation of the MonoGlc-Tyr (Y-59) or MonoGlc-His (H-68) TLSDYNIQKESTLHLVLR analysed by Peaks.

4.7 Bibliography

(1) Arsequell, G.; Espuña, G.; Valencia, G.; Barluenga, J.; Carlon, R. P.; Gonzalez, J. M. First aromatic electrophilic iodination reaction on the solid-phase: Iodination of bioactive peptides. *Tetrahedron Lett.* **1998**, *39*, 7393-7396.

(2) Barluenga, J.; Campos, P. J.; Gonzαlez, J. M.; Asensio, G. A Simple and General Route to Aryl Iodides from Arenes. *J. Chem. Soc. Perkin Trans. I* **1984**, 2623-2624.

(3) Chalker, J. M.; Davis, B. G. Safe and Scalable Preparation of Barluenga's Reagent (Bis(pyridine)iodinium(I) tetrafluoroborate). *Org. Synth.* **2010**, *87*, 288-298.

(4) Espuña, G.; Andreu, D.; Barluenga, J.; Pérez, X.; Planas, A.; Arsequell, G.; Valencia, G. Iodination of Proteins by IPy2BF4, a New Tool in Protein Chemistry. *Biochemistry* **2006**, *45*, 5957-5963.

(5) Espuña, G.; Arsequell, G.; Valencia, G.; Barluenga, J.; Pérez, M.; González, J. M. Control of the iodination reaction on activated aromatic residues in peptides. *Chem. Commun.* **2000**, 1307-1308.

(6) Vilaró, M.; Arsequell, G.; Valencia, G.; Ballesteros, A.; Barluenga, J. Arylation of Phe and Tyr Side Chains of Unprotected Peptides by a Suzuki−Miyaura Reaction in Water. *Org. Lett.* **2008**, *10*, 3243-3245.

(7) Dawson, P. E.; Muir, T. W.; Clark-Lewis, I.; Kent, S. B. H. Synthesis of proteins by native chemical ligation. *Science* **1994**, *266*, 776-778.

(8) Antos, J. M.; Francis, M. B. Transition metal catalyzed methods for site-selective protein modification. *Curr. Opin. Chem. Biol.* **2006**, *10*, 253-262.

(9) Chalker, J. M.; Wood, C. S. C.; Davis, B. G. A Convenient Catalyst for Aqueous and Protein Suzuki-Miyaura Cross-Coupling. *J. Am. Chem. Soc.* **2009**, *131*, 16346-16347.

(10) Johansson Seechurn, C. C.; Kitching, M. O.; Colacot, T. J.; Snieckus, V. Palladium-catalyzed cross-coupling: a historical contextual perspective to the 2010 Nobel Prize. *Angew. Chem. Int. Ed. Engl.* **2012**, *51*, 5062-5085.

(11) Yang, M.; Li, J.; Chen, P. R. Transition metal-mediated bioorthogonal protein chemistry in living cells. *Chem. Soc. Rev.* **2014**, *43*, 6511-6526.

(12) Bernardes, G. J. L.; Chalker, J. M.; Errey, J. C.; Davis, B. G. Facile Conversion of Cysteine and Alkyl Cysteines to Dehydroalanine on Protein Surfaces: Versatile and Switchable Access to Functionalized Proteins. *J. Am. Chem. Soc.* **2008**, *130*, 5052-5053.

(13) Chalker, J. M.; Gunnoo, S. B.; Boutureira, O.; Gerstberger, S. C.; Fernández-González, M.; Bernardes, G. J. L.; Griffin, L.; Hailu, H.; Schofield, C. J.; Davis, B. G. Methods for converting cysteine to dehydroalanine on peptides and proteins. *Chem. Sci.* **2011**, *2*, 1666.

(14) Agard, N. J.; Prescher, J. A.; Bertozzi, C. R. A Strain-Promoted [3 + 2] Azide−Alkyne Cycloaddition for Covalent Modification of Biomolecules in Living Systems. *J. Am. Chem. Soc.* **2004**, *126*, 15046-15047.

(15) Laughlin, S. T.; Baskin, J. M.; Amacher, S. L.; Bertozzi, C. R. In Vivo Imaging of Membrane-Associated Glycans in Developing Zebrafish. *Science* **2008**, *320*, 664-667.

(16) Link, A. J.; Tirrell, D. A. Cell Surface Labeling of Escherichia coli via Copper(I)-Catalyzed [3+2] Cycloaddition. *J. Am. Chem. Soc.* **2003**, *125*, 11164-11165.

(17) McKay, C. S.; Finn, M. G. Click chemistry in complex mixtures: bioorthogonal bioconjugation. *Chemistry & biology* **2014**, *21*, 1075-1101.

(18) Plass, T.; Milles, S.; Koehler, C.; Schultz, C.; Lemke, E. A. Genetically encoded copper-free click chemistry. *Angew. Chem. Int. Ed. Engl.* **2011**, *50*, 3878-3881.

(19) Sletten, E. M.; Bertozzi, C. R. From Mechanism to Mouse: A Tale of Two Bioorthogonal Reactions. *Acc. Chem. Res.* **2011**, *44*, 666-676.

(20) Spicer, C. D.; Davis, B. G. Palladium-Mediated Site-Selective Suzuki-Miyaura Protein Modification at Genetically Encoded Aryl Halides. *Chem. Commun.* **2011**, *47*, 1698-1700.

(21) Spicer, C. D.; Triemer, T.; Davis, B. G. Palladium-Mediated Cell-Surface Labeling. *J. Am. Chem. Soc.* **2012**, *134*, 800-803.

(22) Li, N.; Lim, R. K. V.; Edwardraja, S.; Lin, Q. Copper-Free Sonogashira Cross-Coupling for Functionalization of Alkyne-Encoded Proteins in Aqueous Medium and in Bacterial Cells. *J. Am. Chem. Soc.* **2011**, *133*, 15316-15319.

(23) Hauke, S.; Best, M.; Schmidt, T. T.; Baalmann, M.; Krause, A.; Wombacher, R. Two-step protein labeling utilizing lipoic acid ligase and Sonogashira cross-coupling. *Bioconjug. Chem.* **2014**, *25*, 1632-1637.

(24) Goldstein, G.; Scheid, M.; Hammerling, U.; Schlesinger, D. H.; Niall, H. D.; Boyse, E. A. Isolation of a polypeptide that has lymphocyte-differentiating properties and is probably represented universally in living cells *Proc. Natl. Acad. Sci. U.S.A.* **1975**, *72*, 11-15.

(25) Wilkinson, K. D. The discovery of ubiquitin-dependent proteolysis. *Proc. Natl. Acad. Sci. U.S.A.* **2005**, *102*, 15280-15282.

(26) Popovic, D.; Vucic, D.; Dikic, I. Ubiquitination in disease pathogenesis and treatment. *Nat. Med.* **2014**, *20*, 1242-1253.

(27) FORMA Therapeutics. Protein-Homeostasis-Target-Families. http://www.formatherapeutics.com/our-science/pipeline/protein-homeostasis/protein-homeostasis-target-families.php. **2009**, (accessed on 8th July 2016).

(28) Schneider, T.; Schneider, D.; Rosner, D.; Malhotra, S.; Mortensen, F.; Mayer, T. U.; Scheffner, M.; Marx, A. Dissecting ubiquitin signaling with linkage-defined and protease resistant ubiquitin chains. *Angew. Chem. Int. Ed. Engl.* **2014**, *53*, 12925-12929.

(29) Brzovic, P. S.; Lissounov, A.; Christensen, D. E.; Hoyt, D. W.; Klevit, R. E. A UbcH5/ubiquitin noncovalent complex is required for processive BRCA1-directed ubiquitination. *Mol. Cell* **2006**, *21*, 873-880.

Chapter 5

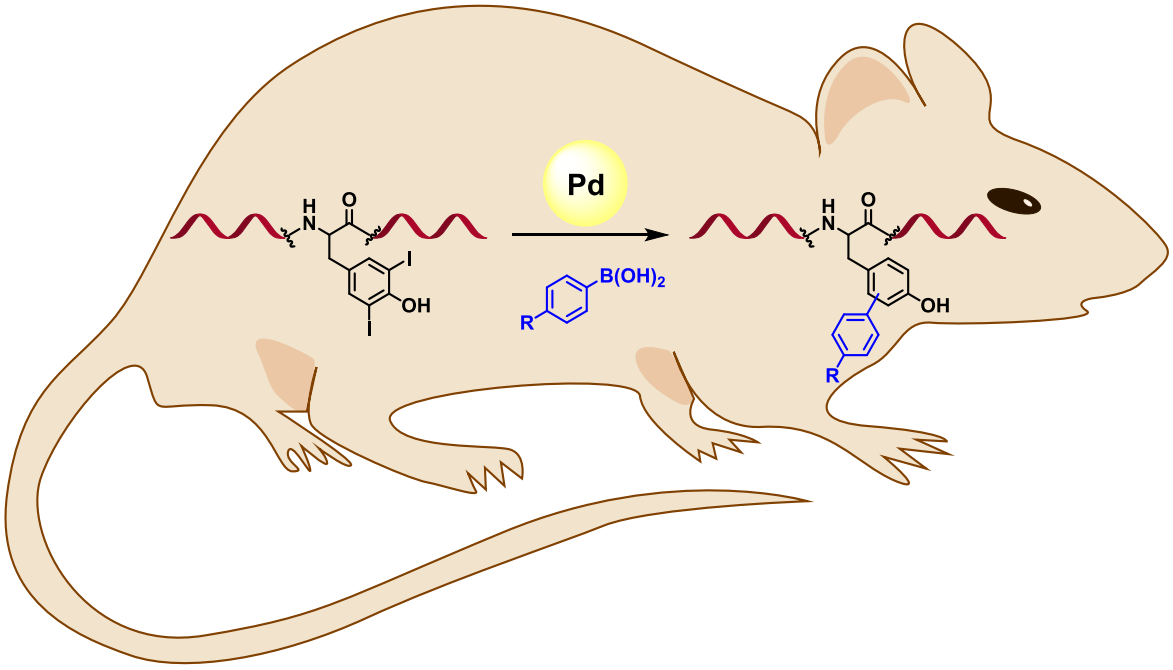

In vivo Applications of Palladium Chemistry in Biological Systems

5.1 Introduction

5.1.1 Thyroglobulin and Thyroid Hormones

5.1.2 Palladium Chemistry to Biology

5.2 Investigation of Palladium Cross-Couplings of Thyroid Hormones

5.3 Investigation of Palladium Cross-Couplings of Thyroglobulin (Tg)

5.3.1 *Ex vivo* Pd-Mediated Reactions of Thyroglobulin (Tg)

5.3.2 *In vivo* Pd-Mediated Reactions of Thyroglobulin (Tg)

5.4 Conclusion

5.5 Experimental

5.6 Bibliography

5.1 Introduction

The aim of this chapter is to investigate the *in vivo* applications of Pd-mediated Suzuki reactions to mammalian living systems as a proof of biocompatibility as well as a preclinical animal study.

5.1.1 Thyroglobulin and Thyroid Hormones

Thyroglobulin (Tg) is a large glycoprotein (330 kDa), highly enriched in the thyroid gland as a precursor for a synthesis of thyroid hormones triiodothyronine (T3) and thyroxine (T4) through iodination and bioconjugation (Figure **5.1**)[1-3]. Tg is a naturally iodinated protein produced in the thyroid follicle with a structure composed of a protein colloid centre surrounded by follicular cells[3]. Around 20-30% of Tg tyrosine residues are iodinated by thyroid peroxidase (TPO), resulting in the formation of C-I bonds on tyrosine residues (including 3-iodotyrosine (MIT) and 3,5-diiodotyrosine (DIT))[1,3-6]. These iodinated tyrosine moieties are enzymatically coupled by TPO, leading to the creation of iodinated bicyclic molecules T3 and T4. The release of thyroid hormones is achieved by proteolysis, which allows these two important molecules to circulate in the bloodstream for regulation of metabolism.

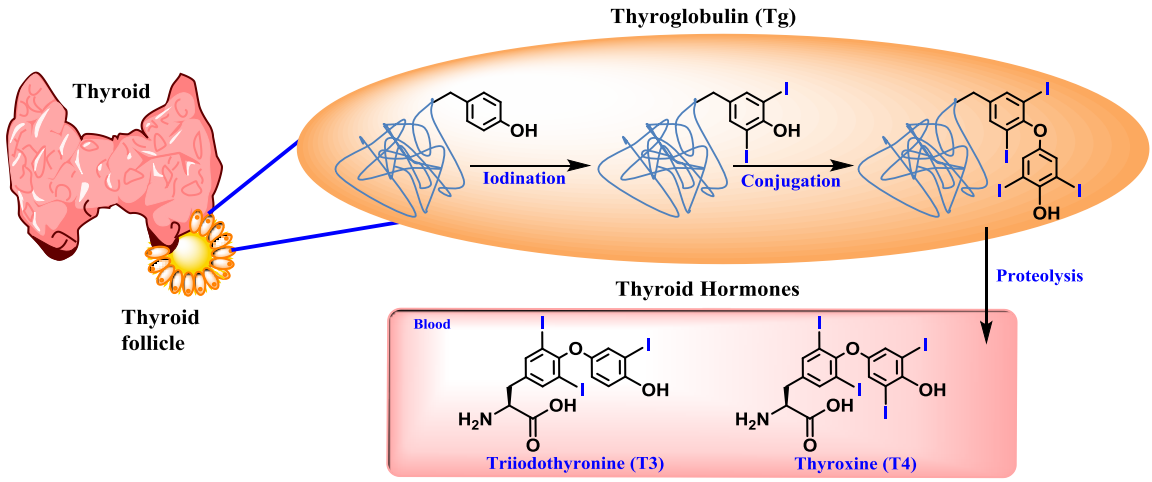

Figure 5.1 Synthesis of thyroglobulin (Tg) in thyroid follicles and a release of thyroid hormones (T3 and T4) into bloodstream by hydrolysis of the iodinated Tg[1,2].

5.1.2 Palladium Chemistry to Biology

Few methods for *in vivo* protein labelling have been reported due to a lack of biocompatibility in biological systems[7-12]. For example, site-selective SPAAC chemical conjugation approach has been demonstrated in the context of protein labelling under *in vivo* conditions by a coupling between the genetically encoded azide tag and the highly strained cyclooctyne probe[13-17]. As such, *in vivo* labelling of iodinated protein species, in particular thyroid hormones (T3/T4) or thyroglobulin (Tg), is challenging under biocompatible conditions. However, advances in this area could allow monitoring of abnormal thyroid functions. Based on Pd-mediated biorthogonal reactions, Chen reported site-specific protein labelling inside *E.coli* bacterial cells through Pd-catalysed Sonogashira cross-coupling by treatment of either GFP or OspF containing a genetically encoded alkyne tag with a *para*-iodophenyl fluorescent probe (Iphe-FL525), in the presence of a $Pd(NO_3)_2$ catalyst (Figure **5.2**)[8].

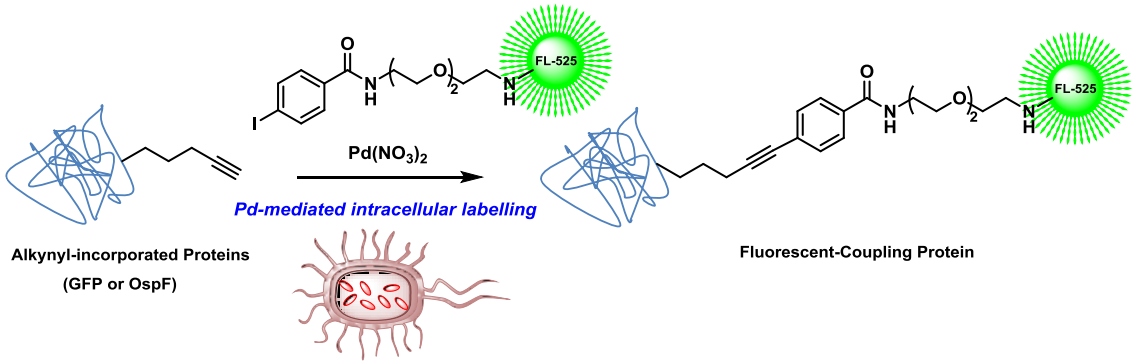

Figure 5.2 Site-specific intracellular protein labelling through Pd-mediated Sonogashira cross-coupling reactions[8].

Bradley reported palladium-mediated intracellular chemistry of fluorescent probes performed in HeLa cells with association of Pd(0) nanoparticle-trapped polystyrene microspheres through either Pd(0)-catalysed cleavage or Suzuki-Miyaura cross-coupling reactions (Figure **5.3**)[11].This work demonstrates the selective transformation of the fluorescent probe by use of the Pd-catalyst inside a cell for visualization of biological processes.

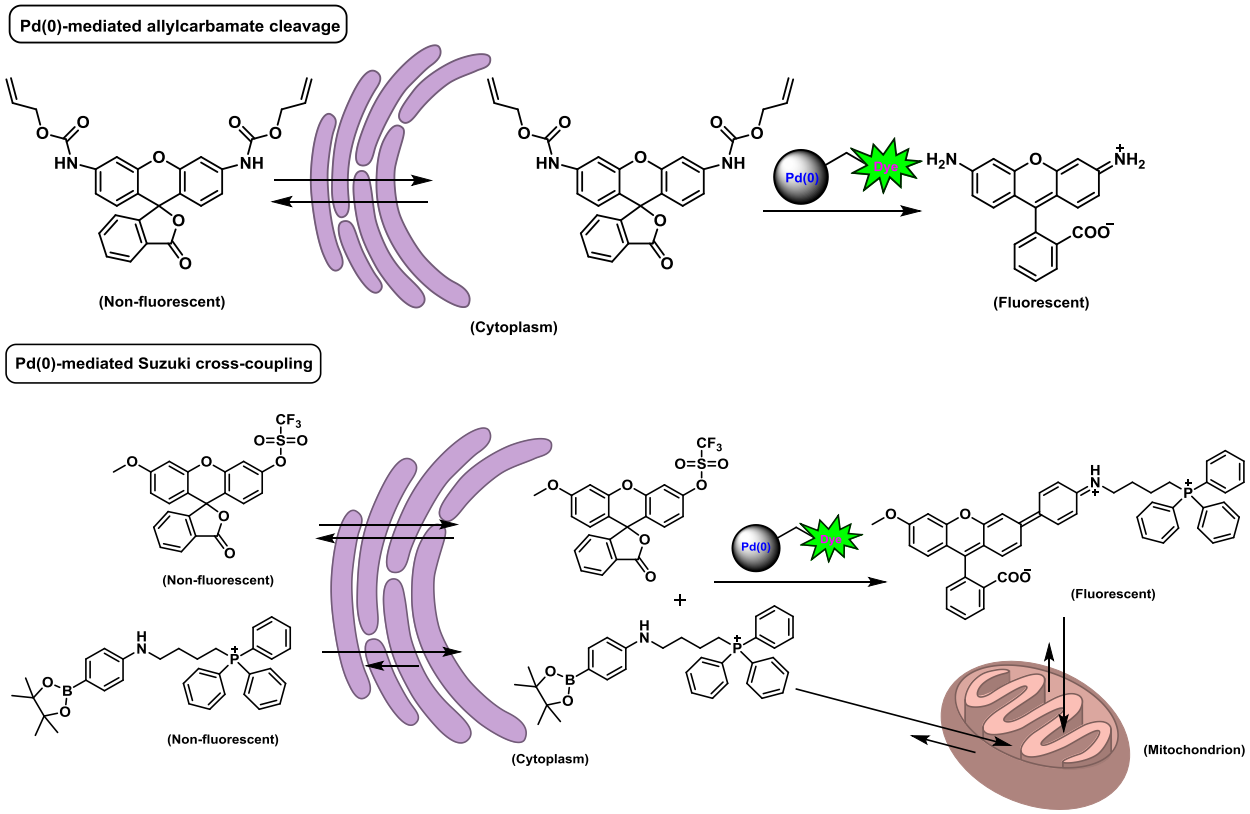

Figure 5.3 Intracellular Pd-mediated reactions of the fluorescent probes in HeLa cells by use of Cy5.5-labelled Pd(0) microspheres through either Pd(0)-mediated cleavage or Suzuki reaction[11].

5.2 Investigation of Palladium Cross-Couplings of Thyroid Hormones

In chapter 4, we were able to show the creation of new C-C bonds at tyrosine and histidine residues of the protein through our Suzuki-Miyaura cross-coupling (SMC) systems. Next, we extended our aqueous Pd-catalysed Suzuki system[9,18-20] to challenging mammalian living organisms by Pd-catalysed Suzuki reactions of either thyroid hormones (T4) or thyroglobulin (Tg) with aromatic boronic acids. This chapter discusses the extension of these reactions to full mammalian tissues. We began our initial study by investigating *ex vivo* SMC reactions by treatment of T4 with $PhB(OH)_2$ performed in simple mimics of circulatory systems. These reactions proceeded in the presence of the $[\mathbf{L2}]_2Pd(OAc)_2$ catalyst (Table **5.1**). However, we found that no formation of the phenyl-coupled T4 could be detected by LC-MS under two reaction conditions: NaP_i buffer, or rat blood plasma (Figure **5.4-5.6**). The ESI-MS spectra showed only peaks of the starting

material (T4) in the form of $[M+H]^+$ (MW : 777.75) and $[M-H+41]^+$ (MW : 818.78, CH_3CN-adduct or Na-adduct $[M+Na]^+ \bullet H_2O$).

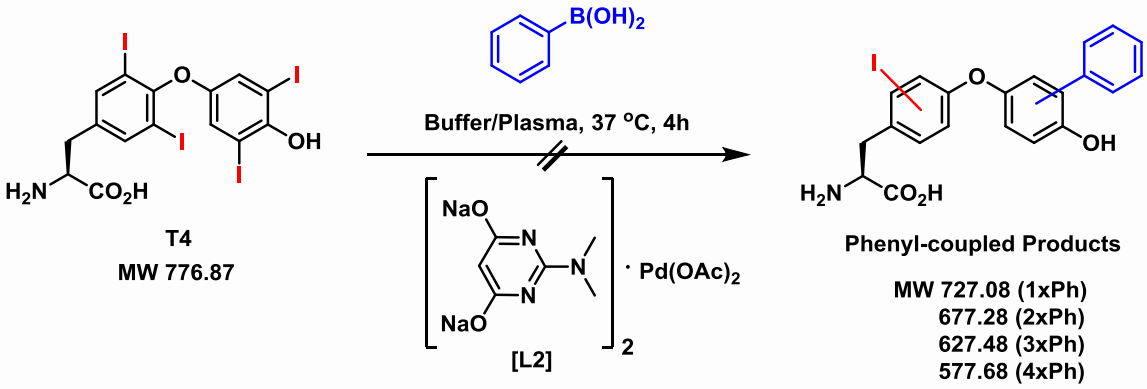

Entry	T4 (equiv.)	$PhB(OH)_2$ (equiv.)	$[L2]_2Pd(OAc)_2$ (equiv.)	Reaction Conditions	ESI-MS
1	1.0 (1.2 µmol)	5.0 (6.0 µmol)	0.2 (0.24 µmol)	50 mM NaP_i	777.75 (SM)
2	1.0 (1.2 µmol)	5.0 (6.0 µmol)	0.2 (0.24 µmol)	50 mM NaP_i + rat plasma (1:1)	777.69 (SM)
3	1.0 (1.2 µmol)	5.0 (6.0 µmol)	0.2 (0.24 µmol)	rat plasma	777.69 (SM)

General conditions: T4 in 0.2 M NaOH (c = 25.0 mg/mL), $PhB(OH)_2$ in 0.2 M NaOH (c = 25.0 mg/mL), $[\mathbf{L2}]_2Pd(OAc)_2$ in 0.1 M NaOH (c = 0.01 M) at 37 °C for 4h unless otherwise indicated.

Table 5.1 Optimisation experiments of the SMC reactions of T4 with $PhB(OH)_2$ in the presence of $[\mathbf{L2}]_2Pd(OAc)_2$ catalyst.

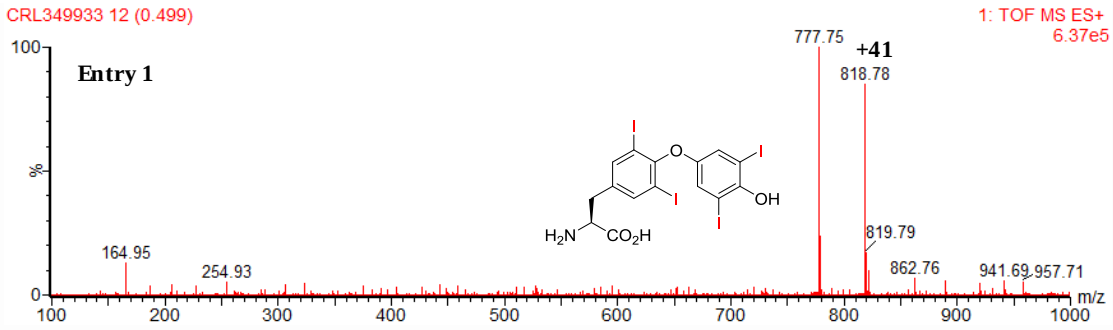

Figure 5.4 ESI-MS spectrum of the unreactive T4 and $[M-H+41]^+$ adduct from treatment of T4 with $PhB(OH)_2$ and $[\mathbf{L2}]_2Pd(OAc)_2$ catalyst in 50 mM NaP_i.

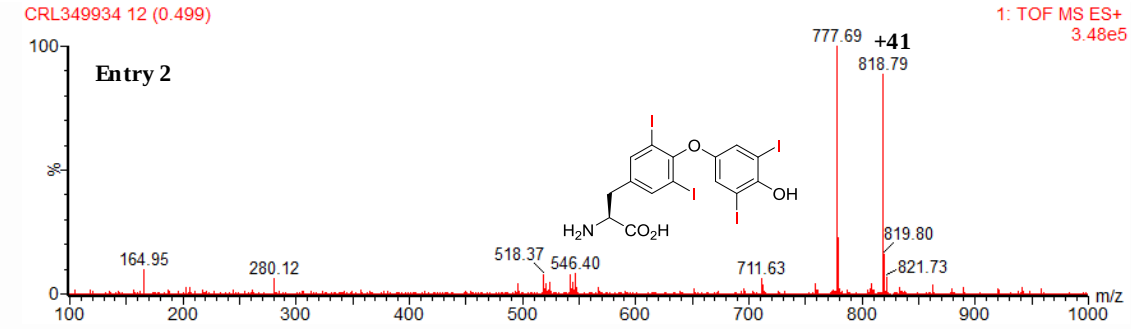

Figure 5.5 ESI-MS spectrum of the unreactive T4 and $[M-H+41]^+$ adduct from treatment of T4 with $PhB(OH)_2$ and $[\mathbf{L2}]_2Pd(OAc)_2$ catalyst in 1:1 ratio of 50 mM NaP_i /rat plasma.

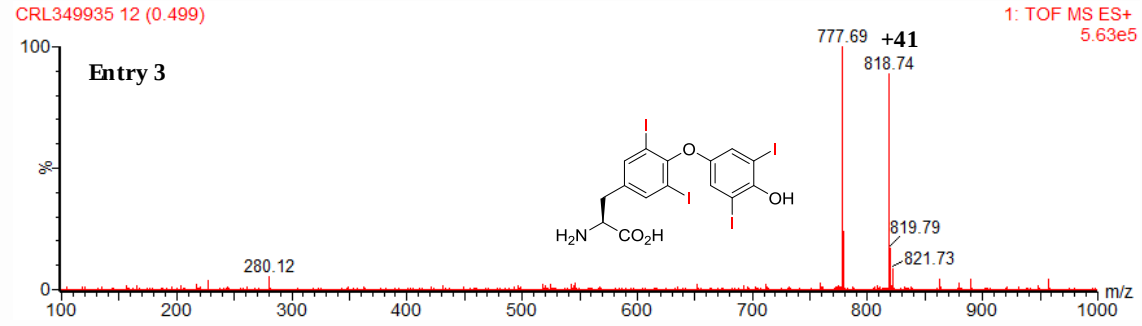

Figure 5.6 ESI-MS spectrum of the unreactive T4 and $[M-H+41]^+$ adduct from treatment of T4 with $PhB(OH)_2$ and $[\mathbf{L2}]_2Pd(OAc)_2$ catalyst in rat plasma.

Since the preliminary study of unprotected T4 showed no formation of the phenyl-coupled products, this might possibly arise from either unproductive coordination of an amine group of the T4 to Pd catalyst, or interference from proteins such as serum albumin, globulin, and fibrinogen which exist in rat blood plasma fluid. Either scenario may adversely affect the reactivity of the Pd catalyst. As a consequence, the BocNH-protected T4 was used to investigate Pd-mediated reactions with similar reaction conditions to natural T4. The BocNH-T4 was treated with phenylboronic acid in the presence of the $[\mathbf{L2}]_2Pd(OAc)_2$, but unfortunately the coupling products were not observed by LC-MS (Table **5.2**).

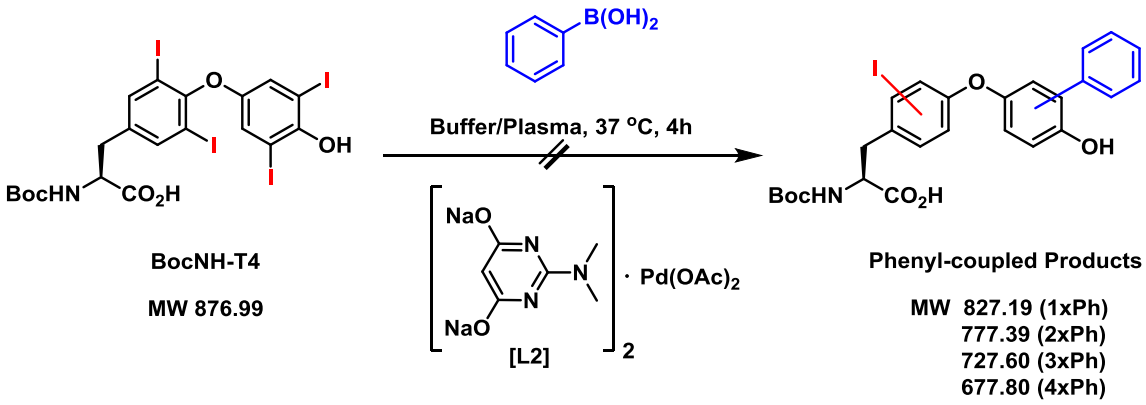

Entry	BocNH-T4 (equiv.)	$PhB(OH)_2$ (equiv.)	$[L2]_2Pd(OAc)_2$ (equiv.)	Reaction Conditions	ESI-MS
1	1.0 (1.2 µmol)	5.0 (6.0 µmol)	0.2 (0.24 µmol)	50 mM NaP_i	875.83 (SM)
2	1.0 (1.2 µmol)	5.0 (6.0 µmol)	0.2 (0.24 µmol)	50 mM NaP_i + plasma (1:1)	875.82 (SM)
3	1.0 (1.2 µmol)	5.0 (6.0 µmol)	0.2 (0.24 µmol)	Rat plasma	875.83 (SM)

General conditions: BocNH-T4 in 0.2 M NaOH (c = 25.0 mg/mL), $PhB(OH)_2$ in 0.2 M NaOH (c = 25.0 mg/mL), $[\mathbf{L2}]_2Pd(OAc)_2$ in 0.1 M NaOH (c = 0.01 M) at 37 °C for 4h unless otherwise indicated.

Table 5.2 Optimisation experiments of the SMC reactions of BocNH-T4 with $PhB(OH)_2$ in the presence of $[\mathbf{L2}]_2Pd(OAc)_2$ catalyst.

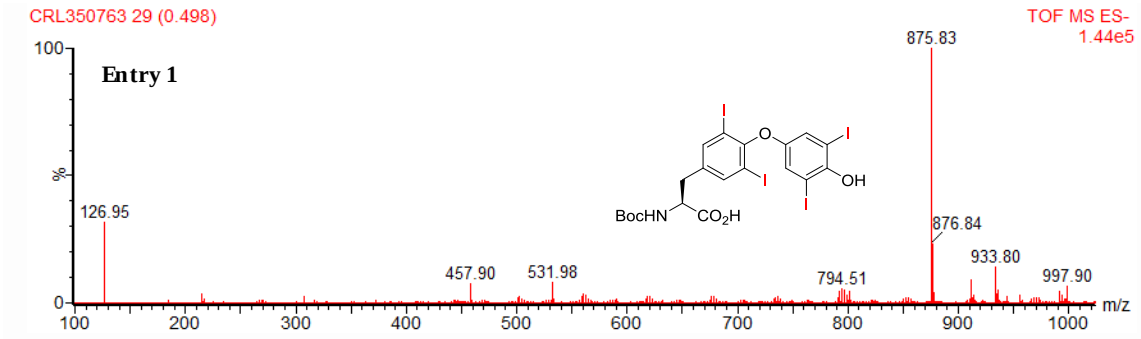

Figure 5.7 ESI-MS spectra of the unreactive BocNH-T4 from treatment of BocNH-T4 with $PhB(OH)_2$ and $[\mathbf{L2}]_2Pd(OAc)_2$ catalyst in 50 mM NaP_i.

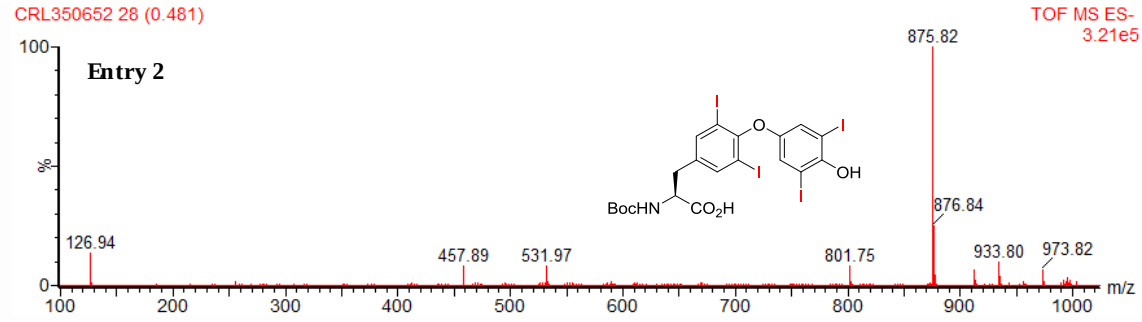

Figure 5.8 ESI-MS spectra of the unreactive BocNH-T4 from treatment of BocNH-T4 with $PhB(OH)_2$ and $[\mathbf{L2}]_2Pd(OAc)_2$ catalyst in 1:1 ratio of 50 mM NaP_i /rat plasma.

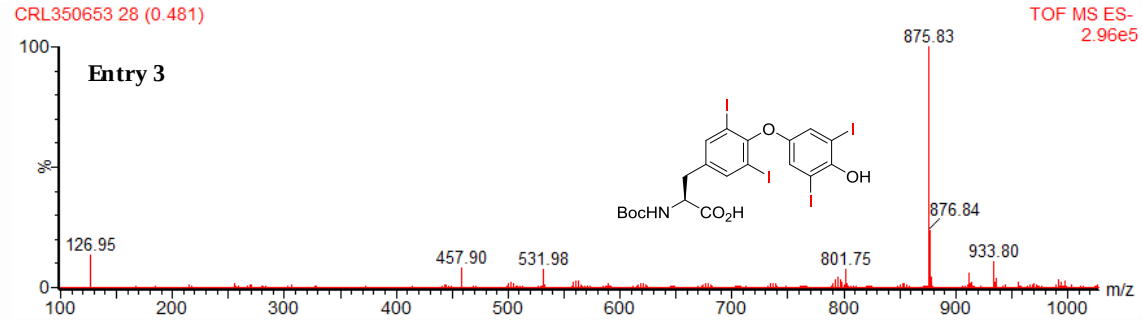

Figure 5.9 ESI-MS spectra of the unreactive BocNH-T4 from treatment of BocNH-T4 with $PhB(OH)_2$ and $[\mathbf{L2}]_2Pd(OAc)_2$ catalyst in rat plasma.

5.3 Investigation of Palladium Cross-Couplings of Thyroglobulin (Tg)

5.3.1 *Ex vivo* Pd-Mediated Reactions of Thyroglobulin (Tg)

Although attempts of Pd-catalysed reactions of the small molecules (T4) failed, we also investigated *ex vivo* Pd cross-coupling of the naturally iodinated thyroglobulin (Tg) through Suzuki-Miyaura reactions. An initial study of the Pd-mediated reactions of Tg (MW ~ 330 kDa) proceeded from treatment of the Tg protein mixture (extracted from the mouse thyroid gland tissue) with biotinylated phenylboronic acid (Table **5.3**). It was found that all protein reactions with a range of Pd catalyst (5-20 µL) and $R\text{-}B(OH)_2$ (0.25-1.0 µL) gave three intense protein bands (MW ≥260 kDa) that were stained by anti-biotin alkaline phosphatase antibody (Figure **5.10**). We could confirm these protein bands belonged to Tg using anti-biotin antibody and MSMS analysis (See experimental details, Table **5.14**). However, some lower-MW protein bands were also detected by this antibody, possibly due to *in vivo* iodination of some other proteins by TPO. These

iodinated proteins could react with biotinylated phenylboronic acid in the presence of the [**L2**]$_2$Pd(OAc)$_2$ catalyst, resulting in observation of protein bands on the membrane.

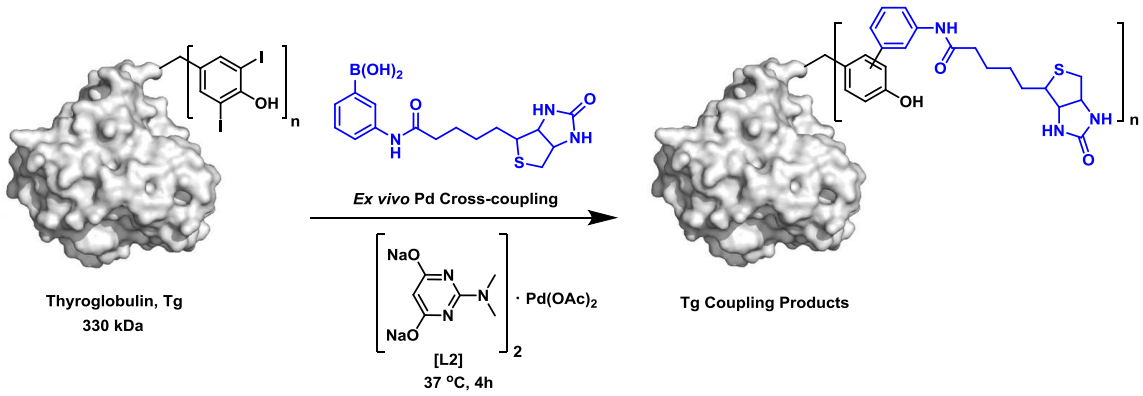

Entry	Tg-mixture (µL)	[L2]$_2$Pd(OAc)$_2$ (µL)	R-B(OH)$_2$ (µL)	Temp	Time	Remarks
1	5	-	-	4°C	4h	Tissue
2	5	-	-	37 °C	4h	Control
3	5	2.5	-	37 °C	4h	Control
4	5	-	0.25	37 °C	4h	Control
5	10	10	0.25 (R = Ph)	37 °C	4h	Reaction
6	10	5	0.25	37 °C	4h	Reaction
7	10	10	0.25	37 °C	4h	Reaction
8	10	20	0.25	37 °C	4h	Reaction
9	10	10	0.50	37 °C	4h	Reaction
10	10	10	1.0	37 °C	4h	Reaction

General conditions: Tg in PBS (pH 7.6), [**L2**]$_2$Pd(OAc)$_2$ in 0.1 M NaOH (c = 0.01 M), biotinylated B(OH)$_2$ in DMSO (c = 50 mg/mL) at 37 °C for 4h, unless otherwise indicated.

Table 5.3 Investigation of *ex vivo* Pd cross-coupling of the Tg mixture with biotin-B(OH)$_2$ in the presence of [**L2**]$_2$Pd(OAc)$_2$.

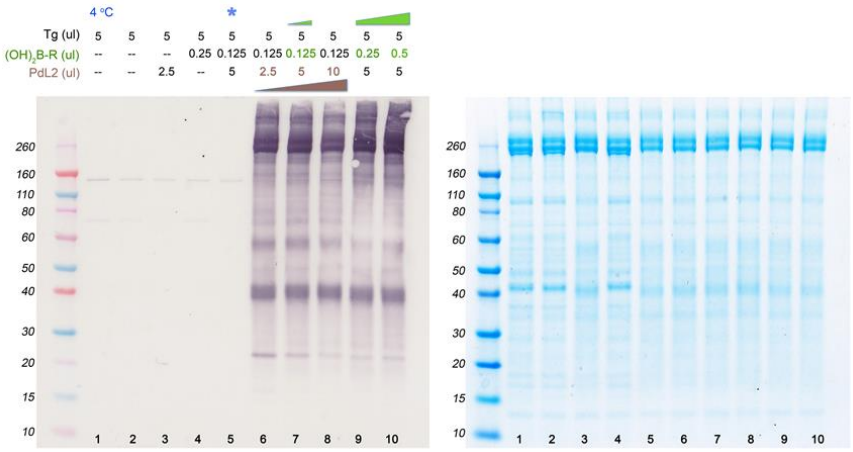

Figure 5.10 Western blot and SDS-PAGE of each reaction mixture stained by anti-biotin alkaline phosphatase antibody.

The treatment of semi-purified Tg (originating from thyroid gland tissue and using a vivaspin column with 100 kDa MW cut-off membrane for a semi-purification) with differently substituted aromatic boronic acids (including biotinylated, coumarinyl and phenyl) is shown in Table **5.4**. After completion of the reaction, each reaction mixture was analysed by SDS-PAGE, and subsequently stained with anti-biotin alkaline phosphatase antibody (Figure **5.11**). It was found that all control reactions showed no Tg protein bands on Western blot, whereas the biotin-coupled Tg was clearly detected by this antibody. As expected, treatment of the Tg with either coumarinyl or phenylboronic acid gave no biotin-specific positive response on the membrane.

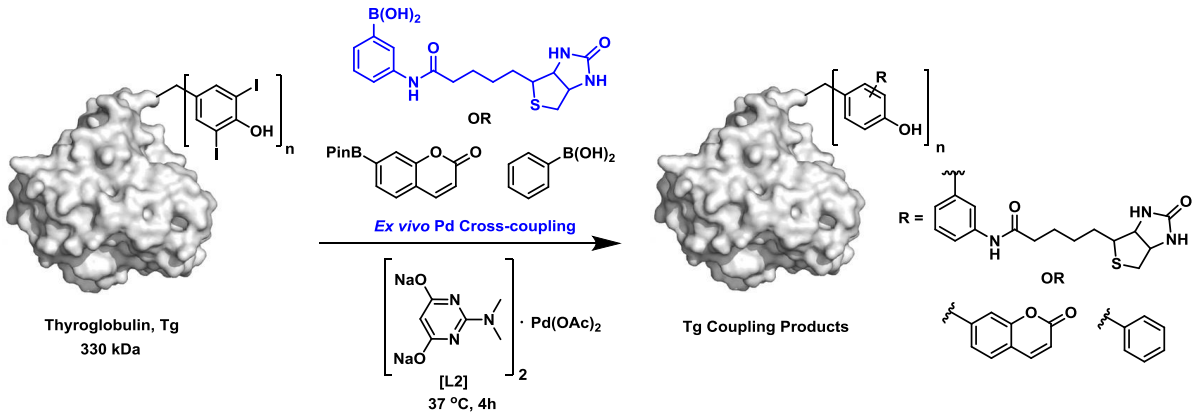

Entry	Purified Tg (equiv.)	$[L2]_2Pd(OAc)_2$ (equiv.)	$R\text{-}B(OH)_2$ (equiv.)	Temp	Time	Remarks
1	1	-	-	4°C	4h	Tissue
2	1	-	-	37 °C	4h	Control
3	1	50	-	37 °C	4h	Control
4	1	-	500 (biotin)	37 °C	4h	Control
5	1	50	500 (biotin)	37 °C	4h	Reaction
6	1	50	500 (coumarin)	37 °C	4h	Reaction
7	1	50	500. (phenyl)	37 °C	4h	Reaction

General conditions: Tg in NaH_2PO_4 (50 mM, pH 8.0 and c = 2.0 mg/mL), $[\mathbf{L2}]_2Pd(OAc)_2$ in 0.1 M NaOH (c = 0.01 M), $R\text{-}B(OH)_2$ in DMSO (c = 50 mg/mL) at 37 °C for 4h, unless otherwise indicated.

Table 5.4 Investigation of *ex vivo* Pd cross-coupling of the purified Tg with different $R\text{-}B(OH)_2$ in the presence of $[\mathbf{L2}]_2Pd(OAc)_2$.

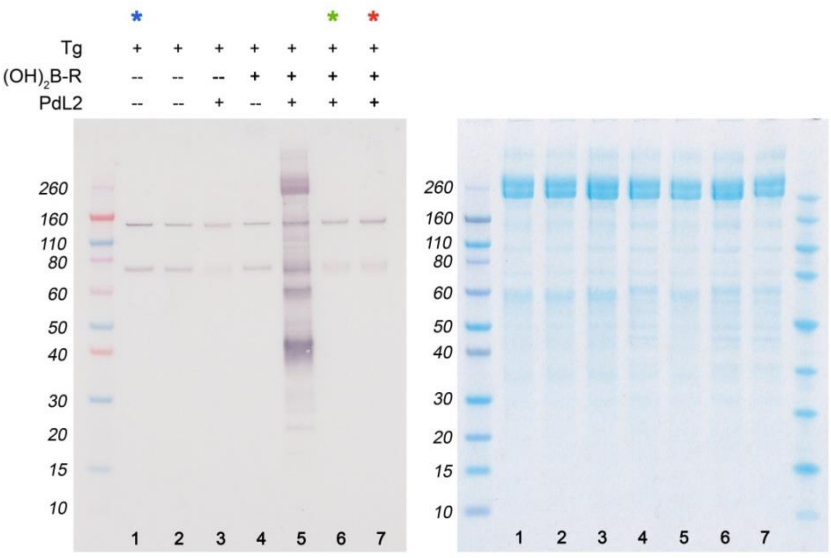

Figure 5.11 Western blot and SDS-PAGE of each reaction mixture by staining with anti-biotin alkaline phosphatase antibody. Lane 5 showed the detection of the biotin-coupled Tg.

Furthermore, a mixture of non-modified proteins extracted from mice thyroid gland tissues was separated by Tris-acetate gel and analysed by MSMS in order to identify specific type of proteins apart from the predominant Tg protein (Figure **5.12** and Table

5.5). It was found that three top protein bands (MW > 225 kDa) correlated to Tg. Medium-sized proteins excised between MW ~ 40-80 kDa were also identified by Mascot database search, especially actin, protein disulphide-isomerase and glucose-regulated protein.

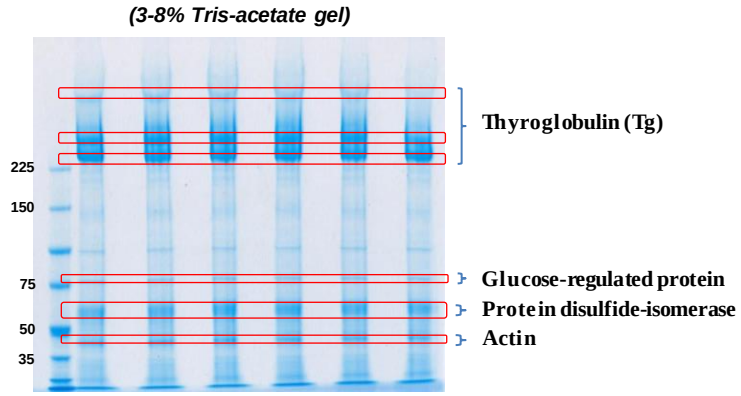

Figure 5.12 Tris-acetate gel(3-8%) shows non-modified proteins extracted from mice thyroid gland tissues.

Entry	Proteins	Protein sequence coverage (%)	Modifications
1	Thyroglobulin (Tg)	93	Iodinated Tyr
2	Glucose-regulated protein (78 kDa)	86	Wild-type
3	Protein disulphide-isomerase	89	Wild-type
4	Actin	97	Wild-type

Table 5.5 Identification of a mixture of proteins from extracts of the thryroid gland tissue separated by 3-8% Tris-acetate gel and analysed by MSMS.

Before we began investigating *in vivo* Suzuki-Miyura reactions of Tg in an animal model, it was important to gain information regarding suitable amounts of the Pd catalyst and boronic acid. Thus, we optimised a model system under *ex vivo* conditions. To determine threshold levels of both reaction factors including boronic acid and $[\mathbf{L2}]_2Pd(OAc)_2$ based on the *ex vivo* assay, we first introduced a biotinylated group into Tg through Suzuki-Miyaura reactions. Through titration experiments, followed by Western blot, we were able to calculate the reaction thresholds for both Pd catalyst and biotinylated boronic acid. All reactions were performed at 37 ^{o}C for 4 h by varying each concentration of either boronic acid or $[\mathbf{L2}]_2Pd(OAc)_2$ (See experimental details, Table

5.10). Each reaction mixture was examined by both SDS-PAGE and Western blot (Figure **5.13**). The intensities of protein bands were measured by ImageJ software, and the plots between intensity *vs* concentration of biotin or Pd catalyst were generated by OriginPro software.

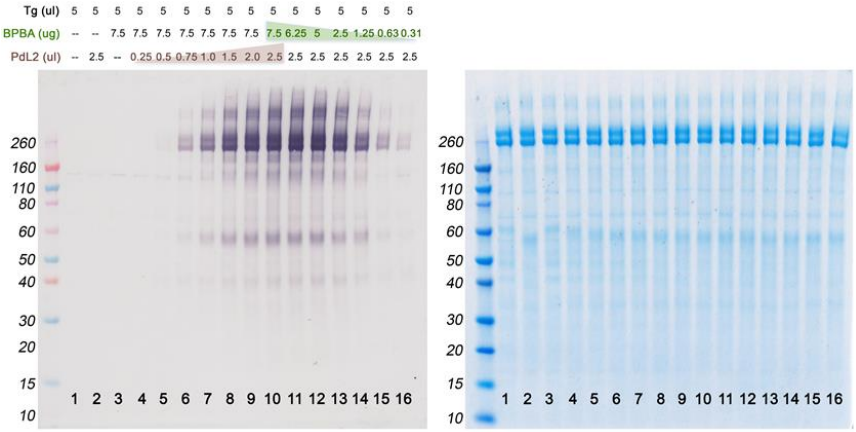

Figure 5.13 Determination of threshold levels of the $[\mathbf{L2}]_2Pd(OAc)_2$ and biotinylated boronic acid for *ex vivo* Suzuki reactions by SDS-PAGE and Western blot (using anti-biotin alkaline phosphatase antibody).

We mainly focused on the results of biotinylated Tg, which indicated that 1.5 mM biotinylated boronic acid and 2.5 mM $[\mathbf{L2}]_2Pd(OAc)_2$ were the minimal operational amounts for Pd-mediated reaction of the Tg under *ex vivo* conditions (Figure **5.14**).

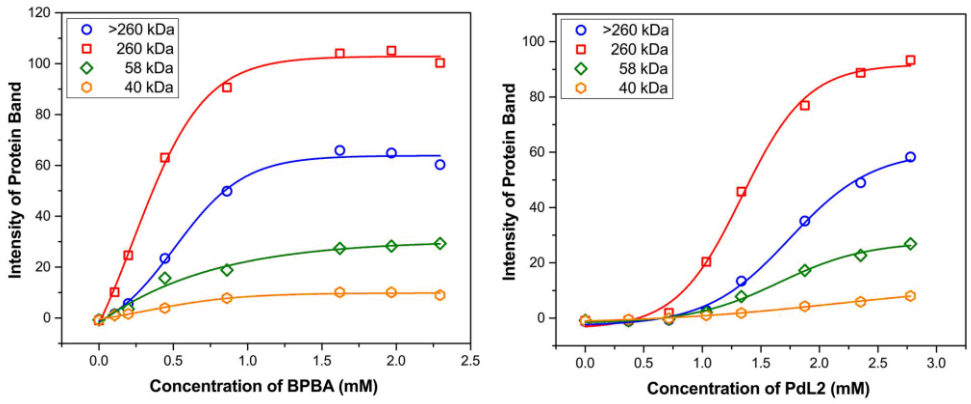

Figure 5.14 Plots between intensity of protein bands (Tg: MW ≥260 kDa, protein disulphide-isomerase: MW ~58 kDa, and actin: MW ~40 kDa) against the concentration of biotinylated boronic acid and $[\mathbf{L2}]_2Pd(OAc)_2$ catalyst.

According to previous experimental results, we further investigated the influence of reaction time by treatment of Tg with certain amounts of boronic acid (1.6 mM) and Pd

catalyst (2.9 mM) performed at 37 °C for 0 - 250 min (See experimental details, Table **5.11**). Each reaction mixture was examined by both Western blot and SDS-PAGE (Figure **5.15**). After calculation and data analysis, it was established that the reactions were complete within 2 h. based on the plots of intensity of protein bands *vs* reaction time (Figure **5.16**).

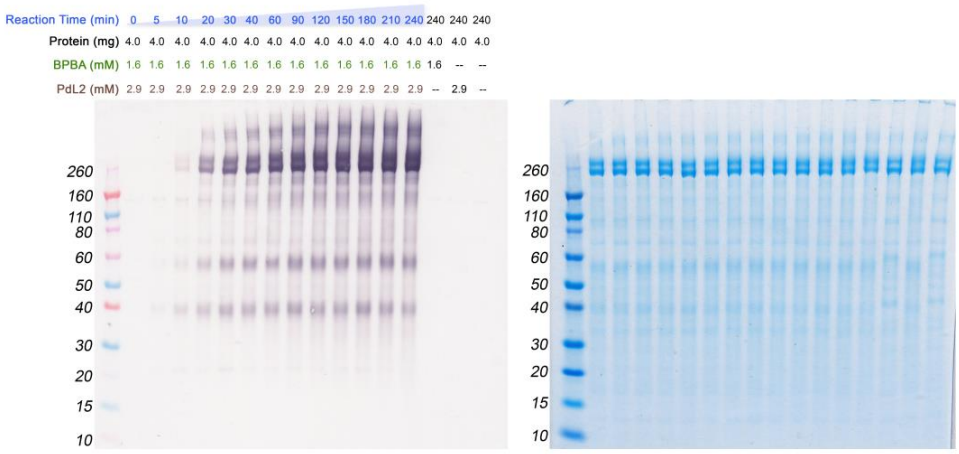

Figure 5.15 Determination of the reaction times of *ex vivo* Suzuki reactions by SDS-PAGE and Western blot (using anti-biotin alkaline phosphatase antibody).

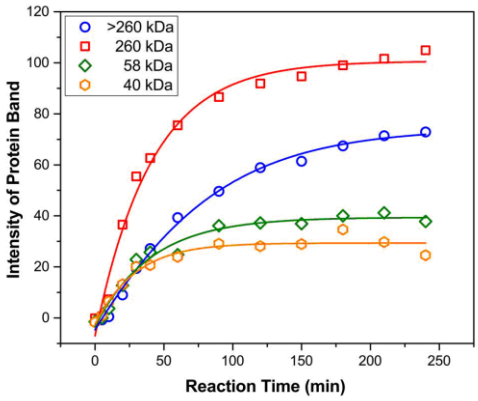

Figure 5.16 Plots between intensity of protein bands (Tg: MW ≥260 kDa, protein disulphide-isomerase: MW ~58 kDa, and actin: MW ~40 kDa) against the reaction times.

For our experiments, the coupling products were analysed by a range of techniques including SDS-PAGE, Western blot and MSMS. In particular, MSMS analysis focused on five possible chemical modifications including monoiodo-Tyr, diiodo-Tyr, monobiotin-Tyr, monobiotin/iodo-Tyr and dibiotin-Tyr. After biotin-streptavidin affinity resin purification, each Tg band was digested and analysed by MSMS to confirm the

presence of biotin-coupled Tg. Fortunately, we found several modifications of the Tg which correlated to the biotin-coupled Tg tyrosine residues (Figures **5.17-5.19**).

Score	Mr(found)	Mr(Calc)	Expect	Modifications	Peptide sequence
57	2057.8180	2057.8207	2.3×10^{-5}	monobiotin / monoiodo-Tyr (Y-1424)	LYFLNGDSFVTSPR
64	1931.9266	1931.9240	5.9×10^{-7}	monobiotin-Tyr (Y-1424)	LYFLNGDSFVTSPR
33	2973.3254	2972.3071	7.4×10^{-4}	dibiotin-Tyr (Y-2657)	AYQGQFSTEEQSLSLKVMQY

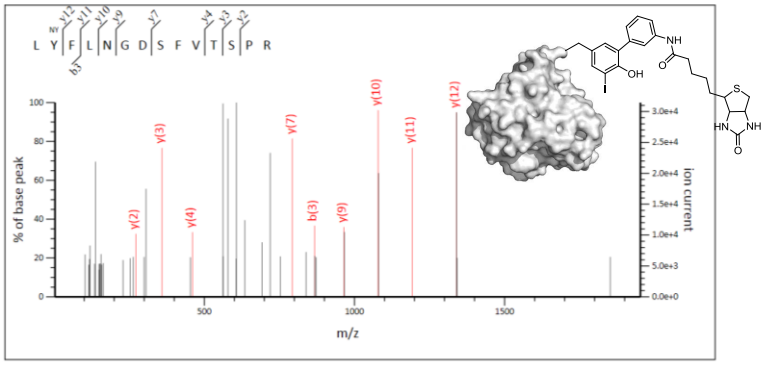

Figure 5.17 Peptide fragmentation (LYFLNGDSFVTSPR) shows a modification site of monobiotin and monoiodo-tyrosine (Tg) using Mascot.

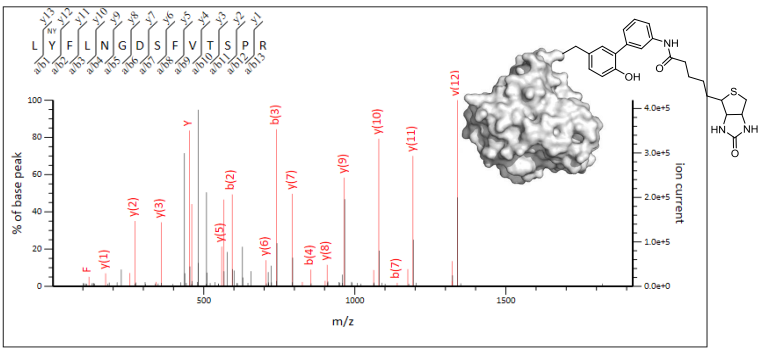

Figure 5.18 Peptide fragmentation (LYFLNGDSFVTSPR) shows a modification site of monobiotin-tyrosine (Tg) using Mascot.

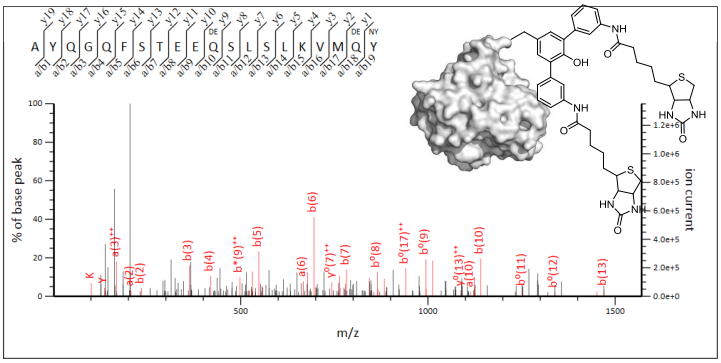

Figure 5.19 Peptide fragmentation (AYQGQFSTEEQSLSLKVMQY) shows a modification site of dibiotin-tyrosine (Tg) using Mascot.

After biotin-streptavidin affinity resin purification, the biotin-coupled Tg protein bands (MW ~260 kDa) were observed using SDS-PAGE. Surprisingly, actin (MW ~40 kDa) also bound to streptavidin resin, leading to a detection of actin protein bands on the SDS-PAGE (Figure **5.20**). The nature of the modified actin was investigated by MSMS analysis, indicating that some tyrosine residues were naturally iodinated and then coupled to the biotinylated phenylboronic acid (Figures **5.21** and **5.22**).

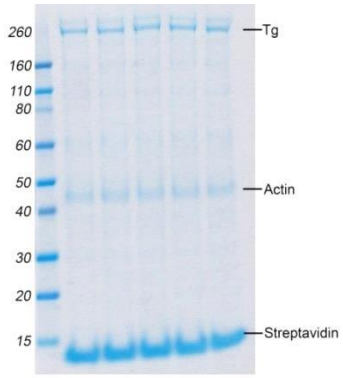

Figure 5.20 Detection of actin protein bands on SDS-PAGE after biotin-streptavidin affinity resin purification.

Score	Mr(found)	Mr(Calc)	Expect	Modifications	Peptide sequence
23	1080.3746	1080.3737	0.066	monoiodo-Tyr (Y-145)	SLYASGRTT
58	1919.8061	1919.8067	8.3×10^{-5}	monoiodo-Tyr (Y-171)	THNVPIYEGYALPHAI
29	1248.3800	1248.3796	0.031	monoiodo-Tyr (Y-364)	KQEYDEAGPS
39	2116.9709	2115.9506	0.0028	dibiotin-Tyr (Y-55)	KDSYVGDEAQSKR
22	1872.9382	1872.9232	0.19	monobiotin-Tyr (Y-168)	NVPIYEGYALPHAI

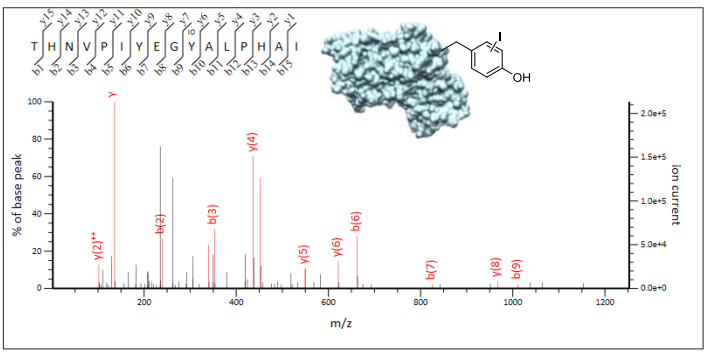

Figure 5.21 Peptide fragmentation (THNVPIYEGYALPHAI) shows a modification site of monoiodo-tyrosine (Tg) using Mascot.

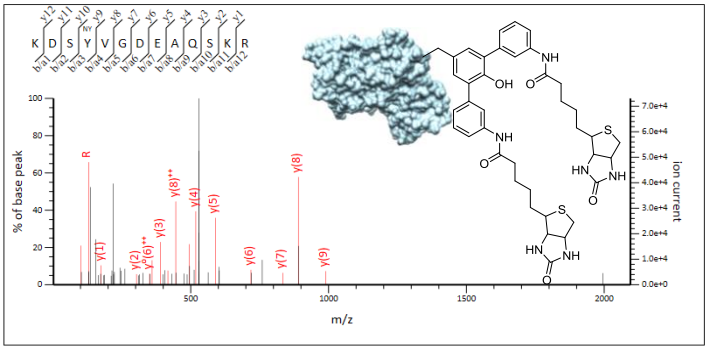

Figure 5.22 Peptide fragmentation (KDSYVGDEAQSKR) shows a modification site of dibiotin-tyrosine (Tg) using Mascot.

5.3.2 *In vivo* Pd-Mediated Reactions of Thyroglobulin (Tg)

Based on our demonstration of protein labelling *ex vivo*, we further extended our aqueous Pd-mediated system to challenging biological systems involving chemical conjugation *in vivo* of some biomacromolecules. This is attractive as a proof of biocompatibility and subsequent application to a preclinical animal study of thyroid activity diagnosis. Our initial investigation of the *in vivo* Pd-mediated cross-coupling of the Tg proceeded from direct injection of each solution of biotinylated phenylboronic acid + Pd catalyst into the thyroid gland (Figure **5.23**). Each reaction was allowed to proceed inside animals at 37 °C for 5h (See experimental details, Table **5.12**). Pre-treated thyroid glands were excised and homogenised in PBS buffer, pH 7.6, then each reaction mixture was run on the SDS-PAGE and Western blot for a detection of the biotin-coupled Tg. Our preliminary results indicated that the presence of weak protein bands at the position of Tg (MW ~260 kDa) (after purification by biotin-streptavidin affinity column) was observed on the membrane using anti-biotin alkaline phosphatase antibody (Figure **5.24**). This indicated that a low level of Pd-mediated Suzuki-Miyaura cross-coupling of Tg occurred under *in vivo* conditions.

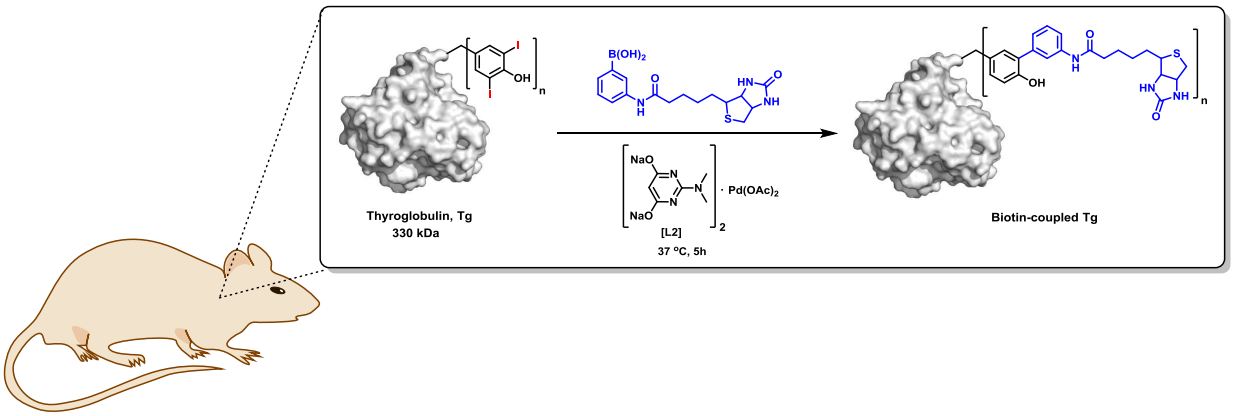

Figure 5.23 A model study of Pd-catalysed protein labelling under *in vivo* conditions by use of our aqueous Pd-mediated cross-coupling system.

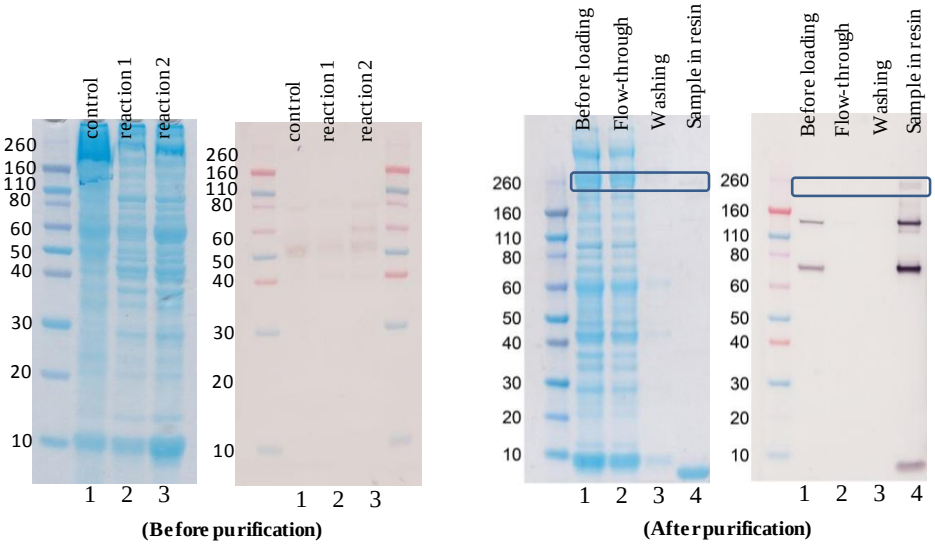

Figure 5.24 SDS-PAGEs and Western blot of the reaction mixture or purified biotinylated Tg stained with anti-biotin alkaline phosphatase antibody.

5.4 Conclusion

Our Pd cross-coupling system is able to show *ex vivo* protein labelling of thyroglobulin (Tg) through Suzuki-Miyaura reactions. Treatment of Tg (originated from thyroid gland tissue) with biotinylated phenylboronic acid gave biotin-coupled products confirmed by anti-biotin alkaline phosphatase antibody. All modified proteins, in particular Tg, were separated by electrophoresis and further analysed by MSMS, indicating that the mixture of the biotin-coupled products included monobiotin-Tyr, dibiotin-Tyr and monoiodo/monobiotin-Tyr (Figure **5.25**). This initial study of the Suzuki reaction under

ex vivo conditions will be useful in a further investigation of *in vivo* applications of Pd-mediated biorthogonal reactions in mammalian living systems. The current *in vivo* experiment exhibited a relatively low level biotinylation of Tg through Suzuki-Miyaura reactions. This reduced efficiency is possibly due to the existence of the circulatory system in living animals, which may cause the dilution of Pd catalyst and biotin boronic acid substrate.

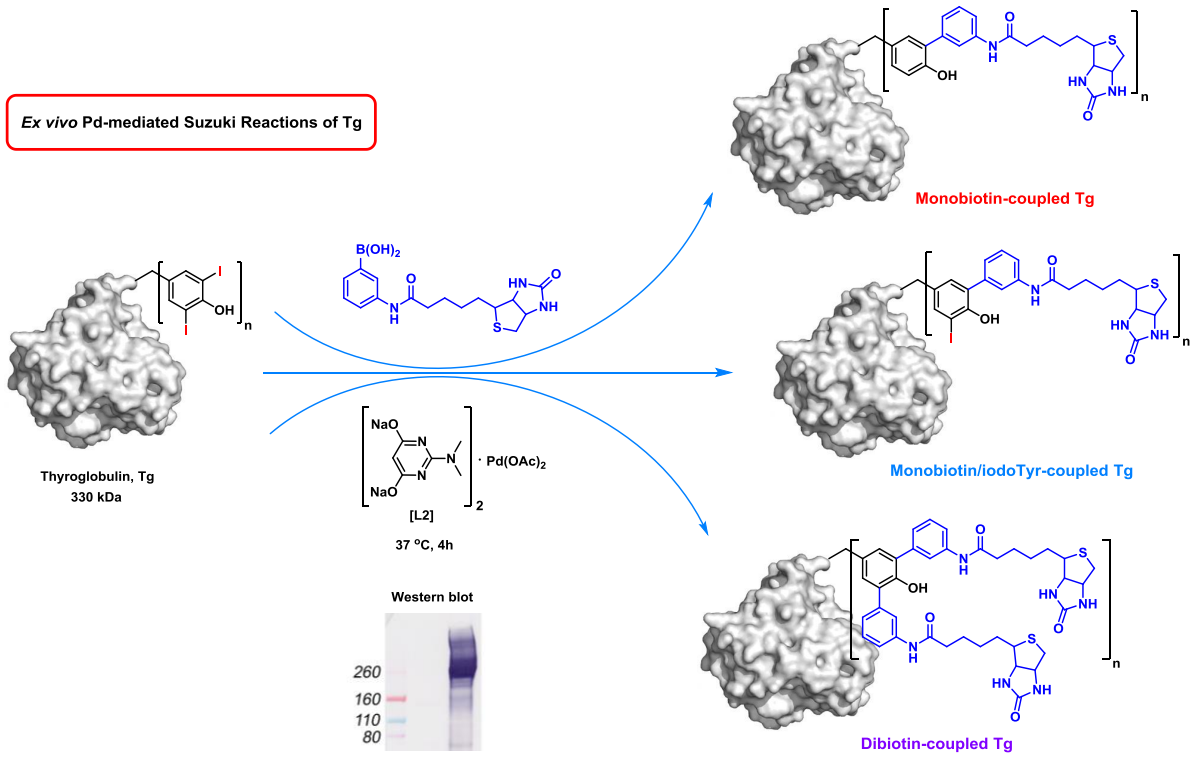

Figure 5.25 *Ex vivo* Pd-mediated reactions of thyroglobulin (Tg) with biotinylated phenylboronic acid through Suzuki-Miyaura reactions. Confirmation of the biotin-coupled products was detected by anti-biotin alkaline phosphatase antibody and also analysed by MSMS.

5.5 Experimental

5.5.1 Palladium Cross-Coupling of Thyroid Hormones

Pd-Mediated Reactions of Thyroxine (T4)

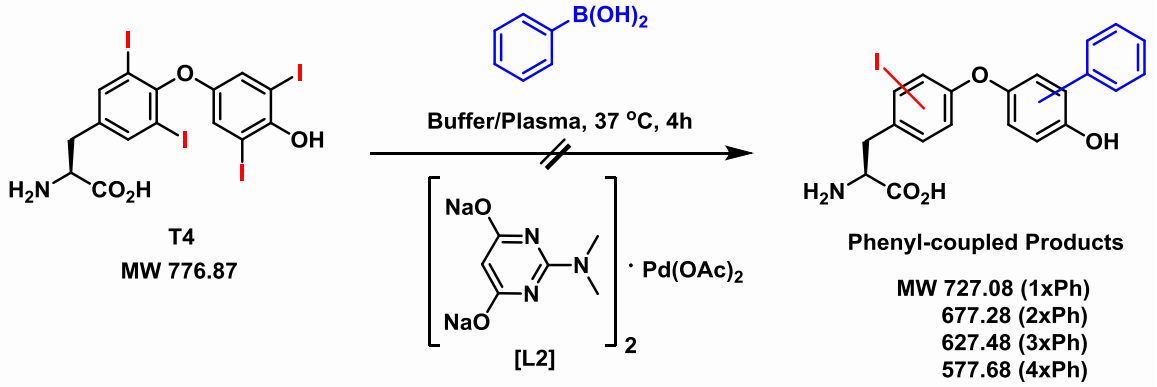

Each aliquot of T4 (1.2 µmol, 12.3 µL from stock solution in 0.2 M NaOH, conc. 25.0 mg/mL) in 50 mM NaH_2PO_4 or 50 mM NaH_2PO_4/rat plasma (1:1) or rat plasma (100 µL) was mixed with a solution of the $PhB(OH)_2$ in 0.2 M NaOH (6.0 µmol, 9.7 µL from stock solution, conc. 25.0 mg/mL) by vortexing briefly. A [**L2**]$_2$Pd(OAc)$_2$ catalyst solution (0.24 µmol, 8 µL, from stock solution in 0.1 M NaOH, conc. 0.01 M) was added to each reaction mixture. After 4 h. of shaking at 37 °C, each aliquot was directly analysed by LC–MS.

Entry	T4 (equiv.)	$PhB(OH)_2$ (equiv.)	[L2]$_2$Pd(OAc)$_2$ (equiv.)	Reaction Conditions	ESI-MS
1	1.0 (1.2 µmol)	5.0 (6.0 µmol)	0.2 (0.24 µmol)	50 mM NaP_i	777.75 (SM)
2	1.0 (1.2 µmol)	5.0 (6.0 µmol)	0.2 (0.24 µmol)	50 mM NaP_i + rat plasma (1:1)	777.69 (SM)
3	1.0 (1.2 µmol)	5.0 (6.0 µmol)	0.2 (0.24 µmol)	rat plasma	777.69 (SM)

General conditions: T4 in 0.2 M NaOH (c = 25.0 mg/mL), $PhB(OH)_2$ in 0.2 M NaOH (c = 25.0 mg/mL), [**L2**]$_2$Pd(OAc)$_2$ in 0.1 M NaOH (c = 0.01 M) at 37 °C for 4h unless otherwise indicated.

Table 5.6 Optimisation experiments of the SMC reactions of T4 with $PhB(OH)_2$ in the presence of [**L2**]$_2$Pd(OAc)$_2$ catalyst.

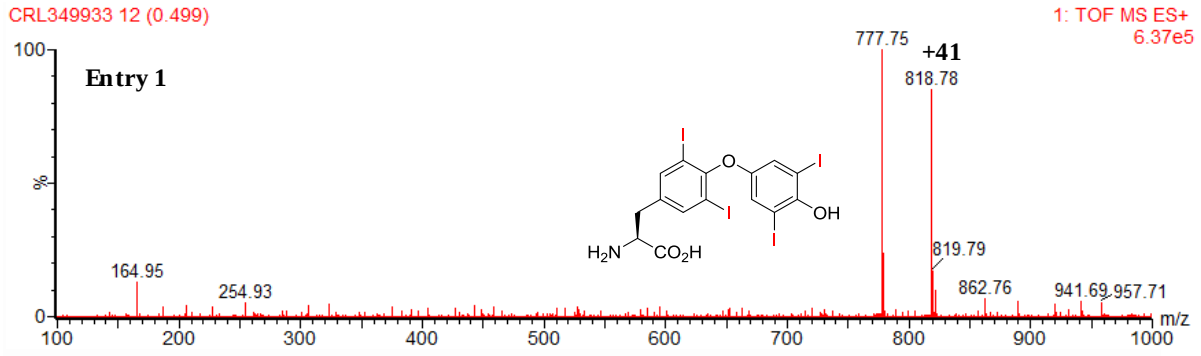

Figure 5.26 ESI-MS spectrum of the unreactive T4 and $[M-H+41]^+$ adduct from treatment of T4 with $PhB(OH)_2$ and $[\mathbf{L2}]_2Pd(OAc)_2$ catalyst in 50 mM NaH_2PO_4.

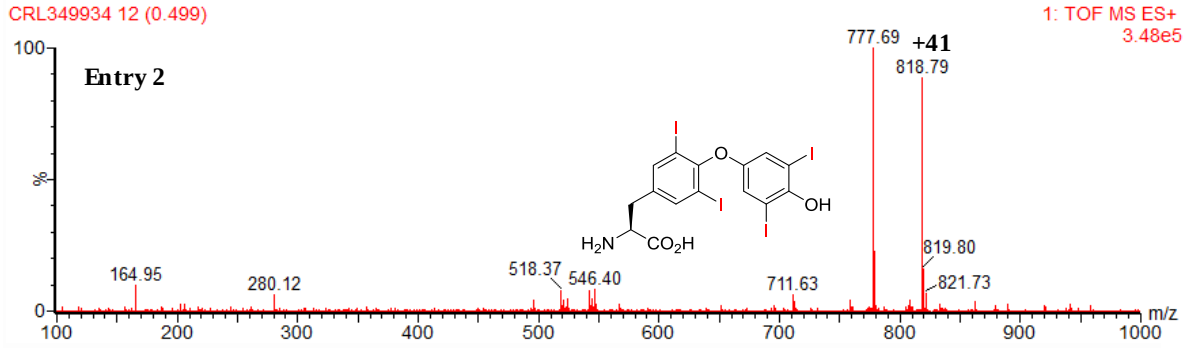

Figure 5.27 ESI-MS spectrum of the unreactive T4 and $[M-H+41]^+$ adduct from treatment of T4 with $PhB(OH)_2$ and $[\mathbf{L2}]_2Pd(OAc)_2$ catalyst in 50 mM NaH_2PO_4/rat plasma (1:1).

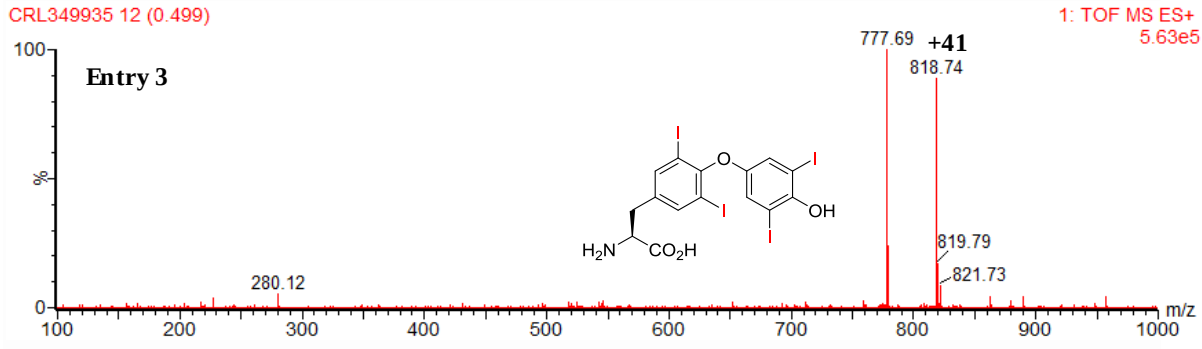

Figure 5.28 ESI-MS spectrum of the unreactive T4 and $[M-H+41]^+$ adduct from treatment of T4 with $PhB(OH)_2$ and $[\mathbf{L2}]_2Pd(OAc)_2$ catalyst in rat plasma.

Pd-Mediated Reactions of the Protected Thyroid Hormone (BocNH-T4)

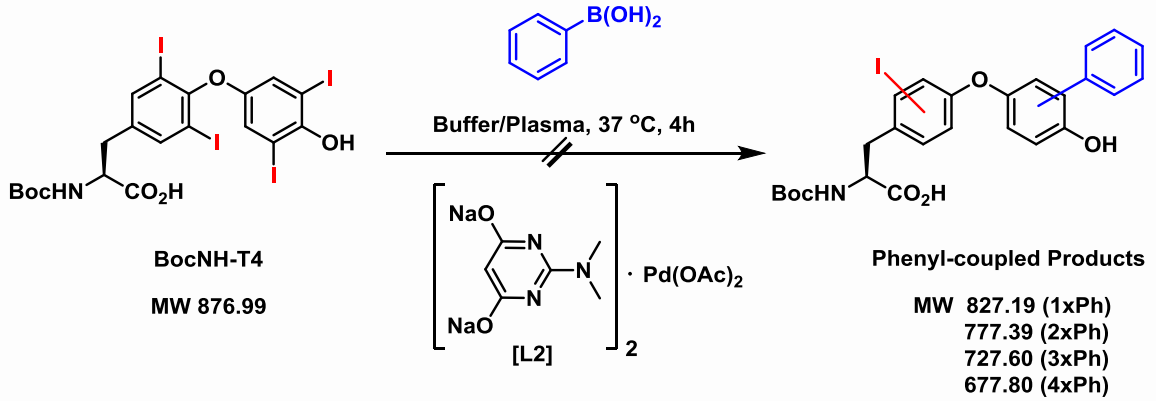

(Same procedure mentioned in section 5.5.1, except for starting materials used in Table **5.7**.)

Entry	BocNH-T4 (equiv.)	$PhB(OH)_2$ (equiv.)	$[L2]_2Pd(OAc)_2$ (equiv.)	Reaction Conditions	ESI-MS
1	1.0 (1.2 µmol)	5.0 (6.0 µmol)	0.2 (0.24 µmol)	50 mM NaP_i	875.83 (SM)
2	1.0 (1.2 µmol)	5.0 (6.0 µmol)	0.2 (0.24 µmol)	50 mM NaP_i + plasma (1:1)	875.82 (SM)
3	1.0 (1.2 µmol)	5.0 (6.0 µmol)	0.2 (0.24 µmol)	Rat plasma	875.83 (SM)

General conditions: BocNH-T4 in 0.2 M NaOH (c = 25.0 mg/mL), $PhB(OH)_2$ in 0.2 M NaOH (c = 25.0 mg/mL), $[\mathbf{L2}]_2Pd(OAc)_2$ in 0.1 M NaOH (c = 0.01 M) at 37 °C for 4h unless otherwise indicated.

Table 5.7 Optimisation experiments of the SMC reactions of the BocNH-T4 with $PhB(OH)_2$ in the presence of $[\mathbf{L2}]_2Pd(OAc)_2$ catalyst.

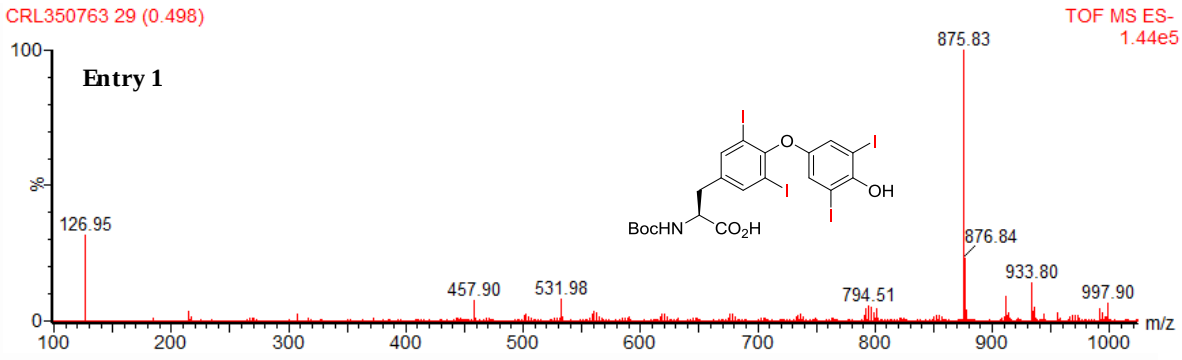

Figure 5.29 ESI-MS spectrum of the unreactive BocNH-T4 from treatment of BocNH-T4 with $PhB(OH)_2$ and $[\mathbf{L2}]_2Pd(OAc)_2$ catalyst in 50 mM NaH_2PO_4.

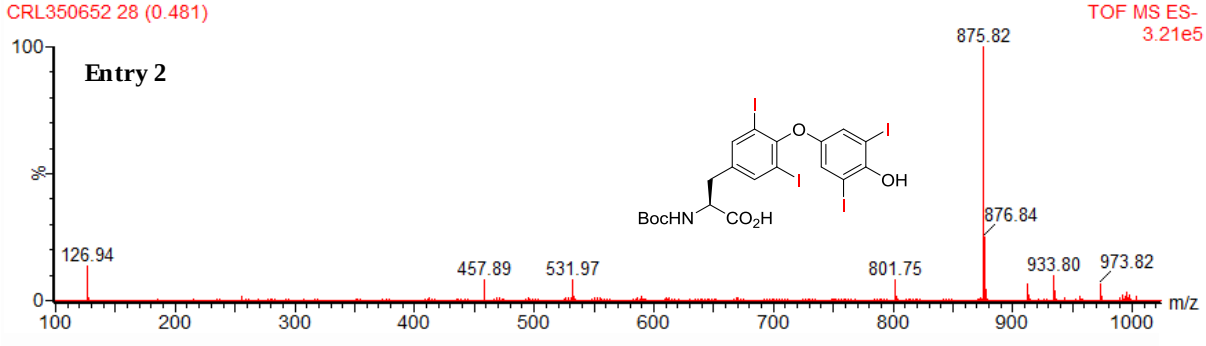

Figure 5.30 ESI-MS spectrum of the unreactive BocNH-T4 from treatment of BocNH-T4 with $PhB(OH)_2$ and $[\mathbf{L2}]_2Pd(OAc)_2$ catalyst in 50 mM NaH_2PO_4/rat plasma (1:1).

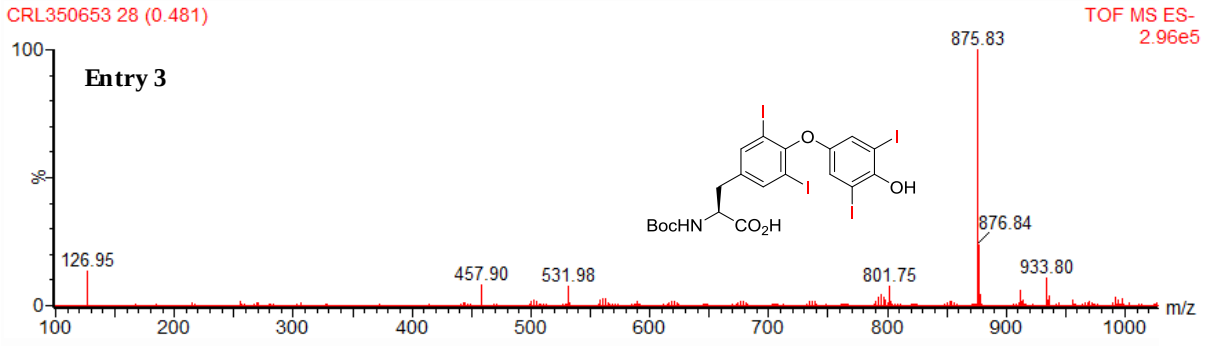

Figure 5.31 ESI-MS spectrum of the unreactive BocNH-T4 from treatment of BocNH-T4 with $PhB(OH)_2$ and $[\mathbf{L2}]_2Pd(OAc)_2$ catalyst in rat plasma.

5.5.2 Palladium Cross-Coupling of Thyroglobulin (Tg)

(Collaboration with Dr. Nan Yang: Department of Chemistry, University of Oxford.)

Ex vivo Suzuki-Miyaura cross-coupling of Tg with boronic acids (I)

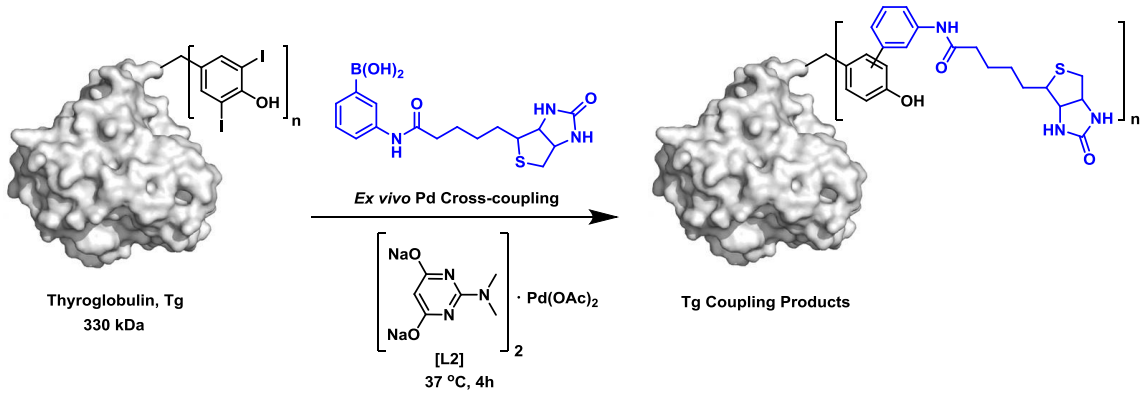

A thyroid gland tissue from mouse was homogenised and re-suspended in 100 µL of PBS buffer, pH 7.6. Each aliquot of the Tg suspension (5.0-10.0 µL) was mixed with a solution of the biotinylated phenylboronic acid in DMSO (0.25-1.0 µL from stock solution, conc. 50 mg/mL) by vortexing briefly. A $[\mathbf{L2}]_2Pd(OAc)_2$ catalyst solution in 0.1

M NaOH (2.5-10.0 µL from stock solution, conc. 0.01 M) was added to each reaction mixture which was vortexed briefly. After 4 h. of shaking at 37°C, each aliquot was analysed by SDS-PAGE and Western blot (using anti-biotin alkaline phosphatase antibody).

Entry	Tg-mixture (µL)	$[L2]_2Pd(OAc)_2$ (µL)	$R\text{-}B(OH)_2$ (µL)	Temp	Time	Remarks
1	5	-	-	4°C	4h	Tissue
2	5	-	-	37 °C	4h	Control
3	5	2.5	-	37 °C	4h	Control
4	5	-	0.25	37 °C	4h	Control
5	10	10	0.25 (R = Ph)	37 °C	4h	Reaction
6	10	5	0.25	37 °C	4h	Reaction
7	10	10	0.25	37 °C	4h	Reaction
8	10	20	0.25	37 °C	4h	Reaction
9	10	10	0.50	37 °C	4h	Reaction
10	10	10	1.0	37 °C	4h	Reaction

General conditions: Tg in PBS (pH 7.6), $[\mathbf{L2}]_2Pd(OAc)_2$ in 0.1 M NaOH (c = 0.01 M), biotinylated $B(OH)_2$ in DMSO (c = 50 mg/mL) at 37 °C for 4h, unless otherwise indicated.

Table 5.8 Investigation of *ex vivo* Pd cross-coupling of Tg mixture with biotin-$B(OH)_2$ in the presence of $[\mathbf{L2}]_2Pd(OAc)_2$.

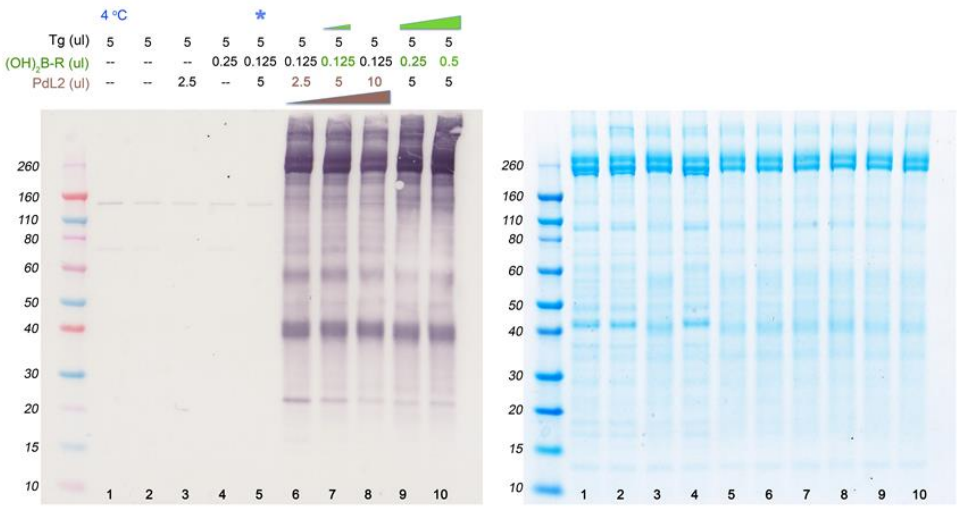

Figure 5.32 Western blot and SDS-PAGE of each reaction mixture stained by anti-biotin alkaline phosphatase antibody.

***Ex vivo* Suzuki-Miyaura cross-coupling of Tg with boronic acids (II)**

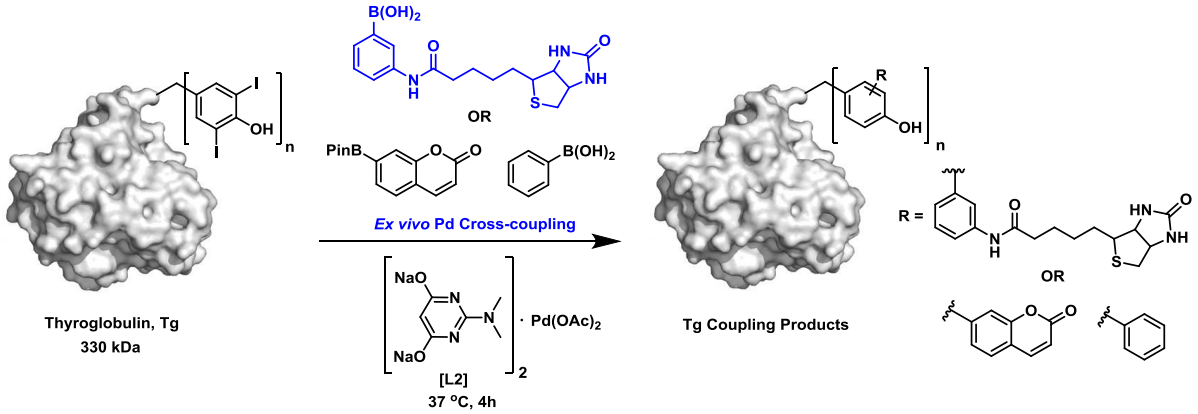

(Same procedure mentioned in section 5.5.2, except for protein/reagents used as follows)

1. Semi-purification of the Tg-mixture by a vivaspin concentrator (100 kDa MWCO) and measurement of its concentration by NanoDrop A_{280} spectrophotometry,
2. A semi-purified Tg (0.06 nmol, 10 µL, 2.0 mg/mL) in PBS buffer, pH 7.6,
3. Each solution of boronic acids in DMSO (30 nmol, 0.55 µL (biotinylated), 0.47 µL (coumarinyl), 0.18 µL (phenyl) from stock solution, conc. = 50 mg/mL), and
4. A [**L2**]$_2$Pd(OAc)$_2$ catalyst solution (3 nmol, 0.3 µL, conc. = 0.01 M).

Entry	Purified Tg (equiv.)	[L2]$_2$Pd(OAc)$_2$ (equiv.)	R-B(OH)$_2$ (equiv.)	Temp	Time	Remarks
1	1	-	-	4°C	4h	Tissue
2	1	-	-	37 °C	4h	Control
3	1	50	-	37 °C	4h	Control
4	1	-	500 (biotinylated)	37 °C	4h	Control
5	1	50	500 (biotinylated)	37 °C	4h	Reaction
6	1	50	500 (coumarinyl)	37 °C	4h	Reaction
7	1	50	500 (phenyl)	37 °C	4h	Reaction

General conditions: Tg in NaH_2PO_4 (50 mM, pH 8.0 and c = 2.0 mg/mL), [**L2**]$_2$Pd(OAc)$_2$ in 0.1 M NaOH (c = 0.01 M), R-B(OH)$_2$ in DMSO (c = 50 mg/mL) at 37 °C for 4h, unless otherwise indicated.

Table 5.9 Investigation of *ex vivo* Pd cross-coupling of the purified Tg with different R-B(OH)$_2$ in the presence of [**L2**]$_2$Pd(OAc)$_2$.

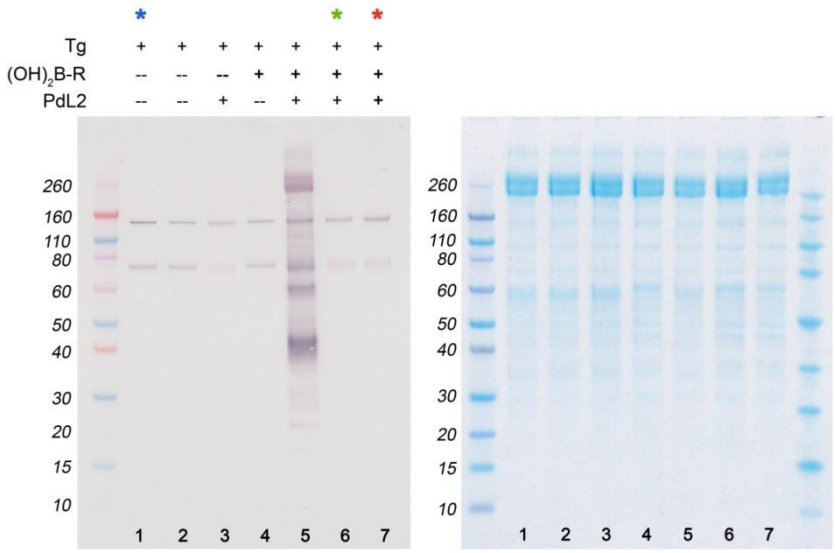

Figure 5.33 Western blot and SDS-PAGE of each reaction mixture by staining with anti-biotin alkaline phosphatase antibody. Lane 5 shows a detection of the biotin-coupled Tg.

Ex vivo Suzuki-Miyaura cross-coupling of Tg with biotin-boronic acids (III)

Determination of threshold levels of Pd catalyst and boronic acid

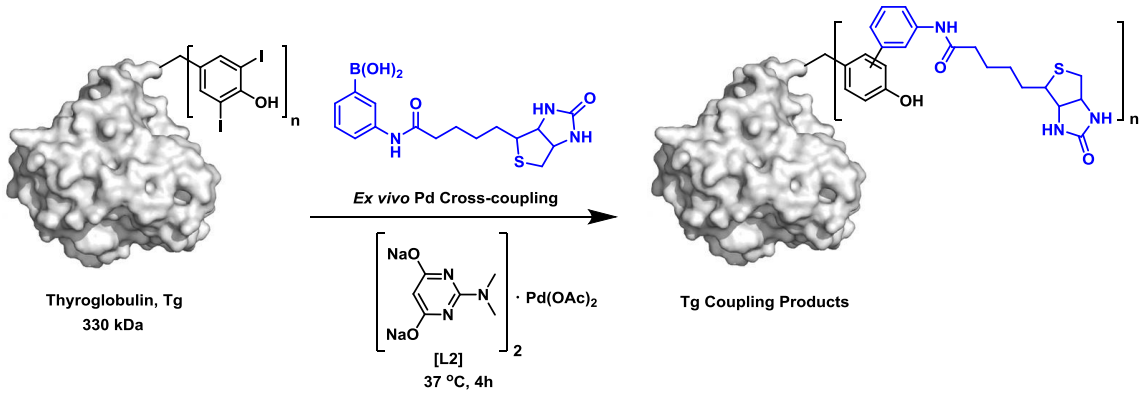

(Same procedure mentioned in section 5.5.2, except for proteins/reagents used in Table **5.10.)**

Entry	Tg-mixture (µL)	$[L2]_2Pd(OAc)_2$ (µL)	$R\text{-}B(OH)_2$ (µL)	Temp (°C)	Time (h)	Remarks
1	5	-	-	37	4	Control
2	5	2.5	-	37	4	Control
3	5	-	1.5	37	4	Control
4	5	0.25	1.5	37	4	Reaction
5	5	0.50	1.5	37	4	Reaction
6	5	0.75	1.5	37	4	Reaction
7	5	1.0	1.5	37	4	Reaction
8	5	1.5	1.5	37	4	Reaction
9	5	2.0	1.5	37	4	Reaction
10	5	2.5	1.5	37	4	Reaction
11	5	2.5	1.25	37	4	Reaction
12	5	2.5	1.0	37	4	Reaction
13	5	2.5	0.5	37	4	Reaction
14	5	2.5	0.25	37	4	Reaction
15	5	2.5	1.25	37	4	Reaction
16	5	2.5	0.625	37	4	Reaction

General conditions: Tg-mixture in NaH_2PO_4 (50 mM, pH 8.0), $[\mathbf{L2}]_2Pd(OAc)_2$ in 0.1 M NaOH (c = 0.01 M), biotinylated $B(OH)_2$ in DMSO (c = 5.0 mg/mL for Entry 3-14 and c = 0.5 mg/mL for Entry 15-16) at 37 °C for 4h, unless otherwise indicated. Final concentrations of each reagent: 0.37-2.778 mM $[\mathbf{L2}]_2Pd(OAc)_2$ and 0.106-2.295 mM biotinylated $B(OH)_2$.

Table 5.10 Investigation of *ex vivo* Pd cross-coupling of the purified Tg with biotin-$B(OH)_2$ in the presence of $[\mathbf{L2}]_2Pd(OAc)_2$.

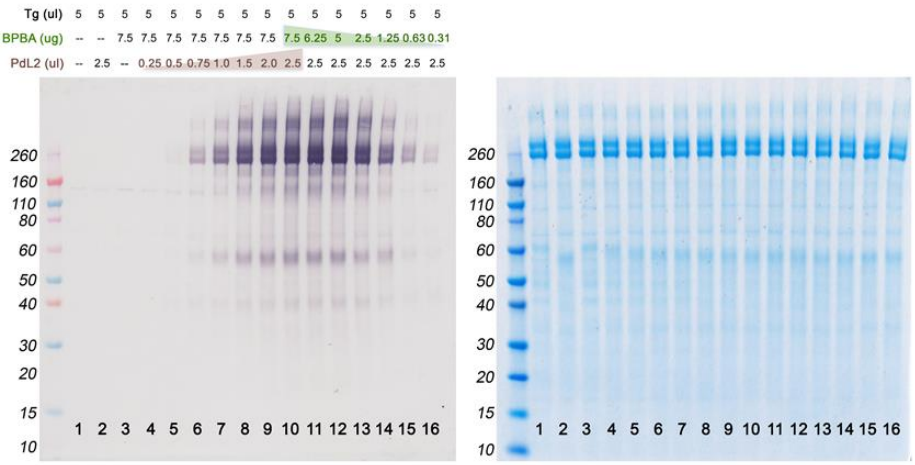

Figure 5.34 Determination of threshold levels of the $[\mathbf{L2}]_2Pd(OAc)_2$ and biotinylated boronic acid for *ex vivo* Suzuki reactions by SDS-PAGE and Western blot (using anti-biotin alkaline phosphatase antibody).

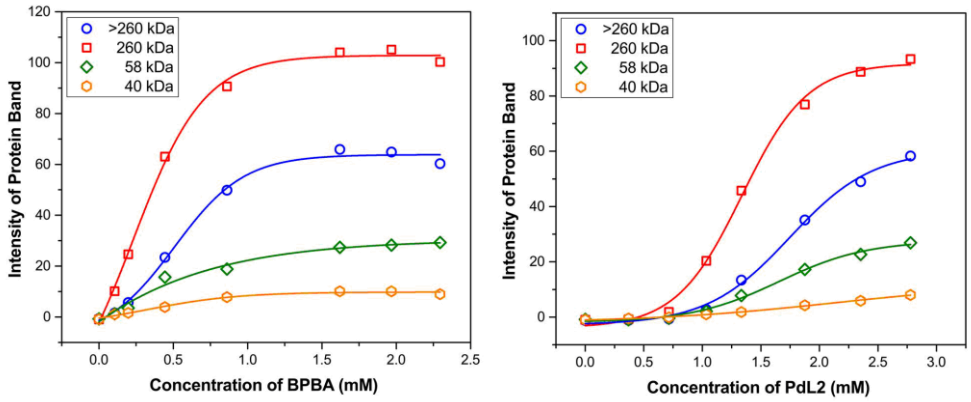

Figure 5.35 Plots between intensity of protein bands against the concentrations of biotinylated boronic acid and [**L2**]$_2$Pd(OAc)$_2$ catalyst.

Ex vivo Suzuki-Miyaura cross-coupling of Tg with biotin-boronic acids (IV) Determination of reaction times

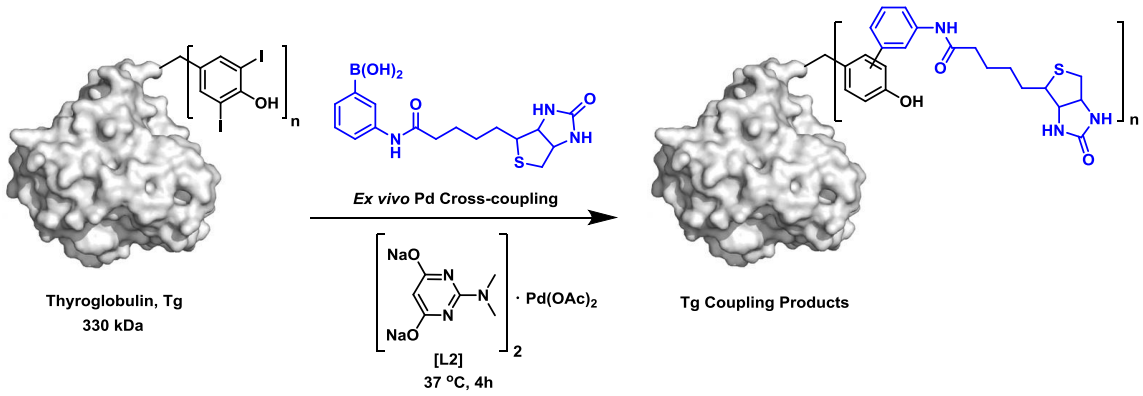

(Same procedure mentioned in section 5.5.2, except for proteins/reagents used in Table **5.11.)**

Entry	Tg-mixture (µL)	$[L2]_2Pd(OAc)_2$ (µL)	$R\text{-}B(OH)_2$ (µL)	Temp (°C)	Time (min)	Remarks
1	5	2.5	1.0	37	0	Control
2	5	2.5	1.0	37	5	Control
3	5	2.5	1.0	37	10	Control
4	5	2.5	1.0	37	20	Reaction
5	5	2.5	1.0	37	30	Reaction
6	5	2.5	1.0	37	40	Reaction
7	5	2.5	1.0	37	60	Reaction
8	5	2.5	1.0	37	90	Reaction
9	5	2.5	1.0	37	120	Reaction
10	5	2.5	1.0	37	150	Reaction
11	5	2.5	1.0	37	180	Reaction
12	5	2.5	1.0	37	210	Reaction
13	5	2.5	1.0	37	240	Reaction
14	5	-	1.0	37	240	Reaction
15	5	2.5	-	37	240	Reaction
16	5	-	-	37	240	Reaction

General conditions: Tg-mixture in NaH_2PO_4 (50 mM, pH 8.0), $[\mathbf{L2}]_2Pd(OAc)_2$ in 0.1 M NaOH (c = 0.01 M), biotinylated $B(OH)_2$ in DMSO (c = 5.0 mg/mL) at 37 °C for 4h, unless otherwise indicated. Final concentrations of each reagent: 2.9 mM $[\mathbf{L2}]_2Pd(OAc)_2$ and 1.6 mM biotinylated $B(OH)_2$.

Table 5.11 Investigation of *ex vivo* Pd cross-coupling of the purified Tg with biotin-$B(OH)_2$ in the presence of $[\mathbf{L2}]_2Pd(OAc)_2$.

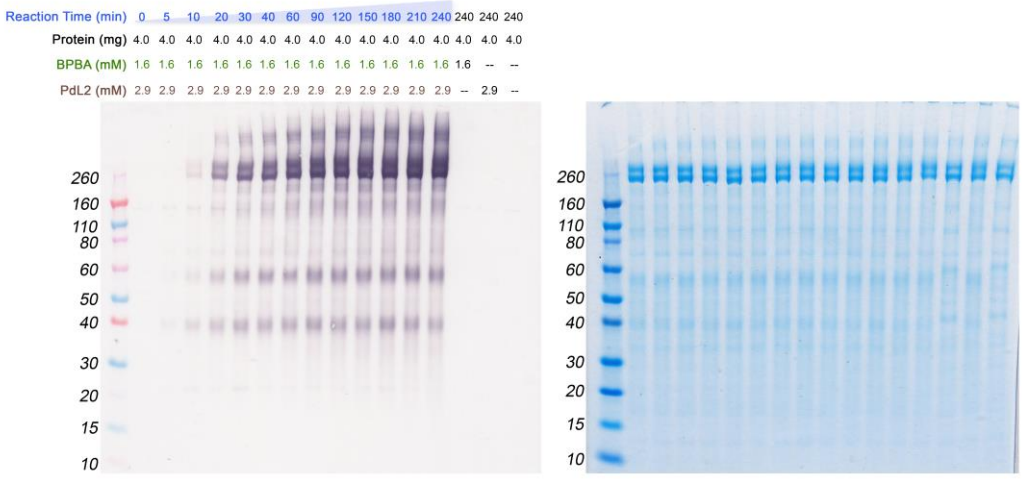

Figure 5.36 Determination of reaction times of *ex vivo* Suzuki reactions by SDS-PAGE and Western blot (using anti-biotin alkaline phosphatase antibody).

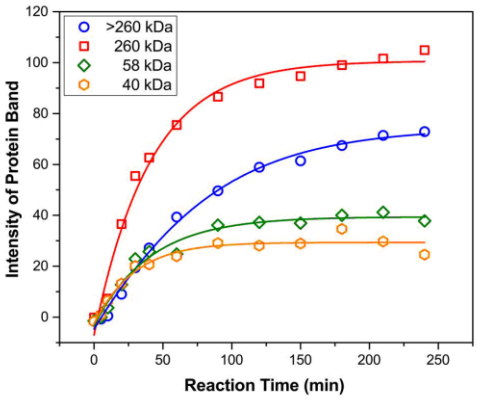

Figure 5.37 Plots between intensity of protein bands against reaction times.

***In vivo* Suzuki-Miyaura cross-coupling of Tg with biotin-boronic acid**

(Collaboration with Prof. Daniel C. Anthony: Department of Pharmacology, University of Oxford, and Dr. Nan Yang: Department of Chemistry, University of Oxford.)

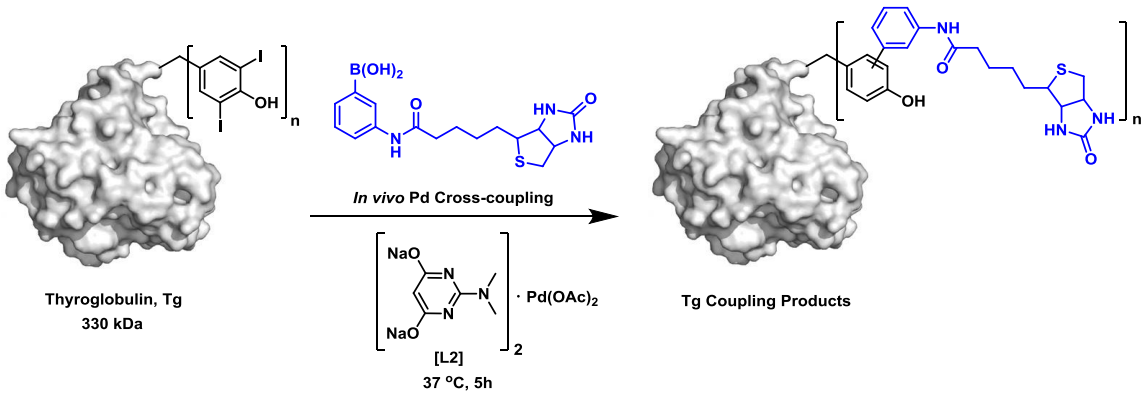

Adult male Sprague Dawley (SD) rats (Harlan, UK, ~300-400 g) were anesthetised using isoflurane for induction and maintenance at 2.5-3.0% in oxygen, and a local lignocaine anaesthesia (100µL) was injected into the skin in the neck and the incision site. All animal experiments performed under a UK Home Office licence and with full ethical approval. The thyroid was exposed by blunt dissection with the aid of a surgical microscope (wildM650, Leica). The reaction components were delivered directly into the thyroid glands over a 5 min period (addition of 10 mM biotinylated phenylboronic acid solution, and subsequent injection of $[\mathbf{L2}]_2Pd(OAc)_2$ solution) (Table **5.12**). All pre-treated animals were maintained in a heated chamber (37 °C) during the reaction periods. After 5 h, the animals were killed by cervical dislocation under deep anaesthesia, and thyroid glands were excised for further analysis. Each excised thyroid gland was

homogenised in PBS buffer, pH 7.6, and each reaction mixture was then run on the SDS-PAGE and subsequently followed by Western blot using anti-biotin alkaline phosphatase antibody for a detection of the biotin-coupled Tg. It was found, in these preliminary experiments, that weak protein bands could be visualised on the membrane post biotin-streptavidin affinity resin purification (Figure **5.38**).

Entry	**$[L2]_2Pd(OAc)_2$ (µL)**	**R-$B(OH)_2$ (µL)**	**Temp (°C)**	**Time (min)**	**Remarks**
1	-	5.0	37	300	Control
2	5.0	5.0	37	300	Reaction 1
3	2x5.0	2x5.0	37	300	Reaction 2

General conditions: [**L2**]$_2$Pd(OAc)$_2$ in 0.1 M NaOH (c = 0.01 M), biotinylated B(OH)$_2$ in DMSO (c = 0.01 M) at 37 °C for 5h, unless otherwise indicated.

Table 5.12 Investigation of *in vivo* Pd cross-coupling of the Tg with biotinylated phenylboronic acid in the presence of [**L2**]$_2$Pd(OAc)$_2$.

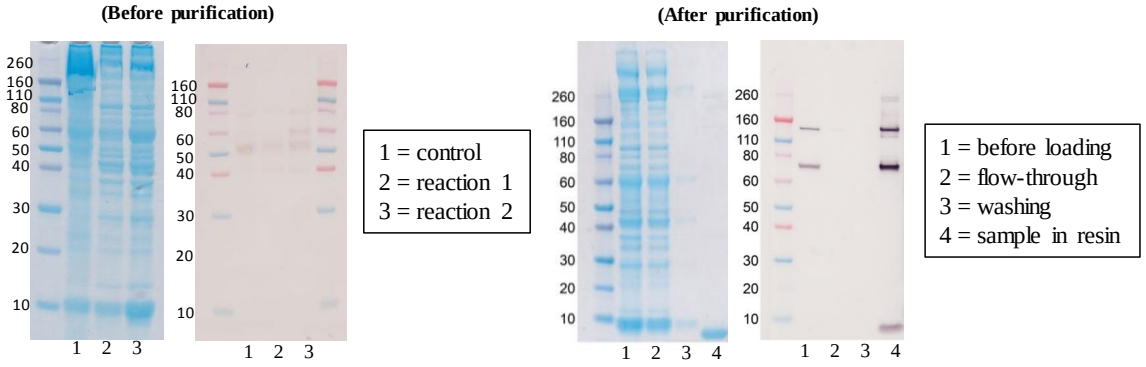

Figure 5.38 SDS-PAGEs and Western blot of the reaction mixture or purified biotinylated Tg (purified by biotin-streptavidin affinity column) stained with anti-biotin alkaline phosphatase antibody.

5.5.3 Western Blot Analysis

(See general experimental considerations in appendix)

Entry	Proteins	Antibodies		Dilution
		Primary	Secondary	
1	Thyroglobulin	Anti-biotin alkaline phosphatase antibody produced in goat	-	1 : 5,000
BCIP/NBT used as an alkaline phosphatase substrate.				

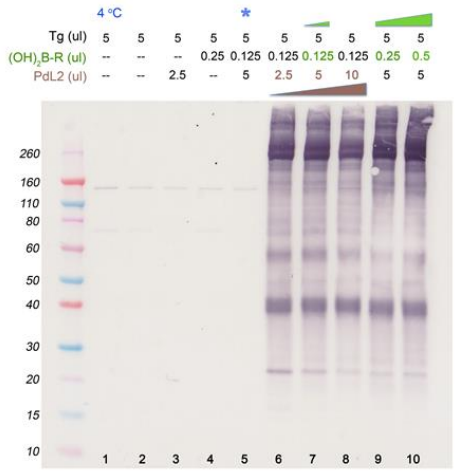

1 = control (Tg, 4 °C)
2 = control (Tg, 37 °C)
3 = control (Tg, PdL2, 37 °C)
4 = control (Tg, R-B(OH)$_2$, 37 °C, R = biotin)
5 = reaction (Tg, PdL2, R-B(OH)$_2$, 37 °C, R = Ph)
6 = reaction (Tg, PdL2, R-B(OH)$_2$, 37 °C, R = biotin)
7 = reaction (Tg, PdL2, R-B(OH)$_2$, 37 °C, R = biotin)
8 = reaction (Tg, PdL2, R-B(OH)$_2$, 37 °C, R = biotin)
9 = reaction (Tg, PdL2, R-B(OH)$_2$, 37 °C, R = biotin)
10 = reaction (Tg, PdL2, R-B(OH)$_2$, 37 °C, R = biotin)

Figure 5.39 Western blot of each reaction mixture stained by anti-biotin alkaline phosphatase antibody produced in goat and visualised by BCIP/NBT alkaline phosphatase substrate.

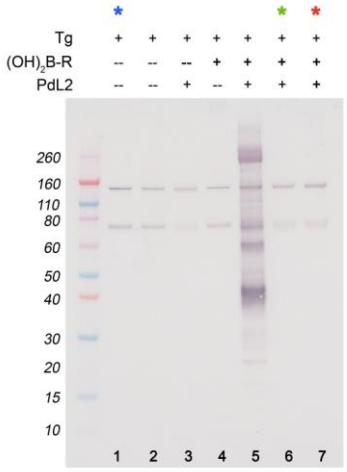

1 = control (Tg, 4 °C)
2 = control (Tg, 37 °C)
3 = control (Tg, PdL2, 37 °C)
4 = control (Tg, R-B(OH)$_2$, 37 °C, R = biotin)
5 = reaction (Tg, PdL2, R-B(OH)$_2$, 37 °C, R = biotin)
6 = reaction (Tg, PdL2, R-B(OH)$_2$, 37 °C, R = coumarin)
7 = reaction (Tg, PdL2, R-B(OH)$_2$, 37 °C, R = phenyl)

Figure 5.40 Western blot of each reaction mixture stained by anti-biotin alkaline phosphatase antibody produced in goat and visualised by BCIP/NBT alkaline phosphatase substrate.

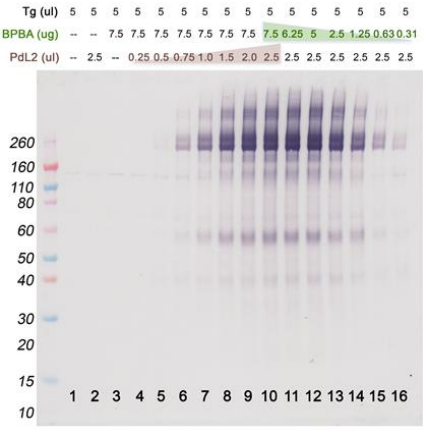

1 = control (Tg, 37 °C)
2 = control (Tg, PdL2 (2.5 μL), 37 °C)
3 = control (Tg, R-B(OH)$_2$ (7.5 μg), 37 °C)
4 = reaction (Tg, PdL2 (0.25 μL), R-B(OH)$_2$ (7.5 μg), 37 °C)
5 = reaction (Tg, PdL2 (0.50 μL), R-B(OH)$_2$ (7.5 μg), 37 °C)
6 = reaction (Tg, PdL2 (0.75 μL), R-B(OH)$_2$ (7.5 μg), 37 °C)
7 = reaction (Tg, PdL2 (1.0 μL), R-B(OH)$_2$ (7.5 μg), 37 °C)
8 = reaction (Tg, PdL2 (1.5 μL), R-B(OH)$_2$ (7.5 μg), 37 °C)
9 = reaction (Tg, PdL2 (2.0 μL), R-B(OH)$_2$ (7.5 μg), 37 °C)
10 = reaction (Tg, PdL2 (2.5 μL), R-B(OH)$_2$ (7.5 μg), 37 °C)
11 = reaction (Tg, PdL2 (2.5 μL), R-B(OH)$_2$ (6.25 μg), 37 °C)
12 = reaction (Tg, PdL2 (2.5 μL), R-B(OH)$_2$ (5.0 μg), 37 °C)
13 = reaction (Tg, PdL2 (2.5 μL), R-B(OH)$_2$ (2.5 μg), 37 °C)
14 = reaction (Tg, PdL2 (2.5 μL), R-B(OH)$_2$ (1.25 μg), 37 °C)
15 = reaction (Tg, PdL2 (2.5 μL), R-B(OH)$_2$ (0.625 μg), 37 °C)
16 = reaction (Tg, PdL2 (2.5 μL), R-B(OH)$_2$ (0.3125 μg), 37 °C)

Figure 5.41 Determination of the threshold levels of the [**L2**]$_2$Pd(OAc)$_2$ and biotinylated boronic acid for *ex vivo* Suzuki reactions by Western blot (stained by anti-biotin alkaline phosphatase antibody produced in goat and visualised by BCIP/NBT alkaline phosphatase substrate).

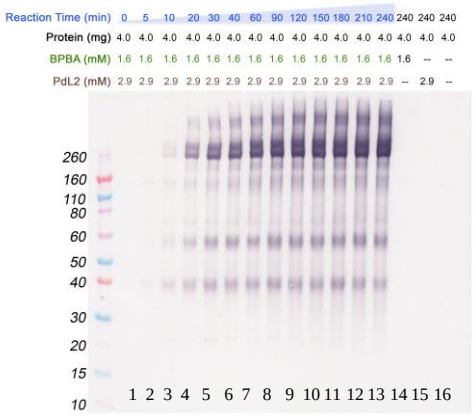

1 = reaction (Tg, PdL2 (2.9 mM), R-B(OH)$_2$ (1.6 mM), 37 °C, 0 min)
2 = reaction (Tg, PdL2 (2.9 mM), R-B(OH)$_2$ (1.6 mM), 37 °C, 5 min)
3 = reaction (Tg, PdL2 (2.9 mM), R-B(OH)$_2$ (1.6 mM), 37 °C, 10 min)
4 = reaction (Tg, PdL2 (2.9 mM), R-B(OH)$_2$ (1.6 mM), 37 °C, 20 min)
5 = reaction (Tg, PdL2 (2.9 mM), R-B(OH)$_2$ (1.6 mM), 37 °C, 30 min)
6 = reaction (Tg, PdL2 (2.9 mM), R-B(OH)$_2$ (1.6 mM), 37 °C, 40 min)
7 = reaction (Tg, PdL2 (2.9 mM), R-B(OH)$_2$ (1.6 mM), 37 °C, 60 min)
8 = reaction (Tg, PdL2 (2.9 mM), R-B(OH)$_2$ (1.6 mM), 37 °C, 90 min)
9 = reaction (Tg, PdL2 (2.9 mM), R-B(OH)$_2$ (1.6 mM), 37 °C, 120 min)
10 = reaction (Tg, PdL2 (2.9 mM), R-B(OH)$_2$ (1.6 mM), 37 °C, 150 min)
11 = reaction (Tg, PdL2 (2.9 mM), R-B(OH)$_2$ (1.6 mM), 37 °C, 180 min)
12 = reaction (Tg, PdL2 (2.9 mM), R-B(OH)$_2$ (1.6 mM), 37 °C, 210 min)
13 = reaction (Tg, PdL2 (2.9 mM), R-B(OH)$_2$ (1.6 mM), 37 °C, 240 min)
14 = control (Tg, R-B(OH)$_2$ (1.6 mM), 37 °C, 240 min)
15 = control (Tg, PdL2 (2.9 mM), 37 °C, 240 min)
16 = control (Tg, 37 °C, 240 min)

Figure 5.42 Determination of the reaction times of *ex vivo* Suzuki reactions by Western blot (stained by anti-biotin alkaline phosphatase antibody produced in goat and visualised by BCIP/NBT alkaline phosphatase substrate).

(Before purification) **(After purification)**

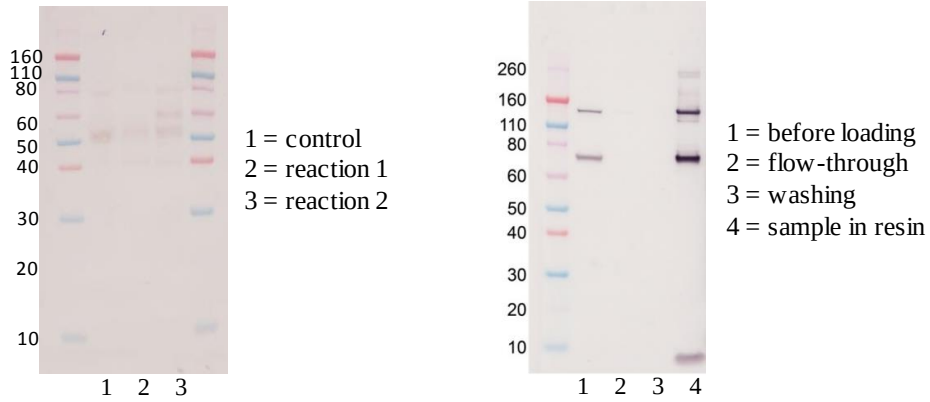

1 = control
2 = reaction 1
3 = reaction 2

1 = before loading
2 = flow-through
3 = washing
4 = sample in resin

Figure 5.43 Western blot of either reaction mixture or purified biotinylated-coupled Tg (from a study of *in vivo* Suzuki reactions) stained with anti-biotin alkaline phosphatase antibody produced in goat and visualised by BCIP/NBT alkaline phosphatase substrate.

5.5.4 Peptide Mapping of the Modified Thyroglobulin and Other Related Proteins

(See general experimental considerations in appendix)

Non-modified Tg and other related proteins

(3-8% Tris-acetate gel)

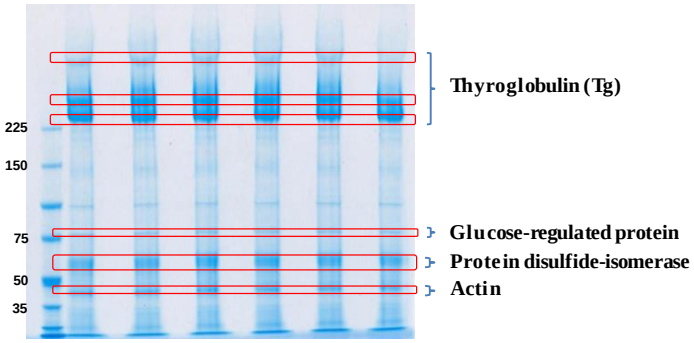

Entry	Proteins	Protein sequence coverage (%)	Modifications
1	Thyroglobulin (Tg)	93	Iodinated Tyr
2	Glucose-regulated protein (78 kDa)	86	Wild-type
3	Protein disulphide-isomerase	89	Wild-type
4	Actin	97	Wild-type

Table 5.13 Identification of each protein from the thyroid gland tissue seperated by Tris-acetate gel and analysed by MSMS.

Thyroglobulin

Protein View: sp|O08710|THYG_MOUSE

Thyroglobulin OS=Mus musculus GN=Tg PE=1 SV=3

Database: UPR_MusMusculus
Score: 14203
Nominal mass (M_r): 311291
Calculated pI: 5.32

Sequence similarity is available as an NCBI BLAST search of sp|O08710|THYG_MOUSE against nr.

Search parameters

Enzyme: No enzyme cleavage specificity.
Fixed modifications: Carbamidomethyl (C)
Variable modifications: Deamidated (N), Deamidated (Q), Oxidation (M), Diiodo (Y)

Protein sequence coverage: 93%

Matched peptides shown in ***bold red***.

```
  1 MTALVLWVST LLSSVCLVAA NIFEYQVDAQ PLRFCELQRE KAFLKQAEYV
 51 PQCSEDGSFQ TVQCQNDGQS CWCVDSDGRE VPGSRQLGRP TVCLSFCQLH
101 KQRILLGSYI NSTDALYLPQ CQDSGNYAPV QCDLQRVQCW CVDTEGMEVY
151 GTRQQGRPTR CPRSCEIRNR RLLHGVGDRS PPQCTADGEF MPVQCKFVNT
201 TDMMIFDLIH NYNRFPDAFV TFSSFRGRFP EVSGYCYCAD SQGRELAETG
251 LELLLDEIYD TIFAGLDQAS TFTQSTMYRI LQRRFLAIQL VISGRFRCPT
301 KCEVEQFAAT RFGHSYIPRC HRDGHYQTVQ CQTEGMCWCV DAQGREVPGT
351 RQQGQPPSCA ADQSCALERQ QALSRFYFET PDYFSPQDLL SSEDRLAPVS
401 GVRSDTSCPP RIKELFVDSG LLRSIAVEHY QRLSESRSLL REAIRAVFPS
451 RELAGLALQF TTNPKRLQQN LFGGTFLANA AQFNLSGALG TRSTFNFSQF
501 FQQFGLPGFL NRDRVTTLAK LLPVRLDSSS TFETLRVSEK TVAMNKRVVG
551 NFGFKVNLQE NQDALKFLVS LLELPEFLVF LQRAVSVPED IARDLGDVME
601 MVFSAQACKQ MPGKFFVPSC TAGGSYEDIQ CYAGECWCVD SRGKELDGSR
651 VRGGRPRCPT KCEKQRAQMQ SLASAQPAGS SFFVPTCTRE GYFLFVQCFN
```

78kDa Glucose-regulated protein

Protein View: sp|P20029|GRP78_MOUSE

78 kDa glucose-regulated protein OS=Mus musculus GN=Hspa5 PE=1 SV=3

Database: UPR_MusMusculus
Score: 1431
Nominal mass (M_r): 72492
Calculated pI: 5.07

Sequence similarity is available as an NCBI BLAST search of sp|P20029|GRP78_MOUSE against nr.

Search parameters

Enzyme: No enzyme cleavage specificity.
Fixed modifications: Carbamidomethyl (C)
Variable modifications: Deamidated (N), Deamidated (Q), Oxidation (M)

Protein sequence coverage: 86%

Matched peptides shown in ***bold red***.

```
  1 MMKFTVVAAA LLLLGAVRAE EEDKKEDVGT VVGIDLGTTY SCVGVFKNGR
 51 VEIIANDQGN RITPSYVAFT PEGERLIGDA AKNQLTSNPE NTVFDAKRLI
101 GRTWNDPSVQ QDIKFLPFKV VEKKTKPYIQ VDIGGGQTKT FAPEEISAMV
151 LTKMKETAEA YLGKKVTHAV VTVPAYFNDA QRQATKDAGT IAGLNVMRII
201 NEPTAAAIAY GLDKREGEKN ILVFDLGGGT FDVSLLTIDN GVFEVVATNG
251 DTHLGGEDFD QRVMEHFIKL YKKKTGKDVR KDNRAVQKLR REVEKAKRAL
301 SSQHQARIEI ESFFEGEDFS ETLTRAKFEE LNMDLFRSTM KPVQKVLEDS
351 DLKKSDIDEI VLVGGSTRIP KIQQLVKEFF NGKEPSRGIN PDEAVAYGAA
401 VQAGVLSGDQ DTGDLVLLDV CPLTLGIETV GGVMTKLIPR NTVVPTKKSQ
451 IFSTASDNQP TVTIKVYEGE RPLTKDNHLL GTFDLTGIPP APRGVPQIEV
501 TFEIDVNGIL RVTAEDKGTG NKNKITITND QNRLTPEEIE RMVNDAEKFA
551 EEDKKLKERI DTRNELESYA YSLKNQIGDK EKLGGKLSSE DKETMEKAVE
601 EKIEWLESHQ DADIEDFKAK KKELEEIVQP IISKLYGSGG PPPTGEEDTS
651 EKDEL
```

Protein disulfide-isomerase

Protein View: sp|P27773|PDIA3_MOUSE

Protein disulfide-isomerase A3 OS=Mus musculus GN=Pdia3 PE=1 SV=2

Database:	UPR_MusMusculus
Score:	1150
Nominal mass (M_r):	57099
Calculated pI:	5.88

Sequence similarity is available as an NCBI BLAST search of sp|P27773|PDIA3_MOUSE against nr.

Search parameters

Enzyme:	No enzyme cleavage specificity.
Fixed modifications:	Carbamidomethyl (C)
Variable modifications:	Deamidated (N), Deamidated (Q), Oxidation (M)

Protein sequence coverage: 89%

Matched peptides shown in ***bold red***.

```
  1 MRFSCLALLP GVALLLASAR LAAASDVLEL TDENFESRVS DTGSAGLMLV
 51 EFFAPWCGHC KRLAPEYEAA ATRLKGIVPL AKVDCTANTN TCNKYGVSGY
101 PTLKIFRDGE EAGAYDGPRT ADGIVSHLKK QAGPASVPLR TEEEFKKFIS
151 DKDASVVGFF RDLFSDGHSE FLKAASNLRD NYRFAHTNIE SLVKEYDDNG
201 EGITIFRPLH LANKFEDKTV AYTEKKMTSG KIKKFIQDSI FGLCPHMTED
251 NKDLIQGKDL LTAYYDVDYE KNAKGSNYWR NRVMMVAKKF LDAGHKLNFA
301 VASRKTFSHE LSDFGLESTT GEVPVVAIRT AKGEKFVMQE EFSRDGKALE
351 QFLQEYFDGN LKRYLKSEPI PESNEGPVKV VVAENFDDIV NEEDKDVLIE
401 FYAPWCGHCK NLEPKYKELG EKLSKDPNIV IAKMDATAND VPSPYEVKGF
451 PTIYFSPANK KLTPKKYEGG RELNDFISYL QREATNPPII QEEKPKKKKK
501 AQEDL
```

Actin

Protein View: sp|P60710|ACTB_MOUSE

Actin, cytoplasmic 1 OS=Mus musculus GN=Actb PE=1 SV=1

Database:	UPR_MusMusculus
Score:	2472
Nominal mass (M_r):	42052
Calculated pI:	5.29

Sequence similarity is available as an NCBI BLAST search of sp|P60710|ACTB_MOUSE against nr.

Search parameters

Enzyme:	No enzyme cleavage specificity.
Fixed modifications:	Carbamidomethyl (C)
Variable modifications:	Deamidated (N), Deamidated (Q), Oxidation (M)

Protein sequence coverage: 97%

Matched peptides shown in ***bold red***.

```
  1 MDDDIAALVV DNGSGMCKAG FAGDDAPRAV FPSIVGRPRH QGVMVGMGQK
 51 DSYVGDEAQS KRGILTLKYP IEHGIVTNWD DMEKIWHHTF YNELRVAPEE
101 HPVLLTEAPL NPKANREKMT QIMFETFNTP AMYVAIQAVL SLYASGRTTG
151 IVMDSGDGVT HTVPIYEGYA LPHAILRLDL AGRDLTDYLM KILTERGYSF
201 TTTAEREIVR DIKEKLCYVA LDFEQEMATA ASSSSLEKSY ELPDGQVITI
251 GNERFRCPEA LFQPSFLGME SCGIHETTFN SIMKCDVDIR KDLYANTVLS
301 GGTTMYPGIA DRMQKEITAL APSTMKIKII APPERKYSVW IGGSILASLS
351 TFQQMWISKQ EYDESGPSIV HRKCF
```

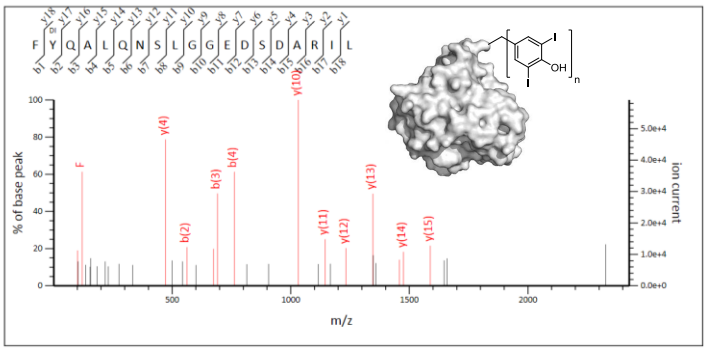

Figure 5.44 Peptide fragmentation of the diiodo-tyrosine FYQALQNSLGGEDSDARIL (Thyroglobulin, Tg) using Mascot.

Modified Tg (biotinylation) and other related proteins

Score	Mr(found)	Mr(Calc)	Expect	Modifications	Peptide sequence
57	2057.8180	2057.8207	2.3 x 10^{-5}	monobiotin / monoiodo-Tyr (Y-1424)	LYFLNGDSFVTS PR
64	1931.9266	1931.9240	5.9 x 10^{-7}	monobiotin-Tyr (Y-1424)	LYFLNGDSFVTS PR
33	2973.3254	2972.3071	7.4 x 10^{-4}	dibiotin-Tyr (Y-2657)	AYQGQFSTEEQ SLSLKVMQY

Table 5.14 Chemical modifications of Tg-mixture after treatment of Tg with biotinylated phenylboronic acid by MSMS analysis.

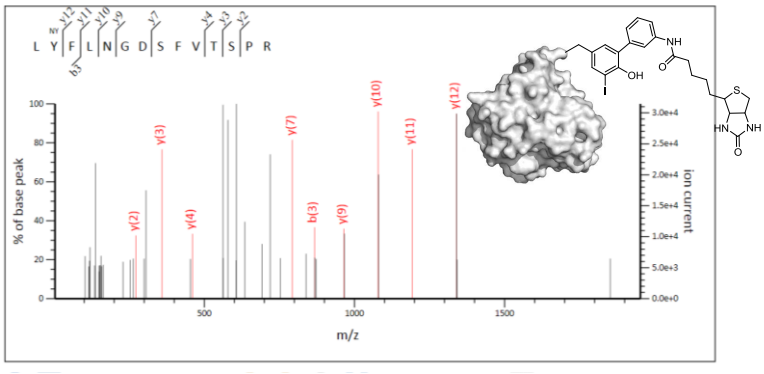

Figure 5.45 Peptide fragmentation of the monobiotin and monoiodo-tyrosine (Y-1424) LYFLNGDSFVTSPR using Mascot.

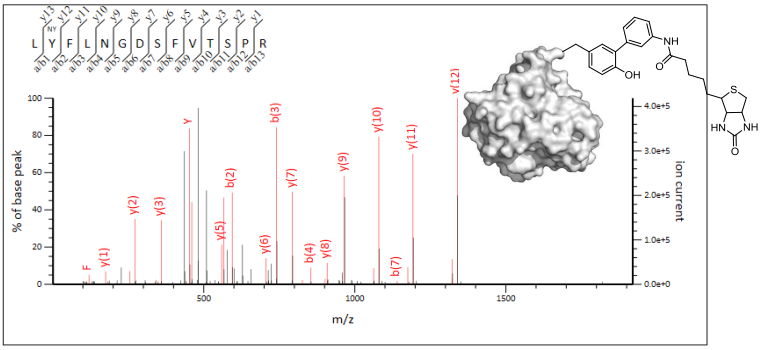

Figure 5.46 Peptide fragmentation of the monobiotin-tyrosine (Y-1424) LYFLNGDSFVTSPR using Mascot.

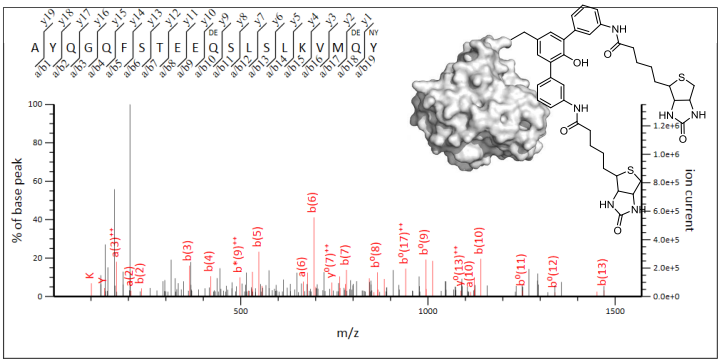

Figure 5.47 Peptide fragmentation of the dibiotin-tyrosine (Y-2657) LYFLNGDSFVTSPR using Mascot.

Actin

Score	Mr(found)	Mr(Calc)	Expect	Modifications	Peptide sequence
23	1080.3746	1080.3737	0.066	monoiodo-Tyr (Y-145)	SLYASGRTT
58	1919.8061	1919.8067	8.3×10^{-5}	monoiodo-Tyr (Y-171)	THNVPIYEGYALPHAI
29	1248.3800	1248.3796	0.031	monoiodo-Tyr (Y-364)	KQEYDEAGPS
39	2116.9709	2115.9506	0.0028	dibiotin-Tyr (Y-55)	KDSYVGDEAQSKR
22	1872.9382	1872.9232	0.19	monobiotin-Tyr (Y-168)	NVPIYEGYALPHAI

Table 5.15 Chemical modifications of the actin after treatment of the actin with biotinylated phenylboronic acid by MSMS analysis.

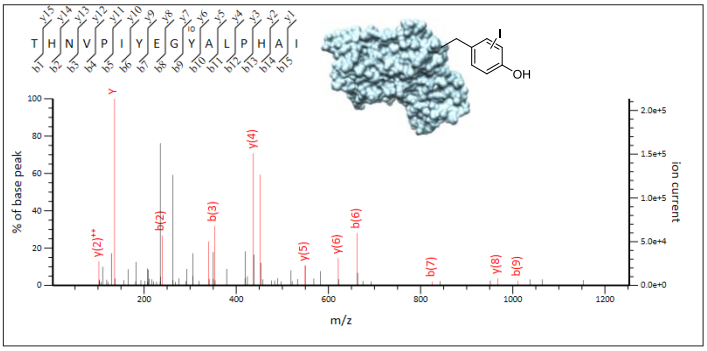

Figure 5.48 Peptide fragmentation of the monoiodo-tyrosine (Y-171) THNVPIYEGYALPHAI using Mascot.

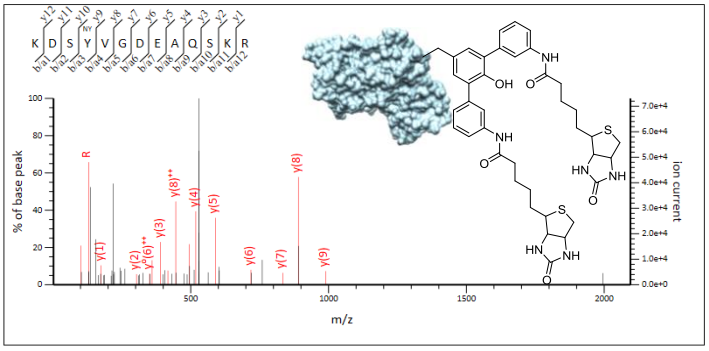

Figure 5.49 Peptide fragmentation of the dibiotin-tyrosine (Y-55) KDSYVGDEAQSKR using Mascot.

5.6 Bibliography

(1) Mondal, S.; Raja, K.; Schweizer, U.; Mugesh, G. Chemistry and Biology in the Biosynthesis and Action of Thyroid Hormones. *Angew. Chem. Int. Ed. Engl.* **2016**, *55*, 7606-7630.

(2) Vali, M.; PRose, N. R.; Caturegli, P. Thyroglobulin as Autoantigen: Structure-Function Relationships. *Rev. Endocr. Metab. Disord.* **2000**, *1*, 69-77.

(3) Deshpande, V.; Venkatesh, S. G. Thyroglobulin, the prothyroid hormone: chemistry, synthesis and degradation. *Biochem. Biophys. Acta* **1999**, *1430*, 157-178.

(4) Dedieu, A.; Gaillard, J. C.; Pourcher, T.; Darrouzet, E.; Armengaud, J. Revisiting iodination sites in thyroglobulin with an organ-oriented shotgun strategy. *J. Biol. Chem.* **2011**, *286*, 259-269.

(5) Dunn, A. D.; Corsi, C. M.; Myers, H. E.; Dunn, J. T. Tyrosine 130 Is an Important Outer Ring Donor for Thyroxine Formation in Thyroglobulin. *J. Biol. Chem.* **1998**, *273*, 25223-25229.

(6) Gentile, F.; Ferranti, P.; Mamone, G.; Malorni, A.; Salvatore, G. Identification of Hormonogenic Tyrosines in Fragment 1218–1591 of Bovine Thyroglobulin by Mass Spectrometry. *J. Biol. Chem.* **1997**, *272*, 639-646.

(7) Li, J.; Chen, P. R. Moving Pd-mediated protein cross coupling to living systems. *Chembiochem.* **2012**, *13*, 1728-1731.

(8) Li, J.; Lin, S.; Wang, J.; Jia, S.; Yang, M.; Hao, Z.; Zhang, X.; Chen, P. R. Ligand-Free Palladium-Mediated Site-Specific Protein Labeling Inside Gram-Negative Bacterial Pathogens. *J. Am. Chem. Soc.* **2013**, *135*, 7330-7338.

(9) Spicer, C. D.; Triemer, T.; Davis, B. G. Palladium-Mediated Cell-Surface Labeling. *J. Am. Chem. Soc.* **2012**, *134*, 800-803.

(10) Yang, M.; Li, J.; Chen, P. R. Transition metal-mediated bioorthogonal protein chemistry in living cells. *Chem. Soc. Rev.* **2014**, *43*, 6511-6526.

(11) Yusop, R. M.; Unciti-Broceta, A.; Johansson, E. M.; Sanchez-Martin, R. M.; Bradley, M. Palladium-mediated intracellular chemistry. *Nat. Chem.* **2011**, *3*, 239-243.

(12) Chankeshwara, S. V.; Indrigo, E.; Bradley, M. Palladium-mediated chemistry in living cells. *Curr. Opin. Chem. Biol.* **2014**, *21*, 128-135.

(13) Chang, P. V.; Prescher, J. A.; Sletten, E. M.; Baskin, J. M.; Miller, I. A.; Agard, N. J.; Lo, A.; Bertozzi, C. R. Copper-free click chemistry in living animals. *Proc. Natl. Acad. Sci. U.S.A.* **2010**, *107*, 1821-1826.

(14) Jewett, J. C.; Sletten, E. M.; Bertozzi, C. R. Rapid Cu-Free Click Chemistry with Readily Synthesized Biarylazacyclooctynones. *J. Am. Chem. Soc.* **2010**, *132*, 3688-3690.

(15) Laughlin, S. T.; Baskin, J. M.; Amacher, S. L.; Bertozzi, C. R. In Vivo Imaging of Membrane-Associated Glycans in Developing Zebrafish. *Science* **2008**, *320*, 664-667.

(16) Plass, T.; Milles, S.; Koehler, C.; Schultz, C.; Lemke, E. A. Genetically encoded copper-free click chemistry. *Angew. Chem. Int. Ed. Engl.* **2011**, *50*, 3878-3881.

(17) Sletten, E. M.; Bertozzi, C. R. From Mechanism to Mouse: A Tale of Two Bioorthogonal Reactions. *Acc. Chem. Res.* **2011**, *44*, 666-676.

(18) Chalker, J. M.; Wood, C. S. C.; Davis, B. G. A Convenient Catalyst for Aqueous and Protein Suzuki-Miyaura Cross-Coupling. *J. Am. Chem. Soc.* **2009**, *131*, 16346-16347.

(19) Dumas, A.; Spicer, C. D.; Gao, Z.; Takehana, T.; Lin, Y. A.; Yasukohchi, T.; Davis, B. G. Self-liganded Suzuki-Miyaura coupling for site-selective protein PEGylation. *Angew. Chem. Int. Ed. Engl.* **2013**, *52*, 3916-3921.

(20) Spicer, C. D.; Davis, B. G. Palladium-Mediated Site-Selective Suzuki-Miyaura Protein Modification at Genetically Encoded Aryl Halides. *Chem. Commun.* **2011**, *47*, 1698-1700.

Appendix

1. General Experimental Considerations

1.1 Instruments and Chemicals/Proteins

1.2 Peptide Mapping of the Modified Proteins

1.3 Western Blot Analysis

2. Optimisation of Protein Fluorination Reactions

2.1 Optimisation of Dehydroalanine (Dha) Formation of Annexin V

2.2 Optimisation of Fluorination Reactions of Annexin V(Dha316)

2.3 Optimisation of [^{18}F]-Radiolabelling of Annexin V(Dha316)

3. Optimisation of Protein Iodination Reactions

3.1 Iodination of Insulin

3.2 Iodination of Monocyte Chemoattractant Protein-1 (MCP-1)

3.3 Iodination of Ubiquitin (UBQ)

4. Optimisation of Palladium-Mediated Reactions of Thyroxine (T4)

4.1 *Ex Vivo* Palladium-Mediated Reactions of T4

4.2 *Ex Vivo* Palladium-Mediated Reactions of BocNH-T4

1. General Experimental Considerations

1.1 Instruments and Chemicals/Proteins

NMR: Nuclear magnetic resonance (NMR) spectra were recorded on a Bruker DPX200 (200MHz), Bruker AVN400 (400 MHz) or Bruker AVII500 (500 MHz) spectrometer as solutions in deuterated dimethylsulfoxide (d_6-DMSO) unless stated otherwise. The chemical shift values for all spectra are given in parts per million (ppm) with coupling constants (*J*) in Hertz (Hz).

IR: Infrared spectra (IR) were recorded on a Bruker Tensor 27 Fourier Transform spectrophotometer using thin films on NaCl plates for liquids and oils and KBr discs for solids and crystals.

Melting point: Melting points (m.p.) were determined in open capillary tubes using a Leica Galen III host stage microscope equipped with a Tesco 720 thermocouple probe and are uncorrected.

Chromatography: Flash column chromatography was carried out using Merck Kieselgel 60 silica and eluted with the solvent system stated. Thin layer chromatography (TLC) was carried out on Merck DC-Alufolien Kieselgel 60F_{254} aluminium-backed silica plates. The plates were developed with an appropriate solvent system then visualized using UV (λ = 254 or 365 nm) and by dipping in a 0.5% $KMnO_4$ in 2.5% $NaHCO_3$ solution or ninhydrin reagent (2 % ninhydrin in ethanol) and drying with a hot air gun.

Chemicals/Proteins: All commercially available compounds and proteins were used without further purification except where stated. Anhydrous dichloromethane was obtained by passing through a modified Grubbs system of alumina columns. Other solvents were purchased as anhydrous solvents. Water refers to distilled water and brine refers to a saturated aqueous solution of sodium chloride. Air or moisture sensitive reactions were carried out in flame dried glassware under a positive flow of nitrogen using standard syringe/septa techniques. Some compounds/proteins were kindly provided by our previous/current members as follows:

Compounds: *N*-Boc-5-chloro-DL-tryptophan, *N*-Boc-6-bromo-DL-tryptophan, *N*HAc-5-chloro-DL-tryptophan, *N*HAc-5-bromo-DL-tryptophan, *N*-Boc-thyroxine (BocNH-T4), coumarinyl boronic acids derivatives, and 1-propyl-β-D-glucopyranose

Proteins: GYG-Y195pIPhe, MBP-E13pIPhe, and MCP-1

Mass spectrometry: Low resolution mass spectrometry (LRMS) was carried out on Waters Micromass LCT Premier TOF spectrometer using electrospray ionisation (ESI) and high resolution mass spectra (HRMS) were obtained on a Bruker MicroTOF ESI mass spectrometer.

Protein Mass spectrometry: Electrospray ionisation mass spectrometry **(**ESI-MS) was obtained using liquid chromatography mass spectrometry (LC-MS), which was performed on a Micromass LCT (ESI TOF-MS) coupled to a Waters Alliance 2790 RP-HPLC using a Phenomenex Jupiter C4 column (250 x 4.6 mm x 5 µm). The mobile phase, containing solvent A (0.1% FA in H_2O) and solvent B (0.1% FA in CH_3CN), was used at a flow rate of 1.0 mL/min. The gradient used to elute the protein was programmed as a 5 min isocratic run of 95% solvent A to 100% solvent B after 15 min, and subsequent isocratic run for 5 min. The system was operated using an electrospray source having with a capillary voltage of 3.2 kV and a cone voltage of 25 V, and the nebuliser having a total flow of N_2 of 600 L/h. Raw ESI-MS data was deconvoluted using the MaxEnt function on MassLynx software v.41 (Waters) according to the manufacturer's instructions.

SDS-PAGE Electrophoresis: Protein samples were run on SDS-PAGEs using Invitrogen system (NuPAGE® Bis-Tris gel and NuPAGE® MES running buffer). SDS-PAGEs were stained by Expedeon Instant Blue™ for visualisation of protein bands.

Circular Dichroism: Circular Dichroism (CD) spectra were recorded on a Chirascan CD Spectrophotometry (Applied Photophysics) in a quartz cuvette (Starna Scientific) with a path length of 1.0 mm.

Microscopy: All HEK293 cells experiments were visualised on a Leica Microsystems SP5 Inverted Confocal Microscope which performed with the pinhole set at 1 Airy diameter. All experiments were gained with the 10x objective lens magnification being achieved with the optical zoom. All fluorescent images, captured at 512x512 pixels at 400 Hz or 1400 Hz capture rates, were processed using Image J. Gains which were kept constant throughout measurements.

Radiochemistry: Reversed phase high performance liquid chromatography (RP-HPLC) UV and radioactivity profiles were generated using a reverse phase Phenomenex Jupiter C4 analytical column (250 x 4.6 mm x 5 µm) which was performed on an Elite LaChrome L-2130 with an Elite LaChrome UV L-2400 detector and an ACE Mate™ Preamplifier, Amplifier, Bias Supply and SCA (925-SCINT) radioactivity detector in

series. The mobile phase, containing solvent A (0.1% TFA in H_2O) and solvent B (0.1% TFA in CH_3CN), was used at a flow rate of 1.0 mL/min. The gradient used to elute the protein was programmed as follows: 95% solvent A (5 min) to 80% solvent B (12 min), hold for 3 min then return to 95 % solvent A (4 min) followed by a final equilibration period of 95% solvent A for 2-5 min.

1.2 Peptide Mapping of Modified Proteins

(Performed and serviced by Marie-Laëtitia Thézénas and Prof. Benedikt M. Kessler: Nuffield Department of Medicine, University of Oxford.)

Sample preparation

Each 20 µL aliquot of the modified proteins (Annexin V, Ubiquitin, Insulin, MCP-1, and Thyroglobulin) in 50 mM NaH_2PO_4 pH 8.0 or appropriate buffers was further processed by tryptic digestion for peptide mapping using the following steps. H_2O (155 µL) and 5 mM DTT (final concentration) were added to the sample which was incubated for 30 minutes at room temperature. A subsequent incubation of 30 minutes was performed after adding 20 mM iodoacetamide (final concentration), and the mixture was then desalted by chloroform methanol precipitation. A solution of 6 M urea in 0.4 M Tris pH 7.4 was used to solubilise the sample pellet. Trypsin (Promega) (all proteins) or elastase (for thyroglobulin), used at a 1:50 ratio (trypsin:protein), was added to the sample 6 times diluted with H_2O, then allowed for an overnight digestion at 37°C. The sample was subsequently desalted by a C18 SEP PAK cartridge (according to Waters' instructions), and was dried via speed vac centrifugation then re-suspended in 20 µL of a mixture of 98% H_2O:2% CH_3CN with 0.1% TFA.

Thyroglobulin subjected to in-gel digestion using the following protocol. The gels pieces (1-2 mm^3) were washed overnight with 1ml of 50 % methanol: 5 % acetic acid in MilliQ-H_2O. The samples were dried twice with 200 µL acetonitrile for 5 min. The protein was then reduced by adding a 10 mM DTT solution on top of the gel for 30 min followed by another 30 minutes incubation with a 50 mM iodoacetamide solution. Samples were then dried for 5 min with acetonitrile rehydrated for 10 min with 100 mM ammonium bicarbonate and re-dried for 5 minutes with acetonitrile. The samples were finally digested overnight at 37°C with 30 µL elastase (2 ng/µL).

LC-MS/MS analysis

The resultant peptides were further analysed by nano–liquid chromatography tandem mass spectrometry (nano–LC-MS/MS) using a Nano-Acquity-UPLC (C18 column with a 75 μm × 250 mm, 1.7 μm particle size; Waters) coupled to an Orbitrap Elite tandem mass spectrometer (Thermo Scientific, Bremen, Germany) with a resolution of 120,000 full-width half maximum at mass/charge 400. Top 20 precursor ion selection and fragmentation were performed in collision-induced dissociation (CID) mode. The samples were loaded in 99.5 % buffer A (0.1% FA in H_2O). The gradient used to elute the peptides started with a 3 minute isocratic gradient composed of 3% buffer B (0.1% FA in CH_3CN), and was subsequently followed by a linear gradient from 3-40% of buffer B for 60 minutes at a flow rate of 250 nL/minute and two washes with 97% of buffer B for 3 minutes. The total length of the analysis was 100 min to allow column re-equilibration. The peptide fragments with desired chemical modifications were determined by either Matrix Science software (Mascot MSMS Ions search) or PEAKS proteomics mass spectrometry software (according to the manufacturer's instructions).

200 ng of peptides were analyzed by tandem mass spectrometry (Q Exactive-HF, Thermo Scientific, Bremen, Germany) coupled with a ultra-high performance liquid chromatography (Dionex Ultimate 3000 UHPLC, Thermo) using a PepMap RSLC column (C18, 2um, 100A, 75um x 50 cm).

The samples were loaded in a 0.1% TFA in 99% H_2O buffer and analysed using a 1 hour linear gradient at a flow rate of 250 nl/minute. The gradient used to elute the peptides started at 3 minutes with 2 % buffer B (0.1% FA and 5% DMSO in CH_3CN) increasing to 5% buffer B by 6 minutes followed by an increase up to 35% by 63 minutes. The column was washed twice for 10 minutes with 99% of buffer B. The total length of the analysis was 100 min to allow column re-equilibration.

The data were acquired with a resolution of 70,000 full-width half maximum at mass/charge 400 with lockmass enabled (445.120025 m/z), Top 15 precursor ion selection, Dynamic Exclusion of 27 seconds and fragmentation performed in Higher-energy C-trap dissociation (HCD) mode with Normalized Collision Energy of 28.

1.3 Western Blot Analysis

Each protein sample run on SDS-PAGE was electroblotted to a nitrocellulose membrane (Invitrogen^{TM}) using iBlot machine (P3 programme, 7 min). The membrane was then transferred into a blocking solution (2.0 g BSA in 40 mL TBST solution) and allowed to gently shake on a rocking table for 1 h at room temperature or overnight at 4°C. The membrane was rinsed with 3 x 20 mL TBST solution, then was soaked in 50 mL TBST solution containing **primary antibody** and 0.5 g BSA. After 1 h gently shaking on the rocking table at room temperature, the membrane was washed with 3 x 20 mL TBST, then was further stained by **secondary antibody** in 50 mL TBST solution containing 0.5 g BSA. The membrane was shaken at room temperature for 1 h, prior to rinsing with 3 x 20 mL TBST. Visualisation of protein bands on the membrane was achieved by dropwise addition of BCIP/NBT alkaline phosphatase substrate. Once protein bands were observed, the membrane was rinsed with 3 x 20 mL H_2O.

Entry	**Proteins**	**Antibodies**		**Dilution**
		Primary	**Secondary**	
1	Annexin V	Anti-human annexin V monoclonal antibody produced in mouse (IgG2a or IgG1)	Anti-mouse IgG (whole molecule) alkaline phosphatase antibody produced in goat	1 : 20,000
2	Annexin V (6xHis-tag) & MBP (6xHis-tag)	Monoclonal anti-polyhistidine alkaline phosphatase antibody produced in mouse	-	1 : 5,000
3	Thyroglobulin	Anti-biotin alkaline phosphatase antibody produced in goat	-	1 : 5,000
BCIP/NBT used as an alkaline phosphatase substrate.				

Table 1.1 Western blot analysis of various proteins using corresponding primary and secondary antibodies.

2. Optimisation of Protein Fluorination Reactions

2.1 Optimisation of Dehydroalanine (Dha) Formation of Annexin V

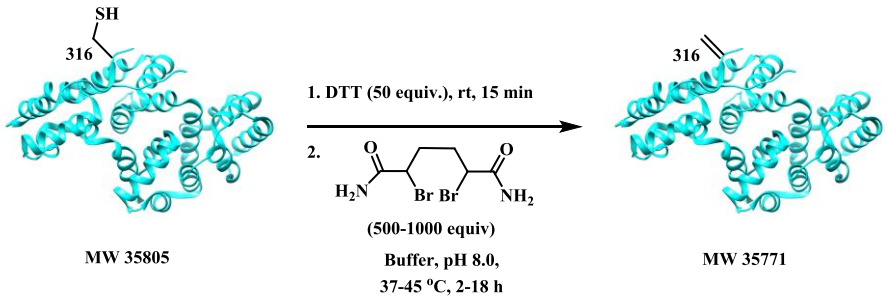

Entry	DBHDA (equiv.)	Buffer, pH 8.0	Temp. (°C)	Reaction times (h)	Results (Da)
1	500	50 mM NaH_2PO_4	37	2	35810 (SM)
2	500			4	35810 (SM)
3	500			18	35810 (SM)
4	2 x 500			2	35810 (SM)
5	2 x 500			4	35810 (SM)
6	2 x 500			18	35810 (SM)
7	2 x 500	50 mM Tris.HCl	37	18	35810 (SM)
8	500	3 M GdmCl	37	2	35774 (Dha)
9	500	50 mM NaH_2PO_4	45	<2	35771 (Dha)

General conditions: ANV(C316) in buffer and DBHDA in DMF at 37-45 °C for 2-18 h unless otherwise indicated.

Table 1.2 Optimisation of Dha formation of annexin V with DBHDA (500-1000 equiv.).

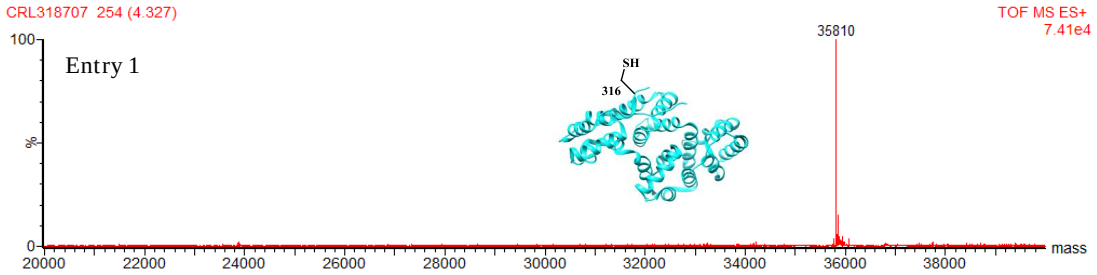

Figure 1.1 ESI-MS spectrum of the annexin V(C316) treated with 500 equiv. DBHDA in 50 mM NaH_2PO_4 at 37 °C for 2h.

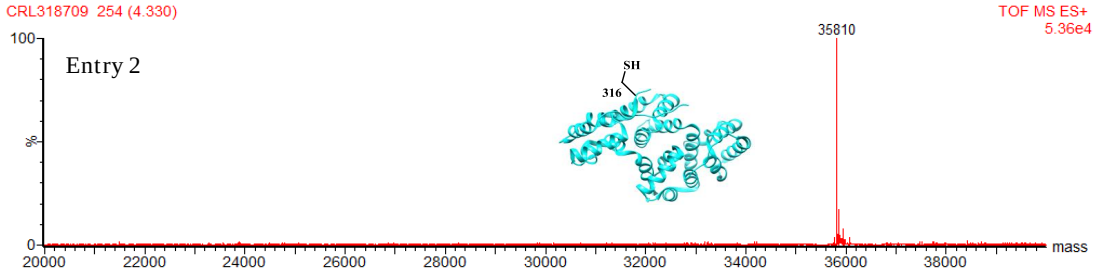

Figure 1.2 ESI-MS spectrum of the annexin V(C316) treated with 500 equiv. DBHDA in 50 mM NaH_2PO_4 at 37 °C for 4h.

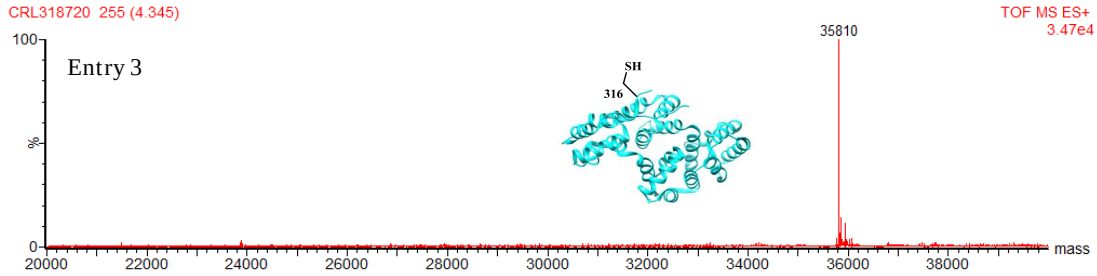

Figure 1.3 ESI-MS spectrum of the annexin V(C316) treated with 500 equiv. DBHDA in 50 mM NaH_2PO_4 at 37 °C for 18h.

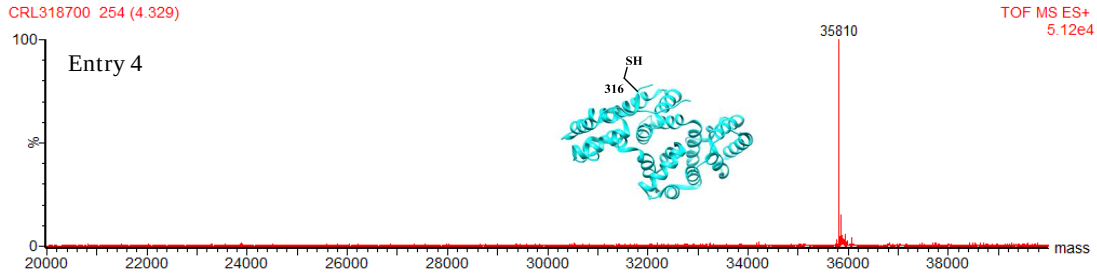

Figure 1.4 ESI-MS spectrum of the annexin V(C316) treated with 2x500 equiv. DBHDA in 50 mM NaH_2PO_4 at 37 °C for 2h.

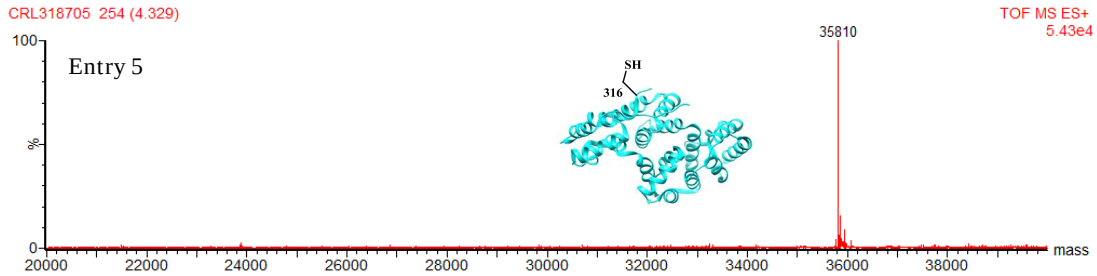

Figure 1.5 ESI-MS spectrum of the annexin V(C316) treated with 2x500 equiv. DBHDA in 50 mM NaH_2PO_4 at 37 °C for 4h.

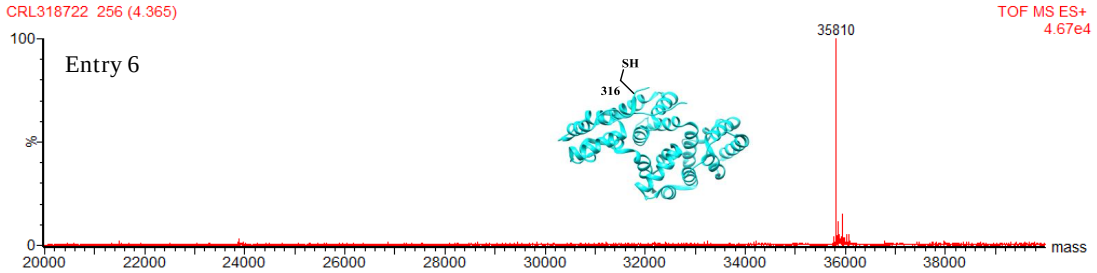

Figure 1.6 ESI-MS spectrum of the annexin V(C316) treated with 2x500 equiv. DBHDA in 50 mM NaH_2PO_4 at 37 °C for 18h.

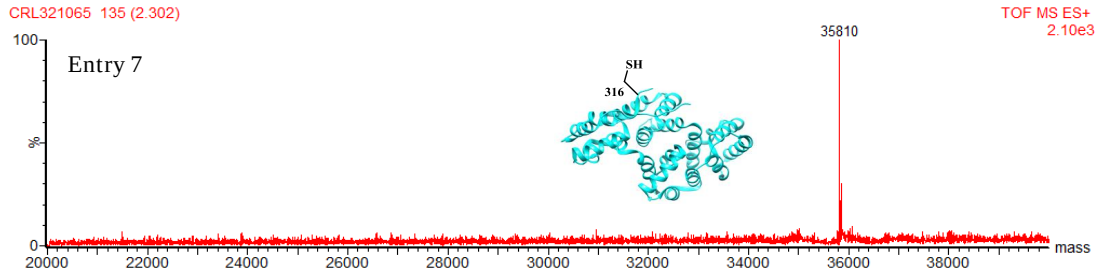

Figure 1.7 ESI-MS spectrum of the annexin V(C316) treated with 2x500 equiv. DBHDA in 50 mM Tris.HCl at 37 °C for 18h.

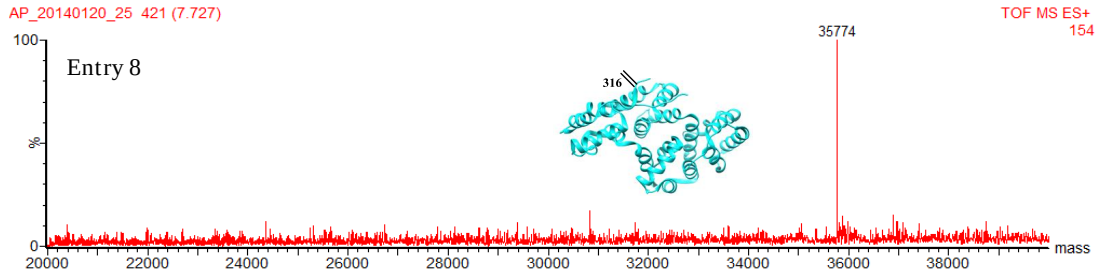

Figure 1.8 ESI-MS spectrum of the annexin V(C316) treated with 500 equiv. DBHDA in 3 M GdmCl at 37 °C for 2h.

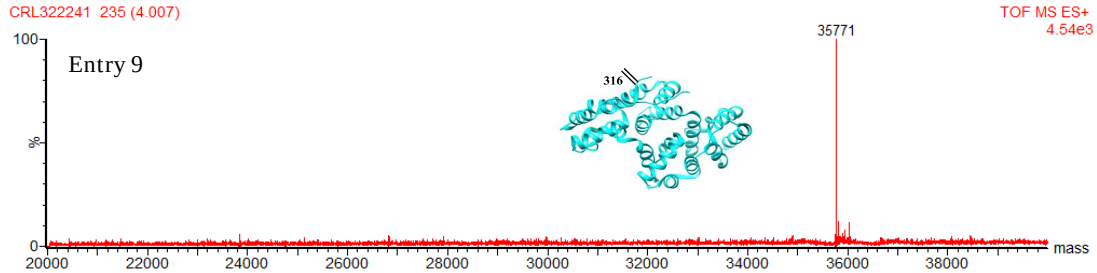

Figure 1.9 ESI-MS spectrum of the annexin V(C316) treated with 500 equiv. DBHDA in 50 mM NaH_2PO_4 at 45°C for 1h 40 min.

2.2 Optimisation of Fluorination Reactions of Annexin V(Dha316)

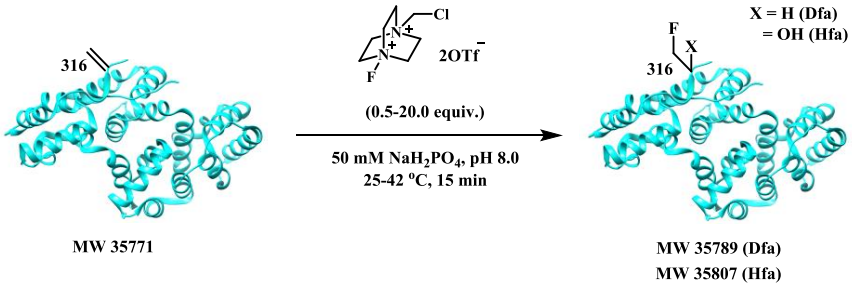

Entry	ANV(Dha316) (equiv.)	Selectfluor *bis*(triflate) (equiv.)	Reaction conditions[a]	Product conversion (%)[b]
1	1.0	0.5	25 °C, 15 min	Dha (69), Dfa (16), Hfa (15)
2	1.0	1.0	25 °C, 15 min	Dha (59), Dfa (25), Hfa (16)
3	1.0	2.0	25 °C, 15 min	Dha (17), Dfa (37), Hfa (32)
4	1.0	0.5	42 °C, 15 min	Dha (63), Dfa (27), Hfa (13)
5	1.0	1.0	42 °C, 15 min	Dha (42), Dfa (39), Hfa (19)
6	1.0	2.0	42 °C, 15 min	Dha (14), Dfa (34), Hfa (34)
7	1.0	5.0	42 °C, 15 min	ND.
8	1.0	20.0	42 °C, 15 min	ND.

General conditions: a). ANV(Dha316) in NaH_2PO_4 (50 mM, pH 8) and Selectfluor *bis*(triflate) in acetone at 42 °C for 15 min unless otherwise indicated. b). Calculated by LC-MS.

Table 1.3 Optimisation of fluorination reactions of ANV(Dha316) using Selectfluor *bis*(triflate) as a fluorinating agent.

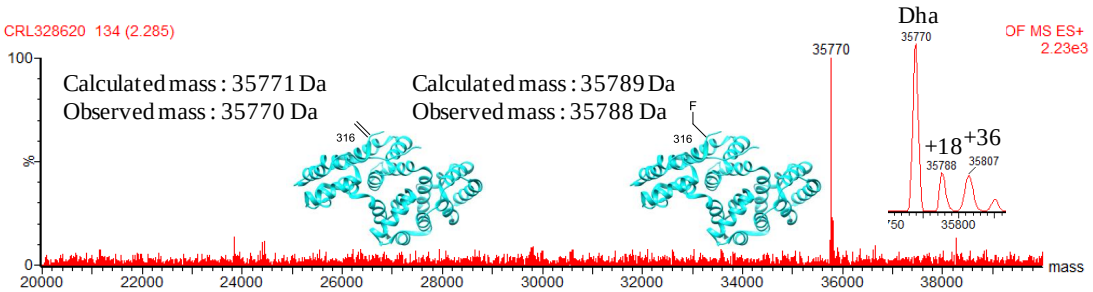

Figure 1.10 ESI-MS spectrum of the annexin V (Dha316) treated with 0.5 equiv. Selectfluor *bis*(triflate) at 25 °C for 15 min.

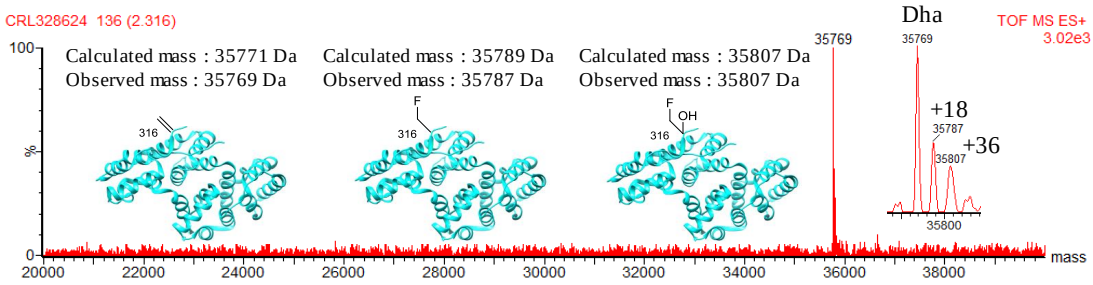

Figure 1.11 ESI-MS spectrum of the annexin V (Dha316) treated with 1.0 equiv. Selectfluor *bis*(triflate) at 25 °C for 15 min.

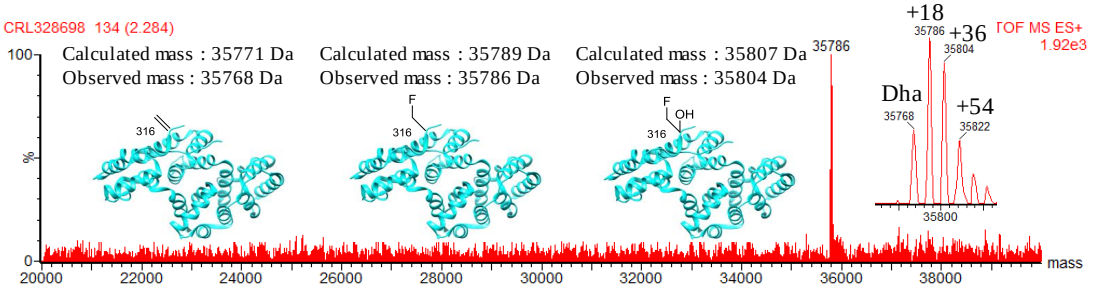

Figure 1.12 ESI-MS spectrum of the annexin V (Dha316) treated with 2.0 equiv. Selectfluor *bis*(triflate) at 25 °C for 15 min.

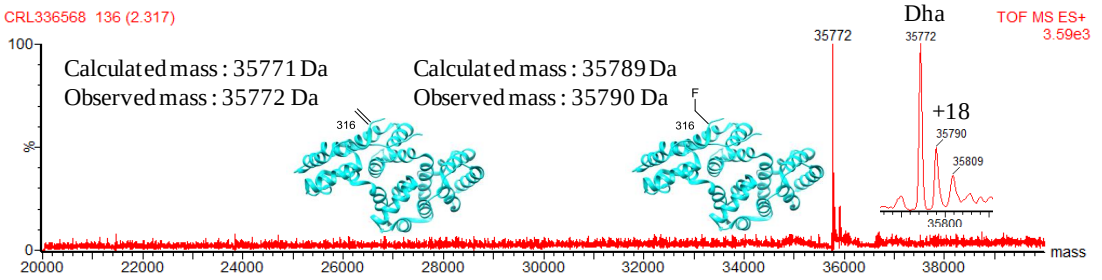

Figure 1.13 ESI-MS spectrum of the annexin V (Dha316) treated with 0.5 equiv. Selectfluor *bis*(triflate) at 42 °C for 15 min.

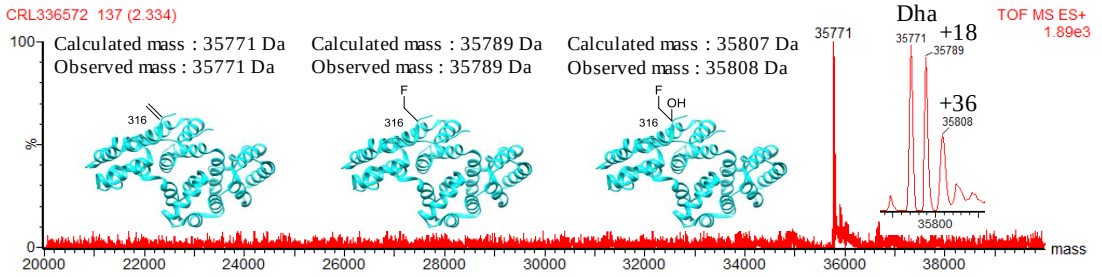

Figure 1.14 ESI-MS spectrum of the annexin V (Dha316) treated with 1.0 equiv. Selectfluor *bis*(triflate) at 42 °C for 15 min.

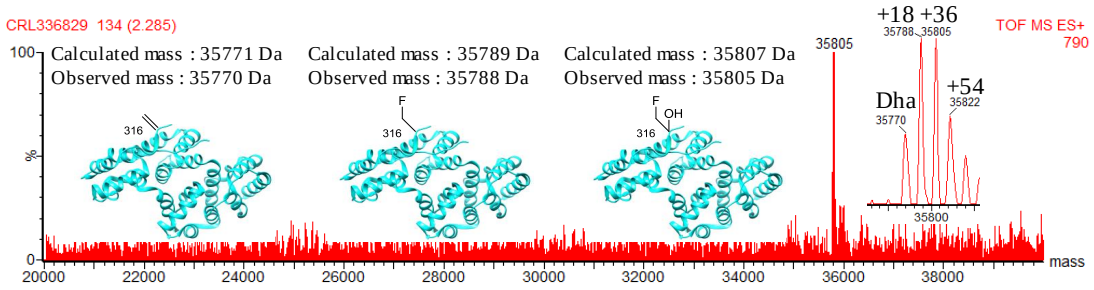

Figure 1.15 ESI-MS spectrum of the annexin V (Dha316) treated with 2.0 equiv. Selectfluor *bis*(triflate) at 42 °C for 15 min.

2.3 Optimisation of [^{18}F]-Radiolabelling of Annexin V(Dha316)

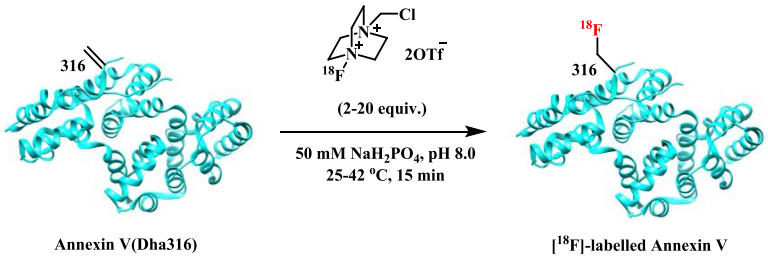

Entry	ANV(Dha316) (equiv.)	Selectfluor *bis*(triflate) (equiv.)	Reaction conditions[a]	Radioactivity (MBq)	Remarks
1	1	2	25 °C, 15 min	0.037	-
2	1	2	37 °C, 15 min	0.100	-
3	1	20	42 °C, 15 min	2.570	-
4	1 (Wild-type)	20	42 °C, 15 min	0.220	Control

General conditions: a). ANV(Dha316) in NaH_2PO_4 (50 mM, pH 8) and Selectfluor *bis*(triflate) in acetone at 25-42 °C for 15 min unless otherwise indicated.

Table 1.4 Optimisation of [^{18}F]-radiolabelling of ANV(Dha316) using [^{18}F]-Selectfluor *bis*(triflate).

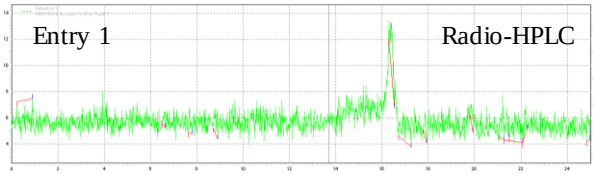

Figure 1.16 Radio-HPLC profile of the annexin V(Dha316) treated with 2 equiv. [^{18}F]-Selectfluor *bis*(triflate) at 25 °C for 15 min.

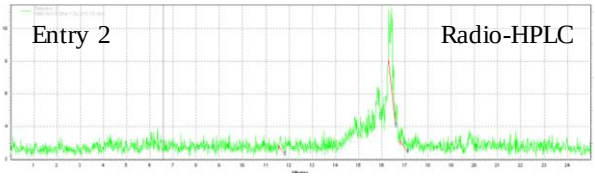

Figure 1.17 Radio-HPLC profile of the annexin V(Dha316) treated with 2 equiv. [^{18}F]-Selectfluor *bis*(triflate) at 37 °C for 15 min.

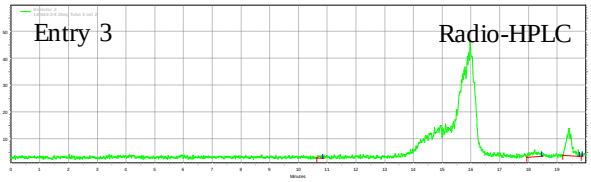

Figure 1.18 Radio-HPLC profile of the annexin V(Dha316) treated with 20 equiv. [^{18}F]-Selectfluor *bis*(triflate) at 42 °C for 15 min.

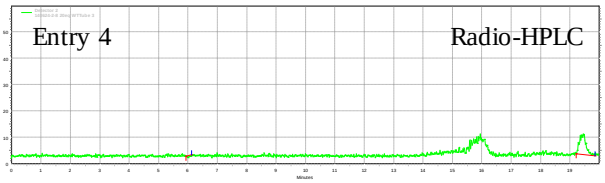

Figure 1.19 Radio-HPLC profile of the annexin V(C316) treated with 20 equiv. [^{18}F]-Selectfluor *bis*(triflate) at 42 °C for 15 min (Control).

3. Optimisation of Protein Iodination Reactions

3.1 Iodination of Insulin

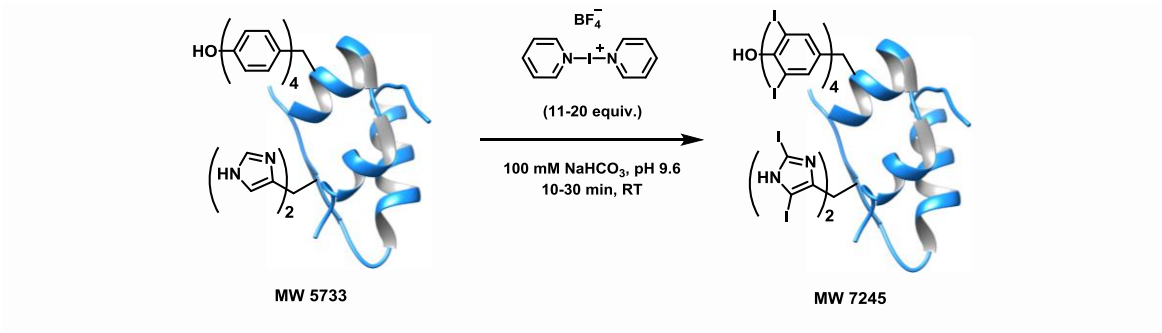

Entry	Insulin (equiv.)	IPy_2BF_4 (equiv.)	Time (min)	Products (Da)
1	1	11	10	5733 (SM), 5859 (1xI), 5985 (2xI), 6110 (3xI), 6237 (4xI), 6363 (5xI), 6489 (6xI), 6614 (7xI), 6741 (8xI)
2	1	11	30	5733 (SM), 5859 (1xI), 5984 (2xI), 6110 (3xI), 6237 (4xI), 6363 (5xI), 6488 (6xI), 6614 (7xI), 6741 (8xI)
3	1	15	10	6237 (4xI), 6362 (5xI), 6488 (6xI), 6614 (7xI), 6740 (8xI), 6866 (9xI), 6992 (10xI), 7118 (11xI), 7244 (12xI)
4	1	20	10	6740 (8xI), 6866 (9xI), 6992 (10xI), 7118 (11xI), 7242 (12xI)

General conditions: Bovine insulin in $NaHCO_3$ (100 mM, pH 9.6) and IPy_2BF_4 in DMF at 25 ^oC for 10-30 min unless otherwise indicated.

Table 1.5 Optimisation of Iodination of insulin with IPy_2BF_4 (11-20 equiv.).

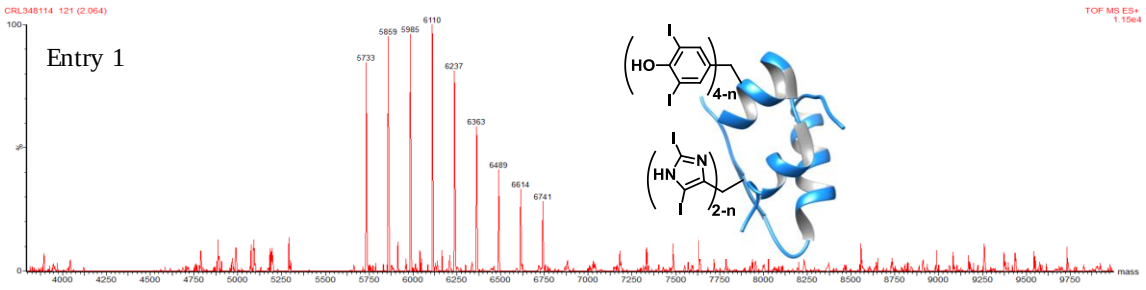

Figure 1.20 ESI-MS spectrum of the insulin treated with 11 equiv. IPy_2BF_4 (10 min).

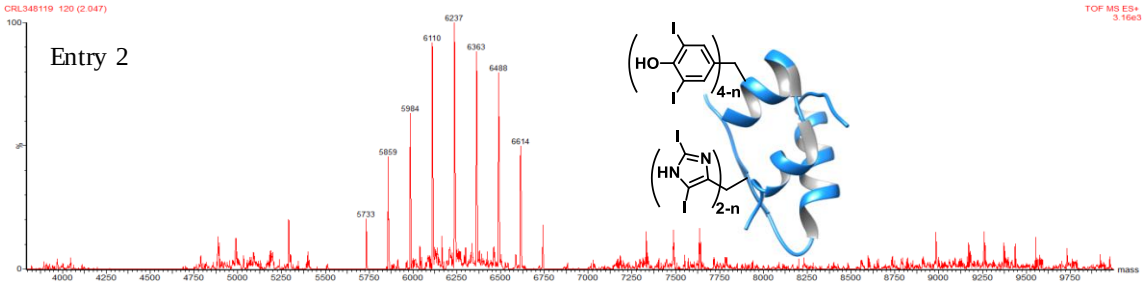

Figure 1.21 ESI-MS spectrum of the insulin treated with 11 equiv. IPy_2BF_4 (30 min).

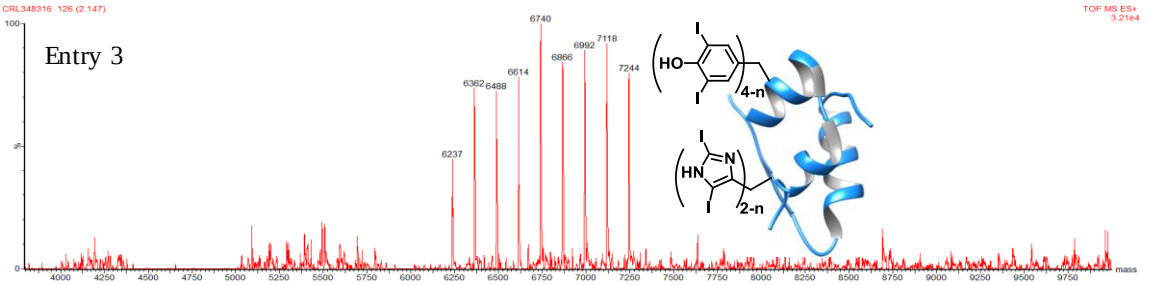

Figure 1.22 ESI-MS spectrum of the insulin treated with 15 equiv. IPy_2BF_4 (10 min).

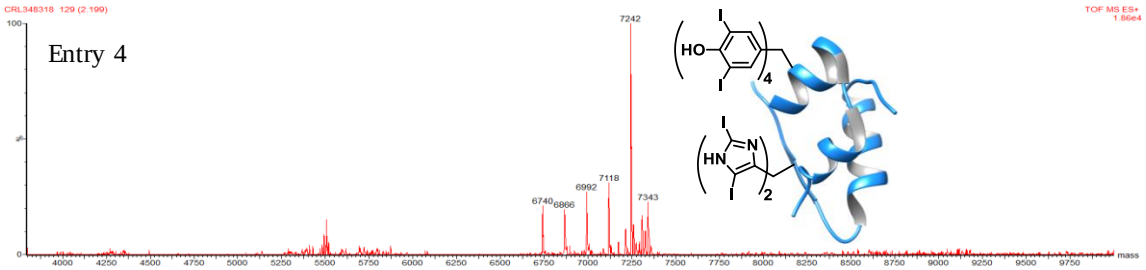

Figure 1.23 ESI-MS spectrum of the insulin treated with 20 equiv. IPy_2BF_4 (10 min).

3.2 Iodination of Monocyte Chemoattractant Protein-1 (MCP-1)

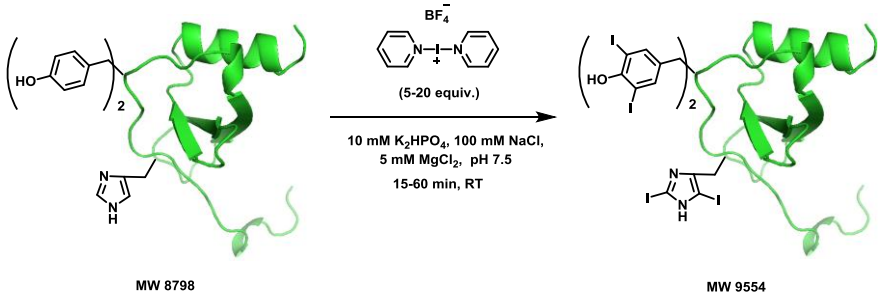

Entry	MCP-1 (equiv.)	IPy_2BF_4 (equiv.)	Time (min)	Products (Da)
1	1	5	15	9044 (2xI), 9170 (3xI), 9296 (4xI), 9422 (5xI)
2	1	5	30	9044 (2xI), 9170 (3xI), 9296 (4xI), 9422 (5xI)
3	1	5	60	9044 (2xI), 9170 (3xI), 9296 (4xI), 9422 (5xI)
4	1	10	30	9425 (5xI), 9551 (6xI)
5	1	20	30	ND.

General conditions: MCP-1 in K_2HPO_4 (10 mM), NaCl (100 mM), $MgCl_2$ (5 mM, pH 7.5) and IPy_2BF_4 in DMF at 25 °C for 15-60 min unless otherwise indicated.
ND. = Not Detectable.

Table 1.6 Optimisation of iodination of MCP-1 with IPy_2BF_4 (5-20 equiv.).

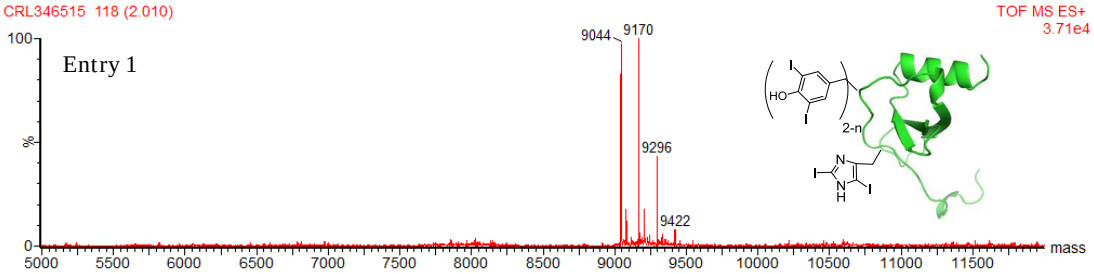

Figure 1.24 ESI-MS spectrum of the MCP-1 treated with 5 equiv. IPy_2BF_4 (15 min).

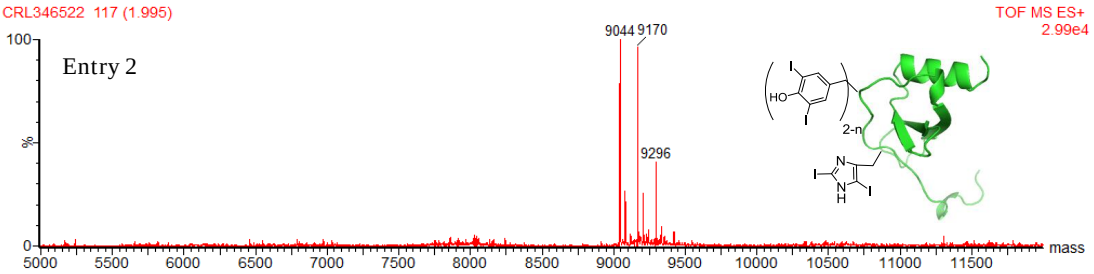

Figure 1.25 ESI-MS spectrum of the MCP-1 treated with 5 equiv. IPy_2BF_4 (30 min).

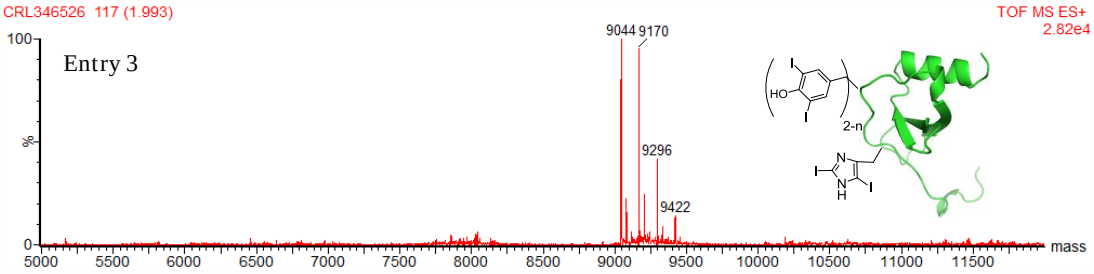

Figure 1.26 ESI-MS spectrum of the MCP-1 treated with 5 equiv. IPy_2BF_4 (60 min).

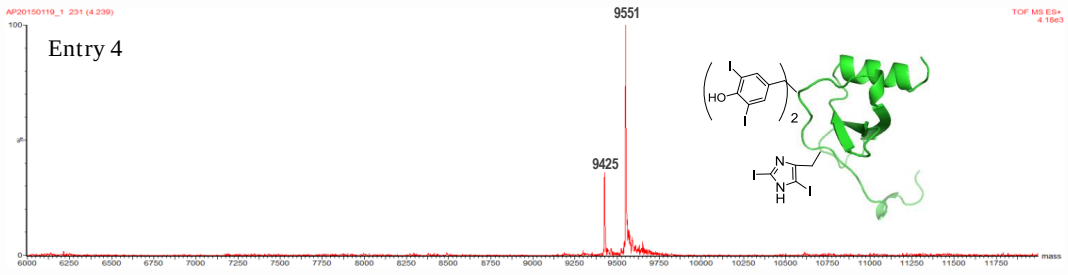

Figure 1.27 ESI-MS spectrum of the MCP-1 treated with 10 equiv. IPy_2BF_4 (30 min).

3.3 Iodination of Ubiquitin (UBQ)

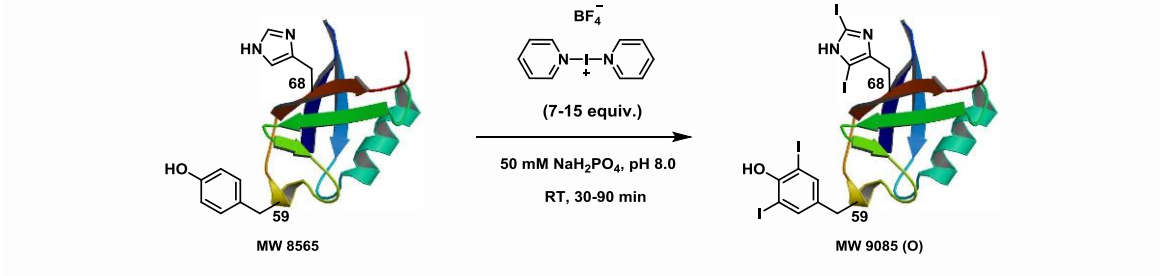

Entry	UBQ (equiv.)	IPy_2BF_4 (equiv.)	Time (min)	Products (Da)
1	1	7	30	8815 (2xI), 8940 (3xI), 9065 (4xI), 9085 (4xI+O)
2	1	7	60	9066 (4xI) , 9084 (4xI+O)
3	1	10	60	9067 (4xI) , 9084 (4xI+O)
4	1	15	60	9067 (4xI) , 9084 (4xI+O)
5	1	15	90	9084 (4xI+O)

General conditions: UBQ in NaH_2PO_4 (50 mM, pH 8) and IPy_2BF_4 in DMF at 25 ^oC for 30-90 min unless otherwise indicated.
O = Oxidised methionine

Table 1.7 Optimisation of iodination of UBQ with IPy_2BF_4 (7-15 equiv.).

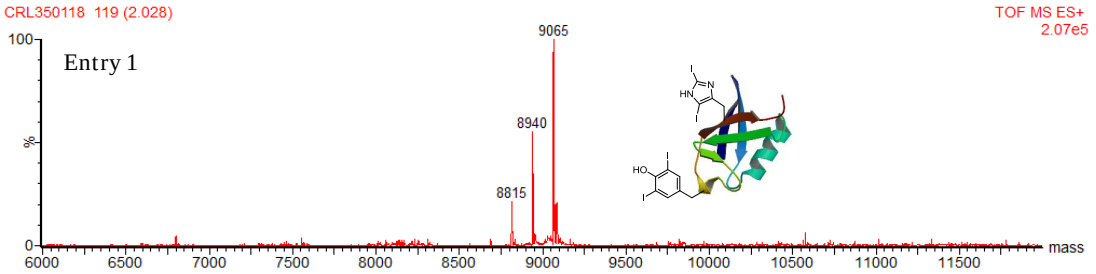

Figure 1.28 ESI-MS spectrum of the ubiquitin treated with 7 equiv. IPy_2BF_4 (30 min).

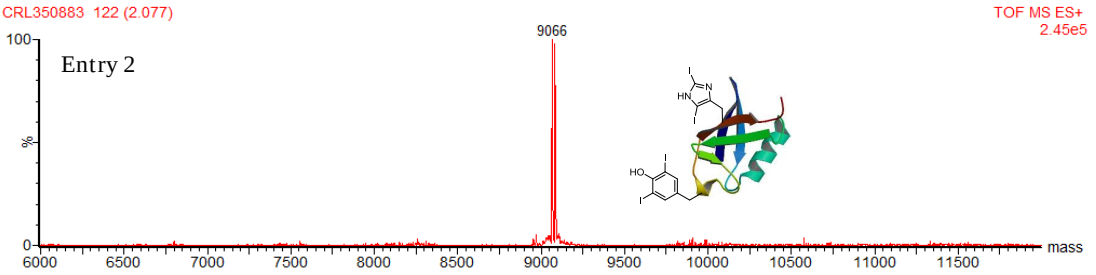

Figure 1.29 ESI-MS spectrum of the ubiquitin treated with 7 equiv. IPy_2BF_4 (60 min).

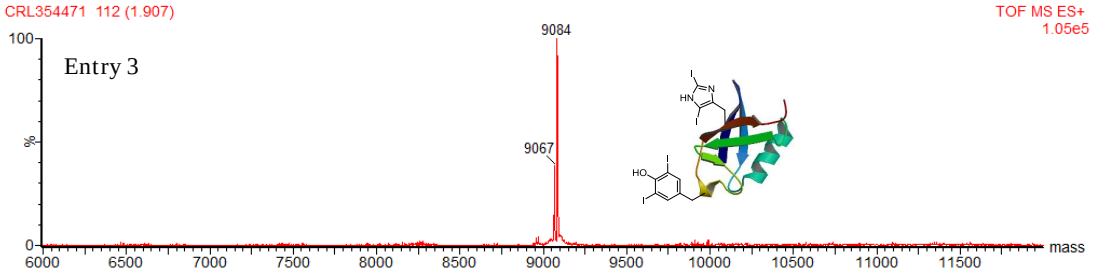

Figure 1.30 ESI-MS spectrum of the ubiquitin treated with 10 equiv. IPy_2BF_4 (60 min).

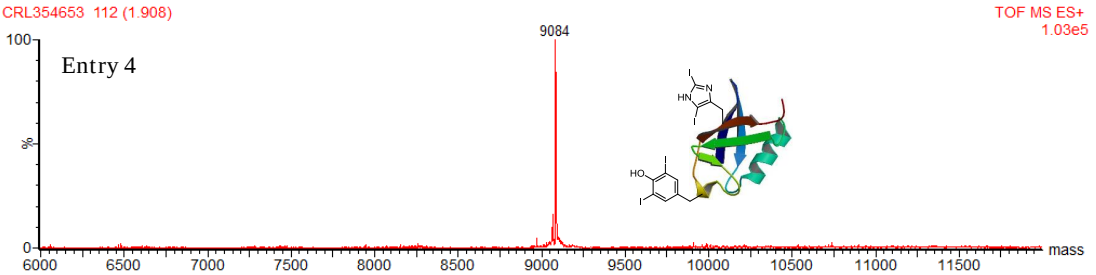

Figure 1.31 ESI-MS spectrum of the ubiquitin treated with 15 equiv. IPy_2BF_4 (60 min).

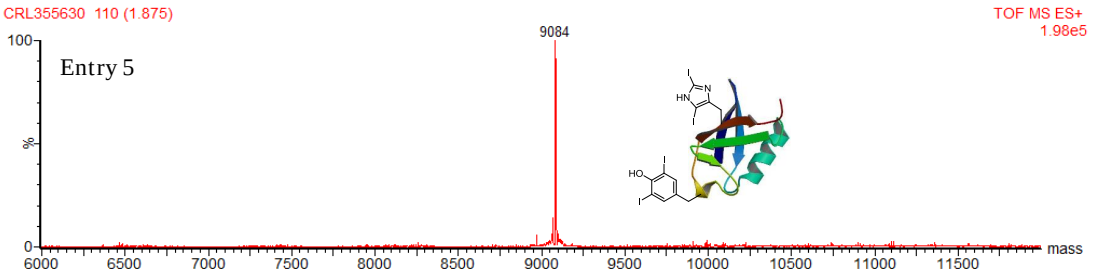

Figure 1.32 ESI-MS spectrum of the ubiquitin treated with 15 equiv. IPy_2BF_4 (90 min).

4. Optimisation of Palladium-Mediated Reactions of Thyroxine (T4)

4.1 *Ex Vivo* Palladium-Mediated Reactions of T4

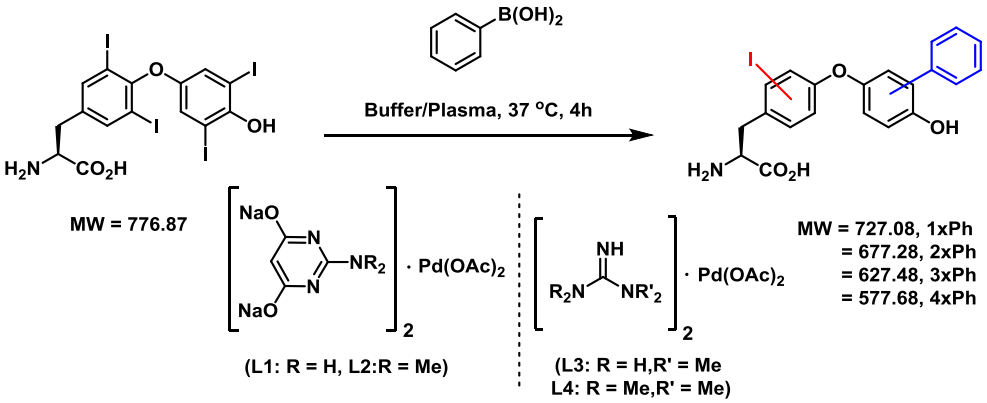

Entry	T4 c=25 mg/mL	$PhB(OH)_2$ c= 25 mg/mL	$(LX)_2Pd(OAc)_2$ 0.01 M	Conditions 37 °C, 4h	ESI-MS
1	1.2 µmol	6.0 µmol	0.24 µmol **L1**	50 mM NaP_i	777.68 (SM)
2	1.2 µmol	6.0 µmol	0.24 µmol **L1**	50 mM NaP_i + plasma (1:1)	777.69 (SM)
3	1.2 µmol	6.0 µmol	0.24 µmol **L1**	Rat plasma	777.74 (SM)
4	1.2 µmol	6.0 µmol	0.24 µmol **L2**	50 mM NaP_i	777.75 (SM)
5	1.2 µmol	6.0 µmol	0.24 µmol **L2**	50 mM NaP_i + plasma (1:1)	777.69 (SM)
6	1.2 µmol	6.0 µmol	0.24 µmol **L2**	Rat plasma	777.69 (SM)
7	1.2 µmol	6.0 µmol	0.24 µmol **L3**	50 mM NaP_i	777.67 (SM)
8	1.2 µmol	6.0 µmol	0.24 µmol **L3**	50 mM NaP_i + plasma (1:1)	777.74 (SM)
9	1.2 µmol	6.0 µmol	0.24 µmol **L3**	Rat plasma	777.74 (SM)
10	1.2 µmol	6.0 µmol	0.24 µmol **L4**	50 mM NaP_i	777.69 (SM)
11	1.2 µmol	6.0 µmol	0.24 µmol **L4**	50 mM NaP_i + plasma (1:1)	777.70 (SM)
12	1.2 µmol	6.0 µmol	0.24 µmol **L4**	Rat plasma	777.74 (SM)

General conditions: T4 in 0.2 M NaOH, $PhB(OH)_2$ in 0.2 M NaOH, $[\mathbf{L1\text{-}L4}]_2Pd(OAc)_2$ in 0.1 M NaOH (c = 0.01 M) at 37 °C for 4h unless otherwise indicated.

Table 1.8 Optimisation experiments of *ex vivo* SMC reactions of T4 with $PhB(OH)_2$ in the presence of $[\mathbf{L1\text{-}L4}]_2Pd(OAc)_2$ catalysts.

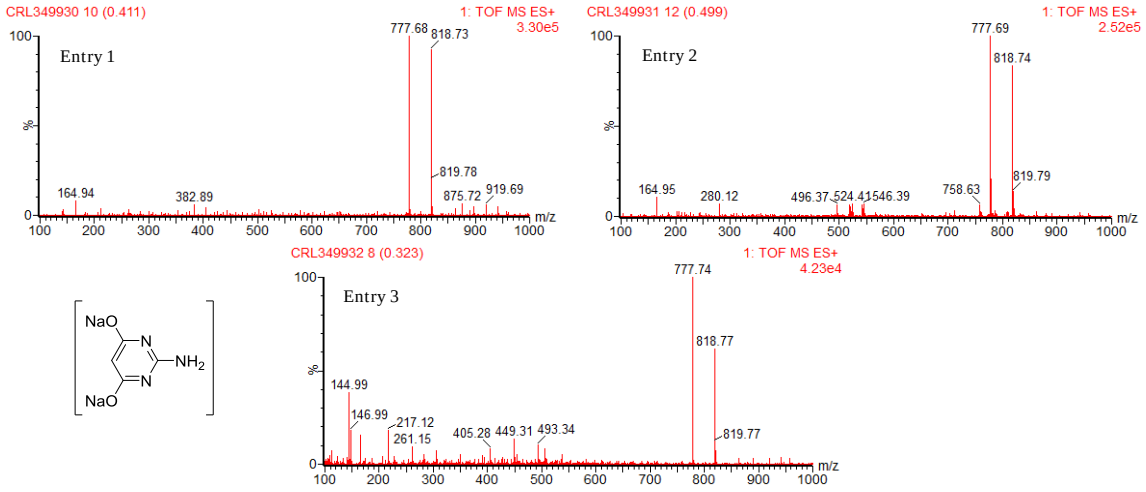

Figure 1.33 ESI-MS spectra of T4 treated with $PhB(OH)_2$ and $[\mathbf{L1}]_2Pd(OAc)_2$ under different conditions (50 mM NaP_i, 1:1 50mM NaP_i/plasma, and plasma, respectively).

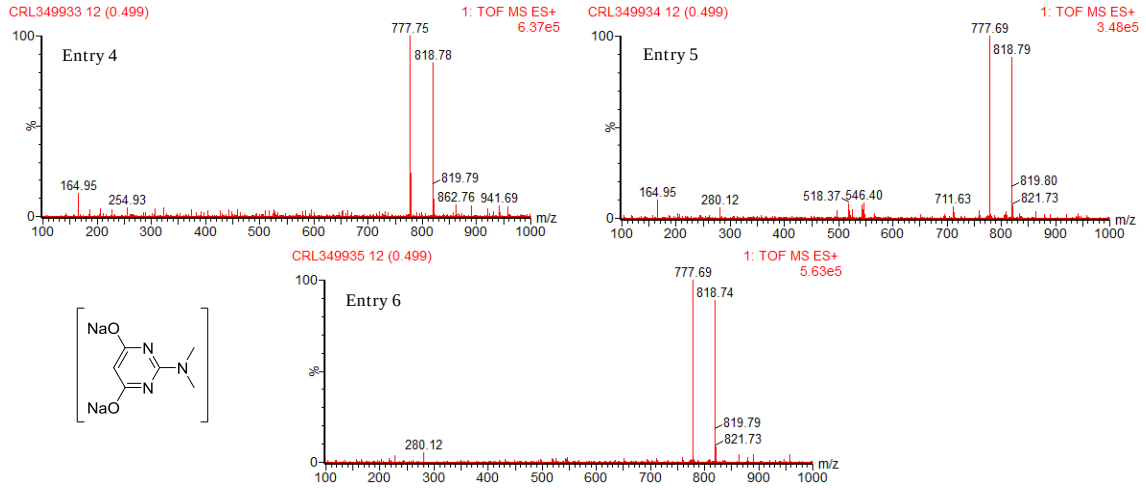

Figure 1.34 ESI-MS spectra of T4 treated with $PhB(OH)_2$ and $[\mathbf{L2}]_2Pd(OAc)_2$ under different conditions (50 mM NaP_i, 1:1 50mM NaP_i/plasma, and plasma, respectively).

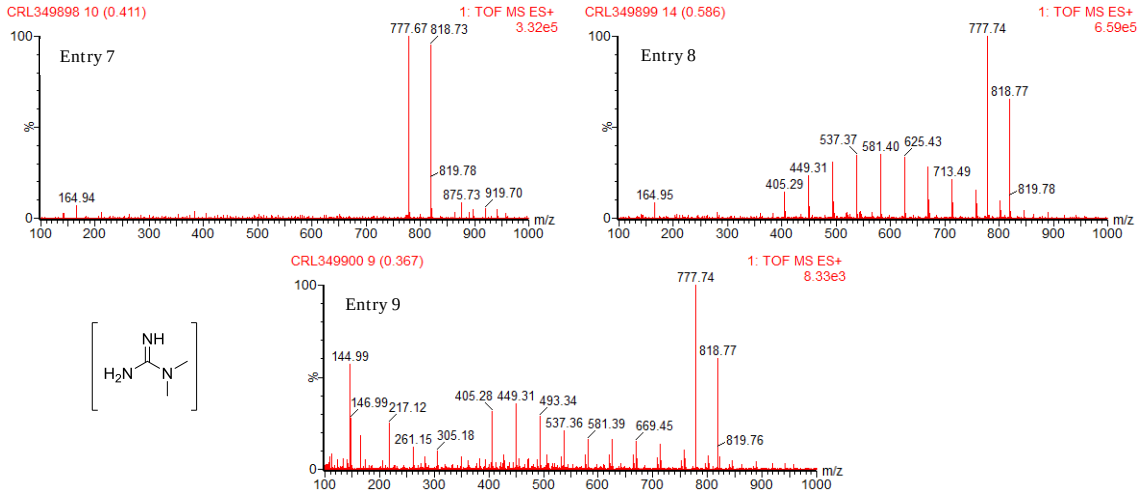

Figure 1.35 ESI-MS spectra of T4 treated with $PhB(OH)_2$ and $[\mathbf{L3}]_2Pd(OAc)_2$ under different conditions (50 mM NaP_i, 1:1 50mM NaP_i/plasma, and plasma, respectively).

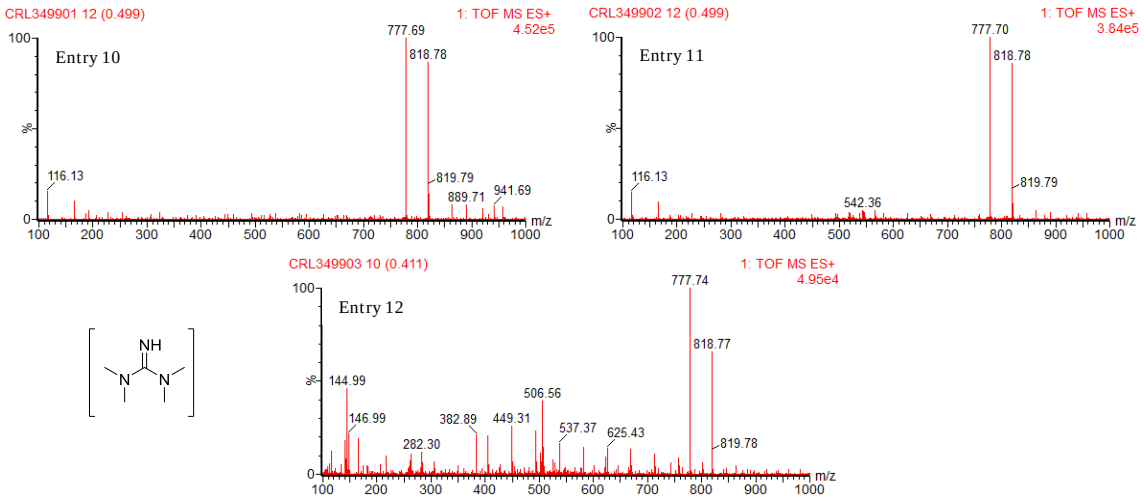

Figure 1.36 ESI-MS spectra of T4 treated with $PhB(OH)_2$ and $[\mathbf{L4}]_2Pd(OAc)_2$ under different conditions (50 mM NaP_i, 1:1 50mM NaP_i/plasma, and plasma, respectively).

4.2 *Ex Vivo* Palladium-Mediated Reactions of BocNH-T4

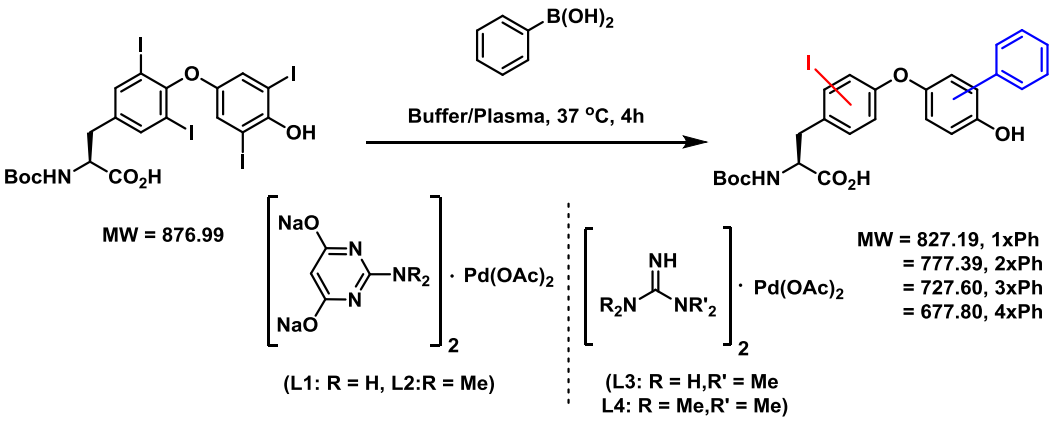

Entry	BocNH -T4 c=25 mg/mL	$PhB(OH)_2$ c= 25 mg/mL	$(LX)_2Pd(OAc)_2$ 0.01 M	Conditions 37 °C, 4h	ESI-MS
1	1.2 µmol	6.0 µmol	0.24 µmol **L1**	50 mM NaP_i	875.81 (SM)
2	1.2 µmol	6.0 µmol	0.24 µmol **L1**	50 mM NaP_i + plasma (1:1)	875.82 (SM)
3	1.2 µmol	6.0 µmol	0.24 µmol **L1**	Rat plasma	875.83 (SM)
4	1.2 µmol	6.0 µmol	0.24 µmol **L2**	50 mM NaP_i	875.83 (SM)
5	1.2 µmol	6.0 µmol	0.24 µmol **L2**	50 mM NaP_i + plasma (1:1)	875.82 (SM)
6	1.2 µmol	6.0 µmol	0.24 µmol **L2**	Rat plasma	875.83 (SM)
7	1.2 µmol	6.0 µmol	0.24 µmol **L3**	50 mM NaP_i	875.82 (SM)
8	1.2 µmol	6.0 µmol	0.24 µmol **L3**	50 mM NaP_i + plasma (1:1)	875.83 (SM)
9	1.2 µmol	6.0 µmol	0.24 µmol **L3**	Rat plasma	875.84 (SM)
10	1.2 µmol	6.0 µmol	0.24 µmol **L4**	50 mM NaP_i	875.84 (SM)
11	1.2 µmol	6.0 µmol	0.24 µmol **L4**	50 mM NaP_i + plasma (1:1)	875.84 (SM)
12	1.2 µmol	6.0 µmol	0.24 µmol **L4**	Rat plasma	875.85 (SM)

General conditions : BocNH-T4 in 0.2 M NaOH, $PhB(OH)_2$ in 0.2 M NaOH, $[\mathbf{L1\text{-}L4}]_2Pd(OAc)_2$ in 0.1 M NaOH (c = 0.01 M) at 37 °C for 4h unless otherwise indicated.

Table 1.9 Optimisation experiments of *ex vivo* SMC reactions of BocNH-T4 with $PhB(OH)_2$ in the presence of $[\mathbf{L1\text{-}L4}]_2Pd(OAc)_2$ catalysts**.**

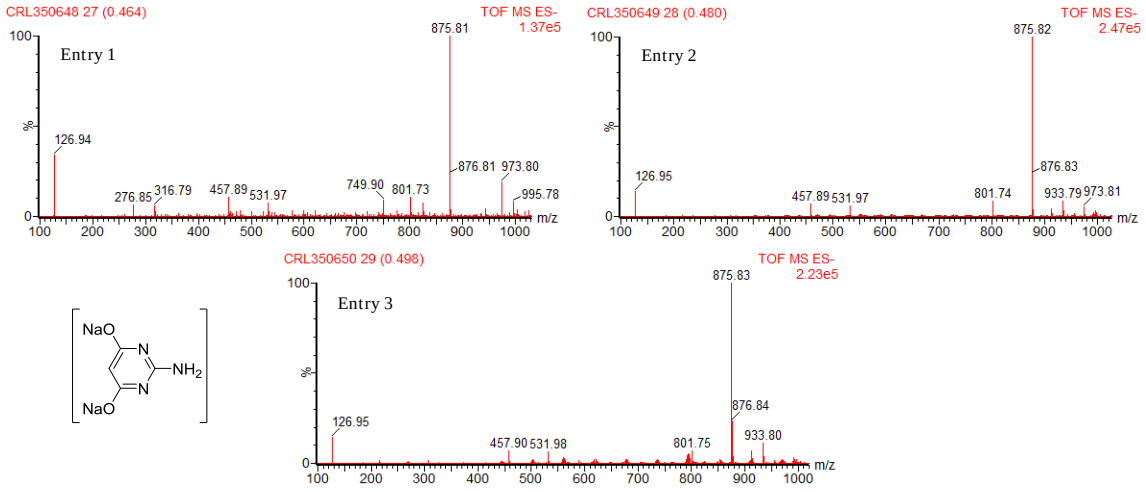

Figure 1.37 ESI-MS spectra of BocNH-T4 treated with $PhB(OH)_2$ and $[\mathbf{L1}]_2Pd(OAc)_2$ under different conditions (50 mM NaP_i, 1:1 50mM NaP_i/plasma, and plasma, respectively).

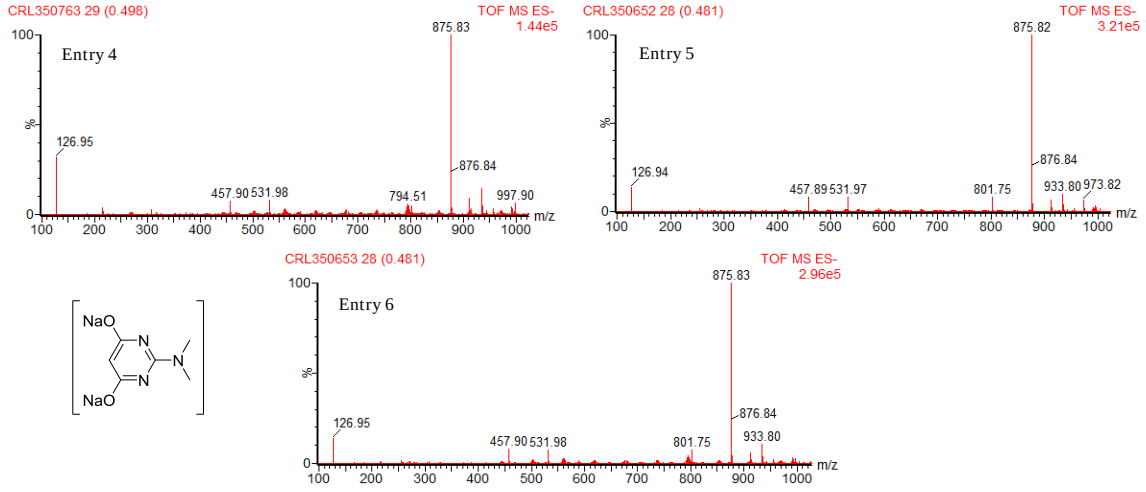

Figure 1.38 ESI-MS spectra of BocNH-T4 treated with $PhB(OH)_2$ and $[\mathbf{L2}]_2Pd(OAc)_2$ under different conditions (50 mM NaP_i, 1:1 50mM NaP_i/plasma, and plasma, respectively).

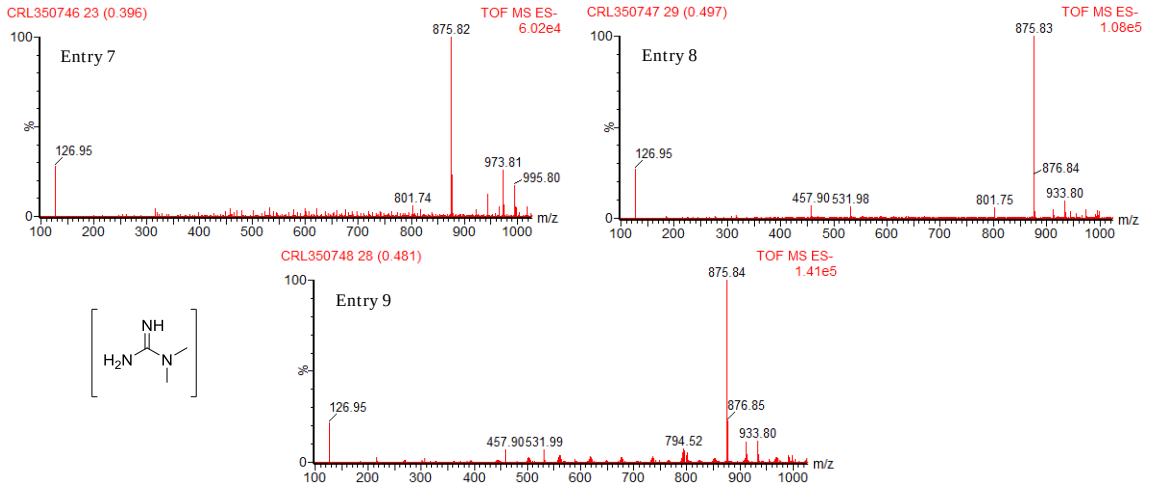

Figure 1.39 ESI-MS spectra of BocNH-T4 treated with $PhB(OH)_2$ and $[\mathbf{L3}]_2Pd(OAc)_2$ under different conditions (50 mM NaP_i, 1:1 50mM NaP_i/plasma, and plasma, respectively).

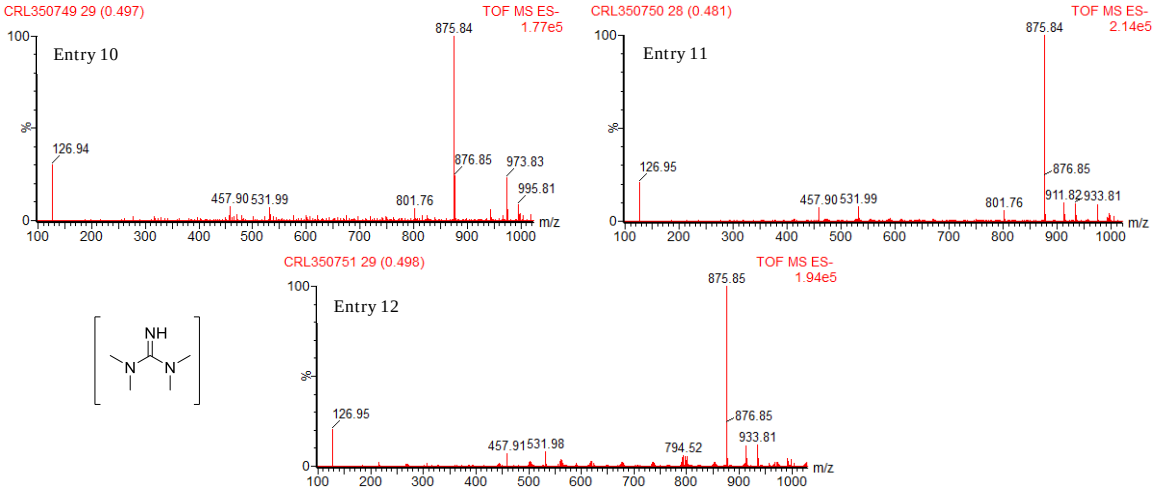

Figure 1.40 ESI-MS spectra of BocNH-T4 treated with $PhB(OH)_2$ and $[\mathbf{L4}]_2Pd(OAc)_2$ under different conditions (50 mM NaP_i, 1:1 50mM NaP_i/plasma, and plasma, respectively).

Title:	The biochemical journal
Article ID:	To be determined
Publication:	Publication1
Publisher:	CCC Republication
Date:	Jan 1, 1984

Order Completed

Thank you for your order.

This Agreement between Anuchit Phanumartwiwath ("You") and Portland Press, Ltd. ("Portland Press, Ltd.") consists of your order details and the terms and conditions provided by Portland Press, Ltd. and Copyright Clearance Center.

License number	Reference confirmation email for license number
License date	Jan 31, 2017
Licensed content publisher	Portland Press, Ltd.
Licensed content title	The biochemical journal
Licensed content date	Jan 1, 1984
Type of use	Thesis/Dissertation
Requestor type	Academic institution
Format	Print, Electronic
Portion	chart/graph/table/figure
Number of charts/graphs/tables/figures	1
Title or numeric reference of the portion(s)	Figure 5 MALDI-TOF mass spectra of PA6 with different Trp analogues digested with trypsin.
Title of the article or chapter the portion is from	Lactococcus lactis as expression host for the biosynthetic incorporation of tryptophan analogues into recombinant proteins.
Editor of portion(s)	Biochemical journal
Author of portion(s)	M. EL Khattabi, M. L. van Roosmalen, D. Jager, H. Metselaar, H. Permentier, K. Leenhouts, and J. Broos
Volume of serial or monograph	409
Page range of portion	193-198
Publication date of portion	01 Jan 2008
Rights for	Main product
Duration of use	Life of current edition
Creation of copies for the disabled	no
With minor editing privileges	yes
For distribution to	Worldwide
In the following language(s)	Original language of publication
With incidental promotional use	no
Lifetime unit quantity of new product	Up to 499
Made available in the following markets	Education
Specified additional information	Minor editing privileges
The requesting person/organization	Anuchit Phanumartwiwath
Order reference number	
Author/Editor	Anuchit Phanumartwiwath
The standard identifier of New Work	PhD thesis/dissertation

Title of New Work	Novel Halogenation and Palladio-Biology Strategies for Biological Probes
Publisher of New Work	University of Oxford
Expected publication date	Feb 2017
Estimated size (pages)	305
Requestor Location	Anuchit Phanumartwiwath St. Cross College, St. Giles Oxford, OX1 3LZ United Kingdom Attn: Anuchit Phanumartwiwath
Billing Type	Invoice
Billing address	Anuchit Phanumartwiwath St. Cross College, St. Giles Oxford, United Kingdom OX1 3LZ Attn: Anuchit Phanumartwiwath
Total (may include CCC user fee)	0.00 USD
Total	0.00 USD

CLOSE WINDOW

Title: Site-Specific Incorporation of Tryptophan Analogues into Recombinant Proteins in Bacterial Cells

Author: Inchan Kwon, David A. Tirrell

Publication: Journal of the American Chemical Society

Publisher: American Chemical Society

Date: Aug 1, 2007

PERMISSION/LICENSE IS GRANTED FOR YOUR ORDER AT NO CHARGE

This type of permission/license, instead of the standard Terms & Conditions, is sent to you because no fee is being charged for your order. Please note the following:

- Permission is granted for your request in both print and electronic formats, and translations.
- If figures and/or tables were requested, they may be adapted or used in part.
- Please print this page for your records and send a copy of it to your publisher/graduate school.
- Appropriate credit for the requested material should be given as follows: "Reprinted (adapted) with permission from (COMPLETE REFERENCE CITATION). Copyright (YEAR) American Chemical Society." Insert appropriate information in place of the capitalized words.
- One-time permission is granted only for the use specified in your request. No additional uses are granted (such as derivative works or other editions). For any other uses, please submit a new request.

If credit is given to another source for the material you requested, permission must be obtained from that source.

BACK | CLOSE WINDOW